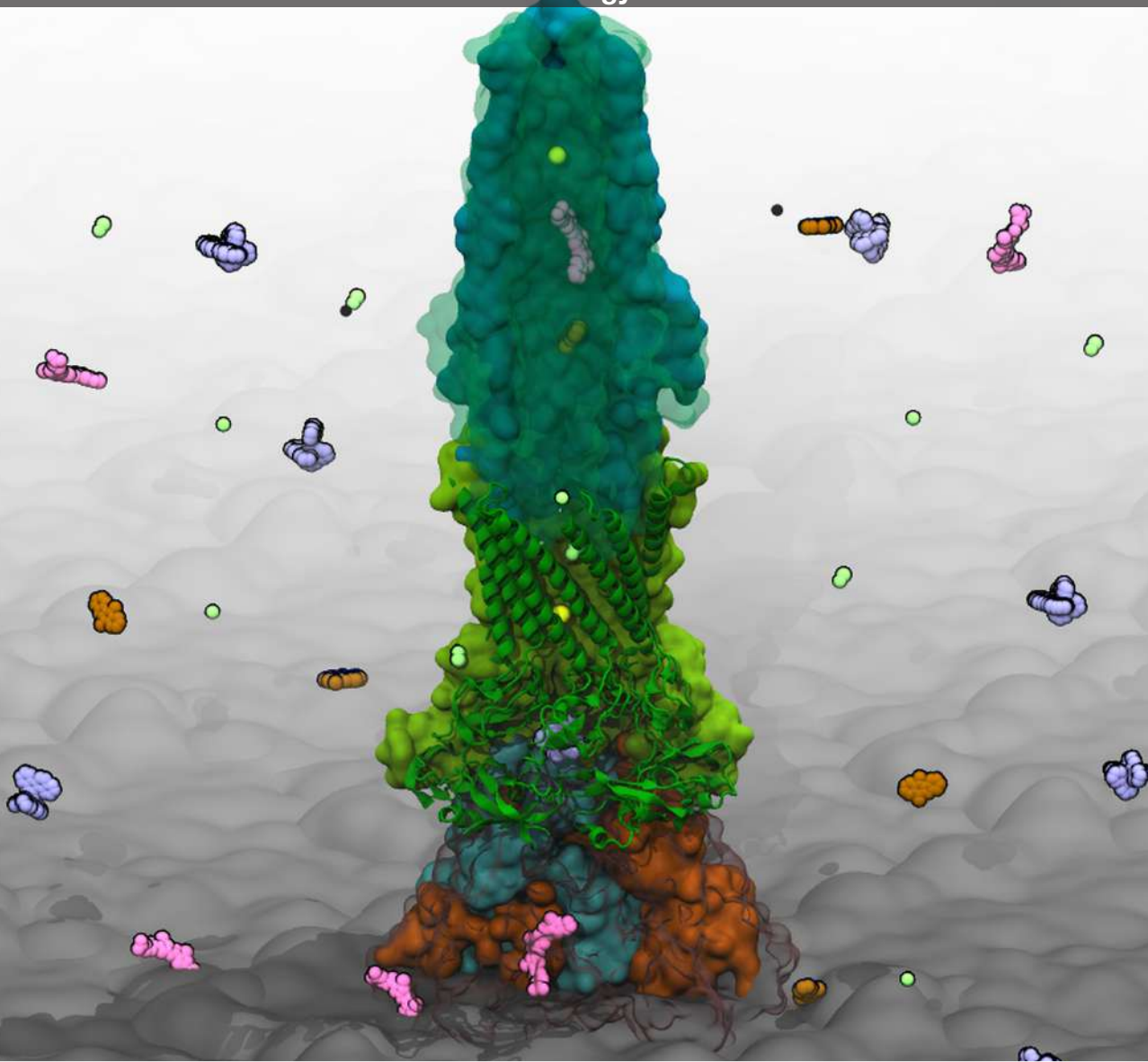


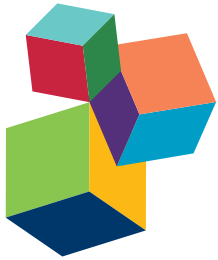
# BAD BUGS IN THE XXIst CENTURY: RESISTANCE MEDIATED BY MULTI-DRUG EFFLUX PUMPS IN GRAM-NEGATIVE BACTERIA

EDITED BY: Attilio Vittorio Vargiu, Klaas Martinus Pos,

Keith Poole and Hiroshi Nikaido

PUBLISHED IN: Frontiers in Microbiology





# frontiers

## **Frontiers Copyright Statement**

© Copyright 2007-2016 Frontiers Media SA. All rights reserved.

All content included on this site, such as text, graphics, logos, button icons, images, video/audio clips, downloads, data compilations and software, is the property of or is licensed to Frontiers Media SA ("Frontiers") or its licensees and/or subcontractors. The copyright in the text of individual articles is the property of their respective authors, subject to a license granted to Frontiers.

The compilation of articles constituting this e-book, wherever published, as well as the compilation of all other content on this site, is the exclusive property of Frontiers. For the conditions for downloading and copying of e-books from Frontiers' website, please see the Terms for Website Use. If purchasing Frontiers e-books from other websites or sources, the conditions of the website concerned apply.

Images and graphics not forming part of user-contributed materials may not be downloaded or copied without permission.

Individual articles may be downloaded and reproduced in accordance with the principles of the CC-BY licence subject to any copyright or other notices. They may not be re-sold as an e-book.

As author or other contributor you grant a CC-BY licence to others to reproduce your articles, including any graphics and third-party materials supplied by you, in accordance with the Conditions for Website Use and subject to any copyright notices which you include in connection with your articles and materials.

All copyright, and all rights therein, are protected by national and international copyright laws.

The above represents a summary only. For the full conditions see the Conditions for Authors and the Conditions for Website Use.

**ISSN 1664-8714**

**ISBN 978-2-88919-931-0**

**DOI 10.3389/978-2-88919-931-0**

## **About Frontiers**

Frontiers is more than just an open-access publisher of scholarly articles: it is a pioneering approach to the world of academia, radically improving the way scholarly research is managed. The grand vision of Frontiers is a world where all people have an equal opportunity to seek, share and generate knowledge. Frontiers provides immediate and permanent online open access to all its publications, but this alone is not enough to realize our grand goals.

## **Frontiers Journal Series**

The Frontiers Journal Series is a multi-tier and interdisciplinary set of open-access, online journals, promising a paradigm shift from the current review, selection and dissemination processes in academic publishing. All Frontiers journals are driven by researchers for researchers; therefore, they constitute a service to the scholarly community. At the same time, the Frontiers Journal Series operates on a revolutionary invention, the tiered publishing system, initially addressing specific communities of scholars, and gradually climbing up to broader public understanding, thus serving the interests of the lay society, too.

## **Dedication to Quality**

Each Frontiers article is a landmark of the highest quality, thanks to genuinely collaborative interactions between authors and review editors, who include some of the world's best academicians. Research must be certified by peers before entering a stream of knowledge that may eventually reach the public - and shape society; therefore, Frontiers only applies the most rigorous and unbiased reviews.

Frontiers revolutionizes research publishing by freely delivering the most outstanding research, evaluated with no bias from both the academic and social point of view.

By applying the most advanced information technologies, Frontiers is catapulting scholarly publishing into a new generation.

## **What are Frontiers Research Topics?**

Frontiers Research Topics are very popular trademarks of the Frontiers Journals Series: they are collections of at least ten articles, all centered on a particular subject. With their unique mix of varied contributions from Original Research to Review Articles, Frontiers Research Topics unify the most influential researchers, the latest key findings and historical advances in a hot research area! Find out more on how to host your own Frontiers Research Topic or contribute to one as an author by contacting the Frontiers Editorial Office: [researchtopics@frontiersin.org](mailto:researchtopics@frontiersin.org)

# BAD BUGS IN THE XXIst CENTURY: RESISTANCE MEDIATED BY MULTI-DRUG EFFLUX PUMPS IN GRAM-NEGATIVE BACTERIA

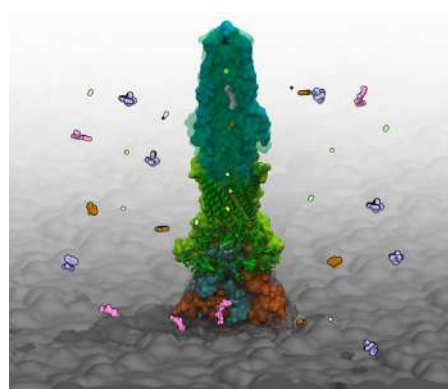
Topic Editors:

**Attilio Vittorio Vargiu**, University of Cagliari, Italy

**Klaas Martinus Pos**, Goethe-University, Germany

**Keith Poole**, Queen's University, Canada

**Hiroshi Nikaido**, University of California, Berkeley, USA



View of the AcrABZ-TolC efflux pump embedded in a model membrane (coordinates of the efflux pump kindly provided by Ben Luisi). The membrane is shown as grey surface, while the half front and the half back parts of the protein assembly are shown in transparent and solid surfaces, respectively. The front monomers of the AcrA hexamer are also shown as cartoons. The Loose, Tight, and Open monomers of AcrB are colored cyan, orange and magenta respectively, while AcrA and TolC proteins are colored green and dark cyan respectively. Different substrates of the pump floating in the periplasmic space are shown with van der Waals spheres.

Image by Attilio Vittorio Vargiu

The discovery of antibiotics represented a key milestone in the history of medicine. However, with the rise of these life-saving drugs came the awareness that bacteria deploy defence mechanisms to resist these antibiotics, and they are good at it. Today, we appear at a crossroads between discovery of new potent drugs and omni-resistant superbugs. Moreover, the misuse of antibiotics in different industries has increased the rate of resistance development by providing permanent selective pressure and, subsequently, enrichment of multidrug resistant pathogens. As a result, antimicrobial resistance has now become an urgent threat to public health worldwide. (<http://www.who.int/drugresistance/documents/surveillancereport/en/>).

The development of multidrug resistance (MDR) in an increasing number of pathogens, including *Pseudomonas*, *Acinetobacter*, *Klebsiella*, *Salmonella*, *Burkholderia*, and other Gram-negative bacteria is a most severe issue. Membrane efflux pump complexes of the Resistance-Nodulation-cell Division (RND) superfamily play a key role in the development of MDR in these bacteria. RND pumps, together with other transporters, contribute to intrinsic and acquired resistance to most, if not all, of the antimicrobial compounds available in our drug arsenal. Given the enormous drug polyspecificity of MDR efflux pumps, studies on their mechanism of action are extremely challenging, and this has negatively impacted both the development of new antibiotics that are able to evade these efflux pumps as well as the design of pump inhibitors.

The collection of articles in this eBook, published as a Research Topic in *Frontiers in Microbiology*, section of Antimicrobials, Resistance, and Chemotherapy, aims to update the reader about the latest advances on the structure and function of RND efflux transporters, their roles in the overall multidrug resistance phenotype of Gram-negative pathogens, and on strategies to inhibit their activities. A deeper understanding of the mechanisms by which RND efflux pumps, alone or synergistically with other efflux pumps, are able to limit the concentration of antimicrobial compounds inside the bacterial cell, may pave the way for new, more directed, inhibitor and antibiotic design to ultimately overcome antimicrobial resistance by Gram-negatives.

**Citation:** Vargiu, A. V., Pos, K. M., Poole, K., Nikaido, H., eds. (2016). *Bad Bugs in the XXIst Century: Resistance Mediated by Multi-Drug Efflux Pumps in Gram-Negative Bacteria*. Lausanne: Frontiers Media. doi: 10.3389/978-2-88919-931-0

# Table of Contents

- 06 Editorial: Bad Bugs in the XXIst Century: Resistance Mediated by Multi-Drug Efflux Pumps in Gram-Negative Bacteria**  
Attilio V. Vargiu, Klaas M. Pos, Keith Poole and Hiroshi Nikaido
- 09 Structural basis of RND-type multidrug exporters**  
Akihito Yamaguchi, Ryosuke Nakashima and Keisuke Sakurai
- 28 Substrate binding accelerates the conformational transitions and substrate dissociation in multidrug efflux transporter AcrB**  
Beibei Wang, Jingwei Weng and Wenning Wang
- 39 Interaction of antibacterial compounds with RND efflux pumps in *Pseudomonas aeruginosa***  
Jürg Dreier and Paolo Ruggerone
- 60 New OprM structure highlighting the nature of the N-terminal anchor**  
Laura Monlezun, Gilles Phan, Houssain Benabdellah, Marie-Bernard Lascombe, Véronique Y. N. Enguéné, Martin Picard and Isabelle Broutin
- 70 Repressive mutations restore function-loss caused by the disruption of trimerization in Escherichia coli multidrug transporter AcrB**  
Zhaoshuai Wang, Meng Zhong, Wei Lu, Qian Chai and Yinan Wei
- 80 Mechanism of coupling drug transport reactions located in two different membranes**  
Helen I. Zgurskaya, Jon W. Weeks, Abigail T. Ntreh, Logan M. Nickels and David Wolloscheck
- 93 Architecture and roles of periplasmic adaptor proteins in tripartite efflux assemblies**  
Martyn F. Symmons, Robert L. Marshall and Vassiliy N. Bavro
- 113 Catch me if you can: a biotinylated proteoliposome affinity assay for the investigation of assembly of the MexA-MexB-OprM efflux pump from *Pseudomonas aeruginosa***  
Véronique Yvette Ntsogo Enguéné, Alice Verchère, Gilles Phan, Isabelle Broutin and Martin Picard
- 121 The ins and outs of RND efflux pumps in Escherichia coli**  
João Anes, Matthew P. McCusker, Séamus Fanning and Marta Martins
- 135 PMQR Genes OqxAB and aac(6')lb-cr accelerate the development of fluoroquinolone resistance in *Salmonella typhimurium***  
Marcus H. Wong, Edward W. Chan, Li Z. Liu and Sheng Chen
- 142 An ace up their sleeve: a transcriptomic approach exposes the AceI efflux protein of *Acinetobacter baumannii* and reveals the drug efflux potential hidden in many microbial pathogens**  
Karl A. Hassan, Liam D. H. Elbourne, Liping Li, Hasinika K. A. H. Gamage, Qi Liu, Scott M. Jackson, David Sharples, Anne-Brit Kolstø, Peter J. F. Henderson and Ian T. Paulsen

- 148** *Efflux-mediated fluoroquinolone resistance in the multidrug-resistant *Pseudomonas aeruginosa* clinical isolate PA7: identification of a novel MexS variant involved in upregulation of the mexEF-oprN multidrug efflux operon*  
Yuji Morita, Junko Tomida and Yoshiaki Kawamura
- 157** *Efflux pump-mediated drug resistance in Burkholderia*  
Nicole L. Podnecky, Katherine A. Rhodes and Herbert P. Schweizer
- 167** *RND-type drug efflux pumps from Gram-negative bacteria: molecular mechanism and inhibition*  
Henrietta Venter, Rumana Mowla, Thelma Ohene-Agyei and Shutao Ma
- 178** *Recent advances toward a molecular mechanism of efflux pump inhibition*  
Timothy J. Opperman and Son T. Nguyen



# Editorial: Bad Bugs in the XXIst Century: Resistance Mediated by Multi-Drug Efflux Pumps in Gram-Negative Bacteria

Attilio V. Vargiu<sup>1\*</sup>, Klaas M. Pos<sup>2</sup>, Keith Poole<sup>3</sup> and Hiroshi Nikaido<sup>4</sup>

<sup>1</sup> Department of Physics, University of Cagliari, Monserrato, Italy, <sup>2</sup> Institute of Biochemistry, Goethe-University, Frankfurt am Main, Germany, <sup>3</sup> Department of Biomedical and Molecular Sciences, Queen's University, Kingston, ON, Canada, <sup>4</sup> Department of Molecular and Cell Biology, University of California, Berkeley, Berkeley, CA, USA

**Keywords:** antibiotic resistance, multi-drug-resistant pathogens, efflux pumps, superbugs, bacterial resistance mechanisms

## The Editorial on the Research Topic

### Bad Bugs in the XXIst Century: Resistance Mediated by Multi-Drug Efflux Pumps in Gram-Negative Bacteria

#### OPEN ACCESS

##### Edited by:

Kunihiro Nishino,  
Osaka University, Japan

##### Reviewed by:

Aixin Yan,  
The University of Hong Kong, China

##### \*Correspondence:

Attilio V. Vargiu  
vargiu@dsf.unica.it

##### Specialty section:

This article was submitted to  
Antimicrobials, Resistance and  
Chemotherapy,  
a section of the journal  
*Frontiers in Microbiology*

**Received:** 06 May 2016

**Accepted:** 17 May 2016

**Published:** 31 May 2016

##### Citation:

Vargiu AV, Pos KM, Poole K and  
Nikaido H (2016) Editorial: Bad Bugs  
in the XXIst Century: Resistance  
Mediated by Multi-Drug Efflux Pumps  
in Gram-Negative Bacteria.  
*Front. Microbiol.* 7:833.

doi: 10.3389/fmicb.2016.00833

The discovery of antibiotics represented a key milestone in the history of medicine. However, with the rise of these life-saving drugs came the awareness that bacteria deploy defense mechanisms to resist these antibiotics, and they are good at it. Today, we appear at a crossroads between discovery of new potent drugs and omni-resistant superbugs. Moreover, the misuse of antibiotics in different industries has increased the rate of resistance development by providing permanent selective pressure and, subsequently, enrichment of multidrug resistant pathogens. As a result, antimicrobial resistance has now become an urgent threat to public health worldwide (<http://www.who.int/drugresistance/documents/surveillancereport/en/>). The development of multidrug resistance (MDR) in an increasing number of pathogens, including *Pseudomonas*, *Acinetobacter*, *Klebsiella*, *Salmonella*, *Burkholderia*, and other Gram-negative bacteria is a serious issue. Membrane efflux pump complexes of the Resistance-Nodulation-Division (RND) superfamily play a key role in the development of MDR in these bacteria. These pumps, together with other transporters, contribute to intrinsic and acquired resistance of bacteria toward most, if not all, of the compounds available in our antimicrobial arsenal. Given the enormous drug polyspecificity of MDR efflux pumps, studies on their mechanism of action are extremely challenging, and this has negatively impacted both on the development of new antibiotics that are able to evade these efflux pumps and on the design of pump inhibitors. The collection of articles in this eBook, published as a Research Topic in *Frontiers in Microbiology*, section of Antimicrobials, Resistance, and Chemotherapy, aims to update the reader about the latest advances on the structure and function of RND efflux transporters, their roles in the overall multidrug resistance phenotype of Gram-negative pathogens, and on the strategies to inhibit their activities.

RND transporters reside in the inner membrane, and in Gram-negative bacteria they form trans-envelope complexes together with periplasmic membrane fusion proteins (MFPs) and outer membrane factors (OMFs). As tripartite entities, these macromolecular complexes are powerful machines that expel multiple antibiotics across outer membranes. In recent years, much of the research efforts have been focused on the structures of the RND, MFP, and the OMF components. The assembly and disassembly of the tripartite efflux pump components is so crucial to their physiological role in resistance, that much research effort has been directed toward both the

elucidation of the structures and functional dynamics of individual components and the *in vivo* and *in vitro* assembly and function of the tripartite systems. X-ray crystallography has provided an understanding of the molecular basis of drug transport by RND-type efflux pumps. Yamaguchi et al. stress critical points related to structure and function of these tripartite pumps, including the lack of consensus on the number of adaptor proteins and the molecular basis for multidrug recognition by two voluminous promiscuous binding pockets in the RND transporter, and they formulate a multisite-drug-oscillation hypothesis to describe their activity. Substrate-mediated conformational changes in RND efflux pumps are also investigated *in silico* by Wang et al. The authors use molecular dynamics simulations of AcrB in complex with substrates to discover an intrinsic allostery in the transport mechanism upon binding of a second substrate. Dreier and Ruggerone analyze how subtle differences in the physicochemical features of antibiotics belonging to the same family determine their diverse susceptibility to efflux mechanisms. They highlight the importance of combining different high-resolution techniques to gain insights on substrate recognition patterns. Broutin and co-workers (Monlezun et al.) focus on the outer membrane channel OprM of *Pseudomonas aeruginosa*, investigating the presence of N-terminal modifications. They present a new X-ray structure solved in a new space group, making it possible to model the N-terminal residue of OprM as a palmitoylated cysteine.

Several factors are critical for the proper function of the tripartite system: drug binding, interaction with MFPs and OMFs, proton relay through the transmembrane domain, and trimerization of the transporter. Regarding the latter process, Wang et al. use AcrAB-TolC of *Escherichia coli* as model to explore the mechanism of function recovery of the AcrB<sub>P223G</sub> variant, which compromises AcrB trimerization and drastically reduces the drug efflux activity. Their study highlights how modulation of several critical factors can lead to the proper functioning of the pump. Zgurskaya et al. further analyze how the reaction cycles of transporters are coupled to the assembly of the trans-envelope complexes. Using a combination of biochemical, genetic and biophysical approaches, the authors reconstruct the sequence of events leading to the assembly of transenvelope drug efflux complexes, and characterize the roles of periplasmic and outer membrane proteins in this process. In particular, they propose that OMF recruitment is triggered by binding of effectors (substrates) to MFP or MFP-RND complexes. Bavro and co-workers investigate in detail the architecture and roles of periplasmic adaptor proteins in tripartite efflux pump assemblies (Symmons et al.). They stress how recognition between the MFPs and OMFs is essential for pump assembly and function, and how targeting this interaction may provide a novel avenue for combating RND pump-mediated multidrug resistance. Picard and co-workers design a new test permitting investigation of the assembly of the MexAB-OprM efflux system of *P. aeruginosa* with only tens of microgram of protein (Ntsogo Enguene et al.). The method relies on the streptavidin-mediated pull-down of OprM proteoliposomes upon interaction with MexAB proteoliposomes

containing biotinylated lipids. Their study gives clear evidence for the importance of MexA in promoting and stabilizing the assembly of the MexAB-OprM complex and the role of the proton motive force on the assembly and disassembly of the efflux pump.

Little of the *in vitro* work makes sense without an understanding of the occurrence, regulation, and interdependence of the efflux pumps in a physiological setting. Martins and co-workers summarize the current knowledge on RND efflux mechanisms in *E. coli*, a bacterium responsible for community and hospital-acquired infections, as well as foodborne outbreaks worldwide (Anes et al.). They review the knowledge on Acriflavine (Acr), Multidrug Transport (Mdt), and Copper transporting (Cus) efflux systems. Chen and collaborators use clinical *Salmonella typhimurium* isolates to demonstrate how acquisition of the plasmid-mediated quinolone resistance (PMQR) genes *oqxAB* and *aac(6')Ib-cr* accelerates the development of fluoroquinolone resistance in this bacterium (Wong et al.). Their analysis reveals that *oqxAB* and *aac(6')Ib-cr* are encoded on plasmids of various sizes and mediate resistance to ciprofloxacin, ultimately facilitating the selection of ciprofloxacin-resistant *S. typhimurium*. In their Perspective, Paulsen and collaborators summarize the current knowledge on the *Acinetobacter* chlorhexidine efflux (Acel) pump, a prototype for a novel family of multidrug efflux pumps conserved in many proteobacterial lineages (Hassan et al.). The discovery of this family raises the possibility that additional undiscovered intrinsic resistance proteins may be encoded in the core genomes of pathogenic bacteria.

Among the mechanisms that are not fully understood is the genetic regulation of efflux pumps. Morita and co-workers identify a novel MexS variant involved in up-regulation of the *mexEF oprN* multidrug efflux operon in a clinical isolate of *P. aeruginosa* displaying multi-drug efflux-mediated resistance to fluoroquinolones, aminoglycosides, and most β-lactams. Their study constitutes the first genetic evidence that a MexS variant causes *mexEF oprN* upregulation in *P. aeruginosa* clinical isolates. If the road toward understanding of efflux-mediated multi-drug resistance in *E. coli*, *Acinetobacter baumannii* and *P. aeruginosa* is rough, the characterization of efflux pumps in many other prominent pathogens, e.g., the members of the genus *Burkholderia*, lags even further behind. As in other non-enteric Gram-negatives, efflux pumps of the resistance nodulation cell division (RND) family are the clinically the most significant efflux systems in this genus. Schweizer and co-workers provide an excellent review of the current knowledge about efflux mechanisms in several *Burkholderia* species (Podnesky et al.).

Last but not least, inhibition of efflux pumps is one of the current strategies being pursued by several groups attempting to reduce the impact of efflux on antimicrobial resistance. Efflux pump inhibitors (EPIs) could be used as adjunctive therapies that would increase the potency of existing antibiotics and decrease the emergence of multidrug-resistant bacteria. In their review, Venter et al. describe how available biochemical and structural information can be translated into the discovery and development of new compounds that could reverse antimicrobial

resistance in Gram-negative pathogens. Opperman and Nguyen analyze in detail the reasons why no compounds have yet progressed into clinical use. One of the major hurdles in the development of EPIs has been the lack of biochemical, computational, and structural methods that could be used to guide rational drug design. The authors review recent reports that have advanced our understanding of the mechanisms of action of several potent EPIs active against RND-type pumps.

In summary, the articles in this research topic serve as a background to the search for a deeper understanding of the mechanisms by which RND efflux pumps limit the concentration of antimicrobial compounds inside the bacterial cell. This knowledge may in turn pave the way for new, more directed inhibitor and antibiotic design to ultimately overcome antimicrobial resistance in Gram-negative pathogens.

## AUTHOR CONTRIBUTIONS

All authors listed, have made substantial, direct and intellectual contribution to the work, and approved it for publication.

## FUNDING

The research of AVV and KMP was conducted as part of the Translocation Consortium ([www.translocation.eu](http://www.translocation.eu)) and has received support from the Innovative Medicines Initiative Joint Undertaking under Grant 115525, resources that are composed of financial contributions from the European Union's Seventh Framework Programme (FP7/2007-2013) and European Federation of Pharmaceutical Industries and Associations (EFPIA) companies. Work in the lab of KP on multidrug efflux is funded by the Canadian Institutes of Health Research and Cystic Fibrosis Canada.

**Conflict of Interest Statement:** The authors declare that the research was conducted in the absence of any commercial or financial relationships that could be construed as a potential conflict of interest.

*Copyright © 2016 Vargiu, Pos, Poole and Nikaido. This is an open-access article distributed under the terms of the Creative Commons Attribution License (CC BY). The use, distribution or reproduction in other forums is permitted, provided the original author(s) or licensor are credited and that the original publication in this journal is cited, in accordance with accepted academic practice. No use, distribution or reproduction is permitted which does not comply with these terms.*

# Structural basis of RND-type multidrug exporters

Akihito Yamaguchi\*, Ryosuke Nakashima and Keisuke Sakurai

Laboratory of Cell Membrane Structural Biology, Institute of Scientific and Industrial Research, Osaka University, Ibaraki, Japan

## OPEN ACCESS

### Edited by:

Attilio Vittorio Vargiu,  
Università' di Cagliari, Italy

### Reviewed by:

Dmitri Debabov,  
NovaBay Pharmaceuticals, USA  
Ashima Kushwaha Bhardwaj,  
Indian Institute of Advanced  
Research, India  
Martin Picard,  
Université Paris Descartes, France

### \*Correspondence:

Akihito Yamaguchi,  
Laboratory of Cell Membrane  
Structural Biology, Institute of  
Scientific and Industrial Research,  
Osaka University, 8-1 Mihogaoka,  
Ibaraki, Osaka 567-0047, Japan  
akihito@sanken.osaka-u.ac.jp

### Specialty section:

This article was submitted to  
Antimicrobials, Resistance and  
Chemotherapy,  
a section of the journal  
*Frontiers in Microbiology*

Received: 31 January 2015

Accepted: 01 April 2015

Published: 20 April 2015

### Citation:

Yamaguchi A, Nakashima R and  
Sakurai K (2015) Structural basis of  
RND-type multidrug exporters.  
*Front. Microbiol.* 6:327.  
doi: 10.3389/fmicb.2015.00327

Bacterial multidrug exporters are intrinsic membrane transporters that act as cellular self-defense mechanism. The most notable characteristics of multidrug exporters is that they export a wide range of drugs and toxic compounds. The overexpression of these exporters causes multidrug resistance. Multidrug-resistant pathogens have become a serious problem in modern chemotherapy. Over the past decade, investigations into the structure of bacterial multidrug exporters have revealed the multidrug recognition and export mechanisms. In this review, we primarily discuss RND-type multidrug exporters particularly AcrAB-TolC, major drug exporter in Gram-negative bacteria. RND-type drug exporters are tripartite complexes comprising a cell membrane transporter, an outer membrane channel and an adaptor protein. Cell membrane transporters and outer membrane channels are homo-trimmers; however, there is no consensus on the number of adaptor proteins in these tripartite complexes. The three monomers of a cell membrane transporter have varying conformations (*access*, *binding*, and *extrusion*) during transport. Drugs are exported following an ordered conformational change in these three monomers, through a functional rotation mechanism coupled with the proton relay cycle in ion pairs, which is driven by proton translocation. Multidrug recognition is based on a multisite drug-binding mechanism, in which two voluminous multidrug-binding pockets in cell membrane exporters recognize a wide range of substrates as a result of permutations at numerous binding sites that are specific for the partial structures of substrate molecules. The voluminous multidrug-binding pocket may have numerous binding sites even for a single substrate, suggesting that substrates may move between binding sites during transport, an idea named as multisite-drug-oscillation hypothesis. This hypothesis is consistent with the apparently broad substrate specificity of cell membrane exporters and their highly efficient ejection of drugs from the cell. Substrates are transported through dual multidrug-binding pockets via the peristaltic motion of the substrate translocation channel. Although there are no clinically available inhibitors of bacterial multidrug exporters, efforts to develop inhibitors based on structural information are underway.

**Keywords:** multidrug exporter, crystal structure, functional-rotation, ACRB, RND, multidrug resistance

## Multidrug Resistance and the Emergence of RND Efflux Pumps

Multidrug resistance of pathogens and cancer cells are serious problem of modern chemotherapy. Multidrug resistance generally reflects the accumulation of many drug resistance factors, e.g.,

enzymes detoxifying antibiotics, mutations in drug targets and permeability barriers. Multidrug exporters are active permeability barriers and, among resistance factors, only multidrug exporters alone can cause multidrug resistance without additional factors (Blair et al., 2014). In many cases, high-level multidrug resistance in pathogens is caused by a synergistic effect of multidrug exporters and the other drug resistance factors (Bhardwaj and Mohanty, 2012).

There are three categories of multidrug efflux transporters (**Figure 1**), that is, transporters driven by ATP-hydrolysis (ABC type), drug/proton or cation antiporters (MFS, MATE, and SMR-types) and tripartite transporters (RND-type), which is also drug/proton antiporter but driven by remote-conformational coupling as mentioned below. ABC (ATP-Binding Cassette)-type exporters including P-glycoprotein was first identified as a multidrug resistance factor in cancer cells (Chen et al., 1986; Gerlach et al., 1986). There are several ABC-type exporters also in bacteria and reported to contribute multidrug resistance mainly in Gram-positive organisms (Luberski et al., 2007). However, the majority of multidrug exporters in bacteria use ion motive force. MFS (Major Facilitator Superfamily)-type drug/proton antiporters (Marger and Saier, 1993) are mainly contribute to multidrug resistance of Gram-positive bacteria. SMR (Small Multidrug Resistance)-type transporters also contribute drug resistance to lipophilic drugs (Grinius and Goldberg, 1994; Paulsen et al., 1996). MATE (Multidrug And Toxic compound Extrusion)-type drug/cation antiporters including NorM contributes multidrug resistance especially in quinolone resistance in some Gram-negative pathogens (Kuroda and Tsuchiya, 2009). MATE-type transporters has also been known in mammalian cells as multidrug and toxin extrusion family (Motohashi and Inui, 2013). However, the major multidrug efflux transporters in Gram-negative bacteria are RND-type exporters (Li and Nikaido, 2015). RND-type exporters have most broad substrate specificity among bacterial multidrug exporters (Elkins and Nikaido, 2002) and the structural studies have been first advanced (Murakami et al., 2002). This review focuses the structural mechanism of RND-type multidrug export.

Gram-negative bacteria tend to exhibit higher tolerance against antibiotics than Gram-positive organisms. The reason for this antibiotic tolerance in Gram-negative bacteria was previously thought to be due to the barrier formed by their outer membranes (Nikaido, 1988). *Pseudomonas aeruginosa* exhibits the highest level of antibiotic tolerance among Gram-negative organisms. Thus, expanding the antibacterial spectrum to target *P. aeruginosa* was one of the most important early antibiotic developments. In the 1970's, porin proteins were identified as molecular sieves by which hydrophilic compounds can penetrate outer membranes (Nikaido and Vaara, 1983). The identification of carbapenem antibiotics, which are efficient against *P. aeruginosa*, represented a major milestone in antibiotic development (Slack, 1981). In the 1980's, there was controversy regarding the efficacy and pore size of the porins of *P. aeruginosa* (Hancock et al., 1979). This controversy seemed to be settled at the end of the 1980's. The pore sizes of the porins of *P. aeruginosa* were shown to be smaller than those of other Gram-negative bacteria, which are only of a sufficient size to allow the

passage of monosaccharides (Yoshihara and Nakae, 1989); one of these porin proteins is specifically permeable to imipenem in molecular size exceeding the upper limit of the molecular sieve (Trias et al., 1989). However, shortly following this controversy, the drug efflux transporter MexAB was identified as a multidrug resistance factor in *P. aeruginosa* (Poole et al., 1993; Li et al., 1994a,b). Mutants that are deficient in these efflux transporters show hypersensitivity to multiple drugs, indicating that the intrinsic drug resistance of *P. aeruginosa* primarily reflects the constitutive expression of intrinsic efflux pumps (Nikaido, 1994). Small pore size of porin proteins also contributes to the drug tolerance of *P. aeruginosa* but the importance is less than efflux transporters (Li et al., 1994a). MexAB functions as a tripartite complex comprising the inner membrane transporter MexB, the outer membrane channel OprM and the adaptor protein MexA. Subsequently, in *E. coli*, AcrAB-TolC was identified as similar multidrug efflux transporter (Okusu et al., 1996) and homologs of AcrAB-TolC are found to be distributed throughout most Gram-negative bacteria (Paulsen et al., 2000). These tripartite exporters were named the RND (resistance/nodulation/division) family (Tseng et al., 1999). Several RND transporters have been identified in *P. aeruginosa* including MexAB-OprM (Li et al., 1995), MexXY-OprM (Mine et al., 1999), MexEF-OprN (Kohler et al., 1997), and MexCD-OprJ (Poole et al., 1996). In *Escherichia coli*, five RND-type drug efflux transporters have been identified (Nishino and Yamaguchi, 2001) including AcrAB-TolC and AcrAD-TolC. All of these transporters in *E. coli* couple with TolC. TolC is a multifunctional outer membrane channel (Buchanan, 2001) that not only couples with RND-type exporters but also with other types of transporters including ABC-type exporters (MacAB) (Kobayashi et al., 2001) and MFS-type exporters (EmrAB and EmrKY) (Furukawa et al., 1993; Kato et al., 2000) and the enterotoxin secretion system (Forman et al., 1995).

Clinical isolates showing multidrug resistance due to the overexpression of intrinsic multidrug exporter genes have been identified (Nikaido, 1998). RND-type multidrug exporters contribute to the multidrug resistance observed in most multidrug-resistant Gram-negative pathogens (Nikaido and Pages, 2012; Blair et al., 2014) and the inhibition of multidrug exporters restores the antibacterial activity of known antibiotics against multidrug pathogens (Pages and Amaral, 2009). Although a number of inhibitors of bacterial multidrug exporters have been developed, there has been no clinically available inhibitor until now (Bhardwaj and Mohanty, 2012). Although the physiological roles and intrinsic substrates of various types of RND-type multidrug exporters are not completely understood, these proteins have some physiological functions, beyond drug resistance 2011 (Piddock, 2006; Alvarez-Ortega et al., 2013). These proteins export intrinsic intracellular toxic metabolites, surround toxic compounds (Thanassi et al., 1997) and microbial toxins (Forman et al., 1995), and play a role in quorum sensing (Minagawa et al., 2012) and bacterial virulence (Nishino et al., 2006). Thus, intrinsic RND-type multidrug exporters likely participate in basic cellular self-defense mechanisms.

Most notably, these proteins demonstrate an extraordinarily wide substrate specificity (Elkins and Nikaido, 2002). The

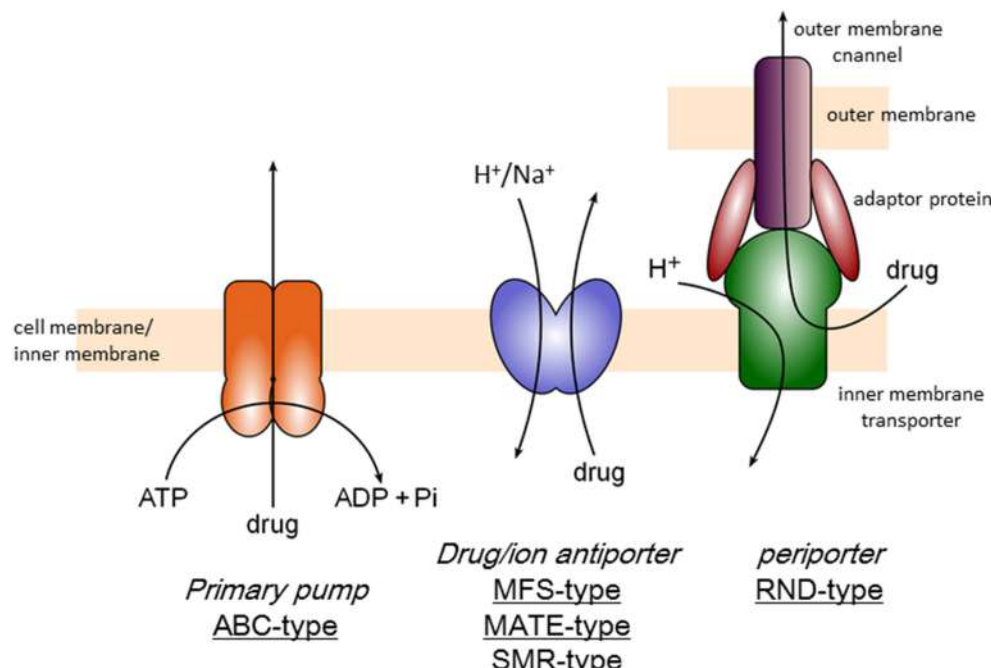


**FIGURE 1 | Classification of multidrug efflux transporters.**

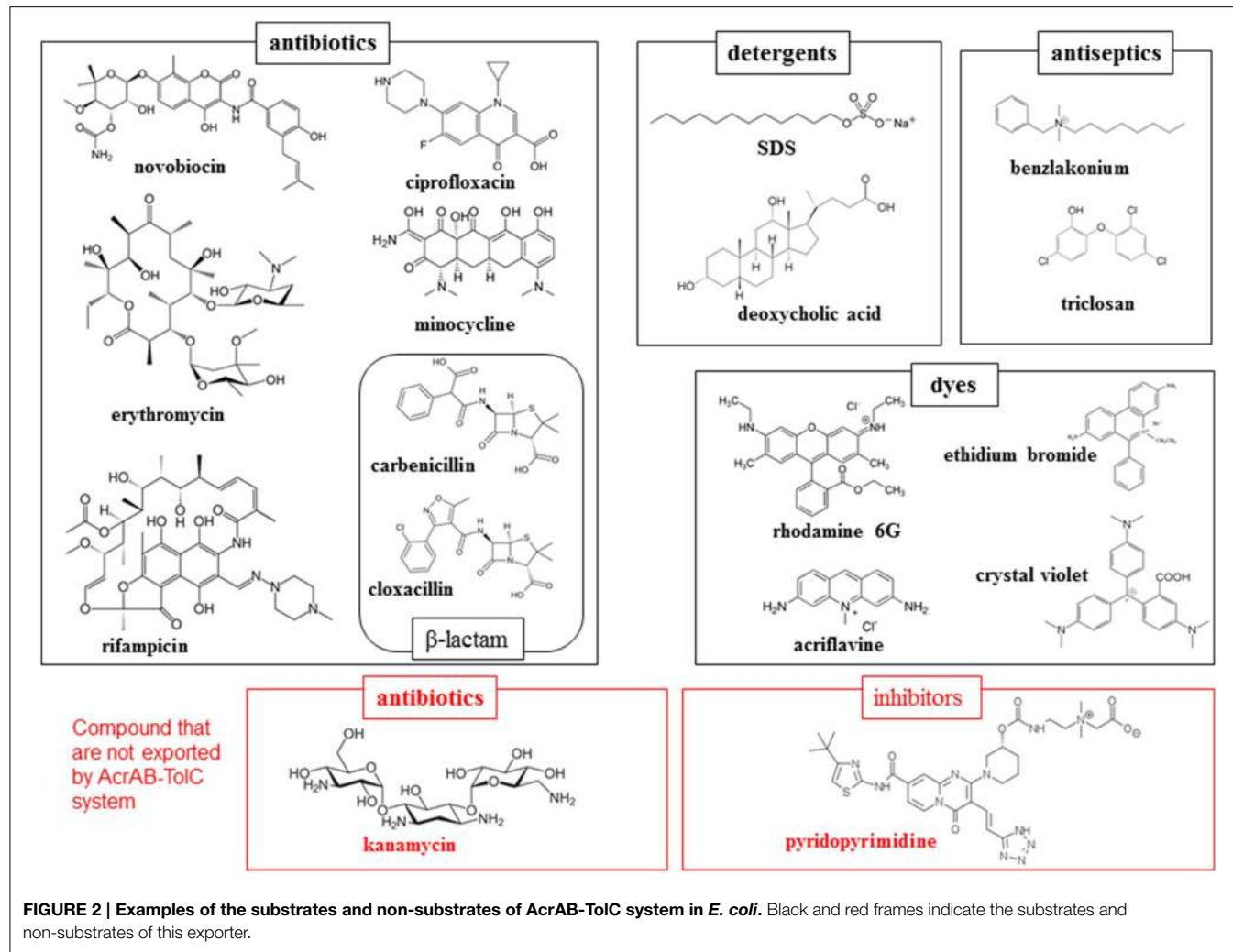
compounds exported through a typical RND-type exporter includes antibiotics, detergents, antiseptics and toxic dyes as well as anionic, cationic, zwitter ionic, and neutral compounds (**Figure 2**). These compounds also include both aromatic and aliphatic compounds. Moreover, there is no common chemical characteristic of these molecules, with the exception of amphiphilic, a characteristics of drugs and cellular toxins that assists them in moving through fluid to the target and in invading cells through the lipid bilayer of the cell membrane. However, multidrug exporters are not non-specific transporters. These proteins do not export nutrients or non-toxic metabolites such as glucose or amino acids. Additionally, these proteins transport a defined spectrum of drugs: e.g., AcrB in *E. coli* and MexB in *P. aeruginosa* do not export aminoglycoside antibiotics such as kanamycin and streptomycin, whereas AcrD in *E. coli* and MexY in *P. aeruginosa* do (Masuda et al., 2000; Elkins and Nikaido, 2002). Various inhibitors are also specific for certain multidrug exporters: e.g., pyridopyrimidine derivatives are potent inhibitors of AcrB and MexB but not MexY (Yoshida et al., 2007). Therefore, multidrug exporters recognize their substrates and are inhibited through specific mechanisms. At the start of the twenty-first century, crystal structure determinations of multidrug exporters first in RND-type (Murakami et al., 2002) followed by ABC-type (Dawson and Locher, 2006) revealed mechanisms of multidrug recognition and the active export of multidrug efflux transporters. In this review, we summarize the structural basis of multidrug recognition and active export, primarily focusing on AcrB and MexB, the most-studied RND-type multidrug exporters. We also discuss future avenues of

research into the structural and mechanical aspects of multidrug exporters.

## X-ray Crystallographic Structure of RND-type Multidrug Exporter

The first X-ray crystallographic structure of a bacterial multidrug exporter AcrB was reported by Murakami et al. (2002), showing a 3.5 Å resolution drug-free homo trimeric structure with a three-fold symmetry axis (R32 crystal). The monomer structure is an impressive shape like a sea horse (**Figure 3A**), having a long hairpin structure. The structure is divided into two parts: the transmembrane domain of approximately 50 Å in thickness and the headpiece protrudes approximately 70 Å into the periplasm. The head piece consists of two domains: the porter (or pore) domain and the TolC-docking domain. The topology diagram of AcrB monomer (**Figure 3B**) has a pseudo-two-fold symmetry. Each of the N- and C-terminal halves comprises six transmembrane helices, two subdomains (PN1 and PN2 or PC1 and PC2) with a  $\beta$ - $\alpha$ - $\beta$  motif in the porter domain and one subdomain (DN or DC) with a short vertical hairpin protruding upward. From the DN subdomain, a long hairpin structure protrudes toward the DC domain of the next monomer.

Three monomers of AcrB are tightly interacted to form a jellyfish or mushroom-like structure (**Figure 4A**). Long hairpins are deeply inserted into the next monomers to form the shape that is likened to the figure called “it takes three to tango” (Lomovslaya et al., 2002). Three PN1 subdomains form a core for the headpiece and the three central  $\alpha$ -helices form a pore-like structure at



the center of the trimer (**Figure 4B**). The funnel-like 30 Å opening at the top of the TolC-docking domain is the same size as the bottom of the TolC channel (Koronakis et al., 2000). In the transmembrane domain, there is a central hole of 30 Å diameter surrounded by three 12- $\alpha$ -helix bundles (**Figure 4C**). The central hole is not a water-filled channel: it is filled with a phospholipid bilayer (Nakashima et al., 2013). There is a central cavity on the putative surface of the phospholipid bilayer in the central hole and below the closed pore-like structure (**Figure 5A**). The central cavity comprises three windows, named vestibules, to the surface of the inner membrane (**Figures 5, 6**). Initially, this central cavity was identified as a substrate binding site, at which the substrates are taken up through vestibules from the outer leaflet of the phospholipid bilayer membrane, bound to the central cavity, transferred through the central pore when it is open, and ultimately extruded from the funnel-like exit at the top of the AcrB trimer into the TolC channel (Murakami et al., 2002). Although the substrate-binding structures of the three-fold symmetry crystals in the central cavity were reported in 2003 (Yu et al., 2003), subsequent studies have not been able to identify significant electron densities of bound drugs in the central cavity

[Pos et al. (2004); Murakami et al. (unpublished observation)] of the symmetric crystal.

## Functional-Rotation Mechanism of Drug Efflux

The physiologically-relevant drug-binding structures of AcrB was determined using C2 crystals, which have no three-fold symmetry (Murakami et al., 2006) (see **Figure 4**, which is the overlay structure of the four drug-bound AcrB structures later determined). Initially, the bound drug was identified using a bromine derivative of minocycline. Unlike symmetric crystals that show three or more bound substrates (Yu et al., 2003, 2005; Drew et al., 2008; Hung et al., 2013), only one drug molecule was bound to the AcrB trimer. The three monomers have different conformations from each other, representing three major steps of drug export, that is, *access*, *binding*, and *extrusion*. The minocycline or doxorubicin molecule bound not to the central cavity (**Figure 4**) but in the phenylalanine-rich pocket at the center of the porter domain between PC1 and PN2 of *binding* monomer (**Figure 4B**). An intramolecular water-accessible channel continued from

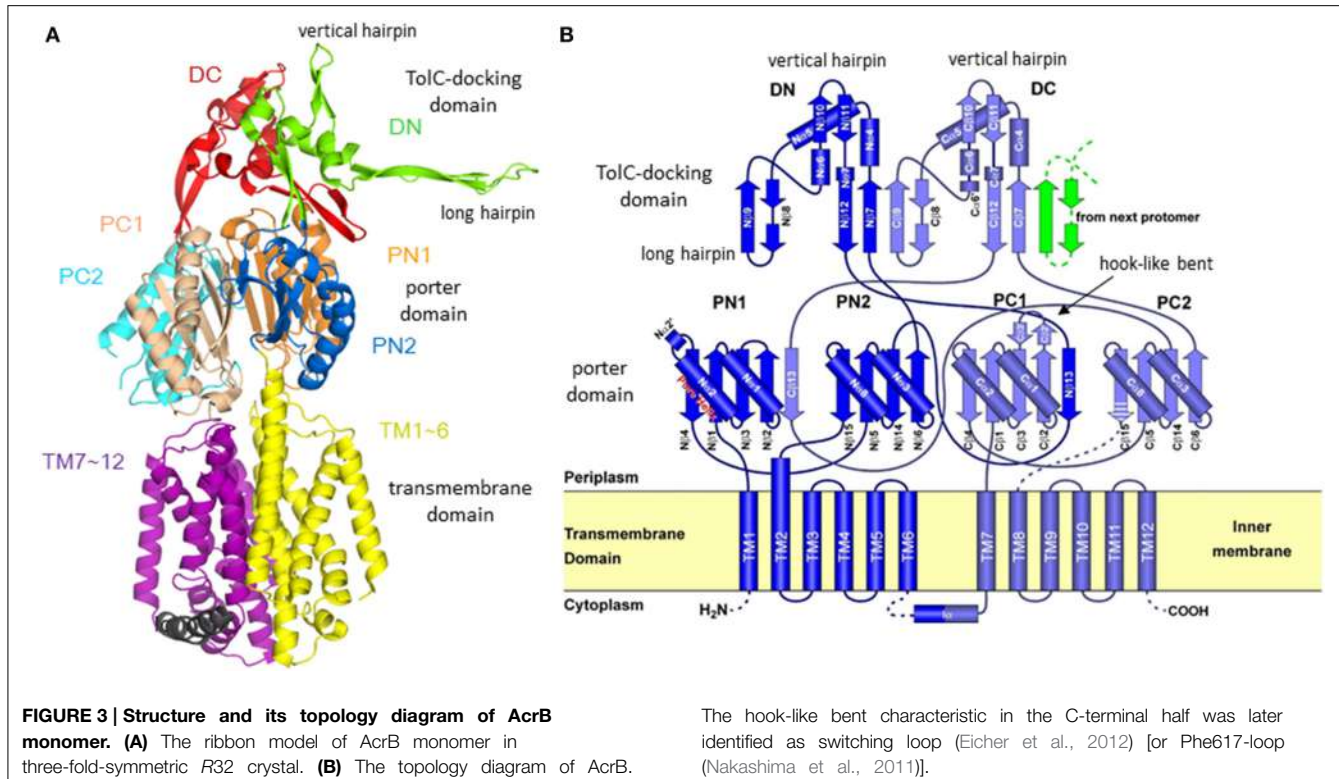


**FIGURE 3 | Structure and its topology diagram of AcrB monomer. (A)** The ribbon model of AcrB monomer in three-fold-symmetric R32 crystal. **(B)** The topology diagram of AcrB.

The hook-like bent characteristic in the C-terminal half was later identified as switching loop (Eicher et al., 2012) [or Phe617-loop (Nakashima et al., 2011)].

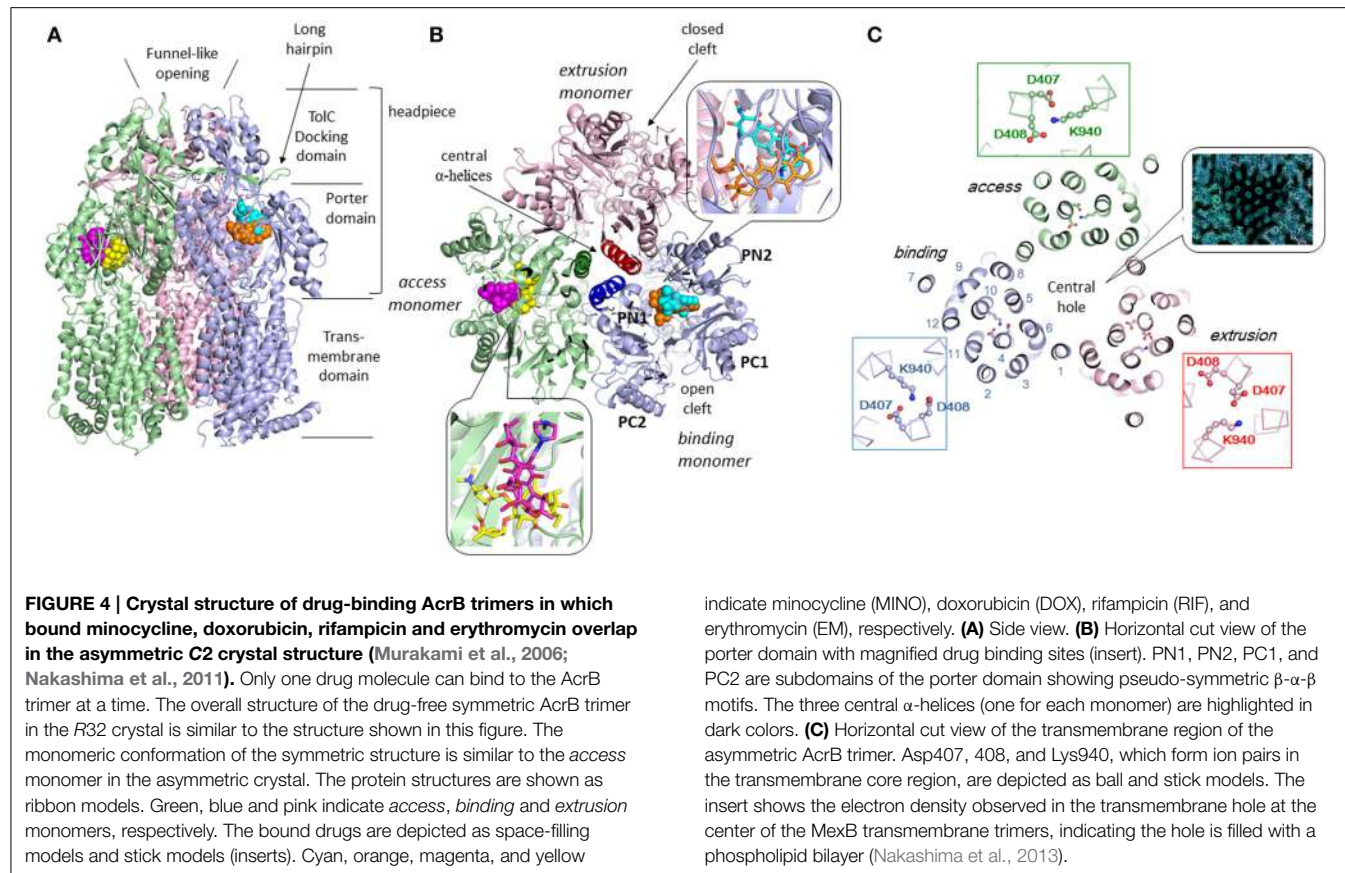
entrances to the minocycline binding pocket (Figure 5). One entrance (entrance 1 in Figure 5) opens to the outer layer of the inner membrane. This inner-membrane entrance is in the vicinity of the “vestibule” that was previously identified as a drug entrance to the central cavity, but the inner-membrane entrance is distinct from this vestibule (Figure 6A). The inner-membrane entrance shows opening and closing movements during drug transport (Figures 6B,C); however, the previously identified “vestibule” is constitutively open. The channel is interrupted at the distal end of the drug-binding pocket by steric hindrance via a central  $\alpha$ -helix of the extrusion monomer (Figure 5B), which is inclined to block the exit from the drug-binding pocket of the *binding* monomer. Thus, the *binding* monomer is in an inside-open form. Notably, the closed-exit conformation of the *binding* monomer reflects the cooperation of the next monomer.

The conformation of the monomer next to the *binding* monomer showed an outside open form. That is, the inner membrane entrance (entrance 1) is closed because of the elongation of N-terminus of TM8 (Figure 6C). The periplasmic entrance (entrance 2) is also closed because the PC2 subdomain swings toward the PC1 subdomain and the outside cleft is closed (Figure 4B). In contrast, the exit is open because the central  $\alpha$ -helix is inclined at 15° away from the exit toward the *binding* monomer and because the PN1 subdomain swings away from the PN2 subdomain (Figures 3B, 4B). Additionally, the binding pocket shrinks because PC1 swings toward PN2. Thus, the bound substrate is squeezed from the binding pocket into the central funnel. This outside-open monomer was identified as the *extrusion* monomer.

The third monomer also has an inside open conformation similar to the *binding* monomer with the exception that the binding pocket is not expanded. Thus, the third monomer is referred to as the *access* monomer. Drugs are transported through concerted sequential conformational changes: *access*, *binding* and *extrusion* (Figures 3B, 4B). The conformational changes of the monomers are inter-dependent, and no two monomers have the same conformation at the same time. This process is referred to as a functional-rotation mechanism (Murakami et al., 2006) (Figure 8).

Symmetric forms of AcrB trimers likely reflect “resting forms”; the conformations of the three symmetric monomers are similar to the *access* monomer of the asymmetric trimers. Regarding the drug-binding symmetric crystal, the bound drugs may not reflect the physiological function. Most likely, the resting form without a substrate is symmetric, and drug binding triggers the conformation change to the asymmetric, functional form. The crystallized asymmetric structure of MexB without drugs contained bound detergent in the drug-binding pocket (Sennhauser et al., 2009). The drug-free asymmetric structure of AcrB may contain a detergent or an intrinsic substrate that has not yet been identified. Most of substrates including drugs, that bind to the AcrB crystal, are difficult to identify because these substrates may be disordered.

Seeger et al. (2006) independently reported the asymmetric structure of drug-free AcrB and Sennhauser et al. (2007) reported the structure of DARPin-bound AcrB. Asymmetric structures have also been reported for MexB (Sennhauser et al., 2009). Functional-rotation mechanism is also supported by the



experiments using covalently-linked AcrB trimer (Takatsuka and Nikaido, 2009) and the experiments using engineered disulfide bonds (Seeger et al., 2008). The functional-rotation mechanism including two or more binding monomers were also proposed (Pos, 2009; Ruggerone et al., 2013) mainly due to explain bi-site activation. However, bi-site activation can be explained by peristaltic mechanism via two drug binding pockets mentioned in the next section. Symmetric drug-binding structures, which have been reported so far (Yu et al., 2003, 2005; Drew et al., 2008; Hung et al., 2013), are completely different from the *binding* monomer of functional-rotation cycle, and no pseudo-two-fold symmetric crystal structure comprising two *binding* monomers or two *access* monomers has been identified. If two of the three monomers have the same conformation at any given moment, then the structural inter-dependence between these monomers will be loose, and one monomer can independently transport drugs. Takatsuka and Nikaido (2009) verified the strict functional-rotation mechanism using covalently linked AcrB trimers that function in intact cells. When one of the three monomer units in the covalently-linked trimers was inactivated through mutations in the proton relay network in the transmembrane region or through disulfide cross-linking of the external cleft in the periplasmic domain, the entire trimeric complex was inactivated. These results clearly indicate that each monomer does not work independently. We believe that each monomer works strictly in concert with the other monomers and all monomers have

different conformations in each other in any moment at the active state until pseudo-two-fold symmetric structure of AcrB will be identified.

## Multi-Pocket Multisite Drug Binding with Multiple-Entrances and the Peristaltic Mechanism of Drug Efflux

Following minocycline and doxorubicin-binding structures, the drug binding structures of AcrB bound to the high molecular mass drugs (HMMD) rifampicin and erythromycin were reported (Nakashima et al., 2011). Similar to the low molecular mass drugs (LMMD) minocycline and doxorubicin, one molecule of rifampicin or erythromycin bound to one AcrB trimer. However, rifampicin and erythromycin binding monomer was not a *binding* monomer but an *access* monomer (**Figures 4A,B**). The rifampicin- and erythromycin-binding pocket is located between PC1 and PC2 in the substrate translocation channel between the entrance(s) and the LMMD binding pocket (**Figure 5**). Thus, the HMMD-binding pocket is referred to as a proximal pocket, and the LMMD-binding pocket is referred to as a distal pocket. Shortly after the report of proximal drug binding (Nakashima et al., 2011; Eicher et al., 2012) independently reported the presence of the proximal pocket in the *access* monomer in which the doxorubicin

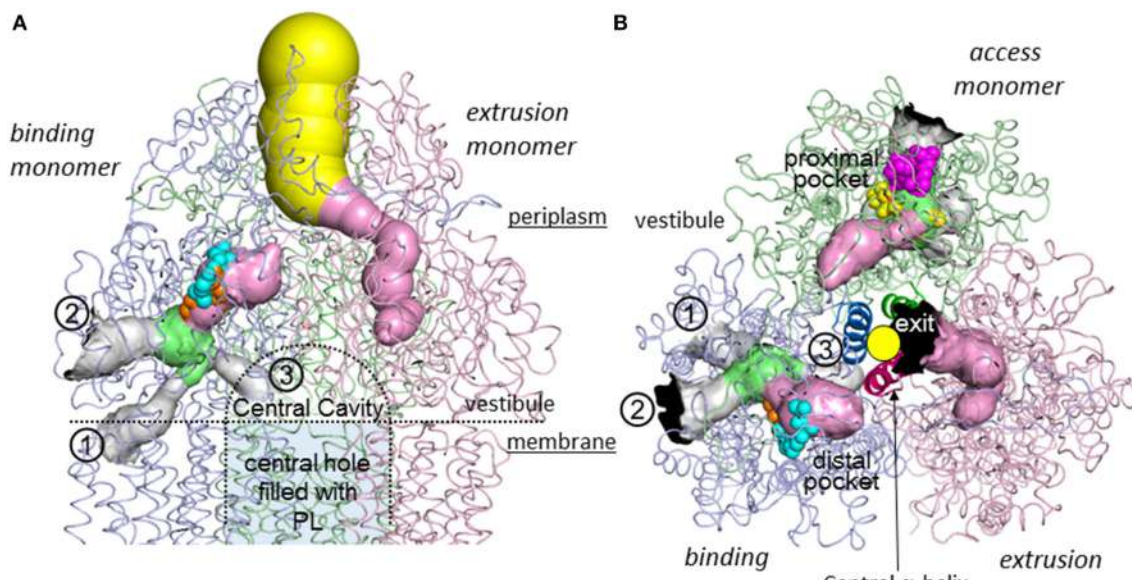


**FIGURE 5 | Intramolecular water-accessible channels in the AcrB trimer** (Nakashima et al., 2011). The channels are shown as colored solid surfaces, as calculated using the CAVER program (Medek et al., 2007). The proximal pocket, distal pocket, entrances and funnel-like exit are depicted in green, pink, gray, and yellow, respectively. The channel apertures at the entrance and exit are depicted in black. (1) Inner membrane entrance (Murakami et al., 2006), (2) periplasmic entrance (Seeger et al., 2006), (3) central cavity entrance (Nakashima et al., 2011). (A) Side view. The channels in the access monomer behind the figure have been omitted. The central cavity

and central hole are depicted as dotted lines. (B) Horizontal cut view of the porter domain. The yellow circle indicates the closed pore-like structure comprising three central  $\alpha$ -helices (depicted as a ribbon model with dense color), which was postulated to be a part of the putative substrate translocation channel during the early stages, however, it was not the case. The central  $\alpha$ -helix of extrusion monomer is inclined 15° toward binding monomer more than the other two  $\alpha$ -helices and, as a result, blocks the exit from the drug binding site. Bound minocycline (cyan), doxorubicin (orange), rifampicin (magenta), and erythromycin (yellow) overlap in the space-filling model.

dimer is bound. The proximal pocket in the *access* monomer is voluminous permitting typical multisite-binding of the HMMDs rifampicin and erythromycin (Figure 4B insert). However, in *access* monomer, the distal pocket is smaller than the proximal pocket. In contrast, in the *binding* monomer, the distal pocket expands and the proximal pocket shrinks. Both pockets are separated by a switch loop (Figure 7). The path under the switch loop is too narrow for the HMMDs to move into the distal pocket. The switch loop swings during the conformational change from the *access* stage to the *binding* stage. HMMDs could be transferred from the proximal pocket to the distal pocket through the swinging of the switch loop and proximal pocket shrinking, followed by distal pocket expansion during the transition from the *access* to the *binding* stages (Nakashima et al., 2011). The importance of switch loop flexibility in export is supported by the fact that when site-directed mutagenesis fixes the loop through the introduction of double proline residues into the loop (Nakashima et al., 2011) or a G616N mutation (Cha et al., 2014), the resultant mutants have completely lost or significantly decreased the drug export activity. The crystal structure revealed that a double proline mutation fixed the loop conformation at a state between the *access* and *binding* stages (Nakashima et al., 2011).

The roles of both pockets have been demonstrated through using site-directed mutagenesis. The resistance of AcrB-expressing *E. coli* cells to erythromycin is not only completely lost after site-directed mutagenesis in the proximal pocket but

also reduced through mutations in the distal pocket. Doxorubicin export activity is lost through mutations in the distal pocket but remains unaffected by proximal mutations. Doxorubicin export is competitively blocked not only by the distal-binding drug minocycline but also by the proximal-binding drugs erythromycin and rifampicin (Nakashima et al., 2011). These observations indicated that both HMMDs and LMMDs are transported through both proximal and distal pockets during export.

The double drug-binding AcrB trimer structure (in which rifampicin binds in the proximal pocket of the *access* monomer and minocycline binds in the distal pocket of the *binding* monomer) was determined. No drugs were detected in the distal pocket of the *access* monomer or the proximal pocket of the *binding* monomer, indicating that the proximal pocket and distal pocket are only activated during the *access* stage and the *binding* stage, respectively (Nakashima et al., 2011). Now the story of drug export is as follows: drugs initially enter the proximal pocket at the *access* stage. At this stage, HMMDs are bound and recognized in the expanded proximal pocket, but LMMDs are hardly or only weakly bound. Subsequently, the drugs are transferred to the distal pocket through the swinging of a switch loop and the relative motion of the subdomains, PC2, PC1, and PN2, resulting in a reduction in the volume of the proximal pocket and the expansion of the distal pocket during the transition from the *access* stage to the *binding* stage. LMMDs

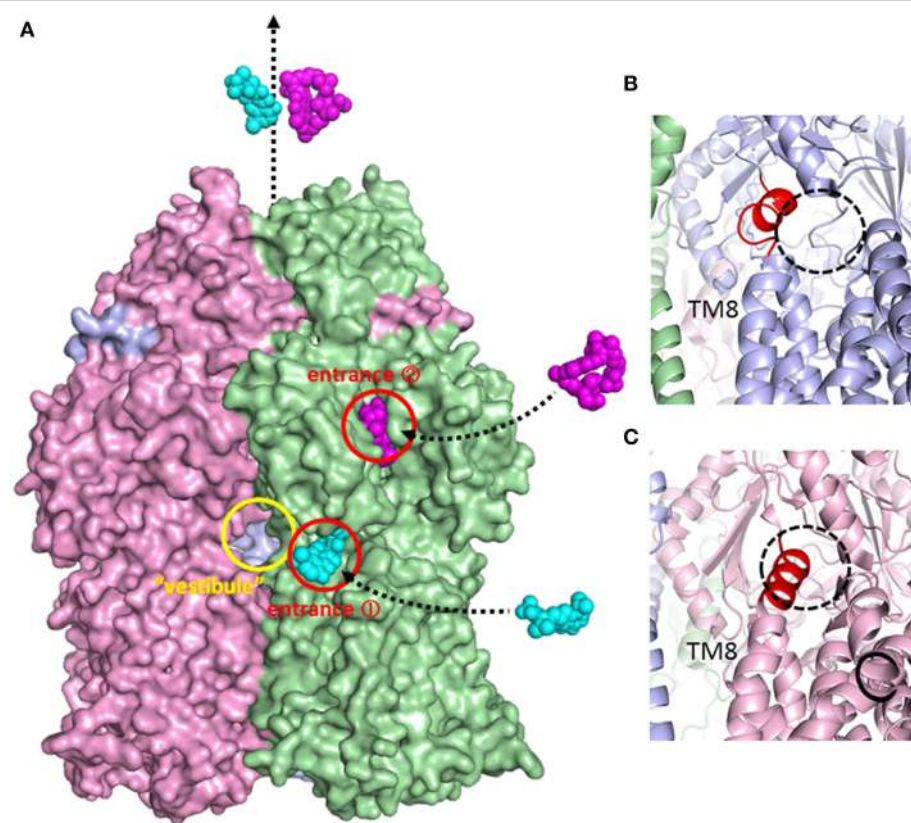


**FIGURE 6 |** Surface model of the AcrB trimer and magnified view of the inner membrane entrance. **(A)** Side view of the AcrB trimer surface model. Access, binding, and extrusion monomers are depicted in green, blue and pink, respectively. The entrances are shown as circles. Minocycline (cyan) and rifampicin (magenta) are illustrated in space-filling models in the

putative drug export route. The “vestibule” indicates window of the central cavity. **(B)** Open inner membrane entrance (entrance 1) of the binding monomer. The untied random coil upon N-terminal of TM8 is depicted in red. **(C)** The closed inner membrane entrance (entrance 1) of the extrusion monomer. The extended  $\alpha$ -helix at the N-terminus of TM8 is depicted in red.

are bound and recognized in the distal pocket: HMMDs are not tightly bound but are instead occluded in the distal pocket because the path under the switch loop is too narrow to permit the return of HMMDs to the proximal pocket. Ultimately, the drugs are squeezed out through the TolC channel via a funnel-like opening as a result of conformational changes at the *extrusion* stage. In other words, drugs are moved through the intramolecular channels by a peristaltic motion of the two tandem drug-binding pockets (**Figure 8**). Multi-pockets having different substrate-binding specificity contribute to expand substrate spectrum.

An AcrB trimer with one drug bound to the *access* monomer and a second drug bound to the *binding* monomer may form the structural basis for the reported allosteric bi-site activation of the AcrAB-TolC pump (Seeger et al., 2006; Pos, 2009). Notably, the dual drug-binding structure does not indicate the presence of two *binding* monomers in one trimer. The two drug binding structures differ: one is an *access* monomer and the other is a *binding* monomer. There is no structural evidence for the presence of two or three *binding* monomers in one trimer.

Sennhauser et al. (2007) reported two possible substrate entrances: the inner-membrane entrance (entrance 1 in **Figure 5**)

and the periplasmic entrance (entrance 2 in **Figure 5**). The inner-membrane entrance is the entrance described by Murakami et al. (2006). The periplasmic entrance is open to the periplasm at the bottom of the cleft between PC1 and PC2. Site-directed mutagenesis revealed that both entrances perform drug export (Husain et al., 2011; Nakashima et al., 2011). The third possible entrance (entrance 3 in **Figure 5**) from the central cavity is also identified (Nakashima et al., 2011); however, there is no evidence that the entrance 3 has any functions. The channels from all three putative drug entrances are merged at the proximal pocket. Molecular simulation studies showed that the inner-membrane entrance and the periplasmic entrance play a role in the export of hydrophobic compounds and hydrophilic compounds, respectively (Yao et al., 2013). Thus, it is reasonable to assume that the outer-layer entrance takes up hydrophobic drugs with relatively low-molecular-mass from the outer layer of the inner membrane (thereby acting as a membrane “vacuum cleaner” mechanism) and that the periplasmic entrance takes up hydrophilic drugs with relatively large molecular mass from the periplasm (acting as a periport). Multi-entrances contribute to expand the physico-chemical characteristics of the substrates.

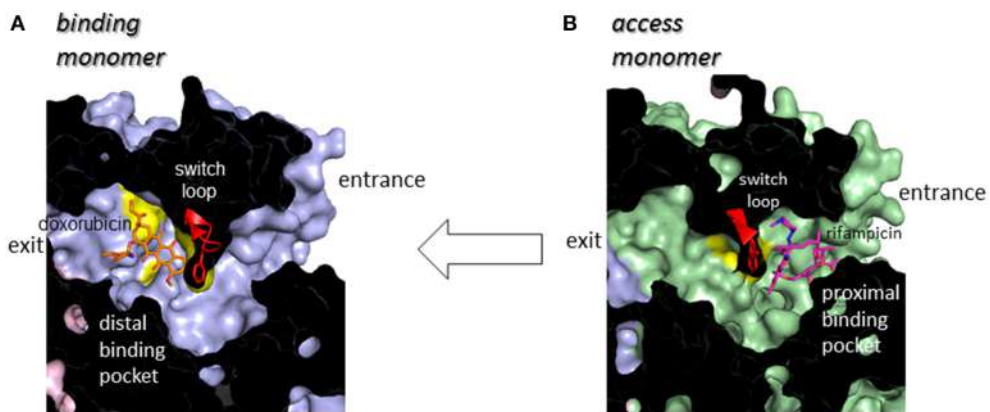


**FIGURE 7 |** Cut view of the transmembrane channels of the *binding monomer* (A) (blue) with bound doxorubicin (orange) and that of the *access monomer* (B) (green) with bound rifampicin (magenta). The switch loop containing Phe617 at the tip is depicted using a red ribbon model.

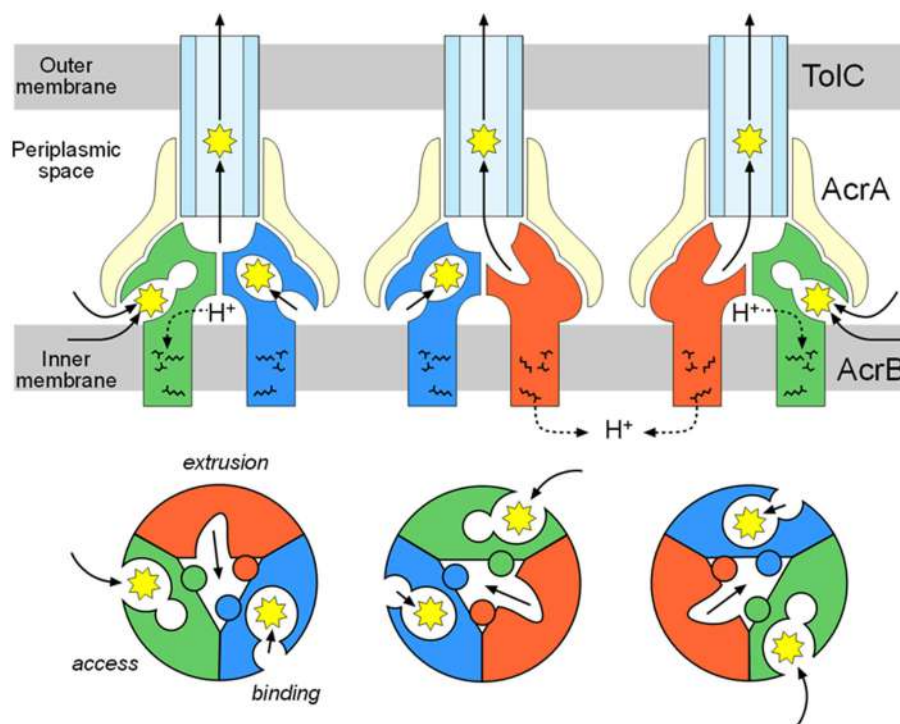


**FIGURE 8 |** Functional-rotation mechanism of drug export mediated through the AcrAB-TolC tripartite complex. The upper and lower panels show side and horizontal views, respectively. The green, blue and red colors

indicate the access, binding and extrusion stages of AcrB, respectively. The yellow and pale blue colors indicate AcrA and TolC, respectively. The jagged circles indicate substrates.

## Structural Basis of Multidrug Recognition

The induced-fit mechanism is one potential mechanism for the enzymatic recognition of multiple substrates with different chemical structures (Vogt et al., 2014). In this mechanism, the size of the substrate binding site and/or the arrangement of amino acid side chains in the binding site changes with the chemical structure of the substrates. In AcrB, the doxorubicin and minocycline binding structures of the distal pocket of the *binding*

monomer, and the rifampicin and erythromycin binding structures of the proximal pocket of the *access* monomer, are not significantly different from each other with the exception of some minor changes in the orientation of the side chains directly interacting with the bound drugs. Thus, although the protein structures of AcrB, including the drug translocation channel, changes considerably during the functional-rotation cycle, the induced-fit mechanism is not the primary mechanism of multidrug recognition.

Multisite drug binding is another potential mechanism of multidrug recognition as has been described for the multidrug-binding transcription regulator QacR (Schumacher et al., 2001). In this mechanism, as mentioned above, the substrate-binding pocket is voluminous, permitting the presence of numerous binding sites for various substrates. The pocket possesses numerous binding sites that correspond to the partial structures of various compounds. The substrates are recognized through permutations of these binding sites. Although minocycline and doxorubicin have a common tetracyclic structure, the binding site of doxorubicin only partially overlaps with that of minocycline in the distal pocket (**Figure 4B** insert). Doxorubicin and minocycline interact with almost different sets of amino acid side chains. Rifampicin and erythromycin show the similar multisite binding in the proximal pocket (**Figure 4B** insert).

Recent molecular dynamics simulations have revealed that a number of structurally-distinct drugs bind to a number of sites that may slightly or substantially differ in the voluminous binding pocket of AcrB (Takatsuka et al., 2010; Vargiu and Nikaido, 2012). Additionally, the presence of two voluminous multisite drug-binding pockets, the proximal and distal pockets, with different substrate specificities greatly contributes to expanding the specificity. Multiple entrances also expand the drug specificity by facilitating drug uptake from two physically different spaces (the outer leaflet of the inner membrane and the periplasm).

Identifying bound drugs in the asymmetric AcrB structure is difficult for most substrates and inhibitors. A drug may not tightly bind to specific sites. However, multidrug exporters exhibit strikingly high efficiency at rejecting substrates. When multidrug exporters are sufficiently expressed, most drug molecules are rejected prior to entering cytoplasm. Experiments using fluorescent dye (**Figure 9**) have shown the drug rejection efficiency of multidrug exporters (Matsumoto et al., 2011). FDG is a pre-fluorescent compound that has no fluorescence itself but demonstrates fluorescein emission when hydrolyzed by intrinsic  $\beta$ -galactosidase in *E. coli*. However, when FDG was added to wild-type *E. coli* cells, almost no fluorescence was observed. In *acrB*-deficient *E. coli* cells, the entire medium was fluorescent, likely reflecting the export of fluorescein from the cell through other RND-type drug exporters that do not completely reject FDG. When *tolC* was deleted, all RND-type exporters became inactive, and the cell body showed strong fluorescence because of fluorescein accumulation in the cell. However, how is this efficient rejection consistent with the apparently weak binding affinity of drugs to multidrug exporters, as predicted in crystallographic studies?

The multisite-drug-oscillation hypothesis may present a possible mechanism that explains the compatibility of high export efficiency with the apparently low affinity of substrate binding to specific sites (**Figure 10**). A recent molecular simulation study (Takatsuka et al., 2010) showed that the voluminous distal binding pocket of AcrB has binding sites for many drugs. These drugs have been classified as groove, cave and mixed binders. Interestingly, there are a number of possible binding sites for a single drug; however, a simulation study indicated that most of the possible binding sites were not equal to the actual site in the crystal. The results of this simulation study suggest that drug molecules

oscillate in this voluminous binding pocket. In this mechanism, when the affinity of binding to each site is low, the total binding efficiency in the pocket may be high. The positions of the substrates that are “oscillating” in the binding pocket are difficult to detect in the crystal structure. Eicher et al. (2012) reported a doxorubicin dimer bound to the proximal pocket of AcrB. The low electron density of proximal doxorubicin molecules might indicate that doxorubicin molecules are not be dimers but instead a mixture of two different doxorubicin-binding AcrB trimers, i.e., each molecule binds at a different site in the proximal pocket. This result may indicate that the doxorubicin molecule oscillates between two binding sites in the proximal pocket and that the average electron density could be apparent in the crystal structure. Substrates tightly bound to one site can be detected, whereas substrates oscillating between multiple sites are rarely detectable in the crystal structure. The apparently fuzzy substrate recognition by AcrB may reflect such a multisite-drug-oscillation mechanism. HMMDs may be occluded without specific binding in the distal pocket (**Figure 10B**).

Rauch proposed the concept of “oscillating drug transporters” in order to explain multi-specificity of P-glycoprotein (Rauch, 2011). However, this “oscillating transporters” model is different from our “drug oscillation” hypothesis. “Oscillating transporters” means that transporter proteins oscillate between open/drug-accepting and closed/drug-expelling conformations in a membrane. Oscillating transporters stochastically catch substrates located in the membrane at the open form and then expels with the protein conformation change by oscillation. Specific drug binding sites are not assumed in oscillating transporter model. In contrast, our “multisite drug-oscillation” hypothesis does not mean transporter protein oscillation but means drug molecule oscillation between numerous drug-binding sites in the voluminous drug binding pockets. Both models can contribute multi-specificity, however, the selectivity of the substrates in the oscillating transporter model depends on the substrate solubility into the membrane. On the other hand, in the drug oscillation model, substrate selectivity depends on the affinity of each drug binding site and this model can explain the difference in the drug specificity between exporters, e.g., aminoglycoside antibiotics are not exported by AcrAB-TolC and MexAB-OprM systems but efficiently exported by MexXY system (Masuda et al., 2000; Elkins and Nikaido, 2002; Lau et al., 2014).

## Remote-Conformational Energy Coupling

Drug efflux by RND-type exporters is driven by the proton motive force (Thanassi et al., 1997; Li et al., 1998; Zgruskaya and Nikaido, 1999). Four essential charged residues, Asp407, Asp408, Lys940 (Lys939 in MexB), and Arg971, in addition to Thr978, are thought to form a transmembrane proton-relay network, based on findings from site-directed mutagenesis (Guan and Nakae, 2001; Su et al., 2006; Takatsuka and Nikaido, 2006). Asp407 and Asp408 in TM4 and Lys940 in TM10 form ion pairs in the transmembrane core (**Figure 4C**) (Murakami et al., 2002, 2006). TM4 and TM10 are located at the center of a 12  $\alpha$ -helix bundle. Arg971 is in the vicinity of the cytoplasmic surface of the membrane (**Figure 11**). Because this putative transmembrane

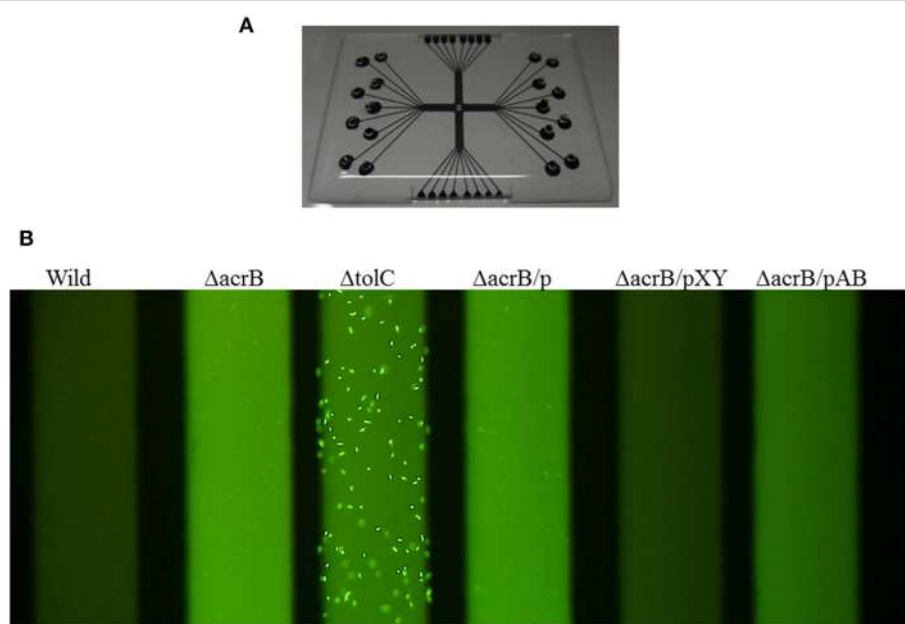


**FIGURE 9 | Fluorescence assay of drug ejection from the cell by multidrug exporters (Matsumoto et al., 2011).** (A) Microfluidics device used in this experiment. *E. coli* cells and the pre-fluorescent dye FDG were mixed and injected to the wells of the device. After incubation, microfluidics tubes were observed by a fluorescence microscope. Upon entering the cytoplasm, FDG is hydrolyzed by intrinsic  $\beta$ -galactosidase and fluorescein is produced. When fluorescein accumulates in the cytoplasm, the cells

fluoresce. When fluorescein is exported from the cytoplasm, the medium fluoresces. (B) Fluorescence of the microfluidics tubes. Wild: wild-type *E. coli* MG1655 cells,  $\Delta$ acrB: acrB-deficient cells,  $\Delta$ tolC: tolC-deficient cells.  $\Delta$ acrB/p,  $\Delta$ acrB/pXY,  $\Delta$ acrB/pAB indicate acrB-deficient cells transformed with vector (pMMB67HE) and the plasmids recombined with *P. aeruginosa* efflux pump genes *mexXY-oprM* and *mexAB-oprM*, respectively (Matsumoto et al., 2011).

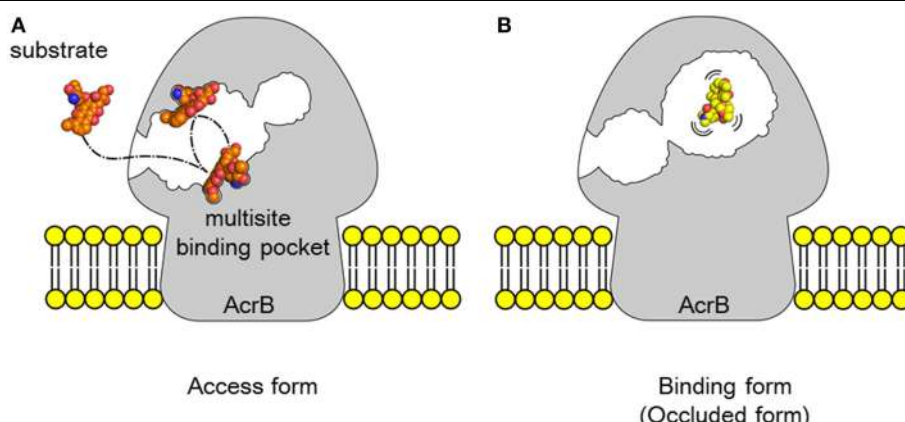


**FIGURE 10 | Multisite-drug-oscillation hypothesis.** (A) Access stage. A drug is oscillating between multiple drug binding sites in the proximal pocket. (B) Binding stage. Most of LMMDs may be oscillating in the distal pocket as

in the proximal pocket but HMMDs may be just occluded in the distal pocket without specific binding sites. Space-filling models in (A,B) show doxorubicin (orange) and erythromycin (yellow), respectively.

proton-relay network is approximately 50 Å apart from the drug binding pocket, the energy coupling must reflect a remote-conformational coupling. In the asymmetric trimer, the  $\epsilon$ -amino group of Lys940 is placed between the carboxyl groups of Asp407 and Asp408 and forms ion pairs in the *access* and *binding* monomers. In *extrusion* monomer, the side chain of Lys940 is twisted approximately 45° clockwise when viewed from the

periplasm, and the ion pairs are abolished (Figure 4C insert) (Murakami et al., 2006), likely reflecting the protonation of the carboxyl group(s). Based on this side chain twisting, a TM bundle of the six N-terminal TMs (TM1-TM6) and a TM bundle of the six C-terminal TMs (TM7-TM12) are also twisted around each other. This bulky twisting movement in the transmembrane region occurs in conjunction with a series of conformational

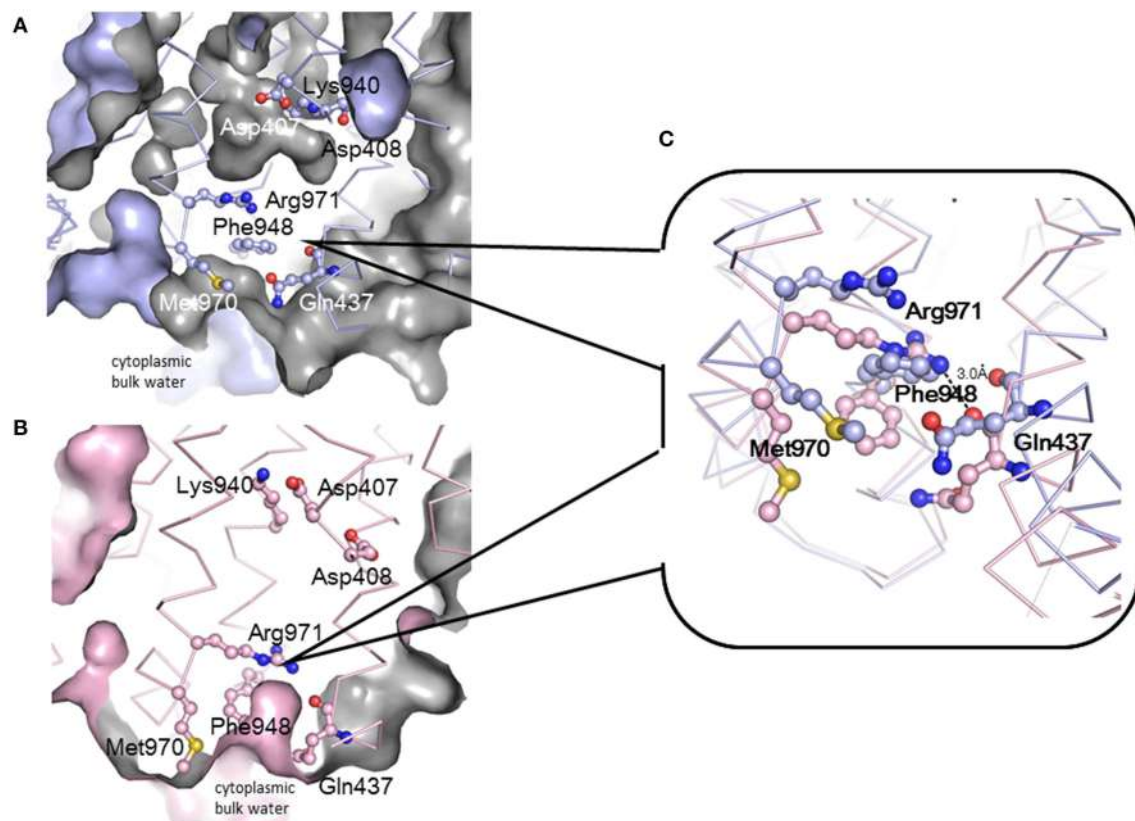


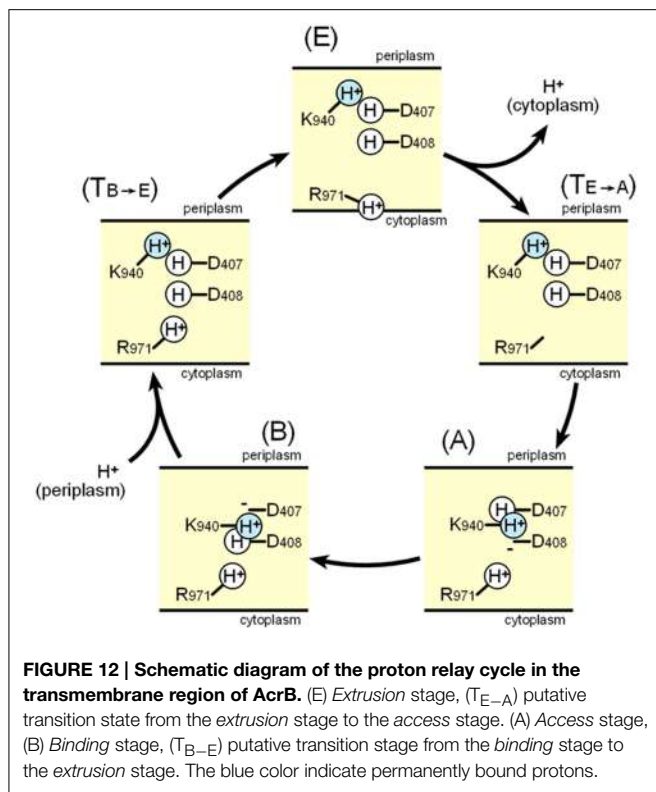
**FIGURE 11 | Conformational changes in transmembrane proton relay residues during the functional-rotation cycle.** (A,B) show cut views of the lower transmembrane regions of the *binding* (blue) (A) and *extrusion* (pink) (B) monomers that have been drawn with  $C\alpha$  traces and the residues associated with proton relay depicted using ball and stick model. Blue and pink surfaces indicate the molecular surface of

AcrB or the inside surface of the intramolecular void space. Gray color indicates the back of the surface or the surface of the intramolecular void space. (C) Magnified overlay of the vicinity of Arg971 in the *binding* and *extrusion* monomers. These figures were drawn based on the crystal structure of the asymmetric AcrB trimer using PyMol (Murakami et al., 2006).

changes that result in the entrance closing, the exit opening and the drug being squeezed from the binding pocket at the *extrusion* stage. During the transition from the *extrusion* stage to the *access* stage, the deprotonation of carboxyl group(s) rebuilds the tripartite ion pairs. To drive drug export via the outside positive proton motive force, protonation during the transition from the *binding* to the *extrusion* stage should occur in the periplasm, and deprotonation during the transition from the *extrusion* to the *access* stage should occur in the cytoplasm. This result suggests an exchange mechanism involving the proton (or water) channel between the inward and outward configurations. Arg971 may be the “valve” that allows switching between inward and outward proton flow. As shown in **Figure 11**, the side chain of Arg971 is bent and is separated from the cytoplasmic bulk water by Phe948 and Met970 in the *binding* monomer (**Figure 11A**). However, this side chain faces the water-accessible void in the center of the transmembrane region that includes the Asp-Lys ion pairs. The void continues to a channel that is connected to the periplasm. Thus, Arg971 can receive a proton from Asp407 and/or Asp408 in the *binding* monomer. In contrast, in the *extrusion* monomer, the guanidino-pentanoic moiety of Arg971 is

extended and slightly slanted downward, followed by the benzene ring of Phe948 and the methylthio-butanoic acid side chain of Met970 being pushed down and away from Arg971 (**Figure 11C**). As a result, the guanidino group of Arg971 is exposed to cytoplasmic bulk water (**Figure 11B**). At the *extrusion* stage, the void in the center of the transmembrane region is not present. Thus, Arg971 is an inside-facing structure from which protons can be released into the cytoplasm.

**Figure 12** shows a potential scheme for proton translocation via the proton relay network based on observations of the crystal structure. Lys940 is postulated to be permanently protonated. All of the residues are protonated at the *extrusion* stage: thus the two aspartates are neutral, and the ion pair is abolished. At this stage, the side chain of Arg971 faces the cytoplasmic bulk water, and protons can be released into the cytoplasm via the proton motive force. Before the *access* stage, there is a transient state  $T_{E-A}$ . The deprotonated guanidino side chain of Arg971 swings away from the bulk water toward the transmembrane core. Next, one proton bound to Asp408 is transferred to Arg971 probably via water molecules, because Arg408 is located closer to Arg971 than Asp407. As a result, Lys-Asp ion pairs are reformed



at the *access* stage. Next, one proton bound to Asp407 is subsequently transferred to Asp408 during the *binding* stage. Subsequently, prior to the *extrusion* stage, an additional transient stage,  $T_{B \rightarrow E}$  is needed, in which Asp407 is protonated from periplasm, tripartite ion pairs are abolished and the side chain of Lys940 swings away from the aspartate pair. There are some transferable proton residues, such as Asp566, Asp924, His338, and Glu346 (Eicher et al., 2014) on the periplasmic side of the transmembrane domain and the water accessible channel continues to the core ion pair region (Fischer and Kandt, 2011), potentially leading to the protonation of Asp407 from periplasm. Subsequently, the conformation returns to the *extrusion* stage via swinging of the protonated Arg971 side chain. In this scheme, one proton flows from the periplasm through Asp407, Asp408, and Arg971 to the cytoplasm in one cycle.

After determining the structures of the asymmetric AcrB trimers and identifying the transmembrane ion pair conformation changes during drug export (Murakami et al., 2006; Seeger et al., 2006; Sennhauser et al., 2007), molecular dynamics studies were performed to reveal the actuating mechanism of AcrB trimers, including an examination of the proton translocation pathway (Fischer and Kandt, 2011; Eicher et al., 2014). Water channels connecting the periplasm to the transmembrane core region were observed, including ion pairs involved at the *binding* and *access* stage, but these disappeared at the *extrusion* stage. The results of these analyses principally support the scheme shown in Figure 12. Eicher et al. (2014) reported changes in the orientation of Arg971 that may allow this amino acid to act as a valve for proton flow. Although Eicher et al. (2014) suggested that two

protons are transported in one cycle (both Asp407 and Asp408 are deprotonated at the *binding* stage and protonated at the *extrusion* stage), it seems difficult to determine how Arg971 mediates the proton relay from the ion pairs to the cytoplasm, when carrying two protons in one cycle. Molecular dynamics simulations have their own limitations and do not necessarily reflect the actual phenomenon. It is likely that there is no need to change the simple one-way model in Figure 12 until experimental data conflicting with the scheme are reported or until detailed structures of the protons are determined.

## Tripartite Structure of RND Exporters and the Drug Sweeping/Extrusion Mode-Switching Hypothesis

The crystal structure of each component of the AcrAB-TolC complex has been determined (Koronakis et al., 2000; Murakami et al., 2002; Mikolosko et al., 2006); however, the complete tripartite crystal structure has not been solved. The crystal structure of a bi-partite complex of the inner membrane transporter and the adaptor protein of RND-type transporters has been solved but only for the CusBA complex (Su et al., 2011). Active forms of AcrB and TolC are most likely trimers (Koronakis et al., 2000; Murakami et al., 2002). The crystal structure of the bottom of native TolC channels is closed; however, this channel should remain open during drug export. The open form of the mutant TolC structure has been experimentally determined (Bavro et al., 2008; Pei et al., 2011). The crystal structures of AcrB and TolC suggest that both trimers directly dock to each other in a top-to-bottom manner (Murakami et al., 2002; Symmons et al., 2009) because the diameter and the shape of the funnel-like opening at the top of the AcrB trimer fit directly into the bottom of the open form of the TolC channel. This direct-docking model is experimentally supported by *in vivo* cross-linking between AcrB and TolC (Tamura et al., 2005; Weeks et al., 2010) and by the *in vitro* detection of the direct AcrB-TolC interaction without AcrA through surface plasmon resonance (Tikhonova et al., 2011).

Regarding AcrA, bi-partite AcrA-AcrB, and AcrA-TolC complexes are detected (Tikhonova and Zgurskaya, 2004; Touze et al., 2004), and AcrA is thought to recruit TolC to form a tripartite complex (Tikhonova et al., 2009). The AcrA structure has four domains: the  $\alpha$ -hairpin, lipoyl,  $\beta$ -barrel, and MP (membrane proximal or  $\beta$ -roll) domains (Mikolosko et al., 2006; Symmons et al., 2009). Cross-linking between AcrA and AcrB showed a 1:1 stoichiometry (Symmons et al., 2009). AcrA-TolC cross linking (Lobedanz et al., 2007) and MexA-OprM (the *P. aeruginosa* homolog) cross linking (Ferrandez et al., 2012) also showed a 1:1 stoichiometry. Thus, the most likely model for the tripartite complex is that three AcrA molecules are attached to the TolC<sub>3</sub>-AcrB<sub>3</sub> direct docking complex (Figure 13A) (Symmons et al., 2009). The  $\alpha$ -hairpins of AcrA interact with TolC, and three other domains interact with the DN and PN2 domains of AcrB.

Although this AcrB<sub>3</sub>-AcrA<sub>3</sub>-TolC<sub>3</sub> direct docking model seems probable on the basis of individual crystal structures and cross-linking experiments, this model was recently challenged in

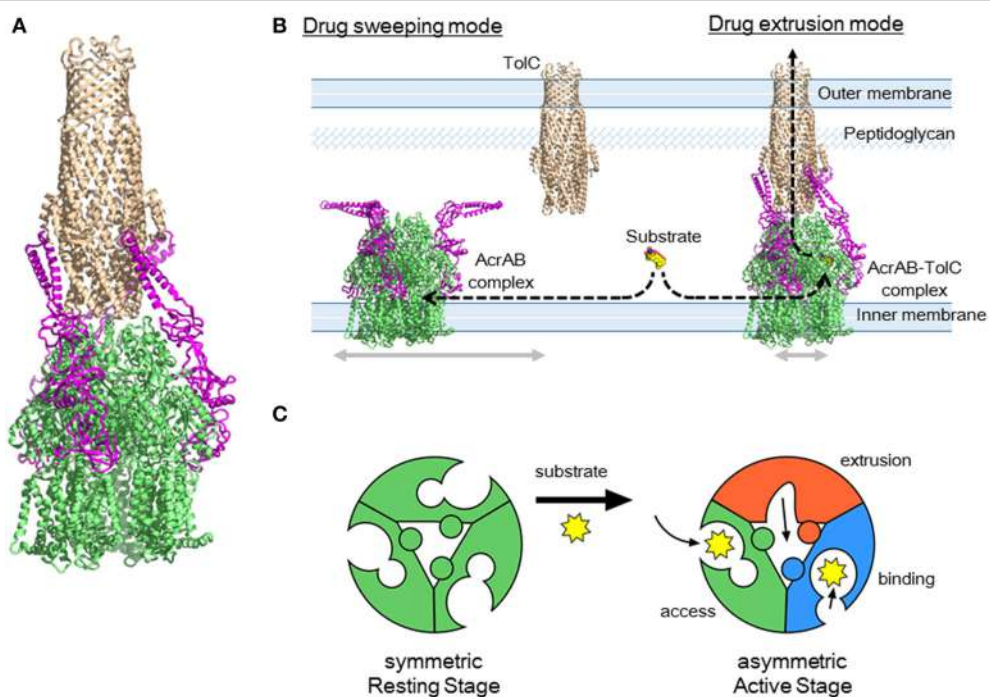


**FIGURE 13 | AcrAB-TolC tripartite complex and the drug sweeping/extrusion mode-switching hypothesis. (A)** Currently postulated structure of the tripartite complex. The TolC (brown) trimer is directly docked with AcrB (green) trimer and three AcrA

(pink) monomers are attached to the side. **(B)** Drug sweeping/extrusion mode-switching hypothesis. **(C)** AcrB trimers switching between the symmetric resting stage (left) and the asymmetric active stage.

electron microscopic images of the AcrAB-TolC complex. Du et al. (2014) obtained *in vitro* images of the reconstituted AcrAB-TolC complex through cryo-electron microscopy and Kim et al. (2015) obtained images using transmission electron microscopy. The images showed the vertical length of the complex was 317 Å, which is significantly longer than that of the TolC-AcrB direct docking model (approximately 270 Å), indicating that the AcrA tube comprising the α-helical and lipoyl domains and a portion of the β-barrel domains is inserted between TolC and AcrB. The images also suggested a TolC<sub>3</sub>-AcrA<sub>6</sub>-AcrB<sub>3</sub> stoichiometry. This indirect docking model is inconsistent with the CusBAC model, on the basis of the crystal structure of the CusBA bipartite complex (Su et al., 2011). To obtain a tripartite complex, Du et al., used two kinds of linker proteins together: AcrA-AcrZ linker proteins and linker proteins in which AcrA is inserted within AcrB. The resultant complexes showed low activity *in vivo*. Kim et al., examined the AcrB-AcrA-AcrA linker protein. These linker proteins may force AcrA into the complex at a AcrA:AcrB stoichiometry being 2:1. Currently, there is no evidence indicating that such an indirect docking form is the active form *in vivo*. Using cryo-electron tomography, Trepout et al. (2010) reported an image of reconstituted MexA-OprM fitting to a 1:1 stoichiometry and suggested a two-step tripartite complex formation model. The indirect-docking complex may be an intermediate step in the formation of an active complex. Regarding the stoichiometry of AcrA in the complex, we recently observed that the AcrB-AcrA one-to-one linker protein exhibits complete

activity in the AcrA/AcrB-deficient base (unpublished observation), suggesting that a 1:1 stoichiometry of AcrA to AcrB is sufficient for drug export. Controversy regarding the stoichiometry and the construction of the tripartite complex will continue until a high-resolution crystal structure is determined.

RND-type multidrug exporters take up substrates from the outer layer of the inner membrane and/or periplasm from dual drug entry points (Sennhauser et al., 2007; Husain et al., 2011; Nakashima et al., 2011). Considering the high efficiency of drug export and the relatively low-level intrinsic expression of RND transporters, each transporter should rapidly sweep the inner membrane through lateral diffusion. However, the lateral movement of the trans-periplasm complex such as AcrAB-TolC is prevented by a peptidoglycan mesh. To both rapidly sweep for substrates and efficiently export these into the TolC channel, it may be necessary to switch between a horizontally-diffusing drug-sweeping mode and the TolC-fixed drug-extrusion mode. Because TolC is a multifunctional outer membrane protein that interacts with a number of inner membrane transporters, complex formation would need to be tentative for optimal functioning (Zgruskaya, 2009).

In the sweeping mode, the inner membrane transporter alone or with adaptor proteins may move laterally via Brownian motion in the lipid bilayer region (Figure 13B). In the absence of substrates, inner membrane transporters are likely symmetric comprising the three monomers being the same access-like structure (Figure 13C). When adaptor proteins are attached to

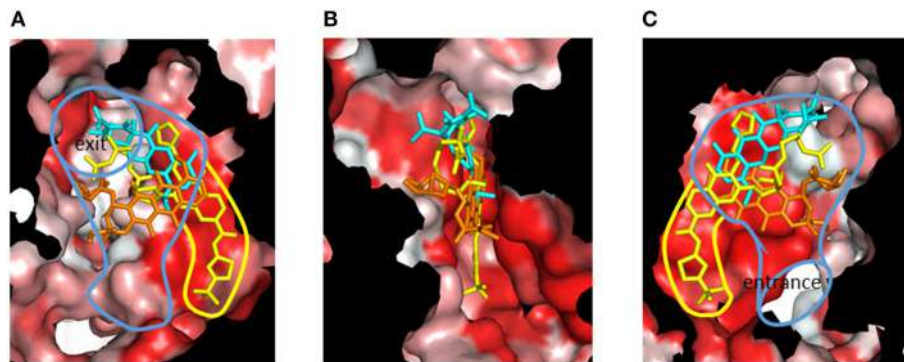


**FIGURE 14 | Cut view of the distal pocket of the AcrB binding monomer in complex with the inhibitor ABI-PP (yellow).** The bound minocycline (cyan) and doxorubicin (orange) are overlaid. **(A)** View toward the exit. **(B)** View looking down the hydrophobic trap (90° rotated from **(A)**)

around the vertical axis. **(C)** View toward the entrance (90° rotated from **(B)** around the vertical axis). The red color indicates Eisenberg's hydrophobicity scale. The blue and yellow curves indicate the drug translocation channel and the hydrophobic trap, respectively.

the moving transporters, the  $\alpha$ -helical moiety is likely to be bent downward. Although the bent conformation of AcrA has not been previously described, this bent-downward structure may be easily accommodated by AcrA because the AcrA structure shows high flexibility between subdomains (Vaccaro et al., 2006). When a substrate binds one of the monomers, the conformation of the trimer changes to the asymmetric form. As a result, AcrA is primed for the recruitment of TolC, followed by tentative tripartite complex formation. Immediately after drug export, the tripartite complexes dissociate. When the substrate concentration is high, the complex may continuously take up substrates without dissociating. This sweeping and extrusion mode exchange hypothesis seems to provide reasonable explanation for the high efficiency of drug efflux through the trans-periplasm complex. FDAP (fluorescence decay after photoconversion) analysis using PA-GFP (photoactivatable-GFP)-labeled AcrB showed the lateral movement of AcrB is more rapid when AcrB is expressed in the *acrB/tolC*-deficient cells than in the *acrB*-deficient cells. AcrB movement is slowed in the presence of proximal binding drugs (unpublished observation). Thus, AcrB is an exciting future target for investigations into how and when tripartite complexes form and what their physiological role(s) is.

## Specific Recognition of Inhibitors

Although RND-type transporters display a broad substrate recognition spectrum, these proteins show strict specificity for some inhibitors. Pyridopyrimidine derivatives are good inhibitors of AcrB and MexB without toxic effects; however, these compounds do not inhibit MexY (Yoshida et al., 2007). The narrow spectrum of pyridopyrimidines limits the clinical usefulness of these molecules. The structural basis of inhibitor specificity has been revealed through an analysis of the inhibitor-bound crystal structure of AcrB and MexB (Nakashima et al., 2013). The pyridopyrimidine derivative ABI-PP binds to the distal pocket of AcrB and MexB. The hydrophobic tail of ABI-PP is inserted into a narrow hydrophobic pit branching off the substrate translocation path (**Figure 14**). The binding site of the relatively hydrophilic

moiety of ABI-PP overlaps with the minocycline and doxorubicin binding sites. The branched pit is inconsistent with a hydrophobic trap in the distal binding pocket (Vargiu et al., 2011). The F610A mutation in this pit caused slip-in of substrates into this pit, resulting in decreased export activity. Phe178 is located at the edge of this pit in AcrB and MexB, and the benzene ring of this amino acid forms  $\pi$ - $\pi$  interactions with the pyridopyrimidine bicyclic ring, thereby stabilizing ABI-PP binding (**Figures 15A,B**). The inhibitory activity of ABI-PP is based on strong binding to this pit, which terminates the functional-rotation cycle because this pit has to become closed off for transition to the *extrusion* stage.

However, in a homology model of MexY, the corresponding position is occupied by tryptophan (Trp177), from which the bulky indolyl side chain protrudes into the pit and sterically hinders ABI-PP binding (**Figure 15C**). When Trp177 of MexY was replaced with phenylalanine by site-directed mutagenesis (**Figure 15D**), the resultant W177F mutant of MexY showed a susceptibility to ABI-PP similar to that observed for AcrB without the loss of drug export activity. In contrast, when Phe178 of AcrB was replaced with tryptophan, the resultant AcrB F178W mutant showed resistance to ABI-PP similar to MexY. The crystal structure of the AcrB F178W mutant was solved and the indolyl side chain of Trp178 protruded into the pit (**Figure 15E**). Thus, ABI-PP specificity is determined by the bulkiness of the side chain at position 178 or 177; however, the MexB F178W mutant remains sensitive to ABI-PP. The crystal structure of the ABI-PP-bound MexB F178W mutant showed that the bulky indolyl side chain is accommodated in parallel to the wall of the pit without projection, thereby contributing to stable binding through  $\pi$ - $\pi$  interactions with the pyridopyrimidine ring (**Figure 15F**).

An *in silico* simulation revealed that the parallel-to-wall arrangement of the indolyl moiety of Trp178 in AcrB is impossible due to steric hindrance from Val139. The pit in MexB is slightly larger than that in AcrB; thus, the parallel arrangement of the indolyl moiety of Trp178 is permitted in MexB but not permitted in AcrB. Ile138 of MexY also sterically hinders the parallel arrangement of the side chain of Trp177. To

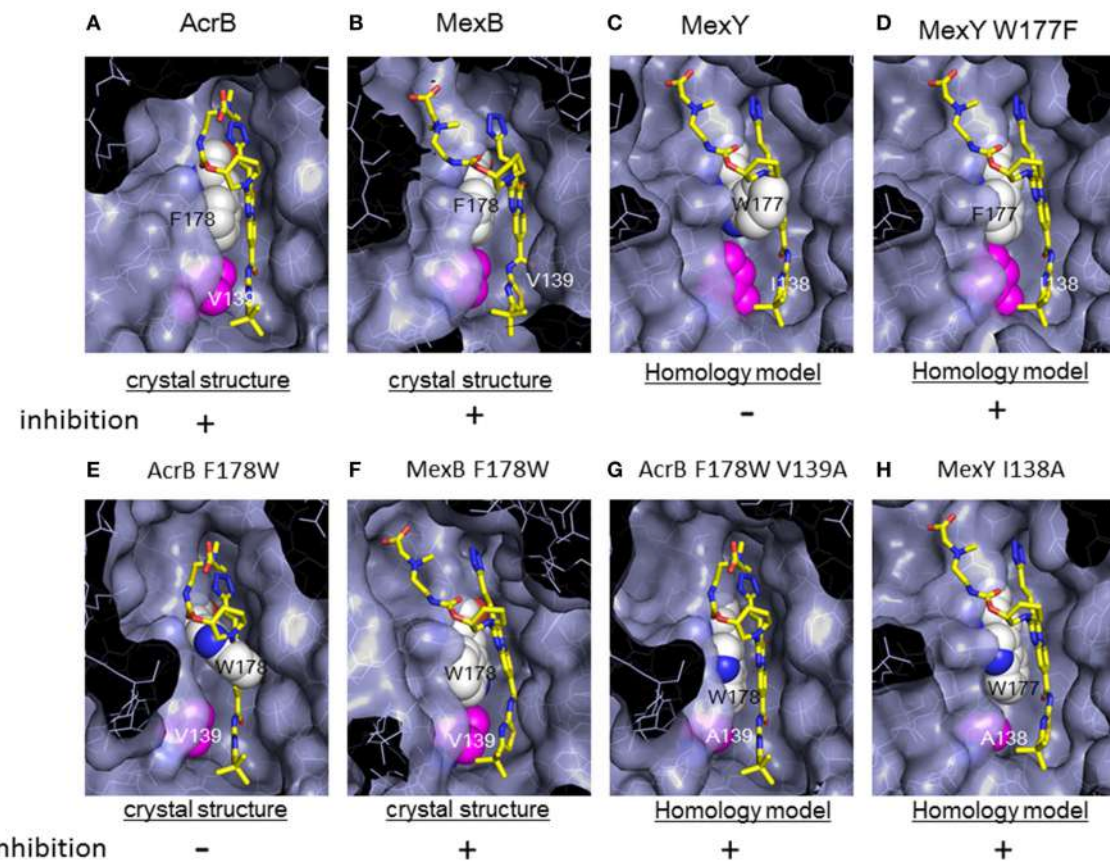


**FIGURE 15 |** Magnified view of the ABI-PP binding site depicted as a surface model. ABI-PP is depicted in a stick model. F178 and W177 are depicted using a white space-filling model. V139, I138, and mutated Ala are depicted shown in magenta in the space-filling model. The symbols + and – indicate inhibition or the lack of inhibition by ABI-PP, respectively. **(A,B,E,F)**

are crystal structures, and **(C,D,G,H)** are homology models. **(A)** ABI-PP-binding AcrB, **(B)** ABI-PP-binding MexB, **(C)** MexY overlapping with ABI-PP, **(D)** MexY W177F overlapping with ABI-PP, **(E)** AcrB F178W overlapping with ABI-PP, **(F)** ABI-PP-binding MexAB F178W, **(G)** AcrB F178W V139A overlapping with ABI-PP, **(H)** MexY I138A overlapping with ABI-PP.

confirm this prediction, the AcrB F178W V139A double mutant and the MexY I138A mutant were constructed (Figures 15G,H). These mutants showed an ABI-PP-sensitive phenotype similar to wild-type AcrB. Thus, the specificity for pyridopyrimidine derivatives is determined by the fit to the hydrophobic pit in the distal binding pocket. The ABI-PP binding structures of AcrB and MexB are the first examples of inhibitor-binding structures of multidrug efflux transporters in physiologically active asymmetric forms. These observations provide information for the development of universal inhibitors that inhibit AcrB, MexB and MexY, through virtual screening and structure-based drug design.

## Concluding Remarks and Future Perspectives

The molecular mechanisms of multidrug recognition and export by RND-type drug exporters have been revealed via crystal structure determinations over past decade. Multidrug recognition is based on multisite drug-binding in voluminous binding pockets.

The presence of two voluminous drug-binding pockets, proximal and distal, significantly expands the substrate specificity of these exporters. Multiple-entrances allow the export of both hydrophobic and hydrophilic compounds. Drug efflux is mediated through functional-rotation mechanism in which three monomers undergo a strictly coordinated sequential conformational change cycle of *access*, *binding* and *extrusion*. During the functional-rotation cycle, no two monomers display the same conformation. The substrates are transported from the entrance to a proximal pocket and then to a distal pocket and finally to a funnel-like exit through the peristaltic motion of the AcrB porter domain. Drug export is driven by the proton motive force via a remote-conformational coupling mechanism. The proton relay cycle in the transmembrane region strictly couples with the functional-rotation cycle in the porter region. Specific inhibitors bind tightly to the deep hydrophobic pit of the multisite drug binding pocket.

Future studies should address questions concerning why it is difficult to identify most bound substrates in the asymmetric structure and how the immobile trans-periplasmic exporter efficiently ejects substrates before they enter the

cytoplasm. The former question could be answered by the multisite-drug-oscillation hypothesis, which is consistent with a broad binding specificity and highly efficient export. The latter question could be addressed by the sweep (moving) and export (fixed) mode-switching hypothesis, which is consistent with the

need for tentative formation of a tripartite complex. However, these hypotheses lack experimental evidence. Addressing these questions is an exciting challenge, which will involve protein dynamics studies and crystal structure determinations of the tripartite complex.

## References

- Alvarez-Ortega, C., Olivares, J., and Martinez, J. L. (2013). RND multidrug efflux pumps: what are they good for? *Front. Microbiol.* 4:7. doi: 10.3389/fmicb.2013.00007
- Bavro, V. N., Pietras, Z., Furnham, N., Perez-Cano, L., Fernandez-Recio, J., Pei, X. Y., et al. (2008). Assembly and channel opening in a bacterial drug efflux machine. *Mol. Cell* 30, 114–121. doi: 10.1016/j.molcel.2008.02.015
- Bhardwaj, A. K., and Mohanty, P. (2012). Bacterial efflux pumps involved in multidrug resistance and their inhibitors: rejuvenating the antimicrobial chemotherapy. *Recent Pat. Antiinfect. Drug Discov.* 7, 73–89. doi: 10.2174/157489112799829710
- Blair, J. M., Richmond, G. E., and Piddock, L. J. (2014). Multidrug efflux pumps in Gram-negative bacteria and their role in antibiotic resistance. *Future Microbiol.* 9, 1165–1177. doi: 10.2217/fmb.14.66
- Buchanan, S. K. (2001). Type I secretion and multidrug efflux transport through the TolC channel-tunnel. *Trends Biochem. Sci.* 26, 3–6. doi: 10.1016/S0968-0004(00)01733-3
- Cha, H. J., Muller, R. T., and Pos, K. M. (2014). Switch loop flexibility affects transport of large drugs by the promiscuous AcrB multidrug efflux transporter. *Antimicrob. Agents Chemother.* 58, 4767–4772. doi: 10.1128/AAC.02733-13
- Chen, C., Chin, J. E., Ueda, K., Clark, D. P., Pastan, I., Gottesman, M. M., et al. (1986). Internal duplication and homology with bacterial transport proteins in the *mdr1* (P-glycoprotein) gene from multidrug resistant human cells. *Cell* 47, 381–389. doi: 10.1016/0092-8674(86)90595-7
- Dawson, R. J., and Locher, K. P. (2006). Structure of a bacterial multidrug ABC transporter. *Nature* 443, 180–185. doi: 10.1038/nature05155
- Drew, D., Klepsch, M. M., Newstead, S., Flraig, R., De Gier, J. W., Iwata, S., et al. (2008). The structure of the efflux pump AcrB in complex with bile acid. *Mol. Membr. Biol.* 25, 677–682. doi: 10.1080/09687680802552257
- Du, D., Wang, Z., James, N. R., Voss, J. E., Klimont, E., Ohene-Agyei, T., et al. (2014). Structure of the AcrAB-TolC multidrug efflux pump. *Nature* 509, 512–515. doi: 10.1038/nature13205
- Eicher, T., Cha, H. J., Seeger, M. A., Brandstätter, L., El-Delik, J., Bohnert, J. A., et al. (2012). Transport of drugs by the multidrug transporter AcrB involves an access and a deep binding pocket that are separated by a switch loop. *Proc. Natl. Acad. Sci. U.S.A.* 109, 5687–5692. doi: 10.1073/pnas.1114944109
- Eicher, T., Seeger, M. A., Anselmi, C., Zhou, W., Brandstätter, L., Verrey, F., et al. (2014). Coupling of remote alternating-access transport mechanisms for protons and substrates in the multidrug efflux pump AcrB. *Elife* 3:e03145. doi: 10.7554/eLife.03145
- Elkins, C. A., and Nikaido, H. (2002). Substrate specificity of the RND-type multidrug efflux pumps AcrB and AcrD of *Escherichia coli* is determined predominantly by two large periplasmic loops. *J. Bacteriol.* 184, 6490–6498. doi: 10.1128/JB.184.23.6490-6499.2002
- Ferrandez, Y., Monlezun, L., Phan, G., Benabdellah, H., Benas, P., Ulryck, N., et al. (2012). Stoichiometry of the MexA-OprM binding, as investigated by blue native gel electrophoresis. *Electrophoresis* 33, 1282–1287. doi: 10.1002/elps.201100541
- Fischer, N., and Kandt, C. (2011). Three ways in, one way out: water dynamics in the transmembrane domains of the inner membrane translocase AcrB. *Proteins* 79, 2871. doi: 10.1002/prot.23122
- Forman, D. T., Martinez, Y., Coombs, G., Torres, A., and Kupersztoch, Y. M. (1995). TolC and DsbA are needed for the secretion of STB, a heat-stable enterotoxin of *Escherichia coli*. *Mol. Microbiol.* 18, 237–245. doi: 10.1111/j.1365-2958.1995.mmi\_18020237.x
- Furukawa, H., Tsay, J. T., Jackowski, S., Takamura, Y., and Rock, C. O. (1993). Thiolactomycin resistance in *Escherichia coli* is associated with the multidrug resistance efflux pump encoded by *emrAB*. *J. Bacteriol.* 175, 3723–3729.
- Gerlach, J. H., Kartner, N., Bell, D. R., and Ling, V. (1986). Multidrug resistance. *Cancer Surv.* 5, 25–46.
- Grinias, L. L., and Goldberg, E. B. (1994). Bacterial multidrug resistance is due to a single membrane protein which functions as a drug pump. *J. Biol. Chem.* 269, 29998–30004.
- Guan, L., and Nakae, T. (2001). Identification of essential charged residues in transmembrane segments of the multidrug transporter MexB of *Pseudomonas aeruginosa*. *J. Bacteriol.* 183, 1734–1739. doi: 10.1128/JB.183.5.1734-1739.2001
- Hancock, R. E., Decad, G. M., and Nikaido, H. (1979). Identification of the protein producing transmembrane diffusion pores in the outer membrane of *Pseudomonas aeruginosa* PAO1. *Biochim. Biophys. Acta* 554, 323–331. doi: 10.1016/0005-2736(79)90373-0
- Hung, L. W., Kim, H. B., Murakami, S., Gupta, G., Kim, C. Y., and Terwilliger, T. C. (2013). Crystal structure of AcrB complexed with linezolid at 3.5 Å resolution. *J. Struct. Funct. Genomics* 14, 71–75. doi: 10.1007/s10969-013-9154-x
- Husain, F., Bikchandani, M., and Nikaido, H. (2011). Vestibules are part of the substrate path in the multidrug efflux transporter AcrB of *Escherichia coli*. *J. Bacteriol.* 193, 5847–5849. doi: 10.1128/JB.05759-11
- Kato, A., Ohnishi, H., Yamamoto, K., Furuta, E., Tanabe, H., and Utsumi, R. (2000). Transcription of *emrKY* is regulated by the EvgA-EvgS two-component system in *Escherichia coli* K12. *Biosci. Biotechnol. Biochem.* 64, 1203–1209. doi: 10.1271/bbb.64.1203
- Kim, J.-S., Jeong, H., Song, S., Kim, H. Y., Lee, K., Hyun, J., et al. (2015). Structure of the tripartite multidrug efflux pump AcrAB-TolC suggests an alternative assembly mode. *Mol. Cells* 38, 180–186. doi: 10.14348/molcells.2015.2277
- Kobayashi, N., Nishino, K., and Yamaguchi, A. (2001). Novel macrolide-specific ABC-type efflux transporter in *Escherichia coli*. *J. Bacteriol.* 183, 5639–5644. doi: 10.1128/JB.183.19.5639-5644.2001
- Kohler, T., Michéa-Hamzehpour, M., Henze, U., Gotoh, N., Curty, L. K., and Pechère, J. C. (1997). Characterization of MexE-MexF-OprN, a positively regulated multidrug efflux system of *Pseudomonas aeruginosa*. *Mol. Microbiol.* 23, 345–354. doi: 10.1046/j.1365-2958.1997.2281594.x
- Koronakis, V., Sharff, A., Koronakis, E., Luisi, B., and Hughes, C. (2000). Crystal structure of the bacterial membrane protein TolC central to multidrug efflux and protein export. *Nature* 405, 914–919. doi: 10.1038/35016007
- Kuroda, T., and Tsuchiya, T. (2009). Multidrug efflux transporters in the MATE family. *Biochim. Biophys. Acta* 1794, 763–768. doi: 10.1016/j.bbapap.2008.11.012
- Lau, C. H., Hughes, D., and Poole, K. (2014). MexY-promoted aminoglycoside resistance in *Pseudomonas aeruginosa*: involvement of a putative proximal binding pocket in aminoglycoside recognition. *MBio* 5:e01068. doi: 10.1128/mBio.01068-14
- Li, X. Z., Livermore, D. M., and Nikaido, H. (1994a). Role of efflux pump(s) in intrinsic resistance of *Pseudomonas aeruginosa*: resistance to tetracycline, chloramphenicol, and norfloxacin. *Antimicrob. Agents Chemother.* 38, 1732–1741. doi: 10.1128/AAC.38.8.1732
- Li, X. Z., Ma, D., Livermore, D. M., and Nikaido, H. (1994b). Role of efflux pump(s) in intrinsic resistance of *Pseudomonas aeruginosa*: active efflux as a contributing factor to beta-lactam. *Antimicrob. Agents Chemother.* 38, 1742–1752. doi: 10.1128/AAC.38.8.1742
- Li, X. Z., and Nikaido, H. (2015). The challenge of efflux-mediated antibiotic resistance in Gram-negative bacteria. *Clin. Microbiol. Rev.* 28, 337–416. doi: 10.1128/CMR.00117-14
- Li, X. Z., Nikaido, H., and Poole, K. (1995). Role of mexA-mex-B-oprM in antibiotic efflux in *Pseudomonas aeruginosa*. *Antimicrob. Agents Chemother.* 39, 1948–1953. doi: 10.1128/AAC.39.9.1948
- Li, X. Z., Zhang, L., and Poole, K. (1998). Role of the multidrug efflux systems of *Pseudomonas aeruginosa* in organic solvent tolerance. *J. Bacteriol.* 180, 2987–2991.

- Lobedanz, S., Bokma, E., Symmons, M. F., Koronakis, E., Hughes, C., and Koronakis, V. (2007). A periplasmic coiled-coil interface underlying TolC recruitment and the assembly of bacterial drug efflux pumps. *Proc. Natl. Acad. Sci. U.S.A.* 104, 4612–4617. doi: 10.1073/pnas.0610160104
- Lomovslaya, O., Zgurskaya, H. I., and Nikaido, H. (2002). It takes three to tango. *Nat. Biotechnol.* 20, 1210–1212. doi: 10.1038/nbt1202-1210
- Luberski, J., Konings, W. N., and Driessens, A. J. M. (2007). Distribution and physiology of ABC-type transporters contributing to multidrug resistance in bacteria. *Microbiol. Mol. Biol. Rev.* 71, 463–476. doi: 10.1128/MMBR.00001-07
- Marger, M. D., and Saier, M. H. Jr. (1993). A major superfamily of transmembrane facilitators that catalyze uniport, symport and antiport. *Trends Biochem. Sci.* 18, 13–20. doi: 10.1016/0968-0004(93)90081-W
- Masuda, N., Sakagawa, E., Ohya, S., Gotoh, N., Tsujimoto, H., and Nishino, T. (2000). Substrate specificities of MexAB-OprM, MexCD-OprJ, and MexXY-OprM efflux pumps in *Pseudomonas aeruginosa*. *Antimicrob. Agents Chemother.* 44, 3322–3327. doi: 10.1128/AAC.44.12.3322-3327.2000
- Matsumoto, Y., Hayama, K., Sakakihara, S., Nishino, K., Noji, H., Iino, R., et al. (2011). Evaluation of multidrug efflux pump inhibitors by a new method using microfluidic channels. *PLoS ONE* 6:e18547. doi: 10.1371/journal.pone.0018547
- Medek, P., Benes, P., and Sochor, J. (2007). Computation of tunnels in protein molecules using Delaunay triangulation. *J. WSCG* 15, 107–114.
- Mikolosko, J., Bobyk, K., Zgurskaya, H. I., and Ghosh, P. (2006). Conformational flexibility in the multidrug efflux system protein AcrA. *Structure* 14, 577–587. doi: 10.1016/j.str.2005.11.015
- Minagawa, S., Inami, H., Kato, T., Sawada, S., Yasuki, T., Miyairi, S., et al. (2012). RND-type efflux pump system MexAB-OprM of *Pseudomonas aeruginosa* selects bacterial languages, 3-oxo-acyl-homoserine lactones, for cell-to-cell communication. *BMC Microbiol.* 12:70. doi: 10.1186/1471-2180-12-70
- Mine, T., Morita, Y., Kataoka, A., Mizushima, T., and Tsuchiya, T. (1999). Expression in *Escherichia coli* of a new multidrug efflux pump, MexXY, from *Pseudomonas aeruginosa*. *Antimicrob. Agents Chemother.* 43, 415–417.
- Motohashi, H., and Inui, K. (2013). Multidrug and toxin extrusion family SLC47: physiological, pharmacokinetic and toxicokinetic importance of MATE1 and MATE2-K. *Mol. Aspects Med.* 34, 661–668. doi: 10.1016/j.mam.2012.11.004
- Murakami, S., Nakashima, R., Yamashita, E., Matsumoto, T., and Yamaguchi, A. (2006). Crystal structures of a multidrug transporter reveal a functionally rotating mechanism. *Nature* 443, 173–179. doi: 10.1038/nature05076
- Murakami, S., Nakashima, R., Yamashita, E., and Yamaguchi, A. (2002). Crystal structure of bacterial multidrug efflux transporter AcrB. *Nature* 419, 587–593. doi: 10.1038/nature01050
- Nakashima, R., Sakurai, K., Yamasaki, S., Hayashi, K., Nagata, C., Hoshino, K., et al. (2013). Structural basis for the inhibition of bacterial multidrug exporters. *Nature* 500, 102–106. doi: 10.1038/nature12300
- Nakashima, R., Sakurai, K., Yamasaki, S., Nishino, K., and Yamaguchi, A. (2011). Structures of the multidrug exporter AcrB reveal a proximal multisite drug-binding pocket. *Nature* 480, 565–569. doi: 10.1038/nature10641
- Nikaido, H. (1988). Bacterial resistance to antibiotics as a function of outer membrane permeability. *J. Antimicrob. Chemother.* 22, 17–22.
- Nikaido, H. (1994). Prevention of drug access to bacterial targets: permeability barriers and active efflux. *Science* 264, 382–388. doi: 10.1126/science.8153625
- Nikaido, H. (1998). Antibiotic resistance caused by gram-negative multidrug efflux pumps. *Clin. Infect. Dis.* 27, S32–S41. doi: 10.1086/514920
- Nikaido, H., and Pages, J.-M. (2012). Broad-specificity efflux pumps and their role in multidrug resistance of Gram-negative bacteria. *FEMS Microbiol. Rev.* 36, 340–363. doi: 10.1111/j.1574-6976.2011.00290.x
- Nikaido, H., and Vaara, M. (1983). Molecular basis of bacterial outer membrane permeability. *Microbiol. Rev.* 49, 1–32.
- Nishino, K., Latifi, T., and Groisman, E. A. (2006). Virulence and drug resistance roles of multidrug efflux systems of *Salmonella enterica* serovar *Typhimurium*. *Mol. Microbiol.* 59, 126–141. doi: 10.1111/j.1365-2958.2005.04940.x
- Nishino, K., and Yamaguchi, A. (2001). Analysis of a complete library of putative drug transporter genes in *Escherichia coli*. *J. Bacteriol.* 183, 5803–5812. doi: 10.1128/JB.183.20.5803-5812.2001
- Okusu, H., Ma, D., and Nikaido, H. (1996). AcrAB efflux pump plays a major role in the antibiotic resistance phenotype of *Escherichia coli* multiple-antibiotic-resistance (Mar) mutants. *J. Bacteriol.* 178, 306–308.
- Pages, J. M., and Amaral, L. (2009). Mechanism of drug efflux and strategies to combat them: challenging the efflux pump of Gram-negative bacteria. *Biochim. Biophys. Acta* 1794, 826–833. doi: 10.1016/j.bbapap.2008.12.011
- Paulsen, I. T., Nguyen, L., Sliwinski, M. K., Rabus, R., and Saier, M. H. Jr. (2000). Microbial genome analyses: comparative transport capabilities in eighteen prokaryotes. *J. Mol. Biol.* 301, 75–100. doi: 10.1006/jmbi.2000.3961
- Paulsen, I. T., Skurray, R. A., Tam, R., Saier, M. H., Turner, R. J., Weiner, J. H., et al. (1996). The SMR family: a novel family of multidrug efflux proteins involved with the efflux of lipophilic drugs. *Mol. Microbiol.* 19, 1167–1175. doi: 10.1111/j.1365-2958.1996.tb02462.x
- Pei, X.-Y., Hinchliffe, P., Symmons, M. F., Koronakis, E., Benz, R., Hughes, C., et al. (2011). Structures of sequential open states in a symmetrical opening transition of the exit duct. *Proc. Natl. Acad. Sci. U.S.A.* 108, 2112–2117. doi: 10.1073/pnas.1012588108
- Piddock, L. J. (2006). Multidrug-resistance efflux pumps – not just for resistance. *Nat. Rev. Microbiol.* 4, 629–636. doi: 10.1038/nrmicro1464
- Poole, K., Gotoh, N., Tsujimoto, H., Zhao, Q., Wada, A., Yamasaki, T., et al. (1996). Overexpression of the mexC-mexD-opr operon in nfx-type multidrug resistant strains of *Pseudomonas aeruginosa*. *Mol. Microbiol.* 21, 713–724. doi: 10.1046/j.1365-2958.1996.281397.x
- Poole, K., Krebes, K., McNally, C., and Neshat, S. (1993). Multiple antibiotic resistance in *Pseudomonas aeruginosa*: evidence for involvement of an efflux operon. *J. Bacteriol.* 175, 7363–7372.
- Pos, K. M. (2009). Drug export mechanism of the AcrB efflux pump. *Biochim. Biophys. Acta* 1794, 782–793. doi: 10.1016/j.bbapap.2008.12.015
- Pos, K. M., Schiefner, A., Seeger, M. A., and Diederichs, K. (2004). Crystallographic analysis of AcrB. *FEBS Lett.* 564, 333–339. doi: 10.1016/S0014-5793(04)00272-8
- Rauch, C. (2011). The “multi” of drug resistance explained by oscillating drug transporters, drug-membrane physical interactions and spatial dimensionality. *Cell Biochem. Biophys.* 61, 103–113. doi: 10.1007/s12013-011-9166-8
- Ruggerone, P., Murakami, S., Pos, K. M., and Vargiu, A. V. (2013). RND efflux pumps: structural information translated into function and inhibition mechanisms. *Curr. Topics Med. Chem.* 13, 3079–3100. doi: 10.2174/15680266113136660220
- Schumacher, M. A., Miller, M. C., Grkovic, S., Brown, M. H., Skurray, R. A., and Brennan, R. G. (2001). Structural mechanisms of QacR induction and multidrug recognition. *Science* 294, 2158–2163. doi: 10.1126/science.1066020
- Seeger, M. A., Schiefner, A., Eicher, T., Verrey, F., Diederichs, K., and Pos, K. M. (2006). Structural asymmetry of AcrB trimer suggests a peristaltic pump mechanism. *Science* 313, 1295–1298. doi: 10.1126/science.1131542
- Seeger, M. A., von Ballmoos, C., Eicher, T., Brandstätter, L., Verrey, F., Diederichs, K., et al. (2008). Engineered disulfide bonds support the functional rotation mechanism of multidrug efflux pump AcrB. *Nat. Struct. Mol. Biol.* 15, 199–205. doi: 10.1038/nsmb.1379
- Sennhauser, G., Amstutz, P., Briand, C., Storchenegger, O., and Grüttner, M. G. (2007). Drug export pathway of multidrug exporter AcrB revealed by DARPin inhibitors. *PLoS Biol.* 5:e7. doi: 10.1371/journal.pbio.0050007
- Sennhauser, G., Bukowska, M. A., Briand, C., and Grüttner, M. G. (2009). Crystal structure of the multidrug exporter MexB from *Pseudomonas aeruginosa*. *J. Mol. Biol.* 389, 134–145. doi: 10.1016/j.jmb.2009.04.001
- Slack, M. P. (1981). Antipseudomonal beta-lactams. *J. Antimicrob. Agents Chemother.* 8, 165–170. doi: 10.1093/jac/8.3.165
- Su, C. C., Li, M., Gu, R., Takatsuka, Y., McDermott, G., Nikaido, H., et al. (2006). Conformation of the AcrB multidrug efflux pump in mutants of the putative proton relay pathway. *J. Bacteriol.* 188, 7290–7296. doi: 10.1128/JB.00684-06
- Su, C. C., Long, F., Zimmermann, M. T., Rajashankar, K. R., Jernigan, R. L., and Yu, E. W. (2011). Crystal structure of the CusBA heavy-metal efflux complex of *Escherichia coli*. *Nature* 470, 558–562. doi: 10.1038/nature09743
- Symmons, M. F., Bokma, E., Koronakis, E., Hughes, C., and Koronakis, V. (2009). The assembled structure of a complete tripartite bacterial multidrug efflux pump. *Proc. Natl. Acad. Sci. U.S.A.* 106, 7173–7178. doi: 10.1073/pnas.0900693106
- Takatsuka, Y., Chen, C., and Nikaido, H. (2010). Mechanism of recognition of compounds of diverse structures by the multidrug efflux pump AcrB of *Escherichia coli*. *Proc. Natl. Acad. Sci. U.S.A.* 107, 6559–6565. doi: 10.1073/pnas.1001460107

- Takatsuka, Y., and Nikaido, H. (2006). Threonine-978 in the transmembrane segment of the multidrug efflux pump AcrB of *Escherichia coli* is crucial for drug transport as a probable component of the proton relay network. *J. Bacteriol.* 188, 7284–7289. doi: 10.1128/JB.00683-06
- Takatsuka, Y., and Nikaido, H. (2009). Covalently linked trimer of the AcrB multidrug efflux pump provides support for the functional rotating mechanism. *J. Bacteriol.* 191, 1729–1737. doi: 10.1128/JB.01441-08
- Tamura, N., Murakami, S., Oyama, Y., Ishiguro, M., and Yamaguchi, A. (2005). Direct interaction of multidrug efflux transporter AcrB and outer membrane channel TolC detected via site-directed disulfide cross linking. *Biochemistry* 44, 11115–11121. doi: 10.1021/bi050452u
- Thanassi, D. G., Cheng, L. W., and Nikaido, H. (1997). Active efflux of bile salts by *Escherichia coli*. *J. Bacteriol.* 179, 2512–2518.
- Tikhonova, E. B., Dastidar, V., Rybenkov, V. V., and Zgurskaya, H. I. (2009). Kinetic control of TolC recruitment by multidrug efflux complexes. *Proc. Natl. Acad. Sci. U.S.A.* 106, 16416–16421. doi: 10.1073/pnas.0906601106
- Tikhonova, E. B., Yamada, Y., and Zgruskaya, H. I. (2011). Sequential mechanism of assembly of multidrug efflux pump AcrAB-TolC. *Chem. Biol.* 18, 454–463. doi: 10.1016/j.chembiol.2011.02.011
- Tikhonova, T., and Zgurskaya, H. I. (2004). AcrA, AcrB, and TolC of *Escherichia coli* form a stable intermembrane multidrug efflux complex. *J. Biol. Chem.* 279, 32116–32124. doi: 10.1074/jbc.M402230200
- Touze, T., Eswaran, J., Bokma, E., Koronakis, E., Hughes, C., and Koronakis, V. (2004). Interactions underlying assembly of the *Escherichia coli* AcrAB-TolC multidrug efflux system. *Mol. Microb.* 53, 697–706. doi: 10.1111/j.1365-2958.2004.04158.x
- Trepout, S., Taveau, J. C., Benabdellah, H., Granier, T., Ducruix, A., Frangakis, A. S., et al. (2010). Structure of reconstituted bacterial membrane efflux pump by cryo-electron tomography. *Biochim. Biophys. Acta* 1798, 1953–1960. doi: 10.1016/j.bbamem.2010.06.019
- Trias, J., Dufresne, J., Levesque, R. C., and Nikaido, H. (1989). Decreased outer membrane permeability in imipenem-resistant mutants of *Pseudomonas aeruginosa*. *Antimicrob. Agents Chemother.* 33, 1202–1206. doi: 10.1128/AAC.33.8.1202
- Tseng, T. T., Gratwick, K. S., Kollman, J., Park, D., Nies, D. H., Goffeau, A., et al. (1999). The RND permease superfamily: an ancient, ubiquitous and diverse family that includes human disease and development proteins. *J. Mol. Microb. Biotechnol.* 1, 107–125.
- Vaccaro, L., Koronakis, V., and Sansom, M. S. P. (2006). Flexibility in a drug transport accessory protein: molecular dynamics simulations of MexA. *Biophys. J.* 91, 558–564. doi: 10.1529/biophysj.105.080010
- Vargiu, A. V., Collu, F., Schulz, R., Pos, K. M., Zacharias, M., Kleinekathöfer, U., et al. (2011). Effect of F610A mutation on substrate extrusion in the AcrB transporter: explanation and rationale by molecular dynamics simulations. *J. Am. Chem. Soc.* 133, 10704–10707. doi: 10.1021/ja202666x
- Vargiu, A. V., and Nikaido, H. (2012). Multidrug binding properties of the AcrB efflux pump characterized by molecular dynamics simulations. *Proc. Natl. Acad. Sci. U.S.A.* 109, 20637–20642. doi: 10.1073/pnas.1218348109
- Vogt, A. D., Pozzi, N., Chen, Z., and Di Cera, E. (2014). Essential role of conformational selection in ligand binding. *Biophys. Chem.* 186, 13–21. doi: 10.1016/j.bpc.2013.09.003
- Weeks, J. W., Celaya-Kolb, T., Pecora, S., and Misra, R. (2010). AcrA suppressor alterations reverse the drug hypersensitivity phenotype of a TolC mutant by inducing TolC aperture opening. *Mol. Microb.* 75, 1468–1483. doi: 10.1111/j.1365-2958.2010.07068.x
- Yao, X.-Q., Kimura, N., Murakami, S., and Takada, S. (2013). Drug uptake pathways of multidrug transporter AcrB studied by molecular simulations and site-directed mutagenesis experiments. *J. Am. Chem. Soc.* 135, 7474–7485. doi: 10.1021/ja310548h
- Yoshida, K., Nakayama, K., Ohtsuka, M., Kuru, N., Yokomizo, Y., Sakamoto, A., et al. (2007). MexAB-OprM specific efflux pump inhibitors in *Pseudomonas aeruginosa*. Part 7: highly soluble and *in vivo* active quaternary ammonium analogue D13-9001, a potential preclinical candidate. *Bioorg. Med. Chem.* 15, 7087–7097. doi: 10.1016/j.bmc.2007.07.039
- Yoshihara, E., and Nakae, T. (1989). Identification of porins in the outer membrane of *Pseudomonas aeruginosa* that form small diffusion pores. *J. Biol. Chem.* 264, 6297–6301.
- Yu, E. W., Aires, J. R., McDermott, G., and Nikaido, H. (2005). A periplasmic drug-binding site of the AcrB multidrug efflux pump: a crystallographic and site-directed mutagenesis study. *J. Bacteriol.* 187, 6804–6815. doi: 10.1128/JB.187.19.6804-6815.2005
- Yu, E. W., McDermott, G., Zgurskaya, H. I., Nikaido, H., and Koshland, D. E. Jr. (2003). Structural basis of multiple drug-binding capacity of the AcrB multidrug efflux pump. *Science* 300, 976–980. doi: 10.1126/science.1083137
- Zgurskaya, H. I. (2009). Multicomponent drug efflux complexes: architecture and mechanism of assembly. *Future Microbiol.* 4, 919–932. doi: 10.2217/fmb.09.62
- Zgurskaya, H. I., and Nikaido, H. (1999). Bypassing the periplasm: reconstitution of the AcrAB multidrug efflux pump of *Escherichia coli*. *Proc. Natl. Acad. Sci. U.S.A.* 96, 7190–7195. doi: 10.1073/pnas.96.13.7190

**Conflict of Interest Statement:** The authors declare that the research was conducted in the absence of any commercial or financial relationships that could be construed as a potential conflict of interest.

Copyright © 2015 Yamaguchi, Nakashima and Sakurai. This is an open-access article distributed under the terms of the Creative Commons Attribution License (CC BY). The use, distribution or reproduction in other forums is permitted, provided the original author(s) or licensor are credited and that the original publication in this journal is cited, in accordance with accepted academic practice. No use, distribution or reproduction is permitted which does not comply with these terms.

# Substrate binding accelerates the conformational transitions and substrate dissociation in multidrug efflux transporter AcrB

Beibei Wang<sup>1</sup>, Jingwei Weng<sup>1\*</sup> and Wenning Wang<sup>1,2\*</sup>

<sup>1</sup> Shanghai Key Laboratory of Molecular Catalysis and Innovative Materials, Department of Chemistry, Fudan University, Shanghai, China, <sup>2</sup> Institutes of Biomedical Sciences, Fudan University, Shanghai, China

## OPEN ACCESS

### Edited by:

Attilio Vittorio Vargiu,  
Università' di Cagliari, Italy

### Reviewed by:

Ulrich Kleinekathöfer,  
Jacobs University Bremen, Germany  
Thomas H. Schmidt,  
University of Bonn, Germany

### \*Correspondence:

Jingwei Weng and Wenning Wang,  
Department of Chemistry,  
Fudan University,  
220 Handan Road,  
Shanghai 200433, China  
jwweng@fudan.edu.cn;  
wnwang@fudan.edu.cn

### Specialty section:

This article was submitted to  
Antimicrobials, Resistance and  
Chemotherapy, a section of the journal  
*Frontiers in Microbiology*

Received: 05 January 2015

Accepted: 27 March 2015

Published: 13 April 2015

### Citation:

Wang B, Weng J and Wang W (2015)  
Substrate binding accelerates the conformational transitions and substrate dissociation in multidrug efflux transporter AcrB.  
*Front. Microbiol.* 6:302.  
doi: 10.3389/fmicb.2015.00302

The tripartite efflux pump assembly AcrAB-TolC is the major multidrug resistance transporter in *E. coli*. The inner membrane transporter AcrB is a homotrimer, energized by the proton movement down the transmembrane electrochemical gradient. The asymmetric crystal structures of AcrB with three monomers in distinct conformational states [access (A), binding (B) and extrusion (E)] support a functional rotating mechanism, in which each monomer of AcrB cycles among the three states in a concerted way. However, the relationship between the conformational changes during functional rotation and drug translocation has not been totally understood. Here, we explored the conformational changes of the AcrB homotrimer during the ABE to BEA transition in different substrate-binding states using targeted MD simulations. It was found that the dissociation of substrate from the distal binding pocket of B monomer is closely related to the concerted conformational changes in the translocation pathway, especially the side chain reorientation of Phe628 and Tyr327. A second substrate binding at the proximal binding pocket of A monomer evidently accelerates the conformational transitions as well as substrate dissociation in B monomer. The acceleration effect of the multi-substrate binding mode provides a molecular explanation for the positive cooperativity observed in the kinetic studies of substrate efflux and deepens our understanding of the functional rotating mechanism of AcrB.

**Keywords:** AcrB, MD simulation, substrate binding, allosteric effect, drug extrusion, positive cooperativity

## Introduction

In Gram-negative bacteria, resistance-nodulation-division (RND) superfamily proteins play a major role in the efflux of a wide range of antibiotics and toxic compounds out of cell. RND superfamily, together with other classes of multidrug efflux pumps, constitute one of the major mechanisms of multidrug resistance (MDR) in bacteria, which represents a serious impediment to improved healthcare (Higgins, 2007). RND transporter is embedded in the inner membrane and works as a drug-proton antiporter. Fueled by proton diffusion down the transmembrane (TM) electrochemical gradient, it collects substrates from the periplasm or the inner leaflet of inner membrane and extrudes them to the lumen of outer membrane component (Nikaido, 1996). The RND transporter AcrB in *Escherichia coli* has been extensively studied as a prototype of the family, which

exports a number of dyes, detergents, chloramphenicol, tetracyclines, macrolides,  $\beta$ -lactams, fluoroquinolones, and organic solvents. It functions in the form of AcrAB-TolC tripartite complex (Zgurskaya and Nikaido, 1999b; Tikhonova and Zgurskaya, 2004; Collu et al., 2012; Du et al., 2014) by working collaboratively with the periplasmic adaptor protein AcrA (Zgurskaya and Nikaido, 1999a; Mikolosko et al., 2006) and the outer membrane protein TolC (Koronakis et al., 2000). As the core of the complex, AcrB is responsible for substrate recognition and energy supplement (Elkins and Nikaido, 2002).

\pi-堆积相互作用捕获底物（Nakashima et al., 2011; Eicher et al., 2012）。

AcrB是高度动态的，其构象变化对于其运输活性至关重要（Takatsuka and Nikaido, 2007, 2009; Seeger et al., 2008）。三种主要构象状态已在不对称晶体结构中识别出来（Murakami et al., 2006; Seeger et al., 2006; Sennhauser et al., 2007; Nakashima et al., 2011; Eicher et al., 2012）。访问（A，也称为松散，L）和结合（B，也称为紧致，T）状态都具有打开的PC1/PC2裂隙和封闭的出口，但两者在结合口袋方面存在差异。DBP在B状态中是完整的，能够容纳底物，而在A

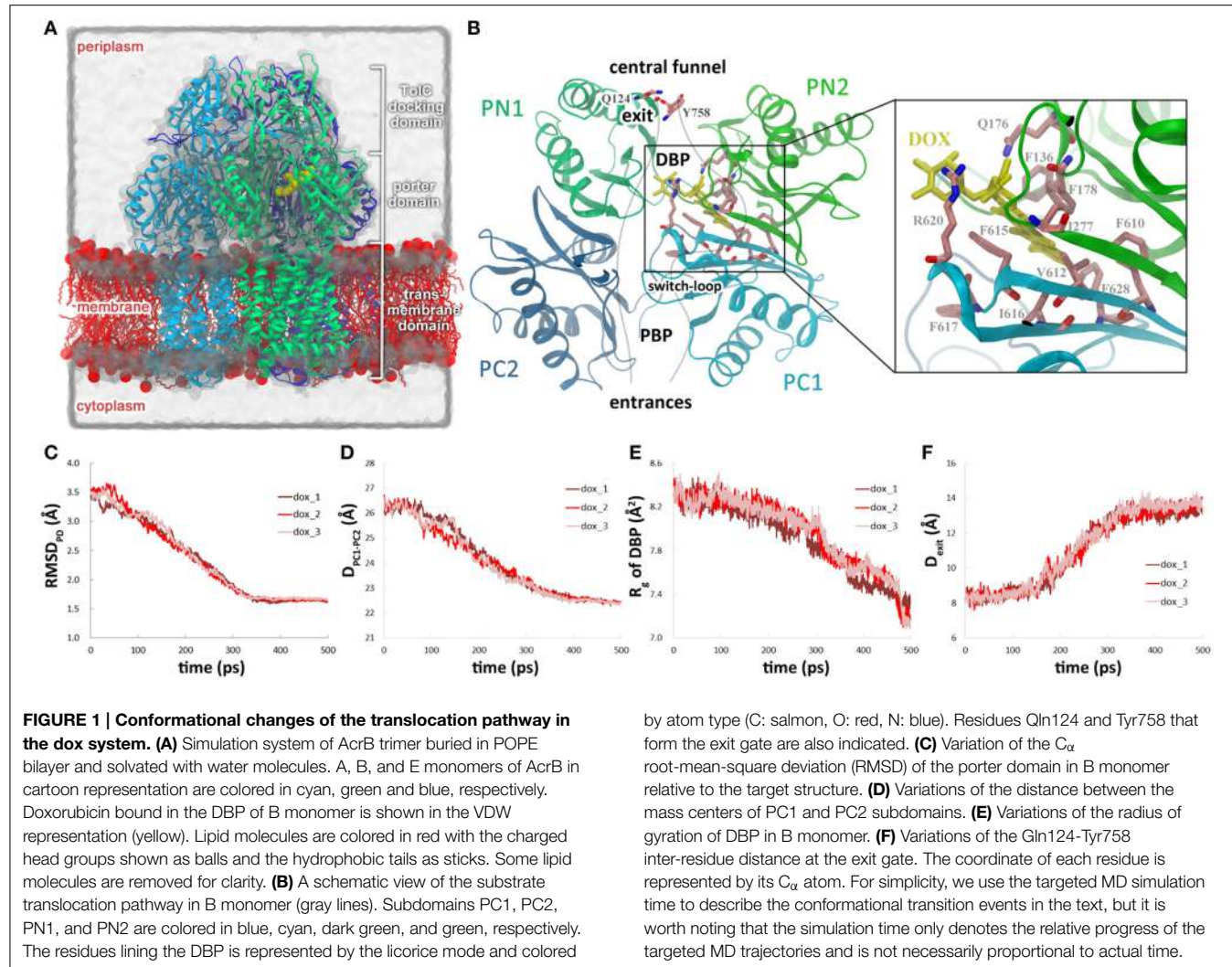
状态，DBP部分塌陷，PBP被发现能够结合底物（Nakashima et al., 2011; Eicher et al., 2012）。挤压（E，也称为开放，O）状态采用一个闭合的PC1/PC2裂隙和一个开放的出口以进行底物挤压。受不对称晶体结构启发，每个亚基被认为在运输期间经历一系列过渡状态，循环从A到B再到E，即功能旋转机制（Murakami et al., 2006; Seeger et al., 2006; Pos, 2009）。该机制还预测每个亚基的过渡状态依赖于其邻居的构象。当A亚基（最初停留在A状态）进化到B状态时，B和E亚基将分别切换到E和A状态，同时完成一个ABE $\rightarrow$ BEA过渡步。

功能旋转机制涉及高度合作的构象变化，其中三个亚基之间存在密切联系。随后的动力学研究确实揭示了底物转运中的正合作性（Nagano and Nikaido, 2009; Lim and Nikaido, 2010）。然而，关于功能旋转和正合作性的详细图景仍然不清楚，特别是AcrB与底物转运动力学之间的关系。分子动力学（MD）模拟是一种强大的工具，可用于提供高时空分辨率的构象变化细节。MD模拟已被用于揭示RND转运蛋白的动力学（Fischer and Kandt, 2013; Yamane et al., 2013），底物运动（Fischer and Kandt, 2011; Feng et al., 2012）以及转运蛋白和底物之间的相互作用网络（Vargiu and Nikaido, 2012; Kinana et al., 2013）。由于常规MD模拟的采样效率问题，一些增强的采样协议，如靶向MD（Ma and Karplus, 1997; Kong et al., 2002; van der Vaart et al., 2004; Compant et al., 2005; Cheng et al., 2006; Weng et al., 2010, 2012），也被实施以提取功能旋转一步中的构象变化细节（Schulz et al., 2010, 2011; Vargiu et al., 2011）。在这项工作中，我们进行了靶向MD模拟来调查构象变化与不同数量的结合底物。结合一或两个分子的多柔比星显示相似的协调构象变化在转运途径中，以及底物从DBP的解离。在两个系统中，Phe628和Tyr327侧链重排与底物解离密切相关。结合第二个底物显然促进了转运途径中的构象变化以及DBP结合底物的解离，解释了正合作性在底物转运中的作用。

## Materials and Methods

### System Setup

晶状学结构（PDBID: 2GIF）被用作所有模拟的起始结构。在晶状学结构中，残基1034–1049在链A和C中缺失，在链B中缺失1046–1049。为了保持蛋白的3-轴对称，我们截断了残基1034–1045在链



B. Since no substrate was cocrystallized in this structure, one doxorubicin was docked into the DBP of B monomer according to the AcrB-doxorubicin complex structure (PDBID: 2DR6). In the simulations with two substrates, the second doxorubicin was docked into the PBP of A monomer by using Autodock (Morris et al., 2009). Default parameters were used for the docking procedure and the center structure of the largest cluster was selected for the simulations.

The AcrB-doxorubicin complex was then buried into a pre-equilibrated palmitoyloleylphosphatidylethanolamine (POPE) bilayer consisting of 512 lipid molecules following the “shrinking” method (Kandt et al., 2007). Additional 10 lipid molecules (5 lipids in the outer leaflet and 5 in the inner leaflet) were manually placed in the central cavity enclosed by the three TM domains. The number of lipids was estimated by the area of the cavity calculated by Hole (Smart et al., 1996) divided by the area per lipid for POPE ( $59 \text{ \AA}^2$ ) (Rappolt et al., 2003). The protein-lipids complex were solvated with a rectangular box of water and neutralized by  $42 \text{ Na}^+$  ions. The box size is  $140 \times 140 \times 160 \text{ \AA}^3$  to keep any atom of protein at least  $10 \text{ \AA}$  away from the edge of

the box. The simulation system contains 320,557 atoms in total (Figure 1A).

## MD Simulations

All simulations were carried out with the parallel MD package NAMD 2.7 (Phillips et al., 2005) with CHARMM27 force field (Feller et al., 1997; MacKerell et al., 1998, 2004). TIP3P model (Jorgensen et al., 1983) was used for water molecules. The CGenFF force field parameters of doxorubicin were derived by using the ParamChem tool (Vanommeslaeghe et al., 2010, 2012; Vanommeslaeghe and MacKerell, 2012). All titratable residues were kept in their default protonation states except Asp407 and Asp408. For these two residues, two different protonation schemes were used. In the first scheme, the protonation states were set according to the asymmetric structure of AcrB (Murakami et al., 2006), i.e., Asp407 and Asp408 were deprotonated in the A and B monomers, and protonated in the E monomer. In the second scheme, Asp407 and Asp408 were protonated in the B monomer and deprotonated in the A and E monomers. The system was maintained at 1.01325 bar by using

the Nosè-Hoover Langevin piston method (Martyna et al., 1994; Feller et al., 1995) and at 300 K by Langevin dynamics with a damping coefficient of 1.0 ps<sup>-1</sup>. Periodic boundary conditions were employed, and the electrostatic interactions were evaluated using the particle-mesh Ewald (PME) method (Darden et al., 1993) with a cutoff of 12 Å and a grid spacing of 1 Å. The van der Waals interactions were switched at 10 Å and truncated at 12 Å. All bonds involving hydrogen atoms were constrained by the SETTLE algorithm (Miyamoto and Kollman, 1992). A time step of 2 fs was used for the conventional MD simulations, and 1 fs was used for the targeted MD simulations.

The whole system was equilibrated for 2 ns with the protein restrained by harmonic forces (the force constant was set to 1000 kcal/mol/Å<sup>2</sup>), followed by a 4 ns run without any restraint. AcrB was stable in the 4 ns NPT run with its C<sub>α</sub> root-mean-square deviation (RMSD) relative to the initial crystal structure fluctuating around 2.2 Å in the last 2 ns. The final structure of the unbiased MD run was used as the initial structure of the targeted MD simulations. The target structure was obtained by setting each monomer to the state of the next functional rotating step, i.e., ABE→BEA.

Targeted MD method propels a known initial structure to a known target structure by using an external potential (Schlitter et al., 1993). The potential decreases the RMSD of the system relative to the target structure toward a preset value at each time step. The potential can be described as:

$$U_{TMD} = \frac{1}{2} \frac{k}{N} [RMSD(t) - RMSD^*(t)]^2$$

where RMSD(t) is the instantaneous best-fit RMSD of the current coordinates to the target coordinates, RMSD\*(t) is the preset RMSD value for the current time step, k is the force constant and N is the number of targeted atoms. The external forces were casted on all heavy atoms of AcrB. A tclForce script was used to perform mass-weighted targeted MD simulations. To assess the influence of parameters on the results, we performed a series of simulations using different force constants ( $k/N = 1, 2$ , and 3 kcal/mol/Å<sup>2</sup>) and different simulation times (500 ps and 1 ns) (Table S1, Supplemental Data).

## Data Analyses

The radius of gyration ( $R_g$ ) of the DBP is defined by all the atoms in the residues 628, 610, 136, 178, 615, 617, 277, 626, 620, 176, and 612 which lies in the vicinity of DBP:

$$R_g = \left( \sum_{i=1}^n \omega(i) (r(i) - r_{mc})^2 \right) / \left( \sum_{i=1}^n \omega(i) \right)$$

where  $r(i)$  is the position of the  $i$ th atom,  $\omega(i)$  is the mass weight and  $r_{mc}$  is the weighted center of the selected atoms. The distance between Gln124 & Tyr758 is defined as the distance between the C<sub>α</sub> atoms of the two residues. All data analysis and molecular structure visualization were conducted by VMD (Humphrey et al., 1996).

## Results

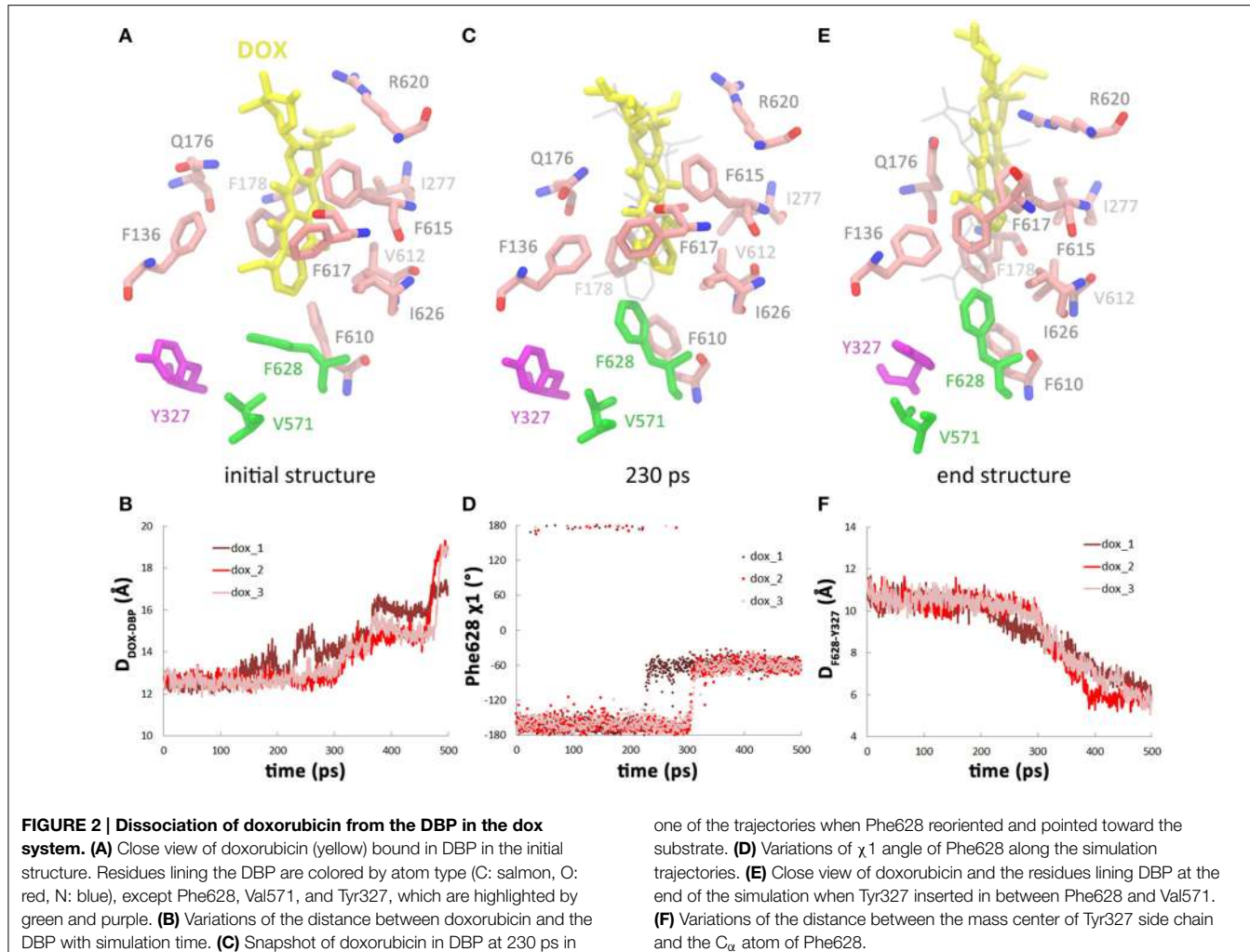
We employed targeted MD simulations to acquire an atomistic view of the conformation changes of AcrB in one functional rotating step. The conformational changes were studied with one doxorubicin bound in the DBP of B monomer (denoted as **dox** hereafter), or with two doxorubicins bound in the DBP of B monomer and in the PBP of A monomer, respectively (denoted as **2dox** hereafter). Three parallel trajectories started with different initial velocities were produced for each system. The results were found to be insensitive to the selection of force constants or time lengths (Table S1, Supplemental Data, see below for details). In the following, we will first introduce the collective and local conformational changes in the translocation pathway and the association of these changes with doxorubicin movement. Then we focus on the effect of the presence of the second doxorubicin by comparing the trajectories of the **dox** and **2dox** systems. For simplicity, we use the targeted MD simulation time to describe the conformational transition events in the text, but it is worth noting that the simulation time only denotes the relative progress of the targeted MD trajectories and is not necessarily proportional to actual time.

### Concerted Conformational Changes in the Translocation Pathway of B Monomer

At the beginning of the simulation, large-scale conformational changes were observed in the porter domain of the B monomer (Figure 1B). In all three trajectories of the **dox** system, the C<sub>α</sub> RMSDs of the porter domain decreased linearly relative to the targeted structure in the first 330 ps, after which the RMSD profiles fluctuated around 1.7 Å till the end of the simulations (Figure 1C). The variations of the porter domain are largely resulted from the relative motions between the subdomains. The motions reduced the distance between the mass centers of PC1 and PC2 subdomains from 26.6 to 22.8 Å in 330 ps (Figure 1D), closing the PC1–PC2 cleft and occluding the translocation pathway toward the entrance (Figure 1B). On the other hand, the DBP shrunk from ~100 ps, with the  $R_g$  decreasing till the end of the simulations (Figure 1E). The decline of  $R_g$  indicates contraction of the middle part of the translocation pathway which would contribute to the dissociation of substrate (see below). During this period, the distance between residues Gln124 and Tyr758, which constrict the exit of drug extrusion (Yao et al., 2013) (Figure 1B) increased from 8.7 to 13.1 Å in about 180 ps (Figure 1F), resulting in the opening of the exit. It is worth noting that the timing of these conformational changes obviously overlap with each other, with the exit gate opening at 155–340 ps (Figure 1F), the PC1/PC2 cleft closing at 50–330 ps (Figure 1D) and the DBP shrinking at 75–500 ps (Figure 1E), indicating concerted conformational motions of the translocation pathway in the first 330 ps of the simulations.

### Dissociation of Doxorubicin from the DBP

As the concerted transmutation of the translocation pathway started in the first 155 ps, the substrate kept stably bound inside the DBP through hydrophobic and π–π interactions with the protein (Figure S1, Supplemental Data). The binding mode in



the simulations is slightly different from the two known binding modes presented in crystal structures (Murakami et al., 2006; Eicher et al., 2012). The position of the amino-sugar moiety was almost invariant, whereas the aglycone moiety showed a new posture by extending directly toward Phe628 rather than pointing toward Phe610 (Eicher et al., 2012) or Phe617 (Murakami et al., 2006) in the crystal structures (Figure S1, Supplemental Data). The diversity of binding mode could be attributed to the differences in the local configuration of the DBP in different crystal structures (see Methods). Similar structural dependence of binding mode was also reported for chloramphenicol in the DBP of AcrB (Vargiu and Nikaido, 2012).

The stable interactions between doxorubicin and DBP were disrupted at 225–300 ps as doxorubicin detached from the binding site. The dissociation of doxorubicin was monitored by the distance between the mass center of doxorubicin and the  $C_\alpha$  atom of Phe628 which lies at the bottom of the DBP (Figure 2A). Two of the trajectories exhibit very similar profiles of substrate motions. The doxorubicin initially stayed in the DBP with the distance fluctuating around 12.5 Å, and detached from the binding site after 300 ps as the distance increased (Table 1, Figure 2B).

pink and red lines). In another trajectory, more evident fluctuations were observed before dissociation, such as the peak at 225 ps on the profile (Figure 2B, brown line). After 275 ps, doxorubicin became fully dissociated from the DBP. At the end of the simulations, a displacement of 5–7 Å toward the exit could be observed and the dissociation is irreversible, as verified by the extended 2-ns simulations with all restraining forces removed (Figure S2, Supplemental Data). Similar extrusion process was also observed by Vargiu et al. using targeted MD simulations (Vargiu et al., 2011).

### Correlation between the Conformational Changes in the DBP and Doxorubicin Dissociation

Further inspection of the trajectories show that the dissociation process of doxorubicin is closely related to the conformational changes of the DBP, especially the side chain orientation of Phe628. The benzyl group of Phe628 originally pointed toward the TM domain at the beginning of the simulations, characterized by the  $\chi_1$  angle of about  $-160^\circ$  (Figure 2A), and then it switched to a new orientation with the  $\chi_1$  angle at

**TABLE 1 | Conformational changes associated with the dissociation of doxorubicin.**

| System <sup>a</sup> | Trajectory | Time of doxorubicin dissociation (ps) <sup>b</sup> | Time of Phe628 side chain reorientation (ps) <sup>c</sup> | Time of Tyr327 side chain insertion (ps) <sup>d</sup> |
|---------------------|------------|--|---|---|
| <b>dox</b>          | 1          | 225, 275   | 225   | 235–500   |
|                     | 2          | 300  | 300   | 300–395   |
|                     | 3          | 300  | 300   | 300–470   |
| <b>2dox</b>         | 1          | 200  | 200   | 200–400   |
|                     | 2          | 225  | 225   | 225–370   |
|                     | 3          | 190  | 190   | 190–420   |

<sup>a</sup>**dox** denotes the simulation system with only one doxorubicin bound in DBP of B monomer, **2dox** denotes the simulation system with a second doxorubicin bound in PBP of A monomer.

<sup>b</sup>Time when doxorubicin detached from the binding pocket. Temporary dissociation leads to more than one dissociation time.

<sup>c</sup>Time when Phe628 reoriented its side chain and pointed toward the substrate.

<sup>d</sup>Time period of the decreasing of the distance between Tyr327 side chain and Phe628 C<sub>α</sub>.

about  $-60^\circ$  (**Figures 2A,C,D**). The reorientation of Phe628 side chain occurred at 300 ps in two of the trajectories (**Figure 2D**, pink and red lines) and at 225 ps in the other (**Figure 2D**, brown line), well consistent with the departure time of doxorubicin (**Table 1**). The close correlation between the two events can be rationalized by the steric hindrance between the bulky side chain of Phe628 and the doxorubicin at binding site (**Figure 2C**), which pushes the substrate from the binding pocket. The importance of Phe628 for substrate dissociation was previously reported by biochemical studies, in which substitution of the bulky side chain reduced the resistance to doxorubicin and other substrates (Husain and Nikaido, 2010; Nakashima et al., 2011).

After the reorientation of Phe628, local conformational rearrangement was observed. The space originally occupied by the benzyl group of Phe628 and the isopropyl group of Val571 (**Figures 2A,C**) was subsequently filled by the phenol group of Tyr327, which is several residues preceding TM2 helix of the TM domain (**Figure 2E**). Interestingly, the rearrangement started almost simultaneously with the reorientation of the Phe628 side chain (**Figure 2F, Table 1**). This implies a functional role of Tyr327 in stabilizing the reorientated conformation of Phe628.

To examine possible influence of TM domain protonation state on substrate dissociation, we produced targeted MD trajectories for AcrB with different protonation state (Table S1, Supplemental Data). It turns out that these trajectories demonstrated very similar features such as substrate dissociation, side chain reorientation of Phe628 and Tyr327 (**Figure S3, Table S1, Supplemental Data**), indicating that the current simulation protocol is insensitive to the changes in protonation state. Different simulation time range (500 ps or 1 ns) and different force constant ( $k/N = 1, 2, \text{ or } 3 \text{ kcal/mol}/\text{\AA}^2$ ) were also tested. These factors do not disturb the correlation between conformational changes in the DBP and substrate dissociation, either (Table S1, Supplemental Data).

## Binding of the Second Doxorubicin Accelerates the Conformational Changes in the Translocation Pathway

To study the effect of multi-substrate binding on the conformational transition, a second doxorubicin was docked into the PBP of A monomer (see Methods) to build the **2dox** system (**Figure 3A**). The position of the docked substrate closely resembles the binding mode of PC1-proximal doxorubicin (**Figure S4, Supplemental Data**) observed in the AcrB-doxorubicin complex structure (Eicher et al., 2012). The presence of the second doxorubicin affects the conformational changes in the translocation pathway in several aspects. First, the closing motion of the PC1/PC2 cleft was antedated, illustrated by the  $\sim 70$  ps earlier decreasing period of the inter-domain distance in the **2dox** system than that in the **dox** system (**Figure 3B**). Secondly, the conformational changes in the DBP were moved ahead as the  $R_g$  decreased to  $7.8 \text{ \AA}$  at about 200 ps in the **2dox** system, instead of at 300 ps in the **dox** system (**Figure 3C**). Finally, the opening motion of the exit was accelerated as the distance between Gln124 and Tyr758 exceeded  $13 \text{ \AA}$  at 220 ps, rather than at 300 ps in the **dox** system (**Figure 3D**). It is worth noting that the **dox** and **2dox** systems share very similar initial and final structures at the PC1/PC2 cleft, the DBP and the exit gate (**Figures 3B–D**), so that the external forces casted on these regions are generally equivalent in both systems (see Methods). The systematic antedate of these events indicates that the conformational changes in the translocation pathway are evidently accelerated by the binding of the second doxorubicin at A monomer.

## Binding of the Second Doxorubicin Facilitates the Dissociation of Doxorubicin

Along with the antedated conformational changes in the translocation pathway, substrate dissociation in the **2dox** system was also earlier than that in the **dox** system. In the three trajectories, irreversible dissociation occurred at 200, 230, and 190 ps, respectively (**Figure 4A**, **Figure S5, Supplemental Data**), about 70 ps earlier than that of the **dox** system on average. Along with substrate dissociation, the change of Phe628  $\chi_1$  angle from  $-160$  to  $-60^\circ$  and the insertion of Tyr327 in between Phe628 and Val571 were also moved ahead to about 200 ps (**Figures 4B,C**). Similar with the **dox** system, there is also a close correlation between substrate dissociation and side chain reorientation of Phe628 and Tyr327 (**Table 1**) and the trend is kept with varied simulation time range or force constant (Table S1, Supplemental Data), indicating that the **2dox** system shares the same mechanism of doxorubicin dissociation in B monomer with the **dox** system.

## Conformational Changes in AcrB Does Not Promote the Transportation of the Second Doxorubicin

The movement of doxorubicin in the PBP of A monomer during the functional rotation was also examined (**Figure 3A**). In contrast to the displacement toward the exit observed for the DBP-bound doxorubicin in B monomer, the PBP-bound doxorubicin in A monomer moved in an opposite direction, further away from the DBP by about  $2 \text{ \AA}$  at the end of the simulations (**Figure 5A**). The slight retrogression of the substrate could be

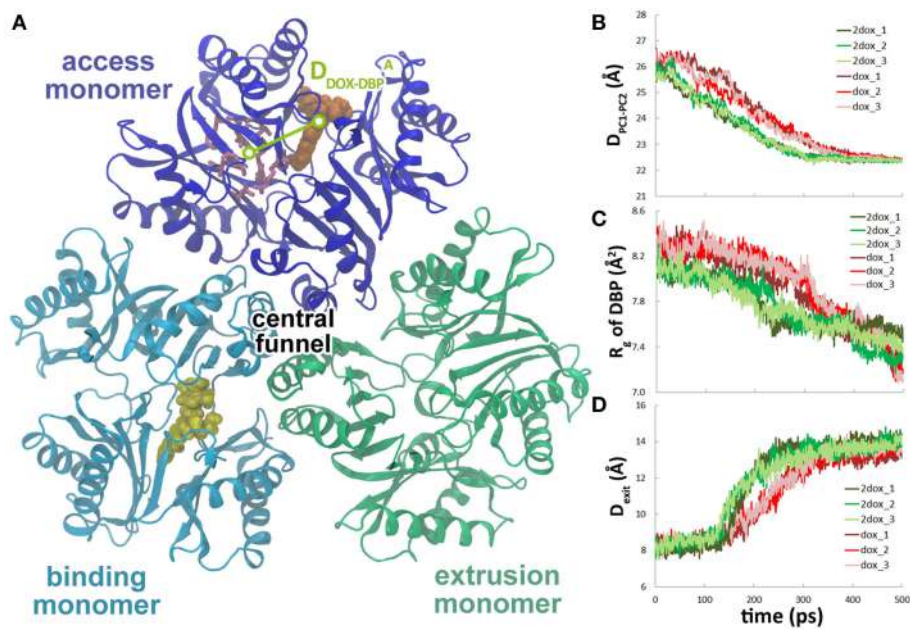


**FIGURE 3 | The second substrate binding at A monomer accelerates the conformational changes of B monomer.** **(A)** Top view of the porter domains with two doxorubicins (yellow and orange) bound in the initial structure of the **2dox** system. The distance between doxorubicin and DBP in A monomer is indicated as  $D_{\text{DOX-DBP}}^{\text{A}}$ . **(B)** Comparison of the variations of  $D_{\text{DOX-DBP}}^{\text{A}} (\text{\AA})$  versus time (ps) for **2dox** and **dox** systems.

the distance between the mass centers of PC1 and PC2 subdomains of B monomer in **dox** and **2dox** systems. **(C)** Comparison of the variations of  $R_g$  of the DBP of B monomer in **dox** and **2dox** systems. **(D)** Comparison of the variations of the Gln124-Tyr758 inter-residue distance at the exit region of B monomer in **dox** and **2dox** systems.

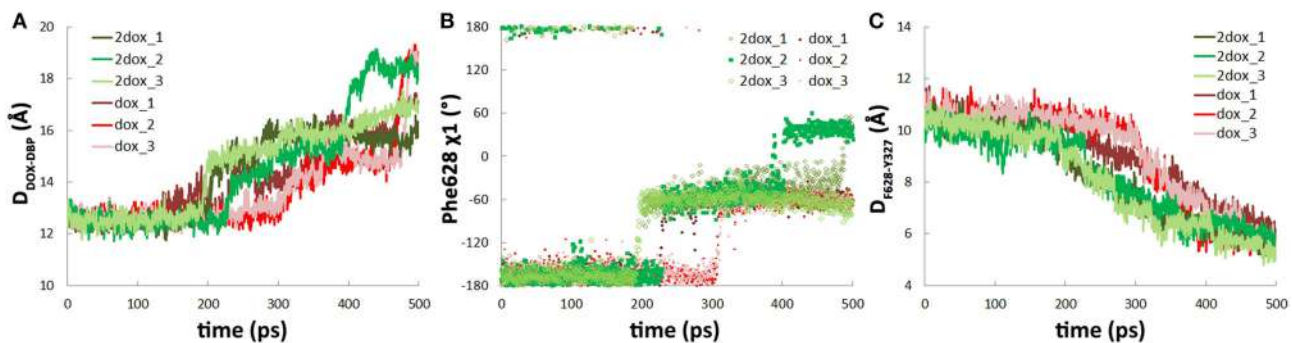


**FIGURE 4 | The second substrate binding at monomer A accelerates the dissociation of doxorubicin from the DBP in monomer B.** **(A)** Comparison of the variations of the distance between doxorubicin and the DBP of monomer B in **dox** and **2dox** systems. **(B)** Comparison of the variations of  $\chi_1$  angle of Phe628 in **dox** and **2dox** systems.

Comparison of the variations of  $\chi_1$  angle of Phe628 in **dox** and **2dox** systems. **(C)** Comparison of the variations of the distance between the mass center of Tyr327 side chain and the  $C_{\alpha}$  atom of Phe628 in **dox** and **2dox** systems.

attributed to the inter-domain motion between PC1 and PC2 subdomains. The PC1/PC2 cleft opened by about 1.5 Å when A monomer evolved toward the B state following the functional rotating mechanism (Figure 5B). The opening motion may weaken the interactions between AcrB and doxorubicin, and leads to the movement of substrate toward the entrance.

## Discussion

The functional rotating mechanism based on the asymmetric structure of AcrB assumes that each monomer cycles among the

three conformational states (A, B, and E) concertedly, facilitating the unidirectional translocation of the substrate toward the outer membrane protein TolC. In this work, we simulated one functional rotating step of AcrB (ABE → BEA) in the context of one or two bound substrates using targeted MD simulations, and provided an atomic spatiotemporal view of the conformational changes and substrate movement.

The targeted MD trajectories demonstrated that the simulation started with conformational changes in the translocation pathway, involving a set of concerted motions such as the closing of the PC1/PC2 cleft (Figure 1D), the shrinking of the DBP

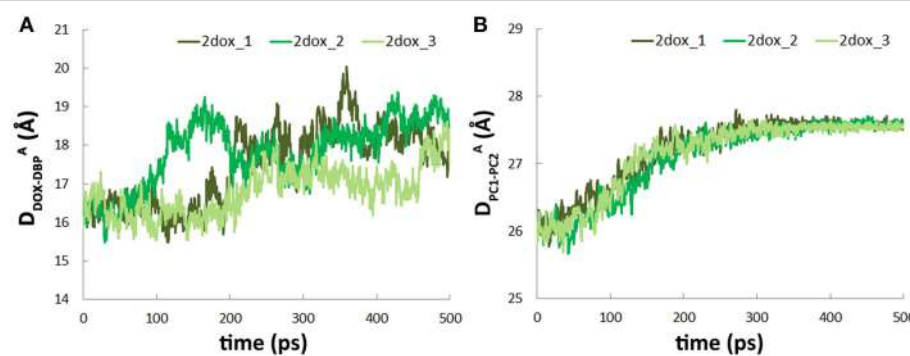


**FIGURE 5 |** Conformational transition of A→B does not facilitate substrate translocation from PBP to DBP. **(A)** Variations of  $D_{DOX-DBP}^A$  along the simulation trajectories. **(B)** Variations of the distance between the mass centers of PC1 and PC2 subdomains in A monomer.

(Figure 1E), and the opening of the exit gate (Figure 1F). In the following 200 ps, however, doxorubicin in DBP did not show evident motions until the dissociation from DBP occurred at 225–300 ps. Therefore, the conformational changes in the translocation pathway are the prerequisite and the driving force for substrate dissociation. Specifically, it has been identified that the side chain reorientation of Phe628 is mainly responsible for substrate dissociation (Figure 2). The importance of Phe628 for substrate transportation is supported by previous biochemical experiments, in which removal of the bulky side chain of Phe628 evidently reduced the resistance to doxorubicin and other substrates of AcrB (Husain and Nikaido, 2010; Nakashima et al., 2011). Similar protein-driven substrate movement was also observed by A. Vargiu et al. using the same method (Schulz et al., 2010; Vargiu et al., 2011) though the atomistic details of protein-substrate interaction are slightly different. Due to the limited simulation time in this work, we did not observe the entire extrusion process of the substrate. Hundreds of nanoseconds or more may be needed for the substrate to overcome the barriers on its way to the central funnel (Ruggerone et al., 2013; Yao et al., 2013).

The functional rotating mechanism of AcrB assumes that the conformational transitions of the three monomers occur in a concerted way, implicating cooperativity in substrate translocation. Kinetic studies of substrate transport of AcrB in intact cells identified positive cooperativities in the efflux of various cephalosporins (Nagano and Nikaido, 2009) and penicillins (Lim and Nikaido, 2010). Efflux could also be stimulated by different kinds of substrates, including solvents (Kinana et al., 2013). The positive cooperativity in substrate efflux could be explained by the simultaneous binding of substrates to PBPs in the B or A monomers. Crystal structures of the AcrB-substrate complex revealed simultaneous substrate binding at DBP of B monomer and at PBP of A monomer (Nakashima et al., 2011; Eicher et al., 2012), implying that the substrate in PBP of A monomer more likely plays a role in stimulating the efflux. Simulations in this study provide the direct evidences that substrate binding at PBP of A monomer indeed stimulates substrate dissociation in B monomer through accelerating the conformational transitions according to the functional rotating mechanism. We noticed that the conformational changes were overall accelerated

by the substrate in A monomer, not just the local changes in DBP (Figure 3). This is in line with the observation that the substrate would not dissociate from the DBP until most of the conformational changes completed during the functional rotation. Therefore, the substrate dissociation is allosterically regulated by the substrate binding in the neighboring monomer. Another possibility we could not rule out, however, is that ligand binding at PBP of the same monomer, i.e., in the B monomer, may also stimulate the substrate extrusion, although the corresponding intermediate state has not been detected in crystallography studies. Yet another mechanism of the positive cooperativity in substrate extrusion proposed by A. Kinana et al. is the direct interference of the stimulator with the substrate through competitive binding at the same DBP of B monomer (Kinana et al., 2013). It is worth noting that in the same study, decreases of Hill coefficients were observed in the presence of the stimulators (Kinana et al., 2013), which supports the allosteric mechanism with stimulators bound at different sites.

Another implication for the observation that substrate binding at A monomer promotes the protein conformational changes is that the functional rotation of AcrB trimer is partly energized by ligand binding in addition to the proton motive force. The accelerated conformational transition indicates that the free energy barrier of this process is lowered upon ligand binding. In other words, substrates are not only passively pumped by the molecular machine of AcrB, but also actively regulate the functional rotation of AcrB trimer. Recent combined crystallography and MD simulation study also suggested that drug binding is the driving force in the A to B (or L to T) transition (Mishra et al., 2014).

An unexpected observation in this work is that the functional rotation did not squeeze the PBP-bound substrate toward DBP during the A-B transition, rather it moved away toward the entrance. This might be attributed to the slight opening of the PC1-PC2 cleft upon A-B transition (Figure 5), suggesting that substrate translocation from PBP to DBP may require temporary closure of the cleft. In line with this, partially closed conformations of the cleft have been observed in monomer A by unbiased substrate-free MD simulations (Fischer and Kandt, 2013). An intermediate state with PC1-PC2

cleft closed was also identified in another RND transporter ZneA (Pak et al., 2013). It is most likely that during the functional rotation, a similar intermediate state between A and B yet identified also exists in AcrB to prevent the back diffusion of the substrate.

Although our simulation was conducted on isolated AcrB, the RND transporter functions together with the periplasmic adaptor protein AcrA and outer membrane protein TolC as a tripartite assembly, and AcrA-Mg<sup>2+</sup> has been reported to strongly accelerate the extrusion of substrate (Zgurskaya and Nikaido, 1999b). These findings raise an issue of whether the acceleration effect of multi-substrate binding observed in our simulation would still work after the association of AcrA-Mg<sup>2+</sup>. The crystal structure of heavy-metal efflux complex CusBA (Su et al., 2011), a homology of AcrAB, and the recently reported pseudo-atomic structure of AcrAB-TolC complex (Du et al., 2014) provide a valuable insight into the acceleration effect of AcrA-Mg<sup>2+</sup>. The structures show that the adaptor protein (CusB or AcrA) forms interactions with the TolC-docking domain and the subdomains PN2, PC1, and PC2 of the RND transporter. A noteworthy feature of the interactions between adaptor protein and RND transporter is that the subdomain PC2 forms much weaker contacts with the adaptor protein than PN2 and PC1 do. Only two residues on PC2 (Arg705 and Leu714) are located within 4 Å of the adaptor protein and they form weak van der Waals interactions. The binding of adaptor protein may restrain the motions in PN2 and PC1, but is less likely to disturb the motions of PC2 and the relative motions

between PC1 and PC2. Since the second substrate in monomer A binds between the PC1 and PC2 subdomains, the adaptor protein may have little influence on the behavior of the second substrate and the accelerated conformational changes brought by its binding. The acceleration effects of AcrA-Mg<sup>2+</sup> and multi-substrate binding may operate simultaneously when AcrB functions. It is worth noting, however, that the above notions are largely derived based on the static structures of CusBA and AcrAB-TolC complexes. Further studies, especially those concerning dynamic properties, are still required to provide a fuller understanding on the molecular mechanism of the acceleration effects.

## Acknowledgments

This work was supported by National Major Basic Research Program of China (2011CB808505, 2014CB910201), National Science Foundation of China (21473034, 21403036), Specialized Research Fund for the Doctoral Program of Higher Education (20130071140004), Science & Technology Commission of Shanghai Municipality (08DZ2270500). We thank the super computer center of Fudan University for their allocation of computer time.

## Supplementary Material

The Supplementary Material for this article can be found online at: <http://www.frontiersin.org/journal/10.3389/fmicb.2015.00302/abstract>

## References

- Cheng, X., Wang, H., Grant, B., Sine, S. M., and McCammon, J. A. (2006). Targeted molecular dynamics study of c-loop closure and channel gating in nicotinic receptors. *PLoS Comput. Biol.* 2:e134. doi: 10.1371/journal.pcbi.0020134
- Collu, F., Vargiu, A. V., Dreier, J., Casella, M., and Ruggerone, P. (2012). Recognition of imipenem and meropenem by the rnd-transporter mexB studied by computer simulations. *J. Am. Chem. Soc.* 134, 19146–19158. doi: 10.1021/ja307803m
- Compoint, M., Picaud, F., Ramseyer, C., and Girardet, C. (2005). Targeted molecular dynamics of an open-state kcsA channel. *J. Chem. Phys.* 122, 134707. doi: 10.1063/1.1869413
- Darden, T., York, D., and Pedersen, L. (1993). Particle mesh ewald - an n.log(n) method for ewald sums in large systems. *J. Chem. Phys.* 98, 10089–10092. doi: 10.1063/1.464397
- Du, D., Wang, Z., James, N. R., Voss, J. E., Klimont, E., Ohene-Agyei, T., et al. (2014). Structure of the acrB-tolC multidrug efflux pump. *Nature* 509, 512–515. doi: 10.1038/nature13205
- Eicher, T., Cha, H. J., Seeger, M. A., Brandstatter, L., El-Delik, J., Bohnert, J. A., et al. (2012). Transport of drugs by the multidrug transporter acrB involves an access and a deep binding pocket that are separated by a switch-loop. *Proc. Natl. Acad. Sci. U.S.A.* 109, 5687–5692. doi: 10.1073/pnas.1114944109
- Elkins, C. A., and Nikaido, H. (2002). Substrate specificity of the rnd-type multidrug efflux pumps acrB and acrD of *Escherichia coli* is determined predominantly by two large periplasmic loops. *J. Bacteriol.* 184, 6490–6498. doi: 10.1128/JB.184.23.6490-6499.2002
- Feller, S. E., Zhang, Y. H., Pastor, R. W., and Brooks, B. R. (1995). Constant-pressure molecular-dynamics simulation - the langevin piston method. *J. Chem. Phys.* 103, 4613–4621. doi: 10.1063/1.470648
- Feller, S. E., Yin, D. X., Pastor, R. W., and MacKerell, A. D. (1997). Molecular dynamics simulation of unsaturated lipid bilayers at low hydration: parameterization and comparison with diffraction studies. *Biophys. J.* 73, 2269–2279. doi: 10.1016/S0006-3495(97)78259-6
- Feng, Z., Hou, T., and Li, Y. (2012). Unidirectional peristaltic movement in multisite drug binding pockets of acrB from molecular dynamics simulations. *Mol. Biosyst.* 8, 2699–2709. doi: 10.1039/c2mb25184a
- Fischer, N., and Kandt, C. (2011). Three ways in, one way out: Water dynamics in the trans-membrane domains of the inner membrane translocase acrB. *Proteins* 79, 2871–2885. doi: 10.1002/prot.23122
- Fischer, N., and Kandt, C. (2013). Porter domain opening and closing motions in the multi-drug efflux transporter acrB. *Biochim. Biophys. Acta* 1828, 632–641. doi: 10.1016/j.bbamem.2012.10.016
- Higgins, C. F. (2007). Multiple molecular mechanisms for multidrug resistance transporters. *Nature* 446, 749–757. doi: 10.1038/nature05630
- Humphrey, W., Dalke, A., and Schulten, K. (1996). Vmd: visual molecular dynamics. *J. Mol. Graph.* 14, 33–38. doi: 10.1016/0263-7855(96)00018-5
- Husain, F., and Nikaido, H. (2010). Substrate path in the acrB multidrug efflux pump of *Escherichia coli*. *Mol. Microbiol.* 78, 320–330. doi: 10.1111/j.1365-2958.2010.07330.x
- Jorgensen, W. L., Chandrasekhar, J., Madura, J. D., Impey, R. W., and Klein, M. L. (1983). Comparison of simple potential functions for simulating liquid water. *J. Chem. Phys.* 79, 926–935. doi: 10.1063/1.445869
- Kandt, C., Ash, W. L., and Tielemans, D. P. (2007). Setting up and running molecular dynamics simulations of membrane proteins. *Methods* 41, 475–488. doi: 10.1016/j.ymeth.2006.08.006
- Kinana, A. D., Vargiu, A. V., and Nikaido, H. (2013). Some ligands enhance the efflux of other ligands by the *Escherichia coli* multidrug pump acrB. *Biochemistry* 52, 8342–8351. doi: 10.1021/bi401303v
- Kong, Y., Shen, Y., Warth, T. E., and Ma, J. (2002). Conformational pathways in the gating of *Escherichia coli* mechanosensitive channel. *Proc. Natl. Acad. Sci. U.S.A.* 99, 5999–6004. doi: 10.1073/pnas.092051099

- Koronakis, V., Sharff, A., Koronakis, E., Luisi, B., and Hughes, C. (2000). Crystal structure of the bacterial membrane protein tolC central to multidrug efflux and protein export. *Nature* 405, 914–919. doi: 10.1038/35016007
- Lim, S. P., and Nikaido, H. (2010). Kinetic parameters of efflux of penicillins by the multidrug efflux transporter acrb-tolc of *Escherichia coli*. *Antimicrob. Agents Chemother.* 54, 1800–1806. doi: 10.1128/AAC.01714-09
- Ma, J., and Karplus, M. (1997). Molecular switch in signal transduction: reaction paths of the conformational changes in ras p21. *Proc. Natl. Acad. Sci. U.S.A.* 94, 11905–11910. doi: 10.1073/pnas.94.22.11905
- MacKerell, A. D., Bashford, D., Bellott, M., Dunbrack, R. L., Evanseck, J. D., Field, M. J., et al. (1998). All-atom empirical potential for molecular modeling and dynamics studies of proteins. *J. Phys. Chem. B* 102, 3586–3616. doi: 10.1021/jp973084f
- MacKerell, A. D., Feig, M., and Brooks, C. L. (2004). Extending the treatment of backbone energetics in protein force fields: limitations of gas-phase quantum mechanics in reproducing protein conformational distributions in molecular dynamics simulations. *J. Comput. Chem.* 25, 1400–1415. doi: 10.1002/jcc.20065
- Martyna, G. J., Tobias, D. J., and Klein, M. L. (1994). Constant-pressure molecular-dynamics algorithms. *J. Chem. Phys.* 101, 4177–4189. doi: 10.1063/1.467468
- Mikolosko, J., Bobyk, K., Zgurskaya, H. I., and Ghosh, P. (2006). Conformational flexibility in the multidrug efflux system protein acra. *Structure* 14, 577–587. doi: 10.1016/j.str.2005.11.015
- Mishra, S., Verhalen, B., Stein, R. A., Wen, P. C., Tajkhorshid, E., and McHaourab, H. S. (2014). Conformational dynamics of the nucleotide binding domains and the power stroke of a heterodimeric abc transporter. *Elife* 3:e02740. doi: 10.7554/elife.02740
- Miyamoto, S., and Kollman, P. A. (1992). Settle – an analytical version of the shake and rattle algorithm for rigid water models. *J. Comput. Chem.* 13, 952–962. doi: 10.1002/jcc.540130805
- Morris, G. M., Huey, R., Lindstrom, W., Sanner, M. F., Belew, R. K., Goodsell, D. S., et al. (2009). Autodock4 and autodocktools4: automated docking with selective receptor flexibility. *J. Comput. Chem.* 30, 2785–2791. doi: 10.1002/jcc.21256
- Murakami, S., Nakashima, R., Yamashita, E., and Yamaguchi, A. (2002). Crystal structure of bacterial multidrug efflux transporter acrb. *Nature* 419, 587–593. doi: 10.1038/nature01050
- Murakami, S., Nakashima, R., Yamashita, E., Matsumoto, T., and Yamaguchi, A. (2006). Crystal structures of a multidrug transporter reveal a functionally rotating mechanism. *Nature* 443, 173–179. doi: 10.1038/nature05076
- Nagano, K., and Nikaido, H. (2009). Kinetic behavior of the major multidrug efflux pump acrb of *Escherichia coli*. *Proc. Natl. Acad. Sci. U.S.A.* 106, 5854–5858. doi: 10.1073/pnas.0901695106
- Nakashima, R., Sakurai, K., Yamasaki, S., Nishino, K., and Yamaguchi, A. (2011). Structures of the multidrug exporter acrb reveal a proximal multisite drug-binding pocket. *Nature* 480, 565–569. doi: 10.1038/nature10641
- Nikaido, H. (1996). Multidrug efflux pumps of gram-negative bacteria. *J. Bacteriol.* 178, 5853–5859.
- Pak, J. E., Ekende, E. N., Kifle, E. G., O'Connell, J. D. 3rd, De Angelis, F., Tessema, M. B., et al. (2013). Structures of intermediate transport states of zne, a zn(ii)/proton antiporter. *Proc. Natl. Acad. Sci. U.S.A.* 110, 18484–18489. doi: 10.1073/pnas.1318705110
- Phillips, J. C., Braun, R., Wang, W., Gumbart, J., Tajkhorshid, E., Villa, E., et al. (2005). Scalable molecular dynamics with namd. *J. Comput. Chem.* 26, 1781–1802. doi: 10.1002/jcc.20289
- Pos, K. M. (2009). Drug transport mechanism of the acrb efflux pump. *Biochim. Biophys. Acta* 1794, 782–793. doi: 10.1016/j.bbapap.2008.12.015
- Rappolt, M., Hickel, A., Bringezu, F., and Lohner, K. (2003). Mechanism of the lamellar/inverse hexagonal phase transition examined by high resolution x-ray diffraction. *Biophys. J.* 84, 3111–3122. doi: 10.1016/S0006-3495(03)70036-8
- Ruggerone, P., Vargiu, A. V., Collu, F., Fischer, N., and Kandt, C. (2013). Molecular dynamics computer simulations of multidrug rnd efflux pumps. *Comput. Struct. Biotechnol. J.* 5:e201302008. doi: 10.5936/csbj.201302008
- Schlitter, J., Engels, M., Kruger, P., Jacoby, E., and Wollmer, A. (1993). Targeted molecular-dynamics simulation of conformational change - application to the t – r transition in insulin. *Mol. Simulat.* 10, 291. doi: 10.1080/08927029308022170
- Schulz, R., Vargiu, A. V., Collu, F., Kleinekathofer, U., and Ruggerone, P. (2010). Functional rotation of the transporter acrb: insights into drug extrusion from simulations. *PLoS Comput. Biol.* 6:e1000806. doi: 10.1371/journal.pcbi.1000806
- Schulz, R., Vargiu, A. V., Ruggerone, P., and Kleinekathofer, U. (2011). Role of water during the extrusion of substrates by the efflux transporter acrb. *J. Phys. Chem. B* 115, 8278–8287. doi: 10.1021/jp200996x
- Seeger, M. A., Schieffner, A., Eicher, T., Verrey, F., Diederichs, K., and Pos, K. M. (2006). Structural asymmetry of acrb trimer suggests a peristaltic pump mechanism. *Science* 313, 1295–1298. doi: 10.1126/science.1131542
- Seeger, M. A., von Ballmoos, C., Eicher, T., Brandstatter, L., Verrey, F., Diederichs, K., et al. (2008). Engineered disulfide bonds support the functional rotation mechanism of multidrug efflux pump acrb. *Nat. Struct Mol. Biol.* 15, 199–205. doi: 10.1038/nsmb.1379
- Seeger, M. A., von Ballmoos, C., Verrey, F., and Pos, K. M. (2009). Crucial role of asp408 in the proton translocation pathway of multidrug transporter acrb: evidence from site-directed mutagenesis and carbodiimide labeling. *Biochemistry* 48, 5801–5812. doi: 10.1021/bi900446j
- Sennhauser, G., Amstutz, P., Briand, C., Storchenegger, O., and Grutter, M. G. (2007). Drug export pathway of multidrug exporter acrb revealed by darpin inhibitors. *PLoS Biol.* 5:e7. doi: 10.1371/journal.pbio.0050007
- Smart, O. S., Neduvilil, J. G., Wang, X., Wallace, B. A., and Sansom, M. S. (1996). Hole: a program for the analysis of the pore dimensions of ion channel structural models. *J. Mol. Graph.* 14, 354–360. doi: 10.1016/S0263-7855(97)00009-X
- Su, C. C., Li, M., Gu, R., Takatsuka, Y., McDermott, G., Nikaido, H., et al. (2006). Conformation of the acrb multidrug efflux pump in mutants of the putative proton relay pathway. *J. Bacteriol.* 188, 7290–7296. doi: 10.1128/JB.00684-06
- Su, C. C., Long, F., Zimmermann, M. T., Rajashankar, K. R., Jernigan, R. L., and Yu, E. W. (2011). Crystal structure of the cuba heavy-metal efflux complex of *Escherichia coli*. *Nature* 470, 558–562. doi: 10.1038/nature09743
- Takatsuka, Y., and Nikaido, H. (2006). Threonine-978 in the transmembrane segment of the multidrug efflux pump acrb of *Escherichia coli* is crucial for drug transport as a probable component of the proton relay network. *J. Bacteriol.* 188, 7284–7289. doi: 10.1128/JB.00683-06
- Takatsuka, Y., and Nikaido, H. (2007). Site-directed disulfide cross-linking shows that cleft flexibility in the periplasmic domain is needed for the multidrug efflux pump acrb of *Escherichia coli*. *J. Bacteriol.* 189, 8677–8684. doi: 10.1128/JB.01127-07
- Takatsuka, Y., and Nikaido, H. (2009). Covalently linked trimer of the acrb multidrug efflux pump provides support for the functional rotating mechanism. *J. Bacteriol.* 191, 1729–1737. doi: 10.1128/JB.01441-08
- Tikhonova, E. B., and Zgurskaya, H. I. (2004). Acra, acrb, and tolC of *Escherichia coli* form a stable intermembrane multidrug efflux complex. *J. Biol. Chem.* 279, 32116–32124. doi: 10.1074/jbc.M402230200
- van der Vaart, A., Ma, J., and Karplus, M. (2004). The unfolding action of groEL on a protein substrate. *Biophys. J.* 87, 562–573. doi: 10.1529.biophysj.103.037333
- Vanommeslaeghe, K., Hatcher, E., Acharya, C., Kundu, S., Zhong, S., Shim, J., et al. (2010). Charmm general force field: a force field for drug-like molecules compatible with the charmm all-atom additive biological force fields. *J. Comput. Chem.* 31, 671–690. doi: 10.1002/jcc.21367
- Vanommeslaeghe, K., and MacKerell, A. D. Jr. (2012). Automation of the charmm general force field (cgenff) i: Bond perception and atom typing. *J. Chem. Inf. Model.* 52, 3144–3154. doi: 10.1021/ci300363c
- Vanommeslaeghe, K., Raman, E. P., and MacKerell, A. D. Jr. (2012). Automation of the charmm general force field (cgenff) ii: Assignment of bonded parameters and partial atomic charges. *J. Chem. Inf. Model.* 52, 3155–3168. doi: 10.1021/ci3003649
- Vargiu, A. V., Collu, F., Schulz, R., Pos, K. M., Zacharias, M., Kleinekathofer, U., et al. (2011). Effect of the f610a mutation on substrate extrusion in the acrb transporter: explanation and rationale by molecular dynamics simulations. *J. Am. Chem. Soc.* 133, 10704–10707. doi: 10.1021/ja202666x
- Vargiu, A. V., and Nikaido, H. (2012). Multidrug binding properties of the acrb efflux pump characterized by molecular dynamics simulations. *Proc. Natl. Acad. Sci. U.S.A.* 109, 20637–20642. doi: 10.1073/pnas.1218348109
- Weng, J., Fan, K., and Wang, W. (2012). The conformational transition pathways of atp-binding cassette transporter btucd revealed by targeted molecular dynamics simulation. *PLoS ONE* 7:e30465. doi: 10.1371/journal.pone.0030465
- Weng, J. W., Fan, K. N., and Wang, W. N. (2010). The conformational transition pathway of atp binding cassette transporter msba revealed by atomistic simulations. *J. Biol. Chem.* 285, 3053–3063. doi: 10.1074/jbc.M109.056432

- Yamane, T., Murakami, S., and Ikeguchi, M. (2013). Functional rotation induced by alternating protonation states in the multidrug transporter acrb: all-atom molecular dynamics simulations. *Biochemistry* 52, 7648–7658. doi: 10.1021/bi400119v
- Yao, X. Q., Kimura, N., Murakami, S., and Takada, S. (2013). Drug uptake pathways of multidrug transporter acrb studied by molecular simulations and site-directed mutagenesis experiments. *J. Am. Chem. Soc.* 135, 7474–7485. doi: 10.1021/ja310548h
- Zgurskaya, H. I., and Nikaido, H. (1999a). Acra is a highly asymmetric protein capable of spanning the periplasm. *J. Mol. Biol.* 285, 409–420. doi: 10.1006/jmbi.1998.2313
- Zgurskaya, H. I., and Nikaido, H. (1999b). Bypassing the periplasm: reconstitution of the acrb multidrug efflux pump of *Escherichia coli*. *Proc. Natl. Acad. Sci. U.S.A.* 96, 7190–7195. doi: 10.1073/pnas.96.13.7190

**Conflict of Interest Statement:** The authors declare that the research was conducted in the absence of any commercial or financial relationships that could be construed as a potential conflict of interest.

Copyright © 2015 Wang, Weng and Wang. This is an open-access article distributed under the terms of the Creative Commons Attribution License (CC BY). The use, distribution or reproduction in other forums is permitted, provided the original author(s) or licensor are credited and that the original publication in this journal is cited, in accordance with accepted academic practice. No use, distribution or reproduction is permitted which does not comply with these terms.

# Interaction of antibacterial compounds with RND efflux pumps in *Pseudomonas aeruginosa*

Jürg Dreier<sup>1\*</sup> and Paolo Ruggerone<sup>2</sup>

<sup>1</sup> Basilea Pharmaceutica International Ltd., Basel, Switzerland, <sup>2</sup> Dipartimento di Fisica, Università di Cagliari – Cittadella Universitaria, Monserrato, Italy

## OPEN ACCESS

### Edited by:

Klaas Martinus Pos,  
Goethe University Frankfurt, Germany

### Reviewed by:

Aixin Yan,  
The University of Hong Kong,  
Hong Kong  
Yuji Morita,  
Aichi Gakuin University, Japan  
Etinosa Igbinosa,  
University of Benin, Nigeria

### \*Correspondence:

Jürg Dreier,  
Basilea Pharmaceutica International  
Ltd., Grenzacherstrasse 487,  
P.O. Box 4005, Basel, Switzerland  
juerg.dreier@basilea.com

### Specialty section:

This article was submitted to  
Antimicrobials, Resistance  
and Chemotherapy,  
a section of the journal  
*Frontiers in Microbiology*

Received: 13 February 2015

Accepted: 16 June 2015

Published: 08 July 2015

### Citation:

Dreier J and Ruggerone P (2015)  
Interaction of antibacterial  
compounds with RND efflux pumps  
in *Pseudomonas aeruginosa*.  
*Front. Microbiol.* 6:660.  
doi: 10.3389/fmicb.2015.00660

*Pseudomonas aeruginosa* infections are becoming increasingly difficult to treat due to intrinsic antibiotic resistance and the propensity of this pathogen to accumulate diverse resistance mechanisms. Hyperexpression of efflux pumps of the Resistance-Nodulation-Cell Division (RND)-type multidrug efflux pumps (e.g., MexAB-OprM), chromosomally encoded by *mexAB-oprM*, *mexCD-oprJ*, *mexEF-oprN*, and *mexXY* (-oprA) is often detected in clinical isolates and contributes to worrying multi-drug resistance phenotypes. Not all antibiotics are affected to the same extent by the aforementioned RND efflux pumps. The impact of efflux on antibiotic activity varies not only between different classes of antibiotics but also between members of the same family of antibiotics. Subtle differences in physicochemical features of compound-pump and compound-solvent interactions largely determine how compounds are affected by efflux activity. The combination of different high-resolution techniques helps to gain insight into the functioning of these molecular machineries. This review discusses substrate recognition patterns based on experimental evidence and computer simulations with a focus on MexB, the pump subunit of the main RND transporter in *P. aeruginosa*.

**Keywords:** efflux, multi-drug resistance, bacteria, RND, substrate recognition, *Pseudomonas aeruginosa*, antibiotic agents, efflux pump inhibitors

## Introduction

Infectious diseases, including bacterial infections, are among the major causes of mortality worldwide (Mason et al., 2003). Infections by multi-drug resistant (MDR) pathogens are especially difficult to treat and are recognized as a major threat (CDC, 2013; Denys and Relich, 2014; Martinez and Baquero, 2014; ECDC, 2015).

The Gram-negative bacterium *Pseudomonas aeruginosa* is frequently involved in healthcare-associated infections like pneumonia, bloodstream infections, urinary tract infections, and surgical site infections (Hidron et al., 2008; Jones et al., 2009; Zhan et al., 2010). About 8% of nosocomial infections reported to the Centers for Disease Control and Prevention in the US are ascribed to *P. aeruginosa*. 13% of the severe cases in the US are caused by MDR isolates and 14% of European isolates reported between 2005 and 2013 had combined resistance to several antibiotics (CDC, 2013; ECDC, 2015). MDR phenotypes have been described for clinical isolates from various places all over the world (Potron et al., 2015). MDR *P. aeruginosa* isolates are sometimes resistant to nearly all classes of antibiotics and have lost susceptibility toward fluoroquinolones, aminoglycosides,

cephalosporins, and carbapenems (Livermore, 2009; Riou et al., 2010; Poole, 2011; Castanheira et al., 2014).

The outer membrane (OM) of Gram-negative bacteria has an asymmetric structure including an outer leaflet made of lipopolysaccharides (LPS), an inner phospholipid leaflet, and porin channels (Kamio and Nikaido, 1976; Nikaido, 2003). Small, hydrophilic compounds can pass the OM by diffusion through the porin channels whereas large and/or hydrophobic compounds have to go through the lipid bilayer (Hancock, 1997; Delcour, 2009). In the *Escherichia coli* OM, there are trimeric porins like OmpF and OmpC present that allow a relatively rapid diffusion of small, hydrophilic substances (Nikaido and Rosenberg, 1983; Cowan et al., 1992; Schulz, 1993). *P. aeruginosa* does not make such trimeric porins but expresses the monomeric porin OprF at a low number with a small opening that only allows slow permeation (Angus et al., 1982; Yoshimura and Nikaido, 1982; Sugawara et al., 2006, 2010). *P. aeruginosa* has also specific channels such as OprD for basic amino acids and peptides, which is the main entry passage of carbapenem antibiotics (Nikaido, 2003). The structure of the OM can be adapted by *P. aeruginosa* to decrease the net negative charge of the LPS in response to cationic peptides such as polymyxin B, which act on the negatively charged LPS (Olaitan et al., 2014). Thus, the OM of *P. aeruginosa* strongly reduces the permeability for most antibiotics and provides an effective and adaptable protection against antibacterial agents (Delcour, 2009; Page, 2012).

Many of the compounds that can pass through the OM are actively transported out of the cell again by efflux pumps. The low permeability of the OM combined with such efflux pumps results in an effective protection against a wide variety of substances including antibiotics (Kumar and Schweizer, 2005; Fernandez and Hancock, 2012). *P. aeruginosa* PAO1 has 12 efflux systems of the Resistance-Nodulation-Cell Division (RND) family (Poole, 2000, 2004, 2005, 2013; Webber and Piddock, 2003; Piddock, 2006; Zechini and Versace, 2009; Fernandez and Hancock, 2012; Nikaido and Pages, 2012; Blair et al., 2014, 2015b; Delmar et al., 2014; Sun et al., 2014), whereof a set of four RND pumps contributes most significantly to antibiotic resistance: MexAB-OprM, MexCD-OprJ, MexEF-OprN, and MexXY-OprM (Fernandez and Hancock, 2012). MexB transports  $\beta$ -lactams including  $\beta$ -lactamase inhibitors and carbapenems (not imipenem), aminoglycosides, fluoroquinolones, tetracyclines, tigecycline, macrolides, amphenicols, novobiocin, sulfonamides, trimethoprim, cerulenin, thiolactomycin, some amphiphilic molecules, disinfectants, dyes, solvents, detergents, and several homoserine lactones involved in quorum sensing [detailed lists of RND substrates are given in (Poole, 2005; Lister et al., 2009) and in Table 1 for dyes described in this review]. MexD recognizes fluoroquinolones, zwitterionic cephalosporins, macrolides, chloramphenicol, trimethoprim, and tetracyclines. MexF accepts fluoroquinolones, chloramphenicol, trimethoprim, and tetracycline as substrates. MexY transports aminoglycosides, fluoroquinolones, macrolides, tetracyclines, tigecycline, and zwitterionic cephalosporins (Morita et al., 2012).

The expression of RND pumps is regulated as a response to external stress factors such as reactive oxygen species (MexAB-OprM, MexXY-OprM), reactive nitrogen species

(MexEF-OprN), and other agents imposing stress to the bacterial cell like membrane damaging agents (MexCD-OprJ) or ribosome blocking substances (MexXY-OprM), (Grkovic et al., 2002; Lister et al., 2009; Morita et al., 2014; Poole, 2014). Thus, efflux pumps may be part of a versatile protection mechanism against cellular stress that works not only in response to naturally occurring signals but also against antibiotics.

Increased pump expression can be linked to decreased porin expression as for example in the *nfxC* mutants of *P. aeruginosa*. In these mutants OprD expression is downregulated, which impairs carbapenem uptake and MexEF-OprN expression is upregulated, which affects fluoroquinolone export (Fukuda et al., 1990, 1995; Davin-Regli et al., 2008; Nishino et al., 2009; Castanheira et al., 2014).

One possibility to circumvent efflux is the development of antibiotics that are not pump substrates, or are only poorly affected by pump activity (e.g., Hayashi et al., 2014). Alternatively, one may look for molecules that inhibit pumps and can be used as adjuvants in combination with antibiotics (e.g., Olivares et al., 2013). For both strategies it is crucial to understand the molecular properties that define pump substrates. This review describes experimental procedures that are sensitive to RND efflux pump activity and allow conclusions on substrate recognition by RND efflux pumps. The described methods include specifically designed efflux assays but also assays which were developed for other purposes than efflux studies but revealed substrates of efflux pumps (e.g., probes for membrane integrity have been found to be efflux pump substrates). Substrate recognition by MexB from *P. aeruginosa* can often not (or not yet) be investigated with the methods described for AcrB in *E. coli* but can be modeled with *in silico* methods based on experimental data. Specific data about substrate recognition by MexB from *P. aeruginosa* are still limited. Therefore we discuss in detail results obtained also for AcrB when they describe similarities between the two RND transporters. It is paradigmatic that to date and to our knowledge there is only a single computational study addressing the molecular aspects of MexB-substrate interactions.

## Impact of Efflux on Antibiotic Activity

A direct impact of efflux on antibiotic activity on *P. aeruginosa* was shown for a core set of RND pumps by efflux-pump deletion mutants and could be confirmed by mutants that overexpress selected RND systems (Li et al., 1995; Lomovskaya et al., 1999; Masuda et al., 2000a; Poole, 2000, 2004, 2005, 2013; Schweizer, 2003). Susceptibility of *P. aeruginosa* towards many antibiotics has been restored when the four systems that are most relevant for antibiotic resistance (MexAB-OprM, MexCD-OprJ, MexEF-OprN, and MexXY-OprM) have been deleted (Morita et al., 2001; Kumar et al., 2006). These *P. aeruginosa* RND pumps have overlapping but not identical substrate ranges as mentioned in the Section *Introduction*. RND efflux pumps have individual substrate specificities that include amphiphilic molecules (e.g., MexB) but also hydrophobic solutes (e.g., MexB, MexD) and the hydrophilic polycationic aminoglycosides (MexY), described to enter cells by a self-promoted mechanism (Hancock, 1997).

**TABLE 1 | Properties of efflux-pump substrates and inhibitors.**

| <b>Compound</b>                                   | <b>logP (o/w)<sup>a</sup></b> | <b>TPSA (Å<sup>2</sup>)<sup>b</sup></b> | <b>MW (Da)<sup>c</sup></b> | <b>PC+<sup>d</sup></b> | <b>PC-<sup>e</sup></b> | <b>Net PC<sup>f</sup></b> | <b>Properties</b>                                      |
|---|-------------------------------|---|----------------------------|------------------------|------------------------|---------------------------|--|
| <b>Inhibitors</b>                                 |                               |   |                            |                        |                        |                           |  |
| D13-9001  | 0.85                          | 210.8                                   | 693.8                      | 9.96                   | -9.96                  | 0                         | Not transported  |
| PABN  | 2.65                          | 149.5                                   | 448.6                      | 9.99                   | -7.99                  | 2                         | Transported  |
| Mefloquin   | 4.27                          | 49.7                                    | 379.3                      | 6.13                   | -5.13                  | 1                         | Quinolone  |
| <b>Substrates acting as inhibitor<sup>g</sup></b> |                               |   |                            |                        |                        |                           |  |
| Minocycline                                       | -0.28                         | 164.6                                   | 457.5                      | 7.11                   | -7.11                  | 0                         | Antibiotic   |
| Trimethoprim                                      | 0.94                          | 106.8                                   | 291.3                      | 5.27                   | -4.28                  | 1                         | Antibiotic   |
| Taurocholate                                      | 2.33                          | 141.0                                   | 514.7                      | 4.79                   | -5.79                  | -1                        | Bile acid  |
| Erythromycin                                      | 2.76                          | 195.1                                   | 734.9                      | 9.73                   | -8.73                  | 1                         | Antibiotic   |
| Glycocholate                                      | 3.15                          | 129.9                                   | 464.6                      | 4.14                   | -5.14                  | -1                        | Bile acid  |
| <b>Substrates</b>                                 |                               |   |                            |                        |                        |                           |  |
| Ceftobiprole                                      | -1.29                         | 213.7                                   | 533.6                      | 9.53                   | -10.5                  | -1                        | Antibiotic   |
| Aztreonam   | -1.03                         | 201.3                                   | 433.4                      | 7.09                   | -9.10                  | -2                        | Antibiotic   |
| Flomoxef  | -0.96                         | 171.8                                   | 495.5                      | 7.34                   | -8.34                  | -1                        | Antibiotic   |
| Cefazolin   | -0.73                         | 158.9                                   | 453.5                      | 5.65                   | -6.65                  | -1                        | Antibiotic   |
| Meropenem   | -0.47                         | 117.6                                   | 383.5                      | 6.09                   | -6.09                  | 0                         | Antibiotic   |
| FDG   | -0.40                         | 234.3                                   | 656.6                      | 10.38                  | -10.4                  | 0                         | Intracellular conversion into a fluorescent product    |
| Moxalactam  | -0.38                         | 212.0                                   | 518.5                      | 7.60                   | -9.60                  | -2                        | Antibiotic   |
| Tigecycline                                       | -0.26                         | 210.3                                   | 586.7                      | 9.99                   | -8.99                  | 1                         | Antibiotic   |
| Cefamandole                                       | -0.18                         | 153.4                                   | 461.5                      | 6.47                   | -7.47                  | -1                        | Antibiotic   |
| (+)-Cerulenin                                     | 0.10                          | 72.7                                    | 223.3                      | 3.39                   | -3.39                  | 0                         | Antibiotic   |
| Cefsulodine                                       | 0.21                          | 187.7                                   | 531.5                      | 9.08                   | -10.1                  | -1                        | Antibiotic   |
| Gemifloxacin                                      | 0.36                          | 125.8                                   | 389.4                      | 6.80                   | -6.81                  | 0                         | Antibiotic   |
| Doxorubicin                                       | 0.51                          | 207.7                                   | 544.5                      | 8.89                   | -7.89                  | 1                         | Anticancer drug, quenched intracellular fluorescence   |
| Cephalotin  | 0.58                          | 115.8                                   | 395.4                      | 5.48                   | -6.48                  | -1                        | Antibiotic   |
| Sulbenicillin                                     | 0.59                          | 140.8                                   | 412.4                      | 5.97                   | -7.97                  | -2                        | Antibiotic   |
| Dodecyl- $\alpha$ -D-maltoside                    | 0.70                          | 178.5                                   | 510.6                      | 7.00                   | -7.00                  | 0                         | Detergent  |
| Levofloxacin                                      | 0.80                          | 76.15                                   | 360.4                      | 4.57                   | -5.58                  | -1                        | Antibiotic   |
| Norfloxacin                                       | 0.85                          | 80.3                                    | 319.3                      | 5.46                   | -5.46                  | 0                         | Antibiotic   |
| Nalidixic acid                                    | 0.88                          | 73.3                                    | 231.2                      | 3.14                   | -4.15                  | -1                        | Antibiotic   |
| Chloramphenicol                                   | 1.10                          | 115.4                                   | 323.1                      | 5.02                   | -5.02                  | 0                         | Antibiotic   |
| Ciprofloxacin                                     | 1.16                          | 80.3                                    | 331.3                      | 5.66                   | -5.66                  | 0                         | Antibiotic   |
| Oxolinic acid                                     | 1.19                          | 78.9                                    | 260.2                      | 3.25                   | -4.25                  | -1                        | Antibiotic   |
| Carbenicillin                                     | 1.23                          | 129.7                                   | 376.4                      | 5.32                   | -7.32                  | -2                        | Antibiotic   |
| Ceftazidime                                       | 1.35                          | 194.1                                   | 545.6                      | 8.68                   | -9.68                  | -1                        | Antibiotic   |
| Resazurin   | 1.79                          | 75.3                                    | 229.2                      | 2.80                   | -2.81                  | 0                         | Intracellular conversion into a fluorescent product    |
| Ala-NAP   | 1.88                          | 56.7                                    | 215.3                      | 4.02                   | -3.02                  | 1                         | Intracellular conversion into a fluorescent product    |
| Cefaloridine                                      | 1.96                          | 93.4                                    | 415.5                      | 6.14                   | -6.14                  | 0                         | Antibiotic   |
| Moxifloxacin                                      | 2.01                          | 89.5                                    | 401.4                      | 5.87                   | -5.87                  | 0                         | Antibiotic   |
| Thiolactomycin                                    | 2.41                          | 34.1                                    | 210.3                      | 2.39                   | -2.39                  | 0                         | Antibiotic   |
| Cloxacillin                                       | 2.67                          | 115.6                                   | 434.9                      | 4.96                   | -5.96                  | -1                        | Antibiotic   |
| Proflavin   | 2.80                          | 66.2                                    | 210.3                      | 4.03                   | -3.03                  | 1                         | Fluorescent probe                                      |
| Pyronin Y   | 2.98                          | 15.5                                    | 267.4                      | 3.14                   | -2.14                  | 1                         | Fluorescent Probe, quenched intracellular fluorescence |
| Nitrocefén  | 3.02                          | 181.2                                   | 515.5                      | 7.20                   | -8.20                  | -1                        | Antibiotic   |
| Clarithromycin                                    | 3.12                          | 184.1                                   | 749.0                      | 9.61                   | -8.61                  | 1                         | Antibiotic   |
| Acriflavine                                       | 3.19                          | 55.9                                    | 224.3                      | 4.06                   | -3.06                  | 1                         | Fluorescent Probe, quenched intracellular fluorescence |
| Leu-NAP   | 3.29                          | 56.7                                    | 257.4                      | 4.02                   | -3.02                  | 1                         | Intracellular conversion into a fluorescent product    |
| Novobiocin  | 3.30                          | 198.9                                   | 611.6                      | 8.03                   | -9.04                  | -1                        | Antibiotic   |
| ANS   | 3.35                          | 63.2                                    | 298.3                      | 3.71                   | -4.71                  | -1                        | Fluorescent Probe, enhanced intracellular fluorescence |
| Nile red  | 3.71                          | 41.9                                    | 318.4                      | 3.38                   | -3.38                  | 0                         | Fluorescent Probe, enhanced intracellular fluorescence |
| Telithromycin                                     | 3.84                          | 173.1                                   | 813.0                      | 9.91                   | -8.91                  | 1                         | Antibiotic   |
| Fluorescein                                       | 4.13                          | 76.0                                    | 332.3                      | 4.16                   | -4.16                  | 0                         | Fluorescent probe                                      |
| DASPEI  | 4.38                          | 7.12                                    | 253.4                      | 3.45                   | -2.45                  | 1                         | Fluorescent Probe, enhanced intracellular fluorescence |

(Continued)

**TABLE 1 | Continued**

| Compound              | logP (o/w) <sup>a</sup> | TPSA (Å <sup>2</sup> ) <sup>b</sup> | MW (Da) <sup>c</sup> | PC+ <sup>d</sup> | PC- <sup>e</sup> | Net PC <sup>f</sup> | Properties   |
|-----------------------|-------------------------|-------------------------------------|----------------------|------------------|------------------|---------------------|--|
| Hoechst H33342        | 4.47                    | 74.3                                | 453.6                | 6.09             | -5.09            | 1                   | Fluorescent Probe, enhanced intracellular fluorescence |
| NPN                   | 4.51                    | 12.0                                | 219.3                | 2.40             | -2.40            | 0                   | Fluorescent Probe, enhanced intracellular fluorescence |
| Rifampicin            | 4.56                    | 221.4                               | 824.0                | 11.1             | -10.1            | 1                   | Antibiotic   |
| Ethidium              | 5.20                    | 55.9                                | 314.4                | 4.66             | -3.66            | 1                   | Fluorescent Probe, enhanced intracellular fluorescence |
| TMA-DPH               | 5.39                    | 0.0                                 | 290.4                | 4.18             | -3.18            | 1                   | Fluorescent Probe, enhanced intracellular fluorescence |
| Rhodamine 6G          | 5.76                    | 59.9                                | 442.6                | 4.23             | -4.24            | 0                   | Fluorescent probe                                      |
| 1,2'-dinaphthylamine  | 5.77                    | 12.0                                | 269.3                | 2.70             | -2.70            | 0                   | Fluorescent Probe, enhanced intracellular fluorescence |
| DiOC <sub>2</sub> (3) | 6.06                    | 29.5                                | 333.4                | 3.79             | -2.79            | 1                   | Fluorescent Probe, enhanced intracellular fluorescence |
| <b>Other</b>          |                         |                                     |                      |                  |                  |                     |  |
| Imipenem              | -0.69                   | 118.3                               | 299.4                | 5.50             | -5.50            | 0                   | Antibiotic, not a substrate                            |
| Resorufin             | 1.49                    | 58.9                                | 213.2                | 2.75             | -2.75            | 0                   | Fluorescent probe                                      |
| Optochin              | 3.75                    | 46.8                                | 341.5                | 4.36             | -3.37            | 1                   | Quinolone  |

Descriptors were calculated for pH 7 using Molecular Operating Environment (MOE), 2013.08; Chemical Computing Group Inc., 1010 Sherbooke St. West, Suite #910, Montreal, QC, Canada, H3A 2R7, 2014.

<sup>a</sup>Logarithm of partition coefficient between n -octanol and water (o/w); <sup>b</sup>Total Polar Surface Area; <sup>c</sup>Molecular Weight; <sup>d</sup>Partial positive charge; <sup>e</sup>Partial negative Charge; <sup>f</sup>net Partial Charge.

<sup>g</sup>Examples for which efflux inhibition was shown are listed. Other substrates may act as inhibitors too.

Note that most antibiotics are amphiphilic compounds with hydrophobic parts that are required to partition into a membrane but that there are considerable differences with regard to the impact of efflux on activity even within classes of antibiotics (Hancock, 1997; Nikaido, 2003; Delcour, 2009; Brown et al., 2014).

An effort to make tetracyclines that are not substrates of tetracycline-specific pumps of the major facilitator superfamily (MFS), led to the development of tigecycline (Chopra, 2002). However, tigecycline was still a substrate of the RND pumps MexY, MexB, and MexD in *P. aeruginosa* (Dean et al., 2003; Visalli et al., 2003; Chollet et al., 2004). This observation illustrates the flexibility of RND efflux pumps but it does not mean that a given RND transporter would accept all antibiotics of the same class. The macrolides erythromycin and clarithromycin have been found to be better substrates of AcrB of *E. coli* and of *Enterobacter aerogenes* than the ketolide telithromycin (Dean et al., 2003; Visalli et al., 2003; Chollet et al., 2004). RND pumps in *P. aeruginosa* have been shown by *in vitro* susceptibility studies to transport substrates of the quinolone family with differential preference (Li et al., 1995; Kohler et al., 1997; Lomovskaya et al., 1999; Masuda et al., 2000a; Griffith et al., 2006; Dunham et al., 2010; Morita et al., 2015). Fluoroquinolones like levofloxacin, ciprofloxacin, norfloxacin, and others, have been reported to be most efficiently exported by MexEF-OprN and MexCD-OprJ and with less efficiency by MexAB-OprM and MexXY-OprM (or OprA). Non-fluorinated quinolones (e.g., nalidixic acid, piromidic acid, pipemidic acid, cinoxacin, oxolinic acid, and flumequine) have been shown to be preferentially transported by MexEF-OprN, less efficiently by MexCD-OprJ and MexAB-OprM, and least efficiently by MexXY-OprM (Kohler et al., 1997; Masuda et al., 2000b). It has been concluded from these results that fluoroquinolones with a positive charge and an electronegative fluorine atom are predominantly recognized by MexCD-OprJ, whereas quinolones without the fluorine atom are preferred substrates of MexEF-OprN. This result was in

agreement with earlier work, suggesting that MexCD-OprJ expels amphiphilic substrates with a positive charge that can partition into a membrane (Masuda et al., 1996; Nikaido, 1996).

Studies on β-lactam efflux by AcrB in *Salmonella enterica* serovar Typhimurium have indicated that RND efflux pumps somehow recognize the hydrophobicity of a substrate (Nikaido et al., 1998; Ferreira and Kiralj, 2004). The studies showed that efflux efficiency varied with the lipophilicity of the β-lactam side chain and that molecules with more hydrophobic side chains were preferred substrates. Further work with β-lactams shed light on substrate specificity among RND pumps in *P. aeruginosa*. MexB transported a broad spectrum of β-lactams including penicillins, cephems, and carbapenems but not imipenem (Masuda et al., 2000b, 2001; Baum et al., 2009). MexD had a slightly narrower spectrum, which excluded the MexB substrates carbenicillin, sulbenicillin, ceftazidime, and moxalactam (Li et al., 1994; Masuda et al., 2000b). MexY had a yet narrower spectrum, which further excluded cefsulodin, flomoxef, and aztreonam (Masuda et al., 2000b; Hocquet et al., 2006). As carbenicillin and sulbenicillin have a negative charge that the other β-lactams in these studies do not have, it seems that MexB accepts substrates with negative charges that MexD and MexY do not recognize. The finding that certain variants of MexD had altered substrate specificity has suggested that the recognition likely takes place via electrostatic interactions. MexD Q45K and MexD E89K with additional positively charged lysine residues have conferred resistance to the negatively charged carbenicillin, aztreonam, and ceftazidime (Mao et al., 2002). A role of charged residues in substrate recognition has been shown for AcrD too based on the fact that the binding pocket of AcrD contains an arginine residue (R625) not found in the mostly hydrophobic pocket of AcrB. Resistance to negatively charged β-lactams increased significantly when an arginine residue was introduced at the corresponding place in AcrB (I626R). Removal of a glutamic acid residue from the AcrB pocket (E673G), a residue not present at this position in AcrD, further enhanced the protective

effect and helped to explain the specificity of AcrD for small hydrophilic substrates such as the anionic  $\beta$ -lactams carbenicillin, aztreonam, and sulbenicillin (Wehmeier et al., 2009; Kobayashi et al., 2014).

Carbapenem activity was not uniformly affected by efflux pumps either. Meropenem was sensitive to overexpression of MexAB-OprM, MexCD-OprJ, or MexXY-OprM, whereas imipenem was not significantly affected (Masuda et al., 2000b; Ong et al., 2007; Riera et al., 2011; Castanheira et al., 2014). Efflux-pump expression levels in clinical isolates of *P. aeruginosa* indicated that MexAB-OprM and MexXY-OprM were most relevant for meropenem activity, followed by MexEF-OprN and with the lowest impact by MexCD-OprJ (Pai et al., 2001; Giske et al., 2005; Riera et al., 2011). A computer simulation of imipenem and meropenem transport by MexB suggested that the hydrophobicity and the flexibility of the side chains were probably responsible for efflux sensitivity (Collu et al., 2012b). The study indicated that the more rigid and hydrophobic tail of meropenem made strong interactions with the hydrophobic lining of the distal binding pocket in MexB (see **Figure 1** for the structure of the transporter with two affinity sites) whereas the flexible and more hydrophilic tail of imipenem prevented this interaction (a detailed description of the extrusion pathway is given in the Section *Computational Study*). The computational results have further suggested that imipenem had no pronounced affinity for any particular site in MexB.

The anti-MRSA cephalosporin ceftobiprole is another  $\beta$ -lactam that is poorly recognized by MexB, MexD, and MexF in *P. aeruginosa* (Baum et al., 2009). Overexpression of these efflux pumps had only the marginal effect on the activity of ceftobiprole of a twofold increase of the minimum inhibitory concentration (MIC). Overexpression of MexXY caused a fourfold to eightfold increase of the MIC. The data have indicated that ceftobiprole was more efficiently transported by MexY than by MexB (Baum et al., 2009).

It should be pointed out that not all efflux substrates can be reliably detected by MIC. MIC may be a misleading indicator for efflux for any antibacterial that is effective at a concentration below the concentration required to reach maximal efflux velocity  $V_{max}$ . For example, AcrB had only a minor effect on the activity of cefaloridine (Nikaido et al., 1998; Mazzariol et al., 2000). Cefaloridine was later shown to be strongly effluxed by AcrB only at concentrations higher than those required to kill bacteria (Nagano and Nikaido, 2009). The discrepancy was explained by the finding that cefaloridine was effluxed with a high  $V_{max}$  but also with a strong positive cooperativity. The cefaloridine concentration required to reach half-maximal velocity (288  $\mu$ M) was much higher than the effective antibacterial dose (Nikaido and Normark, 1987; Nagano and Nikaido, 2009). Note that cefaloridine may not be an exception because other drugs (cephalotin, cefamandole) were also transported in a cooperative manner (Nagano and Nikaido, 2009). The situation may be

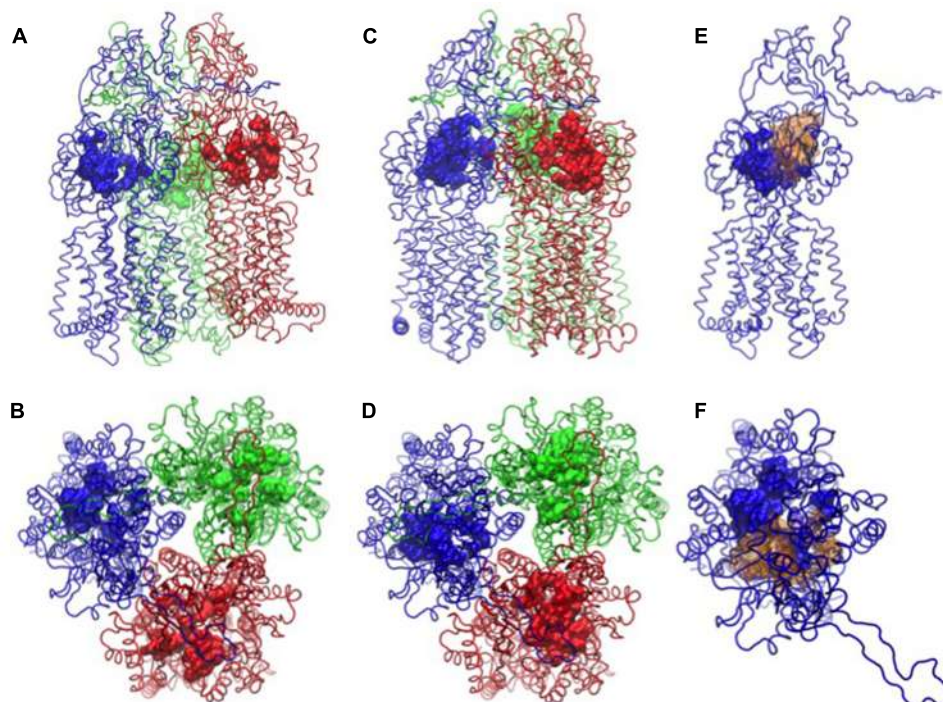


**FIGURE 1 |** Binding pockets of MexB [PDB code: 2V50 (Sennhauser et al., 2009)]. The monomers L, T, and O are in tube representation and colored in blue, red, and green, respectively. In (A,B) side and top views of MexB with the distal binding pocket depicted as surface, in (C,D) the access binding

pocket is highlighted as surface. In (E,F) the side and top views of L monomer are shown with access and distal binding pocket colored as blue and yellow surfaces, respectively. All the atomic-level figures were rendered using Visual Molecular Dynamics (VMD; Humphrey et al., 1996).

different in *P. aeruginosa* because its OM has a lower permeability for  $\beta$ -lactams than the OM of *E. coli* (as explained before). This lower permeability leads to higher MIC and to a stronger impact of efflux than in *E. coli* and thus, less discrepancy between efflux studies and MIC data may be expected.

MIC tests in the presence of the model efflux-pump inhibitor (EPI) phenylalanine-arginine  $\beta$ -naphthylamide (PA $\beta$ N) are often done as a quick check for efflux effects (e.g., Mesaros et al., 2007; Pages et al., 2009; Castanheira et al., 2014). Increased antimicrobial activity (i.e., lower MIC) of an antibiotic in the presence of PA $\beta$ N is taken as an indication that the test compound is an efflux substrate. However, detailed studies with PA $\beta$ N nicely illustrated the complexity of effects that can influence whole cell assays such as MIC determinations. It has already been mentioned in the original publication of PA $\beta$ N that this agent does not only inhibit efflux pumps but also permeabilizes the OM of Gram-negative bacteria (Lomovskaya et al., 2001). This permeabilization property has been confirmed later in separate studies (Iino et al., 2012b; Lamers et al., 2013). Permeabilization of the OM may be mistaken as pump inhibition because facilitated entry of test compounds leads to increased intracellular levels. Pump inhibition and membrane permeabilization by PA $\beta$ N have been shown to be dose-dependent, separable activities in *E. coli* because AcrB and AcrF have been specifically inhibited at low doses of PA $\beta$ N, whereas membrane destabilization has been observed at higher concentrations of PA $\beta$ N (Misra et al., 2015).

The protonophore carbonyl cyanide m-chlorophenylhydrazone (CCCP) is often used in a similar way as PA $\beta$ N to probe for efflux phenomena. RND pumps belong to the class of secondary transporters, which are driven by a transmembrane electrochemical potential of protons (reviewed in Borges-Walmsley et al., 2003; Poole, 2005; Dreier, 2007). CCCP indirectly inhibits secondary efflux pumps by dissipating the proton gradient across the inner membrane (Rosen and Kashket, 1978; Levy, 1992). It should be clear that whole cell assays require thorough controls to avoid confusion of pump inhibition with other effects. Susceptibility tests are useful to investigate general substrate recognition patterns whereas elucidation of detailed efflux mechanisms requires specifically designed assays.

## Efflux Assays

Transport studies generally require at least two compartments and a method to measure concentration changes of a tracer substance. Entire RND efflux systems require three compartments (cytosol, periplasm, and cell exterior), which makes whole bacteria an obvious choice for efflux assays. In principle, cells can be incubated with any pump substrate and efflux can be measured by following the change of substrate concentration inside or outside of the bacteria [e.g., (Kohler et al., 1997; Pumbwe and Piddock, 2000)]. Such a generic method may require the separation of intracellular from extracellular substrate, usually achieved by filtration or centrifugation. Cell lysis may be necessary too before a versatile detection method like liquid chromatography-mass spectrometry (LC-MS) or

high performance liquid chromatography (HPLC) can be applied (e.g., Schumacher et al., 2007; Cai et al., 2009). Homogeneous assays use methods that allow substrate quantification without a separation step, which simplifies applications like time-course transport studies or high-throughput tests. Fluorescence was selected as the method of choice to assess fluoroquinolone accumulation in Gram-negative bacteria based on a comparison of various methods (Mortimer and Piddock, 1991). The study showed that steady-state concentrations and times to reach the steady-state condition varied in a substrate-specific manner within the quinolone family.

Many protocols use molecules whose fluorescent properties are sensitive to their environment and change upon entry into a cell (Figures 2A,B). A prominent example is ethidium bromide (EtBr) since the quantum yield of the fluorescence increases when ethidium intercalates into DNA (LePecq and Paoletti, 1967; Mine et al., 1999; Morita et al., 2001; Li et al., 2003). Active efflux causes reduced intracellular levels of EtBr and as a consequence a decrease of fluorescence whereas inhibition of efflux pumps is recorded as a signal increase (Figure 2A). The same assay principle (Figure 2A) applies to 1-anilinonaphthalene-8-sulphonate (ANS) accumulation because the fluorescence quantum yield increases when ANS binds to hydrophobic structures (e.g., proteins, membranes) in the cell. ANS is a substrate of MexD and has been used to study this transporter in *P. aeruginosa* (Walmsley et al., 1994; Mao et al., 2002; Kamal et al., 2013). Another example is 1,2'-dinaphthylamine which has been used to measure AcrB efflux in *E. coli* because it is a substrate of AcrB and becomes strongly fluorescent when it partitions into a phospholipid bilayer (Bohnert et al., 2011a).

A widely used fluorophore with increased intracellular fluorescence is the bis-benzamide dye Hoechst H33342 which becomes more fluorescent upon binding to DNA (Loontjens et al., 1990). H33342 was successfully used for accumulation studies with several Gram-positive bacteria, Enterobacteriaceae, and *Acinetobacter baumannii* (van den Berg van Saparoea et al., 2005; Garvey and Piddock, 2008; Richmond et al., 2013). Transport of H33342 by intact *P. aeruginosa* has been difficult to measure because of the low OM permeability for such hydrophobic dyes (Loh et al., 1984; Ocaktan et al., 1997; Germ et al., 1999). However, MexB readily transported H33342 when it was expressed in an *E. coli* host (Welch et al., 2010; Ohene-Agyei et al., 2012). This example shows that whole cell assays reflect a sum of events, which often need to be dissected to identify unambiguously substrates of a given efflux pump.

Another group of efflux probes allows efflux measurements based on a signal decrease upon intracellular accumulation (Figure 2B; e.g., Mao et al., 2002; Nakashima et al., 2013). Examples are the anthracycline cancer drug doxorubicin, whose fluorescence is quenched when the drug is internalized, Pyronin Y, whose intracellular fluorescence is quenched because of binding to RNA (Nishino and Yamaguchi, 2002; Nakashima et al., 2013), and acriflavine, whose fluorescence intensity decreases when it is bound to DNA (Chen et al., 2002). Pyronin Y has been successfully used for transport studies with MexD in *P. aeruginosa* (Mao et al., 2002).

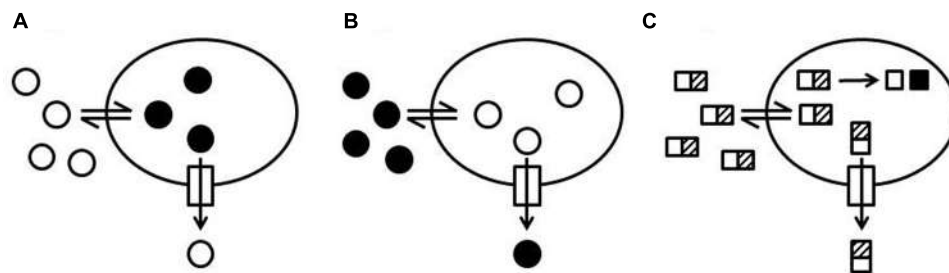


**FIGURE 2 | Schematic representation of efflux assay formats.**

**(A)** Increase of fluorescence intensity upon internalization of a probe. A probe with low fluorescence intensity in the medium surrounding the cells (open circles) is taken up by cells (double arrow). The fluorescence intensity of the probe increases when the probe is internalized (black circles) and interacts with cellular structures such as DNA, proteins, or membranes. Efflux of the probe (arrow through the box to the outside) causes a decrease of the total fluorescence and efflux inhibition causes an increase of the total fluorescence. **(B)** Quenching of fluorescence intensity upon internalization of a probe. A fluorescent probe (black circles) is added to the medium surrounding the cells. The fluorescence intensity of the probe decreases when the probe is taken up by the cells

(open circles) and interacts with cellular structures (e.g., DNA and RNA). Efflux of the probe causes an increase of the total fluorescence and efflux inhibition causes a decrease of the total fluorescence.

**(C)** Intracellular conversion of a probe into a fluorescent product. A non-fluorescent probe (rectangles with a hatched box) is added to the medium surrounding the cells. The probe can penetrate into the cells where it is enzymatically converted (e.g., cleaved or reduced) into a fluorescent product (black squares). The conversion rate of the intact probe into the fluorescent product depends on the intracellular concentration of the intact probe. Efflux of the intact probe slows down the production of the fluorescent product and efflux inhibition increases the rate of fluorescent product generation.

Intracellular conversion of a substrate into a traceable entity is another elegant way to develop homogeneous efflux assays (Figure 2C). The non-fluorescent, blue-colored resazurin (sold under the trade name Alamar Blue®) is reduced to the fluorescent, pink-colored resorufin in live cells by oxidoreductases (Gonzalez and Tarloff, 2001; Rampersad, 2012). The conversion is an indicator mainly for the presence of NADH but also for NADPH and FADH and is routinely used to detect living cells. Resazurin can be used to monitor bacterial growth because conversion rates depend on cell density. However, the method does not work equally well with all microorganisms and is not recommended for *P. aeruginosa*. It was shown that resazurin is a substrate of MexB in *P. aeruginosa* and of AcrB in *E. coli* and it was suggested that efflux pump activity in *P. aeruginosa* may account for the difficulties encountered with resazurin (Vidal-Aroca et al., 2009). Vidal-Aroca et al. (2009) showed that under conditions where *Pseudomonas* do not grow (i.e., in phosphate buffered saline), resazurin can be used to measure efflux pump activity. The assay was useful to identify mefloquine as an inhibitor of MexB and AcrB and to show that optochin, another quinoline derivative, was not an inhibitor of these pumps.

The non-fluorescent alanine- $\beta$ -naphthylamide (Ala-NAP) and leucine- $\beta$ -naphthylamide (Leu-NAP) are enzymatically converted to the highly fluorescent  $\beta$ -naphthylamide by cellular aminopeptidases (Marks et al., 1981; Butler et al., 1993). Assays for RND efflux were developed with Ala-NAP and Leu-NAP and used for the development of peptidomimetic EPI including the model EPI PA $\beta$ N (Lomovskaya et al., 2001; Mao et al., 2002).

Fluorescein-di- $\beta$ -D-galactopyranoside (FDG) is hydrolyzed in the cytoplasm of *E. coli* by  $\beta$ -galactosidase to produce fluorescein (Russo-Marie et al., 1993; Fieldler and Hinz, 1994; Yang and Hu, 2004). Both FDG and fluorescein were shown to be efflux-pump substrates and could be used to develop transport assays

with *E. coli* cells expressing the pseudomonal MexAB-OprM and MexXY-OprM efflux systems (Matsumoto et al., 2011). Intracellular conversion of FDG into fluorescein could even be followed in single-cell mode with a microfluidic device using *E. coli* (Matsumoto et al., 2011; Iino et al., 2012b). FDG cannot be hydrolyzed by *P. aeruginosa* but FDG was useful to study MexB and MexY when they were expressed in an *E. coli* host (Iino et al., 2013). Another approach made use of femtoliter droplet arrays to monitor FDG based efflux in single *E. coli* cells (Iino et al., 2012a, 2013).

The following paragraphs describe fluorescent dyes, which were used as probes for membrane integrity or membrane potential and were later found to be substrates of efflux pumps. The physicochemical properties of these fluorescent dyes provide information on substrate recognition by efflux pumps irrespective of the original use of the probe.

The lipophilic membrane partitioning dye *N*-phenyl-1-naphthylamine (NPN) is useful as a probe for membrane integrity because the amount of NPN that can partition into the phospholipid membrane and hence the fluorescence signal increases when the structure of the OM is disturbed (Loh et al., 1984; Vaara, 1992; Lomovskaya et al., 2001). NPN was shown to be a substrate of AcrB in *E. coli* and of MexB in *P. aeruginosa* (Sedgwick and Bragg, 1996; Ocaktan et al., 1997; Lomovskaya et al., 2001; Murakami et al., 2004; Cai et al., 2009).

Fluorescent potentiometric probes such as the anionic oxonols and the cationic carbocyanines and rhodamines are useful to measure changes of bacterial membrane potentials (Shapiro, 2000). The overall fluorescence signal of these so called slow-response dyes depends on the transmembrane distribution, which is sensitive to changes of the electrochemical potential across the membrane. Rhodamine measurements in *P. aeruginosa* were sensitive to the expression of the RND pumps MexAB-OprM, MexCD-OprJ, and MexHI-OpmD (Morita et al.,

2001; Sekiya et al., 2003). The physicochemical features of these fluorophores, required to partition into a membrane, are apparently recognized by RND efflux-pumps. Indeed, efflux assays were reported in various systems with dyes like the uncharged NPN (MexB of *P. aeruginosa*, AcrB of *E. coli*) or the cationic 1-(4-trimethylammoniumphenyl)-6-phenyl-1,3,5-hexatriene (TMA-DPH, MexB of *P. aeruginosa*) and 2-(4-dimethylamino)styryl-N-ethylpyridinium iodide (DASPEI, AcrB of *E. coli*, MexB of *P. aeruginosa*), (Sedgwick and Bragg, 1996; Ocaktan et al., 1997; Lomovskaya et al., 2001; Murakami et al., 2004; Cai et al., 2009). The properties of the dyes that have been identified as substrates of MexB are listed in **Table 1**.

Substrate export can be directly followed from pre-loaded cells. Alternatively, pump activity can be deduced from intracellular accumulation of externally added substrates, which requires less preparation but reflects efflux in an indirect manner only and includes the hurdle of cellular uptake. Direct efflux measurements require pre-loading of cells with substrate. This extra complication pays off because efflux-related effects can be distinguished from permeation phenomena. The lipophilic dye Nile Red is basically non-fluorescent in aqueous solutions but becomes fluorescent in intracellular, non-polar environments (Greenspan and Fowler, 1985). Nile Red was used for efflux measurements of AcrAB/TolC in *E. coli* (Greenspan and Fowler, 1985; Bohnert et al., 2010, 2011b). When *E. coli* cells were concomitantly loaded with substrate and inhibitor for competition studies, the strongest inhibition was seen with doxorubicin and minocycline, comparable to the effect of PAβN. Many other antibiotics caused slower Nile Red efflux, which is indicative of competitive transport. These results provided further evidence for specific substrate-pump interactions and corroborated the notion of substrate-specific inhibitor efficacy. Adaptation of the Nile Red assay for the use with *P. aeruginosa* would most likely not be straight forward because Nile Red was shown to stain extracellular rhamnolipids made by *P. aeruginosa* (Morris et al., 2011). Strains with deletions of rhamnolipid synthesis genes (rhlAB) may be helpful even if the swarming motility patterns influenced by rhamnolipids would be changed (Deziel et al., 2003; Caiazza et al., 2005). However, pre-loading of *P. aeruginosa* has been achieved with TMA-DPH (Ocaktan et al., 1997). Several other dyes (doxorubicin, rhodamin for YhiUV, NPN, 1,2'-dinaphthylamine and DASPEI for AcrB) have been used to load *E. coli* for efflux assays (Lomovskaya et al., 2001; Nishino and Yamaguchi, 2002; Bohnert et al., 2011a).

Quantitative measurement of substrate transport is crucial for the characterization of efflux pumps. Kinetic analysis of EtBr transport in *E. coli* has shown that uptake rates increased and efflux rates decreased when AcrB was deleted (Xu et al., 2003; Viveiros et al., 2008; Paixao et al., 2009). EtBr transport by MexB has been shown in whole *P. aeruginosa* and an impressive turnover rate of  $500\text{ s}^{-1}$  has been determined for MexB in EtBr efflux assays when the number of pumps was estimated by immunoblotting methods (Ocaktan et al., 1997; Narita et al., 2003). A link of MexCD-OprJ expression with EtBr efflux from *P. aeruginosa* has been demonstrated by Morita et al. (2001, 2003) when they showed that significant EtBr efflux was only measurable after induction

of MexCD-OprJ. MexCD-OprJ expression was inducible with tetraphenyl phosphonium, EtBr, rhodamine 6G, acriflavine, benzalkonium chloride, and chlorhexidine gluconate but not with various antibiotics including substrates of MexD (i.e., norfloxacin, tetracycline, chloramphenicol, streptomycin, or erythromycin).

A thorough quantitative analysis of efflux was achieved with  $\beta$ -lactams and intact *E. coli* cells (Nagano and Nikaido, 2009). The method relies on the hydrolysis of  $\beta$ -lactams by periplasmatic  $\beta$ -lactamases and would probably not be directly applicable to *P. aeruginosa* because of the about 10–100 times lower permeability of the OM for  $\beta$ -lactams (Angus et al., 1982; Yoshimura and Nikaido, 1982; Parr et al., 1987). Under these circumstances it would be very difficult to saturate the efflux pumps and the method may be restricted to a few suitable  $\beta$ -lactams. Hydrolysis rates of  $\beta$ -lactams were measured in intact cells to calculate the periplasmic antibiotic concentration based on known kinetic parameters of  $\beta$ -lactamases. Maximal velocity and dose-response curves depended on the nature of the substrate. Positive cooperativity was detected with cefamandole, cephalotin, and cefaloridin but not with nitrocefin (Nagano and Nikaido, 2009). Cooperativity agrees with the current model of the functional complex of AcrAB-TolC where multiple substrate binding sites reside within three AcrB monomers that adopt different structural conformations in a concerted way during substrate transport (Seeger et al., 2006; Murakami et al., 2006; Sennhauser et al., 2007). Nitrocefin transport was the slowest in the series, which could be explained by the rather strong binding of nitrocefin with its two aromatic rings to AcrB ( $K_m$  of  $5\text{ }\mu\text{M}$ ). No significant efflux could be measured with cefazolin, which has two hydrophilic substituents. Previous work has shown that MIC of cloxacillin, which has a lipophilic side, chain dropped from 256 to  $2\text{ mg/L}$  in *S. enterica* serovar Typhimurium and from 512 to  $2\text{ mg/L}$  in *E. coli* upon inactivation of AcrB whereas no change was observed for the MIC of the hydrophilic cefazolin (Nikaido et al., 1998; Mazzariol et al., 2000). MIC values and efflux studies strongly suggested that AcrB from *E. coli* and *S. enterica* serovar Typhimurium have a preference for hydrophobic  $\beta$ -lactams.

Specific mode-of-action studies ask for less complex assay systems than entire bacterial cells. The activity of different bacterial membrane transporters could be studied with membrane vesicles. Vesicles proved to be very valuable tools for the study of tetracycline-specific pumps (e.g., Yamaguchi et al., 1990). Tetracycline-specific pumps belong to the MFS class of transporters spanning a single cell membrane (Chopra and Roberts, 2001), whereas RND pumps are multi-subunit complexes made of pump subunits (e.g., MexB), an OM channel (e.g., OprM), and an adaptor subunit (e.g., MexA). The pump is formed by three monomers placed in the inner membrane and protrudes into the periplasm (Murakami et al., 2002, 2006; Seeger et al., 2006; Sennhauser et al., 2007, 2009). The OM channel, formed by three monomers, passes the OM linking the periplasmic space with the outside of the cell (Koronakis et al., 2000; Akama et al., 2004a; Phan et al., 2010). The third subunit is an adaptor protein that is required for the assembly of the functional complex which spans the inner membrane, the periplasmic space, and the OM. The stoichiometry of the

subunits (MexB:MexA:OprM or AcrB:AcrA:TolC) is currently discussed with evidence for 3:6:3 (Du et al., 2014, 2015; Kim et al., 2015) or for 3:3:3 (Symmons et al., 2009; Trepout et al., 2010). The models are based on electron microscopy data at resolutions around 20 Å and on docking calculations. A higher-resolution crystal structure of the assembled efflux systems will likely provide a clear-cut response to the controversy regarding the stoichiometry and the construction of the tripartite complex.

The isolated pump subunits AcrB and AcrD from *E. coli* and MexB from *P. aeruginosa* were reconstituted in vesicles (Zgurskaya and Nikaido, 1999; Aires and Nikaido, 2005; Verchère et al., 2014, 2015) but reconstitution of a functional tripartite RND pump complex for *in vitro* transport studies is a truly difficult task that has been achieved only recently (Ntsogou-Enguene et al., 2015; Verchère et al., 2015). Competition studies with AcrB-containing vesicles have indicated that the bile salts taurocholate and glycocholate inhibited transport of a fluorescent phospholipid more efficiently than erythromycin or cloxacillin did (Zgurskaya and Nikaido, 1999). Chloramphenicol was identified in the same study as a substrate that did not inhibit phospholipid efflux. These results suggested that known AcrB substrates were transported with different efficiency reflecting specific substrate recognition patterns. Functional MexAB-OprM complexes have been assembled *in vitro* in a liposome system combining proteoliposomes with OprM and proteoliposomes with MexAB in a way that MexAB-OprM was able to transport EtBr driven by a proton gradient (Ntsogou-Enguene et al., 2015). A related approach used vesicles with MexB and bacteriorhodopsin, a light activated proton pump from *Halobacterium salinarium* (Verchère et al., 2014). Light activation caused bacteriorhodopsin to build up a proton gradient as the energy source for MexB. A change of pH was then taken as indication for substrate transport. The system confirmed that H33342 is a substrate of MexB and suggested that MexA was required for proton-coupled transport.

## Efflux Inhibitors

Many chemically diverse EPI have been reported and their selectivity for pumps can provide insight into specific inhibitor-pump interactions (reviewed in Zechini and Versace, 2009; Van Bambeke et al., 2010). Inhibitors have been derived from natural products, antibiotics, drugs originating from other therapeutic areas or have been newly developed. PAβN and more advanced peptidomimetics of the same series are among the best studied examples (Lomovskaya et al., 2001; Mao et al., 2001; Renau and Lemoine, 2001; Renau et al., 2002; Watkins et al., 2003; Kriengkauykiat et al., 2005). Selectivity for pumps indicated specific inhibitor-pump interactions. For example, PAβN was broadly active against MexAB-OprM, MexEF-OprN, MexCD-OprJ, and MexXY-OprM in *P. aeruginosa* as well as against AcrAB-TolC in several species of the Enterobacteriaceae family while the pyridopyrimidine efflux inhibitor D13-9001 had a much narrower spectrum with specificity for AcrB and MexB (Nakashima et al., 2013). PAβN has been shown to have synergistic activity with levofloxacin against wild-type

*P. aeruginosa* or against *P. aeruginosa* strains overexpressing any of MexAB-OprM, MexCD-OprJ, MexEF-OprM, or MexXY (Lomovskaya et al., 2001). On the other hand, PAβN had no significant effect on carbenicillin or EtBr, which are substrates of MexB too, suggesting multiple binding sites for different substrates. An antagonistic effect of PAβN with aminoglycosides has been observed in the presence of MexXY-OprM, which was explained by the induction of this efflux pump by PAβN (Mao et al., 2001). PAβN was shown to be an efflux substrate likely to act by competition with other substrates for transport (Pages et al., 2005; Lomovskaya and Bostian, 2006; Mahamoud et al., 2007). D13-9001 was hardly transported but was shown to inhibit efflux by high affinity binding to a specific site (Nakashima et al., 2013). Many substances cannot be unambiguously classified as substrates or as inhibitors because there seems to be a gradual transition of properties and many molecules have both characteristics. Minocycline is a substrate of several RND pumps such as AcrB from *E. coli*, *Proteus mirabilis*, *Morganella morganii*, MexB, MexD, and MexY in *P. aeruginosa*, or AdeB and AdeJ in *A. baumannii* (Dean et al., 2003; Visalli et al., 2003; Hirata et al., 2004; Ruzin et al., 2005; Damier-Piolle et al., 2008) but it also acted as an inhibitor of nitrocefin efflux by AcrB (Takatsuka et al., 2010). Trimethoprim, an antibiotic that has been shown to be transported by several RND efflux pumps (i.e., MexB, MexD, and MexF in *P. aeruginosa*, AdeB, AdeJ, AdeG in *A. baumannii*, and BpeF in *Burkholderia pseudomallei*), inhibited the efflux of H33342 by AcrB in *S. enterica* serovar Typhimurium (Kohler et al., 1996; Maseda et al., 2000; Magnet et al., 2001; Coyne et al., 2010; Piddock et al., 2010; Amin et al., 2013; Podneicky et al., 2013). In fact, antibiotics could be modified to become efflux inhibitors as described in the case of fluoroquinolones, tetracyclines, or aminoglycosides (reviewed in Van Bambeke et al., 2010). In general, EPI have aromatic moieties and contain ionizable groups, which are structural features that are reminiscent of substrate characteristics deduced from antibiotic susceptibility tests (Poole, 2004, 2005).

Transport measurements are useful to identify molecules that interact with efflux pumps but investigation of interactions at a molecular level and precise mode-of-action studies require more refined methods.

## Binding Studies and Crystal Structures

Binding of fluorescent substrates to purified AcrB in detergent solution could be measured by fluorescence polarization (Su and Yu, 2007). AcrB bound rhodamine 6G, ethidium, and proflavin, with similar strength ( $K_D$  of 5.5, 8.7, and 14.5  $\mu\text{M}$ , respectively). Binding of ciprofloxacin was significantly weaker with a  $K_D$  of 74.1  $\mu\text{M}$ . Competition studies have indicated that different binding sites may exist for different antibiotics. Experiments with purified AcrB which was immobilized to a surface, yielded  $K_D$  values of 530  $\mu\text{M}$  for novobiocin and of 110  $\mu\text{M}$  for the EPI MC-207,110 (PAβN; Tikhonova et al., 2011). Binding studies confirmed specific interaction of substrates or inhibitors with the pump subunit and revealed substrate-specific variation

of binding strength (Vargiu and Nikaido, 2012; Vargiu et al., 2014).

Many molecules have been described to be efflux substrates or inhibitors but only a small subset thereof could be crystallized in complex with RND pumps (Ruggerone et al., 2013a). Nevertheless, X-ray structures have provided detailed information on substrate-pump interactions (Murakami et al., 2006; Seeger et al., 2006; Sennhauser et al., 2007, 2009; Nakashima et al., 2011; Eicher et al., 2012). A detailed description of the structures is provided in the next section where computational simulation approaches are discussed. The porter domain of the inner membrane transporter protrudes into the periplasmic space (**Figure 1**) and mediates substrate specificity as predicted from genetic studies with AcrB, AcrD, MexB, MexD and MexY (Nikaido, 2011). Gene segments coding for the periplasmatic loops of the pump subunit were swapped between AcrB and AcrD of *E. coli*, between MexB and MexY of *P. aeruginosa*, and between AcrB of *E. coli* and MexB of *P. aeruginosa* (Elkins and Nikaido, 2002; Tikhonova et al., 2002; Eda et al., 2003). Altered substrate specificities of the new constructs suggested that substrate recognition was predominantly determined by the periplasmic region of the pump. Site directed mutagenesis in *P. aeruginosa* confirmed substrate recognition sites in the periplasmatic loops of MexB and MexD (Mao et al., 2002; Middlemiss and Poole, 2004; Wehmeier et al., 2009). Q34K, E89K, and N67K mutations in MexD have led to the transport of negatively charged  $\beta$ -lactams that are not recognized by the wild type transporter (as discussed in the Section *Impact of Efflux on Antibiotic Activity*; Mao et al., 2002). A direct substrate contact for macrolide recognition was proposed for an asparagine residue in a phenylalanine-rich distal binding pocket in MexB (Wehmeier et al., 2009).

The high molecular weight substrates rifampicin, erythromycin, and doxorubicin dimers bound to an access (or proximal) binding pocket (AP) shown in **Figures 1A,B**, which is located close to the protein/periplasm interface (Nakashima et al., 2011; Eicher et al., 2012). The low molecular weight substrates minocycline, dodecyl- $\alpha$ -D-maltoside and doxorubicin have been found in a distal (or deep) binding pocket (DP) displayed in **Figures 1C,D**. AP and DP have also been proposed as two successive locations visited by a substrate during the translocation cycle. The two pockets are separated by a flexible loop (G-loop or switch loop) with two phenylalanine residues (Nakashima et al., 2011; Eicher et al., 2012). Substrate recognition is governed by a phenylalanine-rich hydrophobic region in the distal pocket. Minocycline, rifampicin, and erythromycin, made direct contact with phenylalanine residues (Murakami et al., 2006; Nakashima et al., 2011; Eicher et al., 2012). The MexB-specific pyridopyrimidine efflux inhibitor D13-9001 bound to a narrow pit in the phenylalanine cluster of the distal pocket making  $\pi$ - $\pi$ -stacking interactions (Nakashima et al., 2013). The hydrophilic part of the inhibitor interacted with hydrophilic and ionic residues close to the binding site of minocycline and doxorubicin (Nakashima et al., 2013). Binding to MexY was sterically hindered by a tryptophan in agreement with the phenotypic specificity for MexB over MexY (Nakayama et al., 2003; Yoshida et al., 2007). The binding pocket

of AcrD contains several oxygens in contrast to the mostly hydrophobic pocket of AcrB, which could explain the specificity of AcrD for small basic, hydrophilic substrates such as the anionic  $\beta$ -lactams carbenicillin, aztreonam, and sulbenicillin (Kobayashi et al., 2014). Domain swapping experiments have shown that the specificity of MexB for anionic  $\beta$ -lactams, which are not recognized by MexY, is determined by the periplasmatic domain of the pump subunit (Eda et al., 2003). Although, the complexity of substrate recognition by RND efflux systems has hindered the establishment of a straightforward criterion for the definition of good and poor substrates, it is possible that MexY, as shown for MexD and described before (Mao et al., 2002), does not have the required binding places (i.e., positively charged amino acid residues) in the substrate binding sites to accept negatively charged  $\beta$ -lactams. It cannot be excluded that other, subtle differences in the RND transporter-compound interaction patterns might affect the recognition and the transport at different extrusion stages and positions in the transporters (see **Figure 1** where the different affinity sites are shown). Examples for such subtle but crucial interactions are imipenem and meropenem interacting with MexB (see Section *Computational Study*).

Mutagenesis of D133 in MexY of *P. aeruginosa* (D113A and D133S) has compromised resistance to several aminoglycosides but not to spectinomycin (Lau et al., 2014). The mutation of Y613A in the same protein affected resistance to aminoglycosides but not to erythromycin. This finding supported the view that substrate recognition is governed by binding to specific sites on the extrusion pathway because D133 and Y613 are located in a region of MexY that structurally corresponds to the proximal binding pocket of AcrB.

The experimental data discussed in this review, have provided evidence that hydrophobic moieties are a key property recognized by RND pumps and that hydrophilic parts of a substrate fit into mainly hydrophilic cavities adjacent to a phenylalanine-rich, hydrophobic pocket. Substrates of MexB, which are discussed in this review, are listed in **Table 1**.

## Computational Study

Simulations have reached an impressive maturity as reflected by the increasing number of publications in the field. In particular, a range of simulation techniques have been developed and successfully applied to describe diverse biological systems. Highly precise quantum mechanical techniques (for example see the reviews of Dal Peraro et al., 2007; Zhou et al., 2010; Sgrignani and Magistrato, 2013; Steinbrecher and Elstner, 2013), the classical force-field-based approaches (Kollman et al., 2000), hybrid methods combining appropriate quantum mechanical and classical descriptions (Senn and Thiel, 2009; Steinbrecher et al., 2012) and multi-scale and statistical mechanical methodologies (Kamerlin et al., 2011; Karplus, 2014) are examples of such computational methods.

Although they have been successfully applied to several systems and used to tackle biology-inspired questions, these *in silico* techniques have been barely used to investigate bacterial

efflux systems, in particular members of the RND family. Probably hampered by the lack of crystal structures of the whole systems (the single components have been crystallized) and by the complexity of the machineries (they are tripartite systems), computational studies have addressed RND efflux systems only recently (Collu and Cascella, 2013; Ruggerone et al., 2013a,b). Classical molecular dynamics (MD) simulations represent a particularly promising technique to cast a glimpse on the dynamic behavior of a protein and its immediate micro-environment. MD simulations offer insight into molecular behavior at a temporal and structural accuracy not reached by any other experimental technique today. Continuous improvement of the techniques is pushing the limits of the simulation processes toward longer simulations and thus to a description of increasingly larger biological systems. Extension of the simulation times has improved the quality of the predictions and allowed more robust evaluation of key features such as free energy of binding, interaction patterns, solvent interactions, and interaction lifetimes. Surely, limitations are still present due to the size of many systems and the length of processes of interest, but specific techniques to overcome these drawbacks are under continuous development. As an example of methods used to bridge the time gap between simulated and real processes involving RND efflux systems, we can quote targeted MD simulations (Schlitter et al., 1993), which allows induction of conformational changes between two known states, and metadynamics (Laio et al., 2005; Laio and Gervasio, 2008; Biarnés et al., 2011), which is used to simulate rare events and provides free energy profiles associated with possible processes. Advantages and drawbacks of these biased techniques have been extensively discussed in several publications, to which the interested reader is referred (e.g., Chipot, 2008; Laio and Gervasio, 2008; Markwick and McCammon, 2011; Ovchinnikov and Karplus, 2012 and references therein).

Resistance-Nodulation-Cell Division efflux systems of Gram-negative bacteria form tripartite complexes. The inner-membrane RND transporter and a membrane fusion (adaptor) protein (MFP) connect to a channel that traverses the OM called the outer membrane factor or channel (OMF; Ma et al., 1993; Thanassi et al., 1997; Zgurskaya and Nikaido, 1999; Murakami et al., 2002). Some OMFs such as TolC in *E. coli* are highly versatile and involved in the efflux of both antibiotics and proteins as part of different efflux systems (Akama et al., 2004a; Koronakis et al., 2004; Pietras et al., 2008; Phan et al., 2010; Hinchliffe et al., 2013; Krishnamoorthy et al., 2013). The MFP is suggested to stabilize the assembly of the pump, to contribute to the transfer of efflux-coupled conformational transitions from the RND transporter to the OMF and to affect substrate recognition (Ma et al., 1993; Akama et al., 2004b; Mikolosko et al., 2006). X-ray structures of the individual components of AcrAB-TolC and MexAB-OprM (the two main RND efflux systems of *E. coli* and *P. aeruginosa*, respectively) have been solved by X-ray crystallography, and also computational studies addressing structural and dynamical aspects of these components have been reported in the literature (Vaccaro et al., 2006, 2008; Schulz and Kleinekathöfer, 2009; Schulz et al., 2010, 2011, 2015; Fischer and Kandt, 2011, 2012; Vargiu et al., 2011; Raunest and

Kandt, 2012; Wang et al., 2012; Eicher et al., 2014; Fischer et al., 2014; Blair et al., 2015a). Still open are crucial questions about structure and stoichiometry of the functional assembly (Bavro et al., 2008; Krishnamoorthy et al., 2008; Misra and Bavro, 2009; Symmons et al., 2009; Tikhonova et al., 2011; Xu et al., 2011; Fernandez et al., 2012; Hinchliffe et al., 2013; Du et al., 2014), and also computational studies on the assembly are still in their infancy and limited to static aspects, not least because of the size and complexity of the whole systems (Symmons et al., 2009; Phillips and Gnanakaran, 2015).

The RND inner-membrane transporter subunit is integral to the function of the system. The transporter subunit of the RND-type tripartite complex functions as a proton/drug homotrimeric antiporter and is key for energy transduction and substrate specificity of the entire three-component complex (Murakami, 2008). Structural data have mainly been collected for AcrB, of *E. coli*, and to a lesser extent for MexB, the homolog of AcrB in *P. aeruginosa* (for a recent review, see Ruggerone et al., 2013a). According to crystallographic results, the shape of the protein resembles that of a jellyfish. Viewed orthogonally to the membrane plane, each protomer elongates for ~120 Å, comprising a TM region of ~50 Å composed of 12 α-helices (TM1 to TM12), and a periplasmic headpiece of about 70 Å, the latter being divided into a pore (porter) region and an upper region close to the lower part of the OMF (Murakami, 2008; Eicher et al., 2009).

After the first symmetric structure was solved (Murakami et al., 2002) other crystal structures of AcrB revealed asymmetric conformations of the three monomers in the trimer (Murakami et al., 2006; Seeger et al., 2006; Sennhauser et al., 2007). The three conformations were proposed to represent three consecutive states in a three-step peristaltic mechanism of the substrate translocation [called functional rotation (Murakami et al., 2006) or peristaltic motion (Seeger et al., 2006)]. The postulated functional rotation starts with recognition of substrate at a low affinity site on the L monomer, namely the AP. Global conformational transition converts the L to a T conformation, accompanied by tight binding of the substrate in a designated high-affinity binding pocket, i.e., the DP. Successively, a second peristaltic motion leads to a switch from the T to an O conformation, resulting in the release of the substrate toward the OMF. After substrate release, the O conformation relaxes back to the L conformation restarting the cyclic event. The conversion from the T to the O conformation is suggested to be the major energy-requiring step and should be accompanied by proton binding at the proton translocation site in the TM region. Proton release may occur during conversion from O to L. Computational studies based on targeted MD simulations supported this mechanism and the zipper-like closure of the DP (Schulz et al., 2010).

A 3.0 Å crystal structure of MexB showed the same overall fold as its close homolog AcrB did (Sennhauser et al., 2009). The three monomers constituting MexB assumed an asymmetric conformation supporting the general transport model for this family of multi-drug transporters derived from the AcrB structures (Murakami et al., 2006; Seeger et al., 2006; Sennhauser et al., 2007). However, the conformation of monomer L in MexB

showed significant differences at the periplasmic portal to AcrB. In particular, no access to the binding cavity was observed in this subunit. A clear rationale for this structural difference is missing to date. Sennhauser et al. (2009) proposed, among other things, that the differences might be attributed to the L monomer being trapped in an intermediate conformational state between the extrusion and the binding of the substrates. Alternatively, specific resting states of MexB and of AcrB may account for the observed differences. Recently, Nakashima et al. (2013) solved the structure of MexB in complex with a pyridopyrimidine derivative. This work provided the first structural information on MexB-inhibitor interactions. The authors also crystallized free MexB and found a structure largely similar to that described by Sennhauser et al. (2009). The binding geometry of the pyridopyrimidine derivative to AcrB was also resolved, and showed relevant variations in the conformation of the ligand. These findings highlighted that subtle differences in the mechanisms of drug binding and translocation are relevant for the two pumps.

Several key features of the MexB structure, in particular the AP and DP sites, could be mapped onto the structure of AcrB (Murakami et al., 2006; Nakashima et al., 2011; Eicher et al., 2012). The first and until now the only computational study of antibiotic-MexB interactions was based on these data (Collu et al., 2012b). Collu et al. (2012b) investigated the behavior of two carbapenems, meropenem and imipenem, in the AP and the DP. The two structurally related compounds are differently affected by the RND efflux pumps. The activity of meropenem is significantly reduced by MexAB-OprM efflux whereas the activity of imipenem is not (Masuda and Ohya, 1992; Pai et al., 2001; Pournaras et al., 2005; Walsh and Amyes, 2007). The different sensitivities to RND efflux make imipenem and meropenem attractive candidates for a comparative study of carbapenem-efflux-pump interactions.

Lacking a crystal structure of MexB in complex with the two molecules, the starting configurations for all-atom MD simulations were extracted from docking runs with the ATTRACT package (May and Zacharias, 2008; May et al., 2008; de Vries and Zacharias, 2012). The systems obtained after solvation and equilibration were simulated for 50 ns. A stronger preference of meropenem for the DP than for the AP resulted from the simulations (binding free energies of  $-8.1$  and  $2.4$  kcal mol $^{-1}$ , respectively). Imipenem had nearly the same low affinity for both pockets ( $0.6$  and  $0.4$  kcal mol $^{-1}$ , respectively). This result agreed with microbiological data showing a fourfold to eightfold increase of the MIC of meropenem but no significant change of the imipenem MIC upon overexpression of MexB in *P. aeruginosa* (Eguchi et al., 2007; Ong et al., 2007; Livermore, 2009; Riera et al., 2011). The contacts between meropenem and the DP extracted from the trajectories were qualitatively consistent with the recently determined structure of a MexB-inhibitor complex (Nakashima et al., 2013), suggesting a reliable prediction of the binding structures by the computational protocol of Collu et al. (2012b).

The AP is probably the first internal site to be occupied by compounds during the binding process. At the AP, imipenem and meropenem pointed their  $\beta$ -lactam rings toward the periplasmic region and the entrance to the DP, respectively. These could

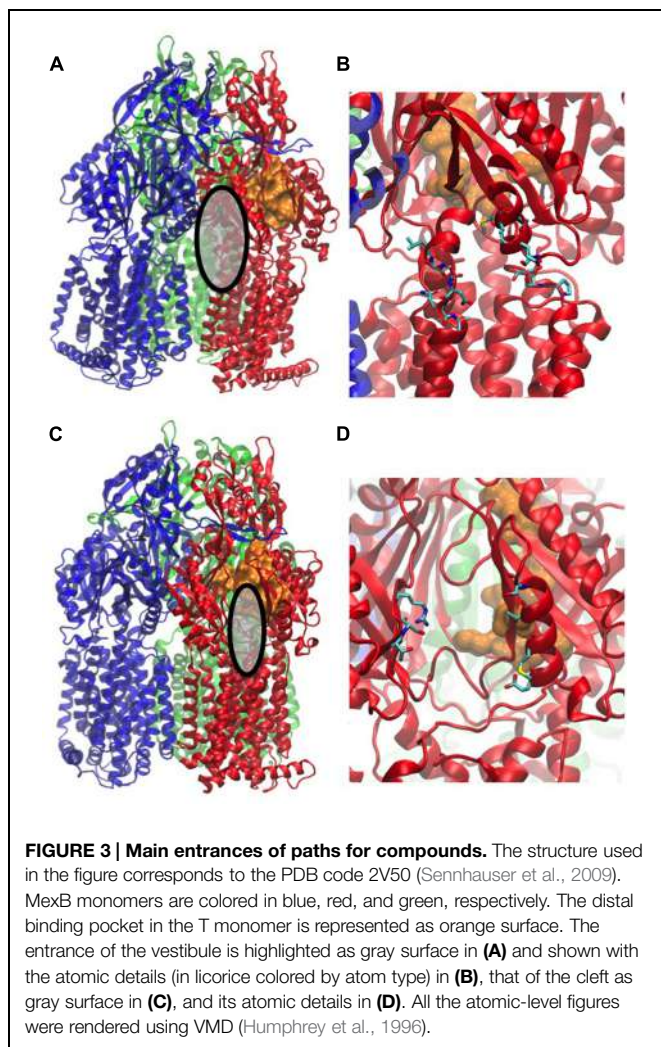
be considered as fingerprints of the different behavior of the two compounds. Meropenem tended to move toward the DP, following the plausible extrusion route, while imipenem had a propensity to reach regions close to the periplasm. Interactions with solvent molecules can be extracted and quantified from the trajectories as a further interesting detail in support of this picture (Serpone et al., 2001; Collu et al., 2012a). Collu et al. (2012a) found that imipenem, unlike meropenem, formed long-lifetime interactions with water molecules inside of MexB.

The docking poses of two compounds in the DP were similar but the 50 ns-long simulations led to different equilibrium binding modes. Meropenem moved in the DP of MexB toward the external channel, assuming a location suitable for extrusion. Imipenem slid away from the entrance to the channel connecting the DP to the extrusion mouth and into a position similar to that assumed by doxorubicin in MD simulations of mutated AcrB F610A (Vargiu et al., 2011). Indeed, Vargiu et al. (2011) found that doxorubicin moved deeper into the DP of a F610A mutant and was not extruded by the induced functional rotation. This was in accordance with reduced doxorubicin MIC (i.e., increased activity) against the F610A variant of AcrB (Bohnert et al., 2008).

The calculated pump interaction patterns have been associated with the different physicochemical properties of the ligand molecules. With its bulky and hydrophobic tail, meropenem established a strong interaction pattern to the aromatic-hydrophobic environment of the DP. Conversely, the more flexible and hydrophilic tail of imipenem had a lower affinity for the DP. Solvent interactions played a major role in the different transport properties of the two carbapenems as well. In fact, the compounds remained highly solvated at all explored binding sites (Collu et al., 2012b). Nonetheless, the water dynamics around meropenem were significantly different in the DP than in the bulk solvent. On the other hand, imipenem showed the same solvent interactions in the DP as in the bulk solvent.

## Paths for Substrate Entry

Substrate uptake by RND pumps is still largely unexplored and to our knowledge, only one computational study has addressed this issue (Yao et al., 2013). The entry of substrates into AcrB was studied by a combination of *in silico* tools and site-directed mutagenesis. The study indicated that uptake pathways of minocycline, acriflavine, and novobiocin differed significantly. Novobiocin is the largest and acriflavin the smallest among the three compounds while minocycline is more hydrophilic than the nearly equally hydrophobic novobiocin and acriflavin. All three molecules are typical substrates of AcrB but they vary in molecular size and hydrophobicity. A ligand-dependent drug uptake mechanism was proposed based on the analysis of the free energy associated with drug movement along AcrB tunnels. Strongly hydrophobic and lipophilic drugs of similar size were preferentially taken up via the vestibule path (the entrance of the vestibule path is shown in Figures 3A,B). This path starts close to the membrane surface at a region between two protomers and goes via the AP to the DP. Other drugs were translocated



through the cleft path starting at a large external indentation of the periplasmic domain, formed by the subdomains PC1 and PC2 of a single AcrB protomer. The cleft path, whose entrance is shown in **Figures 3C,D**, directly connects the periplasm to the DP (Husain and Nikaido, 2010). Smaller drugs were found to favor the vestibule path, while larger compounds preferentially took the cleft path.

The direct simulations identified a novel alternative uptake path, which is not visible in the crystal structure. This third path goes along the bottom of the porter domain toward PC1 and could be validated by site-directed mutagenesis of AcrB in *E. coli*. Mutations of residues located along the path significantly impaired the efflux efficiency. The work of Yao et al. (2013) is of great interest because it combined different techniques to gain insight into an important step of the efflux process. However, it has to be noted that the authors made several approximations. As in all the computational studies described in this review, the partners of the RND transporter (i.e., AcrA and TolC in the present case) were missing. It was also assumed that the drug uptake was mainly driven by hydrophobic interactions. Finally, some of the physicochemical properties such as the ordering of

amphiphilic drugs in the lipid bilayer and the conformational flexibility of drugs with rotatable bonds were neglected. Despite of the necessary approximations, the work of Yao et al. (2013) was an important contribution to the understanding of drug RND efflux. The structures of the L monomers and ligand conformations in co-crystals suggest interesting mechanistic differences between MexB and AcrB (Sennhauser et al., 2009; Nakashima et al., 2013). Thus, a similar study on MexB would be of great interest.

## Conclusion

Much progress has been made in the understanding of the transport mechanism of RND efflux pumps since they were discovered. Genetic and biochemical investigations have provided a good survey of the substrate specificity of different pump complexes in various bacteria. It has become accepted that RND pumps evolved as a first line of bacterial defense against exogenous substances, allowing the development of additional defense strategies (Olivares et al., 2013). Molecules that are able to penetrate the OM are potentially problematic for Gram-negative bacteria. Many sophisticated studies have supported this view as they have indicated that amphiphilic molecules (such as many antibiotics), which are able to pass the OM, are good substrates for export systems (Nikaido, 2011; Nikaido and Pages, 2012). X-ray crystallography has provided highly detailed structural information on binding interactions between pump subunits and substrates (Ruggerone et al., 2013a). It is intriguing that only a handful of a large number of known efflux substrates could be co-crystallized with efflux pumps. Although X-ray structures provide snap-shots of a complex transport mechanism, they have been crucial for the setup of a transport model. Concerning specific experiments aiming at a more direct investigation of efflux dynamics, studies with whole bacteria have been performed. Whole cell efflux assays require thorough controls to rule out non-specific effects that interfere with transport measurements. Such control measurements include the use of membrane-interacting probes to monitor effects on membrane integrity or on the electrochemical potential across the inner membrane. The finding that many of the membrane-interacting probes are efflux substrates too, has confirmed the concept of recognition and export of membrane-active compounds. Based on experimental data, new *in silico* tools have been developed and brought to a point where they can reliably describe or even predict the dynamics of compound extrusion by RND pump subunits.

Substrate recognition by RND efflux pumps is a multi-factorial process that can be measured by different methods as described in this article. MexB, for example, has a broad substrate spectrum including large (e.g., erythromycin) and charged (e.g., aztreonam, PAβN) molecules (see **Table 1**). MexB transports hydrophobic dyes, many of which have been primarily used to study membrane properties, which indicates a preference of this pump for hydrophobic substrates. This is in agreement with the finding that the activity of the hydrophilic antibiotic ceftobiprole is not significantly affected by MexB. Crystal structures and MD simulations of MexB strongly suggested that the DP, lined with

hydrophobic amino acid residues, is the main structural element for the recognition of hydrophobic elements (Collu et al., 2012b; Nakashima et al., 2013). However, hydrophobicity alone is not sufficient to explain substrate recognition by MexB. Imipenem and meropenem have a similar size and hydrophobicity (**Table 1**) but only meropenem is transported by MexB. A computational study revealed that imipenem, unlike meropenem, made no high affinity contacts to the AP or to the DP but instead made long-life interactions with solvent molecules inside MexB and eventually did not enter MexB (Collu et al., 2012b).

The challenge for future studies will be to combine the precision of X-ray structures with the functional relevance of whole cell studies. MD simulations based on experimental data provide a promising tool to complement, integrate and rationalize these data and to shed some light onto this problem.

Despite the advances outlined in the review, dissecting the molecular and conformational steps that regulate transport of substrates by RND pumps is still a very challenging and intriguing task and requires a very efficient interplay between techniques and approaches coming from different fields. The fate of a compound, governed by the action of an RND transporter (i.e., efficiently or poorly transported), is determined by the subtle balance of different molecular contributions that are not necessarily large. The interaction of meropenem and imipenem with MexB described in the Section *Computational Study* is a good example: small differences in flexibility and hydrophobicity are suggested to make the former a good substrate and the latter a poor one. Computational methods can offer insight at a level of accuracy that is not reachable by a single experimental technique but they need a continuous feedback from experiments. Further crystallographic studies of RND pumps in complex with substrates and more accurate modeling techniques with extended simulation times for large proteins are needed in order to achieve full atomic pictures of the

entire tripartite complexes. Efflux kinetics might be affected by several factors that have to be included in the simulations but are not known *a priori* (Kinana et al., 2013). Computer simulations can integrate data from experiments on the molecular level and help to interpret data from whole cell assays (i.e., functional efflux pump ensembles).

The development of novel antibiotics that can bypass the effects of MDR pumps or the development of clinically useful EPI is still a challenging task. Understanding the mechanistic details and the structure-function relationship of bacterial efflux systems, as well as their regulation and the synergistic interactions between the pumps and other resistance mechanisms, is not only scientifically rewarding but can also stimulate applied research for effective new antibacterial drugs.

## Addendum in Proof

While our manuscript was under review two comprehensive review articles by Li et al. (2015) and by Yamaguchi et al. (2015) were published that cover many aspects discussed in our article.

## Acknowledgments

PR has received support from the Innovative Medicines Initiative Joint Undertaking under Grant Agreement n°115525, resources, which are composed of financial contribution from the European Union's seventh framework program (FP7/2007–2013) and from EFPIA companies in kind contribution, as part of the Project TRANSLOCATION (<http://www.imi.europa.eu/content/translocation>).

We want to thank Dr. Stefan Reinelt for help with the calculation of the data in **Table 1** and Dr. Jonathan Thwaite for critically reading the document.

## References

- Aires, J. R., and Nikaido, H. (2005). Aminoglycosides are captured from both periplasm and cytoplasm by the AcrD multidrug efflux transporter of *Escherichia coli*. *J. Bacteriol.* 187, 1923–1929. doi: 10.1128/JB.187.6.1923-1929.2005
- Akama, H., Kanemaki, M., Yoshimura, M., Tsukihara, T., Kashiwagi, T., Yoneyama, H., et al. (2004a). Crystal structure of the drug discharge outer membrane protein, OprM, of *Pseudomonas aeruginosa*: dual modes of membrane anchoring and occluded cavity end. *J. Biol. Chem.* 279, 52816–52819. doi: 10.1074/jbc.C400445200
- Akama, H., Matsuura, T., Kashiwagi, S., Yoneyama, H., Narita, S.-I., Tsukihara, T., et al. (2004b). Crystal structure of the membrane fusion protein, MexA, of the multidrug transporter in *Pseudomonas aeruginosa*. *J. Biol. Chem.* 279, 25939–25942. doi: 10.1074/jbc.C400164200
- Amin, I. M., Richmond, G. E., Sen, P., Koh, T. H., Piddock, L. J., and Chua, K. L. (2013). A method for generating marker-less gene deletions in multidrug-resistant *Acinetobacter baumannii*. *BMC Microbiol.* 13:158. doi: 10.1186/1471-2180-13-158
- Angus, B. L., Carey, A. M., Caron, D. A., Kropinski, A. M., and Hancock, R. E. (1982). Outer membrane permeability in *Pseudomonas aeruginosa*: comparison of a wild-type with an antibiotic-supersusceptible mutant. *Antimicrob. Agents Chemother.* 21, 299–309. doi: 10.1128/AAC.21.2.299
- Baum, E. Z., Crespo-Carbone, S. M., Morrow, B. J., Davies, T. A., Foleno, B. D., He, W., et al. (2009). Effect of MexXY overexpression on ceftobiprole susceptibility in *Pseudomonas aeruginosa*. *Antimicrob. Agents Chemother.* 53, 2785–2790. doi: 10.1128/AAC.00018-09
- Bavro, V. N., Pietras, Z., Furnham, N., Pérez-Cano, L., Fernández-Recio, J., Pei, X. Y., et al. (2008). Assembly and channel opening in a bacterial drug efflux machine. *Mol. Cell.* 30, 114–121. doi: 10.1016/j.molcel.2008.02.015
- Biarnés, X., Bongarzone, S., Vargiu, A. V., Carloni, P., and Ruggerone, P. (2011). Molecular motions in drug design: the coming age of the metadynamics method. *J. Comput. Aided Mol. Des.* 25, 395–402. doi: 10.1007/s10822-011-9415-3
- Blair, J. M., Bavro, V. N., Ricci, V., Modi, N., Cacciottolo, P., Kleinekathfer, U., et al. (2015a). AcrB drug-binding pocket substitution confers clinically relevant resistance and altered substrate specificity. *Proc. Natl. Acad. Sci. U.S.A.* 112, 3511–3516. doi: 10.1073/pnas.1419939112
- Blair, J. M. A., Webber, M. A., Baylay, A. J., Ogbolu, D. O., and Piddock, L. J. V. (2015b). Molecular mechanisms of antibiotic resistance. *Nat. Rev. Microbiol.* 13, 42–51. doi: 10.1038/nrmicro3380
- Blair, J. M., Richmond, G. E., and Piddock, L. J. (2014). Multidrug efflux pumps in Gram-negative bacteria and their role in antibiotic resistance. *Fut. Microbiol.* 9, 1165–1177. doi: 10.2217/fmb.14.66
- Bohnert, J. A., Karamian, B., and Nikaido, H. (2010). Optimized Nile Red efflux assay of AcrAB-TolC multidrug efflux system shows competition

- between substrates. *Antimicrob. Agents Chemother.* 54, 3770–3775. doi: 10.1128/AAC.00620-10
- Bohnert, J. A., Schuster, S., Seeger, M. A., Fähnrich, E., Pos, K. M., and Kern, W. V. (2008). Site-directed mutagenesis reveals putative substrate binding residues in the *Escherichia coli* RND efflux pump AcrB. *J. Bacteriol.* 190, 8225–8229. doi: 10.1128/JB.00912-08
- Bohnert, J. A., Schuster, S., Szymaniak-Vits, M., and Kern, W. V. (2011a). Determination of real-time efflux phenotypes in *Escherichia coli* AcrB binding pocket phenylalanine mutants using a 1,2'-dinaphthylamine efflux assay. *PLoS ONE* 6:e21196. doi: 10.1371/journal.pone.0021196
- Bohnert, J. A., Szymaniak-Vits, M., Schuster, S., and Kern, W. V. (2011b). Efflux inhibition by selective serotonin reuptake inhibitors in *Escherichia coli*. *J. Antimicrob. Chemother.* 66, 2057–2060. doi: 10.1093/jac/dkr258
- Borges-Walmsley, M. I., McKeegan, K. S., and Walmsley, A. R. (2003). Structure and function of efflux pumps that confer resistance to drugs. *Biochem. J.* 376, 313–338. doi: 10.1042/BJ20020957
- Brown, D. G., May-Dracka, T. L., Gagnon, M. M., and Tommasi, R. (2014). Trends and exceptions of physical properties on antibacterial activity for Gram-positive and Gram-negative pathogens. *J. Med. Chem.* 57, 10144–10161. doi: 10.1021/jm501552x
- Butler, M. J., Bergeron, A., Soostmeyer, G., Zimny, T., and Malek, L. T. (1993). Cloning and characterisation of an aminopeptidase P-encoding gene from *Streptomyces lividans*. *Gene* 123, 115–119. doi: 10.1016/0378-1119(93)90549-I
- Cai, H., Rose, K., Liang, L. H., Dunham, S., and Stover, C. (2009). Development of a liquid chromatography/mass spectrometry-based drug accumulation assay in *Pseudomonas aeruginosa*. *Anal. Biochem.* 385, 321–325. doi: 10.1016/j.ab.2008.10.041
- Caiazza, N. C., Shanks, R. M., and O'toole, G. A. (2005). Rhamnolipids modulate swarming motility patterns of *Pseudomonas aeruginosa*. *J. Bacteriol.* 187, 7351–7361. doi: 10.1128/JB.187.21.7351-7361.2005
- Castanheira, M., Deshpande, L. M., Costello, A., Davies, T. A., and Jones, R. N. (2014). Epidemiology and carbapenem resistance mechanisms of carbapenem-non-susceptible *Pseudomonas aeruginosa* collected during 2009–11 in 14 European and Mediterranean countries. *J. Antimicrob. Chemother.* 69, 1804–1814. doi: 10.1093/jac/dku048
- CDC. (2013). US Department of Health and Human Services. Centers for Disease Control and Prevention. *Antibiotic Resistance Threats in the United States*, 2013. Available at: <http://www.cdc.gov/drug-resistance/pdf/arthreats-2013-508.pdf>
- Chen, J., Morita, Y., Huda, M. N., Kuroda, T., Mizushima, T., and Tsuchiya, T. (2002). VmrA a member of a novel class of Na<sup>+</sup>-coupled multidrug efflux pumps from *Vibrio parahaemolyticus*. *J. Bacteriol.* 184, 572–576. doi: 10.1128/JB.184.2.572-576.2002
- Chipot, C. (2008). Free energy calculations applied to membrane proteins. *Methods Mol. Biol.* 443, 121–144. doi: 10.1007/978-1-59745-177-2\_7
- Chollet, R., Chevalier, J., Bryskier, A., and Pages, J. M. (2004). The AcrAB-TolC pump is involved in macrolide resistance but not in telithromycin efflux in *Enterobacter aerogenes* and *Escherichia coli*. *Antimicrob. Agents Chemother.* 48, 3621–3624. doi: 10.1128/AAC.48.9.3621-3624.2004
- Chopra, I. (2002). New developments in tetracycline antibiotics: glycylcyclines and tetracycline efflux pump inhibitors. *Drug Resist. Update* 5, 119–125. doi: 10.1016/S1368-7646(02)00051-1
- Chopra, I., and Roberts, M. (2001). Tetracycline antibiotics: mode of action, applications, molecular biology, and epidemiology of bacterial resistance. *Microbiol. Mol. Biol. Rev.* 65, 232–260. doi: 10.1128/MMBR.65.2.232-260.2001
- Collu, F., and Cascella, M. (2013). Multidrug resistance and efflux pumps: insights from molecular dynamics simulations. *Curr. Top. Med. Chem.* 13, 3165–3183. doi: 10.2174/15680266113136660224
- Collu, F., Ceccarelli, M., and Ruggerone, P. (2012a). Exploring binding properties of agonists interacting with a δ-opioid receptor. *PLoS ONE* 7:e52633. doi: 10.1371/journal.pone.0052633
- Collu, F., Vargiu, A. V., Dreier, J., Cascella, M., and Ruggerone, P. (2012b). Recognition of imipenem and meropenem by the Rnd-transporter MexB studied by computer simulations. *J. Am. Chem. Soc.* 134, 19146–19158. doi: 10.1021/ja307803m
- Cowan, S. W., Schirmer, T., Rummel, G., Steiert, M., Ghosh, R., Paupit, R. A., et al. (1992). Crystal structures explain functional properties of two *E. coli* porins. *Nature* 358, 727–733. doi: 10.1038/358727a0
- Coyne, S., Rosenfeld, N., Lambert, T., Courvalin, P., and Perichon, B. (2010). Overexpression of resistance-nodulation-cell division pump AdeFGH confers multidrug resistance in *Acinetobacter baumannii*. *Antimicrob. Agents Chemother.* 54, 4389–4393. doi: 10.1128/AAC.00155-10
- Dal Peraro, M., Ruggerone, P., Raugei, S., Gervasio, F. L., and Carloni, P. (2007). Investigating biological systems using first principles Car-Parrinello molecular dynamics simulations. *Curr. Opin. Struct. Biol.* 17, 149–156. doi: 10.1016/j.sbi.2007.03.018
- Damier-Piolle, L., Magnet, S., Bremont, S., Lambert, T., and Courvalin, P. (2008). AdeIJK, a resistance-nodulation-cell division pump effluxing multiple antibiotics in *Acinetobacter baumannii*. *Antimicrob. Agents Chemother.* 52, 557–562. doi: 10.1128/AAC.00732-07
- Davin-Regli, A., Bolla, J. M., James, C. E., Lavigne, J. P., Chevalier, J., Garnotel, E., et al. (2008). Membrane permeability and regulation of drug "influx and efflux" in enterobacterial pathogens. *Curr. Drug Targets* 9, 750–759. doi: 10.2174/138945008785747824
- Dean, C. R., Visalli, M. A., Projan, S. J., Sum, P. E., and Bradford, P. A. (2003). Efflux-mediated resistance to tigecycline (GAR-936) in *Pseudomonas aeruginosa* PAO1. *Antimicrob. Agents Chemother.* 47, 972–978. doi: 10.1128/AAC.47.3.972-978.2003
- Delcour, A. H. (2009). Outer membrane permeability and antibiotic resistance. *Biochim. Biophys. Acta* 1794, 808–816. doi: 10.1016/j.bbapap.2008.11.005
- Delmar, J. A., Su, C. C., and Yu, E. W. (2014). Bacterial multidrug efflux transporters. *Annu. Rev. Biophys.* 43, 93–117. doi: 10.1146/annurev-biophys-051013-022855
- Denys, G. A., and Relich, R. F. (2014). Antibiotic resistance in nosocomial respiratory infections. *Clin. Lab. Med.* 34, 257–270. doi: 10.1016/j.cll.2014.02.004
- de Vries, S. J., and Zacharias, M. (2012). Attract-Em: a new method for the computational assembly of large molecular machines using cryo-EM maps. *PLoS ONE* 7:e49733. doi: 10.1371/journal.pone.0049733
- Deziel, E., Lepine, F., Milot, S., and Villemur, R. (2003). rhlA is required for the production of a novel biosurfactant promoting swarming motility in *Pseudomonas aeruginosa*: 3-(3-hydroxyalkanoyloxy)alkanoic acids (HAAs), the precursors of rhamnolipids. *Microbiology* 149, 2005–2013. doi: 10.1099/mic.0.26154-0
- Dreier, J. (2007). "Active Drug Efflux in Bacteria," in: *Enzyme-Mediated Resistance to Antibiotics: Mechanisms, Dissemination, and Prospects for Inhibition*, First Edn, ed. R. A. T. M. E. Bonomo (Washington, DC: ASM Press). doi: 10.1128/9781555815615.ch15
- Du, D., Van Veen, H. W., and Luisi, B. F. (2015). Assembly and operation of bacterial tripartite multidrug efflux pumps. *Trends Microbiol.* 23, 311–319. doi: 10.1016/j.tim.2015.01.010
- Du, D., Wang, Z., James, N. R., Voss, J. E., Klimont, E., Ohene-Agyei, T., et al. (2014). Structure of the AcrAB-TolC multidrug efflux pump. *Nature* 509, 512–515. doi: 10.1038/nature13205
- Dunham, S. A., McPherson, C. J., and Miller, A. A. (2010). The relative contribution of efflux and target gene mutations to fluoroquinolone resistance in recent clinical isolates of *Pseudomonas aeruginosa*. *Eur. J. Clin. Microbiol. Infect. Dis.* 29, 279–288. doi: 10.1007/s10096-009-0852-z
- ECDC. (2015). European Centre for Disease Prevention and Control. Annual Epidemiological Report 2014 Antimicrobial Resistance and Healthcare-Associated Infections, Stockholm.
- Eda, S., Maseda, H., and Nakae, T. (2003). An elegant means of self-protection in gram-negative bacteria by recognizing and extruding xenobiotics from the periplasmic space. *J. Biol. Chem.* 278, 2085–2088. doi: 10.1074/jbc.C200661200
- Eguchi, K., Ueda, Y., Kanazawa, K., Sunagawa, M., and Gotoh, N. (2007). The mode of action of 2-(thiazol-2-ylthio)-1beta-methylcarbenems against *Pseudomonas aeruginosa*: the impact of outer membrane permeability and the contribution of MexAB-OprM efflux system. *J. Antibiot.* 60, 129–135. doi: 10.1038/ja.2007.12
- Eicher, T., Brandstatter, L., and Pos, K. M. (2009). Structural and functional aspects of the multidrug efflux pump AcrB. *Biol. Chem.* 390, 693–699. doi: 10.1515/BC.2009.090
- Eicher, T., Cha, H. J., Seeger, M. A., Brandstatter, L., El-Delik, J., Bohnert, J. A., et al. (2012). Transport of drugs by the multidrug transporter AcrB involves an access

- and a deep binding pocket that are separated by a switch-loop. *Proc. Natl. Acad. Sci. U.S.A.* 109, 5687–5692. doi: 10.1073/pnas.1114944109
- Eicher, T., Seeger, M. A., Anselmi, C., Zhou, W., Brandstatter, L., Verrey, F., et al. (2014). Coupling of remote alternating-access transport mechanisms for protons and substrates in the multidrug efflux pump AcrB. *Elife* 19, 3. doi: 10.7554/eLife.03145
- Elkins, C. A., and Nikaido, H. (2002). Substrate specificity of the RND-type multidrug efflux pumps AcrB and AcrD of *Escherichia coli* is determined predominantly by two large periplasmic loops. *J. Bacteriol.* 184, 6490–6498. doi: 10.1128/JB.184.23.6490-6499.2002
- Fernandez, L., and Hancock, R. E. (2012). Adaptive and mutational resistance: role of porins and efflux pumps in drug resistance. *Clin. Microbiol. Rev.* 25, 661–681. doi: 10.1128/CMR.00043-12
- Ferrandez, Y., Monlezun, L., Phan, G., Benabdellah, H., Benas, P., Ulryck, N., et al. (2012). Stoichiometry of the MexA-OprM binding, as investigated by blue native gel electrophoresis. *Electrophoresis* 33, 1282–1287. doi: 10.1002/elps.201100541
- Ferreira, M. M. C., and Kiralj, R. (2004). QSAR study of  $\beta$ -lactam antibiotic efflux by the multidrug resistance pump AcrB. *J. Chemometr.* 18, 242–252. doi: 10.1002/cem.867
- Fieldler, F., and Hinz, H. (1994). No intermediate channelling in stepwise hydrolysis of fluorescein di-beta-D-galactoside by beta-galactosidase. *Eur. J. Biochem.* 222, 75–81. doi: 10.1111/j.1432-1033.1994.tb18843.x
- Fischer, N., and Kandt, C. (2011). Three ways in, one way out: water dynamics in the trans-membrane domains of the inner membrane translocase AcrB. *Proteins* 79, 2871–2885. doi: 10.1002/prot.23122
- Fischer, N., and Kandt, C. (2012). Porter domain opening and closing motions in the multi-drug efflux transporter AcrB. *Biochim. Biophys. Acta* 1828, 632–641. doi: 10.1016/j.bbapm.2012.10.016
- Fischer, N., Raunest, M., Schmidt, T. H., Koch, D. C., and Kandt, C. (2014). Efflux pump-mediated antibiotics resistance: insights from computational structural biology. *Interdiscip. Sci.* 6, 1–12. doi: 10.1007/s12539-014-0191-3
- Fukuda, H., Hosaka, M., Hirai, K., and Iyobe, S. (1990). New norfloxacin resistance gene in *Pseudomonas aeruginosa* Pao. *Antimicrob. Agents Chemother.* 34, 1757–1761. doi: 10.1128/AAC.34.9.1757
- Fukuda, H., Hosaka, M., Iyobe, S., Gotoh, N., Nishino, T., and Hirai, K. (1995). nfxC-type quinolone resistance in a clinical isolate of *Pseudomonas aeruginosa*. *Antimicrob. Agents Chemother.* 39, 790–792. doi: 10.1128/AAC.39.3.790
- Garvey, M. I., and Piddock, L. J. (2008). The efflux pump inhibitor reserpine selects multidrug-resistant *Streptococcus pneumoniae* strains that overexpress the ABC transporters PatA and PatB. *Antimicrob. Agents Chemother.* 52, 1677–1685. doi: 10.1128/AAC.01644-07
- Germ, M., Yoshihara, E., Yoneyama, H., and Nakae, T. (1999). Interplay between the efflux pump and the outer membrane permeability barrier in fluorescent dye accumulation in *Pseudomonas aeruginosa*. *Biochem. Biophys. Res. Commun.* 261, 452–455. doi: 10.1006/bbrc.1999.1045
- Giske, C. G., Boren, C., Wretlind, B., and Kronvall, G. (2005). Meropenem susceptibility breakpoint for *Pseudomonas aeruginosa* strains hyperproducing mexB mRNA. *Clin. Microbiol. Infect.* 11, 662–669. doi: 10.1111/j.1469-0951.2005.01182.x
- Gonzalez, R. J., and Tarloff, J. B. (2001). Evaluation of hepatic subcellular fractions for Alamar blue and MTT reductase activity. *Toxicol. In Vitro* 15, 257–259. doi: 10.1016/S0887-2333(01)00014-5
- Greenspan, P., and Fowler, S. D. (1985). Spectrofluorometric studies of the lipid probe, nile red. *J. Lipid Res.* 26, 781–789.
- Griffith, D. C., Corcoran, E., Lofland, D., Lee, A., Cho, D., Lomovskaya, O., et al. (2006). Pharmacodynamics of levofloxacin against *Pseudomonas aeruginosa* with reduced susceptibility due to different efflux pumps: do elevated MICs always predict reduced in vivo efficacy? *Antimicrob. Agents Chemother.* 50, 1628–1632. doi: 10.1128/AAC.50.5.1628-1632.2006
- Grkovic, S., Brown, M. H., and Skurray, R. A. (2002). Regulation of bacterial drug export systems. *Microbiol. Mol. Biol. Rev.* 66, 671–701. doi: 10.1128/MMBR.66.4.671-701.2002
- Hancock, R. E. (1997). The bacterial outer membrane as a drug barrier. *Trends Microbiol.* 5, 37–42. doi: 10.1016/S0966-842X(97)81773-8
- Hayashi, K., Fukushima, A., Hayashi-Nishino, M., and Nishino, K. (2014). Effect of methylglyoxal on multidrug-resistant *Pseudomonas aeruginosa*. *Front. Microbiol.* 5:180. doi: 10.3389/fmicb.2014.00180
- Hidron, A. I., Edwards, J. R., Patel, J., Horan, T. C., Sievert, D. M., Pollock, D. A., et al. (2008). NHSN annual update: antimicrobial-resistant pathogens associated with healthcare-associated infections: annual summary of data reported to the National Healthcare Safety Network at the Centers for Disease Control and Prevention, 2006–2007. *Infect. Control. Hosp. Epidemiol.* 29, 996–1011. doi: 10.1086/591861
- Hinchliffe, P., Symmons, M. F., Hughes, C., and Koronakis, V. (2013). Structure and operation of bacterial tripartite pumps. *Annu. Rev. Microbiol.* 67, 221–242. doi: 10.1146/annurev-micro-092412-155718
- Hirata, T., Saito, A., Nishino, K., Tamura, N., and Yamaguchi, A. (2004). Effects of efflux transporter genes on susceptibility of *Escherichia coli* to tigecycline (GAR-936). *Antimicrob. Agents Chemother.* 48, 2179–2184. doi: 10.1128/AAC.48.6.2179-2184.2004
- Hocquet, D., Nordmann, P., El Garch, F., Cabanne, L., and Plesiat, P. (2006). Involvement of the MexXY-OprM efflux system in emergence of ceftazidime resistance in clinical strains of *Pseudomonas aeruginosa*. *Antimicrob. Agents Chemother.* 50, 1347–1351. doi: 10.1128/AAC.50.4.1347-1351.2006
- Humphrey, W., Dalke, A., and Schulten, K. (1996). Vmd: visual molecular dynamics. *J. Mol. Graph.* 14, 33–38. doi: 10.1016/0263-7855(96)00018-5
- Husain, F., and Nikaido, H. (2010). Substrate path in the AcrB multidrug efflux pump of *Escherichia coli*. *Mol. Microbiol.* 78, 320–330. doi: 10.1111/j.1365-2958.2010.07330.x
- Iino, R., Hayama, K., Amezawa, H., Sakakihara, S., Kim, S. H., Matsumono, Y., et al. (2012a). A single-cell drug efflux assay in bacteria by using a directly accessible femtoliter droplet array. *Lab. Chip.* 12, 3923–3929. doi: 10.1039/c2lc40394c
- Iino, R., Nishino, K., Noji, H., Yamaguchi, A., and Matsumoto, Y. (2012b). A microfluidic device for simple and rapid evaluation of multidrug efflux pump inhibitors. *Front. Microbiol.* 3:40. doi: 10.3389/fmicb.2012.00040
- Iino, R., Matsumoto, Y., Nishino, K., Yamaguchi, A., and Noji, H. (2013). Design of a large-scale femtoliter droplet array for single-cell analysis of drug-tolerant and drug-resistant bacteria. *Front. Microbiol.* 4:300. doi: 10.3389/fmicb.2013.00300
- Jones, R. N., Stilwell, M. G., Rhomberg, P. R., and Sader, H. S. (2009). Antipseudomonal activity of piperacillin/tazobactam: more than a decade of experience from the SENTRY Antimicrobial Surveillance Program (1997–2007). *Diagn. Microbiol. Infect. Dis.* 65, 331–334. doi: 10.1016/j.diagmicrobio.2009.06.022
- Kamal, M. Z., Ali, J., and Rao, N. M. (2013). Binding of bis-ANS to *Bacillus subtilis* lipase: a combined computational and experimental investigation. *Biochim. Biophys. Acta* 1834, 1501–1509. doi: 10.1016/j.bbapap.2013.04.021
- Kamerlin, S. C., Vicatos, S., Dryga, A., and Warshel, A. (2011). Coarse-grained (multiscale) simulations in studies of biophysical and chemical systems. *Annu. Rev. Phys. Chem.* 62, 41–64. doi: 10.1146/annurev-physchem-032210-103335
- Kamio, Y., and Nikaido, H. (1976). Outer membrane of *Salmonella typhimurium*: accessibility of phospholipid head groups to phospholipase c and cyanogen bromide activated dextran in the external medium. *Biochemistry* 15, 2561–2570. doi: 10.1021/bi00657a012
- Karplus, M. (2014). Development of multiscale models for complex chemical systems: from  $H^+H(2)$  to biomolecules (Nobel Lecture). *Angew. Chem. Int. Ed. Engl.* 53, 9992–10005. doi: 10.1002/anie.201403924
- Kim, J. S., Jeong, H., Song, S., Kim, H.-Y., Lee, K., Hyun, J., et al. (2015). Structure of the tripartite multidrug efflux pump acrAB-TolC suggests an alternative assembly mode. *Mol. Cells* 38, 180–186. doi: 10.14348/molcells.2015.2277
- Kinana, A. D., Vargiu, A. V., and Nikaido, H. (2013). Some ligands enhance the efflux of other ligands by the *Escherichia coli* multidrug pump AcrB. *Biochemistry* 52, 8342–8351. doi: 10.1021/bi401303v
- Kobayashi, N., Tamura, N., Van Veen, H. W., Yamaguchi, A., and Murakami, S. (2014).  $\beta$ -Lactam selectivity of multidrug transporters AcrB and AcrD resides in the proximal binding pocket. *J. Biol. Chem.* 289, 10680–10690. doi: 10.1074/jbc.M114.547794
- Kohler, T., Kok, M., Michea-Hamzehpour, M., Plesiat, P., Gotoh, N., Nishino, T., et al. (1996). Multidrug efflux in intrinsic resistance to trimethoprim and sulfamethoxazole in *Pseudomonas aeruginosa*. *Antimicrob. Agents Chemother.* 40, 2288–2290.

- Kohler, T., Micheal-Hamzehpour, M., Plesiat, P., Kahr, A. L., and Pechere, J. C. (1997). Differential selection of multidrug efflux systems by quinolones in *Pseudomonas aeruginosa*. *Antimicrob. Agents Chemother.* 41, 2540–2543.
- Kollman, P. A., Massova, I., Reyes, C., Kuhn, B., Huo, S., Chong, L., et al. (2000). Calculating structures and free energies of complex molecules: combining molecular mechanics and continuum models. *Acc. Chem. Res.* 33, 889–897. doi: 10.1021/ar000033j
- Koronakis, V., Eswaran, J., and Hughes, C. (2004). Structure and function of TolC: the bacterial exit duct for proteins and drugs. *Annu. Rev. Biochem.* 73, 467–489. doi: 10.1146/annurev.biochem.73.011303.074104
- Koronakis, V., Sharff, A., Koronakis, E., Luisi, B., and Hughes, C. (2000). Crystal structure of the bacterial membrane protein TolC central to multidrug efflux and protein export. *Nature* 405, 914–919. doi: 10.1038/35016007
- Kriengkauykiat, J., Porter, E., Lomovskaya, O., and Wong-Beringer, A. (2005). Use of an efflux pump inhibitor to determine the prevalence of efflux pump-mediated fluoroquinolone resistance and multidrug resistance in *Pseudomonas aeruginosa*. *Antimicrob. Agents Chemother.* 49, 565–570. doi: 10.1128/AAC.49.2.565–570.2005
- Krishnamoorthy, G., Tikhonova, E. B., Dhamdhare, G., and Zgurskaya, H. I. (2013). On the role of TolC in multidrug efflux: the function and assembly of AcrAB-TolC tolerate significant depletion of intracellular TolC protein. *Mol. Microbiol.* 87, 982–997. doi: 10.1111/mmi.12143
- Krishnamoorthy, G., Tikhonova, E. B., and Zgurskaya, H. I. (2008). Fitting periplasmic membrane fusion proteins to inner membrane transporters: mutations that enable *Escherichia coli* AcrA to function with *Pseudomonas aeruginosa* MexB. *J. Bacteriol.* 190, 691–698. doi: 10.1128/JB.01276-07
- Kumar, A., Chua, K. L., and Schweizer, H. P. (2006). Method for regulated expression of single-copy efflux pump genes in a surrogate *Pseudomonas aeruginosa* strain: identification of the BpeEF-OprC chloramphenicol and trimethoprim efflux pump of *Burkholderia pseudomallei* 1026b. *Antimicrob. Agents Chemother.* 50, 3460–3463. doi: 10.1128/AAC.00440-06
- Kumar, A., and Schweizer, H. P. (2005). Bacterial resistance to antibiotics: active efflux and reduced uptake. *Adv. Drug Deliv. Rev.* 57, 1486–1513. doi: 10.1016/j.addr.2005.04.004
- Laio, A., and Gervasio, F. L. (2008). Metadynamics: a method to simulate rare events and reconstruct the free energy in biophysics, chemistry and material science. *Rep. Prog. Phys.* 71, 126601. doi: 10.1088/0034-4885/71/12/126601
- Laio, A., Rodriguez-Fortea, A., Gervasio, F. L., Ceccarelli, M., and Parrinello, M. (2005). Assessing the accuracy of metadynamics. *J. Phys. Chem. B* 109, 6714–6721. doi: 10.1021/jp045424k
- Lamers, R. P., Cavallari, J. F., and Burrows, L. L. (2013). The efflux inhibitor phenylalanine-arginine beta-naphthylamide (PabetaN) permeabilizes the outer membrane of gram-negative bacteria. *PLoS ONE* 8:e60666. doi: 10.1371/journal.pone.0060666
- Lau, C. H., Hughes, D., and Poole, K. (2014). MexY-promoted aminoglycoside resistance in *Pseudomonas aeruginosa*: involvement of a putative proximal binding pocket in aminoglycoside recognition. *MBio* 5:e01068. doi: 10.1128/mBio.01068-14
- LePecq, J. B., and Paoletti, C. (1967). A fluorescent complex between ethidium bromide and nucleic acids. Physical-chemical characterization. *J. Mol. Biol.* 27, 87–106. doi: 10.1016/0022-2836(67)90353-1
- Levy, S. B. (1992). Active efflux mechanisms for antimicrobial resistance. *Antimicrob. Agents Chemother.* 36, 695–703. doi: 10.1128/AAC.36.4.695
- Li, X. Z., Ma, D., Livermore, D. M., and Nikaido, H. (1994). Role of efflux pump(s) in intrinsic resistance of *Pseudomonas aeruginosa*: active efflux as a contributing factor to beta-lactam resistance. *Antimicrob. Agents Chemother.* 38, 1742–1752. doi: 10.1128/AAC.38.8.1742
- Li, X. Z., Nikaido, H., and Poole, K. (1995). Role of mexA-mexB-oprM in antibiotic efflux in *Pseudomonas aeruginosa*. *Antimicrob. Agents Chemother.* 39, 1948–1953. doi: 10.1128/AAC.39.9.1948
- Li, X. Z., Plesiat, P., and Nikaido, H. (2015). The challenge of efflux-mediated antibiotic resistance in Gram-negative bacteria. *Clin. Microbiol. Rev.* 28, 337–418. doi: 10.1128/CMR.00117-14
- Li, Y., Mima, T., Komori, Y., Morita, Y., Kuroda, T., Mizushima, T., et al. (2003). A new member of the tripartite multidrug efflux pumps, MexVW-OprM, in *Pseudomonas aeruginosa*. *J. Antimicrob. Chemother.* 52, 572–575. doi: 10.1093/jac/dkg390
- Lister, P. D., Wolter, D. J., and Hanson, N. D. (2009). Antibacterial-resistant *Pseudomonas aeruginosa*: clinical impact and complex regulation of chromosomally encoded resistance mechanisms. *Clin. Microbiol. Rev.* 22, 582–610. doi: 10.1128/CMR.00040-09
- Livermore, D. M. (2009). Has the era of untreatable infections arrived? *J. Antimicrob. Chemother.* 64(Suppl. 1), i29–i36. doi: 10.1093/jac/dkp255
- Loh, B., Grant, C., and Hancock, R. E. (1984). Use of the fluorescent probe 1-N-phenylnaphthylamine to study the interactions of aminoglycoside antibiotics with the outer membrane of *Pseudomonas aeruginosa*. *Antimicrob. Agents Chemother.* 26, 546–551. doi: 10.1128/AAC.26.4.546
- Lomovskaya, O., and Bostian, K. A. (2006). Practical applications and feasibility of efflux pump inhibitors in the clinic—a vision for applied use. *Biochem. Pharmacol.* 71, 910–918. doi: 10.1016/j.bcp.2005.12.008
- Lomovskaya, O., Lee, A., Hoshino, K., Ishida, H., Mistry, A., Warren, M. S., et al. (1999). Use of a genetic approach to evaluate the consequences of inhibition of efflux pumps in *Pseudomonas aeruginosa*. *Antimicrob. Agents Chemother.* 43, 1340–1346.
- Lomovskaya, O., Warren, M. S., Lee, A., Galazzo, J., Fronko, R., Lee, M., et al. (2001). Identification and characterization of inhibitors of multidrug resistance efflux pumps in *Pseudomonas aeruginosa*: novel agents for combination therapy. *Antimicrob. Agents Chemother.* 45, 105–116. doi: 10.1128/AAC.45.1.105–116.2001
- Loontiens, F. G., Regenfuss, P., Zechel, A., Dumortier, L., and Clegg, R. M. (1990). Binding characteristics of Hoechst 33258 with calf thymus DNA, poly[d(A-T)], and d(CCGGAATTCCGG): multiple stoichiometries and determination of tight binding with a wide spectrum of site affinities. *Biochemistry* 29, 9029–9039. doi: 10.1021/bi00490a021
- Ma, D., Cook, D. N., Alberti, M., Pon, N. G., Nikaido, H., and Hearst, J. E. (1993). Molecular cloning and characterization of acrA and acrE genes of *Escherichia coli*. *J. Bacteriol.* 175, 6299–6313.
- Magnet, S., Courvalin, P., and Lambert, T. (2001). Resistance-nodulation-cell division-type efflux pump involved in aminoglycoside resistance in *Acinetobacter baumannii* strain BM4454. *Antimicrob. Agents Chemother.* 45, 3375–3380. doi: 10.1128/AAC.45.12.3375–3380.2001
- Mahamoud, A., Chevalier, J., Alibert-Franco, S., Kern, W. V., and Pages, J. M. (2007). Antibiotic efflux pumps in Gram-negative bacteria: the inhibitor response strategy. *J. Antimicrob. Chemother.* 59, 1223–1229. doi: 10.1093/jac/dkl493
- Mao, W., Warren, M. S., Black, D. S., Satou, T., Murata, T., Nishino, T., et al. (2002). On the mechanism of substrate specificity by resistance nodulation division (RND)-type multidrug resistance pumps: the large periplasmic loops of MexD from *Pseudomonas aeruginosa* are involved in substrate recognition. *Mol. Microbiol.* 46, 889–901. doi: 10.1046/j.1365-2958.2002.03223.x
- Mao, W., Warren, M. S., Lee, A., Mistry, A., and Lomovskaya, O. (2001). MexXY-OprM efflux pump is required for antagonism of aminoglycosides by divalent cations in *Pseudomonas aeruginosa*. *Antimicrob. Agents Chemother.* 45, 2001–2007. doi: 10.1128/AAC.45.7.2001-2007.2001
- Marks, N., Suhar, A., and Benuck, M. (1981). Peptide processing in the central nervous system. *Adv. Biochem. Psychopharmacol.* 28, 49–60.
- Markwick, P. R., and McCammon, J. A. (2011). Studying functional dynamics in bio-molecules using accelerated molecular dynamics. *Phys. Chem. Chem. Phys.* 13, 20053–20065. doi: 10.1039/c1cp22100k
- Martinez, J. L., and Baquero, F. (2014). Emergence and spread of antibiotic resistance: setting a parameter space. *Ups. J. Med. Sci.* 119, 68–77. doi: 10.3109/03009734.2014.901444
- Maseda, H., Yoneyama, H., and Nakae, T. (2000). Assignment of the substrate-selective subunits of the MexEF-OprN multidrug efflux pump of *Pseudomonas aeruginosa*. *Antimicrob. Agents Chemother.* 44, 658–664. doi: 10.1128/AAC.44.3.658–664.2000
- Mason, E. O. Jr., Wald, E. R., Bradley, J. S., Barson, W. J., and Kaplan, S. L. (2003). Macrolide resistance among middle ear isolates of *Streptococcus pneumoniae* observed at eight United States pediatric centers: prevalence of M and MLSB phenotypes. *Pediatr. Infect. Dis. J.* 22, 623–627. doi: 10.1097/01.inf.0000073124.06415.93
- Masuda, N., Gotoh, N., Ohya, S., and Nishino, T. (1996). Quantitative correlation between susceptibility and OprJ production in NfxB mutants of *Pseudomonas aeruginosa*. *Antimicrob. Agents Chemother.* 40, 909–913.

- Masuda, N., and Ohya, S. (1992). Cross-resistance to meropenem, cephems, and quinolones in *Pseudomonas aeruginosa*. *Antimicrob. Agents Chemother.* 36, 1847–1851. doi: 10.1128/AAC.36.9.1847
- Masuda, N., Sakagawa, E., Ohya, S., Gotoh, N., and Nishino, T. (2001). Hypersusceptibility of the *Pseudomonas aeruginosa* nfxB mutant to beta-lactams due to reduced expression of the ampC beta-lactamase. *Antimicrob. Agents Chemother.* 45, 1284–1286. doi: 10.1128/AAC.45.4.1284-1286.2001
- Masuda, N., Sakagawa, E., Ohya, S., Gotoh, N., Tsujimoto, H., and Nishino, T. (2000a). Contribution of the MexX-MexY-oprM efflux system to intrinsic resistance in *Pseudomonas aeruginosa*. *Antimicrob. Agents Chemother.* 44, 2242–2246. doi: 10.1128/AAC.44.9.2242-2246.2000
- Masuda, N., Sakagawa, E., Ohya, S., Gotoh, N., Tsujimoto, H., and Nishino, T. (2000b). Substrate specificities of MexAB-OprM, MexCD-OprJ, and MexXY-oprM efflux pumps in *Pseudomonas aeruginosa*. *Antimicrob. Agents Chemother.* 44, 3322–3327. doi: 10.1128/AAC.44.12.3322-3327.2000
- Matsumoto, Y., Hayama, K., Sakaihara, S., Nishino, K., Noji, H., Iino, R., et al. (2011). Evaluation of multidrug efflux pump inhibitors by a new method using microfluidic channels. *PLoS ONE* 6:e18547. doi: 10.1371/journal.pone.0018547
- May, A., Sieker, F., and Zacharias, M. (2008). How to efficiently include receptor flexibility during computational docking. *Curr. Comput. Aided Drug Design* 4, 143–153. doi: 10.2174/157340908784533265
- May, A., and Zacharias, M. (2008). Protein-ligand docking accounting for receptor side chain and global flexibility in normal modes: evaluation on kinase inhibitor cross docking. *J. Med. Chem.* 51, 3499–3506. doi: 10.1021/jm800071v
- Mazzariol, A., Cornaglia, G., and Nikaido, H. (2000). Contributions of the AmpC beta-lactamase and the AcrAB multidrug efflux system in intrinsic resistance of *Escherichia coli* K-12 to beta-lactams. *Antimicrob. Agents Chemother.* 44, 1387–1390. doi: 10.1128/AAC.44.5.1387-1390.2000
- Mesaros, N., Glupczynski, Y., Avrain, L., Caceres, N. E., Tulkens, P. M., and Van Bambeke, F. (2007). A combined phenotypic and genotypic method for the detection of Mex efflux pumps in *Pseudomonas aeruginosa*. *J. Antimicrob. Chemother.* 59, 378–386. doi: 10.1093/jac/dkl504
- Middlemiss, J. K., and Poole, K. (2004). Differential impact of MexB mutations on substrate selectivity of the MexAB-OprM multidrug efflux pump of *Pseudomonas aeruginosa*. *J. Bacteriol.* 186, 1258–1269. doi: 10.1128/JB.186.5.1258-1269.2004
- Mikolosko, J., Bobyk, K., Zgurskaya, H. I., and Ghosh, P. (2006). Conformational flexibility in the multidrug efflux system protein AcrA. *Structure* 14, 577–587. doi: 10.1016/j.str.2005.11.015
- Mine, T., Morita, Y., Kataoka, A., Mizushima, T., and Tsuchiya, T. (1999). Expression in *Escherichia coli* of a new multidrug efflux pump, MexXY, from *Pseudomonas aeruginosa*. *Antimicrob. Agents Chemother.* 43, 415–417.
- Misra, R., and Bavro, V. N. (2009). Assembly and transport mechanism of tripartite drug efflux systems. *Bba Proteins Proteom* 1794, 817–825. doi: 10.1016/j.bbapap.2009.02.017
- Misra, R., Morrison, K. D., Cho, H. J., and Khuu, T. (2015). Importance of real-time assays to distinguish multidrug efflux pump inhibiting and outer membrane destabilizing activities in *Escherichia coli*. *J. Bacteriol.* doi: 10.1128/JB.02456-14 [Epub ahead of print].
- Morita, Y., Komori, Y., Mima, T., Kuroda, T., Mizushima, T., and Tsuchiya, T. (2001). Construction of a series of mutants lacking all of the four major mex operons for multidrug efflux pumps or possessing each one of the operons from *Pseudomonas aeruginosa* PAO1: MexCD-OprJ is an inducible pump. *FEMS Microbiol. Lett.* 202, 139–143. doi: 10.1111/j.1574-6968.2001.tb10794.x
- Morita, Y., Murata, T., Mima, T., Shioota, S., Kuroda, T., Mizushima, T., et al. (2003). Induction of mexcd-oprJ operon for a multidrug efflux pump by disinfectants in wild-type *Pseudomonas aeruginosa* PAO1. *J. Antimicrob. Chemother.* 51, 991–994. doi: 10.1093/jac/dkg173
- Morita, Y., Tomida, J., and Kawamura, Y. (2012). MexXY multidrug efflux system of *Pseudomonas aeruginosa*. *Front. Microbiol.* 3:408. doi: 10.3389/fmicb.2012.00408
- Morita, Y., Tomida, J., and Kawamura, Y. (2014). Responses of *Pseudomonas aeruginosa* to antimicrobials. *Front. Microbiol.* 4:422. doi: 10.3389/fmicb.2013.00422
- Morita, Y., Tomida, J., and Kawamura, Y. (2015). Efflux-mediated fluoroquinolone resistance in the multidrug-resistant *Pseudomonas aeruginosa* clinical isolate PA7: identification of a novel MexS variant involved in upregulation of the mexef-oprN multidrug efflux operon. *Front. Microbiol.* 6:8. doi: 10.3389/fmicb.2015.00008
- Morris, J. D., Hewitt, J. L., Wolfe, L. G., Kamatkar, N. G., Chapman, S. M., Diener, J. M., et al. (2011). Imaging and analysis of *Pseudomonas aeruginosa* swarming and rhamnolipid production. *Appl. Environ. Microbiol.* 77, 8310–8317. doi: 10.1128/AEM.06644-11
- Mortimer, P. G., and Piddock, L. J. (1991). A comparison of methods used for measuring the accumulation of quinolones by *Enterobacteriaceae*, *Pseudomonas aeruginosa* and *Staphylococcus aureus*. *J. Antimicrob. Chemother.* 28, 639–653. doi: 10.1093/jac/28.5.639
- Murakami, S. (2008). Multidrug efflux transporter, AcrB—the pumping mechanism. *Curr. Opin. Struct. Biol.* 18, 459–465. doi: 10.1016/j.sbi.2008.06.007
- Murakami, S., Nakashima, R., Yamashita, E., Matsumoto, T., and Yamaguchi, A. (2006). Crystal structures of a multidrug transporter reveal a functionally rotating mechanism. *Nature* 443, 173–179. doi: 10.1038/nature05076
- Murakami, S., Nakashima, R., Yamashita, E., and Yamaguchi, A. (2002). Crystal structure of bacterial multidrug efflux transporter AcrB. *Nature* 419, 587–593. doi: 10.1038/nature01050
- Murakami, S., Tamura, N., Saito, A., Hirata, T., and Yamaguchi, A. (2004). Extramembrane central pore of multidrug exporter AcrB in *Escherichia coli* plays an important role in drug transport. *J. Biol. Chem.* 279, 3743–3748. doi: 10.1074/jbc.M308893200
- Nagano, K., and Nikaido, H. (2009). Kinetic behavior of the major multidrug efflux pump AcrB of *Escherichia coli*. *Proc. Natl. Acad. Sci. U.S.A.* 106, 5854–5858. doi: 10.1073/pnas.0901695106
- Nakashima, R., Sakurai, K., Yamasaki, S., Hayashi, K., Nagata, C., Hoshino, K., et al. (2013). Structural basis for the inhibition of bacterial multidrug exporters. *Nature* 500, 102–106. doi: 10.1038/nature12300
- Nakashima, R., Sakurai, K., Yamasaki, S., Nishino, K., and Yamaguchi, A. (2011). Structures of the multidrug exporter AcrB reveal a proximal multisite drug-binding pocket. *Nature* 480, 565–569. doi: 10.1038/nature10641
- Nakayama, K., Ishida, Y., Ohtsuka, M., Kawato, H., Yoshida, K., Yokomizo, Y., et al. (2003). MexAB-OprM-specific efflux pump inhibitors in *Pseudomonas aeruginosa*. Part 1: discovery and early strategies for lead optimization. *Bioorg. Med. Chem. Lett.* 13, 4201–4204. doi: 10.1016/j.bmcl.2003.07.024
- Narita, S., Eda, S., Yoshihara, E., and Nakae, T. (2003). Linkage of the efflux-pump expression level with substrate extrusion rate in the MexAB-OprM efflux pump of *Pseudomonas aeruginosa*. *Biochem. Biophys. Res. Commun.* 308, 922–926. doi: 10.1016/S0006-291X(03)01512-2
- Nikaido, H. (1996). Multidrug efflux pumps of gram-negative bacteria. *J. Bacteriol.* 178, 5853–5859.
- Nikaido, H. (2003). Molecular basis of bacterial outer membrane permeability revisited. *Microbiol. Mol. Biol. Rev.* 67, 593–656. doi: 10.1128/MMBR.67.4.593-656.2003
- Nikaido, H. (2011). Structure and mechanism of RND-type multidrug efflux pumps. *Adv. Enzymol. Relat. Areas Mol. Biol.* 77, 1–60. doi: 10.1002/9780470920541.ch1
- Nikaido, H., Basina, M., Nguyen, V., and Rosenberg, E. Y. (1998). Multidrug efflux pump AcrAB of *Salmonella typhimurium* excretes only those beta-lactam antibiotics containing lipophilic side chains. *J. Bacteriol.* 180, 4686–4692.
- Nikaido, H., and Normark, S. (1987). Sensitivity of *Escherichia coli* to various beta-lactams is determined by the interplay of outer membrane permeability and degradation by periplasmic beta-lactamases: a quantitative predictive treatment. *Mol. Microbiol.* 1, 29–36. doi: 10.1111/j.1365-2958.1987.tb00523.x
- Nikaido, H., and Pages, J. M. (2012). Broad-specificity efflux pumps and their role in multidrug resistance of Gram-negative bacteria. *FEMS Microbiol. Rev.* 36, 340–363. doi: 10.1111/j.1574-6976.2011.00290.x
- Nikaido, H., and Rosenberg, E. Y. (1983). Porin channels in *Escherichia coli*: studies with liposomes reconstituted from purified proteins. *J. Bacteriol.* 153, 241–252.
- Nishino, K., Nikaido, E., and Yamaguchi, A. (2009). Regulation and physiological function of multidrug efflux pumps in *Escherichia coli* and *Salmonella*. *Biochim. Biophys. Acta* 1794, 834–843. doi: 10.1016/j.bbapap.2009.02.002
- Nishino, K., and Yamaguchi, A. (2002). EvgA of the two-component signal transduction system modulates production of the yhiuv multidrug transporter in *Escherichia coli*. *J. Bacteriol.* 184, 2319–2323. doi: 10.1128/JB.184.8.2319-2323.2002

- Ntsogo-Enguene, V. Y., Verchère, A., Phan, G., Broutin, I., and Picard, M. (2015). Catch me if you can: a biotinylated proteoliposome affinity assay for the investigation of assembly of the MexA-MexB-OprM efflux pump from *Pseudomonas aeruginosa*. *Front. Microbiol.* 6:541. doi: 10.3389/fmicb.2015.00541
- Ocaktan, A., Yoneyama, H., and Nakae, T. (1997). Use of fluorescence probes to monitor function of the subunit proteins of the MexA-MexB-oprM drug extrusion machinery in *Pseudomonas aeruginosa*. *J. Biol. Chem.* 272, 21964–21969. doi: 10.1074/jbc.272.35.21964
- Ohene-Agyei, T., Lea, J. D., and Venter, H. (2012). Mutations in MexB that affect the efflux of antibiotics with cytoplasmic targets. *FEMS Microbiol. Lett.* 333, 20–27. doi: 10.1111/j.1574-6968.2012.02594.x
- Olaitan, A. O., Morand, S., and Rolain, J. M. (2014). Mechanisms of polymyxin resistance: acquired and intrinsic resistance in bacteria. *Front. Microbiol.* 5:643. doi: 10.3389/fmicb.2014.00643
- Olivares, J., Bernardini, A., Garcia-Leon, G., Corona, F. M. B. S., and Martinez, J. L. (2013). The intrinsic resistome of bacterial pathogens. *Front. Microbiol.* 4:103. doi: 10.3389/fmicb.2013.00103
- Ong, C. T., Tessier, P. R., Li, C., Nightingale, C. H., and Nicolau, D. P. (2007). Comparative in vivo efficacy of meropenem, imipenem, and ceftazidime against *Pseudomonas aeruginosa* expressing MexA-MexB-OprM efflux pumps. *Diagn. Microbiol. Infect. Dis.* 57, 153–161. doi: 10.1016/j.diagmicrobio.2006.06.014
- Ovchinnikov, V., and Karplus, M. (2012). Analysis and elimination of a bias in targeted molecular dynamics simulations of conformational transitions: application to calmodulin. *J. Phys. Chem. B* 116, 8584–8603. doi: 10.1021/jp212634z
- Page, M. G. (2012). The role of the outer membrane of Gram-negative bacteria in antibiotic resistance: Ajax' shield or Achilles' heel? *Handb. Exp. Pharmacol.* 211, 67–86. doi: 10.1007/978-3-642-28951-4\_5
- Pages, J. M., Lavigne, J. P., Leflon-Guibout, V., Marcon, E., Bert, F., Noussair, L., et al. (2009). Efflux pump, the masked side of beta-lactam resistance in *Klebsiella pneumoniae* clinical isolates. *PLoS ONE* 4:e4817. doi: 10.1371/journal.pone.0004817
- Pages, J. M., Masi, M., and Barbe, J. (2005). Inhibitors of efflux pumps in Gram-negative bacteria. *Trends Mol. Med.* 11, 382–389. doi: 10.1016/j.molmed.2005.06.006
- Pai, H., Kim, J., Kim, J., Lee, J. H., Choe, K. W., and Gotoh, N. (2001). Carbapenem resistance mechanisms in *Pseudomonas aeruginosa* clinical isolates. *Antimicrob. Agents Chemother.* 45, 480–484. doi: 10.1128/AAC.45.2.480-484.2001
- Paixao, L., Rodrigues, L., Couto, I., Martins, M., Fernandes, P., De Carvalho, C. C., et al. (2009). Fluorometric determination of ethidium bromide efflux kinetics in *Escherichia coli*. *J. Biol. Eng.* 3, 18. doi: 10.1186/1754-1611-3-18
- Parr, T. R. Jr., Moore, R. A., Moore, L. V., and Hancock, R. E. (1987). Role of porins in intrinsic antibiotic resistance of *Pseudomonas cepacia*. *Antimicrob. Agents Chemother.* 31, 121–123. doi: 10.1128/AAC.31.1.121
- Phillips, J. L., and Gnanakaran, S. (2015). A Data-driven approach to modeling the tripartite structure of multidrug resistance efflux pumps. *Proteins* 83, 43–65. doi: 10.1002/prot.24632
- Piddock, L. J. (2006). Clinically relevant chromosomally encoded multidrug resistance efflux pumps in bacteria. *Clin. Microbiol. Rev.* 19, 382–402. doi: 10.1128/CMR.19.2.382-402.2006
- Piddock, L. J., Garvey, M. I., Rahman, M. M., and Gibbons, S. (2010). Natural and synthetic compounds such as trimethoprim behave as inhibitors of efflux in Gram-negative bacteria. *J. Antimicrob. Chemother.* 65, 1215–1223. doi: 10.1093/jac/dkq079
- Pietras, Z., Bavro, V. N., Furnham, N., Pellegrini-Calace, M., Milner-White, E. J., and Luisi, B. F. (2008). Structure and mechanism of drug efflux machinery in Gram-negative bacteria. *Curr. Drug Targets* 9, 719–728. doi: 10.2174/138945008785747743
- Podneicky, N. L., Wuthiekanun, V., Peacock, S. J., and Schweizer, H. P. (2013). The BpeEF-OprC efflux pump is responsible for widespread trimethoprim resistance in clinical and environmental *Burkholderia pseudomallei* isolates. *Antimicrob. Agents Chemother.* 57, 4381–4386. doi: 10.1128/AAC.00660-13
- Poole, K. (2000). Efflux-mediated resistance to fluoroquinolones in gram-negative bacteria. *Antimicrob. Agents Chemother.* 44, 2233–2241. doi: 10.1128/AAC.44.9.2233-2241.2000
- Poole, K. (2004). Efflux-mediated multiresistance in Gram-negative bacteria. *Clin. Microbiol. Infect.* 10, 12–26. doi: 10.1111/j.1469-0691.2004.00763.x
- Poole, K. (2005). Efflux-mediated antimicrobial resistance. *J. Antimicrob. Chemother.* 56, 20–51. doi: 10.1093/jac/dki171
- Poole, K. (2011). *Pseudomonas aeruginosa*: resistance to the max. *Front. Microbiol.* 2:65. doi: 10.3389/fmicb.2011.00065
- Poole, K. (2013). “*Pseudomonas aeruginosa* efflux pumps,” in: *Microbial Efflux Pumps*, eds E. W. Yu, Q. Zhang, and M. H. Brown (Norfolk: Caister Academic Press).
- Poole, K. (2014). Stress responses as determinants of antimicrobial resistance in *Pseudomonas aeruginosa*: multidrug efflux and more. *Can. J. Microbiol.* 60, 783–791. doi: 10.1139/cjm-2014-0666
- Potron, A., Poirel, L., and Nordmann, P. (2015). Emerging broad-spectrum resistance in *Pseudomonas aeruginosa* and *Acinetobacter baumannii*: mechanisms and epidemiology. *Int. J. Antimicrob. Agents* 45, 568–585. doi: 10.1016/j.ijantimicag.2015.03.001
- Pournaras, S., Maniati, M., Spanakis, N., Ikonomidis, A., Tassios, P. T., Tsakris, A., et al. (2005). Spread of efflux pump-overexpressing, non-metallo-beta-lactamase-producing, meropenem-resistant but ceftazidime-susceptible *Pseudomonas aeruginosa* in a region with blaVIM endemicity. *J. Antimicrob. Chemother.* 56, 761–764. doi: 10.1093/jac/dki296
- Pumbwe, L., and Piddock, L. J. (2000). Two efflux systems expressed simultaneously in multidrug-resistant *Pseudomonas aeruginosa*. *Antimicrob. Agents Chemother.* 44, 2861–2864. doi: 10.1128/AAC.44.10.2861-2864.2000
- Rampersad, S. N. (2012). Multiple applications of Alamar Blue as an indicator of metabolic function and cellular health in cell viability bioassays. *Sensors (Basel)* 12, 12347–12360. doi: 10.3390/s120912347
- Raunest, M., and Kandt, C. (2012). Locked on one side only: ground state dynamics of the outer membrane efflux duct TolC. *Biochemistry* 51, 1719–1729. doi: 10.1021/bi201814s
- Renau, T. E., Leger, R., Yen, R., She, M. W., Flamme, E. M., Sangalang, J., et al. (2002). Peptidomimetics of efflux pump inhibitors potentiate the activity of levofloxacin in *Pseudomonas aeruginosa*. *Bioorg. Med. Chem. Lett.* 12, 763–766. doi: 10.1016/S0960-894X(02)00006-9
- Renau, T. E., and Lemoine, R. C. (2001). Efflux pump inhibitors to address bacterial and fungal resistance. *Drugs Fut.* 26, 1171–1178. doi: 10.1358 dof.2001.026.12.644122
- Richmond, G. E., Chua, K. L., and Piddock, L. J. (2013). Efflux in *Acinetobacter baumannii* can be determined by measuring accumulation of H33342 (bis-benzamide). *J. Antimicrob. Chemother.* 68, 1594–1600. doi: 10.1093/jac/dkt052
- Riera, E., Cabot, G., Mulet, X., Garcia-Castillo, M., Del Campo, R., Juan, C., et al. (2011). *Pseudomonas aeruginosa* carbapenem resistance mechanisms in Spain: impact on the activity of imipenem, meropenem and doripenem. *J. Antimicrob. Chemother.* 66, 2022–2027. doi: 10.1093/jac/dkr232
- Riou, M., Carbonnelle, S., Avrain, L., Mesaros, N., Pirnay, J. P., Bilocq, F., et al. (2010). In vivo development of antimicrobial resistance in *Pseudomonas aeruginosa* strains isolated from the lower respiratory tract of Intensive Care Unit patients with nosocomial pneumonia and receiving antipseudomonal therapy. *Int. J. Antimicrob. Agents.* 36, 513–522. doi: 10.1016/j.ijantimicag.2010.08.005
- Rosen, B. P., and Kashket, E. R. (1978). “Energetics of active transport,” in: *Bacterial Transport*, ed. B. P. Rosen (New York: Marcel Dekker Inc.).
- Ruggerone, P., Murakami, S., Pos, K. M., and Vargiu, A. V. (2013a). Rnd efflux pumps: structural information translated into function and inhibition mechanisms. *Curr. Top. Med. Chem.* 13, 3079–3100. doi: 10.2174/1568026611316660220
- Ruggerone, P., Vargiu, A. V., Collu, F., Fischer, N., and Kandt, C. (2013b). Molecular dynamics computer simulations of multidrug RND efflux pumps. *Computat. Struct. Biotechnol. J.* 5:e201302008. doi: 10.5936/csbj.201302008
- Russo-Marie, F., Roederer, M., Sager, B., Herzenberg, L. A., and Kaiser, D. (1993). Beta-galactosidase activity in single differentiating bacterial cells. *Proc. Natl. Acad. Sci. U.S.A.* 90, 8194–8198. doi: 10.1073/pnas.90.17.8194
- Ruzin, A., Keeney, D., and Bradford, P. A. (2005). AcrAB efflux pump plays a role in decreased susceptibility to tigecycline in *Morganella morganii*. *Antimicrob. Agents Chemother.* 49, 791–793. doi: 10.1128/AAC.49.2.791-793.2005

- Schlitter, J., Engels, M., Kruger, P., Jacoby, E., and Wollmer, A. (1993). Targeted molecular-dynamics simulation of conformational change - application to the T[–]R transition in insulin. *Mol. Simulat.* 10, 291–308. doi: 10.1080/08927029308022170
- Schulz, G. E. (1993). Bacterial porins: structure and function. *Curr. Opin. Cell Biol.* 5, 701–707. doi: 10.1016/0955-0674(93)90143-E
- Schulz, R., and Kleinekathöfer, U. (2009). Transitions between closed and open conformations of TolC: the effects of ions in simulations. *Biophys. J.* 96, 3116–3125. doi: 10.1016/j.bpj.2009.01.021
- Schulz, R., Vargiu, A. V., Collu, F., Kleinekathöfer, U., and Ruggerone, P. (2010). Functional rotation of the transporter AcrB: insights into drug extrusion from simulations. *PLoS Comput. Biol.* 6:e1000806. doi: 10.1371/journal.pcbi.100806
- Schulz, R., Vargiu, A. V., Ruggerone, P., and Kleinekathöfer, U. (2011). Role of water during the extrusion of substrates by the efflux transporter AcrB. *J. Phys. Chem. B* 115, 8278–8287. doi: 10.1021/jp200996x
- Schulz, R., Vargiu, A. V., Ruggerone, P., and Kleinekathöfer, U. (2015). Computational study of correlated domain motions in the acrb efflux transporter. *BioMed. Res. Int.* 12:487298 doi: 10.1155/2015/487298
- Schumacher, A., Trittler, R., Bohnert, J. A., Kummerer, K., Pages, J. M., and Kern, W. V. (2007). Intracellular accumulation of linezolid in *Escherichia coli*, citrobacter freundii and enterobacter aerogenes: role of enhanced efflux pump activity and inactivation. *J. Antimicrob. Chemother.* 59, 1261–1264. doi: 10.1093/jac/dkl380
- Schweizer, H. P. (2003). Efflux as a mechanism of resistance to antimicrobials in *Pseudomonas aeruginosa* and related bacteria: unanswered questions. *Genet. Mol. Res.* 2, 48–62.
- Sedgwick, E. G., and Bragg, P. D. (1996). The role of efflux systems and the cell envelope in fluorescence changes of the lipophilic cation 2-(4-dimethylaminostyryl)-1-ethylpyridinium in *Escherichia coli*. *Biochim. Biophys. Acta* 1278, 205–212. doi: 10.1016/0005-2736(95)00228-6
- Seeger, M. A., Schieferer, A., Eicher, T., Verrey, F., Diederichs, K., and Pos, K. M. (2006). Structural asymmetry of AcrB trimer suggests a peristaltic pump mechanism. *Science* 313, 1295–1298. doi: 10.1126/science.1131542
- Sekiya, H., Mima, T., Morita, Y., Kuroda, T., Mizushima, T., and Tsuchiya, T. (2003). Functional cloning and characterization of a multidrug efflux pump, mexHI-opmD, from a *Pseudomonas aeruginosa* mutant. *Antimicrob. Agents Chemother.* 47, 2990–2992. doi: 10.1128/AAC.47.9.2990-2992.2003
- Senn, H. M., and Thiel, W. (2009). QM/MM methods for biomolecular systems. *Angew. Chem. Int. Ed. Engl.* 48, 1198–1229. doi: 10.1002/anie.200802019
- Sennhauser, G., Amstutz, P., Briand, C., Storchenegger, O., and Grutter, M. G. (2007). Drug export pathway of multidrug exporter AcrB revealed by Darppin inhibitors. *PLoS Biol.* 5:e7. doi: 10.1371/journal.pbio.0050007
- Sennhauser, G., Bukowska, M. A., Briand, C., and Grutter, M. G. (2009). Crystal structure of the multidrug exporter MexB from *Pseudomonas aeruginosa*. *J. Mol. Biol.* 389, 134–145. doi: 10.1016/j.jmb.2009.04.001
- Sgrignani, J., and Magistrato, A. (2013). First-principles modeling of biological systems and structure-based drug-design. *Curr. Comput. Aided Drug Des.* 9, 15–34.
- Shapiro, H. M. (2000). Membrane potential estimation by flow cytometry. *Methods* 21, 271–279. doi: 10.1006/meth.2000.1007
- Steinbrecher, T., and Elstner, M. (2013). QM and QM/MM simulations of proteins. *Methods Mol. Biol.* 924, 91–124. doi: 10.1007/978-1-62703-017-5\_5
- Steinbrecher, T., Prock, S., Reichert, J., Wadhwan, P., Zimpfer, B., Bürck, J., et al. (2012). Peptide-lipid interactions of the stress-response peptide TisB that induces bacterial persistence. *Biophys. J.* 103, 1460–1469. doi: 10.1016/j.bpj.2012.07.060
- Sterpone, F., Ceccarelli, M., and Marchi, M. (2001). Dynamics of hydration in hen egg white lysozyme. *J. Mol. Biol.* 311, 409–419. doi: 10.1006/jmbi.2001.4860
- Su, C. C., and Yu, E. W. (2007). Ligand-transporter interaction in the AcrB multidrug efflux pump determined by fluorescence polarization assay. *FEBS Lett.* 581, 4972–4976. doi: 10.1016/j.febslet.2007.09.035
- Sugawara, E., Nagano, K., and Nikaido, H. (2010). Factors affecting the folding of *Pseudomonas aeruginosa* OprF porin into the one-domain open conformer. *MBio* 1:e00228–10. doi: 10.1128/mBio.00228-10
- Sugawara, E., Nestorovich, E. M., Bezrukova, S. M., and Nikaido, H. (2006). *Pseudomonas aeruginosa* porin OprF exists in two different conformations. *J. Biol. Chem.* 281, 16220–16229. doi: 10.1074/jbc.M600680200
- Sun, J., Deng, Z., and Yan, A. (2014). Bacterial multidrug efflux pumps: mechanisms, physiology and pharmacological exploitations. *Biochem. Biophys. Res. Commun.* 453, 254–267. doi: 10.1016/j.bbrc.2014.05.090
- Symmons, M., Bokma, E., Koronakis, E., Hughes, C., and Koronakis, V. (2009). The assembled structure of a complete tripartite bacterial multidrug efflux pump. *Proc. Natl. Acad. Sci. U.S.A.* 106, 7173–7178. doi: 10.1073/pnas.0900693106
- Takatsuka, Y., Chen, C., and Nikaido, H. (2010). Mechanism of recognition of compounds of diverse structures by the multidrug efflux pump AcrB of *Escherichia coli*. *Proc. Natl. Acad. Sci. U.S.A.* 107, 6559–6565. doi: 10.1073/pnas.1001460107
- Thanassi, D. G., Cheng, L. W., and Nikaido, H. (1997). Active efflux of bile salts by *Escherichia coli*. *J. Bacteriol.* 179, 2512–2518.
- Tikhonova, E. B., Wang, Q., and Zgurskaya, H. I. (2002). Chimeric analysis of the multicomponent multidrug efflux transporters from gram-negative bacteria. *J. Bacteriol.* 184, 6499–6507. doi: 10.1128/JB.184.23.6499-6507.2002
- Tikhonova, E. B., Yamada, Y., and Zgurskaya, H. I. (2011). Sequential mechanism of assembly of multidrug efflux pump AcrAB-TolC. *Chem. Biol.* 18, 454–463. doi: 10.1016/j.chembiol.2011.02.011
- Trepout, S., Taveau, J. C., Benabdellah, H., Granier, T., Ducruix, A., Frangakis, A. S., et al. (2010). Structure of reconstituted bacterial membrane efflux pump by cryo-electron tomography. *Biochim. Biophys. Acta* 1798, 1953–1960. doi: 10.1016/j.bbaram.2010.06.019
- Vaara, M. (1992). Agents that increase the permeability of the outer membrane. *Microbiol. Rev.* 56, 395–411.
- Vaccaro, L., Koronakis, V., and Sansom, M. S. P. (2006). Flexibility in a drug transport accessory protein: molecular dynamics simulations of MexA. *Biophys. J.* 91, 558–564. doi: 10.1529/biophysj.105.080010
- Vaccaro, L., Scott, K. A., and Sansom, M. S. P. (2008). Gating at both ends and breathing in the middle: conformational dynamics of TolC. *Biophys. J.* 95, 5681–5691. doi: 10.1529/biophysj.108.136028
- Van Bambeke, F., Pagès, J.-M., and Lee, V. J. (2010). Inhibitors of bacterial efflux pumps as adjuvant in antibacterial therapy and diagnostic tools for detection of resistance by efflux. *Front. Anti Infect. Drug Discov.* 1: 138–175.
- van den Berg van Saparoea, H. B., Lubelski, J., Van Merkerk, R., Mazurkiewicz, P. S., and Driessens, A. J. (2005). Proton motive force-dependent Hoechst 33342 transport by the ABC transporter LmrA of *Lactococcus lactis*. *Biochemistry* 44, 16931–16938. doi: 10.1021/bi051497y
- Vargiu, A. V., Collu, F., Schulz, R., Pos, K. M., Zacharias, M., Kleinekathöfer, U., et al. (2011). Effect of the F610A mutation on substrate extrusion in the AcrB transporter: explanation and rationale by molecular dynamics simulations. *J. Am. Chem. Soc.* 133, 10704–10707. doi: 10.1021/ja20666x
- Vargiu, A. V., and Nikaido, H. (2012). Multidrug binding properties of the AcrB efflux pump characterized by molecular dynamics simulations. *Proc. Natl. Acad. Sci. U.S.A.* 109, 20637–20642. doi: 10.1073/pnas.1218348109
- Vargiu, A. V., Ruggerone, P., Opperman, T. J., Nguyen, S. T., and Nikaido, H. (2014). Molecular mechanism of Mbx2319 inhibition of *Escherichia coli* AcrB multidrug efflux pump and comparison with other inhibitors. *Antimicrob. Agents Chemother.* 58, 6224–6234. doi: 10.1128/AAC.03283-14
- Verchère, A., Dezi, M., Adrien, V., Broutin, I., and Picard, M. (2015). In vitro transport activity of the fully assembled MexAB-OprM efflux pump from *Pseudomonas aeruginosa*. *Nat. Commun.* 6, 6890. doi: 10.1038/ncomms7890
- Verchère, A., Dezi, M., Broutin, I., and Picard, M. (2014). In vitro investigation of the MexAB efflux pump from *Pseudomonas aeruginosa*. *J. Vis. Exp.* 84:e50894. doi: 10.3791/50894
- Vidal-Aroca, F., Meng, A., Minz, T., Page, M. G., and Dreier, J. (2009). Use of resazurin to detect mefloquine as an efflux-pump inhibitor in *Pseudomonas aeruginosa* and *Escherichia coli*. *J. Microbiol. Methods* 79, 232–237. doi: 10.1016/j.mimet.2009.09.021
- Visalli, M. A., Murphy, E., Projan, S. J., and Bradford, P. A. (2003). AcrAB multidrug efflux pump is associated with reduced levels of susceptibility to tigecycline (GAR-936) in *Proteus mirabilis*. *Antimicrob. Agents Chemother.* 47, 665–669. doi: 10.1128/AAC.47.2.665-669.2003

- Viveiros, M., Martins, A., Paixao, L., Rodrigues, L., Martins, M., Couto, I., et al. (2008). Demonstration of intrinsic efflux activity of *Escherichia coli* K-12 AG100 by an automated ethidium bromide method. *Int. J. Antimicrob. Agents* 31, 458–462. doi: 10.1016/j.ijantimicag.2007.12.015
- Walmsley, A. R., Martin, G. E., and Henderson, P. J. (1994). 8-Anilino-1-naphthalenesulfonate is a fluorescent probe of conformational changes in the D-galactose-H<sup>+</sup> symport protein of *Escherichia coli*. *J. Biol. Chem.* 269, 17009–17019.
- Walsh, F., and Amyes, S. G. (2007). Carbapenem resistance in clinical isolates of *Pseudomonas aeruginosa*. *J. Chemother.* 19, 376–381. doi: 10.1179/joc.2007.19.4.376
- Wang, B., Weng, J., Fan, K., and Wang, W. (2012). Interdomain flexibility and pH-Induced conformational changes of AcrA revealed by molecular dynamics simulations. *J. Phys. Chem. B* 116, 3411–3420. doi: 10.1021/jp212221v
- Watkins, W. J., Landaverry, Y., Leger, R., Litman, R., Renau, T. E., Williams, N., et al. (2003). The relationship between physicochemical properties, in vitro activity and pharmacokinetic profiles of analogues of diamine-containing efflux pump inhibitors. *Bioorg. Med. Chem. Lett.* 13, 4241–4244. doi: 10.1016/j.bmcl.2003.07.030
- Webber, M. A., and Piddock, L. J. (2003). The importance of efflux pumps in bacterial antibiotic resistance. *J. Antimicrob. Chemother.* 51, 9–11. doi: 10.1093/jac/dkg050
- Wehmeier, C., Schuster, S., Fahnrich, E., Kern, W. V., and Bohnert, J. A. (2009). Site-directed mutagenesis reveals amino acid residues in the *Escherichia coli* RND efflux pump AcrB that confer macrolide resistance. *Antimicrob. Agents Chemother.* 53, 329–330. doi: 10.1128/AAC.00921-08
- Welch, A., Awah, C. U., Jing, S., Van Veen, H. W., and Venter, H. (2010). Promiscuous partnering and independent activity of MexB, the multidrug transporter protein from *Pseudomonas aeruginosa*. *Biochem. J.* 430, 355–364. doi: 10.1042/BJ20091860
- Xu, X. H. N., Brownlow, W., Huang, S., and Chen, J. (2003). Single-molecule detection of efflux pump machinery in *Pseudomonas aeruginosa*. *Biochem. Biophys. Res. Commun.* 305, 79–86. doi: 10.1016/S0006-291X(03)00692-2
- Xu, Y., Lee, M., Moeller, A., Song, S., Yoon, B.-Y., Kim, H.-M., et al. (2011). Funnel-like hexameric assembly of the periplasmic adapter protein in the tripartite multidrug efflux pump in gram-negative bacteria. *J. Biol. Chem.* 286, 17910–17920. doi: 10.1074/jbc.M111.238535
- Yamaguchi, A., Nakashima, R., and Sakurai, K. (2015). Structural basis of RND-type multidrug exporters. *Front. Microbiol.* 6:327. doi: 10.3389/fmicb.2015.00327
- Yamaguchi, A., Udagawa, T., and Sawai, T. (1990). Transport of divalent cations with tetracycline as mediated by the transposon Tn10-encoded tetracycline resistance protein. *J. Biol. Chem.* 265, 4809–4813.
- Yang, N. C., and Hu, M. L. (2004). A fluorimetric method using fluorescein di-beta-D-galactopyranoside for quantifying the senescence-associated beta-galactosidase activity in human foreskin fibroblast Hs68 cells. *Anal. Biochem.* 325, 337–343. doi: 10.1016/j.ab.2003.11.012
- Yao, X.-Q., Kimura, N., Murakami, S., and Takada, S. (2013). Drug uptake pathways of multidrug transporter AcrB studied by molecular simulations and site-directed mutagenesis experiments. *J. Am. Chem. Soc.* 135, 7474–7485. doi: 10.1021/ja310548h
- Yoshida, K., Nakayama, K., Ohtsuka, M., Kuru, N., Yokomizo, Y., Sakamoto, A., et al. (2007). MexAB-OprM specific efflux pump inhibitors in *Pseudomonas aeruginosa*. Part 7: highly soluble and in vivo active quaternary ammonium analogue D13-9001, a potential preclinical candidate. *Bioorg. Med. Chem.* 15, 7087–7097. doi: 10.1016/j.bmc.2007.07.039
- Yoshimura, F., and Nikaido, H. (1982). Permeability of *Pseudomonas aeruginosa* outer membrane to hydrophilic solutes. *J. Bacteriol.* 152, 636–642.
- Zechini, B., and Versace, I. (2009). Inhibitors of multidrug resistant efflux systems in bacteria. *Recent Patents Anti Infect. Drug Discov.* 4, 37–50. doi: 10.2174/157489109787236256
- Zgurskaya, H. I., and Nikaido, H. (1999). Bypassing the periplasm: reconstitution of the AcrAB multidrug efflux pump of *Escherichia coli*. *Proc. Natl. Acad. Sci. U.S.A.* 96, 7190–7195. doi: 10.1073/pnas.96.13.7190
- Zhanell, G. G., Decorby, M., Adam, H., Mulvey, M. R., Mccracken, M., Lagace-Wiens, P., et al. (2010). Prevalence of antimicrobial-resistant pathogens in Canadian hospitals: results of the Canadian Ward Surveillance Study (Canward 2008). *Antimicrob. Agents Chemother.* 54, 4684–4693. doi: 10.1128/AAC.00469-10
- Zhou, T., Huang, D., and Caflisch, A. (2010). Quantum mechanical methods for drug design. *Curr. Top. Med. Chem.* 10, 33–45. doi: 10.2174/156802610790232242

**Conflict of Interest Statement:** Jürg Dreier is employee of Basilea Pharmaceutica International Ltd. Paolo Ruggerone declares that the research was conducted in the absence of any commercial or financial relationships that could be construed as a potential conflict of interest.

Copyright © 2015 Dreier and Ruggerone. This is an open-access article distributed under the terms of the Creative Commons Attribution License (CC BY). The use, distribution or reproduction in other forums is permitted, provided the original author(s) or licensor are credited and that the original publication in this journal is cited, in accordance with accepted academic practice. No use, distribution or reproduction is permitted which does not comply with these terms.

# New OprM structure highlighting the nature of the N-terminal anchor

Laura Monlezun<sup>1†</sup>, Gilles Phan<sup>1</sup>, Houssain Benabdellah<sup>2</sup>, Marie-Bernard Lascombe<sup>1</sup>, Véronique Y. N. Enguéné<sup>1</sup>, Martin Picard<sup>1</sup> and Isabelle Broutin<sup>1\*</sup>

<sup>1</sup> Laboratoire de Cristallographie et RMN Biologiques, CNRS UMR 8015, Faculté de Pharmacie, Université Paris Descartes, Paris, France, <sup>2</sup> Laboratoire d'Imagerie Biomédicale, Sorbonne Universités, Université Pierre et Marie Curie Paris 6, CNRS UMR 7371, INSERM U1146, Paris, France

## OPEN ACCESS

### Edited by:

Attilio Vittorio Vargiu,  
Università di Cagliari, Italy

### Reviewed by:

Ashima Kushwaha Bhardwaj,  
Indian Institute of Advanced  
Research, India  
Satoshi Murakami,  
Tokyo Institute of Technology, Japan

### \*Correspondence:

Isabelle Broutin,  
Laboratoire de Cristallographie et  
RMN Biologiques, CNRS UMR 8015,  
Faculté de Pharmacie, Université  
Paris Descartes, 4 Avenue  
de l'Observatoire, 75270 Paris  
Cedex 06, France  
isabelle.broutin@parisdescartes.fr

### †Present address:

Laura Monlezun,  
Division of Molecular Microbiology,  
College of Life Sciences, University  
of Dundee, Dow Street, Dundee DD1  
5EH, UK

### Specialty section:

This article was submitted to  
Antimicrobials, Resistance  
and Chemotherapy,  
a section of the journal  
*Frontiers in Microbiology*

Received: 10 February 2015

Accepted: 19 June 2015

Published: 01 July 2015

### Citation:

Monlezun L, Phan G, Benabdellah H,  
Lascombe M-B, Enguéné VYN,  
Picard M and Broutin I (2015) New  
OprM structure highlighting the nature  
of the N-terminal anchor.  
*Front. Microbiol.* 6:667.  
doi: 10.3389/fmicb.2015.00667

Among the different mechanisms used by bacteria to resist antibiotics, active efflux plays a major role. In Gram-negative bacteria, active efflux is carried out by tripartite efflux pumps that form a macromolecular assembly spanning both membranes of the cellular wall. At the outer membrane level, a well-conserved outer membrane factor (OMF) protein acts as an exit duct, but its sequence varies greatly among different species. The OMFs share a similar tri-dimensional structure that includes a beta-barrel pore domain that stabilizes the channel within the membrane. In addition, OMFs are often subjected to different N-terminal post-translational modifications (PTMs), such as an acylation with a lipid. The role of additional N-terminal anchors is all the more intriguing since it is not always required among the OMFs family. Understanding this optional PTM could open new research lines in the field of antibiotics resistance. In *Escherichia coli*, it has been shown that CusC is modified with a tri-acylated lipid, whereas TolC does not show any modification. In the case of OprM from *Pseudomonas aeruginosa*, the N-terminal modification remains a matter of debate, therefore, we used several approaches to investigate this issue. As definitive evidence, we present a new X-ray structure at 3.8 Å resolution that was solved in a new space group, making it possible to model the N-terminal residue as a palmitoylated cysteine.

**Keywords:** multidrug resistance, efflux pump, membrane protein, post-translational modification, lipoyl, X-ray structure

## Introduction

After several decades of continuous antibiotic therapy success, we are now facing the appearance of multi-drug resistant strains and the near absence of new antibiotic family development for more than 10 years (Fischbach and Walsh, 2009; Hede, 2014). These facts highlight the need for new anti-infection strategies (Walsh, 2003; Olivares et al., 2013), although a promising compound isolated from natural soil bacteria that is able to kill Gram-positive pathogens, was recently reported (Ling et al., 2015). Among the most virulent nosocomial pathogens are *Pseudomonas aeruginosa*, *Escherichia coli*, *Staphylococcus aureus*, *Enterococci*, and *Acinetobacter baumannii* (Poole, 2004; Lister et al., 2009; Bereket et al., 2012; Bayram et al., 2013). These strains have developed several resistance strategies including active efflux pumps (Cattoir, 2004; Li and Nikaido, 2009; Nikaido, 2009; Nikaido and Pages, 2012). In Gram-negative bacteria efflux pumps are multimers of three

**Abbreviations:** BOG, beta-octyl glucopyranoside; DDM, dodecyl maltoside; MexAp, MexA palmitoylated; MexAnp, MexA non palmitoylated; PTM, posttranslational modification.

different proteins that form a long transmembrane scaffold linking the cytoplasm to the outside of the cell (Nikaido and Pages, 2012). These tripartite assemblies are composed of an inner membrane protein from the RND (Resistance Nodulation cell Division) family, which corresponds to the pumping motor that uses the proton-gradient as an energy source; an outer membrane channel from the OMF (Outer Membrane Factor) family; and a periplasmic protein from the MFP (membrane fusion protein) family, anchored to the inner membrane and connecting the other two proteins. In *P. aeruginosa*, up to 12 different pumps have been sequenced (Yen et al., 2002), including OprM<sub>OMF</sub>-MexA<sub>MFP</sub>-MexB<sub>RND</sub> which is one of the most studied pumps because of its constitutive expression whereas the others appear under antibiotic pressure (Li and Poole, 2001; Nakajima et al., 2002; Schweizer, 2003). This study will focus on the versatile membrane channel OprM, which has the ability to work with at least four different pumps, including OprM-MexAB, OprM-MexXY (Aires et al., 1999; Morita et al., 2012), OprM-MexJK (Chuanchuen et al., 2002), and OprM-MexMN (Mima et al., 2005).

The X-ray structure of OprM was solved in two different space groups showing its trimeric nature [Protein Data Bank (PDB) code: 1WP1 (Akama et al., 2004); 3D5K (Phan et al., 2010)]. The architecture of OprM is composed of a beta-barrel domain that is ~40 Å in height spanning the outer membrane and a periplasmic alpha-helical domain that is ~100 Å in length and bears a central buoy. Most of the structure has been determined with the exception of the eleven C-terminal amino acids, which are not visible in the electronic density maps of both structures. In addition, the structure of the post-translational modification (PTM) that covalently links the Cys-terminal residue to a lipoyl has never been properly characterized at any resolution, despite palmitoylation being suggested some time ago (Nakajima et al., 2000). This lipoyl modification is not commonly shared among OMF family members. For instance, the *E. coli* homolog TolC (PDB code: 1EK9, Koronakis et al., 2000), has an N-terminus that is 44 residues shorter and does not begin with a cysteine. Other OMFs with known structures, such as VceC from *Vibrio cholerae* (PDB code: 1YC9, Federici et al., 2005), CusC of the metal effluent pump from *E. coli* (3PIK, Kulathila et al., 2011; 4K7R, Lei et al., 2014a) and CmeC from *E. coli* (4MT4, Su et al., 2014) begin with residues Cys-Ser (Figure 1; Supplementary Figure S1) like OprM. The OMF protein with the most recently solved structure, MtrE (4MT0, Lei et al., 2014b) from *Neisseria gonorrhoeae*, begins with Cys-Thr. The structure of CusC indicates the presence of a di-acylated thiol on the N-terminal cysteine, with or without a supplementary acyl chain on the N-terminal amine (triacylation), depending on the protomer. As the CusC sequence is highly similar to OprM, it has been suggested that the latter may be modified in a similar manner, rather than with only one palmitoyl chain attached by a thio-acyl bound to the N-terminal Cys as previously described (Kulathila et al., 2011). Di-acylation is also found in CmeC, but nothing has been found to be added to the N-terminal cysteine of the MtrE structure. In the VceC structure, the protein sequence was cloned without the first 12 amino acids, therefore, the N-terminal cysteine was not present. In the OprM structure solved in the R32 space group (Akama

et al., 2004), the three monomers were found to be identical by the threefold crystallographic symmetry axis, and despite a resolution of 2.6 Å there was no evidence of lipidation to the thiol or amine of the N-terminal cysteine. The same observation applies to the OprM structure solved at 2.4 Å of resolution (Phan et al., 2010) in which the P2<sub>1</sub>2<sub>1</sub>2<sub>1</sub> space group does not stabilize sufficiently the N-terminal modified cysteine.

Consequently, the N-terminal modification of OMFs remains an open question. Post-translational lipidation is particularly essential for the secretion and localization of some membranous proteins, a process involving different biological modifiers such as palmitoyl acyl transferases (Aicart-Ramos et al., 2011), palmitoyl thioesterases, lipoprotein diacylglycerol transferase or lipoprotein N-acyl transferase (Linder and Deschenes, 2007; Kovacs-Simon et al., 2011; Nakayama et al., 2012). These modifying enzymes could potentially lead to new therapeutic targets. In addition, it is not known why some OMF proteins need to undergo PTM in addition to their *trans*-membrane beta-barrel insertion, or what is the nature of this modification. We asked this question using OprM from *P. aeruginosa* with specific N-terminal chemical probes to investigate whether it is actually palmitoylated via a thio-acyl or subjected to other PTMs, and resolved a new OprM structure in a new crystallographic space group.

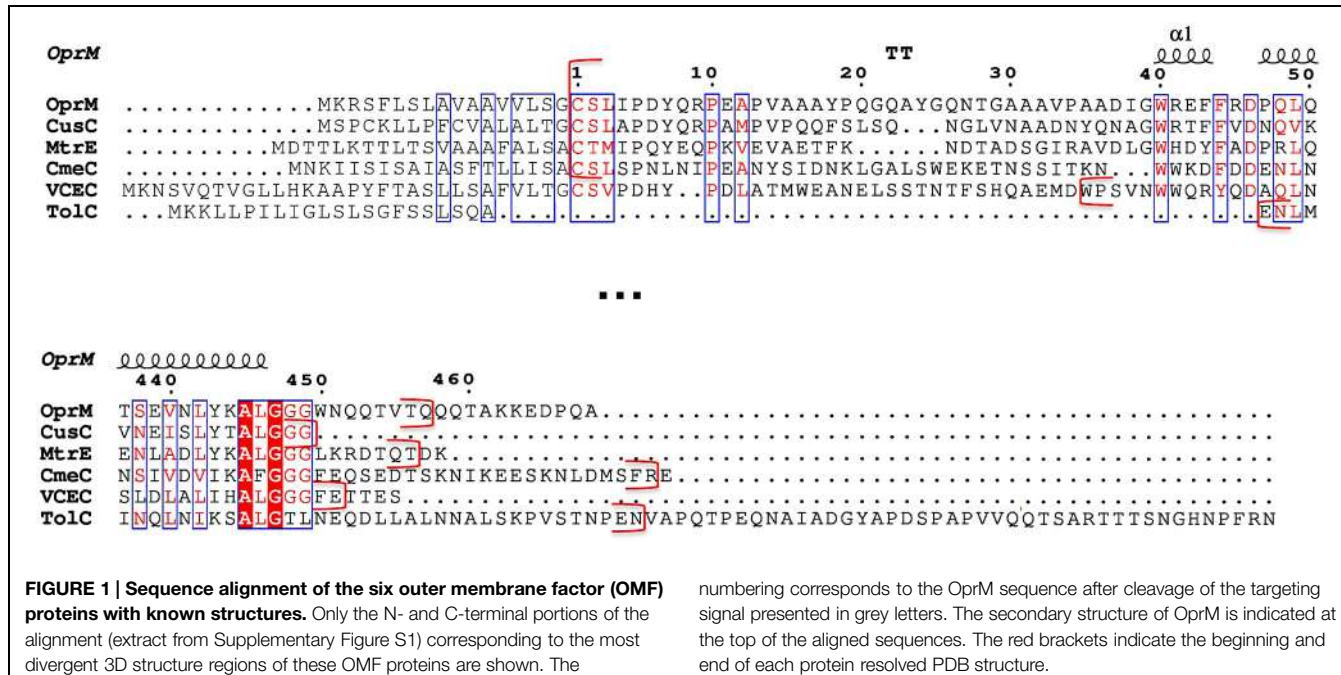
## Materials and Methods

### Expression and Purification of OprM, MexAp, and MexAnp

The three proteins were produced following the protocol described by Phan et al. (2010) and Ferrandez et al. (2012) with some modifications. The protein genes were inserted into the pBAD33-GFPuv plasmid with a C-terminal 6-histidines tag and the N-terminus extremity being dedicated to the signal peptide. For the non-palmitoylated form of MexA (MexAnp), the signal peptide was deleted from the construct, resulting in a non-membranous protein bearing a free N-terminal cysteine. Wt MexA has the same amino acid sequence as MexAnp, but its starting cysteine is palmitoylated after maturation (MexAp).

The plasmids were transformed into the C43-DE3 *E. coli* strain (Miroux and Walker, 1996). For each protein 6 L of cultures were grown; they were begun at OD<sub>600</sub> = 0.05 from dilution of an overnight pre-culture at 37°C in LB medium containing 25 µg/ml chloramphenicol, and were then grown at 30°C. Cells were induced at OD<sub>600</sub> = 0.6–0.8 by the addition of 0.02% L-arabinose and grown for 2 h before centrifugation for 20 min at 9,000 g. The cell pellet was resuspended in 45 ml of buffer containing 20 mM Tris-HCl (pH 8.0), 5 mM MgCl<sub>2</sub>, 1 µl/ml cocktail of anti-protease inhibitors set III (Calbiochem) and 50 units of benzonase (Promega).

Cells were broken using a French pressure cell at 69 MPa and then centrifuged twice for 30 min at 8,500 g to remove inclusion bodies and unbroken cells. As for OprM, the supernatant was applied to a sucrose step gradient (0.5 and 1.5 M) and then centrifuged for 3 h at 200,000 g at 4°C for membrane separation. The pellet, corresponding to the outer membrane fraction, was



re-suspended in a solution containing 20 mM Tris-HCl (pH 8.0), 10% glycerol (v/v) and 2%  $\beta$ OG (w/v) (Anatrace) and then stirred overnight at 23°C. The solubilized membrane proteins were recovered by centrifugation for 30 min at 50,000 g. For MexAp, the lysis supernatant was directly centrifuged at 100,000 g for 1 h at 4°C, and the pellet was resuspended in a solution containing 20 mM Tris-HCl (pH 8.0), 10% glycerol (v/v), 2%  $\beta$ OG (w/v) (Anatrace) 0.2% *N*-lauryl sarkosyl, and 15 mM imidazole, then stirred overnight at 23°C. The solubilized membrane proteins were recovered by centrifugation at 4°C for 1 h at 100,000 g. For MexAnp, because it is produced directly in the cytoplasm, there is no need for a detergent solubilization step. After lysis and centrifugation, 15 mM imidazole was added to the supernatant before loading onto the column. For the three proteins, the same protocol was then used. The proteins were loaded onto a Ni-NTA resin column pre-equilibrated with 20 mM Tris-HCl (pH 8.0), 200 mM NaCl, 10% glycerol (v/v), 15 mM imidazole for MexAnp, the same buffer plus 0.9%  $\beta$ OG (w/v) for OprM, and the addition of 0.2% *N*-lauryl sarkosyl for MexAp. After washing of the column, the proteins were eluted in the same respective buffers containing 300 mM imidazole, and then desalted using a PD-10 desalting column (GE) to remove the imidazole. MexAp and MexAnp were concentrated up to 2.5 mg/ml. OprM was concentrated up to 8 mg/ml using the 30-kDa cutoff Amicon system (Millipore).

## Labeling of the N-Terminal Amine

The fluorescent compound 4-chloro-7-nitrobenzofurazan (NBD-Cl) is a fluorogenic reagent that reacts with protein N-terminal amines but not with lysines in the conditions used as their respective pKa largely differ (Ghosh and Whitehouse, 1968; Bernal-Perez et al., 2012). A NBD-Cl stock solution was prepared in DMSO (dimethylsulfoxide) and 6  $\mu$ M of OprM in 50 mM

numbering corresponds to the OprM sequence after cleavage of the targeting signal presented in grey letters. The secondary structure of OprM is indicated at the top of the aligned sequences. The red brackets indicate the beginning and end of each protein resolved PDB structure.

Hepes buffer (pH 7.5) and 0.05% DDM (w/v) containing 1 mM EDTA was mixed with 0.5 mM of NBD-Cl at 4°C. After 6 h, the reaction was stopped by adding SDS-PAGE loading buffer [60 mM Tris-HCl (pH 6.8), 25% glycerol (v/v), 2% SDS (w/v), 0.1% bromophenol blue (w/v)] and the solution was deposited on an SDS gel together with unmarked OprM protein. The gel was analyzed for fluorescence using a UV transilluminator at an emission wavelength of 504 nm. A clear band was visualized for the labeled OprM.

## Labeling of the N-Terminal Cysteine Sulfur

The fluorescent compound MTS-EMCA [*N*-(2-Methanethiosulfonylethyl)-7-methoxycoumarin-4-acetamide, Toronto Research, Chemicals Inc.] is a sulfhydryl active reagent that covalently attaches to the reduced cysteine via a disulfide bond. 25 mM proteins (MexAp, MexAnp, and OprM) were incubated for 2 h with 2 mM MTS-EMCA in 10 mM HEPES pH 7.5, 150 mM NaCl,  $\beta$ OG 1% (w/v), at room temperature away from light. Reactions were stopped by adding an equivalent volume of SDS-PAGE loading buffer. After electrophoresis, gels were visualized with a UV transilluminator at 312 nm before coomassie blue staining. MTS-EMCA fluorescence appeared for the labeled proteins.

## Crystallization and Data Collection

OprM crystals were grown by vapor diffusion using the hanging drop method. Two different crystal forms were obtained, both leading to the recording of a diffraction dataset after 100s of crystal tests on the different beam lines of both SOLEIL and ESRF synchrotrons. One crystal was obtained in a 1 M sodium citrate (pH 5-6) precipitation solution and was found to belong to the P2<sub>1</sub>2<sub>1</sub>2<sub>1</sub> space group. The structure in this space group has been previously published (Phan et al., 2010). The second

crystal was obtained in 100 mM sodium acetate (pH 4.5), 6% PEG 20 000 (w/v), 300 mM ammonium citrate, 25–30% glycerol (v/v), and 0.9% βOG (w/v). These rhombohedral crystals (100 μm × 100 μm × 30 μm) belong to the C2 space group and diffracted to 3.8 Å resolution. A complete dataset was collected on beamline ID29 (ESRF, Grenoble) with an exposure time of 10 s per degree of oscillation. Owing to its low resolution, this data set has been kept for a long time without solving the structure, but the recent question of the N-terminal modification nature prompted us to ultimately solve the OprM structure in the C2 space group.

## Data processing, Model Building, and Refinement

Reflections were integrated, scaled and reduced using the programs XDS (Kabsch, 1993) and TRUNCATE from the CCP4 suite (1994). Data collection statistics are summarized in **Table 1**.

We have solved the C2 structure of OprM by molecular replacement with PHASER (McCoy et al., 2007) in automatic mode using our previously solved structure (PDB code 3D5K, Phan et al., 2010) as a model. Refinements were conducted using Phenix (Adams et al., 2002) and the protein was rebuilt with COOT (Emsley and Cowtan, 2004). The Bfactors were refined

**TABLE 1 | Crystallographic data and refinement statistics.**

| Data collection   |                      |
|---|----------------------|
| Beamline  | ESRF ID29            |
| X-ray wavelength (Å)                                    | 1.0052               |
| Crystal – detector distance (mm)                        | 400                  |
| Space group   | C2                   |
| Cell dimensions   |                      |
| <i>a</i> , <i>b</i> , <i>c</i> (Å)                      | 152.6, 87.9, 355.9   |
| α, β, γ (°)   | 90, 98.9, 90         |
| Matthews coefficient (Å <sup>3</sup> /Da)               | 3.80                 |
| Solvent content (%)                                     | 67.7                 |
| Resolution (Å) <sup>a</sup>                             | 87.9 – 3.8 (3.9–3.8) |
| Number of reflections                                   | 131 301              |
| Number of unique reflections                            | 40 566 (3571)        |
| R <sub>merge</sub> (%) <sup>a,b</sup>                   | 12.2 (31.2)          |
| Completeness (%) <sup>a</sup>                           | 87.7 (77.9)          |
| Redundancy <sup>a</sup>                                 | 3.2 (3.3)            |
| l/σ <sup>a</sup>  | 8.5 (3.3)            |
| Refinement  |                      |
| R <sub>work</sub> /R <sub>free</sub> (%) <sup>c,d</sup> | 29.7/34.6            |
| Number of residues                                      | 2 741                |
| Number of solvent molecules                             | 0                    |
| Rmsd from ideal values                                  |                      |
| Bonds (Å)   | 0.010                |
| Angles (°)  | 1.400                |
| Mean B-factor (Å) <sup>2</sup>                          | 94.2                 |

<sup>a</sup>Values in brackets correspond to the highest resolution shell.

<sup>b</sup>R<sub>merge</sub> =  $\sum_h \sum_i |I(h)_i - \langle I(h) \rangle| / \sum_h \sum_i \langle I(h) \rangle$  where I(h) is the observed intensity.

<sup>c</sup>R<sub>work</sub> =  $S_{hkl} || F_{obs} || - |F_{calc}| || S_{hkl} | F_{obs} |$ .

<sup>d</sup>R<sub>free</sub> was calculated for 7% of reflections randomly excluded from the refinement.

by groups. These groups were determined after a refinement step using the two Bfactors per residues option, but the resulting structure was not kept for the continuation. The TLS option was not used.

The last 19 C-terminal residues could not be assigned, probably due to the large flexibility of this region. The validity of our model was checked using MolProbity (Davis et al., 2007) and the polygon tool (Urzhumtseva et al., 2009) from Phenix (see Supplementary Figure S3). The OprM structure model of the C2 crystal was deposited in the PDB (4Y1K).

Figures were created with Pymol (DeLano, 2002).

## Sequence Alignment

Sequence alignment of the different OMF proteins whose structures were deposited in the PDB was performed using the program MUSCLE (MUltiple Sequence Comparison by Log-Expectation)<sup>1</sup>. The alignment was submitted to ESPript 3.0 (Robert and Gouet, 2014) for customization.

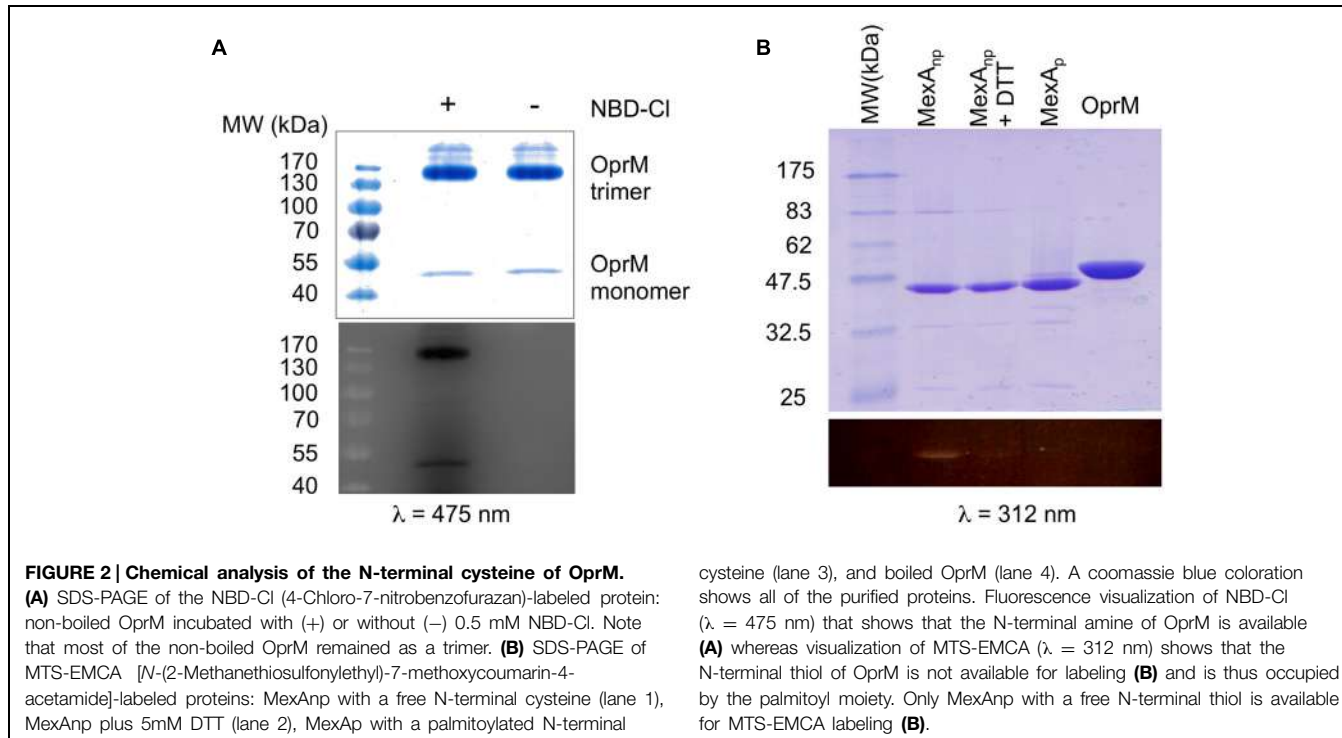
## Results

### Chemical Analysis of the Lipoyl Position

Among the different PTMs that can occur on an N-terminal cysteine (Chalker et al., 2009) N- or S-palmitoylation or acetylation are readily observed (Resh, 1999; Tooley and Schaner Tooley, 2014). As these different modifications are regulated by specific transferases, it is important to characterize the exact nature of OprM PTM. Thus, two questions needed to be clarified: what is the chemical nature of the modification, and which group of the amino acid is modified? To address these two questions, two different types of chemical labeling were performed on purified OprM. To analyze the occupancy of the N-terminal amine, this protein was labeled with the fluorogenic molecule 4-chloro-7-nitrobenzofuran (NBD-Cl) at neutral pH. This molecule has been proven to be a specific probe for the N-terminal amine only (Bernal-Perez et al., 2012). After incubation with NBD-Cl, the protein was analyzed on an SDS gel, revealing a bright fluorescent band when exposed at 475 nm (**Figure 2A**), thus showing that the N-terminal amine of OprM is actually accessible.

Following the same approach, a different probe was used to verify the occupancy of the sulphydryl group of the cysteine. The fluorescent compound MTS-EMCA, which specifically links to this group, was used to label OprM. As a control we also analyzed MexAp (wt palmitoylated MexA), MexAnp (a mutated form of MexA lacking the signal peptide and bearing a free N-terminal cysteine) and MexAnp in the presence of DTT to reverse thiol acylation. After migration on an SDS gel, UV exposure of the gel at 312 nm (**Figure 2B**, lower panel) revealed a bright band for MexAnp and a faint band for MexAnp with DTT but no signal for OprM, demonstrating that the N-terminal cysteine of OprM is occupied on its thiol by lipoyl modification. Therefore, it can be concluded that the lipoyl modification is anchored exclusively to the sulphydryl group of OprM.

<sup>1</sup><http://www.ebi.ac.uk/Tools/msa/muscle/>



As a third approach, measuring the precise protein mass has also been considered. Indeed, in our case, one needs to distinguish between a palmitoyl (chemical composition C<sub>16</sub>H<sub>32</sub>O<sub>2</sub> resulting in a mass of 256 Da) and a tri- or di-acyl that can adopt a variable length. As an example, in the CusC structure can be found a tri-acyl composed of C<sub>19</sub>O<sub>5</sub>H<sub>33</sub> (PDB code: 3PIK) resulting in a mass of 341 Da, or a di-acyl (PDB code: 4K7R) of chemical composition C<sub>14</sub>O<sub>4</sub>H<sub>25</sub>, resulting in a mass of 257 Da, which is close to the mass of a palmitoyl. This result illustrates how difficult it is to obtain an answer using this technique as several combinations result in the same mass and it is necessary to measure mass with a precision as high as one Dalton, which is far to be routinely achieved to date with membrane proteins of that size. Attempts to address this question in the proteolyzed protein using the electrospray and MALDI techniques have been unsuccessful because the N-terminus peptide was not detected despite the use of different protease enzymes, and even thought 90% of the OprM sequence was covered by the analysis (data not shown).

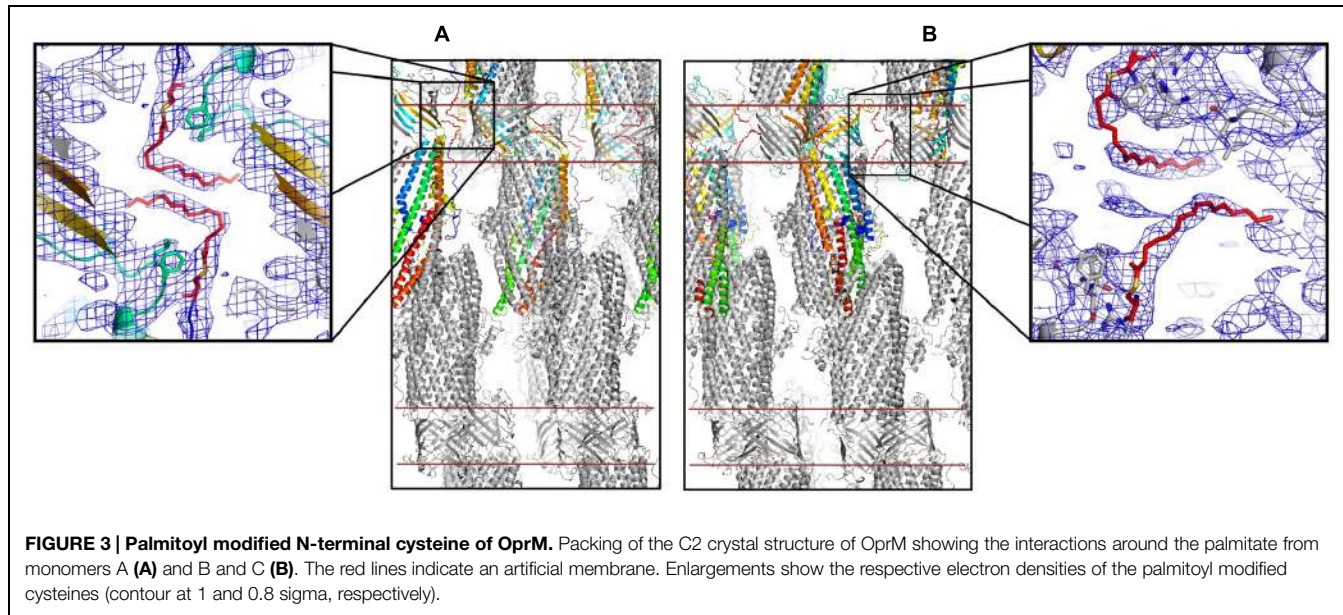
### OprM Crystal Structure in the C2 Space Group and Comparison with the Structure Solved in P2<sub>1</sub>2<sub>1</sub>2<sub>1</sub>

As the question about the nature of the modification remained unanswered, it has been envisaged to refine the OprM crystallographic structure in a different space group, as different crystal packing could stabilize the N-terminus and eventually reveal the complete structure of the added lipid. We previously solved the structure of OprM at 2.4 Å resolution in the P2<sub>1</sub>2<sub>1</sub>2<sub>1</sub> space group (Phan et al., 2010) but this structure showed only the beginning of the N-terminal

cysteine (lane 3), and boiled OprM (lane 4). A coomassie blue coloration shows all of the purified proteins. Fluorescence visualization of NBD-Cl ( $\lambda = 475$  nm) that shows that the N-terminal amine of OprM is available (A) whereas visualization of MTS-EMCA ( $\lambda = 312$  nm) shows that the N-terminal thiol of OprM is not available for labeling (B) and is thus occupied by the palmitoyl moiety. Only MexA<sub>p</sub> with a free N-terminal thiol is available for MTS-EMCA labeling (B).

lipoyl. We previously generated several OprM datasets in the C2 space group, but they were set aside without solving their structures owing to their lower resolution. To investigate the lipoyl structure, we decided to solve the structure of the best diffracting dataset limited to 3.8 Å resolution.

The here-solved structure comprises two trimers in the asymmetric unit with the second trimer being poorly defined. The crystal packing of our C2 OprM structure is slightly different from the P2<sub>1</sub>2<sub>1</sub>2<sub>1</sub> structure (see Supplementary Figure S2) but they share common type I crystal packing in which the homotrimer channels interact in a head-to-head manner through the hydrophobic beta-barrel domains mimicking a lipid bilayer plane. Despite its higher resolution (2.4 Å), the crystal structure of OprM in the P2<sub>1</sub>2<sub>1</sub>2<sub>1</sub> space group does not reveal the entire palmitoyl moiety because all the three N-termini are oriented toward the solvent and this results in high thermal motions. For two monomers, the closest amino acid is located more than 10 Å away from the expected palmitate main chain, and for the third, only the cysteine portion is clearly constrained, but this is not sufficient to build in the palmitoyl tail. In contrast, when stabilized by a more packed environment around the N-terminus, the entire fatty acid chain appears in the density map of the C2 form where two different orientations are observed (Figure 3). This is the sole, but crucial, advantage of this structure, because the crystal packing of OprM is equivalent to that previously published in the R32 space group (Akama et al., 2004) with the exception that the three monomers are not linked by crystallographic symmetries. Attempts were made to highlight some eventual local differences between the monomers even if at low resolution. Superposition of the six different



monomers from the C2 asymmetric unit onto monomer A demonstrates a mean C $\alpha$ -atom RMSD of 0.2 Å for monomers B and C, and 0.58 Å for monomers D, E, and F. These monomer superposition values have to be compared to those obtained for the two other structures of OprM in different space groups (a mean RMSD of 0.50 Å for 440 C $\alpha$  atoms in both cases) and that of the other OMF solved structures (1.87 Å for CmeC for 377 C $\alpha$  atoms, 1.28 Å for CusC on 381 C $\alpha$  atoms, 1.79 Å for VceC on 347 C $\alpha$  atoms, 1.32 Å for MtrE on 383 C $\alpha$  atoms, and 2.47 Å on 321 C $\alpha$  atoms for the closest TolC structure [PDB code: 2VDE (Bavro et al., 2008)]. Although no striking differences among the alternative crystal structures of OprM monomers were revealed, this analysis highlights the highly conserved folding within the OMF family with the most divergent being TolC in accordance with the sequence alignment (Supplementary Figure S1). Thus it appears that the only reason OprM would crystallize in either the R32 or C2 space groups is that the N-terminus lipoyl adopts a different conformation within the three monomers. To understand the different orientations of the palmitoyl, we compared their respective environments (Figure 4). For the three N-termini, the main chain is stabilized by hydrogen bonds with R133 and the carboxyl group of L128. In each case, the palmitoyl tail then turns around two hydrophobic residues, L128 and F129. The palmitoyl from the B monomer (subsequently called Palm-B) is located near the Palm-C of a symmetrical molecule but not close enough to form van der Waals contact because the distance between them is greater than 7 Å. Interestingly, Palm-A instead makes short van der Waals contacts with its own symmetric structure, justifying the quality of the electron density map for this region (see Figure 3) even at low resolution. The quality of the electron density for this particular monomer makes us confident about the exact nature of the fatty acid modification of OprM. As a final control the N-terminal PTMs that were generated in other OMF protein structures, namely CusC and

CmeC (Figure 4E) were superimposed on our structure and these demonstrate a longer acyl chain for OprM, supporting its palmitoyl nature.

## Discussion

Post-translational modifications (PTMs) play an important role in cell life as they govern most signaling events. Among the different PTMs, lipidation ranks as the second most common modification after phosphorylation<sup>2</sup> (dbPTM – database of protein PTMs; Beltrao et al., 2013), anchoring proteins to the membrane and stabilizing their interactions with the lipid bilayer.

It is not well understood why proteins that are embedded within cellular membranes via a large hydrophobic structural domain need supplementary PTMs such as the N-terminal lipidation of OMF proteins. Akama et al. (2004) suggested that these proteins first have to be anchored to the membrane by an N-terminal lipid so that the insertion of their large hydrophobic domain may be triggered. This later step is critical for the correct folding of OMFs. This hypothesis has been reinforced by structural determination of two CusC mutants for which the signal peptide has been conserved but the first cysteine residue after processing is replaced with a serine (C1S-CusC) or is deleted ( $\Delta$ C1-CusC), (Lei et al., 2014a). The structures result in a random folding of the beta-barrel domain of both mutants together with inappropriate opening of the periplasmic helices. These structures support the essential role of OMF N-terminal lipidation in the membrane insertion mechanism; moreover, they also highlight the possible involvement of membrane-interacting components in the OMF opening process and consequently the efflux-pump function.

<sup>2</sup><http://dbptm.mbc.nctu.edu.tw>

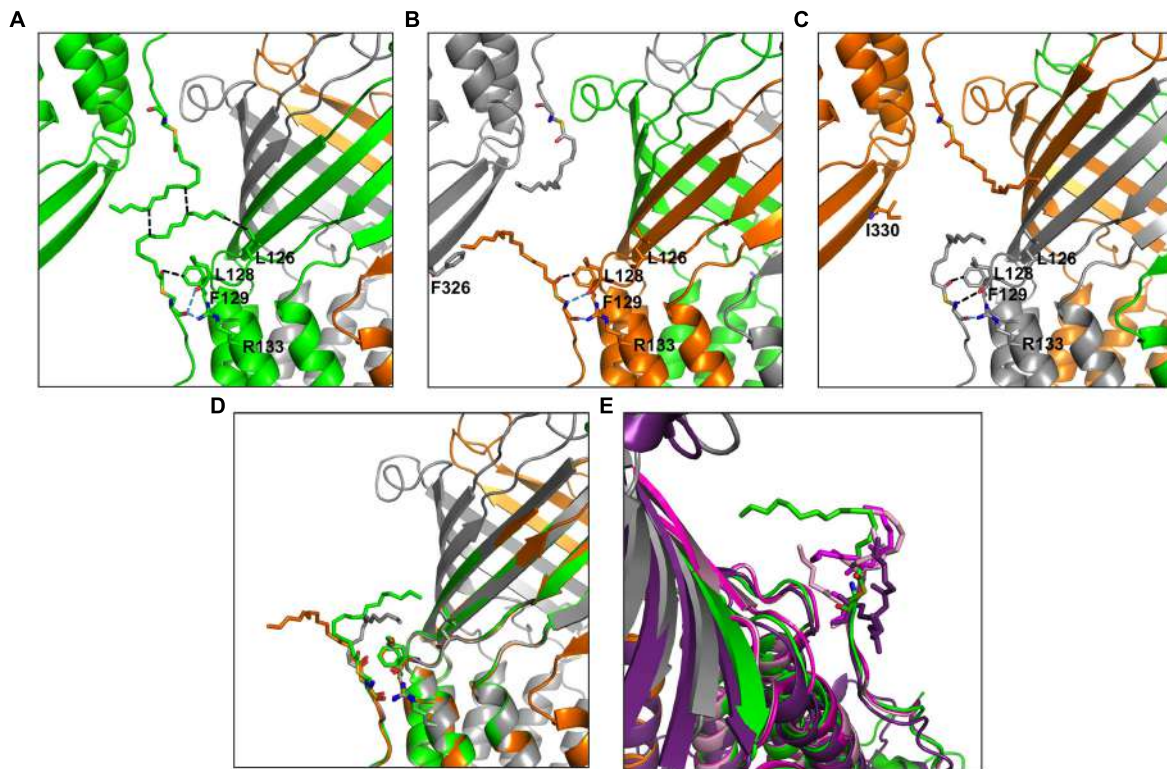


**FIGURE 4 | Environment comparison between palmitates from the three different monomers in the C2 space group. (A–C)** neighboring of the palmitates A, B, and C, respectively. **(D)** Superposition of the three monomers showing different orientations of the palmitate. **(E)** The lipoyl modifications of the CmeC structure (4MT4 in violet) and the two CusC structures (3PIK in light pink, 4K7R in magenta) are superposed on the palmitate from monomer A for length

comparison. Monomer A is shown in green, monomer B is shown in orange, monomer C is shown in gray. The ABC trimer from the asymmetric unit together with the closest monomer from packing is represented in each view. The residues in contact with the palmitates are represented as sticks, and the closest contacts are indicated by dotted lines in black for van der Waals and blue for hydrogen bonds.

In addition to this function, other functions have been attributed to lipid PTMs. It has been shown that the size of the hydrophobic regions of membrane proteins does not necessarily match the thickness of the cellular membrane (Mitra et al., 2004). Additional hydrophobic elements could then help membrane proteins to fit into membranes of variable thickness, which would explain why some proteins require the addition of 16 carbons, whereas others require only fourteen, depending on the transmembrane domain shape and size.

Regarding OprM, several constructs were previously designed for N-terminal labeling, membrane targeting and antibiotic response experiments (Nakajima et al., 2000) and demonstrated that only when residue 18 is a cysteine is the protein labeled by radioactive palmitate and targeted to the outer membrane. Nevertheless, the three tested OprM mutants (C18G, C18F, C18W) were functional, although none were properly targeted to the outer membrane.

Concerning MexA, the MFP component from the OprM-MexAB efflux pump that is also palmitoylated at its N-terminus and attached to the inner membrane, when this PTM is missing MexA becomes unable to interact with OprM as highlighted by *in vitro* blue native gel experiments (Ferrandez et al., 2012).

All of these data highlight interest in the study of these lipoproteins and the protein partners involved in their modification. To gain insight into these lipoproteins, it seemed important to identify which modification occurs on OprM. To that end, we analyzed the chemical accessibility of the N-terminal cysteine thiol and amine using different fluorescent probes, which revealed that only the thiol was occupied. In addition, the nature of the attached lipoyl was proven to be a palmitoyl by our determination of the structure of OprM in a new space group that trapped the lipoyl chain at the interface of one monomer with its own symmetric structure.

We now know the nature of OprM N-terminal PTM, and that other OMFs such as CusC and CmeC from different bacterial strains, have similar but different N-terminal modifications. Nevertheless, if anchorage was important for the function of this class of proteins, why would the analog TolC not undergo PTMs? The sequences of OprM and TolC were submitted to the prediction of palmitoylation site<sup>3</sup>, which confirmed that C18 was a palmitoylation target in OprM and that there was no such site in the TolC sequence. When comparing the structure of TolC with that of OprM, CusC, and CmeC (Figure 5), it appears

<sup>3</sup><http://csspalm.biocuckoo.org/>

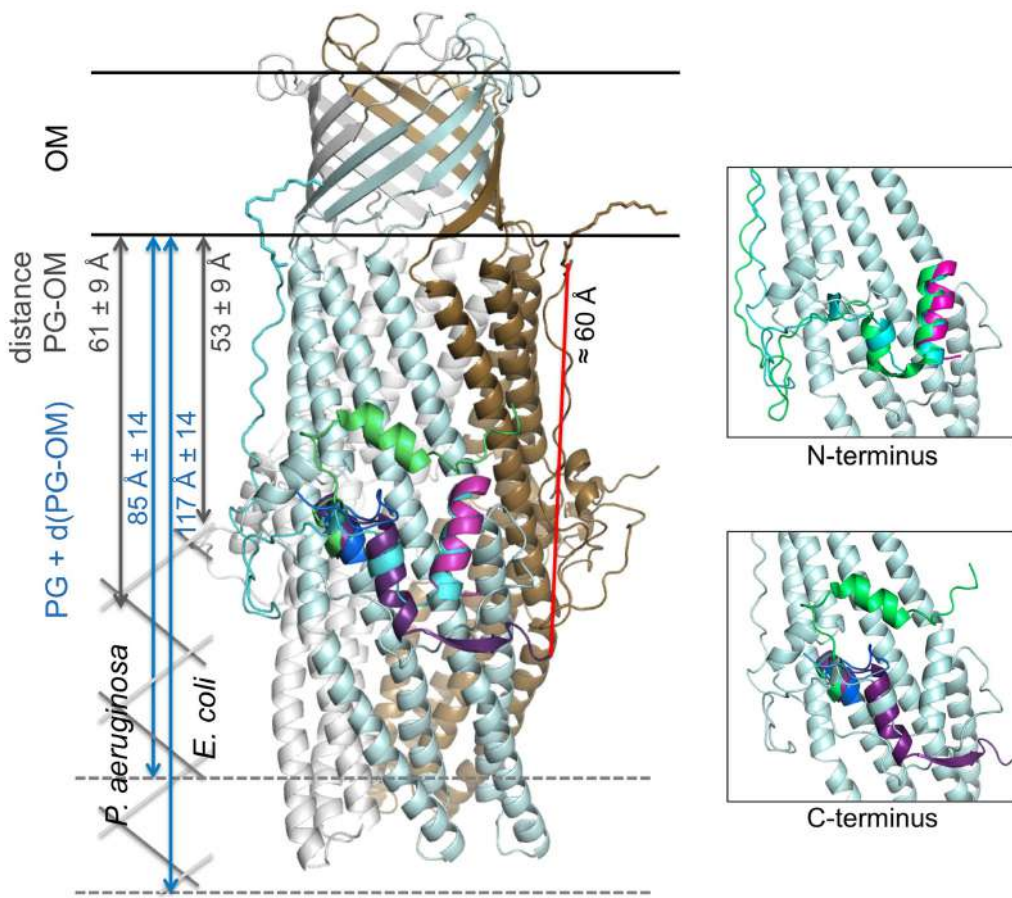


**FIGURE 5 |** Cartoon representation of the C2 OprM structure with the superposition of the N- and C-terminal regions of OprM, TolC and CmeC. The OprM trimer is shown in light blue, gray, and brown. The N-terminal region of OprM is shown in cyan, and its C-terminus is dark blue. The N- and C-termini of TolC are magenta and violet, respectively. Only the C-terminus of CmeC is presented (green) as the N-terminus is similar to that of OprM. The distance between the C-terminal residue present in the TolC

structure and the closest N-terminal cysteine from a monomer in the OprM trimer is indicated (red). For comparison, a schematic drawing of the peptidoglycan (PG) has been added at scale for both *Pseudomonas aeruginosa* and *Escherichia coli* (dimension data are from Matias et al., 2003). Two close-up views of the buoy region with only one OprM monomer are presented for clarity. They correspond to the highlighting of the superposition of the N- and C-termini, respectively.

that only TolC is different at the N-terminus. In particular, TolC is 44 residues shorter in sequence than OprM (Figure 1; Supplementary Figure S1), meaning that the TolC structure starts at the buoy level. Nevertheless, it should be noted that although it possesses a shortened N-terminus, TolC has a longer C-terminal tail (Figure 1; Supplementary Figure S1), which is not present in its solved structure. Even without knowing anything about the role of this long C-terminal region, it can be hypothesized that it could lead to an additional interaction with the membrane. This hypothesis is supported by the fact that the C-terminal structure of CmeC (an OMF protein with the longest C-terminal sequence of those known) is oriented toward the outer membrane, and the C-terminal alpha-helix of TolC is structurally equivalent to the N-terminal alpha-helix of the other OMFs according to structure superposition (Figure 5). In addition, the distance between the last visible C-terminal amino acid of the TolC structure and the membrane proximal N-terminus of the superposed OprM monomer is approximately 60 Å, a distance that could be covered

by a 42 residue-long helix, which corresponds to the number of residues missing at the C-terminus of the TolC construct.

The fact that TolC can be properly inserted in the membrane despite its particularity, the absence of lipid anchor, can be due to the differences in the peptidoglycan (PG) structure between Gram-negative bacteria. The NMR structure of a 2 kDa synthetic fragment composed of NAG-NAM (pentapeptides; Meroueh et al., 2006) allowed to visualize TolC as completely embedded in the PG, its periplasmic alpha-helical domain just flushing the limit of the PG. Measurements of the cell wall dimensions of both *E. coli* and *P. aeruginosa* were performed by cryo-transmission electron microscopy (Matias et al., 2003), revealing large size differences between the different cell wall constituents, particularly the PG. The empty space between the PG and the outer-membrane d(PG-OM), and the total thickness, PG + d(PG-OM), were estimated to be 53 ± 9 and 61 ± 9 Å for d(PG-OM), and 117 ± 14 and 85 ± 14 Å for PG + d(PG-OM) in *E. coli* and *P. aeruginosa*, respectively

(see **Figure 5**). Consequently, TolC is more likely to be tightly embedded in the membrane barrier than OprM. Nevertheless, no published experiments can support these hypotheses to date.

## Conclusion

In this study, we have shown that OprM is palmitoylated at its N-terminal cysteine by thio-palmitoylation. It is now necessary to search for the different proteins involved in this acylation, lipid-transferases, and signal peptidases. These lipoprotein modifiers could represent new interesting targets for the fight against antibiotic resistance.

## Author Contributions

Conceived and designed the experiments: GP, HB, and IB. Performed the experiments: LM, GP, HB, M-BL, YN, and IB. Analyzed the data: LM, GP, HB, M-BL, YN, MP, and IB. Wrote the paper: GP, MP, and IB.

## References

- Adams, P. D., Grosse-Kunstleve, R. W., Hung, L. W., Ioerger, T. R., McCoy, A. J., Moriarty, N. W., et al. (2002). PHENIX: building new software for automated crystallographic structure determination. *Acta Crystallogr. D Biol. Crystallogr.* 58, 1948–1954. doi: 10.1107/S0907444902016657
- Aicart-Ramos, C., Valero, R. A., and Rodriguez-Crespo, I. (2011). Protein palmitoylation and subcellular trafficking. *Biochim. Biophys. Acta* 1808, 2981–2994. doi: 10.1016/j.bbamem.2011.07.009
- Aires, J. R., Kohler, T., Nikaido, H., and Plesiat, P. (1999). Involvement of an active efflux system in the natural resistance of *Pseudomonas aeruginosa* to aminoglycosides. *Antimicrob. Agents Chemother.* 43, 2624–2628.
- Akama, H., Kanemaki, M., Yoshimura, M., Tsukihara, T., Kashiwagi, T., Yoneyama, H., et al. (2004). Crystal structure of the drug discharge outer membrane protein, OprM, of *Pseudomonas aeruginosa*: dual modes of membrane anchoring and occluded cavity end. *J. Biol. Chem.* 279, 52816–52819. doi: 10.1074/jbc.C400445200
- Bavro, V. N., Pietras, Z., Furnham, N., Perez-Cano, L., Fernandez-Recio, J., Pei, X. Y., et al. (2008). Assembly and channel opening in a bacterial drug efflux machine. *Mol. Cell* 30, 114–121. doi: 10.1016/j.molcel.2008.02.015
- Bayram, Y., Parlak, M., Aypak, C., and Bayram, I. (2013). Three-year review of bacteriological profile and antibiogram of burn wound isolates in Van, Turkey. *Int. J. Med. Sci.* 10, 19–23. doi: 10.7150/ijms.4723
- Beltrao, P., Bork, P., Krogan, N. J., and van Noort, V. (2013). Evolution and functional cross-talk of protein post-translational modifications. *Mol. Syst. Biol.* 9, 714. doi: 10.1002/msb.201304521
- Bereket, W., Hemalatha, K., Getenet, B., Wondwossen, T., Solomon, A., Zeynudin, A., et al. (2012). Update on bacterial nosocomial infections. *Eur. Rev. Med. Pharmacol. Sci.* 16, 1039–1044.
- Bernal-Perez, L. F., Prokai, L., and Ryu, Y. (2012). Selective N-terminal fluorescent labeling of proteins using 4-chloro-7-nitrobenzofuran: a method to distinguish protein N-terminal acetylation. *Anal. Biochem.* 428, 13–15. doi: 10.1016/j.ab.2012.05.026
- Cattoir, V. (2004). [Efflux-mediated antibiotics resistance in bacteria]. *Pathol. Biol.* 52, 607–616. doi: 10.1016/j.patbio.2004.09.001
- CCP4 suite. (1994). The CCP4 suite: programs for protein crystallography. *Acta Crystallogr. D Biol. Crystallogr.* 50, 760–763. doi: 10.1107/S0907444994003112
- Chalker, J. M., Bernardes, G. J., Lin, Y. A., and Davis, B. G. (2009). Chemical modification of proteins at cysteine: opportunities in chemistry and biology. *Chem. Asian J.* 4, 630–640. doi: 10.1002/asia.200800427
- Chuanchuen, R., Narasaki, C. T., and Schweizer, H. P. (2002). The MexJK efflux pump of *Pseudomonas aeruginosa* requires OprM for antibiotic efflux but not for efflux of triclosan. *J. Bacteriol.* 184, 5036–5044. doi: 10.1128/JB.184.18.5036-5044.2002
- Davis, I. W., Leaver-Fay, A., Chen, V. B., Block, J. N., Kapral, G. J., Wang, X., et al. (2007). MolProbity: all-atom contacts and structure validation for proteins and nucleic acids. *Nucleic Acids Res.* 35, W375–W383. doi: 10.1093/nar/gkm216
- DeLano, W. L. (2002). *The PyMOL Molecular Graphics System*. Available at: <http://pymol.sourceforge.net/>
- Emsley, P., and Cowtan, K. (2004). Coot: model-building tools for molecular graphics. *Acta Crystallogr. D Biol. Crystallogr.* 60, 2126–2132. doi: 10.1107/S0907444904019158
- Federici, L., Du, D., Walas, F., Matsumura, H., Fernandez-Recio, J., McKeegan, K. S., et al. (2005). The crystal structure of the outer membrane protein VceC from the bacterial pathogen *Vibrio cholerae* at 1.8 Å resolution. *J. Biol. Chem.* 280, 15307–15314. doi: 10.1074/jbc.M500401200
- Ferrandez, Y., Monlezun, L., Phan, G., Benabdellah, H., Benas, P., Ulryck, N., et al. (2012). Stoichiometry of the MexA-OprM binding, as investigated by blue native gel electrophoresis. *Electrophoresis* 33, 1282–1287. doi: 10.1002/elps.201100541
- Fischbach, M. A., and Walsh, C. T. (2009). Antibiotics for emerging pathogens. *Science* 325, 1089–1093. doi: 10.1126/science.1176667
- Ghosh, P. B., and Whitehouse, M. W. (1968). 7-chloro-4-nitrobenzo-2-oxa-1,3-diazole: a new fluorogenic reagent for amino acids and other amines. *Biochem. J.* 108, 155–156.
- Hede, K. (2014). Antibiotic resistance: an infectious arms race. *Nature* 509, S2–S3. doi: 10.1038/509S2a
- Kabsch, W. (1993). Automatic porocessing of rotation diffraction data from crystals of initially unknown symmetry and cell constants. *J. Appl. Crystallogr.* 26, 795–800. doi: 10.1107/S0021889893005588
- Koronakis, V., Sharff, A., Koronakis, E., Luisi, B., and Hughes, C. (2000). Crystal structure of the bacterial membrane protein TolC central to multidrug efflux and protein export. *Nature* 405, 914–919. doi: 10.1038/35016007
- Kovacs-Simon, A., Titball, R. W., and Michell, S. L. (2011). Lipoproteins of bacterial pathogens. *Infect. Immun.* 79, 548–561. doi: 10.1128/IAI.00682-10
- Kulathila, R., Indic, M., and van den Berg, B. (2011). Crystal structure of *Escherichia coli* CusC, the outer membrane component of a heavy metal efflux pump. *PLoS ONE* 6:e15610. doi: 10.1371/journal.pone.0015610
- Lei, H. T., Bolla, J. R., Bishop, N. R., Su, C. C., and Yu, E. W. (2014a). Crystal structures of CusC review conformational changes accompanying

## Acknowledgments

This study was supported by Agence Nationale de la Recherche (Grants ANR-11-BS07-019-04 and ANR-12-BSV8-0010-01). LM was supported by a grant from Vaincre la Mucoviscidose and VE was supported by both Vaincre la Mucoviscidose and the Association Grégory Lemarchal. We acknowledge P. Benas for his assistance in using refinement and building programs. We acknowledge the SOLEIL and the ESRF synchrotrons for providing the synchrotron radiation facilities and thank the technical staff for assistance using beam lines PX1 and ID29. We thank the proteomic plateform from Paris Descartes University (3P5: <http://3p5.medecine.univ-paris5.fr/>) for the mass analysis of OprM.

## Supplementary Material

The Supplementary Material for this article can be found online at: <http://journal.frontiersin.org/article/10.3389/fmib.2015.000667>

- folding and transmembrane channel formation. *J. Mol. Biol.* 426, 403–411. doi: 10.1016/j.jmb.2013.09.042
- Lei, H. T., Chou, T. H., Su, C. C., Bolla, J. R., Kumar, N., Radhakrishnan, A., et al. (2014b). Crystal structure of the open state of the *Neisseria gonorrhoeae* MtrE outer membrane channel. *PLoS ONE* 9:e97475. doi: 10.1371/journal.pone.0097475
- Li, X. Z., and Nikaido, H. (2009). Efflux-mediated drug resistance in bacteria: an update. *Drugs* 69, 1555–1623. doi: 10.2165/11317030-000000000-00000
- Li, X. Z., and Poole, K. (2001). Mutational analysis of the OprM outer membrane component of the MexA-MexB-OprM multidrug efflux system of *Pseudomonas aeruginosa*. *J. Bacteriol.* 183, 12–27. doi: 10.1128/JB.183.1.12-27.2001
- Linder, M. E., and Deschenes, R. J. (2007). Palmitoylation: policing protein stability and traffic. *Nat. Rev. Mol. Cell Biol.* 8, 74–84. doi: 10.1038/nrm2084
- Ling, L. L., Schneider, T., Peoples, A. J., Spoering, A. L., Engels, I., Conlon, B. P., et al. (2015). A new antibiotic kills pathogens without detectable resistance. *Nature* 517, 455–459. doi: 10.1038/nature14098
- Lister, P. D., Wolter, D. J., and Hanson, N. D. (2009). Antibacterial-resistant *Pseudomonas aeruginosa*: clinical impact and complex regulation of chromosomally encoded resistance mechanisms. *Clin. Microbiol. Rev.* 22, 582–610. doi: 10.1128/CMR.00040-09
- Matias, V. R., Al-Amoudi, A., Dubochet, J., and Beveridge, T. J. (2003). Cryo-transmission electron microscopy of frozen-hydrated sections of *Escherichia coli* and *Pseudomonas aeruginosa*. *J. Bacteriol.* 185, 6112–6118. doi: 10.1128/JB.185.20.6112-6118.2003
- McCoy, A. J., Grosse-Kunstleve, R. W., Adams, P. D., Winn, M. D., Storoni, L. C., and Read, R. J. (2007). Phaser crystallographic software. *J. Appl. Crystallogr.* 40, 658–674. doi: 10.1107/S0021889807021206
- Meroueh, S. O., Bencze, K. Z., Hesketh, D., Lee, M., Fisher, J. F., Stemmler, T. L., et al. (2006). Three-dimensional structure of the bacterial cell wall peptidoglycan. *Proc. Natl. Acad. Sci. U.S.A.* 103, 4404–4409. doi: 10.1073/pnas.0510182103
- Mima, T., Sekiya, H., Mizushima, T., Kuroda, T., and Tsuchiya, T. (2005). Gene cloning and properties of the RND-type multidrug efflux pumps MexPQ-OprM and MexMN-OprM from *Pseudomonas aeruginosa*. *Microbiol. Immunol.* 49, 999–1002. doi: 10.1111/j.1348-0421.2005.tb03696.x
- Miroux, B., and Walker, J. E. (1996). Over-production of proteins in *Escherichia coli*: mutant hosts that allow synthesis of some membrane proteins and globular proteins at high levels. *J. Mol. Biol.* 260, 289–298. doi: 10.1006/jmbi.1996.0399
- Mitra, K., Ubarretxena-Belandia, I., Taguchi, T., Warren, G., and Engelmann, D. M. (2004). Modulation of the bilayer thickness of exocytic pathway membranes by membrane proteins rather than cholesterol. *Proc. Natl. Acad. Sci. U.S.A.* 101, 4083–4088. doi: 10.1073/pnas.0307332101
- Morita, Y., Tomida, J., and Kawamura, Y. (2012). MexXY multidrug efflux system of *Pseudomonas aeruginosa*. *Front. Microbiol.* 3:408. doi: 10.3389/fmicb.2012.00408
- Nakajima, A., Sugimoto, Y., Yoneyama, H., and Nakae, T. (2000). Localization of the outer membrane subunit OprM of resistance-nodulation-cell division family multicomponent efflux pump in *Pseudomonas aeruginosa*. *J. Biol. Chem.* 275, 30064–30068. doi: 10.1074/jbc.M005742200
- Nakajima, A., Sugimoto, Y., Yoneyama, H., and Nakae, T. (2002). High-level fluoroquinolone resistance in *Pseudomonas aeruginosa* due to interplay of the MexAB-OprM efflux pump and the DNA gyrase mutation. *Microbiol. Immunol.* 46, 391–395. doi: 10.1111/j.1348-0421.2002.tb02711.x
- Nakayama, H., Kurokawa, K., and Lee, B. L. (2012). Lipoproteins in bacteria: structures and biosynthetic pathways. *FEBS J.* 279, 4247–4268. doi: 10.1111/febs.12041
- Nikaido, H. (2009). Multidrug resistance in bacteria. *Annu. Rev. Biochem.* 78, 119–146. doi: 10.1146/annurev.biochem.78.082907.145923
- Nikaido, H., and Pages, J. M. (2012). Broad-specificity efflux pumps and their role in multidrug resistance of Gram-negative bacteria. *FEMS Microbiol. Rev.* 36, 340–363. doi: 10.1111/j.1574-6976.2011.00290.x
- Olivares, J., Bernardini, A., Garcia-Leon, G., Corona, F., Sanchez, B. M., and Martinez, J. L. (2013). The intrinsic resistome of bacterial pathogens. *Front. Microbiol.* 4:103. doi: 10.3389/fmicb.2013.00103
- Phan, G., Benabdellah, H., Lascombe, M. B., Benas, P., Rety, S., Picard, M., et al. (2010). Structural and dynamical insights into the opening mechanism of *P. aeruginosa* OprM channel. *Structure* 18, 507–517. doi: 10.1016/j.str.2010.01.018
- Poole, K. (2004). Efflux-mediated multiresistance in Gram-negative bacteria. *Clin. Microbiol. Infect.* 10, 12–26. doi: 10.1111/j.1469-0691.2004.00763.x
- Resh, M. D. (1999). Fatty acylation of proteins: new insights into membrane targeting of myristoylated and palmitoylated proteins. *Biochim. Biophys. Acta* 1451, 1–16. doi: 10.1016/S0167-4889(99)00075-0
- Robert, X., and Gouet, P. (2014). Deciphering key features in protein structures with the new ENDscript server. *Nucleic Acids Res.* 42, W320–W324. doi: 10.1093/nar/gku316
- Schweizer, H. P. (2003). Efflux as a mechanism of resistance to antimicrobials in *Pseudomonas aeruginosa* and related bacteria: unanswered questions. *Genet. Mol. Res.* 2, 48–62.
- Su, C. C., Radhakrishnan, A., Kumar, N., Long, F., Bolla, J. R., Lei, H. T., et al. (2014). Crystal structure of the *Campylobacter jejuni* CmeC outer membrane channel. *Protein Sci.* 23, 954–961. doi: 10.1002/pro.2478
- Tooley, J. G., and Schaner Tooley, C. E. (2014). New roles for old modifications: emerging roles of N-terminal post-translational modifications in development and disease. *Protein Sci.* 23, 1641–1649. doi: 10.1002/pro.2547
- Urzhumtseva, L., Afonine, P. V., Adams, P. D., and Urzhumtsev, A. (2009). Crystallographic model quality at a glance. *Acta Crystallogr. D Biol. Crystallogr.* 65, 297–300. doi: 10.1107/S0907444908044296
- Walsh, C. (2003). Where will new antibiotics come from? *Nat. Rev. Microbiol.* 1, 65–70. doi: 10.1038/nrmicro727
- Yen, M. R., Peabody, C. R., Partovi, S. M., Zhai, Y., Tseng, Y. H., and Saier, M. H. (2002). Protein-translocating outer membrane porins of Gram-negative bacteria. *Biochim. Biophys. Acta* 1562, 6–31. doi: 10.1016/S0005-2736(02)00359-0

**Conflict of Interest Statement:** The authors declare that the research was conducted in the absence of any commercial or financial relationships that could be construed as a potential conflict of interest.

Copyright © 2015 Monlezun, Phan, Benabdellah, Lascombe, Enguéne, Picard and Broutin. This is an open-access article distributed under the terms of the Creative Commons Attribution License (CC BY). The use, distribution or reproduction in other forums is permitted, provided the original author(s) or licensor are credited and that the original publication in this journal is cited, in accordance with accepted academic practice. No use, distribution or reproduction is permitted which does not comply with these terms.



# Repressive mutations restore function-loss caused by the disruption of trimerization in *Escherichia coli* multidrug transporter AcrB

Zhaoshuai Wang<sup>†</sup>, Meng Zhong<sup>†</sup>, Wei Lu, Qian Chai and Yinan Wei\*

Department of Chemistry, University of Kentucky, Lexington, KY, USA

**Edited by:**

Hiroshi Nikaido, University of California, Berkeley, USA

**Reviewed by:**

Lei Dai, Iowa State University, USA  
Markus Seeger, University of Zurich, Switzerland

**\*Correspondence:**

Yinan Wei, University of Kentucky, 305 Chemistry-Physics Building, Lexington, KY 40506-0055, USA  
e-mail: yinan.wei@uky.edu

<sup>†</sup>These authors have contributed equally to this work.

AcrAB-TolC and their homologs are major multidrug efflux systems in Gram-negative bacteria. The inner membrane component AcrB functions as a trimer. Replacement of Pro223 by Gly in AcrB decreases the trimer stability and drastically reduces the drug efflux activity. The goal of this study is to identify suppressor mutations that restore function to mutant AcrB<sub>P223G</sub> and explore the mechanism of function recovery. Two methods were used to introduce random mutations into the plasmid of AcrB<sub>P223G</sub>. Mutants with elevated drug efflux activity were identified, purified, and characterized to examine their expression level, trimer stability, interaction with AcrA, and substrate binding. Nine single-site repressor mutations were identified, including T199M, D256N, A209V, G257V, M662I, Q737L, D788K, P800S, and E810K. Except for M662I, all other mutations located in the docking region of the periplasmic domain. While three mutations, T199M, A209V, and D256N, significantly increased the trimer stability, none of them restored the trimer affinity to the wild type level. M662, the only site of mutation that located in the porter domain, was involved in substrate binding. Our results suggest that the function loss resulted from compromised AcrB trimerization could be restored through various mechanisms involving the compensation of trimer stability and substrate binding.

**Keywords:** RND, oligomerization, membrane transporter, efflux pump, protein thermal stability

## INTRODUCTION

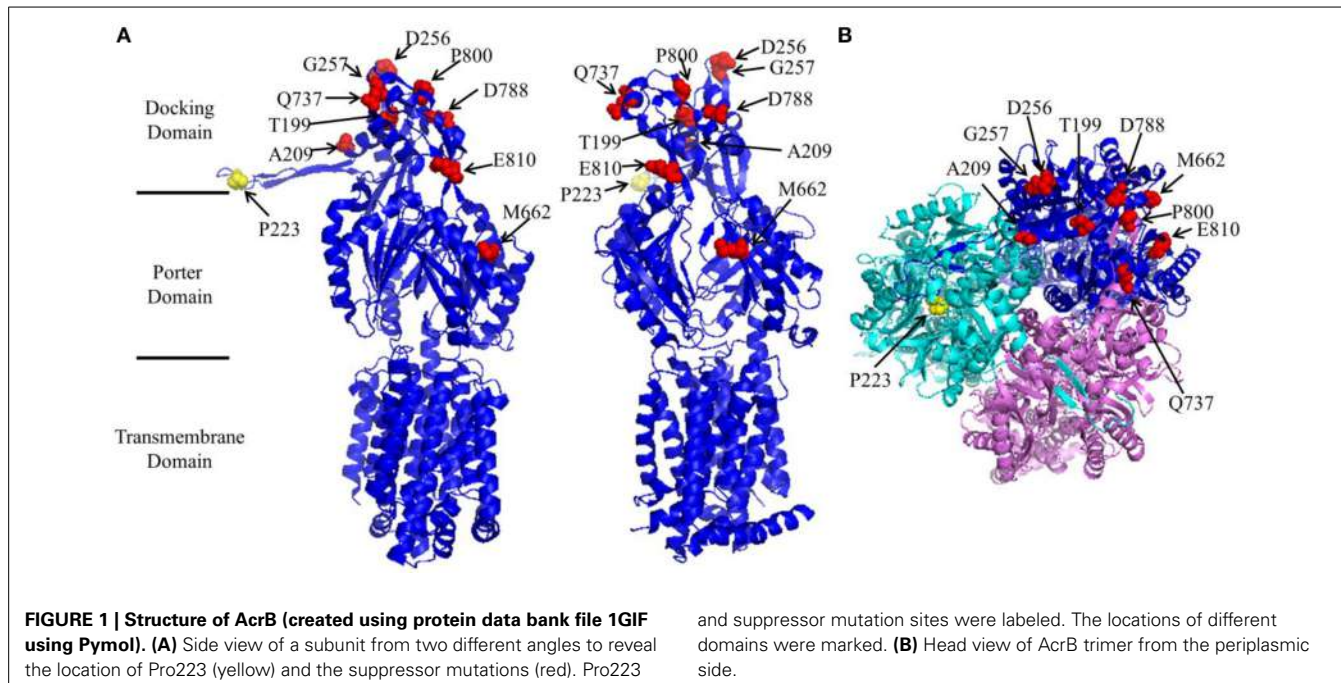
*Escherichia coli* multidrug transporter AcrB and its homologues are the inner membrane component of the Resistance-Nodulation-Division (RND) family transporters in Gram-negative bacteria, which are major players in bacterial multidrug resistance (Blair and Piddock, 2009; Nikaido and Takatsuka, 2009; Nikaido and Pages, 2012; Zgurskaya and Nikaido, 2012). AcrB forms a tripartite pump system with membrane fusion protein (MFP) AcrA and outer membrane protein TolC. In the AcrAB-TolC complex, AcrB determines substrate specificity. The inward proton flow across the cytoplasmic membrane through a proton-relay pathway in the transmembrane domain of AcrB drives the active transport of substrates against their concentration gradient. In the process of substrate efflux, each AcrB monomer rotates through three conformations, access (or loose), binding (or tight), and extrusion (or open) (Murakami et al., 2006; Seeger et al., 2006, 2008; Vargiu and Nikaido, 2012).

AcrB exists and functions as a homotrimer. Each subunit consists of 12 transmembrane helices (TMH), and two large periplasmic loops (LPL) which form a periplasmic domain. Mutations in

the transmembrane domain, including D407A, D408A, K940A, and T978A, disrupt the proton relay network and disable the pump (Su et al., 2006; Eicher et al., 2009; Pos, 2009). The two LPLs exist in between TMH1 and TMH2 (LPL1) and TMH7 and TMH8 (LPL2). The periplasmic domain is further divided into a porter domain and a docking domain (Figure 1). Exchange of AcrB and AcrD periplasmic loops altered the substrate preference of the proteins, suggesting that residues dictating substrate specificity reside in the periplasmic domain (Elkins and Nikaido, 2002). A deep binding pocket was later defined through additional mutational and crystallographic studies (Yu et al., 2005; Sennhauser et al., 2006; Nakashima et al., 2011; Eicher et al., 2012). Depending on where they interact, substrates were divided into two groups: groove binder and cave binder (Bohnert et al., 2010; Takatsuka et al., 2010). Using Bodipy-FL-maleimide labeling, Nikaido and coworkers elucidated the entire substrate translocation pathway (Husain and Nikaido, 2010; Husain et al., 2011). More recently a switching loop was found to separate the binding location of different substrates into two sites, a proximal pocket and a distal pocket (Vargiu and Nikaido, 2012; Kobayashi et al., 2014). While large compounds bind to the proximal pocket before moving toward the exit, smaller substrates bind to the distal pocket.

Crystal structure of the entire AcrAB-TolC complex is not yet available. Two models of interaction have been proposed for AcrAB-TolC and similar tripartite transporters. A wrapping

**Abbreviations:** R6G, Rhodamine 6G; PMSF, phenylmethylsulfonyl fluoride; WT, wild type; DDM, n-dodecylb-D-maltoside; NTA, nitrilotriacetic acid; RND, resistance-nodulation-cell-division; SDS-PAGE, sodium dodecyl sulfate polyacrylamide gel electrophoresis.



model was proposed first, in which the top part of the AcrB periplasmic domain interacts directly with the bottom of the periplasmic domain of TolC and AcrA wraps around the AcrB-TolC complex (Eswaran et al., 2004). Accordingly, the tip of the AcrB periplasmic domain is sometimes referred to as the TolC docking domain. More recently, a bridging model was proposed, in which the hexameric MFP forms a cylindrical bridge to connect the inner membrane protein and outer membrane protein (Xu et al., 2012; Du et al., 2014). In this bridging model, the outer membrane protein does not interact directly with the inner membrane protein.

The proper function of this delicate drug efflux machine requires the accurate assembly of the tripartite complex. While extensive studies have been done on the understanding of substrate binding, proton relay, and interaction between AcrB with AcrA/TolC, much less emphasis have been focused on the investigation of the trimerization of AcrB and how trimerization is correlated with other functional aspects such as interaction with AcrA/TolC and substrate binding (Lu et al., 2014). In each AcrB subunit, a long extended loop inserts into the neighboring subunit, which is important to the formation of AcrB trimer. We have previously created a well-folded monomeric AcrB mutant through truncating 17 residues from the loop (Lu et al., 2011). Later, we found that a single Pro223 to Gly mutation is sufficient to disrupt trimerization and lead to a drastic loss of activity (Yu et al., 2011). AcrB<sub>P223G</sub> has low trimer affinity and its function can be partially restored through stabilizing the trimer via the introduction of an inter-subunit disulfide bond (Yu et al., 2011). To understand interactions that stabilize AcrB trimer, we conducted random mutagenesis experiments to identify suppressor mutations that restore functions to AcrB<sub>P223G</sub>. Nine single-site suppressor mutations were identified. These suppressor mutants were purified and

characterized to investigate the potential mechanisms of function restoration.

## MATERIALS AND METHODS

### RANDOM MUTAGENESIS OF AcrB AND MUTANTS SCREENING

Random mutagenesis of AcrB was achieved by two methods, hydroxylamine hydrochloride treatment and error-prone PCR. Chemical mutagenesis by hydroxylamine hydrochloride was performed as described with slight modifications (Middlemiss and Poole, 2004). Plasmid pQE70-acrB<sub>P223G</sub> was constructed in a previous study (Yu et al., 2011). pQE70-acrB<sub>P223G</sub> was incubated in a potassium phosphate buffer (44 mM, pH 6.0) containing 5 mM EDTA and 0.46 M hydroxylamine hydrochloride at 70°C for 40 min. To quench the reaction, Tris-Cl (pH 8.0) and EDTA were added to the mixture to final concentrations of 90 and 9 mM, respectively. Treated plasmid was purified using a gel extraction kit (Qiagen, CA) and used for transformation.

Error prone PCR was carried out using GeneMorph II EZClone domain mutagenesis kit following the manufacturer's instruction (Agilent Technologies, Inc., Clara, CA). pQE70-AcrB<sub>P223G</sub> was amplified using Mutazyme II DNA polymerase with two pairs of primers. Primers PP1 (5'-atgcctaattcttatcga tcgc-3') and PP2 (5'-AACGGCGTGGTG TCGTATGG-3') were used to introduce mutations into the first large periplasmic loop of AcrB. Primers PP3 (5'-cggtgatctgactccagtc-3') and PP4 (5'- ATCGACCAGCTCTCGT ACAG-3') were used to introduce mutations in the second large periplasmic loop. PCR products were separated and purified by gel electrophoresis. The purified PCR product was used as mega-primers and pQE70-AcrB<sub>P223G</sub> was used as the template during the following EZClone reaction. DpnI was then added to digest the template plasmid.

Mutated plasmids generated through hydroxylamine treatment or error-prone PCR were used to transform *E. coli*

BW25113Δ*acrB* through electroporation. The resultant cells were incubated with 1 mL LB broth with shaking at 37°C for 1 h before plated on LB agar plates containing 100 μg/mL ampicillin, 50 μg/mL kanamycin, and 16–32 μg/mL AcrB substrate erythromycin. Plasmids were extracted from colonies that were able to grow on the erythromycin plates and retransformed into BW25113Δ*acrB* strain. Drug susceptibility was tested. Plasmids that conferred decreased susceptibility were sequenced. Forty two suppressor clones were sequenced. Each mutations identified were further confirmed by introducing into P223G through site directed mutagenesis. Mutations yield false positive results were excluded. Nine unique single mutations that could restore P223G activity were identified. T199M were identified 14 times, D256N 6 times, M662I 2 times, D788K 2 times, and each of the other five mutations were only identified once. We have also observed the G223P back-to wild type mutation twice.

#### DRUG SUSCEPTIBILITY ASSAY OF AcrB MUTANTS

AcrB activities were examined using a drug susceptibility assay. The minimum inhibitory concentrations (MIC) of different strains were measured as described (Takatsuka and Nikaido, 2009). Plasmids encoding different AcrB constructs were used to transform BW25113Δ*acrB*. Freshly transformed cells were plated on LB-agarose plates containing 100 μg/mL ampicillin and 50 μg/mL kanamycin. The same ampicillin and kanamycin concentrations were used throughout the study. A single colony was used to inoculate LB media supplemented with ampicillin and kanamycin. The exponential-phase cultures of different strains were diluted to an OD<sub>600nm</sub> unit of 0.1 using LB broth. 2 μL of this culture was spotted onto a series of LB-agar plate containing the indicated concentration of AcrB substrates. The agar plates were incubated at 37°C overnight and the lowest concentration of substrate that fully inhibited the bacteria growth was recorded as the MIC. BW25113Δ*acrB* strains transformed with plasmid-encoded wild type AcrB or AcrB<sub>P223G</sub> were used as the positive and negative controls, respectively. Each experiment was repeated at least three times.

#### BLUE NATIVE PAGE ANALYSIS OF WILD TYPE AND MUTANT AcrB

Protein purification was conducted as described (Lu et al., 2011). BN-PAGE analysis were performed as described (Wittig et al., 2006). A phosphate buffer (20 mM NaPi, 100 mM NaCl, 0.03% w/v DDM, pH 7.9) was used throughout the study unless otherwise noted. Purified protein samples were mixed with blue native loading buffer to reach a final concentration of 0.02 M 6-aminoocaproic acid, 1% dodecylmaltoside, 5% glycerol, 0.1% Coomassie brilliant blue G-250, pH 7.0. Protein samples were loaded to a 4–15% polyacrylamide gradient gel. Electrophoresis was performed using a running buffer (50 mM Tricine, 7.5 mM imidazole, 0.02% Coomassie brilliant blue G-250, pH 7.0) at 15 mA, in the 4°C refrigerator for 2 h. Protein bands were visualized after Coomassie blue stain. Band intensity was quantified using the software ImageJ.

#### AcrA AND AcrB INTERACTION

pQE70-AcrB and its mutants were transformed into BW25113Δ*acrB* to study *in vivo* interaction between AcrB

and AcrA. Dithiobis succinimidyl propionate (DSP) crosslinking and co-purification were performed as described with slight modifications (Zgurskaya and Nikaido, 2000). Cells were cultured overnight in 50 mL LB supplemented with ampicillin and kanamycin before harvested and washed with 5 mL phosphate buffer twice. The pellet was resuspended in 5 mL phosphate buffer containing 4 mM DSP, and incubated at 37°C for 30 min. Tris was added to a final concentration of 50 mM to quench the reaction. Proteins were purified using metal affinity chromatography as described (Yu et al., 2011). After elution, dithiothreitol (DTT) was added to the sample to a final concentration of 50 mM to reduce the disulfide bond in the DSP linker. Finally, the samples were subjected to SDS-PAGE and Western blot analyses using anti-AcrA antibody.

#### FLUORESCENT LABELING

BODIPY-FL-maleimide labeling was conducted following published method (Husain and Nikaido, 2010; Husain et al., 2011). BW25113Δ*acrB* cells harboring plasmids encoded AcrB mutants were cultured overnight at 37°C. Ten mL culture were harvested by centrifugation at 4000 × g for 5 min, washed twice using 10 mL of buffer A (50 mM potassium phosphate, 0.5 mM MgCl<sub>2</sub>, pH 7.0), and resuspended in 5 mL of the same buffer containing 0.4% glucose and 6 μM BODIPY-FL-maleimide. The mixture was shaken at room temperature for 1 h. Next, Cells were harvested by centrifugation, washed with 5 mL buffer A supplemented with 0.4% glucose, and then washed again with 5 mL buffer A. AcrB was then purified normally and resolved using SDS-PAGE. Fluorescence images were collected using a Typhoon Phosphor Imager with the excitation wavelength of 488 nm. The gel was then stained with Coomassie blue stain and imaged under white light. Band intensities were quantified using ImageJ (Rasband, 1997–2012; Schneider et al., 2012).

#### STRUCTURAL CHARACTERIZATION USING CIRCULAR DICHROISM (CD) AND FLUORESCENCE SPECTROSCOPY

CD spectra of purified wild type AcrB and its mutants were collected as described (Lu et al., 2011). CPM was from Invitrogen (GRAND ISLAND, NY). The CPM reactivity experiment was conducted as described in literature with minor modifications (Alexandrov et al., 2008). Briefly, a DMSO solution of CPM was freshly made at a concentration of 4.0 mg/mL. It was diluted in phosphate buffer by 40-fold to make a work solution, which was kept on ice during the experiment. 30 μL of the CPM working solution was mixed with 570 μL phosphate buffer in which the final concentration of protein was 4 μM. The fluorescence signal excited at 387 nm and emitted at 463 nm was monitored upon heating. Fluorescence emission intensity was normalized against the maximum intensity. Each experiment was performed at least three times.

## RESULTS

#### IDENTIFICATION OF SINGLE POINT SUPPRESSOR MUTATIONS THAT RESTORE ACTIVITY TO AcrB<sub>P223G</sub>

In a previous study we found that mutation of P223 into Gly reduced the activity of AcrB to a level close to that of the *acrB* knockout strain (Yu et al., 2011). P223 locates close to the tip

of a long protruding loop critical for AcrB trimerization. The mutation had little effect on proteins structure except that purified AcrB<sub>P223G</sub> migrated mainly as a monomer in BN-PAGE. In addition, the observed function loss could be partially restored by the introduction of a pair of strategically placed Cys residues and the formation of inter-subunit disulfide bond, indicating that the disruption of trimerization was a major cause of function loss in AcrB<sub>P223G</sub> (Yu et al., 2011). In this study, random mutagenesis was conducted to identify suppressor mutations that restore function to AcrB<sub>P223G</sub>. Plasmid encoding AcrB<sub>P223G</sub> was first subjected to random mutagenesis, and then transformed into BW25113ΔacrB and plated onto LB agar plate containing 16 or 32 μg/mL erythromycin. Erythromycin is a well-established AcrB substrate. Here we chose to use erythromycin mainly due to the large difference of MIC between BW25113ΔacrB containing WT AcrB (128 μg/mL) and AcrB<sub>P223G</sub> (8 μg/mL).

Two methods were used to introduce random mutations into AcrB<sub>P223G</sub>, hydroxylamine hydrochloride treatment and error prone PCR. The hydroxylamine hydrochloride method is biased, as it only results in transition from C to T and G to A (Middlemiss and Poole, 2004). Two suppressor mutations, T199M and D256N, were recovered using this method. The error-prone PCR method generated a more uniform spectrum of mutations with equivalent mutation rates. Two pairs of primers, PP1/PP2 and PP3/PP4 were used to introduce random mutations into two periplasmic regions: between residues 30–332 and residues 494–889. We focused our search in the two long loops that form the periplasmic domain. With this method, we rediscovered T199M and D256N, and seven additional single point suppressor mutations including A209V, G257V, M662I, Q737L, D788K, P800S, and E810K.

To confirm that the decreased drug susceptibility was actually caused by the restoration of AcrB activity, we introduced these suppressor mutations through site directed mutagenesis into plasmid pQE70-AcrB<sub>P223G</sub> and transformed the resultant plasmids into BW25113ΔacrB for activity assay. Drug susceptibilities were measured for four AcrB substrates, including erythromycin, novobiocin, tetracycline, and tetraphenylphosphonium. BW25113ΔacrB transformed with pQE70-AcrB, pQE70-AcrB<sub>P223G</sub>, or the empty plasmid pQE70 were used as controls. MICs of the mutants and controls were shown in **Table 1**. For all AcrB substrates tested, the additional suppressor mutation greatly enhanced the activity of AcrB<sub>P223G</sub>.

A closer inspection reveals that there were several different MIC patterns for the nine suppressor mutants: (a) T199M, G257V, Q737L, D788K, and E810K restored the MIC to all four tested antibiotics to comparable levels. (b) For A209V, M662I, and P800S, the MICs to erythromycin were almost fully recovered (8-folds), but only limited effects were observed (2-folds) for the other three antibiotics. (c) For D256N, the MIC to erythromycin was only partially recovered (4-folds), but for other three antibiotics the recovery effect was quite obvious. To understand the mechanism of function restoration, we mapped the suppressor mutations (red) as well as P223 (yellow) onto the crystal structure of AcrB (**Figure 1**). Eight out of the nine suppressor mutations located in the top part (docking domain) of the periplasmic domain. The only exception is M662, which is in the

middle of the periplasmic domain (porter domain). Thus, eight out of nine suppressor mutations (other than M662I) are located distant from the substrate translocation pathway, and thus are not likely to be directly involved in interaction with substrates. These mutations might have led to subtle changes of the substrate translocation pathway through certain allosteric effect and subsequently resulted in the observed difference.

## SEQUENCE ALIGNMENT OF SUPPRESSOR MUTATIONS

To probe the potential role of these suppressor mutations, we aligned the *E. coli* AcrB sequence with 13 homologues. **Table 2** showed the residues occupying these locations in all sequences together with their consensus score (Waterhouse et al., 2009). Substitutions identified in the suppressor mutation were also included. Although overall the sequence of AcrB is highly conserved among Gram-negative bacteria, most suppressor mutation sites were poorly conserved as revealed by the low consensus scores. This is a reasonable observation since mutation of highly conserved sites by itself might cause function loss as they are likely to play important roles in structure and function.

## EFFECT OF SUPPRESSOR MUTATION ON PROTEIN EXPRESSION

To determine the effects of additional mutations on AcrB<sub>P223G</sub>, we first examined the expression level of these double mutants. Plasmid encoding each mutant was transformed into BW25113ΔacrB for protein expression under the basal condition. Membrane vesicles were then extracted from the same amount of cells and subjected to Western blot analysis using an anti-AcrB antibody. We have previously demonstrated that AcrB<sub>P223G</sub> expressed at a similar level as the wild type AcrB (Yu et al., 2011). Here we found that all mutant except for AcrB<sub>P223G/D256N</sub> expressed at levels similar to that of the wild type AcrB and AcrB<sub>P223G</sub> (Figure S1). The expression level of AcrB<sub>P223G/D256N</sub> was approximately three folds higher than AcrB<sub>P223G</sub>. The exact reason for the observed increase of expression level is not clear.

**Table 1 | MIC (μg/mL) of BW25113ΔacrB harboring the indicated plasmids.**

| Plasmids                          | MIC (μg/mL) |     |      |     |
|-----------------------------------|-------------|-----|------|-----|
|                                   | Ery         | Nov | Tet  | TPP |
| pQE70-AcrB                        | 128         | 320 | 2.56 | 640 |
| pQE70-AcrB <sub>P223G</sub>       | 8           | 40  | 0.64 | 20  |
| pQE70-AcrB <sub>P223G/T199M</sub> | 128         | 160 | 2.56 | 640 |
| pQE70-AcrB <sub>P223G/A209V</sub> | 64          | 80  | 1.28 | 40  |
| pQE70-AcrB <sub>P223G/D256N</sub> | 32          | 160 | 2.56 | 320 |
| pQE70-AcrB <sub>P223G/G257V</sub> | 64          | 160 | 2.56 | 160 |
| pQE70-AcrB <sub>P223G/M662I</sub> | 128         | 80  | 1.28 | 160 |
| pQE70-AcrB <sub>P223G/Q737L</sub> | 64          | 160 | 2.56 | 160 |
| pQE70-AcrB <sub>P223G/D788K</sub> | 128         | 160 | 2.56 | 320 |
| pQE70-AcrB <sub>P223G/P800S</sub> | 64          | 80  | 1.28 | 80  |
| pQE70-AcrB <sub>P223G/E810K</sub> | 128         | 160 | 2.56 | 320 |

Drugs tested were Ery, erythromycin; Nov, novobiocin; TPP, tetraphenylphosphonium; and Tet, tetracycline.

**Table 2 | Sequence alignment of AcrB with homologs at sites that restored AcrB<sub>P223G</sub> activity.**

| Residue number                  | 199 | 209 | 256 | 257 | 662 | 737 | 788 | 800 | 810 |
|---------------------------------|-----|-----|-----|-----|-----|-----|-----|-----|-----|
| AcrB ( <i>E. coli</i> )         | T   | A   | D   | G   | M   | Q   | D   | P   | E   |
| Replaced by                     | M   | V   | N   | V   | I   | L   | K   | S   | K   |
| AcrD ( <i>E. coli</i> )         | T   | S   | D   | G   | V   | L   | Y   | S   | G   |
| AcrF ( <i>E. coli</i> )         | T   | V   | D   | G   | V   | A   | L   | F   | Y   |
| MexB ( <i>P. aeruginosa</i> )   | T   | A   | D   | G   | M   | A   | W   | F   | Y   |
| AcrB ( <i>H. pylori</i> )       | D   | V   | I   | G   | V   | Q   | E   | R   | P   |
| AcrB ( <i>Y. pestis</i> )       | T   | I   | D   | G   | V   | A   | W   | F   | Y   |
| AcrB ( <i>V. cholera</i> )      | V   | S   | G   | D   | Q   | I   | W   | Q   | E   |
| AcrB ( <i>K. pneumonia</i> )    | T   | A   | D   | G   | V   | A   | W   | F   | Y   |
| AdeB ( <i>A. baumannii</i> )    | L   | R   | T   | N   | P   | D   | G   | Q   | R   |
| AmeB ( <i>A. tumefaciens</i> )  | T   | Q   | G   | A   | I   | D   | N   | S   | S   |
| TtgB ( <i>P. Putida</i> )       | T   | A   | D   | G   | V   | L   | Y   | S   | G   |
| CmeB ( <i>C. coli</i> )         | G   | V   | N   | E   | G   | M   | N   | T   | V   |
| AmrB ( <i>P. aeruginosa</i> )   | A   | H   | G   | G   | N   | M   | E   | K   | I   |
| MtrD ( <i>N. meningitidis</i> ) | A   | N   | S   | N   | V   | G   | V   | T   | T   |
| Consensus score                 | 3   | 2   | 3   | 4   | 4   | 3   | 2   | 2   | 0   |

Replacement residues identified in suppressor mutants were also shown.

### EFFECT OF SUPPRESSOR MUTATION ON TRIMER STABILITY

BN-PAGE was used to compare the trimer stability of each mutant. We have previously shown that while freshly purified wild type AcrB migrates predominantly as trimers, AcrB<sub>P223G</sub> migrates predominantly as monomers (Yu et al., 2011). **Figure 2A** showed the representative gel images of the BN-PAGE results of the repressor mutants. AcrB<sub>P223G</sub> and wild type AcrB were also shown as controls. Protein band intensities in the gel were quantified using ImageJ and trimer to monomer ratios were shown in **Figure 2B**. Two observations could be made: first, the trimer stability of all repressor mutants were much lower than that of the wild type AcrB; second, among the 9 suppressors, only three showed a significant increase of trimer stability, including AcrB<sub>T199M/P223G</sub>, AcrB<sub>A209V/P223G</sub>, and AcrB<sub>D256N/P223G</sub>. Other six mutations caused decreases in trimer stability as compared to AcrB<sub>P223G</sub>, especially in the case of AcrB<sub>Q737L/P223G</sub>. This result was a surprise since we expected the suppressor mutations to recover the MIC of AcrB<sub>P223G</sub> through increasing the trimer stability.

### INTERACTION WITH AcrA

The majority of mutations occurred at the top of the periplasmic domain in AcrB, the interaction site of AcrB with AcrA and/or TolC. A crosslinking protocol has been previously developed by Tikhonova et al. to demonstrate that AcrA and AcrB make direct contact (Zgurskaya and Nikaido, 2000; Tikhonova and Zgurskaya, 2004). To verify if these mutations have any impact on AcrA-AcrB interaction, we treated BW25113ΔacrB cells expressing different AcrB constructs with chemical crosslinker DSP, purified proteins using metal affinity chromatography, cleaved the disulfide bond in the crosslinker, and examined the quantity of AcrA co-purified with AcrB. The level of AcrA co-purified was revealed through anti-AcrA Western blot analysis, while the amount of purified AcrB was examined through staining a duplicate gel with Coomassie blue stain. Representative gel images were showed in

**Figure 3.** BW25113ΔacrB transformed with pQE70 vector were used as a negative control to confirm that the signal was not from non-specific interaction of AcrA with the Ni-nitrilotriacetic acid (NTA) resin. Little signal could be detected for the negative control, suggesting AcrA did not retain on Ni-NTA resin without being cross-linked with AcrB.

The relative amounts of AcrA crosslinked to AcrB<sub>P223G</sub> and wild type AcrB were similar, indicating that the P223G mutation, while decreased the trimer stability and compromised drug efflux activity, could still bind effectively to AcrA. The relative levels of AcrA cross-linked with all suppressor mutants tested were not significantly different from that of wild type AcrB or AcrB<sub>P223G</sub>. These results suggest that interaction with AcrA was not affected by the initial P223G mutation. Therefore, function restoration in the suppressor mutants was not likely through strengthening the interaction with AcrA.

### M662 IS ON THE SUBSTRATE TRANSLOCATION PATHWAY

Of all suppressor mutants, AcrB<sub>P223G/M662I</sub> is especially interesting. M662I is the only mutation that occurred in the AcrB porter domain. Nikaido and coworkers have developed a BODIPY-FL-maleimide labeling method to probe the substrate translocation pathway in AcrB periplasmic domain and proved that Phe664 and Phe666 were involved in substrate binding (Husain and Nikaido, 2010; Husain et al., 2011). In this method, a Cys was introduced at a target location. BODIPY-FL-maleimide selectively reacts with Cys introduced along the substrate translocation pathway. We speculate that Met662 was involved in substrate binding based on its location in the AcrB structure. To test the hypothesis, we conducted Bodipy-FL-maleimide labeling of a Cys introduced to replace M662 (**Figure 4**). Although there are two intrinsic cysteines in AcrB, both of them are distant from the translocation pathway. Thus, they were used as the negative control to confirm that BODIPY-FL-maleimide specifically label Cys at the substrate binding site. For positive control, we used AcrB<sub>F664C</sub>,

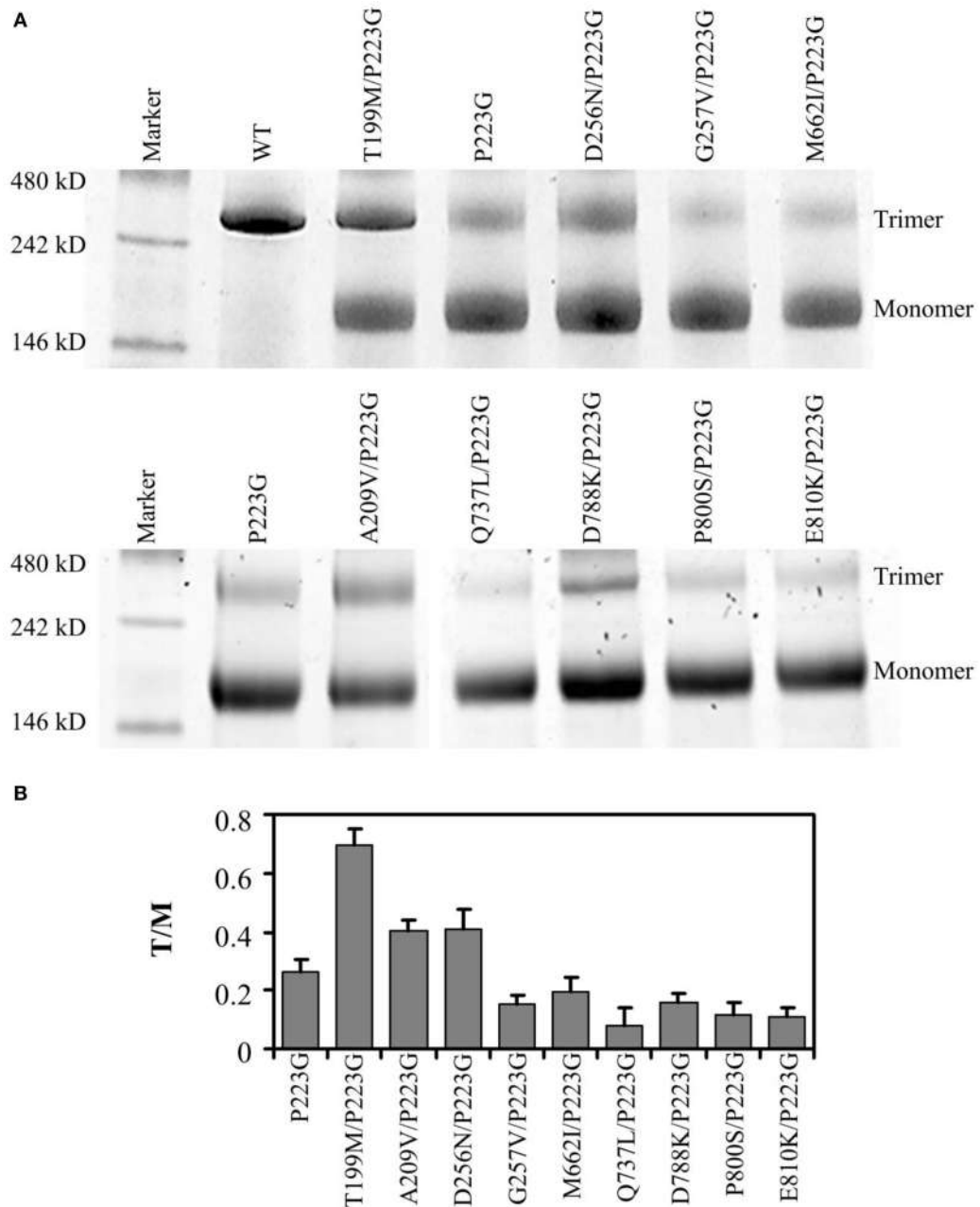


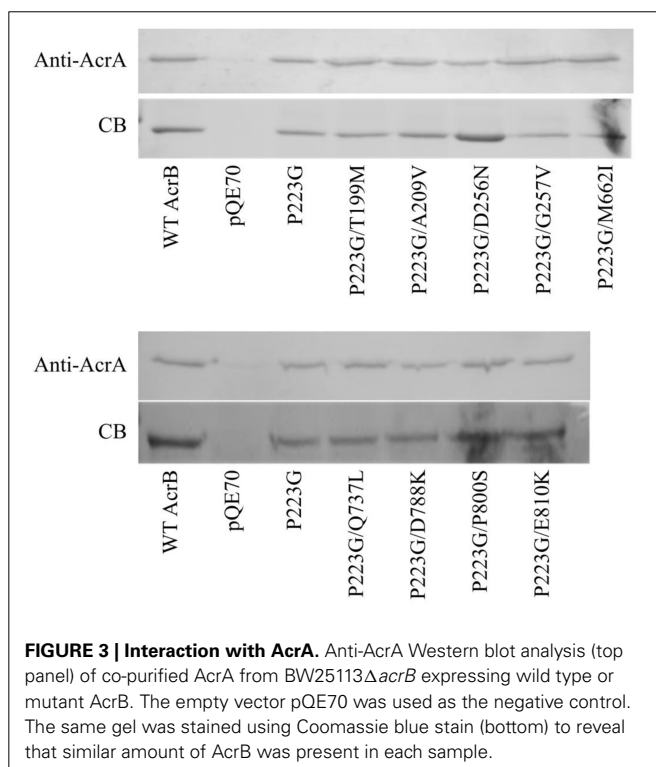
**FIGURE 2 | Quarternary structure analysis. (A)** Representative images of BN-PAGE analyses of wild type (WT) and mutant AcrB. **(B)** Trimer to monomer ratio for each mutant was derived from the BN-PAGE analysis. Experiments were repeated three times. The average value and standard deviation were shown.

a previously confirmed substrate-binding residue (Husain and Nikaido, 2010). As expected, no labeling was observed in wild type AcrB while AcrB<sub>F664C</sub> was labeled well. AcrB<sub>M662C</sub> could also be labeled by BODIPY-FL-maleimide, suggesting Met662 was indeed involved in substrate binding, most likely at the entrance of the drug translocation pathway. The relative level of labeling was weaker in AcrB<sub>M662C</sub> as compared to AcrB<sub>F664C</sub>, suggesting that substrate interaction at this site was not as strong.

#### M662I MUTATION IMPROVES SUBSTRATE BINDING IN THE DEEP BINDING POCKET OF AcrB<sub>P223G</sub>

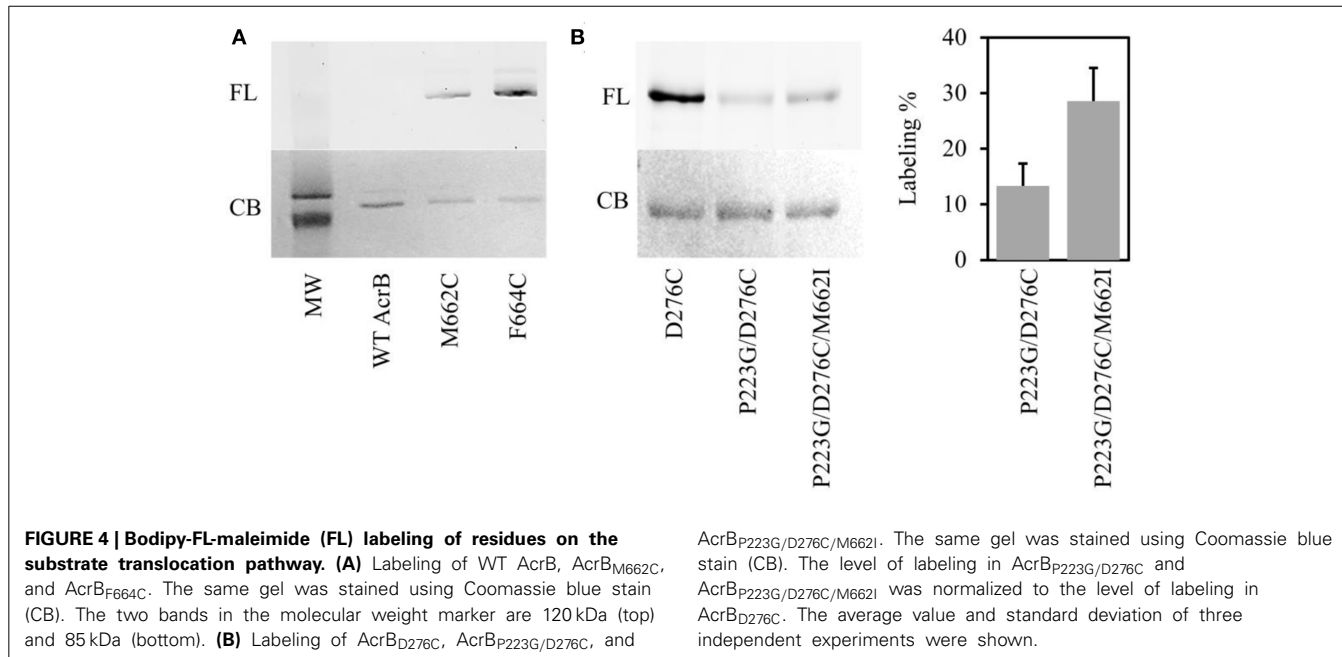
To investigate the potential effect of M662I mutation on substrate accessibility to the translocation pathway, we investigated the level of labeling of a previously verified site in the deep binding pocket, D276C (Husain and Nikaido, 2010; Lu et al., 2014). We performed BODIPY-FL-maleimide labeling in AcrB<sub>D276C</sub>, AcrB<sub>P223G/D276C</sub> and AcrB<sub>P223G/D276C/M662I</sub> (Figure 4B). The level of labeling was normalized to the labeling level in AcrB<sub>D276C</sub>.

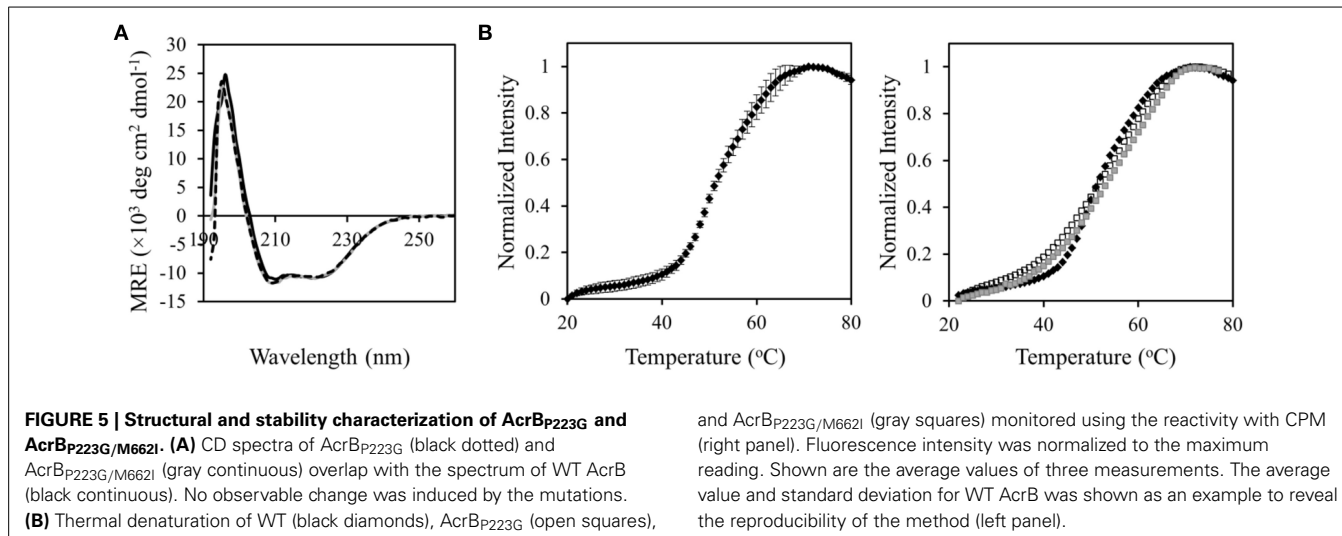
In AcrB<sub>P223G/D276C</sub>, the level of labeling was approximately  $14 \pm 4\%$  of the level of labeling in AcrB<sub>D276C</sub>. The suppressor mutation, AcrB<sub>P223G/D276C/M662I</sub>, improved the labeling level to  $28 \pm 5\%$ , approximately twice of the level in AcrB<sub>P223G/D276C</sub>. This result is consistent with the observed partial recovery of drug efflux activity in the repressor mutant.



#### M662I MUTATION DID NOT AFFECT THE OVERALL STRUCTURE NOR IMPROVE THE STABILITY OF AcrB<sub>P223G</sub>

To further elucidate the mechanism of function restoration, we compared the structure and stability of AcrB<sub>P223G/M662I</sub> with those of AcrB<sub>P223G</sub>. CD spectra of both mutants overlap well on top of the spectrum of wild type AcrB, indicating that the overall conformation was not affected by P223G, nor the additional M662I mutations (Figure 5A). Next, we examined the stability of the proteins. In a previous study, we measured the thermal denaturation profiles of wild type AcrB and AcrB<sub>P223G</sub> using a thermal denaturation method monitoring the CD signal at 222 nm (Yu et al., 2011). No significant difference was observed, indicating that either the two proteins have similar stability, or the technique is not sensitive to the intended measurement. Here we compared the stability of the proteins using a fluorescence labeling method (Alexandrov et al., 2008). Unfolding was monitored via the exposure of Cys residues upon heating and the subsequent reaction with N-[4-(7-diethylamino-4-methyl-3-coumarinyl) phenyl] maleimide (CPM). CPM is a thiol specific probe whose fluorescence emission intensity increased drastically upon reaction with a sulphydryl group in a protein. The formation of a thioether and the concurrent attachment to the protein is revealed by a surge of fluorescence emission at 463 nm (excited at 387 nm). Since free Cys residues are usually found in the hydrophobic core of a folded protein structure, the unfolding of the protein exposes the Cys and greatly accelerates the thiol-specific reaction. The thermal denaturation of wild type AcrB revealed a fluorescence surge as approximately 52°C (Figure 5). The transition temperatures of the two mutants were similar as the transition temperature of the wild type protein, while the slopes were less steep, indicating a less cooperative unfolding behavior. This difference could be due to a decrease of trimer stability, as the thermal denaturation experiment monitors the global unfolding of the protein including trimer dissociation and





protomer unfolding. The unfolding profiles of AcrB<sub>P223G</sub> and AcrB<sub>P223G/M662I</sub> were very similar, indicating that the restoration of function was not a result of improving structural stability.

## DISCUSSION

Several factors are critical for the proper function for AcrB: drug binding, interaction with AcrA and TolC, proton relay through the transmembrane domain, and AcrB trimerization. In this study, we identified nine single suppressor mutations that could restore function to AcrB<sub>P223G</sub>. Trimer affinity of purified mutants was examined using BN-PAGE. Three mutants had higher trimer stability than AcrB<sub>P223G</sub>, while remained drastically lower than that of the wild type AcrB. For the rest of the mutant, trimer stability was not improved. They are likely to restore functions through alternative mechanisms. However, it is possible that *in vivo* in bacterial cells these mutations could enhance trimer stability as a secondary effect of other interactions, such as binding with AcrA/TolC or substrate.

The next factor we tested was the interaction with partner proteins. We chose to investigate the interaction with AcrA since AcrA and AcrB make direct contact according to both the wrapping model and bridging model, while TolC does not interact directly with AcrB in the bridging model. We found that AcrB<sub>P223G</sub> and all suppressor mutants could be crosslinked with similar amount of AcrA as wild type AcrB, suggesting that the loss of function in AcrB<sub>P223G</sub> was not likely an effect on disruption of AcrA interaction and the restoration of function was not an effect of improving interaction with AcrA.

Finally we focused on the study of one suppressor mutant, M662I, which is at the porter domain and close to the substrate translocation pathway. Using a fluorescent labeling experiment, we found that M662 was involved in substrate binding. Substrate binding in AcrB involves mainly hydrophobic interactions. Ile is slightly more hydrophobic than Met according to hydrophobicity scales generated by different studies (Rose et al., 1985; White and Wimley, 1999). It is interesting to notice that such a small change of hydrophobicity could significantly increase the MIC for all substrates tested. We further measured the level of labeling of

residue in the deep binding pocket, D276C. We found that the M662I mutation doubled the relative level of labeling at this site on the P223G background. Finally, we confirmed that the additional M662I mutation did not induce an observable change on AcrB<sub>P223G</sub> structure and stability.

While ligand-induced oligomerization has been observed in many receptor and signaling proteins, the ligand binding sites in these cases usually locate at the inter-subunit interface (Sigalov, 2010; Atanasova and Whitty, 2012). In AcrB, the substrate translocation pathway, including M662, is distant from the inter-subunit interface. Therefore, the potential effect on AcrB trimer stability, if any, has to be allosteric. Interaction between neighboring subunits in an AcrB trimer is clearly critical for function. During drug efflux each subunit adopts a different conformation and cycles through the three conformations in turn. Recently Pos and co-workers determined the structure of AcrB at high enough resolution to resolve unambiguously the side chains of critical residues involved in proton translocation in the transmembrane domain and rationalized how the cross-talk among protomers across the trimerization interface might lead to a more kinetically efficient efflux system (Eicher et al., 2014). Therefore, each subunit has to be able to “sense” the state of its neighbors and undergoes conformational change in a concerted manner. A key element differentiates the various conformational states is the mode of interaction with the substrate. Therefore, it is possible that improved interaction with substrate could enhance efflux activity either directly through more efficient uptake or indirectly via increasing trimer affinity. Interestingly, some ligands are found to enhance the transport of other ligands by AcrB, suggesting that ligand binding could potentially play a more active role in efflux (Kinana et al., 2013).

For the rest of the repressor mutant, it remains unclear how these mutations restored the function loss in AcrB<sub>P223G</sub>. Middlemiss and Poole conducted a random mutagenesis study to identify residues that are critical to the function of MexB, a close homolog of AcrB (Middlemiss and Poole, 2004). Most mutations that affected function were mapped to regions of MexB predicted to be involved in trimerization or interaction with MexA. In the

same study, five suppressor mutations were identified to restore the activity of the MexB<sub>G220S</sub>, which was proposed to cause function loss via disruption of trimerization. Interestingly, similar as our observation in this study that all suppressor mutants identified, E796K, V203M/G581D, A737V, L738F, and D793N, locate in the docking area of the periplasmic domain. Protein-protein interaction during the assembly of the functional pump, including the intra-species interaction (trimerization of AcrB or MexB) and inter-species interaction with partner proteins (AcrA and/or TolC, MexA and/or OprM), seem to be correlated. The inter-species interaction may, to some degree, strengthen the intra-species interaction and compensate for function loss as a result of compromised trimerization. Finally, we have to acknowledge the limitation of the method we used to probe protein trimer stability using purified protein samples. It is possible that the suppressor mutations might have a more drastic effect on improving trimer stability in the cell membrane, and thus compensating for the loss of activity by directly improving the interaction between neighboring substrates in a trimer.

## FUNDING

We thank the National Science Foundation (MCB-1158036, Yinan Wei) and National Institute of Health (1R21AI103717, Yinan Wei) for supporting this work.

## ACKNOWLEDGMENT

We acknowledge the University of Kentucky Center for Structure Biology for the usage of the Typhoon Phosphorimager.

## SUPPLEMENTARY MATERIAL

The Supplementary Material for this article can be found online at: <http://www.frontiersin.org/journal/10.3389/fmibc.2015.00004/abstract>

## REFERENCES

- Alexandrov, A. I., Mileni, M., Chien, E. Y.T., Hanson, M. A., and Stevens, R. C. (2008). Microscale fluorescent thermal stability assay for membrane proteins. *Structure* 16, 351–359. doi: 10.1016/j.str.2008.02.004
- Atanasova, M., and Whitty, A. (2012). Understanding cytokine and growth factor receptor activation mechanisms. *Crit. Rev. Biochem. Mol. Biol.* 47, 502–530. doi: 10.3109/10409238.2012.729561
- Blair, J. M. A., and Piddock, L. J. V. (2009). Structure, function and inhibition of RND efflux pumps in Gram-negative bacteria: an update. *Curr. Opin. Microbiol.* 12, 512–519. doi: 10.1016/j.mib.2009.07.003
- Bohnert, J. A., Karamian, B., and Nikaido, H. (2010). Optimized nile red efflux assay of AcrAB-TolC multidrug efflux system shows competition between substrates. *Antimicrob. Agents Chemother.* 54, 3770–3775. doi: 10.1128/AAC.00620-10
- Du, D., Wang, Z., James, N. R., Voss, J. E., Klimont, E., Ohene-Agyei, T., et al. (2014). Structure of the AcrAB-TolC multidrug efflux pump. *Nature* 509, 512–515. doi: 10.1038/nature13205
- Eicher, T., Brandstatter, L., and Pos, K. M. (2009). Structural and functional aspects of the multidrug efflux pump AcrB. *Biol. Chem.* 390, 693–699. doi: 10.1515/BC.2009.090
- Eicher, T., Cha, H., Seeger, M. A., Brandstatter, L., El-Delik, J., Bohnert, J. A., et al. (2012). Transport of drugs by the multidrug transporter AcrB involves an access and a deep binding pocket that are separated by a switch-loop. *Proc. Natl. Acad. Sci. U.S.A.* 109, 5687–5692. doi: 10.1073/pnas.1114944109
- Eicher, T., Seeger, M. A., Anselmi, C., Zhou, W., Brandstätter, L., Verrey, F., et al. (2014). Coupling of remote alternating-access transport mechanisms for protons and substrates in the multidrug efflux pump AcrB. *ELIFE* 3:e03145. doi: 10.7554/eLife.03145
- Elkins, C. A., and Nikaido, H. (2002). Substrate specificity of the RND-type multidrug efflux pumps AcrB and AcrD of *Escherichia coli* is determined predominately by two large periplasmic loops. *J. Bacteriol.* 184, 6490–6498. doi: 10.1128/JB.184.23.6490-6498.2002
- Eswaran, J. E., Koronakis, M. K., Hughes, H. C., and Koronakis, V. (2004). Three's company: component structures bring a closer view of tripartite drug efflux pumps. *Curr. Opin. Struct. Biol.* 14, 741–747. doi: 10.1016/j.sbi.2004.10.003
- Husain, F., Bikhchandani, M., and Nikaido, H. (2011). Vestibules are part of the substrate path in the multidrug efflux transporter AcrB of *Escherichia coli*. *J. Bacteriol.* 193, 5847–5849. doi: 10.1128/JB.05759-11
- Husain, F., and Nikaido, H. (2010). Substrate path in the AcrB multidrug efflux pump of *Escherichia coli*. *Mol. Microbiol.* 78, 320–330. doi: 10.1111/j.1365-2958.2010.07330.x
- Kinana, A. D., Varqiu, A. V., and Nikaido, H. (2013). Some ligands enhance the efflux of other ligands by the *Escherichia coli* multidrug pump AcrB. *Biochemistry* 52, 8342–8351. doi: 10.1021/bi401303v
- Kobayashi, N., Tamura, N., van Veen, H. W., Yamaguchi, A., and Murakami, S. (2014).  $\beta$ -Lactam selectivity of multidrug transporters AcrB and AcrD resides in the proximal binding pocket. *J. Biol. Chem.* 289, 10680–10690. doi: 10.1074/jbc.M114.547794
- Lu, W., Zhong, M., Chai, Q., Wang, Z., Yu, L., and Wei, Y. (2014). Functional relevance of AcrB trimerization in pump assembly and substrate binding. *PLoS ONE* 9:e89143. doi: 10.1371/journal.pone.0089143
- Lu, W., Zhong, M., and Wei, Y. (2011). Folding of AcrB subunit precedes trimerization. *J. Mol. Biol.* 411, 264–274. doi: 10.1016/j.jmb.2011.05.042
- Middlemiss, J. K., and Poole, K. (2004). Differential impact of MexB mutations on substrate selectivity of the MexAB-OprM multidrug efflux pump of *Pseudomonas aeruginosa*. *J. Bacteriol.* 186, 1258–1269. doi: 10.1128/JB.186.5.1258-1269.2004
- Murakami, S., Nakashima, R., Yamashita, E., Matsumoto, T., and Yamaguchi, A. (2006). Crystal structure of a multidrug transporter reveals a functionally rotating mechanism. *Nature* 443, 173–179. doi: 10.1038/nature05076
- Nakashima, R., Sakurai, K., Yamasaki, S., Nishino, K., and Yamaguchi, A. (2011). Structures of the multidrug exporter AcrB reveal a proximal multisite drug-binding pocket. *Nature* 480, 565–569. doi: 10.1038/nature10641
- Nikaido, H., and Pages, J. M. (2012). Broad-specificity efflux pumps and their role in multidrug resistance of Gram-negative bacteria. *FEMS Microbiol. Rev.* 36, 340–363. doi: 10.1111/j.1574-6976.2011.00290.x
- Nikaido, H., and Takatsuka, Y. (2009). Mechanisms of RND multidrug efflux pumps. *Biochim. Biophys. Acta* 1794, 769–781. doi: 10.1016/j.bbapap.2008.10.004
- Pos, K. M. (2009). Drug transport mechanism of the AcrB efflux pump. *Biochim. Biophys. Acta* 5, 782–793. doi: 10.1016/j.bbapap.2008.12.015
- Rasband, W. S. (1997–2012). *ImageJ*. Bethesda, MD: U. S. National Institutes of Health. Available online at: <http://imagej.nih.gov/ij/>
- Rose, G. D., Geselowitz, A. R., Lesser, G. J., Lee, R. H., and Zehfus, M. H. (1985). Hydrophobicity of amino acid residues in globular proteins. *Science* 229, 834–838. doi: 10.1126/science.4023714
- Schneider, C. A., Rasband, W. S., and Eliceiri, K. W. (2012). NIH Image to ImageJ: 25 years of image analysis. *Nat. Methods* 9, 671–675. doi: 10.1038/nmeth.2089
- Seeger, M. A., Schiefner, A., Eicher, T., Verrey, F., Diederichs, K., and Pos, K. M. (2006). Structural asymmetry of AcrB trimer suggests a peristaltic pump mechanism. *Science* 313, 1295–1298. doi: 10.1126/science.1131542
- Seeger, M. A., von Ballmoos, C., Eicher, T., Brandstatter, L., Verrey, F., Diederichs, K., et al. (2008). Engineered disulfide bonds support the functional rotation mechanism of multidrug efflux pump AcrB. *Nat. Struct. Mol. Biol.* 15, 199–205. doi: 10.1038/nsmb.1379
- Sennhauser, G., Amstutz, P., Briand, C., Storchenecker, O., and Grutter, M. G. (2006). Drug export pathway of multidrug exporter AcrB revealed by DARPin inhibitors. *PLoS Biol.* 5:e7. doi: 10.1371/journal.pbio.0050007
- Signalov, A. B. (2010). Protein intrinsic disorder and oligomericity in cell signaling. *Mol. BioSyst.* 6, 451–461. doi: 10.1039/b916030m
- Su, C., Li, M., Gu, R., Takatsuka, Y., McDermott, G., Nikaido, H., et al. (2006). Conformation of the AcrB multidrug efflux pump in mutants of the putative proto relay pathway. *J. Bacteriol.* 188, 7290–7296. doi: 10.1128/JB.00684-06
- Takatsuka, Y., Chen, C., and Nikaido, H. (2010). Mechanism of recognition of compounds of diverse structures by the multidrug efflux pump AcrB of *Escherichia coli*. *Proc. Natl. Acad. Sci. U.S.A.* 107, 6559–6565. doi: 10.1073/pnas.1001460107

- Takatsuka, Y., and Nikaido, H. (2009). Covalently linked trimer of the AcrB multidrug efflux pump provides support for the functional rotating mechanism. *J. Bacteriol.* 191, 1729–1737. doi: 10.1128/JB.01441-08
- Tikhonova, E. B., and Zgurskaya, H. I. (2004). AcrA, AcrB, and TolC of *Escherichia coli* form a stable intermembrane multidrug efflux complex. *J. Biol. Chem.* 279, 32116–32124. doi: 10.1074/jbc.M402230200
- Vargiu, A. V., and Nikaido, H. (2012). Multidrug binding properties of the AcrB efflux pump characterized by molecular dynamics simulations. *Proc. Natl. Acad. Sci. U.S.A.* 109, 20637–20642. doi: 10.1073/pnas.1218348109
- Waterhouse, A. M., Procter, J. B., Martin, D. M. A., Clamp, M., and Barton, G. J. (2009). Jalview version 2 – a multiple sequence alignment editor and analysis workbench. *Bioinformatics* 25, 1189–1191. doi: 10.1093/bioinformatics/btp033
- White, S. H., and Wimley, W. C. (1999). Membrane protein folding and stability: physical principles. *Annu. Rev. Biophys. Biomol. Struct.* 28, 319–365. doi: 10.1146/annurev.biophys.28.1.319
- Wittig, I., Braun, H., and Schagger, H. (2006). Blue native PAGE. *Nat. Protoc.* 1, 418–428. doi: 10.1038/nprot.2006.62
- Xu, Y., Moeller, A., Jun, S. Y., Le, M., Yoon, B. Y., Kim, J. S., et al. (2012). Assembly and channel opening of outer membrane protein in tripartite drug efflux pumps of Gram-negative bacteria. *J. Biol. Chem.* 287, 11740–11750. doi: 10.1074/jbc.M111.329375
- Yu, E. W., Aires, J. R., McDermott, G., and Nikaido, H. (2005). A periplasmic drug binding site of the AcrB multidrug efflux pump: a crystallographic and site-directed mutagenesis study. *J. Bacteriol.* 187, 6804–6815. doi: 10.1128/JB.187.19.6804–6815.2005
- Yu, L., Lu, W., and Wei, Y. (2011). AcrB trimer stability and efflux activity, insight from mutagenesis studies. *PLoS ONE* 6:e28390. doi: 10.1371/journal.pone.0028390
- Zgurskaya, H. I., and Nikaido, H. (2000). Cross-linked complex between oligomeric periplasmic lipoprotein AcrA and the inner-membrane-associated multidrug efflux pump AcrB from *Escherichia coli*. *J. Bacteriol.* 182, 4264–4267. doi: 10.1128/JB.182.15.4264–4267.2000
- Zgurskaya, H. I., and Nikaido, H. (2012). Multidrug resistance mechanisms: drug efflux across two membranes. *Mol. Microbiol.* 37, 219–225. doi: 10.1046/j.1365-2958.2000.01926.x

**Conflict of Interest Statement:** The authors declare that the research was conducted in the absence of any commercial or financial relationships that could be construed as a potential conflict of interest.

Received: 25 November 2014; accepted: 03 January 2015; published online: 22 January 2015.

Citation: Wang Z, Zhong M, Lu W, Chai Q and Wei Y (2015) Repressive mutations restore function-loss caused by the disruption of trimerization in *Escherichia coli* multidrug transporter AcrB. *Front. Microbiol.* 6:4. doi: 10.3389/fmicb.2015.00004

This article was submitted to Antimicrobials, Resistance and Chemotherapy, a section of the journal *Frontiers in Microbiology*.

Copyright © 2015 Wang, Zhong, Lu, Chai and Wei. This is an open-access article distributed under the terms of the Creative Commons Attribution License (CC BY). The use, distribution or reproduction in other forums is permitted, provided the original author(s) or licensor are credited and that the original publication in this journal is cited, in accordance with accepted academic practice. No use, distribution or reproduction is permitted which does not comply with these terms.



# Mechanism of coupling drug transport reactions located in two different membranes

Helen I. Zgurskaya\*, Jon W. Weeks, Abigail T. Ntreh, Logan M. Nickels and David Wolloscheck

Department of Chemistry and Biochemistry, University of Oklahoma, Norman, OK, USA

**Edited by:**

Hiroshi Nikaido, University of California, Berkeley, USA

**Reviewed by:**

Herbert P. Schweizer, Colorado State University, USA

William William Shafer, Emory University School of Medicine, USA

**\*Correspondence:**

Helen I. Zgurskaya, Department of Chemistry and Biochemistry, University of Oklahoma, 101 Stephenson Parkway, Norman, OK 73072, USA

e-mail: elenaz@ou.edu

Gram-negative bacteria utilize a diverse array of multidrug transporters to pump toxic compounds out of the cell. Some transporters, together with periplasmic membrane fusion proteins (MFPs) and outer membrane channels, assemble trans-envelope complexes that expel multiple antibiotics across outer membranes of Gram-negative bacteria and into the external medium. Others further potentiate this efflux by pumping drugs across the inner membrane into the periplasm. Together these transporters create a powerful network of efflux that protects bacteria against a broad range of antimicrobial agents. This review is focused on the mechanism of coupling transport reactions located in two different membranes of Gram-negative bacteria. Using a combination of biochemical, genetic and biophysical approaches we have reconstructed the sequence of events leading to the assembly of trans-envelope drug efflux complexes and characterized the roles of periplasmic and outer membrane proteins in this process. Our recent data suggest a critical step in the activation of intermembrane efflux pumps, which is controlled by MFPs. We propose that the reaction cycles of transporters are tightly coupled to the assembly of the trans-envelope complexes. Transporters and MFPs exist in the inner membrane as dormant complexes. The activation of complexes is triggered by MFP binding to the outer membrane channel, which leads to a conformational change in the membrane proximal domain of MFP needed for stimulation of transporters. The activated MFP-transporter complex engages the outer membrane channel to expel substrates across the outer membrane. The recruitment of the channel is likely triggered by binding of effectors (substrates) to MFP or MFP-transporter complexes. This model together with recent structural and functional advances in the field of drug efflux provides a fairly detailed understanding of the mechanism of drug efflux across the two membranes.

**Keywords:** Gram-negative bacteria, antibiotic resistance, drug efflux, periplasmic membrane fusion proteins

## TRANSPORTERS

Multidrug resistance or polyspecific transporters (MDRs) are present in all living systems. However, they are particularly abundant and diverse in bacteria and comprise 2–7% of the total bacterial protein content (Saier and Paulsen, 2001). Such putative MDRs are identified based on sequence similarity with experimentally confirmed transporters able to handle multiple substrates. Most of these substrates are hydrophobic or amphipathic molecules often containing weakly basic moieties. Other substrates are organic cations with a permanent charge distributed over a large hydrophobic surface (Hall et al., 1998; Zgurskaya and Nikaido, 2000b).

Functional studies and subsequent phylogenetic analysis demonstrated that bacterial MDR transporters can be organized into several evolutionary distinct protein families that significantly differ in bioenergetics, structure and transport mechanism (Saier and Paulsen, 2001). Most of MDRs are found in three large and diverse superfamilies: ABC (ATP-binding Cassette) (Higgins and Linton, 2004), MF (Major Facilitator) (Saier et al., 1999) and RND (Resistance-Nodulation-Cell Division) (Tseng et al.,

1999). In addition, some MDRs form a core of smaller superfamilies: SMR (Small Multidrug Resistance) family [now part of the DMT (Drug/metabolite Transporter) superfamily] (Chung and Saier, 2001) and MATE (Multidrug and Toxic Extrusion) family [recently joined the MOP (Multidrug/Oligosaccharidyl-lipid/Polysaccharide) superfamily] (Hvorup et al., 2003). Just recently, a new family of transporters involved in efflux of cyclohexidine has been identified in *Acinetobacter* spp. (Hassan et al., 2013).

ABC MDRs (as all other members of this superfamily) are primary active transporters which couple substrate translocation with binding and hydrolysis of ATP. MDRs in all the other superfamilies are secondary transporters which utilize electrochemical gradients of ions (most frequently protons but sometimes sodium) to transport their diverse substrates. Both primary and secondary transporters are ubiquitous in bacteria, however their relative presence seems to correlate with energy generation: fermentative bacteria tend to rely more on the primary transporters while genomes of aerobic bacteria contain somewhat more secondary transporters (Paulsen et al., 1998, 2000).

## EFFLUX ACROSS CYTOPLASMIC MEMBRANES

At least three steps are common to various transporters during transport across cytoplasmic membranes: (i) binding of a substrate on the cytoplasmic or periplasmic side of the membrane, (ii) conformational changes in a transporter leading to re-orientation of the binding site to the other side of the membrane, and (iii) the release of the substrate. The conformational change leading to reorientation of substrate binding sites and relaxation of a transporter are usually energy-dependent steps, which is provided by either ATP hydrolysis (ABC pumps) or by a proton motive force (PMF) or sodium motive force. The basic mechanism of energization of transporters by ATP and PMF are well understood on examples of ABC and MF transporters (Davidson et al., 2008; Fluman and Bibi, 2009) but require further analyses in other transporters such as those belonging to the RND superfamily (Eicher et al., 2014).

The directionality of the transport is defined by binding affinity on either side of the membrane and the transport reaction is thought to be reversible at least in the case of PMF-dependent pumps (Smirnova et al., 2011; Fluman et al., 2012). However, RND pumps seem to be uni-directional with some of them transporting substrates only across the outer membrane (Nikaido and Pages, 2012). In these transporters, the substrate binding site is located in the periplasmic domain and is separated from the proton translocation pathway. Other RND pumps, such as the metal efflux pump CusBAC from *E. coli*, transport substrates across both the cytoplasmic and the outer membranes. This transporter comprises a network of methionine and charged residues traversing the transmembrane and periplasmic domains and involved in metal binding and transport (Su et al., 2011, 2012).

Transporters belonging to the same family of proteins are capable of efflux either alone or in complexes with accessory proteins. Mechanisms of transporters that function in complexes with other proteins are likely to be very similar to single-component ones. Studies of various transporters suggested that accessory proteins located in the periplasm and in the outer membrane enable high affinities toward substrates and also couple transport reactions separated in two different membranes.

## EFFLUX ACROSS OUTER MEMBRANES

Efflux is most effective when working in cooperation with other resistance mechanisms. Reduced uptake across the outer membrane of Gram-negative bacteria, which is a significant permeability barrier for both hydrophilic and hydrophobic compounds, constitutes such a mechanism (Sen et al., 1988; Sanchez et al., 1997). To take advantage of the reduced uptake, some Gram-negative MDR pumps extrude their substrates across the outer membrane directly into the external medium.

Permeability constants of amphiphilic antibiotics across cytoplasmic and outer membranes often differ by several orders of magnitude. Therefore, efflux is most effective when antibiotics are transported across the outer membrane back into the external medium. Among various MDRs, some transporters belonging to RND, ABC, and MF superfamilies utilize energy conserved in ATP or in the PMF of the cytoplasmic membrane to transport drugs across the outer membrane, which is energy deficient. This transduction of energy is possible because of the association between

the transporters and two types of accessory proteins: the periplasmic Membrane Fusion Proteins (MFP) and the outer membrane channels (OMFs) (Paulsen et al., 1997).

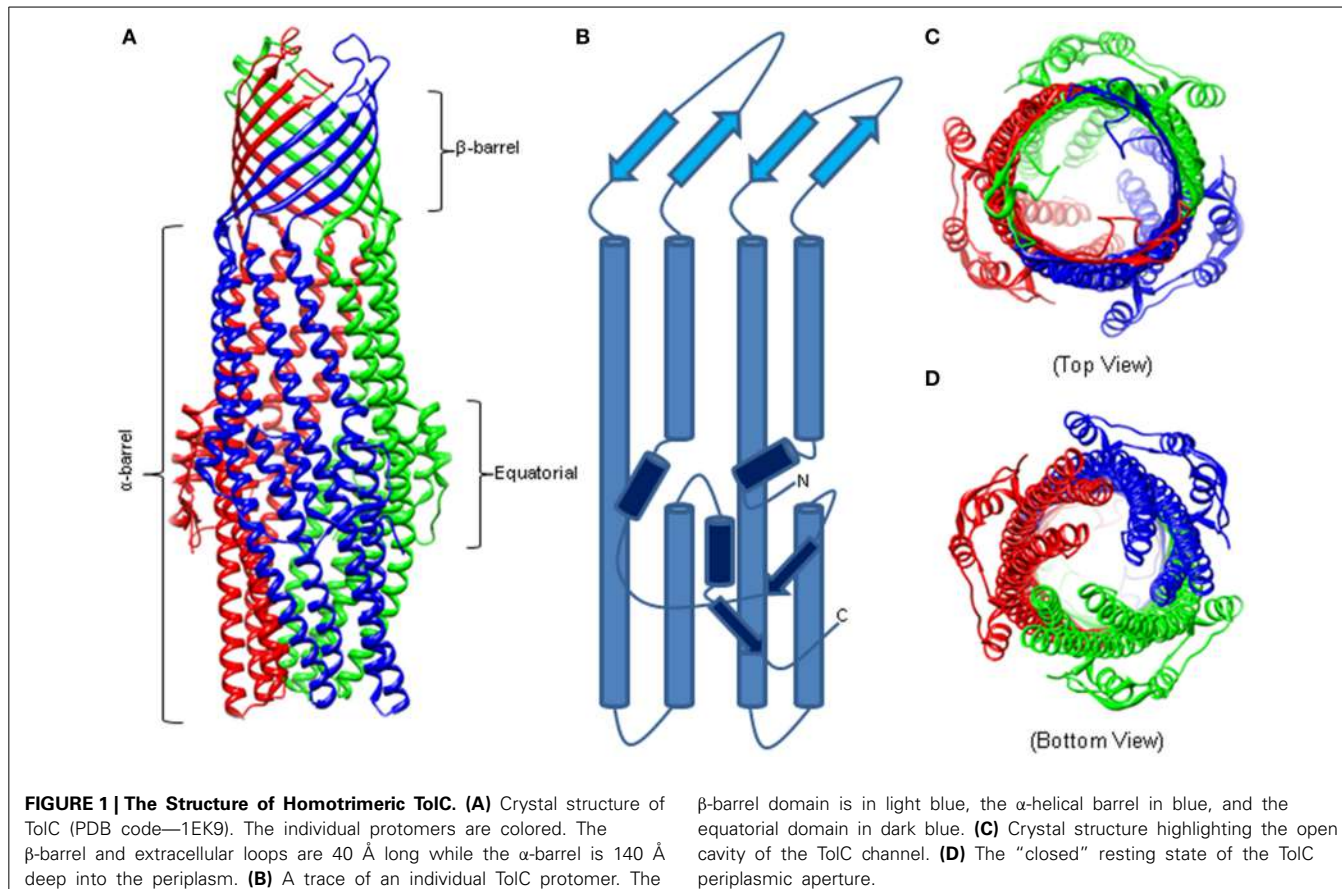
Importantly, the trans-envelope efflux of antibiotics contributes to resistance in clinical settings. In clinical *Escherichia coli* and *Klebsiella pneumoniae* isolates, fluoroquinolone resistance is linked to overproduction of AcrAB efflux pump, and multiple efflux pumps, including MexAB-OprM, confer antibiotic resistance in *Pseudomonas aeruginosa* (Ziha-Zarifi et al., 1999; Padilla et al., 2010; Swick et al., 2011). Also in *P. aeruginosa*, elevated expression of MexXY is the major cause of aminoglycoside resistance in the absence of modifying enzymes (Poole and Srikumar, 2001). The unquestionably significant impact of multidrug efflux pumps on the effectiveness of antibiotics in clinical settings makes them attractive targets for inhibition (Lomovskaya et al., 2008a,b). This review is focused on the mechanism of coupling drug transport reactions in the cytoplasmic and outer membranes. This critical step in drug efflux could be targeted for development of effective inhibitors of efflux pumps.

## OUTER MEMBRANE CHANNELS

The outer membrane of Gram-negative bacteria is an asymmetric lipid bilayer, which significantly slows down diffusion of drugs and bile salts into the cell. Although the inner leaflet of the outer membrane is composed of glycerophospholipids, the major components of cytoplasmic membranes, the outer leaflet is composed of lipopolysaccharides (LPS) which are largely responsible for the low permeability characteristic (Tommassen, 2010; Gessmann et al., 2014). Of the five existing families of Gram-negative outer membrane channels (Hagan et al., 2011), only proteins belonging to the Outer Membrane Factor (OMF) family associate with periplasmic MFPs and active transporters to drive the extrusion of ions, drugs, peptides and other substrates across the outer membrane (Yen et al., 2002). During transport, OMFs are believed to transition between the “open” and “closed” conformational states. In the resting state, the channel is in the “closed” conformation and is not permeable to most of its substrates. Induction of the conformational changes necessary to “open” the periplasmic aperture of OMFs is credited to the MFPs, which also stabilize the trans-envelope protein complexes and enable export of various substrates through OMFs (Matias et al., 2003; Lobedanz et al., 2007; Tikhonova et al., 2009).

## OMF STRUCTURE

Similar to other outer membrane proteins, OMFs have a signature  $\beta$ -barrel domain but these proteins also have unique features befitting their functions in the trans-envelope transport. The first OMF purified and characterized was the homotrimeric TolC from *E. coli* that functions with various drug efflux pumps of RND (e.g., AcrAB), ABC (e.g., MacAB) and MF (e.g., EmrAB) superfamilies (Figure 1) (Koronakis et al., 2000). TolC is a 12  $\beta$ -strand barrel, which is 30 Å wide and contains six asymmetric loops exposed to the cell surface. The  $\beta$ -barrel extends into the periplasm as an  $\alpha$ -barrel of 140 Å long. The  $\alpha$ -barrel is formed by 12  $\alpha$ -helices—six continuous and six discontinuous—that share similar sequences and inter-helical interactions, yet one pair of helices is inclined by  $-20^\circ$  with respect to the molecular threefold



axis. The introduced curvature yields a “closed” aperture of the periplasmic end of TolC. The  $\alpha$ -barrel domain is belted by an  $\alpha/\beta$  structure that comprises the equatorial domain.

TolC homologs crystallized since then, MtrE, VceC, OprM, and CusC, conserve closely the  $\alpha$ - and  $\beta$ -barrel architecture (Akama et al., 2004a; Federici et al., 2005; Kulathila et al., 2011; Lei et al., 2014). The equatorial domain is also retained but with significant variation, particularly in the C terminus (Federici et al., 2005; Kulathila et al., 2011). Highlighting the important role of the equatorial domain, mutations in the N and C termini attenuate the function of TolC (Yamanaka et al., 2002, 2004; Bokma et al., 2006; Krishnamoorthy et al., 2013).

Most of the available structures of OMFs, including TolC, OprM and CusC are closed at one or both sides. Several structures of the TolC variants, in which the opening of the TolC exit duct was forced by removal of key interactions, have been reported (Andersen et al., 2002; Bavro et al., 2008; Pei et al., 2011). A network of inter- and intra-protoomer bonds that constrains the inner and outer coiled coils in their closed conformation is centered at four key residues: Thr152, Asp153, Tyr362, and Arg367. Disruption of key hydrogen bonds and salt bridges involving these residues allowed movement of the inner coiled coils and widened the periplasmic pore (Andersen et al., 2002). Structural characterization of these TolC mutants presented sequential snapshots of both symmetrical and asymmetrical openings of the entrance aperture, revealing that relaxation of the constraining network

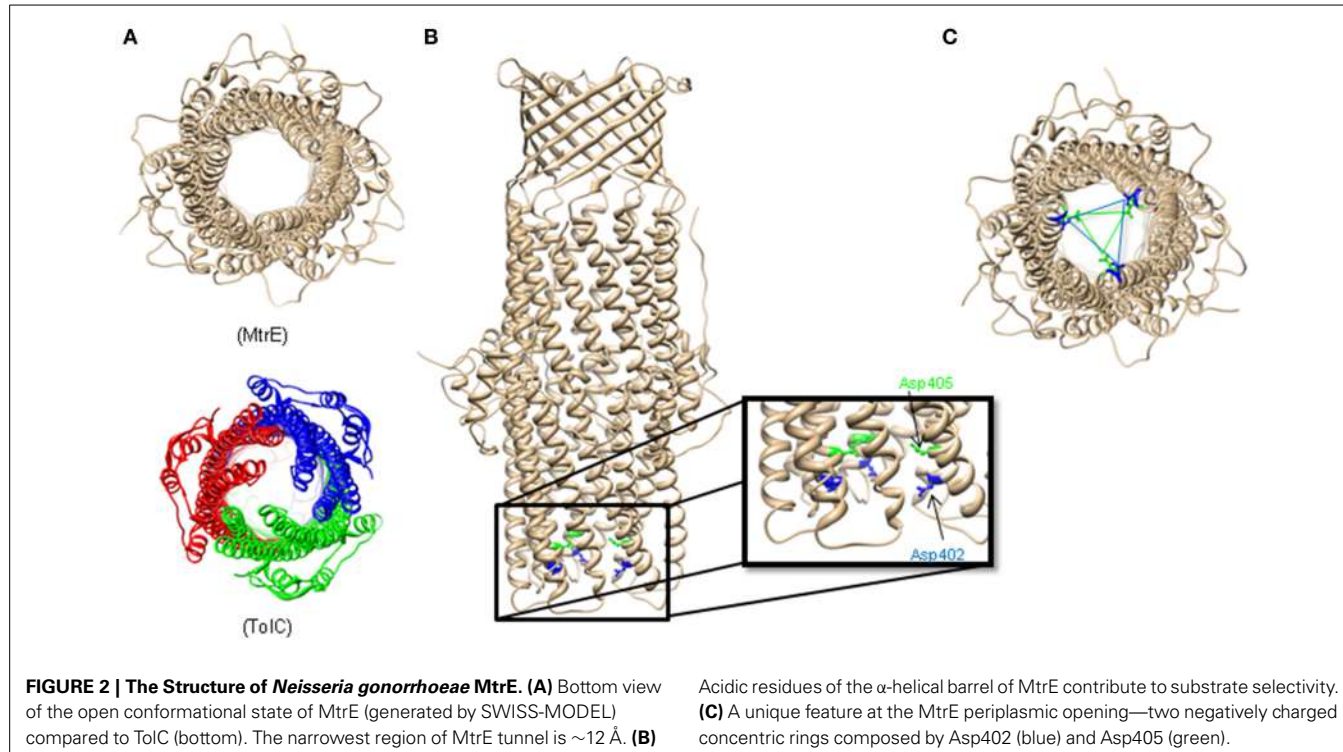
allows both a twist and dilation at the entrance (Bavro et al., 2008; Pei et al., 2011). These studies also suggested that interactions with transporters and periplasmic proteins are likely to contribute significantly to opening of the channel.

Surprisingly, the crystal structure of MtrE showed that this channel is open all the way from the outer membrane surface and down to the tip of the  $\alpha$ -helical periplasmic domain (Figure 2) (Lei et al., 2014). The widest section of the channel is located at the external surface of the outer membrane, with the internal diameter of ~22 Å. Hence, MtrE could be a highly dynamic channel spontaneously transitioning between the closed and open states. Like TolC and other OMFs, MtrE also contains an aspartate ring at its periplasmic entrance. Each protomer of MtrE contributes Asp402 and Asp405 to form two concentric circles of negative charges in the inner cavity of MtrE, which could contribute to the selectivity of the channel (Figure 2).

#### PROPOSED MECHANISM

The structural and functional studies suggested that opening of the channel could be achieved by interrupting inter- and intramolecular interactions that stabilize the resting state. Interactions with both a transporter and a MFP were considered as driving forces for OMF transition into the open state.

The *E. coli* K-12 periplasm is estimated to range ~18–23 nm (Matias et al., 2003). In case of RND-containing complexes, the periplasmic portion of the AcrB transporter is large enough to



reach halfway across the periplasm and contact TolC directly (Murakami et al., 2002). If AcrB and TolC structures are docked in a tip-to-tip manner the complex spans ~17 nm of the periplasm and the drug exit funnel of AcrB is sealed by the periplasmic duct of TolC preventing the escape of substrates into periplasm (Murakami et al., 2002; Symmons et al., 2009). This model has found a support at both the genetic and biochemical levels. Binding experiments showed that the transporter-channel AcrB-TolC pair forms a highly dynamic complex, even in the absence of MFP AcrA (Tikhonova et al., 2011). An “open” TolC variant containing Tyr362 to Phe and Arg367 to Glu substitutions (TolCYFRE) showed significantly lower affinity to AcrB (Tikhonova et al., 2011), suggesting that opening of the channel could lead to destabilization of interactions, disengagement of the complex and channel closing. The proposed AcrB-TolC interface is formed by AcrB  $\beta$ -hairpins extending from its TolC-docking domain. Genetic studies showed that these hairpins play an important role in the functional assembly of the pump complex by stabilizing interactions with TolC (Weeks et al., 2014). However such a limited interface could initiate the opening of the channel but is not sufficient to release interactions that keep the channel in its closed state (Weeks et al., 2010). Interestingly, in the assembled tri-partite AcrAB-TolC complex, AcrB and TolC do not contact each other (Du et al., 2014). Also, transporters belonging to ABC and MF superfamilies of proteins lack the large periplasmic domains of AcrB and do not interact with OMF directly (Lu and Zgurskaya, 2013). Hence the transporter-channel interface, if formed, is not a requirement for assembling a functional complex. This function is assigned to MFPs that play a critical role in coupling transport reactions separated in two different membranes.

## COUPLING OF TWO MEMBRANES: PERIPLASMIC MEMBRANE FUSION PROTEINS

MFPs play an important functional role in trans-envelope drug efflux: (i) by stimulating the efflux activities of transporters and (ii) by engaging OMFs and opening them for substrates to be expelled from the cell (Zgurskaya et al., 2009). *In vitro* reconstitution studies showed that the stimulating activities of MFP are a common feature of transporters belonging to various protein families. *E. coli* AcrA, that functions with the RND pump AcrB, and MacA, a subunit of the ABC-type MacB transporter, both stimulate activities of their cognate transporters located in the inner membrane (Zgurskaya and Nikaido, 1999b; Tikhonova et al., 2007). On the other hand, MFPs mediate and stabilize the functional interactions between transporters and OMFs and in doing so, presumably transmit energy from the energized transporter to the closed OMF in order to open the channel and allow the diffusion of substrates through the OMF into the extracellular medium. It is thought that this transfer of energy is mediated by conformational energy and movement of the MFPs.

## STRUCTURE OF MFPs

While amino acid conservation among MFPs is relatively low, their structures are conserved. Typical MFPs are highly elongated proteins, and adopt a linear conformation that extends from the outer leaflet of the inner membrane deep into the periplasm to meet the OMF (Zgurskaya and Nikaido, 1999a; Mikolosko et al., 2006). This linear structure comprises up to four characteristic domains. Starting at the inner membrane, the domains are the membrane proximal (MP),  $\beta$ -barrel, lipoyl, and  $\alpha$ -helical hairpin domains (Figure 3). While these domains are arranged in a linear

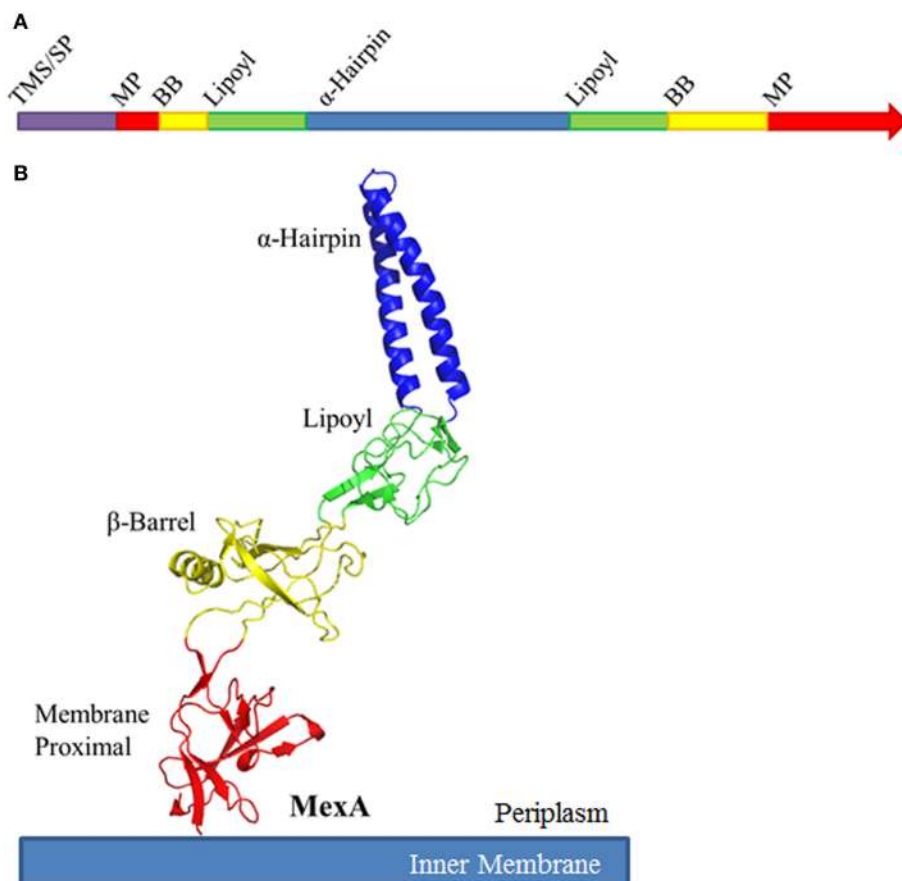


**FIGURE 3 | Schematic organization of Membrane Fusion Proteins.**

**(A)** Typical membrane fusion proteins (MFPs) contain four domains which are broken and distributed between the N- and C-halves of the protein. As MFPs are periplasmic proteins, they contain an N-terminal transmembrane segment (TMS) or signal peptide (SP). The N-terminal half of the protein encodes for a small portion of the membrane proximal (MP) and  $\beta$ -barrel domains (BB), half of the lipoyl domain and one of the  $\alpha$ -helices of the  $\alpha$ -helical domain. The C-terminal half encodes for the second  $\alpha$ -helix, the second half of the lipoyl domain

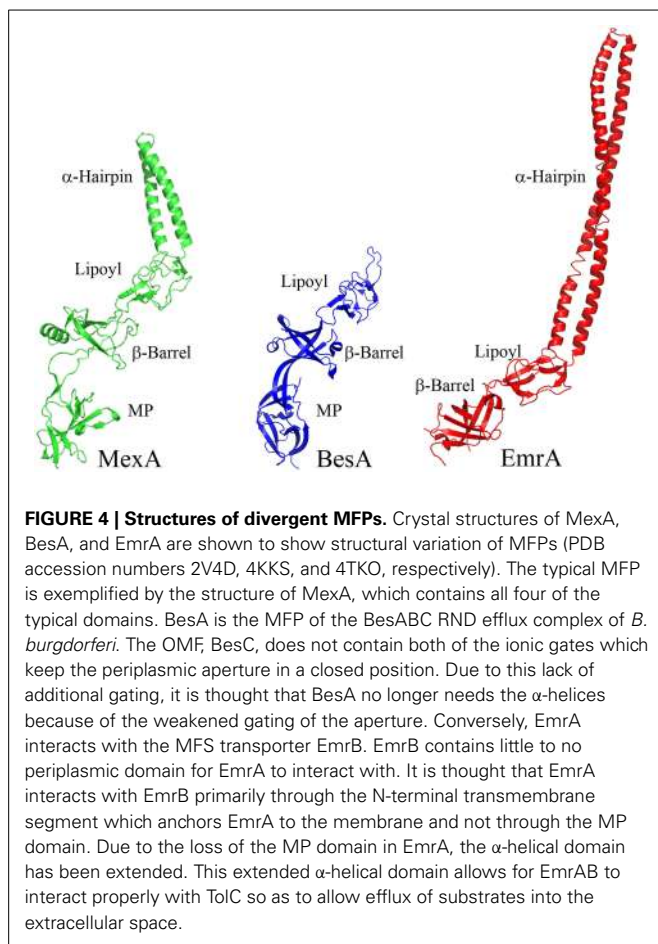
and the majority of the BB and MP domains. **(B)** When folded, MFPs form an elongated structure with four unique domains. From the inner membrane, the domains are organized as MP, BB, lipoyl and  $\alpha$ -helical. The domains are separated by short flexible linkers. Due to the flexibility of these linker regions, MFPs are capable of dramatic variation in structure, likely to allow for conformational changes which transmit energy from the IMP to the OMF. The MP, BB, and lipoyl domains are primarily comprised of  $\beta$ -sheets, while the  $\alpha$ -helical domain is typically a single pair of anti-parallel  $\alpha$ -helices connected by a single turn.

manner, the N-terminal and C-terminal halves of the protein fold in upon each other to complete the structure.

The MP,  $\beta$ -barrel and the lipoyl domains are mostly  $\beta$ -sheet structures. The  $\alpha$ -hairpin domain, unlike the other three domains, consists of two anti-parallel coiled-coils separated by a single turn. The domains are linked by flexible unstructured regions which give the overall protein its conformational flexibility and allow for a high degree of movement believed to be important for functional interactions with transporters and OMFs.

The  $\alpha$ -helical hairpins oligomerize and assemble a funnel-like structure that interacts with an OMF. The MP,  $\beta$ -barrel, and possibly the lipoyl domain are responsible for interactions with the cognate transporter. In addition, some MFPs, such as MacA, contain N-terminal transmembrane domains (TMD) that interact with transporters within the cytoplasmic membrane (Tikhonova et al., 2007). However, in many other MFPs this TMD is replaced

by a lipid modification that anchors the protein into the membrane. As the different families of transporters vary in sizes of domains exposed to the periplasm, MFPs and their domains which interact with specific transporters also vary. For example, MF transporters such as *E. coli* EmrB are thought to have little to no periplasmic extrusions (**Figure 4**). Accordingly, its cognate MFP, EmrA, lacks a MP domain and contains a very long  $\alpha$ -hairpin sufficient to span the periplasm and bind TolC (Hinchliffe et al., 2014). On the other side of the MFP diversity spectrum is BesA, the MFP of *Borrelia burgdorferi* BesABC complex, which lacks an  $\alpha$ -hairpin domain all together (Greene et al., 2013). The exact reasons for the lack of the  $\alpha$ -hairpin remains unclear, but it could be due to the fact that OMF, BesC, lacks the aspartate ring in the periplasmic duct of the channel suggesting that MFP binding to the periplasmic tip of BesA could be sufficient to trigger opening of the channel (Bunikis et al., 2008).



## INTERACTIONS BETWEEN MFPs AND OTHER COMPLEX COMPONENTS

### Oligomerization of MFPs

MFPs oligomerize independently of interactions with their cognate IMPs and OMFs. The first evidence of MFP oligomerization came from *in vivo* cross-linking studies of AcrA and HlyD (Thanabalu et al., 1998; Zgurskaya and Nikaido, 2000a). More recently, structural studies showed that in crystals MFPs such as *P. aeruginosa* MexA and *E. coli* MacA, and AcrA, all have repeating dimer pairs (Akama et al., 2004b; Mikolosko et al., 2006; Yum et al., 2009). AcrA is a dimer of dimers, MacA forms a hexameric funnel-like structure, whereas MexA has sets of dimers aligned with one another creating a sheet, which wraps upon itself in an asymmetric fashion. These structures suggested that the MFPs could function as dimers, but the strongest evidence for a dimer as a functional unit of MFPs was collected by biochemical and genetic studies (Mima et al., 2007; Tikhonova et al., 2009, 2011; Xu et al., 2011a).

For MFPs which interact with RND transporters (e.g., MexA and AcrA), the MFP oligomerization was treated more as an artifact of crystallization, partly due to the fact that hydrodynamic studies and the size exclusion chromatography studies showed only monomers in solution (Zgurskaya and Nikaido, 1999a; Tikhonova et al., 2009). However, kinetic studies established that MFPs that function with transporters belonging to

different protein families all oligomerize, albeit to a different degree (Tikhonova et al., 2009). EmrA and MacA, MFPs functioning with MFS and ABC transporters, respectively, form more stable oligomers and with a higher affinity than AcrA. This result suggested that interactions with the periplasmic domains of AcrB stabilize the oligomeric state of AcrA. In contrast, MFPs that function with transporters lacking large periplasmic domains have a strong propensity to self-oligomerization. These studies suggested that oligomerization of MFPs is needed to seal the gap between their cognate transporters and TolC.

Further *in vivo* (construction of genetic fusions, Xu et al., 2011a) and *in vitro* (binding affinities of stabilized dimers Tikhonova et al., 2011) studies showed that the functional unit of MFPs is a dimer, which assembles into a trimer of dimers when in the complex. Perhaps the most natural evidence of MFP dimers, as functional units, is the *P. aeruginosa* triclosan-specific TriABC-OpmH complex. Mima et al. (2007) identified this complex through a screen for increasing triclosan resistance and discovered that TriA and TriB are unique MFPs which are both required for functionality of the complex.

### Interactions between MFPs and transporters

Physical interactions between MFPs and transporters remain a subject of intense investigation using such approaches as crystallography, mutagenesis, surface plasmon resonance, isothermal calorimetry, chemical crosslinking, co-purification, and chimeric protein studies (Weeks et al., 2010, 2014; Su et al., 2011; Tikhonova et al., 2011; Xu et al., 2011a,b). Symmons et al. (2009) proposed the first model of AcrAB-TolC complex based on crystal structures of individual components, *in vivo* chemical crosslinking and molecular docking analyses. In this model, the AcrA molecule occupies the AcrB surface between the PN2 and PC2 subdomains, extending up along the DN subdomain. The MP,  $\beta$ -barrel, and lipoyl domains of AcrA are modeled to interface with AcrB. Interestingly the PC1 and PC2 cleft of AcrB has been proposed to be one of the main entrance tunnels which substrates use to enter into the drug binding pocket (Pos, 2009). This further suggested that MFPs could stimulate activities of their cognate transporters by participating in drug binding.

In the co-crystal structure of the metal efflux pump CusBA, the two CusB protomers are positioned substantially higher on the surface of the CusA transporter than in the cross-linking based model of AcrAB described above (Symmons et al., 2009; Su et al., 2011). Here, the MP and  $\beta$ -barrel domains of CusB interface primarily with the DN and DC subdomains of CusA and only make limited contacts with the top portions of the PN2, PC1, and PC2 subdomains. The authors were able to define two different types of MFP-transporter interactions. The first CusB molecule primarily engages CusA through an extensive network of salt bridges. Conversely, the second CusB molecule interacts with CusA primarily through a network of hydrogen bonding. In addition, the two CusB are staggered: one of the two molecules sits slightly higher on the surface of CusA. In this arrangement, the MP domain of CusB molecule 1 fits into a pocket formed between the MP and  $\beta$ -barrel domains of molecule 2. When compared with the cross-linking based model of AcrAB, CusB molecule 1 is positioned similar to AcrA with the exception that

the lipoyl domain of CusB does not interface with the transporter and its MP occupies the position of  $\beta$ -barrel domain of AcrA. This upward shift also tilts the MFPs and gives them a different overall structure; CusB has a sickle shape as observed in crystal structures of other MFPs including MacA, AcrA, and MexA. The recently reported cryo-EM-based structure of the complete AcrAB-TolC complex shows similar positioning of AcrA on AcrB transporter (Du et al., 2014). However, only lipoyl domains of AcrA contribute to AcrA oligomerization and there are no contacts between the MP domains of AcrA.

In various models of MFP-transporter complexes, at least two domains of MFP directly contact a transporter: the MP domain and the  $\beta$ -barrel. Functional importance of these domains in various MFPs has been supported by genetic and biochemical studies (Elkins and Nikaido, 2003; Tikhonova et al., 2007; Ge et al., 2009; Modali and Zgurskaya, 2011). Mutagenesis of the C-terminal domains of MacA and AcrA identified conserved glycine residues important for the functional interactions between these MFPs and the cognate components of the complexes. A substitution of Gly353 with Cys leads to inactivation of MacA, and prevents stimulation of the MacB ATPase activity, but not physical interactions with MacB or TolC (Modali and Zgurskaya, 2011). An analogous alteration in AcrA, Gly363 to Cys, prevented functional, but not physical interaction with AcrB and TolC (Ge et al., 2009). Limited proteolysis studies both *in vivo* and *in vitro* showed that these substitutions affect conformations of the MP domains of AcrA and MacA. Although EmrA does not have a MP domain, its C-terminal signature residues of the MFP family of proteins are incorporated into the  $\beta$ -barrel (Zgurskaya et al., 2009; Hinchliffe et al., 2014).

### Conformational changes and effectors

Early hydrodynamic and EPR studies pointed to significant structural flexibility of MFPs (Zgurskaya and Nikaido, 1999a; Ip et al., 2003). In the presence of magnesium ions, the highly asymmetric shape of AcrA was found to be more compact, whereas mildly acidic pH restrained significantly conformational dynamics of this protein. The X-ray structure of AcrA suggested that these conformational changes could involve the  $\alpha$ -hairpin, which undergoes an  $\sim 15^\circ$  rotation between the two most dissimilar molecules (Mikolosko et al., 2006). In addition, the refined full structure of MexA showed that the MP domain is also mobile and that in one of the MexA protomers this domain is twisted by  $85^\circ$  clockwise relative to the  $\beta$ -barrel domain (Symmons et al., 2009). Additionally, when the lipoyl domains of MexA were superimposed, the  $\alpha$ -hairpins exhibited  $\sim 35^\circ$  of rotation while the  $\beta$ -barrel and MP domains underwent an additional  $\sim 25^\circ$  of rotation. Molecular dynamics simulations of MexA and AcrA supported the high inter-domain flexibility of MFPs (Vaccaro et al., 2006; Wang et al., 2012). *In vivo* proteolysis studies however, pointed onto the MP domains of AcrA and MacA that undergo significant conformational changes and that these changes are detected only when all three components of complexes are present and functional (Ge et al., 2009; Modali and Zgurskaya, 2011; Lu and Zgurskaya, 2012).

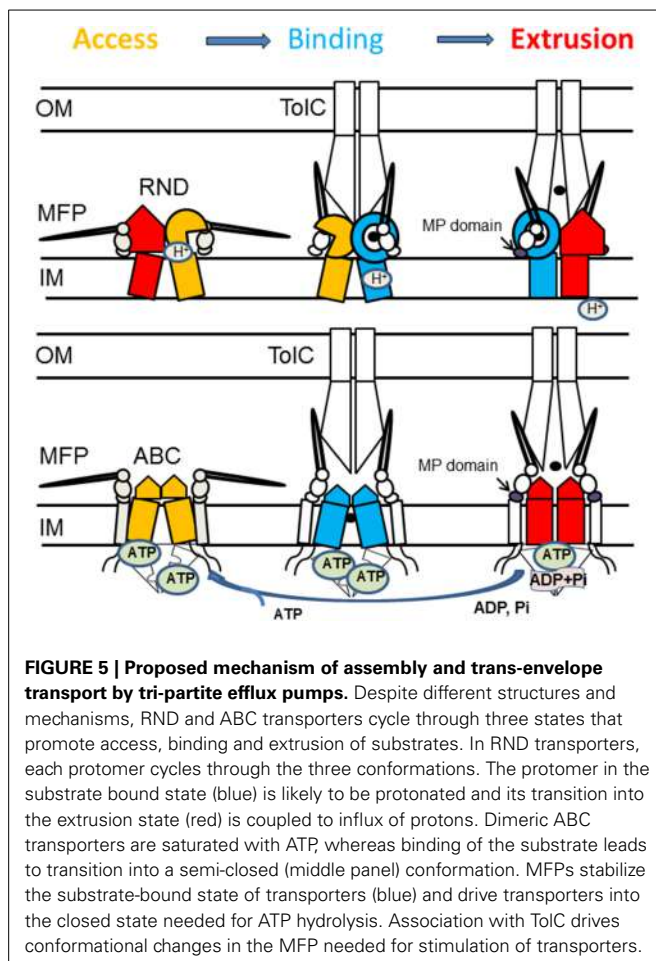
The protonation/deprotonation of His285 was proposed to underlie the pH-regulated conformational dynamics of AcrA by

disturbing the local hydrogen bond interactions (Wang et al., 2012). Interestingly, in a heavy metal MFP ZneB, the same His residue is a part of the metal-binding site (De Angelis et al., 2010). In MacA, the patch of positively charged residues located at the interface between  $\beta$ -barrel and the MP domains are important for both binding to core LPS and functionality of the pump, suggesting that LPS could be a substrate of MacAB-TolC (Lu and Zgurskaya, 2013). In addition, kinetic experiments showed that AcrA and other MFPs show differential binding affinities to OMF and transporters depending on pH (Tikhonova et al., 2009, 2011). Hence, the changes of pH in the periplasm accompanying the drug efflux or binding of substrates/effectors could act as a signal to trigger the action of MFPs, which undergo reversible conformational rearrangement.

Several genetic screens with defective complexes were carried out to identify gain-of-function suppressor mutations in MFPs. Surprisingly, most of such suppressors were mapped to the  $\beta$ -barrel domains of MFPs, which do not contact OMFs directly and suppress the defects in complexes through the contact with transporter and long range conformational changes in the protein. Suppressors of defects in MexB transporter mapped to the  $\beta$ -barrel domain of MexA were found to increase the stability of MexA binding to MexB (Nehme and Poole, 2007). An analogous study of an assembly defective TolC mutant also gave rise to gain-of-function suppressor mutations within the  $\beta$ -barrel domain of AcrA (Gerken and Misra, 2004). One such suppressor of the defective TolC mutant was AcrA<sub>L222Q</sub>, which is itself labile and subject to degradation if not in a functional complex with AcrB and TolC (Weeks et al., 2010). It is thought that this mutant protein is in a conformation which AcrA assumes transiently during typical complex assembly and drug efflux; however, when locked into this conformation, the protein becomes highly sensitized to proteolytic degradation by the periplasmic protease DegP. Other AcrA  $\beta$ -barrel mutants suppressed a TolC mutant defective in functional interactions with AcrA and AcrB presumably by controlling the opening of TolC channel (Weeks et al., 2010), or enabled functioning of a hybrid AcrA-MexB-TolC efflux complex (Krishnamoorthy et al., 2008).

### PROPOSED MECHANISM OF TRANS-ENVELOPE DRUG EFFLUX

Studies discussed above suggest that efflux complexes assembled with transporters belonging to various protein families utilize the same mechanism of transport across the outer membrane and that MFPs play an important role in the functional communication between transporters and OMF. Although molecular details of how ABC, MF, and RND transporters bind their substrates and transport them to the OMFs differ significantly between members of different families, all these transporters cycle through three states that promote access, binding and extrusion of substrates (Figure 5). The function of MFPs is to couple these transitions in transporter to opening of OMFs and transport of substrates across the outer membrane. Most of the investigations were done on either RND or ABC efflux complexes but it is likely that the same conclusions apply to MF complexes. The major findings on the mechanism of MFPs in transport could be summarized in the following conclusions:



1. MFP-transporter interactions are sensitive to conformational changes in transporters. When MacB transporter was trapped in different conformations by mutations or by the presence of nucleotide analogs, the affinity of association between MFP MacA and MacB increased upon ATP binding but remained unchanged during ATP hydrolysis (Lu and Zgurskaya, 2012). Similarly, the interactions between the MFP AcrA and the RND transporter AcrB are most stable when AcrB is in its protonated state (Janganan et al., 2013). These results suggested that MFPs act on the pre-translocation “Binding” state of transporters (Figure 5).
2. Stimulation of transporters is coupled to a conformational change in the C-terminal domain of MFPs. Reconstitution studies showed that interactions between MFPs and transporters increase the rates of transport and energy consumption (Zgurskaya and Nikaido, 1999b; Tikhonova et al., 2007). Further studies of MacAB and AcrAB showed that the C-terminal domains of MFPs are critical for their ability to stimulate transporters (Ge et al., 2009; Modali and Zgurskaya, 2011). These domains of MFPs interface with periplasmic domains of transporters and undergo conformational changes needed for stimulation of transporters. Studies of MacAB-TolC suggested that MFPs stimulate ABC transporters by stabilizing the closed pre-ATP hydrolysis conformation (Modali

and Zgurskaya, 2011). Assuming conservation of the mechanism, we propose that in the case of RND transporters, MFPs stabilize the binding-to-extrusion transition that precedes the transmembrane proton transfer (Figure 5).

3. Interaction with OMF is needed for conformational changes in MFPs. The *in vivo* proteolysis approach showed that *in vivo* conformational changes in MFPs occur only in the presence of TolC (Ge et al., 2009; Modali and Zgurskaya, 2011). The TolC-induced conformational changes in MFPs were further linked to stimulation of activities of transporters by MFPs and to stabilization of tri-partite complexes *in vitro*. Taken together these results support the model that *in vivo* MFPs exist in stable complexes with transporters and that association with OMF triggers the conformational changes in MFPs needed for stimulation of transporters (Figure 5).
4. Interactions between transporters and OMFs are dynamic. Current models postulate that OMF association with an MFP-transporter complex leads to opening of the channel (Weeks et al., 2010; Janganan et al., 2013). In the docked models of AcrAB-TolC, TolC is in the open conformation (Symmons et al., 2009; Du et al., 2014). The dilation of the TolC channel in the assembled complex is apparently driven by energy-dependent conformational changes in MFP-transporter complexes (Janganan et al., 2013). The open and closed conformers of TolC stabilized by mutations can be readily distinguished *in vivo* by drug susceptibility, proteolytic and thiol labeling profiles (Krishnamoorthy et al., 2013). However, the interactions with TolC are highly dynamic and the life-time of TolC-containing complexes is very short (Tikhonova et al., 2009, 2011). Thus, TolC binding to the inner membrane complexes is transient.

Based on the data described above, we propose that reaction cycles of transporters are tightly coupled to the assembly of the trans-envelope complexes. Transporters and MFPs exist in the inner membrane as inactive complexes (Figure 5). The activation of complexes is triggered by MFP binding to OMF, which leads to a conformational change in MFP needed for stimulation of transporters. The activated MFP-transporter complex engages an OMF to expel substrates across the outer membrane. The recruitment of an OMF is likely triggered by binding of effectors (substrates) to MFP or MFP-transporter complex. This possibility has been discussed before for the *P. aeruginosa* MexJK pump where experimental evidence strongly suggests that the MexJK complex recruits either OprM or OpmH in a substrate-dependent manner (Chuanchuen et al., 2005).

## NON-TYPICAL DRUG EFFLUX TRANSPORTERS

The discussed above MFP-transporter complexes have a three-fold symmetry befitting the trimeric architecture of OME. However, asymmetric assemblies like RND transporters MdtABC or TriABC are also broadly represented in bacterial genomes. The mechanism and the requirement for asymmetry in such complexes remain unclear.

MdtB and MdtC share only 50% sequence identity with each other. The expression of both MdtB and MdtC together with the MFP MdtA leads to a decreased drug susceptibility of *E. coli*

to SDS, novobiocin, cloxacillin, and several bile salts (Baranova and Nikaido, 2002; Nagakubo et al., 2002; Kim et al., 2010; Kim and Nikaido, 2012). The expression of MdtAB does not yield a functional transporter, but expression of MdtAC resulted in partial activity: a drug resistant phenotype against bile salts. Co-purification experiments and protein fusion studies suggest that MdtBC associates as a  $B_2C$  complex (Kim et al., 2010). Furthermore, there is convincing evidence that MdtB and MdtC fulfill distinctly different roles for the transporter. Site-directed mutagenesis studies have shown that a mutation in the proton relay network of MdtB abolishes functionality of the complex to a greater extent than corresponding mutations in MdtC (Kim et al., 2010). On the other hand, mutations in the proposed drug binding pocket and 3D docking studies on homology models indicate that substrates bind primarily to MdtC (Kim and Nikaido, 2012). The proton relay network in MdtB is thus thought to provide the energy required for a conformational change in MdtC resulting in removal of substrates (Mima et al., 2009). This arrangement differs from the current model of drug expulsion in homotrimeric RND transporters, in which each protomer is functionally identical. MuxABC-OpmB in *P. aeruginosa* similarly includes two RND components in a single operon MuxB and MuxC. In this system, both peptides are necessary in order to observe drug resistance against a range of antibiotics including novobiocin and carbenicillin (Mima et al., 2009; Yang et al., 2011).

In some complexes, the asymmetry arises through heterooligomerization of MFPs. TriABC-OpmH from *P. aeruginosa* requires two MFPs TriA and TriB that share 36% sequence identity with each other (Mima et al., 2007). TriABC-OpmH provides resistance to triclosan with both TriA and TriB required for efflux

(Mima et al., 2007). TriA and TriB presumably form either a trimer or dimers or a hetero-oligomeric hexamer. Since both MFPs share relatively little sequence identity and each of them is required for activity, it is likely that they serve different functions for the transporter.

Some transporters include a fourth unique component in their operons. These proteins are typically not required for functionality of the complex, however their presence modifies the activity of the transporter. The best characterized efflux pumps with a fourth component are the ABC transporter YknWXYZ from *B. subtilis* (see below) (Yamada et al., 2012), MexGHI-OpmD from *P. aeruginosa* (Aendekerk et al., 2002) and CusF-CusBAC from *E. coli* (Kim et al., 2011) (Figure 6). In addition, there are small ~50 aa long peptides like AcrZ from *E. coli* that binds to AcrAB-TolC and modifies its substrate specificity (Hobbs et al., 2012).

MexGHI-OpmD is required for virulence of *P. aeruginosa* and its overproduction decreases susceptibilities to norfloxacin, ethidium bromide, acriflavine, and rhodamine 6G (Aendekerk et al., 2002, 2005; Sekiya et al., 2003). The complex is thought to be involved in the translocation of quorum sensing molecules that upregulate the transcription of virulence factors. MexH, MexI and OpmD are MFP, RND, and OMF respectively, whereas MexG is a small 16.2 kDa protein of unknown function. According to sequence analysis it is proposed to be a membrane protein comprising four transmembrane  $\alpha$ -helices. MexHI-OpmD is functional without MexG but the latter is required for full functionality of the complex (Sekiya et al., 2003). Homologs of MexG exist in other Gram-negative bacteria that are also encoded in operons with RND transporters, suggesting that the requirement for the fourth component is

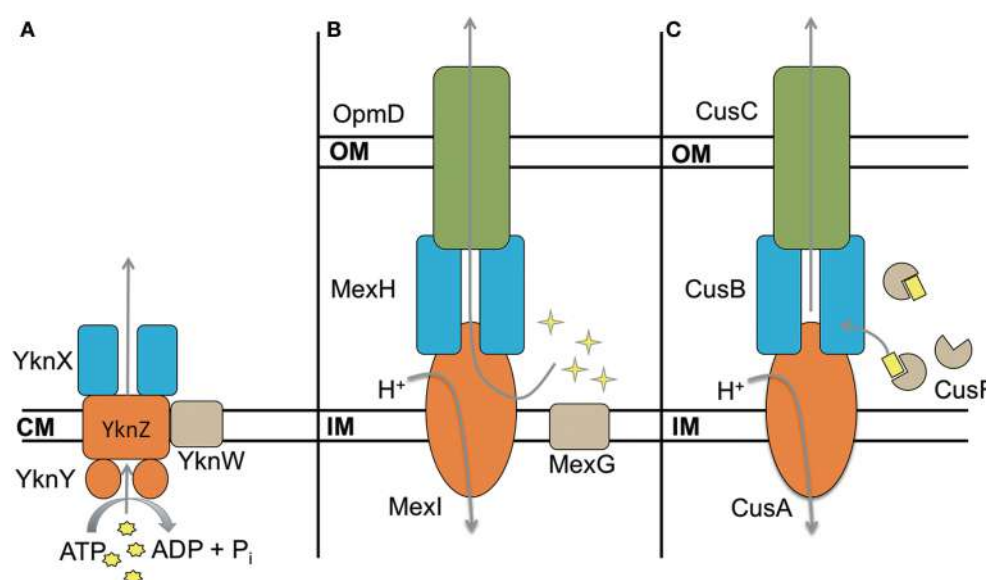


**FIGURE 6 | Four component transporters.** **(A)** ATP type transporter YknWXYZ from *B. subtilis*. YknW is thought to associate with the YknXYZ complex and seems to be essential for the transporter (Yamada et al., 2012). **(B)** MexGHI-OpmD is an RND transporter in *P. aeruginosa* that is involved in virulence (Aendekerk et al., 2002, 2005). MexG is proposed to be located in

the inner membrane and contributes to the functionality of MexHI-OpmD (Sekiya et al., 2003). **(C)** RND transporter CusBAC-CusF from *E. coli*. CusF is a metal chaperon that is thought to donate Cu(I) to the MFP CusB (Argüello et al., 2011; Mealman et al., 2011; Padilla-Benavides et al., 2014). Shapes in yellow represent the corresponding substrates for each transporter.

conserved. More work is needed to elucidate the role of MexG homologs.

The existence of asymmetric and four-component complexes implies that current models of the MFP-dependent transport may be incomplete. It is possible that the asymmetry and additional components split functional roles of subunits and promote one of the transition states. What step(s) in the transport could be enhanced by additional subunits? In case of MFPs, this could be the separation of roles in the stimulation of a transporter and the recruitment/opening of OMF. In transporters, this could be an added substrate specificity or a separation of energy transduction and substrate translocation as suggested for MdtBC (Nagakubo et al., 2002; Kim et al., 2010). It is also possible that the hetero-oligomerization of transporters and MFPs as well as additional components might serve similar roles in the transport cycle such as modulation of transporter affinities to substrates and/or MFPs and OMFs. In this way, asymmetry might increase the specificity of a MFP-transporter complex to an OMF, which in turn could be a way to control the activity of the transporter.

## MFP-DEPENDENT TRANSPORTERS OF GRAM-POSITIVE BACTERIA

Although MFPs are ubiquitous in efflux complexes that function in the context of two membranes, these proteins are also present in Gram-positive bacteria, which typically lack an outer membrane. Overall, the structures of cell envelopes of Gram-positive bacteria are poorly characterized, and while Gram-positive and Gram-negative cell envelopes share some characteristics, they are chemically and compositionally distinct. MFPs are required for functions of many transporters in Gram-positive bacteria that are involved in drug resistance, membrane biogenesis, and protein secretion (Butcher and Helmann, 2006; Yamada et al., 2012; Freudl, 2013).

Sequence homology and modeling indicate that MFPs from Gram-positive bacteria share the same general architecture as Gram-negative MFPs (Figure 3). The conservation of the  $\alpha$ -hairpin region in Gram-positive MFPs is puzzling, as the region is thought to be the major contributor toward interactions between the MFP and OMF in Gram-negative transporters. The best characterized complex is *B. subtilis* YknWXYZ known to provide resistance against the endogenously-produced toxin SdpC, which lyses surrounding cells, freeing nutrients and allowing the cell to delay sporulation (Butcher and Helmann, 2006). YknWXYZ shows homology to other ABC-type transporters such as MacAB-TolC of *E. coli*, and in addition to the MFP YknX, contains the components YknYZ and YknW (Figure 6). YknY and YknZ are an ATPase and a permease components of the transporter. YknW contains four transmembrane domains, and shares homology with the Yip1 family of proteins which are involved with vesicular transport in yeast. YknW was shown to affect the oligomeric state of YknX, or possibly YknX and YknYZ interactions (Yamada et al., 2012). This furthers the idea that the MFP-transporter interface is largely dependent on conformational changes within the MFP, and that stimulation of these changes can be conferred by proteins other than the transporter and OMF.

The functions of Gram-positive MFPs in transporter cycles await further studies. However, activities of Gram-negative MFPs

are not limited to that of engaging an outer membrane channel and some of such activities could be also characteristic of Gram-positive MFPs. First, similar to Gram-negative MFPs, YknX and other Gram-positive MFPs are expected to be conformationally flexible. A wide range of MFPs movement (Mikolosko et al., 2006; Vaccaro et al., 2006; Wang et al., 2012) has been proposed to be important for stimulation of transporter activities, assembly of functional complexes and substrate extrusion. Second, MFPs of metal-exporting transporters are known to bind their substrates. The MFP ZneB from the *Cupriavidus metallidurans* ZneCAB export complex is known to exhibit structural changes upon binding its substrate zinc (De Angelis et al., 2010), the MFP CusB of the efflux complex CusBAC has been shown to bind its substrate, copper (Su et al., 2009; Delmar et al., 2013), and the MFP MacA binds a core LPS molecule, a putative substrate (Lu and Zgurskaya, 2013). It is possible that Gram-positive MFPs also receive substrates from their cognate transporters and then release them into the external medium. Finally, MFPs have also been proposed to stabilize or destabilize certain conformations of the transporter, moving the complex through the transport process. Hence, MFPs in Gram-positive cell envelopes, as in the context of Gram-negative cell envelopes, are likely to play an active role in the transport process. Interestingly, the predicted MFP of an ABC-type transporter DSY0927 from *Desulfitobacterium hafniense* is a fusion of two different MFPs. The N-terminal half of the protein shows homology to MF-type MFPs and does not have a coiled-coil domain, whereas the C-terminal half of the protein shares more characteristics of an RND-type MFP (Zgurskaya et al., 2009). This finding further suggests that similar to Gram-negatives, Gram-positive MFPs likely function as dimers, with each MFP molecule attaining a specific role in the transport cycle.

## CONCLUSIONS

The proposed model together with recent structural and functional advances provides a fairly detailed understanding of the mechanism of drug efflux across the two membrane envelopes of Gram-negative bacteria. Allosteric inhibitors that target specific conformations of MFPs and prevent these proteins from binding to OMF and activation of transporters could be effective in potentiation of activities of antibiotics. Further studies are needed: (i) to identify MFP-transporter and MFP-OMF molecular interfaces that are critical for activation of efflux and (ii) to characterize conformational transitions in all components of the complexes leading to efflux across the outer membrane. Non-typical transporters could be powerful tools in understanding how the trans-envelope efflux is achieved. There is a significant gap in knowledge about functions of MFPs in the context of Gram-positive cell envelopes.

## ACKNOWLEDGMENTS

Studies in Zgurskaya lab are sponsored by the Department of the Defense, Defense Threat Reduction Agency and by the National Institute of Health (grant AI052293). The content of the information does not necessarily reflect the position or the policy of the federal government, and no official endorsement should be inferred.

## REFERENCES

- Aendekerk, S., Diggle, S. P., Song, Z., Hoiby, N., Cornelis, P., Williams, P., et al. (2005). The MexGHI-OpmD multidrug efflux pump controls growth, antibiotic susceptibility and virulence in *Pseudomonas aeruginosa* via 4-quinolone-dependent cell-to-cell communication. *Microbiology* 151(Pt 4), 1113–1125. doi: 10.1099/mic.0.27631-0
- Aendekerk, S., Ghysels, B., Cornelis, P., and Baysse, C. (2002). Characterization of a new efflux pump, MexGHI-OpmD, from *Pseudomonas aeruginosa* that confers resistance to vanadium. *Microbiology* 148(Pt 8), 2371–2381.
- Akama, H., Kanemaki, M., Yoshimura, M., Tsukihara, T., Kashiwagi, T., Yoneyama, H., et al. (2004a). Crystal structure of the drug discharge outer membrane protein, OprM, of *Pseudomonas aeruginosa*: dual modes of membrane anchoring and occluded cavity end. *J. Biol. Chem.* 279, 52816–52819. doi: 10.1074/jbc.C400445200
- Akama, H., Matsuura, T., Kashiwagi, S., Yoneyama, H., Narita, S., Tsukihara, T., et al. (2004b). Crystal structure of the membrane fusion protein, MexA, of the multidrug transporter in *Pseudomonas aeruginosa*. *J. Biol. Chem.* 279, 25939–25942. doi: 10.1074/jbc.C400164200
- Andersen, C., Koronakis, E., Bokma, E., Eswaran, J., Humphreys, D., Hughes, C., et al. (2002). Transition to the open state of the TolC periplasmic tunnel entrance. *Proc. Natl. Acad. Sci. U.S.A.* 99, 11103–11108. doi: 10.1073/pnas.162039399
- Argüello, J. M., González-Guerrero, M., and Raimunda, D. (2011). Bacterial transition metal P1B-ATPases: transport mechanism and roles in virulence. *Biochemistry* 50, 9940–9949. doi: 10.1021/bi201418k
- Baranova, N., and Nikaido, H. (2002). The baeSR two-component regulatory system activates transcription of the yegMNOB (mdtABCD) transporter gene cluster in *Escherichia coli* and increases its resistance to novobiocin and deoxycholate. *J. Bacteriol.* 184, 4168–4176. doi: 10.1128/JB.184.15.4168-4176.2002
- Bavro, V. N., Pietras, Z., Furnham, N., Perez-Cano, L., Fernandez-Recio, J., Pei, X. Y., et al. (2008). Assembly and channel opening in bacterial drug efflux machine. *Mol. Cell* 30, 114–121. doi: 10.1016/j.molcel.2008.02.015
- Bokma, E., Koronakis, E., Lobedanz, S., Hughes, C., and Koronakis, V. (2006). Directed evolution of a bacterial efflux pump: adaptation of the *E. coli* TolC exit duct to the *Pseudomonas* MexAB translocase. *FEBS Lett.* 580, 5339–5343. doi: 10.1016/j.febslet.2006.09.005
- Bunikis, I., Denker, K., Ostberg, Y., Andersen, C., Benz, R., and Bergstrom, S. (2008). An RND-type efflux system in *Borrelia burgdorferi* is involved in virulence and resistance to antimicrobial compounds. *PLoS Pathog.* 4:e1000009. doi: 10.1371/journal.ppat.1000009
- Butcher, B. G., and Helmann, J. D. (2006). Identification of *Bacillus subtilis* sigma-dependent genes that provide intrinsic resistance to antimicrobial compounds produced by Bacilli. *Mol. Microbiol.* 60, 765–782. doi: 10.1111/j.1365-2958.2006.05131.x
- Chuanchuen, R., Murata, T., Gotoh, N., and Schweizer, H. P. (2005). Substrate-dependent utilization of OprM or OpmH by the *Pseudomonas aeruginosa* MexJK efflux pump. *Antimicrob. Agents and Chemother.* 49, 2133–2136. doi: 10.1128/AAC.49.5.2133-2136.2005
- Chung, Y. J., and Saier, M. H. Jr. (2001). SMR-type multidrug resistance pumps. *Curr. Opin. Drug Discov. Devel.* 4, 237–245.
- Davidson, A. L., Dassa, E., Orelle, C., and Chen, J. (2008). Structure, function, and evolution of bacterial ATP-binding cassette systems. *Microbiol. Mol. Biol. Rev.* 72, 317–364. doi: 10.1128/MMBR.00031-07
- De Angelis, F., Lee, J. K., O'Connell, J. D., Miercke, L. J. W., Verschueren, K. H., Srinivasan, V., et al. (2010). Metal-induced conformational changes in ZneB suggest an active role of membrane fusion proteins in efflux resistance systems. *Proc. Natl. Acad. Sci.* 107, 11038–11043.
- Delmar, J. A., Su, C. C., and Yu, E. W. (2013). Structural mechanisms of heavy-metal extrusion by the Cus efflux system. *Biometals* 26, 593–607. doi: 10.1007/s10534-013-9628-0
- Du, D., Wang, Z., James, N. R., Voss, J. E., Klimont, E., Ohene-Agyei, T., et al. (2014). Structure of the AcrAB-TolC multidrug efflux pump. *Nature* 509, 512–515. doi: 10.1038/nature13205
- Eicher, T., Seeger, M. A., Anselmi, C., Zhou, W., Brandstatter, L., Verrey, F., et al. (2014). Coupling of remote alternating-access transport mechanisms for protons and substrates in the multidrug efflux pump AcrB. *eLife* 3:e03145. doi: 10.7554/eLife.03145
- Elkins, C. A., and Nikaido, H. (2003). Chimeric analysis of AcrA function reveals the importance of its C-terminal domain in its interaction with the AcrB multidrug efflux pump. *J. Bacteriol.* 185, 5349–5356. doi: 10.1128/JB.185.18.5349-5356.2003
- Federici, L., Du, D., Walas, F., Matsumura, H., Fernandez-Recio, J., McKeegan, K. S., et al. (2005). The crystal structure of the outer membrane protein VceC from the bacterial pathogen Vibrio cholerae at 1.8 Å resolution. *J. Biol. Chem.* 280, 15307–15314. doi: 10.1074/jbc.M500401200
- Fluman, N., and Bibi, E. (2009). Bacterial multidrug transport through the lens of the major facilitator superfamily. *Biochim. Biophys. Acta* 1794, 738–747. doi: 10.1016/j.bbapap.2008.11.020
- Fluman, N., Ryan, C. M., Whitelegge, J. P., and Bibi, E. (2012). Dissection of mechanistic principles of a secondary multidrug efflux protein. *Mol. Cell* 47, 777–787. doi: 10.1016/j.molcel.2012.06.018
- Freudl, R. (2013). Leaving home ain't easy: protein export systems in Gram-positive bacteria. *Res. Microbiol.* 164, 664–674. doi: 10.1016/j.resmic.2013.03.014
- Ge, Q., Yamada, Y., and Zgurskaya, H. (2009). The C-terminal domain of AcrA is essential for the assembly and function of the multidrug efflux pump AcrAB-TolC. *J. Bacteriol.* 191, 4365–4371. doi: 10.1128/JB.00204-09
- Gerken, H., and Misra, R. (2004). Genetic evidence for functional interactions between TolC and AcrA proteins of a major antibiotic efflux pump of *Escherichia coli*. *Mol. Microbiol.* 54, 620–631. doi: 10.1111/j.1365-2958.2004.04301.x
- Gessmann, D., Chung, Y. H., Danoff, E. J., Plummer, A. M., Sandlin, C. W., Zaccai, N. R., et al. (2014). Outer membrane β-barrel protein folding is physically controlled by periplasmic lipid head groups and BamA. *Proc. Natl. Acad. Sci. U.S.A.* 111, 5878–5883. doi: 10.1073/pnas.1322473111
- Greene, N. P., Hinchliffe, P., Crow, A., Ababou, A., Hughes, C., and Koronakis, V. (2013). Structure of an atypical periplasmic adaptor from a multidrug efflux pump of the spirochete *Borrelia burgdorferi*. *FEBS Lett.* 587, 2984–2988. doi: 10.1016/j.febslet.2013.06.056
- Hagan, C. L., Silhavy, T. J., and Kahne, D. (2011). Beta-barrel membrane protein assembly by the bam complex. *Annu. Rev. Biochem.* 80, 189–210. doi: 10.1146/annurev-biochem-061408-144611
- Hall, J. A., Davidson, A. L., and Nikaido, H. (1998). Preparation and reconstitution of membrane-associated maltose transporter complex of *Escherichia coli*. *Methods Enzymol.* 292, 20–29. doi: 10.1016/S0076-6879(98)92004-3
- Hassan, K. A., Jackson, S. M., Penesyan, A., Patching, S. G., Tetu, S. G., Eijkelpamp, B. A., et al. (2013). Transcriptomic and biochemical analyses identify a family of chlorhexidine efflux proteins. *Proc. Natl. Acad. Sci. U.S.A.* 110, 20254–20259. doi: 10.1073/pnas.1317052110 doi: 10.1073/pnas.1317052110
- Higgins, C. F., and Linton, K. J. (2004). The ATP switch model for ABC transporters. *Nat. Struct. Mol. Biol.* 11, 918–926. doi: 10.1038/nsmb836
- Hinchliffe, P., Greene, N. P., Paterson, N. G., Crow, A., Hughes, C., and Koronakis, V. (2014). Structure of the periplasmic adaptor protein from a major facilitator superfamily (MFS) multidrug efflux pump. *FEBS Lett.* 588, 3147–3153. doi: 10.1016/j.febslet.2014.06.055
- Hobbs, E. C., Yin, X., Paul, B. J., Astarita, J. L., and Storz, G. (2012). Conserved small protein associates with the multidrug efflux pump AcrB and differentially affects antibiotic resistance. *Proc. Natl. Acad. Sci. U.S.A.* 109, 16696–16701. doi: 10.1073/pnas.1210093109
- Hvorup, R. N., Winnen, B., Chang, A. B., Jiang, Y., Zhou, X. F., Saier, M. H., et al. (2003). The multidrug/oligosaccharidyl-lipid/polysaccharide (MOP) exporter superfamily. *Eur. J. Biochem.* 270, 799–813. doi: 10.1046/j.1432-1033.2003.03418.x
- Ip, H., Stratton, K., Zgurskaya, H., and Liu, J. (2003). pH-induced conformational changes of AcrA, the membrane fusion protein of *Escherichia coli* multidrug efflux system. *J. Biol. Chem.* 278, 50474–50482. doi: 10.1074/jbc.M305152200
- Janganan, T. K., Bavro, V. N., Zhang, L., Borges-Walmsley, M. I., and Walmsley, A. R. (2013). Tripartite efflux pumps: energy is required for dissociation, but not assembly or opening of the outer membrane channel of the pump. *Mol. Microbiol.* 88, 590–602. doi: 10.1111/mmi.12211
- Kim, E.-H., Nies, D. H., McEvoy, M. M., and Rensing, C. (2011). Switch or funnel: how RND-type transport systems control periplasmic metal homeostasis. *J. Bacteriol.* 193, 2381–2387. doi: 10.1128/JB.01323-10
- Kim, H. S., Nagore, D., and Nikaido, H. (2010). Multidrug efflux pump MdtBC of *Escherichia coli* is active only as a B2C heterotrimer. *J. Bacteriol.* 192, 1377–1386. doi: 10.1128/JB.01448-09
- Kim, H. S., and Nikaido, H. (2012). Different functions of MdtB and MdtC subunits in the heterotrimeric efflux transporter MdtB(2)C complex of *Escherichia coli*. *Biochemistry* 51, 4188–4197. doi: 10.1021/bi300379y

- Koronakis, V., Sharff, A., Koronakis, E., Luisi, B., and Hughes, C. (2000). Crystal structure of the bacterial membrane protein TolC central to multidrug efflux and protein export. *Nature* 405, 914–919. doi: 10.1038/35016007
- Krishnamoorthy, G., Tikhonova, E. B., Dhamdhare, G., and Zgurskaya, H. I. (2013). On the role of TolC in multidrug efflux: the function and assembly of AcrAB-TolC tolerate significant depletion of intracellular TolC protein. *Mol. Microbiol.* 87, 982–997. doi: 10.1111/mmi.12143
- Krishnamoorthy, G., Tikhonova, E. B., and Zgurskaya, H. I. (2008). Fitting periplasmic membrane fusion proteins to inner membrane transporters: mutations that enable *Escherichia coli* AcrA to function with *Pseudomonas aeruginosa* MexB. *J. Bacteriol.* 190, 691–698. doi: 10.1128/JB.01276-07
- Kulathila, R., Indic, M., and van den Berg, B. (2011). Crystal structure of *Escherichia coli* CusC, the outer membrane component of a heavy metal efflux pump. *PLoS ONE* 6:e15610. doi: 10.1371/journal.pone.0015610
- Lei, H. T., Chou, T. H., Su, C. C., Bolla, J. R., Kumar, N., Radhakrishnan, A., et al. (2014). Crystal structure of the open state of the *Neisseria gonorrhoeae* MtrE outer membrane channel. *PLoS ONE* 9:e97475. doi: 10.1371/journal.pone.0097475
- Lobedanz, S., Bokma, E., Symmons, M. F., Koronakis, E., Hughes, C., and Koronakis, V. (2007). A periplasmic coiled-coil interface underlying TolC recruitment and the assembly of bacterial drug efflux pumps. *Proc. Natl. Acad. Sci. U.S.A.* 104, 4612–4617. doi: 10.1073/pnas.0610160104
- Lomovskaya, O., Zgurskaya, H. I., and Bostian, K. A. (2008a). “Bacterial multidrug transporters: molecular and clinical aspects,” in *Transporters as Drug Carriers. Methods and Principles in Medicinal Chemistry*, Vol. 33, eds G. F. Ecker and P. Chiba (Weinheim: Wiley and Sons), 121–158.
- Lomovskaya, O., Zgurskaya, H. I., Bostian, K. A., and Lewis, K. (2008b). “Multidrug efflux pumps: structure, mechanism, and inhibition,” in *Bacterial Resistance to Antimicrobials*, eds R. G. Wax, K. Lewis, A. A. Salyers, and H. Taber (Boca, CA; Raton; London; New York, NY: CRC Press), 45–69.
- Lu, S., and Zgurskaya, H. I. (2012). Role of ATP binding and hydrolysis in assembly of MacAB-TolC macrolide transporter. *Mol. Microbiol.* 86, 1132–1143. doi: 10.1111/mmi.12046
- Lu, S., and Zgurskaya, H. I. (2013). MacA, a periplasmic membrane fusion protein of the macrolide transporter MacAB-TolC, binds lipopolysaccharide core specifically and with high affinity. *J. Bacteriol.* 195, 4865–4872. doi: 10.1128/JB.00756-13
- Matias, V. R., Al-Amoudi, A., Dubochet, J., and Beveridge, T. J. (2003). Cryo-transmission electron microscopy of frozen-hydrated sections of *Escherichia coli* and *Pseudomonas aeruginosa*. *J. Bacteriol.* 185, 6112–6118. doi: 10.1128/JB.185.20.6112-6118.2003
- Mealman, T. D., Bagai, I., Singh, P., Goodlett, D. R., Rensing, C., Zhou, H., et al. (2011). Interactions between CusF and CusB identified by NMR spectroscopy and chemical cross-linking coupled to mass spectrometry. *Biochemistry* 50, 2559–2566. doi: 10.1021/bi102012j
- Mikolosko, J., Bobyk, K., Zgurskaya, H. I., and Ghosh, P. (2006). Conformational flexibility in the multidrug efflux system protein AcrA. *Structure* 14, 577–587. doi: 10.1016/j.str.2005.11.015
- Mima, T., Joshi, S., Gomez-Escalada, M., and Schweizer, H. P. (2007). Identification and characterization of TriABC-OpmH, a triclosan efflux pump of *Pseudomonas aeruginosa* requiring two membrane fusion proteins. *J. Bacteriol.* 189, 7600–7609. doi: 10.1128/JB.00850-07
- Mima, T., Kohira, N., Li, Y., Sekiya, H., Ogawa, W., Kuroda, T., et al. (2009). Gene cloning and characteristics of the RND-type multidrug efflux pump MuxABC-OpmB possessing two RND components in *Pseudomonas aeruginosa*. *Microbiology* 155(Pt 11), 3509–3517. doi: 10.1099/mic.0.031260-0
- Modali, S. D., and Zgurskaya, H. I. (2011). The periplasmic membrane proximal domain of MacA acts as a switch in stimulation of ATP hydrolysis by MacB transporter. *Mol. Microbiol.* 81, 937–951. doi: 10.1111/j.1365-2958.2011.07744.x
- Murakami, S., Nakashima, R., Yamashita, E., and Yamaguchi, A. (2002). Crystal structure of bacterial multidrug efflux transporter AcrB. *Nature* 419, 587–593. doi: 10.1038/nature01050
- Nagakubo, S., Nishino, K., Hirata, T., and Yamaguchi, A. (2002). The putative response regulator BaeR stimulates multidrug resistance of *Escherichia coli* via a novel multidrug exporter system, MdtABC. *J. Bacteriol.* 184, 4161–4167. doi: 10.1128/JB.184.15.4161-4167.2002
- Nehme, D., and Poole, K. (2007). Assembly of the MexAB-OprM multidrug pump of *Pseudomonas aeruginosa*: component interactions defined by the study of pump mutant suppressors. *J. Bacteriol.* 189, 6118–6127. doi: 10.1128/JB.00718-07
- Nikaido, H., and Pages, J. M. (2012). Broad-specificity efflux pumps and their role in multidrug resistance of Gram-negative bacteria. *FEMS Microbiol. Rev.* 36, 340–363. doi: 10.1111/j.1574-6976.2011.00290.x
- Padilla, E., Llobet, E., Doménech-Sánchez, A., Martínez-Martínez, L., Bengoechea, J. A., and Alberti, S. (2010). *Klebsiella pneumoniae* AcrAB efflux pump contributes to antimicrobial resistance and virulence. *Antimicrob. Agents Chemother.* 54, 177–183. doi: 10.1128/AAC.00715-09
- Padilla-Benavides, T., Arguello, J. M., George, T. A. M., and McEvoy, M. M. (2014). Mechanism of ATPase-mediated Cu<sup>+</sup> export and delivery to periplasmic chaperones: the interaction of *Escherichia coli* CopA and CusF. *J. Biol. Chem.* 289, 20492–20501. doi: 10.1074/jbc.M114.577668
- Paulsen, I. T., Brown, M. H., and Skurray, R. A. (1998). Characterization of the earliest known *Staphylococcus aureus* plasmid encoding a multidrug efflux system. *J. Bacteriol.* 180, 3477–3479.
- Paulsen, I. T., Nguyen, L., Sliwinski, M. K., Rabus, R., and Saier, M. H. Jr. (2000). Microbial genome analyses: comparative transport capabilities in eighteen prokaryotes. *J. Mol. Biol.* 301, 75–100. doi: 10.1006/jmbi.2000.3961
- Paulsen, I. T., Park, J. H., Choi, P. S., and Saier, M. H. Jr. (1997). A family of gram-negative bacterial outer membrane factors that function in the export of proteins, carbohydrates, drugs and heavy metals from gram-negative bacteria. *FEMS Microbiol. Lett.* 156, 1–8. doi: 10.1016/S0378-1097(97)00379-0
- Pei, X. Y., Hinchliffe, P., Symmons, M. F., Koronakis, E., Benz, R., Hughes, C., et al. (2011). Structures of sequential open states in a symmetrical opening transition of the TolC exit duct. *Proc. Natl. Acad. Sci. U.S.A.* 108, 2112–2117. doi: 10.1073/pnas.1012588108
- Poole, K., and Srikumar, R. (2001). Multidrug efflux in *Pseudomonas aeruginosa*: components, mechanisms and clinical significance. *Curr. Top. Med. Chem.* 1, 59–71. doi: 10.2147/1568026013395605
- Pos, K. M. (2009). Drug transport mechanism of the AcrB efflux pump. *Biochim. Biophys. Acta* 1794, 782–793. doi: 10.1016/j.bbapap.2008.12.015
- Saier, M. H. Jr., Beatty, J. T., Goffeau, A., Harley, K. T., Heijne, W. H., Huang, S. C., et al. (1999). The major facilitator superfamily. *J. Mol. Microbiol. Biotechnol.* 1, 257–279.
- Saier, M. H. Jr., and Paulsen, I. T. (2001). Phylogeny of multidrug transporters. *Semin. Cell Dev. Biol.* 12, 205–213. doi: 10.1006/scdb.2000.0246
- Sanchez, L., Pan, W., Vinas, M., and Nikaido, H. (1997). The acrAB homolog of *Haemophilus influenzae* codes for a functional multidrug efflux pump. *J. Bacteriol.* 179, 6855–6857.
- Sekiya, H., Mima, T., Morita, Y., Kuroda, T., Mizushima, T., and Tsuchiya, T. (2003). Functional cloning and characterization of a multidrug efflux pump, mexHI-opmD, from a *Pseudomonas aeruginosa* mutant. *Antimicrob. Agents Chemother.* 47, 2990–2992. doi: 10.1128/AAC.47.9.2990-2992.2003
- Sen, K., Hellman, J., and Nikaido, H. (1988). Porin channels in intact cells of *Escherichia coli* are not affected by Donnan potentials across the outer membrane. *J. Biol. Chem.* 263, 1182–1187.
- Smirnova, I., Kasho, V., and Kaback, H. R. (2011). Lactose permease and the alternating access mechanism. *Biochemistry* 50, 9684–9693. doi: 10.1021/bi2014294
- Su, C. C., Long, F., Lei, H. T., Bolla, J. R., Do, S. V., Rajashankar, K. R., et al. (2012). Charged amino acids (R83, E567, D617, E625, R669, and K678) of CusA are required for metal ion transport in the Cus efflux system. *J. Mol. Biol.* 422, 429–441. doi: 10.1016/j.jmb.2012.05.038
- Su, C. C., Long, F., Zimmermann, M. T., Rajashankar, K. R., Jernigan, R. L., and Yu, E. W. (2011). Crystal structure of the CusBA heavy-metal efflux complex of *Escherichia coli*. *Nature* 470, 558–562. doi: 10.1038/nature09743
- Su, C. C., Yang, F., Long, F., Reyen, D., Routh, M. D., Kuo, D. W., et al. (2009). Crystal structure of the membrane fusion protein CusB from *Escherichia coli*. *J. Mol. Biol.* 393, 342–355. doi: 10.1016/j.jmb.2009.08.029
- Swick, M. C., Morgan-Linnell, S. K., Carlson, K. M., and Zechiedrich, L. (2011). Expression of multidrug efflux pump genes acrAB-tolC, mdfA, and norE in *Escherichia coli* clinical isolates as a function of fluoroquinolone and multidrug resistance. *Antimicrob. Agents Chemother.* 55, 921–924. doi: 10.1128/AAC.00996-10
- Symmons, M. F., Bokma, E., Koronakis, E., Hughes, C., and Koronakis, V. (2009). The assembled structure of a complete tripartite bacterial

- multidrug efflux pump. *Proc. Natl. Acad. Sci. U.S.A.* 106, 7173–7178. doi: 10.1073/pnas.0900693106
- Thanabalu, T., Koronakis, E., Hughes, C., and Koronakis, V. (1998). Substrate-induced assembly of a contiguous channel for protein export from *E.coli*: reversible bridging of an inner-membrane translocase to an outer membrane exit pore. *EMBO J.* 17, 6487–6496. doi: 10.1093/embj/17.22.6487
- Tikhonova, E. B., Dastidar, V., Rybenkov, V. V., and Zgurskaya, H. I. (2009). Kinetic control of TolC recruitment by multidrug efflux complexes. *Proc. Natl. Acad. Sci. U.S.A.* 106, 16416–16421. doi: 10.1073/pnas.0906601106
- Tikhonova, E. B., Devroy, V. K., Lau, S. Y., and Zgurskaya, H. I. (2007). Reconstitution of the *Escherichia coli* macrolide transporter: the periplasmic membrane fusion protein MacA stimulates the ATPase activity of MacB. *Mol. Microbiol.* 63, 895–910. doi: 10.1111/j.1365-2958.2006.05549.x
- Tikhonova, E. B., Yamada, Y., and Zgurskaya, H. I. (2011). Sequential mechanism of assembly of multidrug efflux pump AcrAB-TolC. *Chem. Biol.* 18, 454–463. doi: 10.1016/j.chembiol.2011.02.011
- Tommassen, J. (2010). Assembly of outer-membrane proteins in bacteria and mitochondria. *Microbiology* 156, 2587–2596. doi: 10.1099/mic.0.042689-0
- Tseng, T. T., Gratwick, K. S., Kollman, J., Park, D., Nies, D. H., Goffeau, A., et al. (1999). The RND permease superfamily: an ancient, ubiquitous and diverse family that includes human disease and development proteins. *J. Mol. Microbiol. Biotechnol.* 1, 107–125.
- Vaccaro, L., Koronakis, V., and Sansom, M. S. (2006). Flexibility in a drug transport accessory protein: molecular dynamics simulations of MexA. *Biophys. J.* 91, 558–564. doi: 10.1529/biophysj.105.080010
- Wang, B., Weng, J., Fan, K., and Wang, W. (2012). Interdomain flexibility and pH-induced conformational changes of AcrA revealed by molecular dynamics simulations. *J. Phys. Chem. B* 116, 3411–3420. doi: 10.1021/jp212221v
- Weeks, J. W., Bavro, V. N., and Misra, R. (2014). Genetic assessment of the role of AcrB beta-hairpins in the assembly of the TolC-AcrAB multidrug efflux pump of *Escherichia coli*. *Mol. Microbiol.* 91, 965–975. doi: 10.1111/mmi.12508
- Weeks, J. W., Celaya-Kolb, T., Pecora, S., and Misra, R. (2010). AcrA suppressor alterations reverse the drug hypersensitivity phenotype of a TolC mutant by inducing TolC aperture opening. *Mol. Microbiol.* 75, 1468–1483. doi: 10.1111/j.1365-2958.2010.07068.x
- Xu, Y., Lee, M., Moeller, A., Song, S., Yoon, B. Y., Kim, H. M., et al. (2011a). Funnel-like hexameric assembly of the periplasmic adapter protein in the tripartite multidrug efflux pump in gram-negative bacteria. *J. Biol. Chem.* 286, 17910–17920. doi: 10.1074/jbc.M111.238535
- Xu, Y., Song, S., Moeller, A., Kim, N., Piao, S., Sim, S. H., et al. (2011b). Functional implications of an intermeshing cogwheel-like interaction between TolC and MacA in the action of macrolide-specific efflux pump MacAB-TolC. *J. Biol. Chem.* 286, 13541–13549. doi: 10.1074/jbc.M110.202598
- Yamada, Y., Tikhonova, E. B., and Zgurskaya, H. I. (2012). YknWXYZ is an unusual four-component transporter with a role in protection against sporulation-delaying-protein-induced killing of *Bacillus subtilis*. *J. Bacteriol.* 194, 4386–4394. doi: 10.1128/JB.00223-12
- Yamanaka, H., Morisada, N., Miyano, M., Tsuge, H., Shinoda, S., Takahashi, E., et al. (2004). Amino-acid residues involved in the expression of the activity of *Escherichia coli* TolC. *Microbiol. Immunol.* 48, 713–722. doi: 10.1111/j.1348-0421.2004.tb03593.x
- Yamanaka, H., Nomura, T., Morisada, N., Shinoda, S., and Okamoto, K. (2002). Site-directed mutagenesis studies of the amino acid residue at position 412 of *Escherichia coli* TolC which is required for the activity. *Microb. Pathog.* 33, 81–89. doi: 10.1006/mpat.2002.0519
- Yang, L., Chen, L., Shen, L., Surette, M., and Duan, K. (2011). Inactivation of MuxABC-OpmB transporter system in *Pseudomonas aeruginosa* leads to increased ampicillin and carbenicillin resistance and decreased virulence. *J. Microbiol.* 49, 107–114. doi: 10.1007/s12275-011-0186-2
- Yen, M.-R., Peabody, C. R., Partovi, S. M., Zhai, Y., Tseng, Y.-H., and Saier, M. H. Jr. (2002). Protein-translocating outer membrane porins of Gram-negative bacteria. *Biochim. Biophys. Acta* 1562, 6–31. doi: 10.1016/S0005-2736(02)00359-0
- Yum, S., Xu, Y., Piao, S., Sim, S. H., Kim, H. M., Jo, W. S., et al. (2009). Crystal structure of the periplasmic component of a tripartite macrolide-specific efflux pump. *J. Mol. Biol.* 387, 1286–1297. doi: 10.1016/j.jmb.2009.02.048
- Zgurskaya, H. I., and Nikaido, H. (1999a). AcrA is a highly asymmetric protein capable of spanning the periplasm. *J. Mol. Biol.* 285, 409–420. doi: 10.1006/jmbi.1998.2313
- Zgurskaya, H. I., and Nikaido, H. (1999b). Bypassing the periplasm: reconstitution of the AcrAB multidrug efflux pump of *Escherichia coli*. *Proc. Natl. Acad. Sci. U.S.A.* 96, 7190–7195. doi: 10.1073/pnas.96.13.7190
- Zgurskaya, H. I., and Nikaido, H. (2000a). Cross-linked complex between oligomeric periplasmic lipoprotein AcrA and the inner-membrane-associated multidrug efflux pump AcrB from *Escherichia coli*. *J. Bacteriol.* 182, 4264–4267. doi: 10.1128/JB.182.15.4264-4267.2000
- Zgurskaya, H. I., and Nikaido, H. (2000b). Multidrug resistance mechanisms: drug efflux across two membranes. *Mol. Microbiol.* 37, 219–225. doi: 10.1046/j.1365-2958.2000.01926.x
- Zgurskaya, H. I., Yamada, Y., Tikhonova, E. B., Ge, Q., and Krishnamoorthy, G. (2009). Structural and functional diversity of bacterial membrane fusion proteins. *Biochim. Biophys. Acta* 1794, 794–807. doi: 10.1016/j.bbapap.2008.10.010
- Ziha-Zarifi, I., Llanes, C., Kohler, T., Pechere, J. C., and Plesiat, P. (1999). *In vivo* emergence of multidrug-resistant mutants of *Pseudomonas aeruginosa* overexpressing the active efflux system MexA-MexB-OprM. *Antimicrob. Agents Chemother.* 43, 287–291.
- Conflict of Interest Statement:** The authors declare that the research was conducted in the absence of any commercial or financial relationships that could be construed as a potential conflict of interest.
- Received:** 06 January 2015; **accepted:** 26 January 2015; **published online:** 24 February 2015.
- Citation:** Zgurskaya HI, Weeks JW, Ntreh AT, Nickels LM and Wolloscheck D (2015) Mechanism of coupling drug transport reactions located in two different membranes. *Front. Microbiol.* 6:100. doi: 10.3389/fmicb.2015.00100
- This article was submitted to Antimicrobials, Resistance and Chemotherapy, a section of the journal *Frontiers in Microbiology*.
- Copyright © 2015 Zgurskaya, Weeks, Ntreh, Nickels and Wolloscheck. This is an open-access article distributed under the terms of the Creative Commons Attribution License (CC BY). The use, distribution or reproduction in other forums is permitted, provided the original author(s) or licensor are credited and that the original publication in this journal is cited, in accordance with accepted academic practice. No use, distribution or reproduction is permitted which does not comply with these terms.

# Architecture and roles of periplasmic adaptor proteins in tripartite efflux assemblies

Martyn F. Symmons<sup>1</sup>, Robert L. Marshall<sup>2</sup> and Vassiliy N. Bavro<sup>2\*</sup>

<sup>1</sup> Department of Veterinary Medicine, University of Cambridge, Cambridge, UK, <sup>2</sup> Institute of Microbiology and Infection, University of Birmingham, Birmingham, UK

## OPEN ACCESS

### Edited by:

Attilio Vittorio Vargiu,  
Università di Cagliari, Italy

### Reviewed by:

Herbert P. Schweizer,  
Colorado State University, USA  
William William Shafer,  
Emory University School of Medicine,  
USA

### \*Correspondence:

Vassiliy N. Bavro,  
Institute of Microbiology and Infection,  
University of Birmingham,  
Birmingham B15 2TT, UK  
v.bavro@bham.ac.uk

### Specialty section:

This article was submitted to  
Antimicrobials, Resistance  
and Chemotherapy,  
a section of the journal  
Frontiers in Microbiology

**Received:** 26 March 2015

**Accepted:** 08 May 2015

**Published:** 28 May 2015

### Citation:

Symmons MF, Marshall RL  
and Bavro VN (2015) Architecture  
and roles of periplasmic adaptor  
proteins in tripartite efflux assemblies.  
Front. Microbiol. 6:513.  
doi: 10.3389/fmicb.2015.00513

Recent years have seen major advances in the structural understanding of the different components of tripartite efflux assemblies, which encompass the multidrug efflux (MDR) pumps and type I secretion systems. The majority of these investigations have focused on the role played by the inner membrane transporters and the outer membrane factor (OMF), leaving the third component of the system – the *Periplasmic Adaptor Proteins* (PAPs) – relatively understudied. Here we review the current state of knowledge of these versatile proteins which, far from being passive linkers between the OMF and the transporter, emerge as active architects of tripartite assemblies, and play diverse roles in the transport process. Recognition between the PAPs and OMFs is essential for pump assembly and function, and targeting this interaction may provide a novel avenue for combating multidrug resistance. With the recent advances elucidating the drug efflux and energetics of the tripartite assemblies, the understanding of the interaction between the OMFs and PAPs is the last piece remaining in the complete structure of the tripartite pump assembly puzzle.

**Keywords:** periplasmic adaptor proteins, TolC, drug efflux pumps, type I secretion system, antibiotic resistance, membrane proteins, membrane transport, RND family pumps

## Introduction – Components of Tripartite Pump Assemblies and Specificity

Gram-negative bacteria have to export a number of cargoes across their double membrane, which presents a formidable barrier for free diffusion of molecules. Amongst a number of secretion systems (Gerlach and Hensel, 2007; Christie et al., 2014; Minamino, 2014; Nivaskumar and Francetic, 2014; Thomas et al., 2014; van Ulsen et al., 2014; Zoued et al., 2014), tripartite efflux assemblies have particular importance for multidrug resistance, a growing global problem (Silver, 2011; Piddock, 2012).

Tripartite assemblies are a heterogeneous group of *multidrug efflux* and *type I secretion systems* which draws from several different families of primary and secondary inner-membrane transporters (MFS, ABC and RND). With the help of the so-called *periplasmic adaptor proteins* (PAPs), the inner-membrane transporters are linked to the *outer membrane factors* (OMFs) of the TolC family to create continuous conduits from the cytoplasm to the extracellular space, shown in **Figure 1** (Misra and Bavro, 2009; Hinchliffe et al., 2013; Blair et al., 2014, 2015; Zgurskaya et al., 2015). These are involved in transport of cargoes that vary in size from single ions to large proteins, which could reach over 100 kDa (Kaur et al., 2012). In addition, a fourth transmembrane

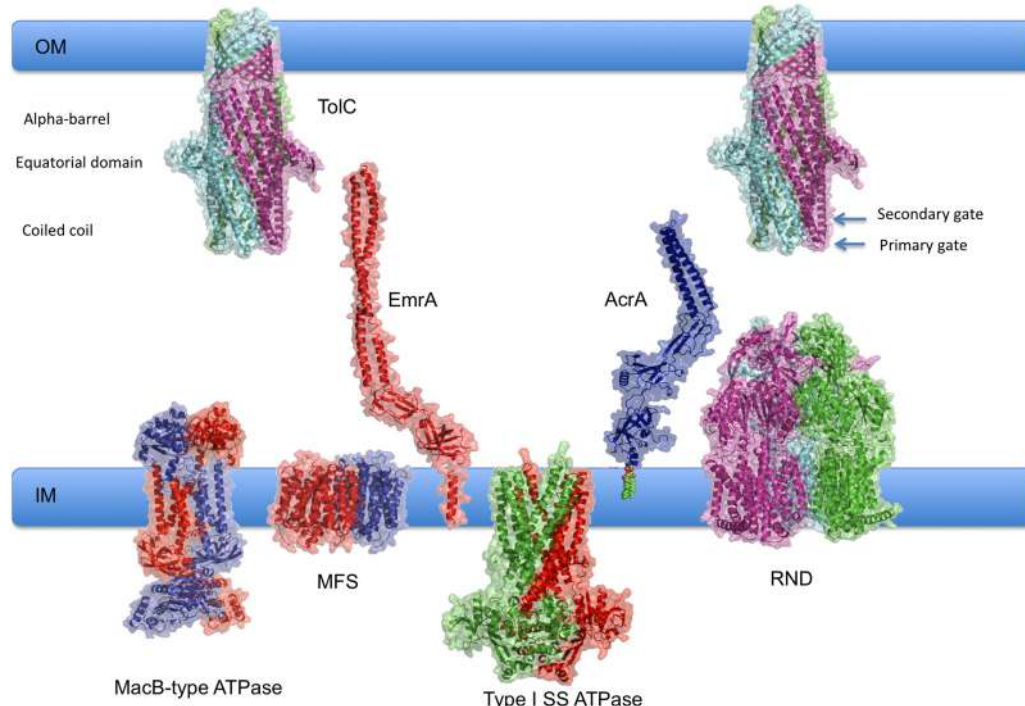


**FIGURE 1 | Overview of tripartite assemblies engaged in efflux and type I secretion.** Schematic diagram of pump components showing their relative sizes and respective membrane locations. Representative experimental structures of RND transporter MtrD (4MT1.pdb); MFS transporter EmrD (2GFP.pdb); the OMF TolC (2VDD.pdb) and periplasmic adaptor protein (PAPs) EmrA (4TK0.pdb) have been used. Type I SS ATPase refers to ABC-transporters, such as HlyB, that are associated with Type I Secretion systems. Evaluative models of the components for

which experimental structures are currently unavailable have been generated using homology modeling with I-TASSER (Yang et al., 2015) and manual optimisation using Coot (Emsley et al., 2010). The following templates were used: MacB (3FTJ.pdb); for HlyB (3ZUA.pdb; 2FF7.pdb; 2HYD), AcrA was modeled based on the experimental structure by Mikolosko et al. (2006) 2F1M.pdb. 3D structures in this manuscript were rendered using PyMOL (The PyMOL Molecular Graphics System, Schrödinger, LLC.).

component is sometimes present in the complex, e.g., YajC (Törnroth-Horsefield et al., 2007) or AcrZ (Hobbs et al., 2012). These small proteins are entirely  $\alpha$ -helical and bind the transporter within the inner membrane (Törnroth-Horsefield et al., 2007; Du et al., 2014). These proteins appear to be non-essential, but may play a modulatory role, affecting the efflux profile of the pump (Törnroth-Horsefield et al., 2007; Hobbs et al., 2012).

### Tripartite Efflux Assemblies and their Transporters

Multidrug efflux-pumps are grouped into a number of families including the primary transporters of the ABC-family [e.g., MacB (Kobayashi et al., 2003)], and secondary transporters which encompass the large group of RND-pumps (Eicher et al., 2014), major facilitator family (MFS), and a number of others, such as MATE, SM (Piddock, 2006; Bavro et al., 2008; Zgurskaya et al., 2015), and the recently discovered PACE family (Hassan et al., 2013, 2015). Of these, only the ABC, RND and MFS groups have been reported to participate in tripartite assemblies and associate with PAPs.

While the roles of the OMFs and transporters have been subject of much scrutiny (Koronakis et al., 2004; Zgurskaya et al.,

2011; Ruggerone et al., 2013; Eicher et al., 2014; Wong et al., 2014; Du et al., 2015), the role of the PAPs has remained more obscure. Recent advances indicate that these diverse modular proteins, far from being passive linkers of the outer and inner membranes, are central players in the efflux and transport processes, including cargo recognition and selection, control of energy flow, and emerge as the main architects of the tripartite assemblies. As the phylogenetic connections of PAPs have been subject to thorough review (Zgurskaya et al., 2009), we will focus on summarizing the advances in structural knowledge of the PAP family and how it helps to better understand their function in the context of the complete pump assembly. Our analyses presented here indicate that adaptors possess a highly modular organization with structural domains shared beyond the adaptor protein group and re-used in a number of other protein components of transport and regulatory systems.

### The Outer Membrane Component – TolC

The OMFs, which are the outer membrane components of tripartite pumps, are trimeric integral membrane proteins. Although TolC was identified as a colicin-susceptibility factor in the early 1970s (Whitney, 1971), its association with multidrug efflux pumps was not conclusively proven until the mid-1990s

(Fralick, 1996), when the whole family was described as membrane channels, or OMFs (Paulsen et al., 1997).

The structure of the prototypical member of the family, TolC, was solved by Koronakis et al. (2000) over a decade ago. Since then, the structural gallery has been expanded with the OprM (Akama et al., 2004; Phan et al., 2010); CusC (Kulathila et al., 2011; Lei et al., 2014a); VceC (Federici et al., 2005); MtrE (Lei et al., 2014b); and CmeC (Su et al., 2014). A detailed description of the structures of the OMF family is provided elsewhere (see Misra and Bavro, 2009; Hincliffe et al., 2013) and a comprehensive review provides an overview of the functional characteristics of the family (Zgurskaya et al., 2011).

Outer membrane factors have a  $\beta$ -barrel domain resembling the porin fold, which, unlike the canonical porins is formed by all three subunits, each of which contributes four  $\beta$ -strands to form a pseudo-continuous barrel. In addition, OMFs possess a unique periplasmic domain, which, like the  $\beta$ -barrel, is a pseudo-continuous structure built with the participation of all three protomers. Unlike the  $\beta$ -barrel domain, the periplasmic part is almost entirely  $\alpha$ -helical (Koronakis et al., 1997, 2000). The upper half of the periplasmic extension takes the form of an  $\alpha$ -barrel domain (Calladine et al., 2001), while in the lower half this is an arrangement of coiled-coil hairpins – each subunit contributing two pairs of helices. This arises from the fact that each of the TolC protomers is itself a product of internal gene duplication, manifesting as a structural repeat, which effectively gives the TolC trimer a pseudo-sixfold symmetry. The overall  $\beta$ -barrel: $\alpha$ -barrel:coiled-coil architecture has been conserved in other TolC homologues crystallized since then, but some of the members, e.g., OprM, also present a flexible N-terminal tail, which is often lipidated and inserted in the outer membrane (Akama et al., 2004). Finally, in some OMFs the N-and C-terminal elements form an ‘equatorial domain’ about halfway up the periplasmic part of the protein.

In the original crystal structure of the TolC the coiled coils of the periplasmic domain curve inward below the level of the equatorial domain to give a closed pore extended into the periplasm (Koronakis et al., 2000). *In vitro* studies of the TolC channel in isolation showed that it is predominantly closed with only very short stochastic opening sequences, and exhibiting strong cation selectivity (Andersen et al., 2002b). The closure at the tip of the channel was revealed to be maintained by an elaborate network of charged interactions, involving D153, R367, Y362, which when disrupted resulted in leaky channel phenotypes (Andersen et al., 2002a; Augustus et al., 2004; Bavro et al., 2008). This network has also been analyzed by *in silico* molecular dynamics studies, which hinted toward the possibility of asymmetric channel opening (Schulz and Kleinekathöfer, 2009), and indicate that the channel may open more than seen in “open state” crystal structures (Bavro et al., 2008; Pei et al., 2011). Two aspartates of each monomer (D371 and D374), facing into the channel lumen at successive helical turns were identified as responsible for this cation selectivity (Andersen et al., 2002b). Similar constrictions are a common feature in the family and were observed in other members – including OprM and VceC (Akama et al., 2004; Federici et al., 2005). The nature of the selectivity

gate may vary – such as in VceC, in which there is a hydrophobic constriction.

Bavro et al. (2008) suggested that the lower ion-bridges can be destabilized by direct interaction with transporters with large periplasmic domains, such as the RND family. The report also noted that the Asp-rings are too far up the channel to be directly affected by the transporter and are likely “unlocked” via interaction with the tip of the PAP. As successful unlocking of these bridges would be a requirement for productive transport, Bavro et al. (2008) designated them the “primary” and “secondary gates,” respectively. The designation indicates the sequence of cargo passage through these constrictions, although the order of their unlocking remains unclear.

## Determinants of OMF Specificity

While the adaptors and transporters are often encoded on the same operon, working in well-defined pairs that often stay associated even in the absence of substrate (Thanabalu et al., 1998; Zgurskaya and Nikaido, 2000), the outer membrane is served by only a handful of TolC-family members (Piddock, 2006; Zgurskaya et al., 2011). A consequence of this is that a number of different PAPs have to be able to bind to a single OMF, leading to “promiscuity” on the side of the OMF – in *Salmonella* at least 7 different efflux systems converge toward TolC (Horiyama et al., 2010). While a number of PAPs are able to function with a common OMF, this does not translate into total promiscuity; OMFs from one organism are not usually able to complement non-cognate systems. Even within one organism there is clear differentiation between systems on the basis of their OMF composition. As a result of this the focus of the search for determinants of specificity has justly fallen on to the OMF-adaptor interaction.

Periplasmic adaptor proteins successfully recognize and couple a limited set of OMFs to a diverse range of transporters, with high fidelity and selectivity of assembly. How they achieve this is one of the last remaining questions in the structure of efflux pumps. The answer has important medical implications due to the involvement of these complexes in both multidrug resistance and virulence (Nishino et al., 2006; Li and Nikaido, 2009; Nikaido and Pagès, 2012; Piddock, 2012, 2014).

## PAPs – Architecture and Structural Connections

### Discovery of the PAPs

The PAPs were initially identified as “membrane fusion proteins” (MFPs) based on perceived sequence similarity to *bona fide* viral MFPs, namely paramyxoviral SV5 fusion protein, and correspondingly a membrane fusion function was also ascribed (Dinh et al., 1994). The later description of the 3D structures of both MFPs and the paramyxoviral trimeric fusion protein (1ZTM.pdb) demonstrated a lack of general structural similarity between the two classes of proteins (Akama et al., 2004; Higgins et al., 2004b; Yin et al., 2005; Mikolosko et al., 2006). We show later that although viral MFPs and bacterial PAPs are generally dissimilar, one specific domain of the viral fusion protein

structure can indeed be matched to a small domain in many PAPs. The inferred fusion function was never experimentally detected in the PAP family. Despite this, the term MFP has persisted, and can still be found widely in the literature. To avoid confusion we will use the alternative term “PAPs.”

## PAP Structures Solved to Date

The adaptor proteins were the last component of the tripartite pumps to be characterized structurally. In Akama et al. (2004) and Higgins et al. (2004b) the structure of the MexA from *Pseudomonas aeruginosa* became the first member of the family to be crystallized (1VF7.pdb and 1T5E.pdb), followed by the structure of AcrA (2F1M.pdb; Mikolosko et al., 2006). All of these structures were missing a significant region, later called the membrane proximal domain (MPD), which due to its highly flexible nature didn’t become available until re-refinement of the MexA structure by Symmons et al. (2009; 2V4D.pdb).

In quick succession, the MacA structures from *Escherichia coli* (3FPP.pdb) and *Actinobacillus actinomycetemcomitans* (4DK0.pdb) were solved (Yum et al., 2009; Xu et al., 2012), followed by a number of metal pump-associated PAPs – CusB alone (3H94.pdb; 3OOC.pdb; 3OPO.pdb; 3OW7.pdb; Su et al., 2009); ZneB from *Cupriavidus metallidurans* (3LLN.pdb; De Angelis et al., 2010); as well as the CusBA complex (4DNR.pdb; 3T51.pdb; 3T53.pdb; 3T56.pdb; 3NE5.pdb; 4DNT.pdb; 4DOP.pdb; Su et al., 2011, 2012). The partial structure of the *Campylobacter jejuni* AcrA in a glycosylated state has also been determined by NMR (2K32.pdb; 2K33.pdb; Slynsko et al., 2009). In addition, the structure of the PAP (BACEGG\_01895) from a putative efflux pump from *Bacteroides eggerthii* DSM 20697 (4L8J.pdb) has become available from a structural genomics effort. Last year saw the report of the first MFS-transporter associated PAP – EmrA from *Aquifex aeolicus* (Hinchliffe et al., 2014), as well as a non-typical PAP lacking the  $\alpha$ -hairpin domain, BesA (Greene et al., 2013), widening our picture of structural diversity of the family.

There are now example structures available of PAPs from RND systems, both small molecules and metals, and ABC-efflux systems, but to date no structure of a PAP from a Type I system.

## General Architecture and Domain Organization of PAPs

Adaptor proteins are elongated molecules composed of a number of well-defined structural modules. Some modules are universal while others are only shared within a subset of the family. PAP structures show a ‘hairpin like’ arrangement in which the polypeptide passes from the inner-membrane outward to contact the outer membrane component and then back to the inner membrane (**Figure 2**). A topological analysis of domains in a complete adaptor (**Figure 2**, which has ZneB as an example) clearly shows how each domain is constructed from structural elements from the N- and C-terminal halves of the protein.

The central section of the majority of solved adaptors is an  $\alpha$ -helical hairpin forming a coiled-coil arrangement. This is of variable length and in the PAP of one system (BesA) it is dispensed with entirely (Greene et al., 2013). The coiled-coil is extended and shortened by insertion or deletion of heptad repeats

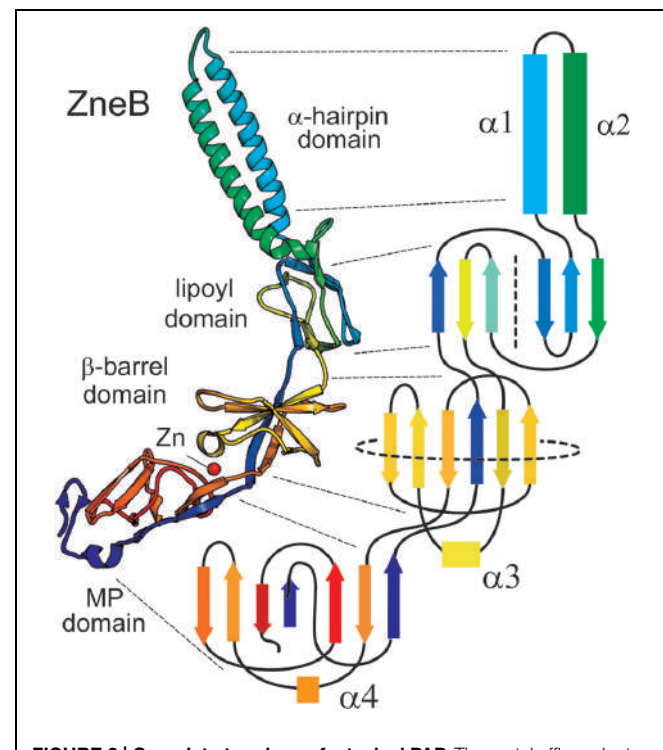


**FIGURE 2 | Complete topology of a typical PAP.** The metal efflux adaptor ZneB is shown here in schematic form (**left**) colored from blue (N-terminal) through red (C-terminal). The overall topology is presented alongside (**right**) in equivalent colors for the  $\beta$ -strands and  $\alpha$ -helices of each of the domains. The lipoyl domain has been flattened into two halves separated by a dotted line; and the  $\beta$ -barrel domain has also been flattened out as indicated by the circular dotted line.

in the two  $\alpha$ -helices. In the case of the metal efflux adaptor CusB, the hairpin is observed to be folded back on itself to generate a shortened four helical bundle (Su et al., 2009). In some PAPs the  $\alpha$ -hairpin is extended by a further  $\alpha$ -helical section constructed from paired  $\alpha$ -helices. Similar to the helices in the TolC  $\alpha$ -barrel, these run anti-parallel but without the marked twist of the coiled-coil helices. Crystal contacts in several PAP structures produce a six-membered barrel from these pairs of helices (see Yum et al., 2009, for example). This was suggested to function as a periplasmic channel assembly complementing the TolC periplasmic tunnel, based on similarity of their diameters although definitive evidence is not yet available.

Adjacent to the hairpin and its helical extension is a domain that was predicted and subsequently shown structurally to be homologous to biotin/lipoyl carrier domains in dehydrogenase enzymes (Johnson and Church, 1999; Higgins et al., 2004a). These domains consist of a  $\beta$ -sandwich of two interlocking motifs of four  $\beta$ -strands (**Figure 2**). Strikingly the  $\alpha$ -hairpin is an extension from the same loop in this domain that contains the lysine which is modified with the lipoyl group in the dehydrogenase subunit. However, the PAP lipoyl domain does not contain the signature modified lysine, as the hairpin extension is spliced *en lieu* of the loop that harbors it. While the exact functional role of this domain is still to be established, analysis of mutations targeting it suggest that it has a role in

stabilizing the complex assembly. This may be achieved either by interaction with the transporter, as indicated by cross-linking of the AcrA lipoyl domain to AcrB (e.g., Symmons et al., 2009), or by self-association, which would explain the loss of hexamerization of DevB when its lipoyl domain is disrupted (Staron et al., 2014).

The next domain in PAPs is a  $\beta$ -barrel consisting of six antiparallel  $\beta$ -strands capped by a single  $\alpha$ -helix. The overall topology of this barrel (**Figure 2** presents a limited 2D depiction) is also similar to enzyme ligand-binding domains such as the flavin adenine nucleotide-binding domain of flavodoxin reductase and ribokinase enzymes, and also to domains with odorant-binding properties (Higgins et al., 2004a).

A fourth domain present in some PAPs is the MPD (Symmons et al., 2009). Even when present, this is often ill-defined owing to its highly flexible connection to the  $\beta$ -barrel. Although it is constructed largely from the C-terminal elements of the protein, and has been termed ‘C-terminal domain’, it also incorporates the N-terminal  $\beta$ -strand, which provides the direct link to the inner membrane. The first example of a MPD structure was revealed only after re-refinement of MexA crystal data, showing a  $\beta$ -roll that is topologically related to the adjacent  $\beta$ -barrel domain, suggesting that it is likely to be the result of a domain duplication event.

Periplasmic adaptor proteins are anchored to the inner membrane either by an N-terminal transmembrane helix or, when no transmembrane helix is present, by N-terminal cysteine lipidation (e.g., triacylation or palmitoylation) following processing by signal peptidase 2.

Periplasmic adaptor proteins associated with the heavy metal efflux (HME) family of RND transporters may also present additional N- and C-terminal domains. Involvement of the latter in metal-chaperoning function has been demonstrated in the SilB adaptor protein from *Cupriavidus metallidurans* CH34 (Bersch et al., 2011). These domains also present themselves as stand-alone proteins (e.g., CusF of *E. coli*) and possess a unique metal-binding  $\beta$ -barrel fold (Loftin et al., 2005; Xue et al., 2008). The domain of the SilB metal-efflux adaptor has been solved separately from the full length SilB adaptor.

The possible conformational transitions associated with ion binding in CusB have recently been revealed by modeling of the N-terminal domains based on extensive homology modeling combined with molecular dynamics and NMR spectroscopy data (Ucisik et al., 2013). Despite these advances there is limited structural data on the N-terminal domains at present. However, the CusB N-terminal domain can be modeled as shown in **Figure 3** with the methionine residues implicated in metal binding clustered at one end of the domain.

## Structural Similarities Suggest Domain Duplications

**Figures 4A,B** show the comparison of the detailed topology of the  $\beta$ -barrel and the MPDs from MexA. The key conserved elements in these domains is the combination of a  $\beta$  strand with a helix or helical turn (shown in green) followed by a  $\beta$ -meander (yellow, orange, red). The subsequent  $\beta$ -hairpin strands (magenta, purple) and an N-terminal strand (blue) are associated with this  $\beta$ -meander in the complete barrel domain. In

contrast the MPD has a split in the barrel giving a  $\beta$ -roll structure. There is a characteristic folding over of the  $\beta$ -hairpin (**Figure 4B**, magenta, purple) and the N-terminal strand (blue) is also split so that it interacts with both halves of the MP domain.

Strikingly this combination of a  $\beta$ -meander with a  $\beta$ -hairpin is also observed in domain I of a viral fusion glycoprotein (**Figure 4C**, Fusion GP DI domain, from 2B9B.pdb) although the helix has been lost in this case. The resemblance is increased by the fact that the viral domain also shares the involvement of a separate, more N-terminal, strand. It is not clear if this structural similarity is in fact owing to evolutionary homology. However, it is possible that this structural resemblance underpins the original sequence similarity that motivated the name MFP for the adaptor protein family.

There is also a distant resemblance between the barrel/MP domain and the CusF metallochaperone topologies. This is shown in **Figure 4D**. Again there is no helical element and further there is no involvement of an N-terminal strand. Instead the barrel is completed by the  $\beta$ -hairpin (magenta, purple) folding back over the  $\beta$ -meander. The resulting topology is known from many OB-fold domains (Murzin, 1993), but may possibly have arisen as a special example of that fold in the case of the metal-efflux adaptors.

## Flexible Linkers in Periplasmic Adaptor Protein Structure

Owing to the hairpin-like pathway of the polypeptide chain through the PAP structure the linkers between each domain consist of two anti-parallel strands or turns. These are flexible but have distinctive structures with some degree of inter-strand hydrogen bonding. Comparing different PAP structures and also separate examples from different crystal environments shows these linkers can accommodate a range of both angular and rotational flexibility between adjacent domains.

These linkers are likely to allow the domains to optimize their individual interactions both with each other and with the inner and outer membrane components. This may be of significance as the TolC outer membrane exit duct undergoes conformational change on opening while the inner membrane transporter can undergo conformational changes as part of its pumping cycle. The associated PAPs must accommodate these conformational changes while retaining contact with the other pump components.

## Structural Homology and Evolutionary Connections of Periplasmic Adaptor Protein Domains

Periplasmic adaptor protein structures revealed that they have a common modular architecture. Far from being unique, their domains and linkers appear to be shared with other, highly diverse protein families, some of which are involved in bacterial tripartite systems and their regulation. Suggested structural relations of the adaptor domains to other proteins are shown in **Figure 5**.

It has been previously observed that the  $\alpha$ -helical domains of particular PAPs resemble inverted versions of the TolC domains (Symmons et al., 2009). Strikingly the polypeptide also follows

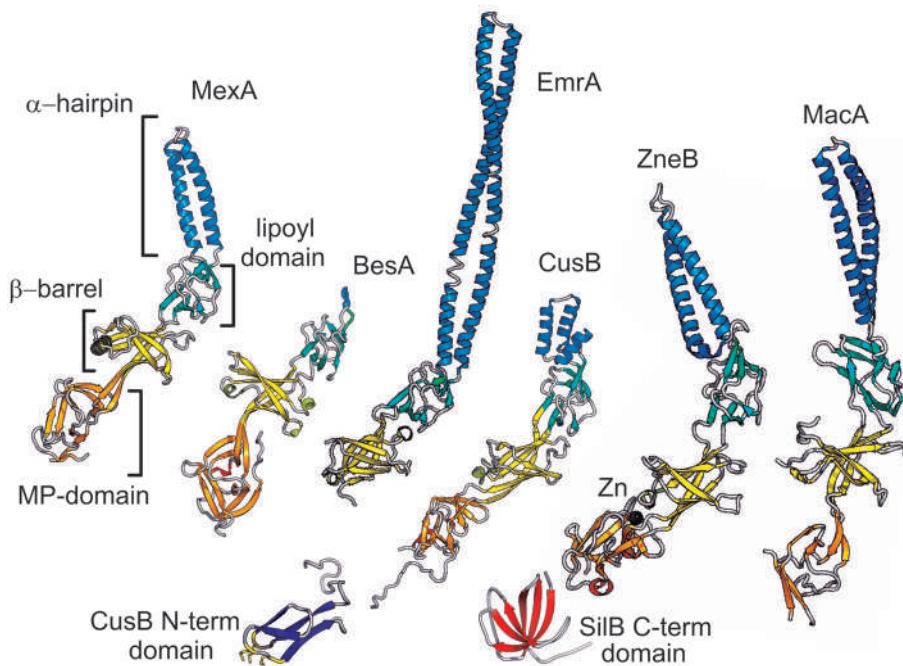


**FIGURE 3 | Representative PAPs.** Selected examples of the PAP family are shown in schematic representation. The domains of MexA (RND adaptor) are indicated and colored orange for the MP domain, yellow for the barrel domain, green for the lipoyl, and blue for the hairpin. The equivalent domains in other examples are colored similarly. BesA (RND),

which lacks the hairpin domain, EmrA (an MFS adaptor) which does not have an MP domain. CusB and ZneB are metal RND efflux pump adaptors some of which have additional domains represented here: the CusB N-terminal domain; and the SIlB C-terminal domain. Finally the MacA ABC adaptor is shown.

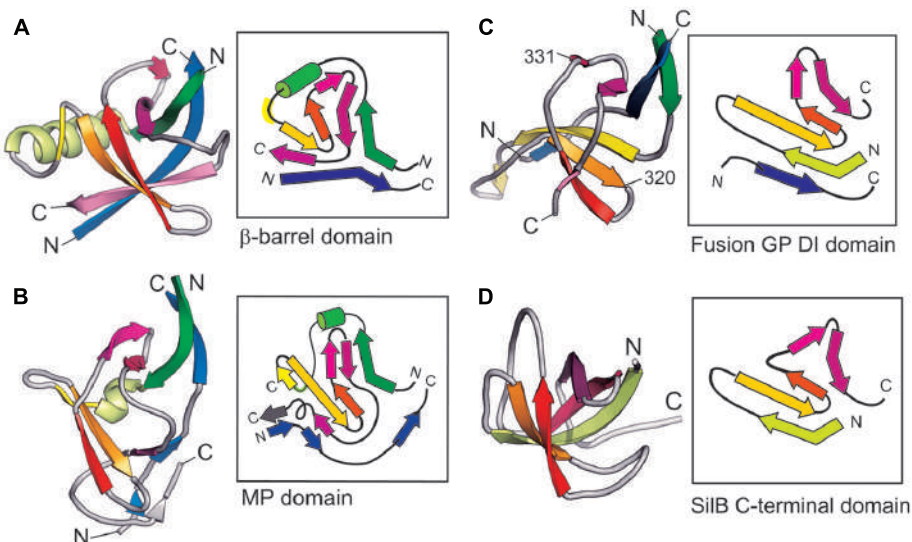
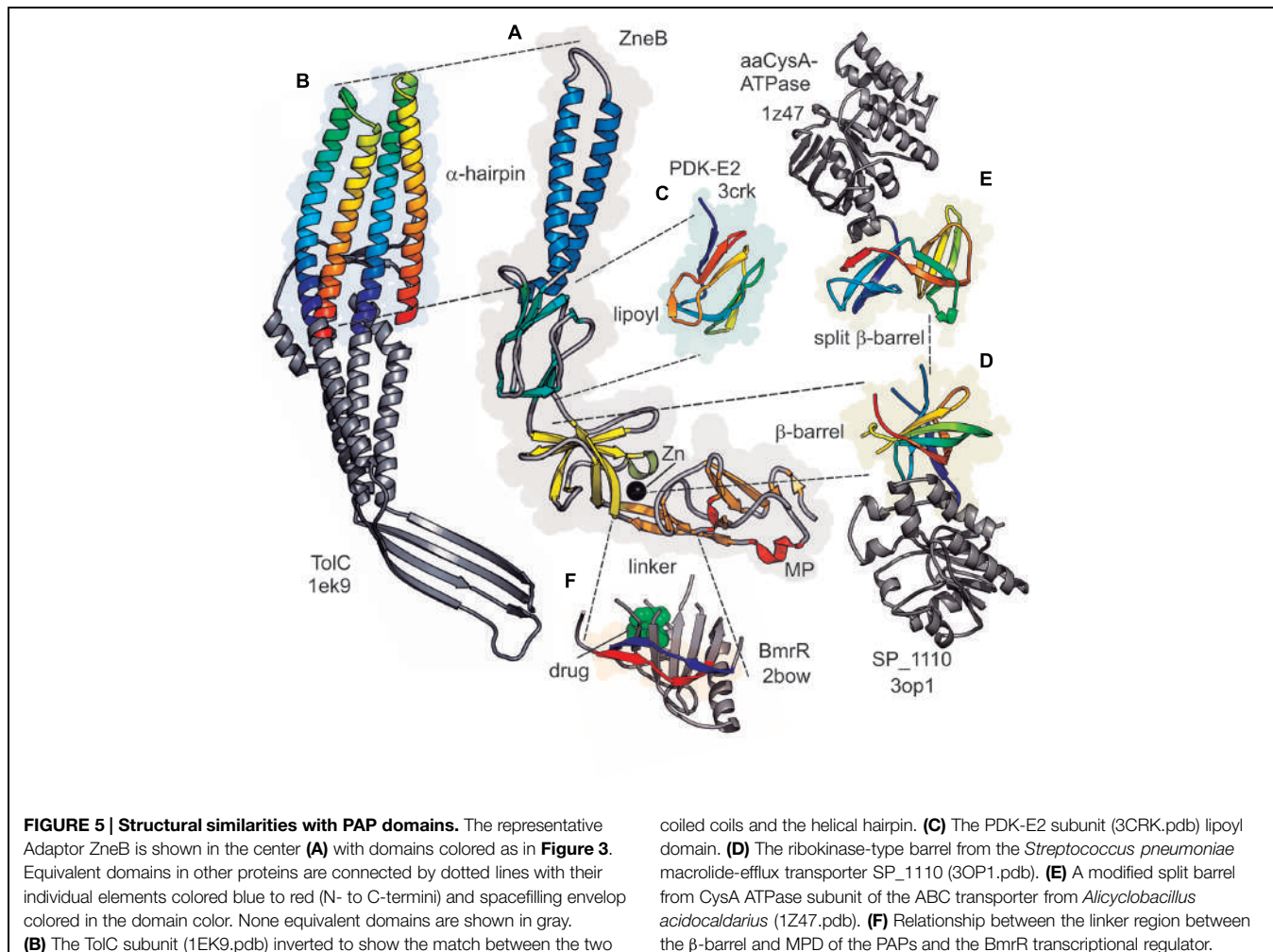


**FIGURE 4 | Topological organization of PAP domains.** Side-by-side comparison of typical adaptor domains compared as 3D schematics colored from N- to C-terminal together with highly simplified topological diagrams in the same colors. **(A)** MexA β-barrel domain. **(B)** MexA MP domain. **(C)** Viral Fusion Glycoprotein DI domain (from 2B9B.pdb). **(D)** SIlB C-terminal domain.

a similar pathway outward and back through each domain. The backbone of the α-helical hairpin domain from PAPs can be superimposed on both coiled-coils of TolC (Figure 5B) when inverted and viewed in an equivalent orientation. Furthermore,

the α-helical hairpin extension domain of adaptors such as EmrA (Figure 3) and MacA is highly similar to the untwisted pairs of α-helices in the TolC α-barrel. Indeed MacA and related PAPs are observed to form a barrel-like hexameric assembly that



superimposes very well on the complete lower part of the TolC trimer.

The lipoyl domain of PAPs was named owing to its sequence homology to the section of dehydrogenase enzymes (Johnson and Church, 1999). This homology was confirmed by the structure of MexA and subsequent adaptors showing that this region of the PAPs is topologically equivalent to those in lipoyl domains of dehydrogenases. This is clear when they are presented side-by-side in matching orientations, e.g., alongside the pyruvate dehydrogenase kinase (**Figure 5C**).

The β-barrel domain, adjacent to the lipoyl in the PAP structure, shares the topology of a barrel in ribokinase enzymes and lipid-binding proteins (Higgins et al., 2004b). It is intriguing that in one case such ribokinase-like barrel domain is also associated with a macrolide efflux protein of a Gram-positive organism – SP\_1110 from *Streptococcus pneumoniae* (pdb structure 3OP1, compared with the adaptor in **Figure 5D**). A splitting of this barrel is observed in the cytoplasmic regulatory domain of another structurally characterized ABC transporter system – namely the sulfate transporter from *Alicyclobacillus acidocaldarius* CysA (**Figure 5E**). There, a partial duplication and rearrangement of the barrel strands in the CysA subunit may be

recapitulating the changes in adaptor domain from a barrel to an MPD (Scheffel et al., 2005, 1Z47.pdb, **Figure 5E**).

These ribokinase-like domains are present in ABC-ATPases of the CUT1 and MOI subfamilies (Diederichs et al., 2000), which have been suggested to be involved in regulatory processes. Furthermore there is some evidence that these domains may play a role in signal transduction (Scheffel et al., 2005). Sequence alignments indicate (data not shown) that there is a high probability of a similar fold existing in MacB-type ATPases. While the evolutionary connection between these ABC-transporter associated domains and the β-barrel domain in PAPs remain to be fully established, the structural match is rather striking and would be consistent with the modular re-use of structures in these systems.

It is notable, that ribokinase-like domains reappear in some flagellar basal body assembly proteins (see Supplementary Figure S1). The C-domain of the flagellar protein FlgT from *Vibrio* (3W1E.pdb; Terashima et al., 2013), the role of which is not completely clear, but which has a remarkable structural connection to the N-terminal domain of the β-subunit of F1-ATPase, the catalytic subunit of the ATP synthase complex. Despite lacking a discernible sequence homology, the FlgT

exhibits the same topology as the PAP  $\beta$ -barrel domains and is comprised of six  $\beta$ -strands forming a barrel, topped with a helix (see Supplementary Figure S1A). Interestingly, FlgA, a different flagellar P-ring associated protein, displays a topologically different, but structurally equivalent domain (3TEE.pdb; Supplementary Figure S1B), which, however, lacks a full complement of  $\beta$ -strands, leaving it incomplete.

Another example of possible structural re-use is provided by the extended linker between the barrel domain and the MPD, in those PAPs which have the latter feature. This linker, although an apparently simple arrangement of two antiparallel  $\beta$ -strands, provides conformational adaptability to allow the flexible arrangement of the barrel and MPD relative to each other. This has been suggested to help maintain association with the inner membrane transporter domains during pumping activity (Symmons et al., 2009). Intriguingly, however, a very similar extended linker connects the two halves of the intracellular regulatory domain from the transcriptional repressor protein BmrR in *Bacillus* (Figure 5F, 2BOW.pdb, Zheleznova et al., 1999). The BmrR repressor regulates the expression of a drug efflux system (Kumar et al., 2013), and the domain containing the ‘linker’ element is implicated in drug sensing (bound drug shown as spacefilling atoms, Figure 5F). It may therefore be possible that the linker element may have been reused during evolution of the regulatory system.

One final overall structural similarity which is difficult to ignore, is between the overall architecture of PAP assemblies and the packing of the domains of flagellin to give flagella assemblies (Yonekura et al., 2003). Although the detailed topology and connectivity differs from that of PAPs (Figure 2), the overall arrangement of a central paired helices surrounded by small  $\beta$ -stranded domains is similar. In the case of flagellin the polypeptide also passes as a hairpin through the domains – but in contrast to adaptors it starts and ends in the helical section. Thus it may hint at a deep evolutionary relationship between drug efflux assemblies and flagella together with type III secretion structures.

## Models of Full-Pump Assembly and the Respective Role of PAPs in them

While structures of isolated components of the tripartite pumps are available for a number of different species and transporter types, the actual mode of association remains an area of active debate. The RND transporter family was the first group of transporters associated with tripartite pumps for which structures became available, influencing early models of assembly. RND pumps are specific for toxic substrates and largely belong to one of two families: the HME family and the multidrug hydrophobe/amphiphile efflux-1 (HAE1) family, both of which have unique PAPs.

RND HAE1 transporters are trimeric assemblies, with each protomer consisting of a transmembrane domain containing 12 transmembrane  $\alpha$ -helices and characteristic two large hydrophilic loops that comprise the substrate-binding porter (or pore) domain and the OMF-coupling docking domain

(Murakami et al., 2002). The HME pumps have a very similar trimeric assembly (Long et al., 2010), while the general protomer architecture is also shared with SecDF family as well as with the mycobacterial MmpL family of transporters (Tsukazaki et al., 2011; Varela et al., 2012).

## Deep Interpenetration Models

As soon as the AcrB structure became available it was speculated that TolC and AcrB might come into direct contact (Murakami et al., 2002), based on the apparent spatial compatibility of their apex regions. When the first OprM structures became available this idea was further reinforced by Akama et al. (2004), who pointed out the complementarity of the hydrophobic residues present in RND transporters and OMFs. Such direct interaction has been unequivocally demonstrated by *in vivo* crosslinking by Tamura et al. (2005). As mentioned before, the initial idea of PAP function ascribed them membrane-fusion protein like qualities, and suggested that they literally bring the two membranes together (Dinh et al., 1994). In prescient analysis, Johnson and Church (1999) dismissed the fusion protein connection, and suggested for the first time not only the organization of tandem repeats of the TolC-family, but also the potential for the formation of helical bundles between the OMPs and adaptor proteins to stabilize the complete assembly.

Taking into account the then-available MexA structures and this suggestion, Akama et al. (2004), Fernandez-Recio et al. (2004), and Higgins et al. (2004a) proposed the first fully assembled models of the tripartite pump. These models all featured deep interpenetration between the helical hairpin of the PAP and the coiled-coil domain of OMF, but differed wildly in terms of stoichiometry, presenting respectively 3:9:3, 3:6:3, and 3:3:3 options, although Akama et al. (2004) even suggested that up to 12 PAP protomers could be accommodated.

The 3:3:3 model of Fernandez-Recio et al. (2004), featuring a direct interaction between the RND transporter and TolC, has become one of the most popular models of pump assembly and provided the foundation for a number of other models (e.g., Symmons et al., 2009) sharing the same lateral inter-helical bundling between the PAP and OMF, collectively referred to here as “deep-interpenetration” models. These models (for example the AcrAB-TolC model of Figure 5A) are supported by direct evidence from cross-linking studies and a number of gain-of-function analyses, which will be discussed in detail below.

The debate on the stoichiometry of the pumps is still not fully settled. However, following the description of MacA hexameric organization in isolation (Yum et al., 2009); the CusBA crystal structure solution demonstrating a trimer of dimers of CusB (Su et al., 2011); and the direct crosslinking of the PAP hairpins to both grooves of the OMF (Janganan et al., 2011a), the 3:6:3 models have come to dominate the field. Furthermore, the existence of fused dimeric PAPs such as DSY0927 from *Desulfobacterium hafniense* (Zgurskaya et al., 2009); existence of MDR pumps with multiple PAPs such as TriABC (Mima et al., 2007) as well as functional complementation using fused dimeric AcrA constructs (Xu et al., 2011a) strongly support the idea of a trimer of PAP dimers as the most likely functional assembly.

## Tip to Tip Models of Assembly

Higgins et al. (2004a) were the first to propose lack of direct interaction between the RND transporter and TolC, still maintaining a deep interpenetration model. This idea had a dramatic makeover with the determination of the MacA structure, which was used for a radically new model of interaction (Yum et al., 2009).

The crystal structure of MacA shows the same general configuration as other PAPs at the level of the monomer (Yum et al., 2009). However, due to crystal packing it forms a hexameric tube-like structure, which the authors proposed to be the functional quaternary structure and to be maintained through interactions between the  $\beta$ -barrel domains. As the tube formed from the hairpins was approximately the same diameter as the  $\alpha$ -barrel of TolC, they hypothesized that the  $\alpha$ -barrels of these oligomeric assemblies may sit one atop the other to form a continuous channel. Following the structure being solved, a new conserved motif was identified at the tip region of the PAP hairpin – the ‘RLS motif’ – which was proposed to be common and essential (Xu et al., 2010). This RLS motif has been studied in various PAPs, with most of the mutations affecting it reported to abolish function and binding of PAP to OMF (Kim et al., 2010; Xu et al., 2010, 2011b; Lee et al., 2012; Song et al., 2014).

The next important advance came when the structure of CusB in isolation and as part of the CusBA complex were resolved in quick succession (Su et al., 2009, 2011), revealing for the first time a binary PAP-RND transporter complex, which presented a 2:1 PAP:transporter stoichiometry. Despite the marked difference of its hairpin domains from those of canonical adaptors, CusB was found to form a ring atop the CusA transporter, with an aperture too narrow to accommodate its cognate OMF CusC, which is structurally very similar to TolC. Extrapolating the structure of a complex of multidrug RND transporter (such as AcrB or MexB) with its associated PAP that has a prominent  $\alpha$ -helical domain from that of the CusBA complex reinforced the idea that in such RND-based pumps the OMF does not contact the transporter and may interact with the PAPs in a tip-to-tip fashion. However, while CusB forms a hexameric ring atop CusA, the helices of CusB-hairpins appear to be folded away from the CusC OMF (Su et al., 2011).

Crystallographic pursuit of the structure of the complete tripartite complex has been complicated by the transient nature of the inter-component interactions making the isolation of sufficient quantities of monodisperse complexes suitable for crystallographic studies problematic. Thus most of the recent efforts to reconstitute the full complex for structural studies have focused on single particle reconstructions, which required engineering of the components of the complex for increased stability. This approach achieved a major breakthrough by visualizing a complete assembly for the first time, based on cryo-electron microscopy reconstruction, which appears to support a model resembling the prototypical tip-to-tip yet also displaying some limited interpenetration between the tip regions of the PAPs to OMF (Du et al., 2014; **Figure 6**). At the same time, a negative stain EM reconstruction claimed that a canonical tip-to-tip interaction may take place (Kim et al., 2015).

## Functional and Biophysical Evidence Supporting Different Modes of Assembly

While providing crucial new insights, the recent EM studies used heavily engineered chimeric protein assemblies shown to have only limited functional activity (Du et al., 2014). An earlier EM-tomography study using non-modified MexA–MexB proteins reconstituted into membranes was unable to distinguish between tip-to-tip and deep-interpenetration models (Trépout et al., 2010). These observations call into question whether the conformations being stabilized in these assemblies represent a functional state of the activated pump or perhaps an inactive intermediate. While the question of the architecture of the functional assembly awaits its final solution we systematize the available evidence in the context of each of the models, focusing on the OMF-PAP interaction.

The two different models of OMF-PAP interaction predict dramatically different binding interfaces. In the deep-interpenetration model there are large helical bundling interfaces. This creates two degenerate interfaces, which closely resemble each other, but are not identical. In some systems, such as triclosan pump TricABC-OpmH, each of the grooves is occupied by separate PAPs (Mima et al., 2007), but in the majority of cases a single PAP seals the assembly. This introduces a requirement for some sequence-tolerance of the side of the PAP hairpin, which has to bind two slightly different grooves on the OMF. At the same time, the extended nature of the interface would be more tolerant to single substitutions and some level of promiscuity is expected between related protein pairs. Indeed, a number of studies have reported that the non-cognate OMFs and PAPs assemble, although not always into functional complexes (Bokma et al., 2006; Stegmeier et al., 2006; Vediappan et al., 2006; Krishnamoorthy et al., 2008; Yoshihara et al., 2009). The hypothesis that the hairpin of the PAP requires a specific interaction with some residues on the surface of the OMF to unlock the “gates” logically expects a limited number of “discriminator” residues to be present to allow differentiation between productive and non-productive complexes (Bavro et al., 2008). Such interpretation is consistent with the study by Stegmeier et al. (2006), which demonstrated a clear separation between interaction and functionality, as WT AcrA could be cross-linked to both TolC and OprM via the DSP reagent, which has a 12 Å spacer arm, but could only confer drug resistance when used with TolC. Similarly, Bokma et al. (2006) also distinguished functional activity from association, as MexA and TolC could be cross-linked whilst being unable to form a functional complex.

While the non-cognate hairpins of the PAPs may not function *ad hoc* due to incompatibility with these residues, one can also expect that the incompatibility in such a scenario could be overcome by adaptation of the interface, e.g., via mutation of these key discriminator residues (Bokma et al., 2006; Vediappan et al., 2006). To the contrary, the very limited interface of the tip-to-tip models should be much more sensitive to single substitutions specifically at the tip regions of the PAP and the OMF, and as these are expected to be the only determinants of specificity as well as binding affinity, the compensatory mutations would be expected to also map to the same region.

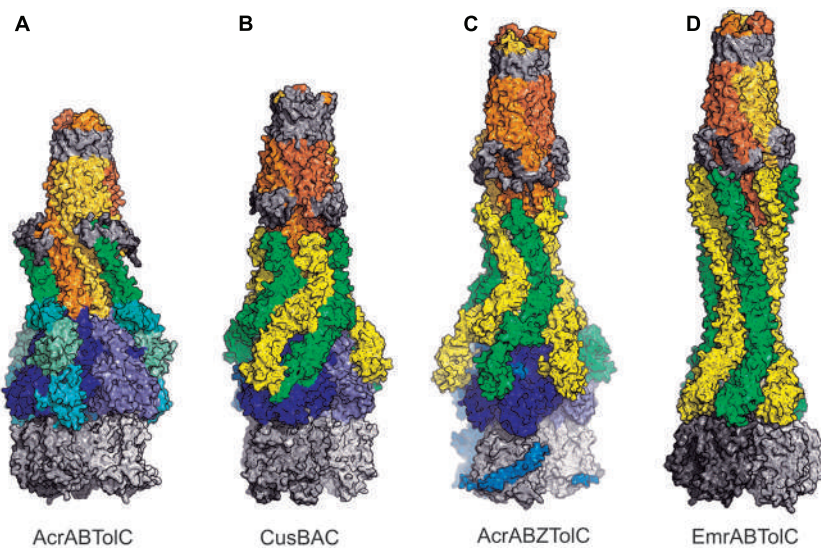


**FIGURE 6 | Assembled models of pumps.** OMF subunits are shown as gold or orange shades except for the beta-barrel in the outer membrane and the equatorial domain, which are in gray. AcrB and CusA trimeric RND transporters are blue for its periplasmic domains, gray for its membrane domains. EmrA MFS transporter is in gray (a dimer is shown for size comparison). Adaptors are in shades of green or yellow around the OMF. **(A)** AcrABToIC model based on site specific cross-linking data (Symmons et al., 2009). Domains of the AcrB are distinguished by green shades. **(B)** CusBAC model based on the docking in Su et al. (2011).

This is based on the maximum interpenetration without alteration in the CusB hairpin domains. Closer approach of the CusC and CusA is possible after re-alignment of the adaptor tips. **(C)** AcrABZToIC model based on fitting to single-particle CryoEM envelope (Du et al., 2014). The AcrZ subunit, to which one copy of AcrA was fused, is shown in light-blue. **(D)** EmrABToIC model suggested by the structure of Hinchliffe et al. (2014) and constructed by docking six EmrA subunits based on the arrangement of helices in the ToIC trimer (**Figure 5B**). Further interpenetration would be possible after re-alignment of the adaptor tips.

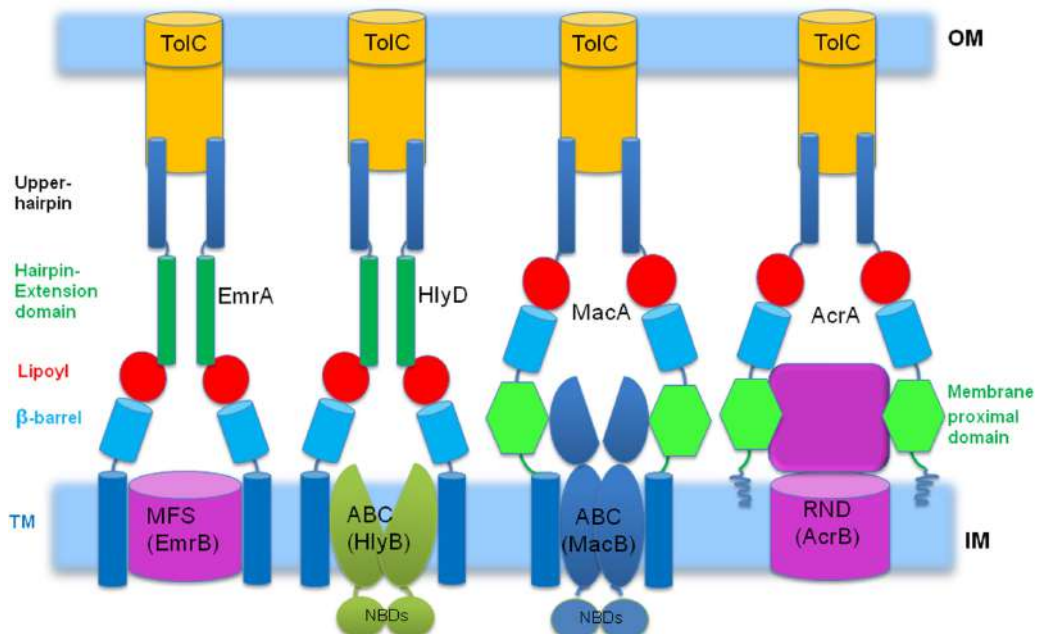


**FIGURE 7 | Schematic representation of the proposed pattern of pairing between PAPs and specific transporters, highlighting domains involved.**

We propose that the type of the transporter is strongly linked to the particular architecture of the PAP. This emerging logic allows predicting the type of the transporter based purely on the architecture of the PAP, e.g., membrane proximal domains are only found in PAPs that work with transporters with

prominent periplasmic domains, suggesting a role in substrate presentation (see main text for details). In contrast, PAPs which pair with transporters with cytoplasmic cargo access require TM (transmembrane) domains to communicate with the transporter as well as hairpin-extension domains to ensure safe conduit for their cargoes through the periplasm. NBD, nucleotide binding domains.

## Evidence from Cross-Reactivity

The concept of simultaneously maintaining both specificity and promiscuity may be thought of as a suited key system, in which the locks are analogous to OMFs and keys analogous to PAPs, whereby locks and keys can be suited to different security levels. Using the same analogy, a functional key fits, turns and unlocks the gate, while a number of similarly shaped keys would only fit the keyhole [e.g., the examples provided by Stegmeier et al. (2006) and Bokma et al. (2006)].

A good illustration for the concept is provided by the existence, within a single species, of PAPs that have multiple cognate OMFs, such as MdsA of *Salmonella*, which can use both MdsC and TolC (Horiyama et al., 2010; Song et al., 2014). In such an analogy MdsA is a more universal key than AcrA, opening more locks; MdsC here would appear to be a more secure lock than TolC, being opened only by one key rather than by many. This can easily be explained using the idea of extended interfaces with discriminator residues. Here, TolC and MdsC would have some discriminator(s) in common; however, the MdsC would have extra, which can only be recognized by MdsA.

The keys analogy would also predict that in some cases there is an odd chance that an OMF may function with a non-cognate PAP from a different species. An example of this is VceAB of *Vibrio*, which pairs with TolC in AcrAB-deficient *E. coli* (Vediyappan et al., 2006). As the reverse is not true (AcrAB cannot function with VceC), VceC could be likened to MdsC, as possessing a higher level of security than TolC, likely due to an extra set of discriminator residues.

A clear demonstration of the importance of the hairpin for the selection of partners can be obtained from domain swap experiments. If a PAP hairpin contains the entire lock-fitting features of a key, then hairpin swapping would change the OMF-binding profile of one PAP to that of another. A study by Stegmeier et al. (2006), which analyzed MexA hairpins grafted onto AcrA, demonstrated that such chimeras can cause gain of function with a non-cognate OMF, but do not necessarily cause loss of function with the cognate OMF. In the case of a stringent fit, one may expect that MexA should also be capable of at least partially functioning with TolC, as AcrA(MexA-hairpin) can. It is therefore surprising that MexAB cannot function with TolC unless directed evolution is used (Bokma et al., 2006), hinting that additional levels of compatibility checks may be in place.

## Evidence from Adaptive Mutagenesis

Since non-cognate PAPs present imperfect keys, directed evolution could help identify discriminator residues. However, the distribution of these gain-of-function mutants would be expected to be markedly different under the different models of assembly. In the report from Bokma et al. (2006), several mutations required to adapt TolC to MexAB occurred in the  $\beta$ -barrel and are difficult to visualize as interacting with any other component of the efflux machinery in either model. However, the study also found a number of mutations in the  $\alpha$ -helical regions of the OMF both at the tip and high up the coiled-coil domain, consistent with deep interpenetration. An alternative explanation for the gain-of-function may be that the mutations cause the channel to become leaky, such that they do not require

opening by the PAP. Similarly, gain of function mutations in VceC allowing it to function with AcrAB are spread around the lower portion of the  $\alpha$ -barrel (Vediyappan et al., 2006), but are not confined to the tip. One (V445E) affects the hydrophobic gate of VceC in the equivalent position to D374 in TolC (Koronakis et al., 2000; Federici et al., 2005), and would likely introduce a similar acidic-residue ring. The existence of compensatory mutations far away from the tip region is difficult to reconcile with the tip-to-tip models, as the functional interaction, and hence its loss, is supposed to be restricted to the limited tip region. Hence, a gain of function would be expected to arise at the same interface. In stark contrast the majority of the Vediyappan et al. (2006) mutations map to the inside of the channel, ruling out their role in direct engagement with the PAP.

## Evidence from Compensatory Mutations

Similar to directed evolution of non-cognate OMF-PAP pairs, the mapping and characterization of the gain of function mutations that compensate defects on either of the components of the pump complex provide powerful tools for studying the mode of their interaction. Weeks et al. (2010) reported on the effects of extensive mutagenesis of the periplasmic turn connecting the first two helices of the TolC channel, which, in the strict tip-to-tip models of interaction comprises almost half of the expected docking site for the PAP. Due to the very limited size of the tip, one might expect the mutagenesis to cause severe disruption of the interaction, however, this isn't the case. Even when the signature sequence GLVA was substituted to a poly-Ala the OMF retained wild-type functionality, and only mutation of all four positions to AGSG caused loss of function. This insensitivity implies either extensive structural redundancy or potentially a different mode of interaction between the OMF and the PAP taking place. That conclusion is further reinforced by the isolation of AcrA suppressors of the AGSG, which were shown to dilate the TolC aperture in an AcrB-dependent manner. Furthermore, this did not require energy input from AcrB, as the induction of leakiness was also present in AcrB D407 mutant, lacking functional proton coupling (Weeks et al., 2010). Interestingly, out of the six compensatory mutations isolated, only a single one, T111P, was located at the hairpin.

The location of multiple compensatory PAP mutations at the level of the RND-transporter suggests that the rescue of efflux function may occur via stabilization of the PAP-transporter interaction, leading to extended lifetime of the efflux complex. This is consistent with the observation that AcrA-recruitment of proteinase sensitive TolC mutant P246R/S350C into complexes protects it from degradation (Gerken and Misra, 2004; Weeks et al., 2014). Similar observations have been made by Nehme and Poole (2007), who reported that RND transporter mutation (MexB G220S), which caused a loss of transporter-PAP association and resulted in drug sensitivity, was compensated by mutations in the  $\alpha$ -barrel of the OMF promoting increased stability of OMF-PAP association. Mutation at the tip of MexA  $\alpha$ -hairpin (V129M) compromised the *in vivo* interaction with OprM resulting in drug hypersensitivity, which may hint at a tip-to-tip interaction. However, that

phenotype was restored by the T198I and F439I substitutions 5 helical turns up the  $\alpha$ -barrel of OprM, consistent with the hairpin domain mediating MexA binding to this region of OprM in a lateral fashion (Nehme and Poole, 2007). Furthermore, the association between the mutant MexA and OprM was not affected, indicating that impacted gating, rather than disrupted complex formation, caused the observed efflux defects.

### Cross-Linking Data

Usage of heterobifunctional cross-linkers with different spacer lengths achieved *in vivo* cross-linking of PAPs to OMFs (Lobedanz et al., 2007). In these studies, cysteine residues introduced along the entire length of the N-terminal helix of the AcrA hairpin could crosslink to TolC, when using a 6.8 Å linker arm. This suggests that the residue eight helical turns from the PAP tip must lie less than 7 Å from TolC. The residue one helical turn further from the tip could only be cross-linked to TolC with the longer (15.6 Å) linker arm. These results suggest a deep interpenetration of at least six helical turns. Introduction of a cysteine in TolC, six helical turns from the helical tip, could also be cross-linked to AcrA via the short-spacer linker. At the same time a TolC D121C mutation, seven helical turns from the tip, could not be cross-linked with either linker. Given that a D121N mutation was identified as an adapting mutation that enables TolC to function with MexAB (Bokma et al., 2006), a charged residue may be involved in maintaining the PAP association.

### Evidence from Direct-Residue Interactions

Interpretation of the data generated by heterobifunctional cross-linking is complicated by the uncertainty introduced by the length of the spacers and the involvement of large side-chains, e.g., Lys and Arg. It is more difficult to refute results from direct spontaneous Cys–Cys cross-linking and functional complementation. One example of a direct interaction between the OMF and the PAP was described by Bavro et al. (2008) in the case of the K383 (TolC)-D149 (AcrA) functional pair. Mutation of each of the residues in isolation caused hypersensitivity to the AcrB substrate novobiocin, presumably due to abolition of the OMF-PAP association. The functional activity could be restored when the reciprocal mutations were introduced into the respective proteins, suggesting a direct interaction between the two. Mutation of the equivalent residue to K383 in the Neisserial ortholog MtrE (E434) similarly causes hypersensitivity to substrate drugs, but also makes the cells sensitive to the influx-dependent vancomycin, indicating that the mutation causes the OMF channel to become leaky (Janganan et al., 2011b). Importantly, vancomycin hypersensitivity was only observed when the OMF was co-expressed with the PAP, suggesting that their interaction is required to provoke channel opening (Janganan et al., 2011a, 2013).

Several other MtrE mutations affecting efflux have been identified, all of which map to the surface of its  $\alpha$ -barrel, up to eight helical turns from its periplasmic tip-region. The loss of efflux function was not related to the failure of association, as binary OMF-PAP complex formation was not affected, as demonstrated by isothermal calorimetry (ITC) and pull-down

assays (Janganan et al., 2011b). Furthermore, introduction of MtrC E149C and MtrE K390C resulted in formation of intermolecular Cys–Cys bridging *in vivo*, locking the OMF channel in an open conformation thus causing increased vancomycin sensitivity (Janganan et al., 2011a).

These results, combined with the similar cross-linking studies of AcrAB (Symmons et al., 2009), served as the principle source of the refined deep-interpenetration model of pump assembly.

### Evidence from Structural Biology Studies

Unlike the deep-interpenetration model, which was primarily derived from *in vivo* functional and cross-linking assays, the main support for the tip-to-tip model came from *in vitro* structural studies of isolated components. While CusBA crystallographic complex is sometimes considered as supportive of tip-to-tip assembly due to the narrow aperture of the ring of the PAPs which may imply that there is no direct contact between the transporter and the OMF, the organization of the CusB hexamer is rather different from that in the MacA structure (Yum et al., 2009; Su et al., 2011, 2012). It is in fact a trimer of dimers, and the hairpins of the PAP in the case of CusB are pointing away from the center, without participating in tubular formation. Also, the very size of the CusB hairpin dictates a necessary adjustment of the OMF-interaction distance for a productive complex to form in a tip-to-tip model as evidenced on **Figure 6**.

Apart from the crystal structures of MacA and CusBA, the majority of these studies included different degrees of usage of chimeric proteins. Chimeric constructs of *Actinobacillus actinomycetemcomitans* (Aa) MacA on which the tip region was replaced by the tip regions of the TolC  $\alpha$ -barrel have been analyzed for structural formation with wild-type *E. coli* MacA by electron microscopy, and showed dumbbell-shaped structures with a central bulge (Xu et al., 2011b). Similar studies, replacing the hairpin tip of *E. coli* MacA with that of MexA or AcrA and the hairpin tip of AaMacA with the tip regions of the OprM or TolC  $\alpha$ -barrel showed the same bulged dumbbell-shaped structures (Xu et al., 2011a, 2012). In all of these studies the bulges in the structures were modeled as an intermeshing of the tip regions of the two proteins, with the OMF aperture fully opened. The MexA-OprM docking model suggested possible interacting positions, with the RLS motif formed of R119, L123 and S130 of the MexA proposed to interact with the OprM backbone carbonyl groups, V201/V408, and S138 of OprM, respectively, with additional hydrophobic support from MexA L122 with OprM V199/T406 (Xu et al., 2012).

The recent electron microscopy studies of complete assemblies have provided the most compelling support for the tip-to-tip interactions to date (Du et al., 2014; Kim et al., 2015; **Figure 6**). It is notable that the two models derived from these EM-reconstructions differ slightly on the level of OMF-PAP interaction. While Kim et al. (2015) have put forward an orthodox tip-to-tip interaction, where only the RLS motif and the turns of the TolC channel seem to interact, the envelope provided by Du et al. (2014) appears to allow for at least partial interpenetration of the OMF and the PAP. Thus this latter model might be able to rationalize at least some of the evidence presented above, and is compatible with the direct disruption of secondary gates by the

PAP. However, in common with earlier such models it rules out a direct interaction with the RND-class transporters (Du et al., 2014).

### Evidence from *In Vitro* Binary Interactions between Components

Apart from EM studies, some support for the tip-to-tip interactions comes from recent SPR studies of the *Anabaena* DevBCA ABC-transporter system, the PAP in which is DevB, was reported to require the tip-regions of TolC for binding (Staron et al., 2014). However, surface plasmon resonance (SPR) studies of a number of PAPs as well as TolC, have detected direct interaction of the OMF with the RND transporters which possess large periplasmic domains, independently of the PAP (Tikhonova et al., 2011). The binding is enhanced by low pH, dependent on lipidation and reported to be of nanomolar affinity. Mutations affecting the aperture of the TolC channel by disruption of the primary gates resulted in decreased binding to AcrB and AcrA, implying that the tip regions were indeed specifically engaging under the test conditions (Tikhonova et al., 2011).

Isothermal calorimetry measurements of binding of the PAP MtrC and OMF MtrE showed that the PAP hairpins in isolation bind the MtrE channel with around fivefold higher affinity than the full-length MtrC. This could be increased to 100-fold (13 mM) when a leaky E434K OMF mutant is used as a partner (Janganan et al., 2011b).

### Evidence from RLS Conservation and Diversity of the PAP Hairpins

Although the proposed RLS motif seems to be widely conserved between different pump systems (Kim et al., 2010; Xu et al., 2010), this conservation is not absolute, and deviation from the canonical sequence has been reported, e.g., in the HlyD family of PAPs (Lee et al., 2012). Some other TolC-binding PAPs in *E. coli* do not seem to possess identifiable RLS sequence altogether – e.g., CvaA (Hwang et al., 1997), suggesting that an alternative interaction can take place at least in some instances. The EM analysis of chimeric constructs, implies that at least part of the interaction is backbone mediated (Xu et al., 2011a, 2012), which seemingly contradicts the strict requirement for RLS conservation.

Perhaps the biggest challenge for the tip-to-tip model is the existence of efflux assemblies lacking not just the RLS motif but the entire hairpin, such as the *Borrelia burgdorferi* BesA, which is associated with the RND transporter BesB (Bunikis et al., 2008; Greene et al., 2013). While such an assembly may still be reconciled with a deep-interpenetration model where the RND participates in direct binding with the OMP, it is fully incompatible with the current tip-to-tip models. Furthermore, consistent with the hypothesis that one of the main roles of the PAP hairpin domain is to unlock the secondary gates of the OMF, uniquely the TolC homologue BesC associated with this hairpin-less efflux system has a disrupted gate system.

### Evidence of Equatorial Domain Involvement

One of the adapted lines from Bokma et al. (2006) that contained two mutations in TolC that greatly increased its functionality

with MexA may have increased the propensity for cross-linking. This double mutation increased antibiotic resistance in an additive fashion compared to individual mutations, though one (V198D, in the equatorial domain) had a greater effect than the other (Q142R, at the tip region), suggesting a role for the equatorial domain in determining specificity. It was shortly after determination of the TolC structure (Koronakis et al., 2000), that evidence first arose suggesting the equatorial domain may be involved in OMF function (Yamanaka et al., 2001, 2002). These equatorial domain mutations affected function without affecting stability or folding of TolC, as shown by cross-linking and immunoblotting. Evidence for the significance of the equatorial domain has also been found in the OMF AatA, where positions F381, L382 and L383 have been shown as essential for Aap secretion (Iwashita et al., 2006). These positions mapped to the equatorial domain as based on the homology model of AatA (Nishi et al., 2003). It is also notable that, pairing with a PAP lacking a hairpin domain altogether, BesC not only lacks primary gates but the C-terminal domain is also truncated (Bunikis et al., 2008; Greene et al., 2013). The significance of the equatorial domain has also been shown in the OMF OprM, in which C-terminal truncation impairs the ability of OprM and VceAB to form a functional complex (Bai et al., 2010, 2014).

### Evidence from TolC-AcrB Direct Interactions

As both AcrB and TolC protrude into the periplasm from the inner and outer membrane respectively, Murakami et al. (2002) suggested that they directly dock with each other at their periplasmic tips, which have remarkably similar spatial-dimensions and structural complementarity. The suggested TolC-docking site of AcrB covers part of the “TolC-docking domain,” and features two  $\beta$ -hairpin extensions, while TolC contributes two homologous helical turns. This idea was reinforced by direct *in vivo* Cys–Cys cross-linking of the periplasmic turns of the TolC with these  $\beta$ -hairpins (Tamura et al., 2005), even in the absence of AcrA. Consistent with Tamura’s findings, AcrA-AcrB association was found to be independent of the AcrB  $\beta$ -hairpins, however, TolC is lost from the complex when the  $\beta$ -hairpins of the tip of the periplasmic domain of AcrB are deleted (Weeks et al., 2014). Similar to Tamura, earlier reports using cross-linking via DSP showed that the AcrB-TolC proximity was independent of AcrA, although the authors did not detect a direct AcrB-TolC interaction when using isothermal titration calorimetry (Touzé et al., 2004).

### Additional Lines of Evidence

The demonstration that tandem fusions of AcrA provide functional complementation to AcrA deletion, suggesting that PAP dimers may be the functional units for complex assembly is often taken as supporting the tip-to-tip model (Xu et al., 2011a). However, it can equally be accommodated into deep-interpenetration models. The existence of the functional dimeric unit of the PAP has been confirmed by SPR (Tikhonova et al., 2011).

The remaining evidence for how the complex assembles, while strongly favoring the deep-interpenetration model does not, however, disprove the tip-to-tip model entirely. It is still

plausible that this model may represent an intermediate step in binding, as initially suggested by the creators of the tip-to-tip model (Yum et al., 2009).

## Functional Roles of PAPs Beyond Structural Assembly

### Energy Independence of Assembly

Effective efflux is dependent on energy provision by the transporters, and could be abrogated by proton gradient decouplers such as CCCP (carbonyl cyanide 3-chlorophenylhydrazone) and/or non-hydrolysable ATP-analogs. Given this, it has been anticipated that energy is also required for the formation of the complex, and likely conformational changes in the transporter are relayed to the OMF channel, *via* the PAP, causing its opening. However, several studies have provided evidence that this may not be the case. Several binary interaction studies in the absence of active energy sources have been able to demonstrate successful PAP-OMF association *in vitro*, including EM-studies of reconstituted complexes (Trépout et al., 2010), ITC (Janganan et al., 2011b), and SPR (Tikhonova et al., 2011; Lu and Zgurskaya, 2013). Some early studies on the Type I secretion system HlyBCD have suggested that the assembly of the complex is nucleotide-independent, while the secretion of the HlyA cargo required HlyB-mediated ATP hydrolysis (Thanabalu et al., 1998).

Crucial evidence came from studying the RND MtrCDE system in *Neisseria*, where the opening of the OMF channel was demonstrated to be dependent on the functional interaction with the PAP (Janganan et al., 2013). This interaction was found to cause the E434K mutant of the MtrE to become vancomycin sensitive, but only when co-expressed with full-length cognate PAP. This interaction was transporter independent, and did not require energy. Furthermore, when a transporter mutant lacking a functional proton-relay was introduced the vancomycin sensitivity was greatly diminished, while the sensitivity to drugs translocated by AcrB remained the same, suggesting that a full, but non-productive efflux complex is assembled, sequestering the otherwise leaky channels. Similar effects were reported for AcrAB-TolC by Weeks et al. (2010).

These results suggest that energy is required for the efflux and disassembly of the pump complex, but not for the association between its components. This provides rationale for future design of peptidomimetic drugs to target the assembly interface of efflux complexes at the level of PAP association. Similar approaches have been shown to be effective in targeting the LptD assembly of *Pseudomonas* (Srinivas et al., 2010).

### Active Participation of Adaptor Proteins in Transport Activity of the IMPs

The participation of the PAPs in transport activity may broadly be split into two major actions – namely affecting energy generation and transduction, and participation in cargo selection and presentation to the transporter. The active role of PAPs in regulating the transporter energy cycles was initially demonstrated for the ABC transporters. The PAP MacA has been shown to be critical for ATPase activity of MacB (Tikhonova et al.,

2007; Lin et al., 2009; Modali and Zgurskaya, 2011). Modali and Zgurskaya (2011) further narrowed down the region responsible for this activation to the MPD, and proposed that the MacA adaptor protein promotes the transporter MacB transition to a closed ATP-bound state, similar to the structurally unrelated periplasmic solute binding proteins, such as TroA (Deka et al., 1999).

The role of PAPs in activation of proton-motive force driven transporters is less well explored. This is mainly due to the difficulties in reconstituting active systems utilizing proton-motive force. However, it is emerging that PAPs play a significant role in stimulation of the efflux activity and consumption of the gradient as exemplified by the reconstitution of MexA-MexB into liposomes (Verchère et al., 2012). MexA dramatically increased the activity of MexB only when the substrate was also present, confirming and expanding the results of earlier AcrA-AcrB liposome reconstitution assays (Zgurskaya and Nikaido, 1999). These results invite the exciting speculation that one of the roles of PAPs could be to serve as checkpoints for successful drug loading into the transporter, to prevent unproductive cycling without cargo that may deplete the proton gradient.

In order to effectively fulfill such checkpoint function, the PAP may be expected to participate in cargo binding and selection, and there is mounting evidence from different systems to support such a hypothesis. One early report described substrate-induced conformational changes in the MFS-associated EmrA from Trp-fluorescence analysis (Borges-Walmsley et al., 2003).

### Heavy Metal Efflux

The heavy metal efflux (HME) pumps have been instrumental for establishing the active role of the PAPs in the transport process. De Angelis et al. (2010) demonstrated that the PAP ZneB of the ZneCAB heavy-metal efflux system from *Cupriavidus metallidurans* specifically binds Zn<sup>2+</sup> ions in the interface between the β-barrel and MPD domains. Binding is associated with a significant conformational change and on this basis it was suggested that the PAP may play an active role in the presentation of the substrate to the transporter ZneA. Similar action has since been confirmed in the Cu(I)/Ag(I) efflux pump CusCFBA which is composed of the OMF CusC, the RND-transporter CusA, metallochaperone CusF, and the PAP CusB. CusF and CusB have been shown by NMR spectroscopy to freely exchange Ag(I) and Cu(I) toward equilibrium in highly specific protein–protein interactions (Bagai et al., 2008; Mealman et al., 2011). Similar organization has been found in the PAP SilB from *Cupriavidus metallidurans* CH34 which has a C-terminal-extension domain homologous to CusF (Bersch et al., 2011).

Metal co-ordination appears to be accomplished by methionine clusters, in both the chaperones and the transporter (e.g., CusA) as identified by X-ray crystallography and NMR and by mass-spectrometry and X-ray absorption spectroscopy (Su et al., 2011; Mealman et al., 2012), creating an ion-transport relay. The latter study also demonstrated that the N-terminal 61 residues of CusB are sufficient to bind metal and provide partial metal resistance *in vivo*. It has also been shown that the N-terminal domain acquires the metal from

the metallochaperone (CusF) and is able to pass it on to the transporter (Mealman et al., 2012; Chacon et al., 2014). In that study, CusB was found to directly activate the CusA pump.

### RND Efflux Pumps

The involvement of the PAPs in the cargo selectivity in the RND multidrug efflux pumps is less studied, but some indication of their role could be found from studies of non-cognate PAP complementation. Change of the substrate profile brought by the PAP change was clearly demonstrated by the complementation analysis of AcrA interactions with MexB (Krishnamoorthy et al., 2008). In this system AcrA was able to provide near wild-type resistance to SDS, and partial to novobiocin and ethidium bromide, while nalidixic acid, lincomycin, and erythromycin proved highly toxic, suggesting that the change of PAP resulted in a shift of substrate specificity of the pump.

### Interactions within the Membrane

As mentioned previously, some adaptor proteins contain N-terminal membrane spanning domains, and these have been suggested to interact within the membrane with their cognate transporters (Tikhonova et al., 2007). This is likely the prime way of communication between transporters that lack any periplasmic protrusions and are fully submerged in the membrane, such as the canonical ABC transporters and MFS transporters. In HlyD, a  $\Delta$ -N45 construct lacking the N-terminal cytoplasmic helix failed to recruit TolC or activate the HlyB ATPase, suggesting that a transmembrane communication takes place (Balakrishnan et al., 2001).

### Importance of the C-Terminal Domain of the PAP

Elkins and Nikaido (2003) showed that the C-terminal part of the PAP plays a role in the recognition of the transporter. The region identified encompasses the majority of the MPD, consistent with that identified by Ge et al. (2009), showed that a single G363C substitution in the MPD dramatically impairs the multidrug efflux activity of AcrAB-TolC. The importance of the MPD has also been noted in the ABC-transporter associated MacA, where substitutions in the MPD affected LPS binding as well as general activity of the pump, including macrolide efflux (Lu and Zgurskaya, 2013). One interesting observation from earlier work (Tikhonova et al., 2002), showed that a small region of the RND transporter was crucial for binding with the PAP. Mapping this region to the available binary complex of CusBA (Su et al., 2011), shows that the equivalent sequence in the CusA overlaps with its docking site for the CusB MPD. Interestingly, the bound protomers of CusB display significant conformational discrepancy at their respective binding sites. The corresponding region would also be close to suggested drug-acquisition sites in AcrB (Pos, 2009). This raises the intriguing speculation that the MPDs may be actively sensing the state of the transporter, translating it into communicable conformational change.

It is notable, that MPDs appear exclusively in PAPs associated with RND- and ABC-transporters that feature prominent periplasmic domains. As these classes of transporters are also

known to acquire their efflux substrates from the periplasmic space or the outer leaflet of the cytoplasmic membrane, we propose that the role of the MPDs in these systems may be associated with active cargo presentation and regulation of energy-coupling of the transport cycling.

ATPase activation of the transporter and active involvement of the adaptor in cargo binding and presentation is not limited to transporters with large periplasmic domains. Direct binding of cargo to HlyD has been reported (Balakrishnan et al., 2001). Substrate binding was not dependent on the N-terminal helical domain, as HlyD was still able to associate with both substrate and TolC. However, the substrate transport was impaired, suggesting that this region may play an active role in assembly and stimulation of the ATPase activity of the HlyB transporter. The recruitment of TolC to preassembled HlyBD was promoted by cargo binding (Thanabalu et al., 1998; Benabdellah et al., 2003). Such recruitment may result from conformation changes in the PAP, as suggested from crystallographic and molecular dynamics studies (Mikolosko et al., 2006; Vaccaro et al., 2006; Wang et al., 2012), where the PAP hairpin flexes relative to other domains in a pH-dependent fashion (Ip et al., 2003), which may mimic *in vivo* functional binding to cargo and/or transporter. Furthermore, it has been reported that mutations in the PAP HlyD affected folding of the substrate (Pimenta et al., 2005). One such mutation maps within the hairpin domain, highlighting a role of hairpins in folding, perhaps by creation of a “foldase” cage, which may explain the presence of these domains in Gram-positive organisms.

### PAPs in Gram-Positive Organisms

The very existence of PAPs in Gram-positive organisms suggests that their roles must be much more diverse than just bridging between the transporter and OMF. Based on the same logic it may also be expected that the ones present would be lacking  $\alpha$ -hairpin domains. This has proven not to be the case, however, and genome analysis studies have revealed a number of PAPs are indeed present in Gram-positive organisms (Zgurskaya et al., 2009), contrary to the early expectations (Dinh et al., 1994).

While in some cases it is difficult to establish functionality of these genes, which may have been acquired via a lateral gene transfer and are dormant in the genome – e.g., in the case of *Enterococcus gallinarum* EGD-AAK12ERE46183.1 which shows up to 82% identity to the MFS-associated EmRA hairpin domain; there are a number of *bona fide* secretion systems in firmicutes that require PAPs for function. ABC associated PAPs similar to HlyD could be readily identified, e.g., MknX from *Bacillus*. Another wide spread system is the mesentericin Y105 secretion pump which is built around the MesD-type ABC transporter (Aucher et al., 2005). The gene encoding this transporter pairs with the *mesE* gene, which appears to encode a PAP resembling HlyD. Some examples include MesE from *Leuconostoc mesenteroides* (Q10419.1), PlnH from *Lactobacillus plantarum* (WP\_015379778.1); SppE from *Lactobacillus sakei* (CAA86947.1). The list could be expanded by

the related Streptococcal competence protein ComB, as well as the *Enterococcal* iron ABC transporter (WP\_025481776.1), and *Carnobacterium maltaromaticum* CbaC (AAF18149.1).

These PAPs possess extremely large hairpin domains, which is difficult to rationalize if the only function of the hairpin is OMF-transporter bridging. However, as mentioned above it may have a role in folding the nascent polypeptide chain of the cargo. Preservation of the large hairpins in PAPs such as MdtN in *Virgibacillus halodenitrificans* showing high similarity to the PAPs associated with MFS transporters [e.g., EmrX-MdtN-MdtP(OMF) in *E. coli*] is more difficult to explain and requires further studies.

A rather unusual case is presented by the *Bacillus subtilis* YknX (BSU14350), which seems to function with a multi-component ABC-transporter, YknZYW, involved in the resistance to antimicrobial killing factor SdPC (Yoshida et al., 2000; Yamada et al., 2012). This system contains a permease, YknZ, which binds to the transmembrane regulator YknW, while ATPase activity provided by a separately coded YknY powers the full assembly (Zgurskaya et al., 2015). All these permeases appear to belong to the FtsX family (Crawford et al., 2011), which also includes MacB and similarly some of them occur also as gene fusions with the AAA-ATPase (e.g., YknU BSU14320 and YknV BSU14330). It is worth reminding that the FtsX-like transporters (including MacB) seem to possess regulatory domains with the ribokinase-fold with striking similarity to the  $\beta$ -barrel domain of PAPs (see Figure 5). Adding to the similarity with MacAB, the PAP YknX also has a prominent  $\alpha$ -hairpin domain. Furthermore, it also contains, so far uniquely amongst the Gram-positive PAPs, a MPD. As we will demonstrate in the final chapter, the presence of certain domains can serve as a reliable diagnostic for the pairing of the PAP with its transporter.

## Transporter Type Determines the Domain Organization of the Associated PAPs

Our structural analysis of the available PAP-transporter pairs in combination with the examination of the available biochemical evidence, leads us to believe that there is a very clear pattern of structural matching of specific PAP domain combinations to certain transporter types, summarized in Figure 7.

This pairing is far from random and most likely underlies a functional connection between the domains in question. We have identified that MPDs occur without exception in PAPs paired with transporters possessing large periplasmic domains and which are suggested to load their cargo either exclusively or preferentially from the periplasm or the outer leaflet of the inner membrane, such as RND-transporters and MacB-family of ABC transporters. There are two likely explanations for this – one is that due to purely spatial requirements the MPDs are required as “spacers” to prevent displacement of the PAP by the large transporter, which would prevent the PAP from reaching from the inner membrane to the OMF. An alternative and, in light of the increasing amount of functional data, more likely explanation is that the MPDs

critically complement the cargo selection and presentation to the transporters.

Similarly, the requirement for effective sealing of the transport conduit in PAP-transporter combinations, such as MFS and ABC-transporters of the Type I Secretion System where the transporter lacks a pronounced periplasmic domain, necessitates an introduction of the recognizable “hairpin extension” subdomain (Hinchliffe et al., 2014). The predicted rigidity of these  $\alpha$ -tubular conduits also makes it difficult to imagine major conformational changes being easily communicated through to the OMF channel causing its opening.

Ultimately, none of the evidence provided above proves conclusively either of the models of OMF-PAP association. However, while structural biology seemingly gives us a hint toward the tip-to-tip interaction taking place, the ability of such interactions to provide sufficient energy for stabilization of a large multi-protein assembly, which also undergoes significant conformational changes during its transport cycle, is still called into question, especially in light of the wealth of functional data.

## Conclusion

Recent data have shown the PAPs to be a versatile group of proteins which, far from being passive linkers between the OMF and the energized inner-membrane transporters actively control the tripartite complex assembly. They play an active role in assembly energetics and cargo selection and presentation, while at the same time providing highly specific differentiation between a number of homologous partners to provide high fidelity and specificity of transport.

Our analysis has expanded the current understanding of structural relations of the multiple domains of these highly modular proteins, and revealed some unexpected connections linking them to other secretion systems and transporters. Finally, we have identified a pattern in the domain organization of the PAP families, which underlies their functional association with their cognate transporters.

Summing up the available data also shows that despite these recent advances, the ultimate answer of the complete pump architecture remains elusive.

## Acknowledgments

We are grateful to Prof. Ben Luisi (University of Cambridge) for the provision of the model of the complete AcrABZ-TolC assembly from cryo-EM studies and to Dr Mark Webber (University of Birmingham) for critical discussion of the manuscript. VB is supported by Birmingham Fellowship. RM is supported by EPSRC studentship.

## Supplementary Material

The Supplementary Material for this article can be found online at: <http://journal.frontiersin.org/article/10.3389/fmich.2015.00513/abstract>

## References

- Akama, H., Kanemaki, M., Yoshimura, M., Tsukihara, T., Kashiwagi, T., Yoneyama, H., et al. (2004). Crystal structure of the drug discharge outer membrane protein, OprM, of *Pseudomonas aeruginosa* – dual modes of membrane anchoring and occluded cavity end. *J. Biol. Chem.* 279, 52816–52819. doi: 10.1074/jbc.C400445200
- Andersen, C., Hughes, C., and Koronakis, V. (2002a). Electrophysiological behavior of the TolC channel-tunnel in planar lipid bilayers. *J. Membr. Biol.* 185, 83–92. doi: 10.1007/s00232-001-0113-2
- Andersen, C., Koronakis, E., Hughes, C., and Koronakis, V. (2002b). An aspartate ring at the TolC tunnel entrance determines ion selectivity and presents a target for blocking by large cations. *Mol. Microbiol.* 44, 1131–1139. doi: 10.1046/j.1365-2958.2002.02898.x
- Aucher, W., Lacombe, C., Héquet, A., Frère, J., and Berjeaud, J. M. (2005). Influence of amino acid substitutions in the leader peptide on maturation and secretion of mesentericin Y105 by *Leuconostoc mesenteroides*. *J. Bacteriol.* 187, 2218–2223. doi: 10.1128/JB.187.6.2218-2223.2005
- Augustus, A. M., Celaya, T., Husain, F., Humbard, M., and Misra, R. (2004). Antibiotic-sensitive TolC mutants and their suppressors. *J. Bacteriol.* 186, 1851–1860. doi: 10.1128/JB.186.6.1851-1860.2004
- Bagai, I., Rensing, C., Blackburn, N. J., and McEvoy, M. M. (2008). Direct metal transfer between periplasmic proteins identifies a bacterial copper chaperone. *Biochemistry* 47, 11408–11414. doi: 10.1021/bi801638m
- Bai, J., Bhagavathi, R., Tran, P., Muzzarelli, K., Wang, D., and Fralick, J. A. (2014). Evidence that the C-terminal region is involved in the stability and functionality of OprM in *E. coli*. *Microbiol. Res.* 169, 425–431. doi: 10.1016/j.micres.2013.08.006
- Bai, J., Mosley, L., and Fralick, J. A. (2010). Evidence that the C-terminus of OprM is involved in the assembly of the VceAB-OprM efflux pump. *FEBS Lett.* 584, 1493–1497. doi: 10.1016/j.febslet.2010.02.066
- Balakrishnan, L., Hughes, C., and Koronakis, V. (2001). Substrate-triggered recruitment of the TolC channel-tunnel during type I export of hemolysin by *Escherichia coli*. *J. Mol. Biol.* 313, 501–510. doi: 10.1006/jmbi.2001.5038
- Bavro, V. N., Pietras, Z., Furnham, N., Perez-Cano, L., Fernandez-Recio, J., Pei, X. Y., et al. (2008). Assembly and channel opening in a bacterial drug efflux machine. *Mol. Cell* 30, 114–121. doi: 10.1016/j.molcel.2008.02.015
- Benabdellah, H., Kiontke, S., Horn, C., Ernst, R., Blight, M., Holland, I., et al. (2003). A specific interaction between the NBD of the ABC-transporter HlyB and a C-terminal fragment of its transport substrate haemolysin A. *J. Mol. Biol.* 327, 1169–1179. doi: 10.1016/S0022-2836(03)00204-3
- Bersch, B., Derfoufi, K., De Angelis, F., Auquier, V., Ekende, E. N., Mergeay, M., et al. (2011). Structural and metal binding characterization of the C-terminal metallochaperone domain of membrane fusion protein SilB from *Cupriavidus metallidurans* CH34. *Biochemistry* 50, 2194–2204. doi: 10.1021/bi200005k
- Blair, J. M. A., Richmond, G. E., and Piddock, L. J. V. (2014). Multidrug efflux pumps in Gram-negative bacteria and their role in antibiotic resistance. *Future Microbiol.* 9, 1165–1177. doi: 10.2217/FMB.14.66
- Blair, J. M. A., Webber, M. A., Baylay, A. J., Ogbolu, D. O., and Piddock, L. J. V. (2015). Molecular mechanisms of antibiotic resistance. *Nat. Rev. Microbiol.* 13, 42–51. doi: 10.1038/nrmicro3380
- Bokma, E., Koronakis, E., Lobedanz, S., Hughes, C., and Koronakis, V. (2006). Directed evolution of a bacterial efflux pump: adaptation of the *E. coli* TolC exit duct to the *Pseudomonas* MexAB translocase. *FEBS Lett.* 580, 5339–5343. doi: 10.1016/j.febslet.2006.09.005
- Borges-Walmsley, M., Beauchamp, J., Kelly, S., Jumel, K., Candlish, D., Harding, S., et al. (2003). Identification of oligomerization and drug-binding domains of the membrane fusion protein EmrA. *J. Biol. Chem.* 278, 12903–12912. doi: 10.1074/jbc.M209457200
- Bunikis, I., Denker, K., Ostberg, Y., Andersen, C., Benz, R., and Bergstrom, S. (2008). An RND-type efflux system in *Borrelia burgdorferi* is involved in virulence and resistance to antimicrobial compounds. *PLoS Pathog.* 4:e1000009. doi: 10.1371/journal.ppat.1000009
- Calladine, C., Sharff, A., and Luisi, B. (2001). How to untwist an alpha-helix: structural principles of an alpha-helical barrel. *J. Mol. Biol.* 305, 603–618. doi: 10.1006/jmbi.2000.4320
- Chacon, K. N., Mealman, T. D., McEvoy, M. M., and Blackburn, N. J. (2014). Tracking metal ions through a Cu/Ag efflux pump assigns the functional roles of the periplasmic proteins. *Proc. Natl. Acad. Sci. U.S.A.* 111, 15373–15378. doi: 10.1073/pnas.1411475111
- Christie, P. J., Whitaker, N., and Gonzalez-Rivera, C. (2014). Mechanism and structure of the bacterial type IV secretion systems. *Biochim. Biophys. Acta* 1843, 1578–1591. doi: 10.1016/j.bbamcr.2013.12.019
- Crawford, M. A., Lowe, D. E., Fisher, D. J., Stibitz, S., Plaut, R. D., Beaber, J. W., et al. (2011). Identification of the bacterial protein FtsX as a unique target of chemokine-mediated antimicrobial activity against *Bacillus anthracis*. *Proc. Natl. Acad. Sci. U.S.A.* 108, 17159–17164. doi: 10.1073/pnas.1108495108
- De Angelis, F., Lee, J. K., O'Connell, J. D. III, Miercke, L. J. W., Verschueren, K. H., Srinivasan, V., et al. (2010). Metal-induced conformational changes in ZneB suggest an active role of membrane fusion proteins in efflux resistance systems. *Proc. Natl. Acad. Sci. U.S.A.* 107, 11038–11043. doi: 10.1073/pnas.1003908107
- Deka, R., Lee, Y., Haghman, K., Shevchenko, D., Lingwood, C., Hasemann, C., et al. (1999). Physicochemical evidence that *Treponema pallidum* TroA is a zinc-containing metalloprotein that lacks porin-like structure. *J. Bacteriol.* 181, 4420–4423.
- Diederichs, K., Diez, J., Greller, G., Müller, C., Breed, J., Schnell, C., et al. (2000). Crystal structure of MalK, the ATPase subunit of the trehalose/maltose ABC transporter of the archaeon *Thermococcus litoralis*. *EMBO J.* 19, 5951–5961. doi: 10.1093/emboj/19.22.5951
- Dinh, T., Paulsen, I. T., and Saier, M. H. (1994). A family of extracytoplasmic proteins that allow transport of large molecules across the outer membranes of Gram-negative bacteria. *J. Bacteriol.* 176, 3825–3831.
- Du, D., van Veen, H. W., and Luisi, B. F. (2015). Assembly and operation of bacterial tripartite multidrug efflux pumps. *Trends Microbiol.* 23, 311–319. doi: 10.1016/j.tim.2015.01.010
- Du, D., Wang, Z., James, N. R., Voss, J. E., Klimont, E., Ohene-Agyei, T., et al. (2014). Structure of the AcrAB-TolC multidrug efflux pump. *Nature* 509, 512–515. doi: 10.1038/nature13205
- Eicher, T., Seeger, M. A., Anselmi, C., Zhou, W., Brandstatter, L., Verrey, F., et al. (2014). Coupling of remote alternating-access transport mechanisms for protons and substrates in the multidrug efflux pump AcrB. *Elife* 3, e03145. doi: 10.7554/elife.03145
- Elkins, C., and Nikaido, H. (2003). Chimeric analysis of AcrA function reveals the importance of its C-terminal domain in its interaction with the AcrB multidrug efflux pump. *J. Bacteriol.* 185, 5349–5356. doi: 10.1128/JB.185.18.5349-5356.2003
- Emsley, P., Lohkamp, B., Scott, W. G., and Cowtan, K. (2010). Features and development of Coot. *Acta Cryst.* 66, 486–501. doi: 10.1107/S0907444910007493
- Federici, L., Du, D., Walas, F., Matsumura, H., Fernandez-Recio, J., McKeegan, K., et al. (2005). The crystal structure of the outer membrane protein VceC from the bacterial pathogen *Vibrio cholerae* at 1.8 angstrom resolution. *J. Biol. Chem.* 280, 15307–15314. doi: 10.1074/jbc.M500401200
- Fernandez-Recio, J., Walas, F., Federici, L., Pratap, J., Bavro, V., Miguel, R., et al. (2004). A model of a transmembrane drug-efflux pump from Gram-negative bacteria. *FEBS Lett.* 578, 5–9. doi: 10.1016/j.febslet.2004.10.097
- Fralick, J. A. (1996). Evidence that TolC is required for functioning of the Mar/AcrAB efflux pump of *Escherichia coli*. *J. Bacteriol.* 178, 5803–5805.
- Ge, Q., Yamada, Y., and Zgurskaya, H. (2009). The C-terminal domain of AcrA is essential for the assembly and function of the multidrug efflux pump AcrAB-TolC. *J. Bacteriol.* 191, 4365–4371. doi: 10.1128/JB.00204-09
- Gerken, H., and Misra, R. (2004). Genetic evidence for functional interactions between TolC and AcrA proteins of a major antibiotic efflux pump of *Escherichia coli*. *Mol. Microbiol.* 54, 620–631. doi: 10.1111/j.1365-2958.2004.04301.x
- Gerlach, R. G., and Hensel, M. (2007). Protein secretion systems and adhesins: the molecular armory of Gram-negative pathogens. *Int. J. Med. Microbiol.* 297, 401–415. doi: 10.1016/j.ijmm.2007.03.017
- Greene, N. P., Hincliffe, P., Crow, A., Ababou, A., Hughes, C., and Koronakis, V. (2013). Structure of an atypical periplasmic adaptor from a multidrug efflux pump of the spirochete *Borrelia burgdorferi*. *FEBS Lett.* 587, 2984–2988. doi: 10.1016/j.febslet.2013.06.056
- Hassan, K. A., Jackson, S. M., Penesyan, A., Patching, S. G., Tetu, S. G., Eijkeliamp, B. A., et al. (2013). Transcriptomic and biochemical analyses identify a family of chlorhexidine efflux proteins. *Proc. Natl. Acad. Sci. U.S.A.* 110, 20254–20259. doi: 10.1073/pnas.1317052110

- Hassan, K. A., Liu, Q., Henderson, P. J. F., and Paulsen, I. T. (2015). Homologs of the *Acinetobacter baumannii* Acel transporter represent a new family of bacterial multidrug efflux systems. *Mbio* 6, e01982-14. doi: 10.1128/mBio.01982-14
- Higgins, M., Bokma, E., Koronakis, E., Hughes, C., and Koronakis, V. (2004a). Structure of the periplasmic component of a bacterial drug efflux pump. *Proc. Natl. Acad. Sci. U.S.A.* 101, 9994–9999. doi: 10.1073/pnas.0400375101
- Higgins, M., Eswaran, J., Edwards, P., Schertler, G., Hughes, C., and Koronakis, V. (2004b). Structure of the ligand-blocked periplasmic entrance of the bacterial multidrug efflux protein TolC. *J. Mol. Biol.* 342, 697–702. doi: 10.1016/j.jmb.2004.07.088
- Hinchliffe, P., Greene, N. P., Paterson, N. G., Crow, A., Hughes, C., and Koronakis, V. (2014). Structure of the periplasmic adaptor protein from a major facilitator superfamily (MFS) multidrug efflux pump. *FEBS Lett.* 588, 3147–3153. doi: 10.1016/j.febslet.2014.06.055
- Hinchliffe, P., Symmons, M. F., Hughes, C., and Koronakis, V. (2013). Structure and operation of bacterial tripartite pumps. *Annu. Rev. Microbiol.* 67, 221–242. doi: 10.1146/annurev-micro-092412-155718
- Hobbs, E. C., Yin, X. F., Paul, B. J., Astarita, J. L., and Storz, G. (2012). Conserved small protein associates with the multidrug efflux pump AcrB and differentially affects antibiotic resistance. *Proc. Natl. Acad. Sci. U.S.A.* 109, 16696–16701. doi: 10.1073/pnas.1210093109
- Horiyama, T., Yamaguchi, A., and Nishino, K. (2010). TolC dependency of multidrug efflux systems in *Salmonella enterica* serovar Typhimurium. *J. Antimicrob. Chemother.* 65, 1372–1376. doi: 10.1093/jac/dkq160
- Hwang, J., Zhong, X., and Tai, P. (1997). Interactions of dedicated export membrane proteins of the colicin V secretion system: CvaA, a member of the membrane fusion protein family, interacts with CvaB and TolC. *J. Bacteriol.* 179, 6264–6270.
- Ip, H., Stratton, K., Zgurskaya, H., and Liu, J. (2003). pH-induced conformational changes of AcrA, the membrane fusion protein of *Escherichia coli* multidrug efflux system. *J. Biol. Chem.* 278, 50474–50482. doi: 10.1074/jbc.M305152200
- Iwashita, M., Nishi, J., Wakimoto, N., Fujiyama, R., Yamamoto, K., Tokuda, K., et al. (2006). Role of the carboxy-terminal region of the outer membrane protein AatA in the export of dispersin from enteroaggregative *Escherichia coli*. *FEMS Microbiol. Lett.* 256, 266–272. doi: 10.1111/j.1574-6968.2006.00123.x
- Janganan, T. K., Bavro, V. N., Zhang, L., Borges-Walmsley, M. I., and Walmsley, A. R. (2013). Tripartite efflux pumps: energy is required for dissociation, but not assembly or opening of the outer membrane channel of the pump. *Mol. Microbiol.* 88, 590–602. doi: 10.1111/mmi.12211
- Janganan, T. K., Bavro, V. N., Zhang, L., Matak-Vinkovic, D., Barrera, N. P., Venien-Bryan, C., et al. (2011a). Evidence for the assembly of a bacterial tripartite multidrug pump with a stoichiometry of 3:6:3. *J. Biol. Chem.* 286, 26900–26912. doi: 10.1074/jbc.M111.246595
- Janganan, T. K., Zhang, L., Bavro, V. N., Matak-Vinkovic, D., Barrera, N. P., Burton, M. F., et al. (2011b). Opening of the outer membrane protein channel in tripartite efflux pumps is induced by interaction with the membrane fusion partner. *J. Biol. Chem.* 286, 5484–5493. doi: 10.1074/jbc.M110.187658
- Johnson, J. M., and Church, G. M. (1999). Alignment and structure prediction of divergent protein families: periplasmic and outer membrane proteins of bacterial efflux pumps. *J. Mol. Biol.* 287, 695–715. doi: 10.1006/jmbi.1999.2630
- Kaur, S. J., Rahman, M. S., Ammerman, N. C., Beier-Sexton, M., Ceraul, S. M., Gillespie, J. J., et al. (2012). TolC-dependent secretion of an ankyrin repeat-containing protein of *Rickettsia typhi*. *J. Bacteriol.* 194, 4920–4932. doi: 10.1128/JB.00793-12
- Kim, H., Xu, Y., Lee, M., Piao, S., Sim, S., Ha, N., et al. (2010). Functional relationships between the AcrA hairpin tip region and the TolC aperture tip region for the formation of the bacterial tripartite efflux pump AcrAB-TolC. *J. Bacteriol.* 192, 4498–4503. doi: 10.1128/JB.00334-10
- Kim, J., Jeong, H., Song, S., Kim, H., Lee, K., Hyun, J., et al. (2015). Structure of the tripartite multidrug efflux pump AcrAB-TolC suggests an alternative assembly mode. *Mol. Cells* 38, 180–186. doi: 10.14348/molcells.2015.2277
- Kobayashi, N., Nishino, K., Hirata, T., and Yamaguchi, A. (2003). Membrane topology of ABC-type macrolide antibiotic exporter MacB in *Escherichia coli*. *FEBS Lett.* 546, 241–246. doi: 10.1016/S0014-5793(03)00579-9
- Koronakis, V., Eswaran, J., and Hughes, C. (2004). Structure and function of TolC: the bacterial exit duct for proteins and drugs. *Annu. Rev. Biochem.* 73, 467–489. doi: 10.1146/annurev.biochem.73.011303.074104
- Koronakis, V., Li, J., Koronakis, E., and Stauffer, K. (1997). Structure of TolC, the outer membrane component of the bacterial type I efflux system, derived from two-dimensional crystals. *Mol. Microbiol.* 23, 617–626. doi: 10.1046/j.1365-2958.1997.d01-1880.x
- Koronakis, V., Sharff, A., Koronakis, E., Luisi, B., and Hughes, C. (2000). Crystal structure of the bacterial membrane protein TolC central to multidrug efflux and protein export. *Nature* 405, 914–919. doi: 10.1038/35016007
- Krishnamoorthy, G., Tikhonova, E. B., and Zgurskaya, H. I. (2008). Fitting periplasmic membrane fusion proteins to inner membrane transporters: mutations that enable *Escherichia coli* AcrA to function with *Pseudomonas aeruginosa* MexB. *J. Bacteriol.* 190, 691–698. doi: 10.1128/JB.01276-07
- Kulathila, R., Kulathila, R., Indic, M., and van den Berg, B. (2011). Crystal structure of *Escherichia coli* CusC, the outer membrane component of a heavy metal efflux pump. *PLoS ONE* 6:e15610. doi: 10.1371/journal.pone.0015610
- Kumar, S., Mukherjee, M. M., and Varela, M. F. (2013). Modulation of bacterial multidrug resistance efflux pumps of the major facilitator superfamily. *Int. J. Bacteriol.* 2013, pii: 204141. doi: 10.1155/2013/204141
- Lee, M., Jun, S., Yoon, B., Song, S., Lee, K., and Ha, N. (2012). Membrane fusion proteins of type I secretion system and tripartite efflux pumps share a binding motif for TolC in Gram-negative bacteria. *PLoS ONE* 7:e40460. doi: 10.1371/journal.pone.0040460
- Lei, H., Bolla, J. R., Bishop, N. R., Su, C., and Yu, E. W. (2014a). Crystal structures of CusC review conformational changes accompanying folding and transmembrane channel formation. *J. Mol. Biol.* 426, 403–411. doi: 10.1016/j.jmb.2013.09.042
- Lei, H., Chou, T., Su, C., Bolla, J. R., Kumar, N., Radhakrishnan, A., et al. (2014b). Crystal structure of the open state of the *Neisseria gonorrhoeae* MtrE outer membrane channel. *PLoS ONE* 9:e97475. doi: 10.1371/journal.pone.0097475
- Li, X., and Nikaido, H. (2009). Efflux-mediated drug resistance in bacteria: an update. *Drugs* 69, 1555–1623. doi: 10.2165/11317030-000000000-00000
- Lin, H. T., Bavro, V. N., Barrera, N. P., Frankish, H. M., Velamakkanni, S., van Veen, H. W., et al. (2009). MacB ABC transporter is a dimer whose ATPase activity and macrolide-binding capacity are regulated by the membrane fusion protein MacA. *J. Biol. Chem.* 284, 1145–1154. doi: 10.1074/jbc.M806964200
- Lobedanz, S., Bokma, E., Symmons, M. F., Koronakis, E., Hughes, C., and Koronakis, V. (2007). A periplasmic coiled-coil interface underlying TolC recruitment and the assembly of bacterial drug efflux pumps. *Proc. Natl. Acad. Sci. U.S.A.* 104, 4612–4617. doi: 10.1073/pnas.0610160104
- Loftin, I., Franke, S., Roberts, S., Weichsel, A., Heroux, A., Montfort, W., et al. (2005). A novel copper-binding fold for the periplasmic copper resistance protein CusF. *Biochemistry* 44, 10533–10540. doi: 10.1021/bi050827b
- Long, F., Su, C., Zimmermann, M. T., Boyken, S. E., Rajashankar, K. R., Jernigan, R. L., et al. (2010). Crystal structures of the CusA efflux pump suggest methionine-mediated metal transport. *Nature* 467, 484–488. doi: 10.1038/nature09395
- Lu, S., and Zgurskaya, H. I. (2013). MacA, a periplasmic membrane fusion protein of the macrolide transporter MacAB-TolC, binds lipopolysaccharide core specifically and with high affinity. *J. Bacteriol.* 195, 4865–4872. doi: 10.1128/JB.00756-13
- Mealman, T. D., Bagai, I., Singh, P., Goodlett, D. R., Rensing, C., Zhou, H., et al. (2011). Interactions between CusF and CusB identified by NMR spectroscopy and chemical cross-linking coupled to mass spectrometry. *Biochemistry* 50, 2559–2566. doi: 10.1021/bi102012j
- Mealman, T. D., Zhou, M., Affandi, T., Chacon, K. N., Aranguren, M. E., Blackburn, N. J., et al. (2012). N-terminal region of CusB is sufficient for metal binding and metal transfer with the metallochaperone CusF. *Biochemistry* 51, 6767–6775. doi: 10.1021/bi300596a
- Mikolosko, J., Bobyk, K., Zgurskaya, H. I., and Ghosh, P. (2006). Conformational flexibility in the multidrug efflux system protein AcrA. *Structure* 14, 577–587. doi: 10.1016/j.str.2005.11.015
- Mima, T., Joshi, S., Gomez-Escalada, M., and Schweizer, H. P. (2007). Identification and characterization of TriABC-OpmH, a triclosan efflux pump of *Pseudomonas aeruginosa* requiring two membrane fusion proteins. *J. Bacteriol.* 189, 7600–7609. doi: 10.1128/JB.00850-07
- Minamino, T. (2014). Protein export through the bacterial flagellar type III export pathway. *Biochim. Biophys. Acta* 1843, 1642–1648. doi: 10.1016/j.bbamcr.2013.09.005

- Misra, R., and Bavro, V. N. (2009). Assembly and transport mechanism of tripartite drug efflux systems. *Biochim. Biophys. Acta* 1794, 817–825. doi: 10.1016/j.bbapap.2009.02.017
- Modali, S. D., and Zgurskaya, H. I. (2011). The periplasmic membrane proximal domain of MacA acts as a switch in stimulation of ATP hydrolysis by MacB transporter. *Mol. Microbiol.* 81, 937–951. doi: 10.1111/j.1365-2958.2011.07744.x
- Murakami, S., Nakashima, R., Yamashita, E., and Yamaguchi, A. (2002). Crystal structure of bacterial multidrug efflux transporter AcrB. *Nature* 419, 587–593. doi: 10.1038/nature01050
- Murzin, A. (1993). Ob(oligonucleotide oligosaccharide binding)-fold - common structural and functional solution for non-homologous sequences. *EMBO J.* 12, 861–867.
- Nehme, D., and Poole, K. (2007). Assembly of the MexAB-OprM multidrug pump of *Pseudomonas aeruginosa*: component interactions defined by the study of pump mutant suppressors. *J. Bacteriol.* 189, 6118–6127. doi: 10.1128/JB.00718-07
- Nikaido, H., and Pagès, J. (2012). Broad-specificity efflux pumps and their role in multidrug resistance of Gram-negative bacteria. *FEMS Microbiol. Rev.* 36, 340–363. doi: 10.1111/j.1574-6976.2011.00290.x
- Nishi, J., Sheikh, J., Mizuguchi, K., Luisi, B., Burland, V., Boutin, A., et al. (2003). The export of coat protein from enteropathogenic *Escherichia coli* by a specific ATP-binding cassette transporter system. *J. Biol. Chem.* 278, 45680–45689. doi: 10.1074/jbc.M306413200
- Nishino, K., Latifi, T., and Groisman, E. (2006). Virulence and drug resistance roles of multidrug efflux systems of *Salmonella enterica* serovar Typhimurium. *Mol. Microbiol.* 59, 126–141. doi: 10.1111/j.1365-2958.2005.04940.x
- Nivaskumar, M., and Francetic, O. (2014). Type II secretion system: a magic beanstalk or a protein escalator. *Biochim. Biophys. Acta-Mol. Cell Res.* 1843, 1568–1577. doi: 10.1016/j.bbamcr.2013.12.020
- Paulsen, I., Park, J., Choi, P., and Saier, M. (1997). A family of Gram-negative bacterial outer membrane factors that function in the export of proteins, carbohydrates, drugs and heavy metals from Gram-negative bacteria. *FEMS Microbiol. Lett.* 156, 1–8. doi: 10.1016/S0378-1097(97)00379-0
- Pei, X., Hinchliffe, P., Symmons, M. F., Koronakis, E., Benz, R., Hughes, C., et al. (2011). Structures of sequential open states in a symmetrical opening transition of the TolC exit duct. *Proc. Natl. Acad. Sci. U.S.A.* 108, 2112–2117. doi: 10.1073/pnas.1012588108
- Phan, G., Benabdellah, H., Lascombe, M., Benas, P., Rety, S., Picard, M., et al. (2010). Structural and dynamical insights into the opening mechanism of *P. aeruginosa* OprM channel. *Structure* 18, 507–517. doi: 10.1016/j.str.2010.01.018
- Piddock, L. J. V. (2006). Multidrug-resistance efflux pumps - not just for resistance. *Nat. Rev. Microbiol.* 4, 629–636. doi: 10.1038/nrmicro1464
- Piddock, L. J. V. (2012). The crisis of no new antibiotics-what is the way forward? *Lancet Infect. Dis.* 12, 249–253. doi: 10.1016/S1473-3099(11)70316-4
- Piddock, L. J. V. (2014). Understanding the basis of antibiotic resistance: a platform for drug discovery. *Microbiology* 160, 2366–2373. doi: 10.1099/mic.0.082412-0
- Pimenta, A., Racher, K., Jamieson, L., Blight, M., and Holland, I. (2005). Mutations in HlyD, part of the type 1 translocator for hemolysin secretion, affect the folding of the secreted toxin. *J. Bacteriol.* 187, 7471–7480. doi: 10.1128/JB.187.21.7471-7480.2005
- Pos, K. M. (2009). Drug transport mechanism of the AcrB efflux pump. *Biochim. Biophys. Acta* 1794, 782–793. doi: 10.1016/j.bbapap.2008.12.015
- Ruggerone, P., Murakami, S., Pos, K. M., and Vargiu, A. V. (2013) RND efflux pumps: structural information translated into function and inhibition mechanisms. *Curr. Top. Med. Chem.* 13, 3079–3100. doi: 10.2174/15680266113136660220
- Scheffel, F., Demmer, U., Warkentin, E., Hülsmann, A., Schneider, E., and Ermler, U. (2005). Structure of the ATPase subunit CysA of the putative sulfate ATP-binding cassette (ABC) transporter from *Alicyclobacillus acidocaldarius*. *FEBS Lett.* 579, 2953–2958. doi: 10.1016/j.febslet.2005.04.017
- Schulz, R., and Kleinekathöfer, U. (2009). Transitions between closed and open conformations of TolC: the effects of ions in simulations. *Biophys. J.* 96, 3116–3125. doi: 10.1016/j.bpj.2009.01.021
- Silver, L. L. (2011). Challenges of antibacterial discovery. *Clin. Microbiol. Rev.* 24, 71–109. doi: 10.1128/CMR.00030-10
- Slynko, V., Schubert, M., Numao, S., Kowarik, M., Aebi, M., and Allain, F. H. (2009). NMR structure determination of a segmentally labeled glycoprotein using in vitro glycosylation. *J. Am. Chem. Soc.* 131, 1274–1281. doi: 10.1021/ja808682v
- Song, S., Hwang, S., Lee, S., Ha, N., and Lee, K. (2014). Interaction mediated by the putative tip regions of MdsA and MdsC in the formation of a *Salmonella*-specific tripartite efflux pump. *PLoS ONE* 9:e100881. doi: 10.1371/journal.pone.0100881
- Srinivas, N., Jetter, P., Ueberbacher, B. J., Werneburg, M., Zerbe, K., Steinmann, J., et al. (2010). Peptidomimetic antibiotics target outer-membrane biogenesis in *Pseudomonas aeruginosa*. *Science* 327, 1010–1013. doi: 10.1126/science.1182749
- Staron, P., Forchhammer, K., and Maldener, I. (2014). Structure-function analysis of the ATP-driven glycolipid efflux pump DevBCA reveals complex organization with TolC/HgdD. *FEBS Lett.* 588, 395–400. doi: 10.1016/j.febslet.2013.12.004
- Stegmeier, J. F., Polleichtner, G., Brandes, N., Hotz, C., and Andersen, C. (2006). Importance of the adaptor (membrane fusion) protein hairpin domain for the functionality of multidrug efflux pumps. *Biochemistry* 45, 10303–10312. doi: 10.1021/bi060320g
- Su, C., Long, F., Lei, H., Bolla, J. R., Do, S. V., Rajashankar, K. R., et al. (2012). Charged amino acids (R83, E567, D617, E625, R669, and K678) of CusA are required for metal ion transport in the Cus efflux system. *J. Mol. Biol.* 422, 429–441. doi: 10.1016/j.jmb.2012.05.038
- Su, C., Long, F., Zimmermann, M. T., Rajashankar, K. R., Jernigan, R. L., and Yu, E. W. (2011). Crystal structure of the CusBA heavy-metal efflux complex of *Escherichia coli*. *Nature* 470, 558–562. doi: 10.1038/nature09743
- Su, C., Radhakrishnan, A., Kumar, N., Long, F., Bolla, J. R., Lei, H., et al. (2014). Crystal structure of the *Campylobacter jejuni* CmeC outer membrane channel. *Protein Sci.* 23, 954–961. doi: 10.1002/pro.2478
- Su, C., Yang, F., Long, F., Reyen, D., Routh, M. D., Kuo, D. W., et al. (2009). Crystal structure of the membrane fusion protein CusB from *Escherichia coli*. *J. Mol. Biol.* 393, 342–355. doi: 10.1016/j.jmb.2009.08.029
- Symmons, M. F., Bokma, E., Koronakis, E., Hughes, C., and Koronakis, V. (2009). The assembled structure of a complete tripartite bacterial multidrug efflux pump. *Proc. Natl. Acad. Sci. U.S.A.* 106, 7173–7178. doi: 10.1073/pnas.0900693106
- Tamura, N., Murakami, S., Oyama, Y., Ishiguro, M., and Yamaguchi, A. (2005). Direct interaction of multidrug efflux transporter AcrB and outer membrane channel TolC detected via site-directed disulfide cross-linking. *Biochemistry* 44, 11115–11121. doi: 10.1021/bi050452u
- Terashima, H., Li, N., Sakuma, M., Koike, M., Kojima, S., Homma, M., et al. (2013). Insight into the assembly mechanism in the supramolecular rings of the sodium-driven *Vibrio* flagellar motor from the structure of FlgT. *Proc. Natl. Acad. Sci. U.S.A.* 110, 6133–6138. doi: 10.1073/pnas.1222655110
- Thanabalu, T., Koronakis, E., Hughes, C., and Koronakis, V. (1998). Substrate-induced assembly of a contiguous channel for protein export from *E. coli*: reversible bridging of an inner-membrane translocase to an outer membrane exit pore. *EMBO J.* 17, 6487–6496. doi: 10.1093/emboj/17.22.6487
- Thomas, S., Holland, I. B., and Schmitt, L. (2014). The type 1 secretion pathway – the hemolysin system and beyond. *Biochim. Biophys. Acta.* 1843, 1629–1641. doi: 10.1016/j.bbamcr.2013.09.017
- Tikhonova, E. B., Devroy, V. K., Lau, S. Y., and Zgurskaya, H. I. (2007). Reconstitution of the *Escherichia coli* macrolide transporter: the periplasmic membrane fusion protein MacA stimulates the ATPase activity of MacB. *Mol. Microbiol.* 63, 895–910. doi: 10.1111/j.1365-2958.2006.05549.x
- Tikhonova, E., Wang, Q., and Zgurskaya, H. (2002). Chimeric analysis of the multicomponent multidrug efflux transporters from Gram-negative bacteria. *J. Bacteriol.* 184, 6499–6507. doi: 10.1128/JB.184.23.6499-6507.2002
- Tikhonova, E. B., Yamada, Y., and Zgurskaya, H. I. (2011). Sequential mechanism of assembly of multidrug efflux pump AcrAB-TolC. *Chem. Biol.* 18, 454–463. doi: 10.1016/j.chembiol.2011.02.011
- Törnroth-Horsefield, S., Gourdon, P., Horsefield, R., Brive, L., Yamamoto, N., Mori, H., et al. (2007). Crystal structure of AcrB in complex with a single transmembrane subunit reveals another twist. *Structure* 15, 1663–1673. doi: 10.1016/j.str.2007.09.023
- Touzé, T., Eswaran, J., Bokma, E., Koronakis, E., Hughes, C., and Koronakis, V. (2004). Interactions underlying assembly of the *Escherichia coli* AcrAB-TolC multidrug efflux system. *Mol. Microbiol.* 53, 697–706. doi: 10.1111/j.1365-2958.2004.04158.x

- Trépout, S., Taveau, J., Benabdellah, H., Granier, T., Ducruix, A., Frangakis, A. S., et al. (2010). Structure of reconstituted bacterial membrane efflux pump by cryo-electron tomography. *Biochim. Biophys. Acta.* 1798, 1953–1960. doi: 10.1016/j.bbapmem.2010.06.019
- Tsukazaki, T., Mori, H., Echizen, Y., Ishitani, R., Fukai, S., Tanaka, T., et al. (2011). Structure and function of a membrane component SecDF that enhances protein export. *Nature* 474, 235–238. doi: 10.1038/nature09980
- Ucisik, M. N., Chakravorty, D. K., and Merz, K. M. Jr. (2013). Structure and dynamics of the N-terminal domain of the Cu(I) binding protein CusB. *Biochemistry* 52, 6911–6923. doi: 10.1021/bi400606b
- Vaccaro, L., Koronakis, V., and Sansom, M. (2006). Flexibility in a drug transport accessory protein: molecular dynamics simulations of MexA. *Biophys. J.* 91, 558–564. doi: 10.1529/biophysj105.080010
- van Ulzen, P., Rahman, S. U., Jong, W. S. P., Daleke-Schermerhorn, M. H., and Luirink, J. (2014). Type V secretion: from biogenesis to biotechnology. *Biochim. Biophys. Acta.* 1843, 1592–1611. doi: 10.1016/j.bbamcr.2013.11.006
- Varela, C., Rittmann, D., Singh, A., Krumbach, K., Bhatt, K., Eggeling, L., et al. (2012). MmpL genes are associated with mycolic acid metabolism in *Mycobacteria* and *Corynebacteria*. *Chem. Biol.* 19, 498–506. doi: 10.1016/j.chembiol.2012.03.006
- Vediappan, G., Borisova, T., and Fralick, J. (2006). Isolation and characterization of VceC gain-of-function mutants that can function with the AcrAB multiple-drug-resistant efflux pump of *Escherichia coli*. *J. Bacteriol.* 188, 3757–3762. doi: 10.1128/JB.00038-06
- Verchère, A., Broutin, I., and Picard, M. (2012). Photo-induced proton gradients for the in vitro investigation of bacterial efflux pumps. *Sci. Rep.* 2:306. doi: 10.1038/srep00306
- Wang, B., Weng, J., Fan, K., and Wang, W. (2012). Interdomain flexibility and pH-induced conformational changes of AcrA revealed by molecular dynamics simulations. *J. Phys. Chem. B* 116, 3411–3420. doi: 10.1021/jp212221v
- Weeks, J. W., Bavro, V. N., and Misra, R. (2014). Genetic assessment of the role of AcrB beta hairpins in the assembly of the TolC-AcrAB multidrug efflux pump of *Escherichia coli*. *Mol. Microbiol.* 91, 965–975. doi: 10.1111/mmi.12508
- Weeks, J. W., Celaya-Kolb, T., Pecora, S., and Misra, R. (2010). AcrA suppressor alterations reverse the drug hypersensitivity phenotype of a TolC mutant by inducing TolC aperture opening. *Mol. Microbiol.* 75, 1468–1483. doi: 10.1111/j.1365-2958.2010.07068.x
- Whitney, E. N. (1971). The tolC locus in *Escherichia coli* K12. *Genetics* 67, 39–53.
- Wong, K., Ma, J., Rothnie, A., Biggin, P. C., and Kerr, I. D. (2014). Towards understanding promiscuity in multidrug efflux pumps. *Trends Biochem. Sci.* 39, 8–16. doi: 10.1016/j.tibs.2013.11.002
- Xu, Y., Lee, M., Moeller, A., Song, S., Yoon, B., Kim, H., et al. (2011a). Funnel-like hexameric assembly of the periplasmic adapter protein in the tripartite multidrug efflux pump in Gram-negative bacteria. *J. Biol. Chem.* 286, 17910–17920. doi: 10.1074/jbc.M111.238535
- Xu, Y., Song, S., Moeller, A., Kim, N., Piao, S., Sim, S., et al. (2011b). Functional implications of an intermeshing cogwheel-like interaction between TolC and MacA in the action of macrolide-specific efflux pump MacAB-TolC. *J. Biol. Chem.* 286, 13541–13549. doi: 10.1074/jbc.M110.202598
- Xu, Y., Moeller, A., Jun, S., Le, M., Yoon, B., Kim, J., et al. (2012). Assembly and channel opening of outer membrane protein in tripartite drug efflux pumps of Gram-negative bacteria. *J. Biol. Chem.* 287, 11740–11750. doi: 10.1074/jbc.M111.329375
- Xu, Y., Sim, S., Song, S., Piao, S., Kim, H., Jin, X. L., et al. (2010). The tip region of the MacA alpha-hairpin is important for the binding to TolC to the *Escherichia coli* MacAB-TolC pump. *Biochem. Biophys. Res. Commun.* 394, 962–965. doi: 10.1016/j.bbrc.2010.03.097
- Xue, Y., Davis, A. V., Balakrishnan, G., Stasser, J. P., Staehlin, B. M., Focia, P., et al. (2008). Cu(I) recognition via cation-pi and methionine interactions in CusF. *Nat. Chem. Biol.* 4, 107–109. doi: 10.1038/nchembio.2007.57
- Yamada, Y., Tikhonova, E. B., and Zgurskaya, H. I. (2012). YknWXYZ is an unusual four-component transporter with a role in protection against sporulation-delaying-protein-induced killing of *Bacillus subtilis*. *J. Bacteriol.* 194, 4386–4394. doi: 10.1128/JB.00223-12
- Yamanaka, H., Izawa, H., and Okamoto, K. (2001). Carboxy-terminal region involved in activity of *Escherichia coli* TolC. *J. Bacteriol.* 183, 6961–6964. doi: 10.1128/JB.183.23.6961-6964.2001
- Yamanaka, H., Nomura, T., Morisada, N., Shinoda, S., and Okamoto, K. (2002). Site-directed mutagenesis studies of the amino acid residue at position 412 of *Escherichia coli* TolC which is required for the activity. *Microb. Pathog.* 33, 81–89. doi: 10.1006/mpat.2002.0519
- Yang, J., Yan, R., Roy, A., Xu, D., Poisson, J., and Zhang, Y. (2015). The I-TASSER suite: protein structure and function prediction. *Nat. Methods* 12, 7–8. doi: 10.1038/nmeth.3213
- Yin, H., Paterson, R., Wen, X., Lamb, R., and Jardetzky, T. (2005). Structure of the uncleaved ectodomain of the paramyxovirus (hPIV3) fusion protein. *Proc. Natl. Acad. Sci. U.S.A.* 102, 9288–9293. doi: 10.1073/pnas.0503989102
- Yonekura, K., Maki-Yonekura, S., and Namba, K. (2003). Complete atomic model of the bacterial flagellar filament by electron cryomicroscopy. *Nature* 424, 643–650. doi: 10.1038/nature01830
- Yoshida, K., Fujita, Y., and Ehrlich, S. (2000). An operon for a putative ATP-binding cassette transport system involved in acetoin utilization of *Bacillus subtilis*. *J. Bacteriol.* 182, 5454–5461. doi: 10.1128/JB.182.19.5454-5461.2000
- Yoshihara, E., Eda, S., and Kaitou, S. (2009). Functional interaction sites of OprM with MexAB in the *Pseudomonas aeruginosa* multidrug efflux pump. *FEMS Microbiol. Lett.* 299, 200–204. doi: 10.1111/j.1574-6968.2009.01752.x
- Yum, S., Xu, Y., Piao, S., Sim, S., Kim, H., Jo, W., et al. (2009). Crystal structure of the periplasmic component of a tripartite macrolide-specific efflux pump. *J. Mol. Biol.* 387, 1286–1297. doi: 10.1016/j.jmb.2009.02.048
- Zgurskaya, H. I., Krishnamoorthy, G., Ntreh, A., and Lu, S. (2011). Mechanism and function of the outer membrane channel TolC in multidrug resistance and physiology of enterobacteria. *Front. Microbiol.* 2:189. doi: 10.3389/fmicb.2011.00189
- Zgurskaya, H., and Nikaido, H. (1999). Bypassing the periplasm: reconstitution of the AcrAB multidrug efflux pump of *Escherichia coli*. *Proc. Natl. Acad. Sci. U.S.A.* 96, 7190–7195. doi: 10.1073/pnas.96.13.7190
- Zgurskaya, H., and Nikaido, H. (2000). Cross-linked complex between oligomeric periplasmic lipoprotein AcrA and the inner-membrane-associated multidrug efflux pump AcrB from *Escherichia coli*. *J. Bacteriol.* 182, 4264–4267. doi: 10.1128/JB.182.15.4264-4267.2000
- Zgurskaya, H. I., Weeks, J. W., Ntreh, A. T., Nickels, L. M., and Wolloscheck, D. D. (2015). Mechanism of coupling drug transport reactions located in two different membranes. *Front. Microbiol.* 6:100. doi: 10.3389/fmicb.2015.00100
- Zgurskaya, H. I., Yamada, Y., Tikhonova, E. B., Ge, Q., and Krishnamoorthy, G. (2009). Structural and functional diversity of bacterial membrane fusion proteins. *Biochim. Biophys. Acta* 1794, 794–807. doi: 10.1016/j.bbapap.2008.10.010
- Zheleznova, E., Markham, P., Neyfakh, A., and Brennan, R. (1999). Structural basis of multidrug recognition by BmrR, a transcription activator of a multidrug transporter. *Cell* 96, 353–362. doi: 10.1016/S0092-8674(00)80548-6
- Zoued, A., Brunet, Y. R., Durand, E., Aschtgen, M., Logger, L., Douzi, B., et al. (2014). Architecture and assembly of the type VI secretion system. *Biochim. Biophys. Acta.* 1843, 1664–1673. doi: 10.1016/j.bbamcr.2014.03.018

**Conflict of Interest Statement:** The authors declare that the research was conducted in the absence of any commercial or financial relationships that could be construed as a potential conflict of interest.

Copyright © 2015 Symmons, Marshall and Bavro. This is an open-access article distributed under the terms of the Creative Commons Attribution License (CC BY). The use, distribution or reproduction in other forums is permitted, provided the original author(s) or licensor are credited and that the original publication in this journal is cited, in accordance with accepted academic practice. No use, distribution or reproduction is permitted which does not comply with these terms.

# Catch me if you can: a biotinylated proteoliposome affinity assay for the investigation of assembly of the MexA-MexB-OprM efflux pump from *Pseudomonas aeruginosa*

OPEN ACCESS

**Edited by:**

Klaas M. Pos,

Goethe University Frankfurt, Germany

**Reviewed by:**

Vishvanath Tiwari,

Central University of Rajasthan, India

Dinesh Sriramulu,

Shres Consultancy (Life Sciences),

India

Markus Seeger,

University of Zurich, Switzerland

**\*Correspondence:**

Martin Picard,

Laboratoire de Cristallographie et RMN Biologiques, Faculté de Pharmacie de Paris, UMR 8015 CNRS – Université Paris 089

Descartes, 4, Avenue de l'Observatoire, 75270 Paris Cedex

06, France

martin.picard@parisdescartes.fr

<sup>†</sup> These authors have contributed equally to this work.**Specialty section:**

This article was submitted to

Antimicrobials, Resistance and

Chemotherapy,

a section of the journal

Frontiers in Microbiology

**Received:** 13 February 2015**Accepted:** 16 May 2015**Published:** 02 June 2015**Citation:**Enguéné VYN, Verchère A, Phan G, Broutin I and Picard M (2015) Catch me if you can: a biotinylated proteoliposome affinity assay for the investigation of assembly of the MexA-MexB-OprM efflux pump from *Pseudomonas aeruginosa*. *Front. Microbiol.* 6:541.

doi: 10.3389/fmicb.2015.00541

Véronique Yvette Ntsogo Enguéné<sup>†</sup>, Alice Verchère<sup>†</sup>, Gilles Phan, Isabelle Broutin and Martin Picard\*

Laboratoire de Cristallographie et RMN Biologiques, Faculté de Pharmacie de Paris, UMR 8015 CNRS – Université Paris 089 Descartes, Paris, France

Efflux pumps are membrane transporters that actively extrude various substrates, leading to multidrug resistance (MDR). In this study, we have designed a new test that allows investigating the assembly of the MexA-MexB-OprM efflux pump from the Gram negative bacteria *Pseudomonas aeruginosa*. The method relies on the streptavidin-mediated pull-down of OprM proteoliposomes upon interaction with MexAB proteoliposomes containing a biotin function carried by lipids. We give clear evidence for the importance of MexA in promoting and stabilizing the assembly of the MexAB-OprM complex. In addition, we have investigated the effect of the role of the lipid anchor of MexA as well as the role of the proton motive force on the assembly and disassembly of the efflux pump. The assay presented here allows for an accurate investigation of the assembly with only tens of microgram of protein and could be adapted to 96 wells plates. Hence, this work provides a basis for the medium-high screening of efflux pump inhibitors (EPIs).

**Keywords:** multidrug resistance, efflux pump, membrane protein, proteoliposome, macro-molecular assembly

## Introduction

In Gram-negative bacteria, efflux transporters play a major role in the emergence of antibiotic resistance thanks to their ability to export drugs out of the cell (Nikaido, 2009). They are organized as tripartite systems where the RND pump (member of the Resistance, Nodulation, cell Division family) is located in the inner membrane and works in conjunction with a periplasmic protein belonging to the MFP family (Membrane Fusion Protein family), and an outer membrane channel (from the OMF, outer membrane factor family). The cytoplasmic inner membrane protein acts as an energy-dependent pump with broad substrate specificity. The outer membrane protein acts as a porin whereas the third one is thought to stabilize the whole complex. The understanding of these pumps has been largely improved thanks to the publication of high-resolution structures of the various components (Hinchliffe et al., 2013) but the overall mechanism of assembly as well as the stoichiometry of assembly is still a matter of controversy. Two main models have been suggested for a complete

**Abbreviations:** BOG, beta-octyl glucopyranoside; DDM, dodecyl maltoside; EthB, Ethidium bromide. DOPC, 1,2-dioleoyl-sn-glycero-3-phosphocholine; DOPE, 1,2-dioleoyl-sn-glycero-3-phosphoethanolamine; RND, Resistance, Nodulation, cell Division family; OMF, outer membrane factor family; MFP, Membrane Fusion family; ITC, isothermal titration calorimetry; SPR, surface plasmon resonance.

description of the pump assembly. In the first one there is a direct docking of the RND protein on the OMF. In this model, three or six copies of the MFP stabilize the complex. This direct docking model has been comforted by the characterization of a direct interaction between AcrB and TolC by cross-linking (Tamura et al., 2005; Symmons et al., 2009; Weeks et al., 2010) and by *in vitro* surface plasmon resonance (SPR; Tikhonova et al., 2011). A second model where the MFP, assembled in a funnel-like conformation with a stoichiometry of 6- 12 copies acts as a bridge between the RND and the OMF, has been comforted by recent electron microscopy studies (Trépout et al., 2010; Du et al., 2014; Kim et al., 2015). This controversy builds up on a series of biochemical and biophysical characterizations. Indeed it is known for long that a genuine tripartite complex can be purified, without prior cross-linking, simply by using a hexahistidine tag on each of the proteins (Tikhonova and Zgurskaya, 2004). The assembly can be also studied *in vivo*, by screening mutants and assessing their ability to restore resistance against antibiotics (see, e.g., Nehme and Poole, 2007) or by taking advantage of the sensitivity of bacterial cells to vancomycin, a very large antibiotic that cannot penetrate the cell by slow passive diffusion (Bayro et al., 2008). Gram negative bacteria are not sensitive to vancomycin but become so if the OMF were to open upon assembly, thereby allowing the antibiotic to diffuse inside the cell. This strategy has been used to study the efflux pump MtrC-MtrD-MtrE (respectively MFP-RND-OMF) from *Neisseria gonorrhoea* (Janganan et al., 2013). The assembly has also been studied *in vitro* by isothermal titration calorimetry (ITC), a technique that allowed for the evaluation of the affinity between components and the establishment of a four-stage model where four sequential, non-cooperative, binding sites are suggested (Touzé et al., 2004). Following similar lines, the assembly of the whole complex has been studied by (SPR; Tikhonova et al., 2011). Upon injection of the protein partners (premixed or in a sequenced manner) on a biochip onto which AcrB was adsorbed, they could monitor assembly in real time. The tripartite complex successfully formed only when the partners were mixed in following a specific sequence of events.

In spite of the valuable and continued efforts for understanding how a tripartite efflux pump assembles, the development of original solutions compatible with medium-high screening of inhibitors is lacking. Antibiotic resistance is an increasing threat complicated by the scarcity of new anti-infective drug families under development. Hence, finding new ways to inhibit efflux pumps is a very promising and important endeavor because it was shown that such inhibitors restore the activity of antibiotics (Lomovskaya et al., 2006; Pages and Amaral, 2009). Lately, we have described a new protocol where transport through the whole pump could be monitored by use of proteoliposomes and respective fluorescent probes liable to report the activity of each partner of the pump (Verchère et al., 2015). As a complementary approach we present here a new strategy that allows investigating the formation of efflux pumps.

## Materials and Methods

1,2-dioleoyl-sn-glycero-3-phosphocholine (DOPC) and 1,2-dioleoyl-sn-glycero-3-phosphoethanolamine-N-(cap biotinyl;

DOPE, cap biotin) were purchased from Avanti Polar Lipids (reference: 850375C and 870273C, respectively). SM<sub>2</sub> Bio-beads were obtained from Bio-Rad (reference 152-3920). n-dodecyl-β-D-maltopyranoside (DDM) and n-octyl-β-D-glucopyranoside (β-OG) was purchased from Anatrace (reference D310LA and O311, respectively).

## Production, Purification of MexB

MexB was purified following the protocol described in (Mokhonov et al., 2005), with minor modifications. Heterologous expression was performed in a C43 ΔAcrB strain. A pre-culture was grown overnight at 37°C under agitation at 200 rpm and inoculated at OD<sub>600nm</sub> = 0.05 in 2xTY medium containing 100 μg/mL of ampicillin. Cells were grown to OD<sub>600nm</sub> = 0.6 at 30°C at 200 rpm and then cooled down at 4°C for 30 min. Isopropyl β-D-1-thiogalactopyranoside (IPTG) was added (1 mg/mL final) and growth was continued overnight at 20°C. Cells were then lysed thanks to a cell-disrupter (Cell-D from Constant LTD) at 4°C after two passages at 2.4 kbar. Membranes were collected upon centrifugation at 100,000 g during 1 h at 4°C. Solubilization was performed overnight at 4°C in 10 mM Bis-Tris pH 7.4; glycerol 20%, 10 mM imidazole and 500 mM NaCl at a 2:1 detergent-to-protein ratio (protein concentration was determined using the Bicinchoninic acid test from Sigma). Purification was performed by affinity chromatography followed by a gel filtration (superose 6 HR, GE).

## Production, Purification of MexA

MexA was purified following the protocol described in (Akama et al., 2004) with minor modifications. Heterologous expression was performed in a C43 ΔAcrB strain. A pre-culture was grown overnight at 37°C under agitation at 200 rpm and inoculated at OD<sub>600nm</sub> = 0.05 in 2xTY medium containing 25 μg/mL of chloramphenicol. Cells were grown to OD<sub>600nm</sub> = 0.6 at 30°C at 200 rpm and then cooled down at 4°C for 30 min. Arabinose was added (0.02% final, w/v) and growth was continued during 2.5 h at 30°C. Cells were then lysed thanks to a cell-disrupter (Cell-D from Constant LTD) at 4°C after two passages at 2.4 kbar. Membranes were collected upon centrifugation at 100,000 g during 1 h at 4°C. Solubilization was performed overnight at room temperature in 20 mM Tris-HCl pH 8, glycerol 10%, 15 mM imidazole at a 40:1 detergent-to-protein ratio (protein concentration was determined using the Bicinchoninic acid test from Sigma). Purification was performed by affinity chromatography followed by a gel filtration (superose 6 HR, GE). A truncated form of MexA “cysteine-less,” named MexAmp, without its first 24 residues, has been generated in the laboratory in order to produce and purify a non-palmitoylated, soluble version of the protein.

## Production, Purification of OprM

OprM is purified following the protocol described in (Phan et al., 2010) with minor modifications. In brief, the procedure was exactly that described above for MexA except that an additional solubilization step is added on the membrane pellet: N-octylpolyoxyethylene (C<sub>8</sub>POE) is added (2% final, w/v) and the mixture was incubated 30 min at 37°C. C<sub>8</sub>POE is a detergent

that has been shown to specifically solubilize bacterial inner membranes.

### Production, Purification of the RNA Scaffold

Purification of the RNA scaffold, dubbed ref-f, was performed as described in Ponchon et al. (2013). Heterologous expression was achieved in XL1 cells. A pre-culture was grown 10 h at 37°C under shaking at 200 rpm and inoculated at OD<sub>600nm</sub> = 0.05 in LB medium containing 100 µg/mL of ampicillin. Cells were grown overnight to OD<sub>600nm</sub> = 3 at 37°C at 200 rpm. The expression of ref-f is induced by the addition of 1 mM of IPTG. After 3 h, cells were centrifuged at 7000 g, during 20 min at room temperature. Pellets were re-suspended in 1 L of buffer containing 20 mM Tris, 200 mM NaCl and centrifuged at 7000 g, during 20 min, again at room temperature. Pellets were re-suspended in 40 mM of MgSO<sub>4</sub>, 50 mM Na<sub>3</sub>Citrate pH 5.6. RNA was extracted upon incubation with 40 mL of phenol during 2 h under gentle stirring at room temperature. The mixture was centrifuged 15 min at 3200 g. The supernatant was incubated with two volumes of ethanol and 1/20 of NaCl 5 M, a precipitate was formed and the mixture was centrifuged 5 min at 3200 g. The pellet was dried under the fume hood for 5 min and 10 mL of distilled water was added. The RNA was then purified by anion exchange chromatography.

### Preparation of Unilamellar Vesicles

A mix of lipids consisting of DOPC and DOPE with cap biotin at a 20:1 w/w ratio were dissolved in 25 mM HEPES pH7, 100 mM K<sub>2</sub>SO<sub>4</sub> and 2 mM MgSO<sub>4</sub>, to a final concentration of 1 mg/mL. The suspension was then heated for 10 min at 37°C. This solution was then sonicated for 10 min with 30' pulse/30' pause cycles. Liposomes were subsequently passed through 200 nm membranes and then 100 nm membranes thanks to an extruder from Avanti (20 pass for each type of membrane). The homogeneity of the suspension was controlled by Dynamic Light scattering (DLS, Nanosizer Malvern).

### Reconstitution of the Proteins

Liposomes were first solubilized at a 1:1 detergent to lipid ratio (w/w). Solubilization was performed using β-OG for 1 h at 20°C under gentle agitation. Proteins were added to the solubilized liposome suspension at the following lipid-to-protein ratio (w/w): MexB 1:20; MexA, 1:30; OprM, 1:20. OprM proteoliposomes were prepared in the presence of ref-f at 3 mg/ml: MexAB proteoliposomes were prepared in the presence of 3 mM pyranine. Detergent removal was achieved upon 3 consecutive additions of Bio-beads (previously washed with methanol, ethanol and water) at a Bio-bead: detergent ratio of 20 (w/w) for at 1 h at 20°C, followed by an eventual addition, overnight, at the same ratio. MexAB proteoliposomes were purified from untrapped pyranine using a PD-10 desalting column (GE Healthcare). OprM proteoliposomes were purified from untrapped RNA using source Q column (GE Healthcare).

The efficiency of the reconstitution is controlled by running a discontinuous sucrose gradient formed of five layers (60, 20, 10, 5 and 2.5% sucrose). After ultracentrifugation of liposomes on this sucrose gradient overnight at 100,000 g, non-incorporated

proteins are found at the bottom of the tube, while proteoliposomes are trapped at a sucrose interface that corresponds to their intrinsic density. Empty liposomes are recovered higher in the gradient. Different gradient fractions are collected gently and analyzed on SDS-PAGE using Coomassie staining.

### Ethidium Bromide Transport

Ethidium bromide (EthB) transport was measured as previously described (Verchère et al., 2015). Fluorescence measurements were conducted at 25°C using a SAFAS-Xenius spectrofluorimeter. The measurements were performed using the dual-wavelength mode, with excitation and emission wavelengths set at 300 nm and 600 nm, respectively, for the recording of EthB fluorescence and at 455 nm and 509 nm for the recording of pyranine fluorescence. Bandwidths were set at 10 nm. 100 µL of OprM proteoliposomes and 100 µL of MexAB proteoliposomes were mixed and diluted with 800 µL of the liposome reconstitution buffer (25 mM Hepes pH7, 100 mM K<sub>2</sub>SO<sub>4</sub>, 2 mM MgSO<sub>4</sub>). The system was then incubated until a steady baseline was obtained. EthB was then added at 5 µM and a pH jump was performed after 20 min incubation.

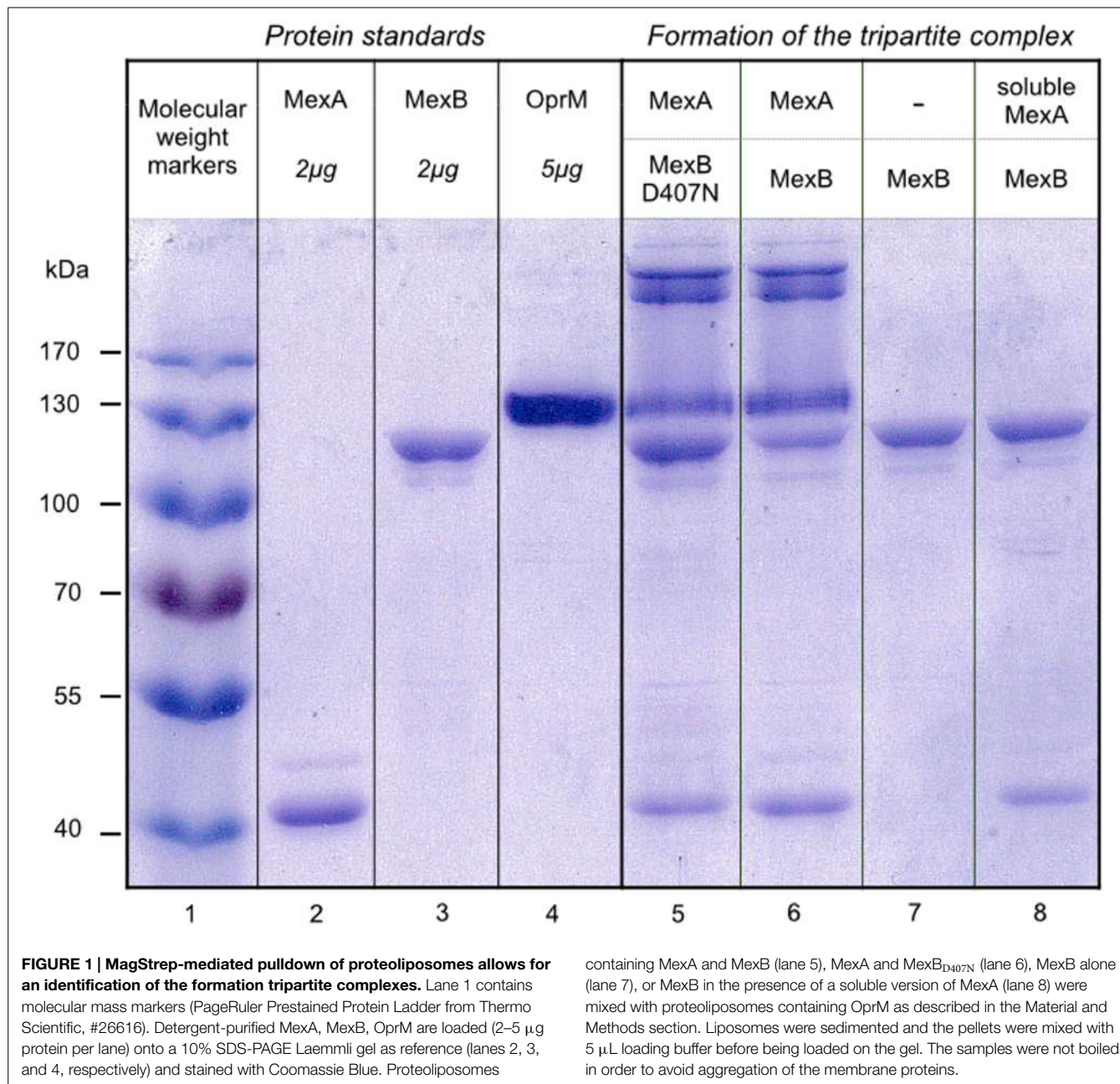
### Pull Down Assay

100 µL of the respective liposomes were mixed and the suspension was then complemented with 800 µL of the liposome reconstitution buffer (25 mM Hepes pH7, 100 mM K<sub>2</sub>SO<sub>4</sub>, 2 mM MgSO<sub>4</sub>), when the assembly is performed under non-energized conditions (see § Investigation of the assembly) or with 800 µL of a buffer containing 20 mM Mes Tris pH6, 100 mM K<sub>2</sub>SO<sub>4</sub>, 2 mM MgSO<sub>4</sub> when the assembly is performed under pH gradient conditions (see § Liposome pull down as a complementary approach to a transport assay, below). Both buffers have been tuned in order to have the same osmolarity, as measured by a cryoscopic Osmometer (Fisher Scientific, reference: 11900557). Then, the liposomes are incubated for 20 min at room temperature. Finally, 5 µL of MagStrep resin (MagStrep “type2HC” high capacity beads, IBA) at 5% (50 mg/mL) was added and the suspension was then placed on a magnetic separator (IBA, ref. 2-1602-000) in order to magnetize down the MexAB-biotin enriched-proteoliposomes and their potential interacting partner. Within a couple of minutes, the target proteins are specifically pelleted. The corresponding pellets were washed twice with 1 ml of 100 mM Tris HCl pH8, 150 mM NaCl before being resuspended directly in a 5X acrylamide gel loading buffer. The proteins were revealed on 10% gels by Laemmli-type SDS-PAGE (Laemmli, 1970) and stained with Coomassie blue.

## Results

### Investigation of the Assembly

Streptavidin- or streptactin-coated beads are classically used to purify biotinylated proteins, or proteins containing a strep tag, by affinity chromatography procedures. Here, we take advantage of streptavidin-coated magnetic beads to specifically sediment MexAB proteoliposomes containing biotinylated lipids. As can be seen **Figure 1**, when MexAB proteoliposomes are preincubated with OprM proteoliposomes, OprM is eventually found in the



pellet after sedimentation by the streptavidin-coated magnetic beads, thereby providing a clear evidence of the assembly *in vitro* (see the presence of MexA, MexB, and OprM, lane 6, by comparison with the protein standards lane 2, 3, and 4, respectively). Note that in addition to the presence of OprM itself, one can see complexes of very high molecular mass in the upper part of the gel. These complexes were extracted from the gel, incubated for 1.5 h in water at room temperature and treated under mild heating conditions (60°C for 15 min in SDS PAGE loading dye). This revealed that the high molecular mass complexes were OprM aggregates (data no shown). As a control, we have performed the same experiment in the absence of MexA. MexA is a periplasmic protein that is covalently attached to the membrane via a lipid

anchor. When MexB is reconstituted in the absence of MexA, OprM is not found in the pellet (lane 7), in accordance with the well-documented role of MexA on the formation of the pump. Interestingly, when a soluble version of MexA is added on the latter system, the formation of the complex is not restored (lane 8). Once again, this result is reminiscent with studies that showed that the absence of the lipid anchor severely impairs the ability for the efflux pump to form (Ferrandez et al., 2012). It must be put forward that the soluble version of MexA does not restore the ability to form the complex but is nevertheless able to bind to MexB, as both MexA and MexB are identified on lane 8. Finally, we also decided to study if the complex can form if the experiment is performed in the presence of an inactive version of MexB, mutated

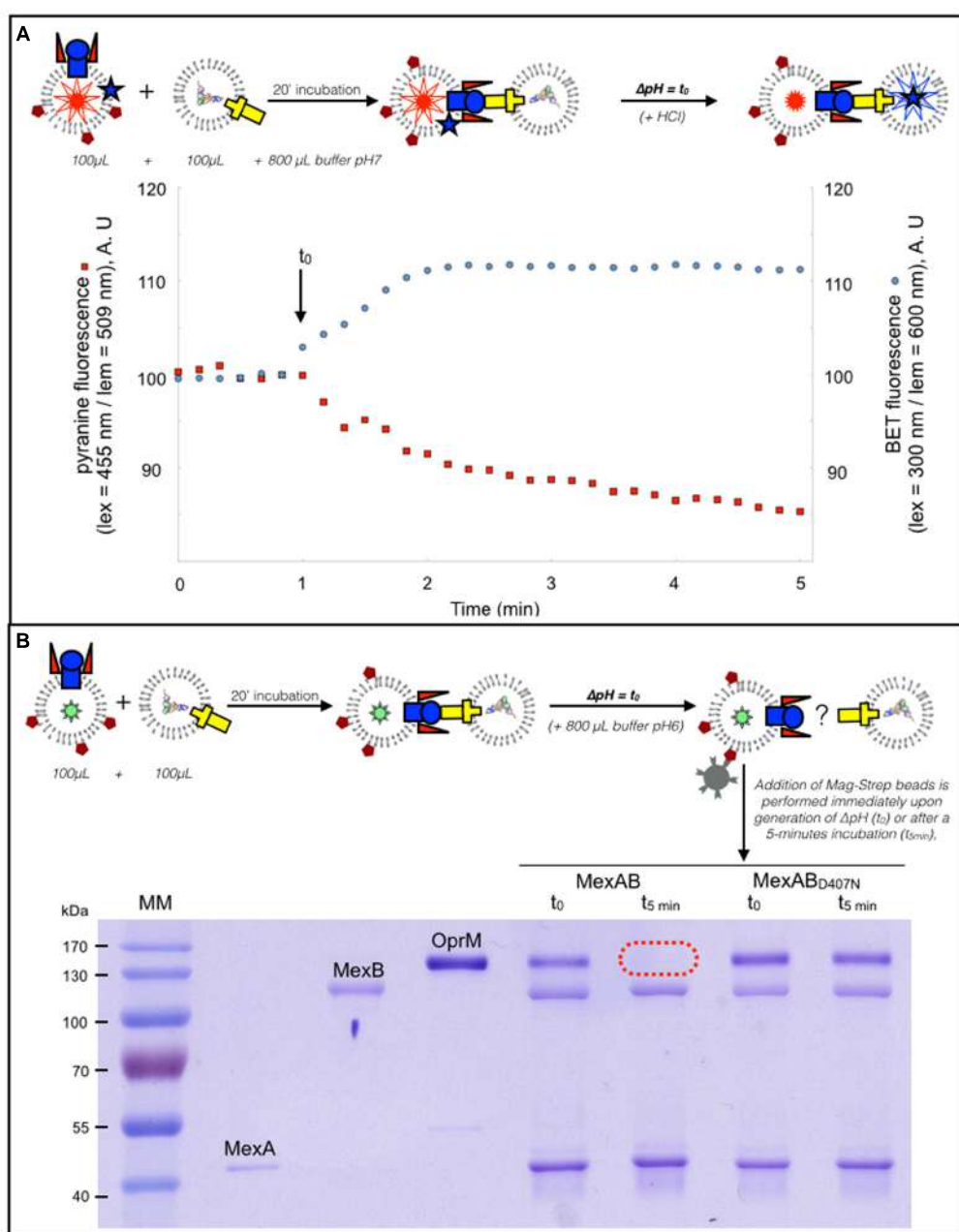


**FIGURE 2 |** The pull down assay can be adapted in conditions mimicking the transport. **(A)** Dual wavelength fluorescence monitoring of transport. Fluorescence measurements were conducted with excitation and emission wavelengths set for the recording of EthB and pyranine fluorescence. OprM proteoliposomes and of MexAB proteoliposomes were mixed and incubated with EthB (5 µM) and a pH jump, indicated by an arrow, was performed after 20 min incubation. The concomitant fluorescence variations of pyranine (see **A**, red trace) and EthB (see **A**, blue trace) is the proof of actual transport of the substrate from one vesicle to the other.

**(B)** MagStrep-mediated pulldown of proteoliposomes under conditions of a pH gradient. The liposomes used in the experiment shown **(A)** were enriched with biotinylated lipids in order to investigate the kinetics of the tripartite complex assembly in the context of transport. Samples were prepared as described in the Material and Methods section and were incubated for 20 min before being diluted with a buffer containing 20 mM Mes Tris pH 6, 100 mM K<sub>2</sub>SO<sub>4</sub>, 2 mM MgSO<sub>4</sub> in order to generate a pH gradient. Streptavidin-coated magnetic beads were then added either immediately ( $t_0$ ) or after a 5-min incubation ( $t = 5$  min).

in the proton relay pathway (D407N mutant, Guan and Nakae, 2001; Su et al., 2006; Takatsuka and Nikaido, 2006), and in the presence of the palmitoylated version of MexA. Lane 5 shows

that the complex does form in this condition showing that the mutation, located in the transmembrane part of the protein, does not affect the formation of the pump.

## Liposome Pull Down as a Complementary Approach to a Transport Assay

We have previously shown that transport through the whole tripartite pump can be measured thanks to the use of proteoliposomes loaded with fluorescent probes that report the activity of MexB and OprM (Verchère et al., 2015). In brief, MexA and MexB are reconstituted in proteoliposomes containing pyranine, while OprM is reconstituted in another kind of proteoliposome in which RNA is encapsulated. Besides, EthB, a substrate of the pump that has DNA-intercalating properties is incubated with the proteins. Pyranine is a pH-dependent probe which fluorescence decreases when pH decreases. EthB fluorescence increases significantly upon intercalation into nucleic acids. Because the pump is energized by the proton motive force (Thanassi et al., 1997; Li et al., 1998; Zgurskaya and Nikaido, 1999), transport can be triggered by generating a change in the pH in the external medium (the pH jump is indicated by an arrow, **Figure 2A**). Efflux is monitored by measuring the simultaneous fluorescence variations of pyranine (see **Figure 2A**, red trace) and EthB (see **Figure 2A**, blue trace): the concomitant fluorescence variations indicate actual transport of the substrate from one vesicle to the other (the increase of EthB fluorescence is ascribed to the intercalation into RNA), mediated by an active transport through the pump (the decrease of pyranine fluorescence is the result of proton counter-transport, hence the acidification of the liposome, by MexB). If the same experiment is now performed in the presence of proteoliposomes where the MexAB<sub>D407N</sub> inactive mutant is used, both the pyranine and EthB fluorescence signals remain steady (see Verchère et al., 2015). The liposomes used in the experiment shown **Figure 2A** were enriched with biotinylated lipids in order to investigate the kinetics of the tripartite complex assembly in the context of transport, using the pull-down protocol on the very same proteoliposome preparation. To that purpose the proteoliposomes were incubated as described in the previous paragraph except that the buffer used to dilute the liposomes was now more acidic than that in which the proteoliposomes were prepared. As a consequence, a pH gradient is generated across the liposome membrane. As can be seen in **Figure 2B**, the tripartite complex is observed upon generation of the pH gradient, as OprM is detected together with MexA and MexB (see “MexAB samples” prepared at  $t_0$ ). However, after transport has reached steady state (i.e., within a couple of minutes), the complex has seemingly disappeared. Indeed, OprM does no longer interact with MexAB (see the “MexAB samples” prepared at  $t = 5$  min). Interestingly, when the same experiment is performed in the presence of the D407N mutant, the complex remains stable (see “MexAB<sub>D407N</sub> samples” prepared at  $t_0$  and at  $t = 5$  min).

## Discussion

### An Original Technique Allowing to Monitor Transport and Assembly

The formation of the macromolecular complex formed by MexA, MexB, and OprM has been studied for long, by use of various biochemical and biophysical techniques. These studies made it possible to understand key aspects of the mechanism of an efflux

pump but they are rather demanding in term of protein quantity (ITC) and methodology (in SPR, the target protein must be attached on the sensor chip and must remain stable throughout the whole titration experiment). As presented here, our protocol is much more versatile, it is compatible with a medium-large screening of potential inhibitors as it does not require large amounts of protein (typically 10 µg of protein is necessary for one measurement). Finally, this protocol can be scaled up in 96-wells. In such a case, SDS-PAGE would not be the best identification option but we have adapted the protocol by using OprM proteoliposomes enriched with lipids grafted with a rhodamine function. In such a context, the purple color of the liposomes remains in the supernatant when the complex is not formed, the purple color being lost in the pellet if the complex forms (data not shown). Hence, the assembly could be simply monitored by colorimetry. Our methodology finds its limit in being only qualitative. Indeed, the variability of the efficiency of reconstitution, and the reproducibility of the procedure (washing of the pellets, resuspension in the loading buffer) precludes from any quantitative conclusion. Hence, we can not claim any information on the stoichiometry.

### Role of MexA

The results presented **Figure 1** show that MexA is absolutely necessary for the assembly, a result in accordance with previous results. Tikhonova et al. (2011) showed that if an His-tag is located on AcrA or AcrB, a tripartite complex can be purified in measurable quantities from bacterial native membranes. However, if the His-tag is placed on TolC, only traces of the complex are purified. AcrA is thus indispensable for AcrB to co-fractionate with OprM (Tikhonova and Zgurskaya, 2004). The interaction between the different partners has also been investigated using ITC, which allows evaluating the affinity between two components (Touzé et al., 2004). When the interaction between AcrB and TolC is investigated by ITC measurement, no stable interaction is detected. This was interpreted by the fact that AcrA is required for the interaction between AcrB and TolC.

Finally, the efflux pump MtrC-MtrD-MtrE (respectively MFP-RND-OMF) from *Neisseria gonorrhoea* has also been intensely investigated *in vivo* by Janganan et al. (2013). They made use of vancomycin susceptibility to monitor the assembly of the OMF with its RND and MFP partners (Janganan et al., 2013). Gram negative bacteria are not susceptible to vancomycin but become so if the OMF were to open and let the antibiotic diffuse inside the cell. Interestingly if the MFP is expressed together with the OMF, cells become sensitive to vancomycin, meaning that the MFP is required for the OMF to open. Note that, it was shown that a truncated version of the MFP, consisting of the alpha helical hairpin domain only, is not able to open the OMF. Finally the assembly of the whole complex was monitored by SPR (Tikhonova et al., 2011), showing that AcrA-AcrB and AcrA-TolC complexes can be detected. If palmitoylated AcrA and TolC are premixed and then injected on AcrB adsorbed on solid support, the complex does not form, probably because TolC inhibits the interaction between AcrB and AcrA.

The reason for the fact that the soluble MexA does not restore the formation of the complex remains an open question. It could very well be that this construction is intrinsically unable to make

the pump assemble but one can also imagine that this inability to form a complex is purely thermodynamic. Indeed, the lipid anchor may be present for restricting the diffusion of the protein to a two-dimensional space, thereby allowing a more probable interaction with MexB. However, the role of the N-terminal lipid part of AcrA, was investigated in real time by SPR (Tikhonova et al., 2011) and it was shown that when the MFP lacks its lipid anchor, no oligomerization of the MFP is detected. Considering that AcrA binds AcrB as a dimer, it seems probable that the lipid anchor has a genuine effect on the assembly. We have to stress that the observation that the soluble version of MexA is nevertheless able to bind MexB (see **Figure 1**, lane 8) is in contradiction with the fact that Tikhonova et al. showed that the binding of soluble AcrA to AcrB is very weak at pH7.5 and pH6.

### Role of pmf on the Assembly

We show that the mutation within the proton relay pathway does not impair the assembly, which indicates that the efflux pump assembly does not require transport activity. Again, this result is in line with the work of Tikhonova and Zgurskaya regarding the assembly of the AcrAB-TolC pump from native bacterial membranes (Tikhonova and Zgurskaya, 2004) where they showed that if the corresponding non-functional mutant of AcrB (AcrB Asp408Ala) is expressed, the complex is still co-purified. Besides, if the proton motive force is disrupted in the cells (using CCCP, valinomycin and/or nigericin) the complex is also co-purified.

### Role of pmf on the Disassembly

In a remarkable series of papers, Bavro et al. (2008) previously investigated the energy dependence of the pump assembly, by use of non-functional mutants of MtrD mutated in residues involved in the proton-transducing pathway (Asp405, Asp406, and Lys948). If these mutants are expressed with the MFP and the OMF, cells remain insensitive to vancomycin; indicating that the efflux pump must dissociate under the proton motive force. Although very elegant, this conclusion is indirect and is realized in the context of the bacteria where additional factors could be

suspected. **Figure 2** provides direct and non-ambiguous support for the fact that the proton motive force indeed promotes disassembly of the complex, as evidenced by i) the disappearing of OprM when the wild type pump has reached its steady state and ii) by the maintaining of the assembly when the D407N mutant, defective in proton translocation, is used.

## Conclusion

We were able to detect the assembly of an efflux pump after it has been reconstituted into proteoliposomes. We could discriminate between conditions that allow, or favor, the formation of the complex and could also confirm that MexA is mandatory for the assembly to take place. Hence, this is in accordance with several studies obtained in recent years on that matter. Our reconstitution method and the subsequent characterization approach described in the present work allow us to consider further studies of reconstitutions including proteins mutated at various positions, in order to shed light on the actual determinants of transport in a simple system in a bottom-up approach.

## Author Contributions

Conceived and designed the experiments: MP. Performed the experiments: YN, AV, MP. Wrote the paper: AV, GP, IB, MP.

## Acknowledgments

This study was supported by the Agence Nationale de la Recherche (ANR-12-BSV8-0010-01). YN was supported by both Vaincre la Mucoviscidose and the Association Grégory Lemarchal. AV was supported by a grant from Région Ile-de-France (DIM-Malinf 110058). We thank Klaas Martinus Pos for providing us the C43 ΔAcrB strain and Henrietta Venter for the D407N MexB plasmid. We thank Manuela Dezi for her help in the purification of the proteins, and Houssain Benabdellah, Arnaud Ducruix and Philippe Bénas for their helpful comments on the manuscript. We thank Nathalie Sisattana for technical assistance.

## References

- Akama, H., Matsuura, T., Kashiwagi, S., Yoneyama, H., Narita, S.-I., Tsukihara, T., et al. (2004). Crystal structure of the membrane fusion protein, MexA, of the multidrug transporter in *Pseudomonas aeruginosa*. *J. Biol. Chem.* 279, 25939–25942. doi: 10.1074/jbc.C400164200
- Bavro, V. N., Pietras, Z., Furnham, N., Pérez-Cano, L., Fernández-Recio, J., Pei, X. Y., et al. (2008). Assembly and channel opening in a bacterial drug efflux machine. *Mol. Cell* 30, 114–121. doi: 10.1016/j.molcel.2008.02.015
- Du, D., Wang, Z., James, N. R., Voss, J. E., Klimont, E., Ohene-Agyei, T., et al. (2014). Structure of the AcrAB-TolC multidrug efflux pump. *Nature* 509, 512–515. doi: 10.1038/nature13205
- Ferrandez, Y., Monlezun, L., Phan, G., Benabdellah, H., Benas, P., Ulryck, N., et al. (2012). Stoichiometry of the MexA-OprM binding, as investigated by blue native gel electrophoresis. *Electrophoresis* 33, 1282–1287. doi: 10.1002/elps.201100541
- Guan, L., and Nakae, T. (2001). Identification of essential charged residues in transmembrane segments of the multidrug transporter MexB of *Pseudomonas aeruginosa*. *J. Bacteriol.* 183, 1734–1739. doi: 10.1128/JB.183.5.1734-1739.2001
- Hinchliffe, P., Symmons, M. F., Hughes, C., and Koronakis, V. (2013). Structure and operation of bacterial tripartite pumps. *Annu. Rev. Microbiol.* 67, 221–242. doi: 10.1146/annurev-micro-092412-155718
- Janganan, T. K., Bavro, V. N., Zhang, L., Borges-Walmsley, M. I., and Walmsley, A. R. (2013). Tripartite efflux pumps: energy is required for dissociation, but not assembly or opening of the outer membrane channel of the pump. *Mol. Microbiol.* 88, 590–602. doi: 10.1111/mmi.12211
- Kim, J.-S., Jeong, H., Song, S., Kim, H.-Y., Lee, K., Hyun, J., et al. (2015). Structure of the tripartite multidrug efflux pump AcrAB-TolC suggests an alternative assembly mode. *Mol. Cells* 38, 180–186. doi: 10.14348/molcells.2015.2277
- Laemmli, U. K. (1970). Cleavage of structural proteins during the assembly of the head of bacteriophage T4. *Nature* 227, 680–685.
- Li, X. Z., Zhang, L., and Poole, K. (1998). Role of the multidrug efflux systems of *Pseudomonas aeruginosa* in organic solvent tolerance. *J. Bacteriol.* 180, 2987–2991.
- Lomovskaya, O., Zgurskaya, H. I., Totrov, M., and Watkins, W. J. (2006). Waltzing transporters and “the dance macabre” between humans and bacteria. *Nat. Rev. Drug Discov.* 6, 56–65. doi: 10.1038/nrd2200
- Mokhonov, V., Mokhonova, E., Yoshihara, E., Masui, R., Sakai, M., Akama, H., et al. (2005). Multidrug transporter MexB of *Pseudomonas aeruginosa*: overexpression, purification, and initial structural characterization. *Error* 40, 91–100. doi: 10.1016/j.pep.2004.10.002
- Nehme, D., and Poole, K. (2007). Assembly of the MexAB-OprM multidrug pump of *Pseudomonas aeruginosa*: component interactions defined by the study

- of pump mutant suppressors. *J. Bacteriol.* 189, 6118–6127. doi: 10.1128/JB.00718-07
- Nikaido, H. (2009). Multidrug resistance in bacteria. *Annu. Rev. Biochem.* 78, 119–146. doi: 10.1146/annurev.biochem.78.082907.145923
- Pages, J. M., and Amaral, L. (2009). Mechanism of drug efflux and strategies to combat them: challenging the efflux pump of Gram-negative bacteria. *Biochim. Biophys. Acta* 1794, 826–833. doi: 10.1016/j.bbapap.2008.12.011
- Phan, G., Benabdellah, H., Lascombe, M.-B., Benas, P., Rety, S., Picard, M., et al. (2010). Structural and dynamical insights into the opening mechanism of *P. aeruginosa* OprM Channel. *Structure* 18, 507–517. doi: 10.1016/j.str.2010.01.018
- Ponchon, L., Catala, M., Seijo, B., El Khouri, M., Dardel, F., Nonin-Lecomte, S., et al. (2013). Co-expression of RNA-protein complexes in *Escherichia coli* and applications to RNA biology. *Nucleic Acids Res.* 41, e150–e150. doi: 10.1093/nar/gkt576
- Su, C. C., Li, M., Gu, R., Takatsuka, Y., McDermott, G., Nikaido, H., et al. (2006). Conformation of the AcrB multidrug efflux pump in mutants of the putative proton relay pathway. *J. Bacteriol.* 188, 7290–7296. doi: 10.1128/JB.00684-06
- Symmons, M. F., Bokma, E., Koronakis, E., Hughes, C. and Koronakis, V. (2009). The assembled structure of a complete tripartite bacterial multidrug efflux pump. *Proc. Natl. Acad. Sci.* 106, 7173–7178.
- Takatsuka, Y., and Nikaido, H. (2006). Threonine-978 in the transmembrane segment of the multidrug efflux pump AcrB of *Escherichia coli* is crucial for drug transport as a probable component of the proton relay network. *J. Bacteriol.* 188, 7284–7289. doi: 10.1128/JB.00683-06
- Tamura, N., Murakami, S., Oyama, Y., Ishiguro, M., and Yamaguchi, A. (2005). Direct interaction of multidrug efflux transporter acrB and outer membrane channel tolC detected via site-directed disulfide cross-linking<sup>†</sup>. *Biochemistry* 44, 11115–11121. doi: 10.1021/bi050452u
- Thanassi, D. G., Cheng, L. W., and Nikaido, H. (1997). Active efflux of bile salts by *Escherichia coli*. *J. Bacteriol.* 179, 2512–2518.
- Tikhonova, E. B., Yamada, Y., and Zgurskaya, H. I. (2011). Sequential mechanism of assembly of multidrug efflux pump AcrAB-TolC. *Chem. Biol.* 18, 454–463. doi: 10.1016/j.chembiol.2011.02.011
- Tikhonova, E. B., and Zgurskaya, H. I. (2004). AcrA, AcrB, and TolC of *Escherichia coli* form a stable intermembrane multidrug efflux complex. *J. Biol. Chem.* 279, 32116–32124. doi: 10.1074/jbc.M402230200
- Touzé, T., Eswaran, J., Bokma, E., Koronakis, E., Hughes, C., and Koronakis, V. (2004). Interactions underlying assembly of the *Escherichia coli* AcrAB-TolC multidrug efflux system. *Mol. Microbiol.* 53, 697–706. doi: 10.1111/j.1365-2958.2004.04158.x
- Trépout, S., Taveau, J. C., Benabdellah, H., Granier, T., Ducruix, A., Frangakis, A. S., et al. (2010). Structure of reconstituted bacterial membrane efflux pump by cryo-electron tomography. *Biochim. Biophys. Acta* 1798, 1953–1960. doi: 10.1016/j.bbapap.2010.06.019
- Verchère, A., Dezi, M., Adrien, V., Broutin, I., and Picard, M. (2015). *In vitro* transport activity of the fully assembled MexAB-OprM efflux pump from *Pseudomonas aeruginosa*. *Nat. Commu.* 6, 6890. doi: 10.1038/ncomms7890
- Weeks, J. W., Celaya-Kolb, T., Pecora, S., and Misra, R. (2010). AcrA suppressor alterations reverse the drug hypersensitivity phenotype of a TolC mutant by inducing TolC aperture opening. *Mol. Microb.* 75, 1468–1483. doi: 10.1111/j.1365-2958.2010.07068.x
- Zgurskaya, H. I., and Nikaido, H. (1999). Bypassing the periplasm: reconstitution of the AcrAB multidrug efflux pump of *Escherichia coli*. *Proc. Natl. Acad. Sci. U.S.A.* 96, 7190–7195. doi: 10.1073/pnas.96.13.7190

**Conflict of Interest Statement:** The authors declare that the research was conducted in the absence of any commercial or financial relationships that could be construed as a potential conflict of interest.

Copyright © 2015 Enguéné, Verchère, Phan, Broutin and Picard. This is an open-access article distributed under the terms of the Creative Commons Attribution License (CC BY). The use, distribution or reproduction in other forums is permitted, provided the original author(s) or licensor are credited and that the original publication in this journal is cited, in accordance with accepted academic practice. No use, distribution or reproduction is permitted which does not comply with these terms.

# The ins and outs of RND efflux pumps in *Escherichia coli*

João Anes, Matthew P. McCusker, Séamus Fanning and Marta Martins\*

UCD Centre for Food Safety, School of Public Health, Physiotherapy and Population Science, UCD Centre for Molecular Innovation and Drug Discovery, University College Dublin, Dublin, Ireland

## OPEN ACCESS

### Edited by:

Attilio Vittorio Vargiu,  
Università degli Studi di Cagliari, Italy

### Reviewed by:

Rajeev Misra,  
Arizona State University, USA  
Kunihiro Nishino,  
Osaka University, Japan

### \*Correspondence:

Marta Martins,  
UCD Centre for Food Safety, School  
of Public Health, Physiotherapy  
and Population Science, UCD Centre  
for Molecular Innovation and Drug  
Discovery, University College Dublin,  
Room S1.06, Science Centre South  
Belfield, Dublin 4, Ireland  
marta.martins@ucd.ie

### Specialty section:

This article was submitted to  
Antimicrobials, Resistance  
and Chemotherapy,  
a section of the journal  
*Frontiers in Microbiology*

Received: 14 March 2015

Accepted: 28 May 2015

Published: 10 June 2015

### Citation:

Anes J, McCusker MP, Fanning S  
and Martins M (2015) The ins  
and outs of RND efflux pumps  
in *Escherichia coli*.  
*Front. Microbiol.* 6:587.  
doi: 10.3389/fmicb.2015.00587

Infectious diseases remain one of the principal causes of morbidity and mortality in the world. Relevant authorities including the WHO and CDC have expressed serious concern regarding the continued increase in the development of multidrug resistance among bacteria. They have also reaffirmed the urgent need for investment in the discovery and development of new antibiotics and therapeutic approaches to treat multidrug resistant (MDR) bacteria. The extensive use of antimicrobial compounds in diverse environments, including farming and healthcare, has been identified as one of the main causes for the emergence of MDR bacteria. Induced selective pressure has led bacteria to develop new strategies of defense against these chemicals. Bacteria can accomplish this by several mechanisms, including enzymatic inactivation of the target compound; decreased cell permeability; target protection and/or overproduction; altered target site/enzyme and increased efflux due to over-expression of efflux pumps. Efflux pumps can be specific for a single substrate or can confer resistance to multiple antimicrobials by facilitating the extrusion of a broad range of compounds including antibiotics, heavy metals, biocides and others, from the bacterial cell. To overcome antimicrobial resistance caused by active efflux, efforts are required to better understand the fundamentals of drug efflux mechanisms. There is also a need to elucidate how these mechanisms are regulated and how they respond upon exposure to antimicrobials. Understanding these will allow the development of combined therapies using efflux inhibitors together with antibiotics to act on Gram-negative bacteria, such as the emerging globally disseminated MDR pathogen *Escherichia coli* ST131 (O25:H4). This review will summarize the current knowledge on resistance-nodulation-cell division efflux mechanisms in *E. coli*, a bacteria responsible for community and hospital-acquired infections, as well as foodborne outbreaks worldwide.

**Keywords:** *Escherichia coli*, efflux pumps, antimicrobial resistance, antibiotics, biocides

## Introduction

*Escherichia coli* is a well-recognized human pathogen. While most strains do not cause disease, some serotypes are pathogenic. *E. coli* is the most common cause of UTIs worldwide, but can

**Abbreviations:** ABC, ATP-binding cassette; EPI, efflux pump inhibitor; HGT, horizontal gene transfer; MATE, multidrug and toxic compound extrusion; MDR, multidrug resistant; MFP, membrane fusion protein; OMP, outer membrane protein; PMF, proton-motive force; RND, resistance-nodulation-cell division; SMR, small multidrug resistance; UTI, urinary tract infection.

also cause bacteraemia and neonatal meningitis as well as serious food-borne infections. The recent emergence of specific serotypes such as O157:H7, responsible for food- and water-borne outbreaks in Europe (Monea et al., 2010; Pennington, 2014) and the U.S. (Centers for Disease Control and Prevention [CDC], 2006), and the enterohaemorrhagic *E. coli* O104:H4 that caused the 2011 German outbreak, resulting in 53 deaths (Radosavljevic et al., 2014), pose a serious threat to public health. More recently, the worldwide pandemic clone *E. coli* O25:H4 ST131 has emerged harboring CTX-M-type beta-lactamases as well as several virulence genes that result in a MDR phenotype (Olesen et al., 2013).

Treatment of *E. coli* infections depends on the diagnosis. Antibiotic therapy normally involves the administration of co-trimoxazole, nitrofurantoin, or a fluoroquinolone and only in life-threatening situations a third-generation cephalosporin can be administered (Piddock, 2006). The extensive use of fluoroquinolone-based antimicrobials, has been a major driver in the development of antibiotic resistant *E. coli* strains (Cagnacci et al., 2008; Lamikanra et al., 2011; Matsumura et al., 2013; Michael et al., 2014).

Antimicrobial resistance has been considered the new challenge of the 21st century (World Health Organization (WHO), 2014). The increased level of resistance to antimicrobial agents has raised serious questions concerning the way in which these therapeutic compounds are being used (Gilbert and McBain, 2001). Global organizations have expressed their concern on this issue, suggesting that increased focus and efforts are required to address this challenge (World Health Organization (WHO), 2014). The intensive use of antimicrobial compounds in the human clinical setting and in animals as growth promoters (Castanon, 2007) or as a preventive measure against infection, is considered to be one of the root causes for selection of resistant bacteria. The constant exposure to sub-lethal concentrations of antimicrobial compounds, along with commonly used biocides for disinfection processes, can play an important role in the selection and emergence of resistant strains (Andersson and Hughes, 2014; Capita et al., 2014). The use of certain antibiotics, specifically fluoroquinolones, has led to an increase in MDR phenotypes associated with the overexpression of efflux pumps (Wang et al., 2001). In addition, the presence of naturally occurring heavy metals and the use of chemicals in agriculture for fertilization of the soil can also induce the expression of efflux pumps in environmental strains leading to cross-resistance (Peltier et al., 2010). Strengthening our understanding of these resistance mechanisms will contribute to the development of new compounds that can ultimately help to overcome this challenge.

## Mechanisms of Antimicrobial Resistance

Gram-negative bacteria, like *E. coli*, have several mechanisms of resistance when it comes to surviving the selective pressure exerted by antimicrobial agents. Some mechanisms can be definitive whereas others may reverse when the selective pressure is released or completely removed. Resistance can occur due to:

- (i) accumulation of mutations involved in specific antimicrobial targets (e.g., mutations in quinolone resistance-determining regions (QRDRs) in *gyrA*, *gyrB*, *parE*, and *parC* genes) (Moon et al., 2010);
- (ii) antimicrobial inactivation/modification (e.g., production of β-lactamase enzymes; Poole, 2002);
- (iii) acquisition of mobile genetic elements such as plasmids, transposons, or integrons acquired by HGT (Carraro et al., 2014; Gillings, 2014);
- (iv) alteration in the cell wall composition (e.g., lipopolysaccharide modification; Gunn, 2001);
- (v) reduced expression of cell wall porins, resulting in decreased influx of antimicrobials (Masi and Pagès, 2013); and
- (vi) over-expression of efflux pumps (Wang et al., 2001).

## Efflux Pumps

Classically, efflux pumps can be classified into five different families: the ABC superfamily; the major facilitator superfamily (MFS); the MATE family; the SMR family and the RND family (Poole, 2007; Li and Nikaido, 2009; Delmar et al., 2014). Recently, the proteobacterial antimicrobial compound efflux (PACE) family was identified in some Gram-negative bacteria. However, *E. coli* strains do not seem to encode PACE efflux proteins unless carried by mobile genetic elements (Hassan et al., 2015a,b). While all the efflux pump families are well distributed among Gram-negative bacteria, RND are responsible for the extrusion of a broad range of compounds (Nikaido and Pagès, 2012). Depending on the efflux mechanism different energy sources can be used. ABC transporters for instance, use ATP as the energy source for extrusion of toxic compounds (Lubelski et al., 2007), whereas MATE pumps are driven by  $\text{Na}^+/\text{H}^+$  drug antiport systems (Alvarez-Ortega et al., 2013). The MFS, SMR, and RND pumps are PMF driven, which means that these are dependent on the pH gradient. For instance, *E. coli* has been shown to be able to extrude ethidium bromide more efficiently at lower pH values when compared to higher pH values (Martins et al., 2009; Amaral et al., 2011).

## RND General Structure and Substrates

Resistance-nodulation-cell division transporters operate as part of a tripartite system composed of the RND pump located in the inner membrane, a periplasmic adaptor protein from the MFP family and an OMP belonging to the outer membrane factor (OMF) family located in the outer membrane (Nikaido, 2011). The OMP TolC, for example, works in combination with other RND, ABC, and MFS efflux pumps (Tanabe et al., 2009; Turlin et al., 2014). The absence of any of these components renders the entire complex non-functional. Nonetheless, the efflux systems show a cooperative interaction between them and can act sequentially when one fails (Lee et al., 2000; Tal and Schuldiner, 2009). RND transporters can be classified into two different subfamilies according to their substrates, the hydrophobic and amphiphilic efflux RND (HAE-RND) family and the heavy metal efflux RND (HME-RND) family (Nies, 2003). In *E. coli* there are five efflux transporters that belong to the HAE-RND

subfamily, AcrAB (Tikhonova and Zgurskaya, 2004; Pos, 2009), AcrAD (Rosenberg et al., 2000; Elkins and Nikaido, 2002), AcrEF (Nishino and Yamaguchi, 2001), MdtAB (Baranova and Nikaido, 2002; Nagakubo et al., 2002), and MdtEF (Kobayashi et al., 2006; Zhang et al., 2011). In contrast, there is only one efflux transporter that belongs to the HME-RND, the CusCFBA (Su et al., 2011a; Chacón et al., 2014; Delmar et al., 2014).

## Acriflavine (Acr) Efflux System

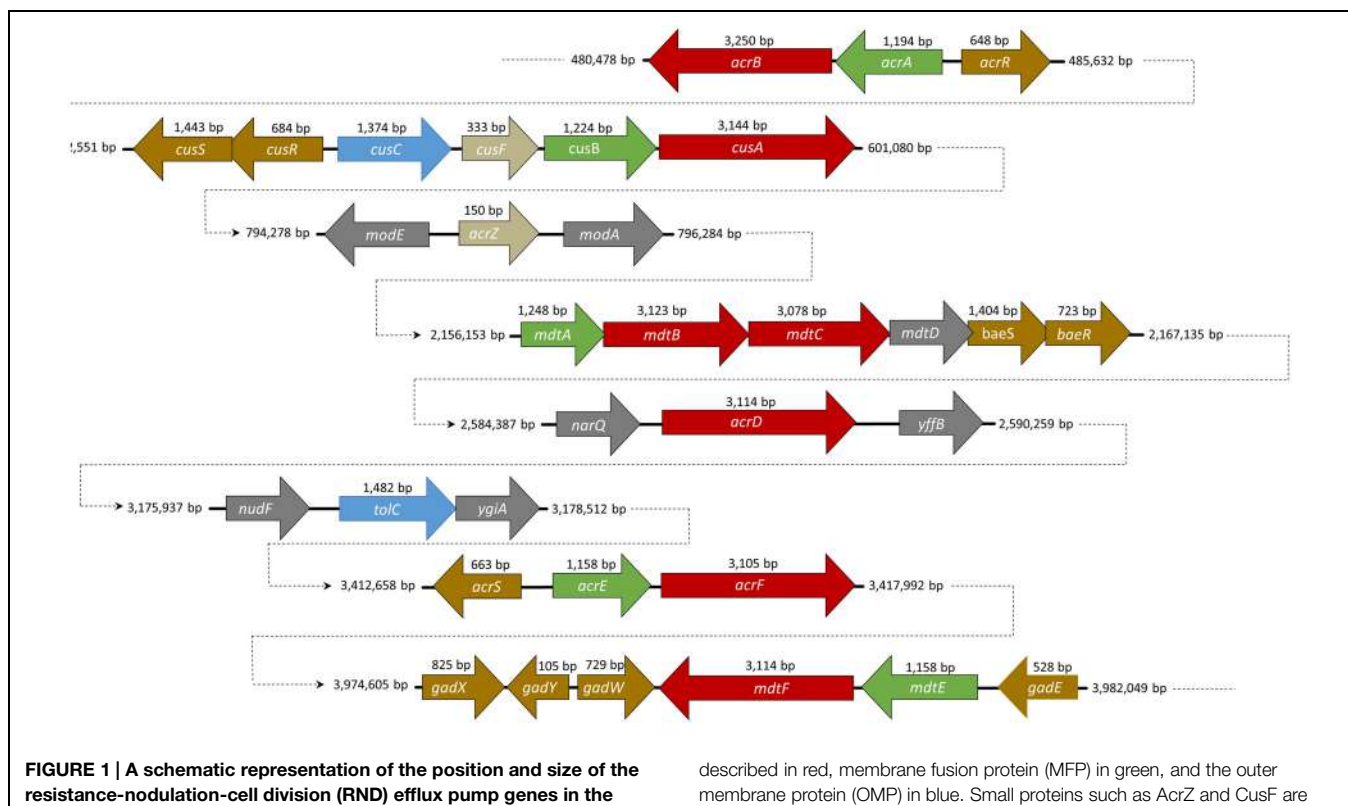
AcrAB is encoded in a single operon for the RND and the MFP, under the control of the transcriptional repressor, AcrR and AcrS (Wang et al., 2001; Hirakawa et al., 2008; **Figure 1**). SdiA (Wei et al., 2001) and CpxRA (Yang et al., 2014) have also been shown to regulate expression of *acrAB*. The outer membrane component, TolC, is coded elsewhere on the chromosome (Fralick, 1996) and is part of the *marA/soxS/rob* regulon (Warner and Levy, 2010).

In the last years, there has been more evidence favoring a stoichiometry of 3:6:3, comprising an AcrB trimer, an AcrA hexamer and a TolC trimer (Tikhonova et al., 2011; Xu et al., 2011; Du et al., 2014). However, the functional stoichiometry remains unclear and under some controversy (Zgurskaya and Nikaido, 2000; Fernandez-Recio et al., 2004; Symmons et al., 2009).

The RND protein AcrB is composed of 1,049 amino acids and is distributed throughout the transmembrane domain and

the large periplasmic domain (Husain and Nikaido, 2010; **Figure 2A**). The first symmetrical crystal structure for AcrB protein was resolved by Murakami et al. (2002) at a 3.5 Å resolution in which three AcrB protomers were organized as a homotrimer. Co-crystallization of AcrB with several ligands (including 6-rhodamine 6G, ethidium, dequalinium and ciprofloxacin) showed that these ligands bind near the transmembrane domain and in various positions within the binding pocket. The binding is established primarily through hydrophobic, aromatic stacking, and van der Waals interactions (Yu et al., 2003). Asymmetric crystal structures of AcrB were later resolved using minocycline, doxorubicin (Murakami et al., 2006), ethidium, dequalinium (Seeger et al., 2006), and designed ankyrin repeat proteins (DARPins), the latter being an inhibitor designed specifically for AcrB, as a substrate (Sennhauser et al., 2007).

The asymmetric structure obtained indicated that each protomer takes on a different conformation, which is related to a different stage of the ligand binding and extrusion mechanism (**Figure 2B**). One of the monomers presents a loose (L) conformation. Here, the substrates can enter from three different open channels (**Figures 2A,B**; 1, 2, and 3). Substrates can enter via the lower external depression or cleft (**Figures 2A,B**; 1) in the periplasmic side close to the outer leaflet away from the membrane surface. Substrates can also enter through the vestibule, located between the protomers (**Figures 2A,B**; 2), facing toward the periplasm, close to the external surface of the membrane bilayer (Murakami et al., 2006; Sennhauser et al., 2007). The last channel (**Figures 2A,B**; 3) in which substrates



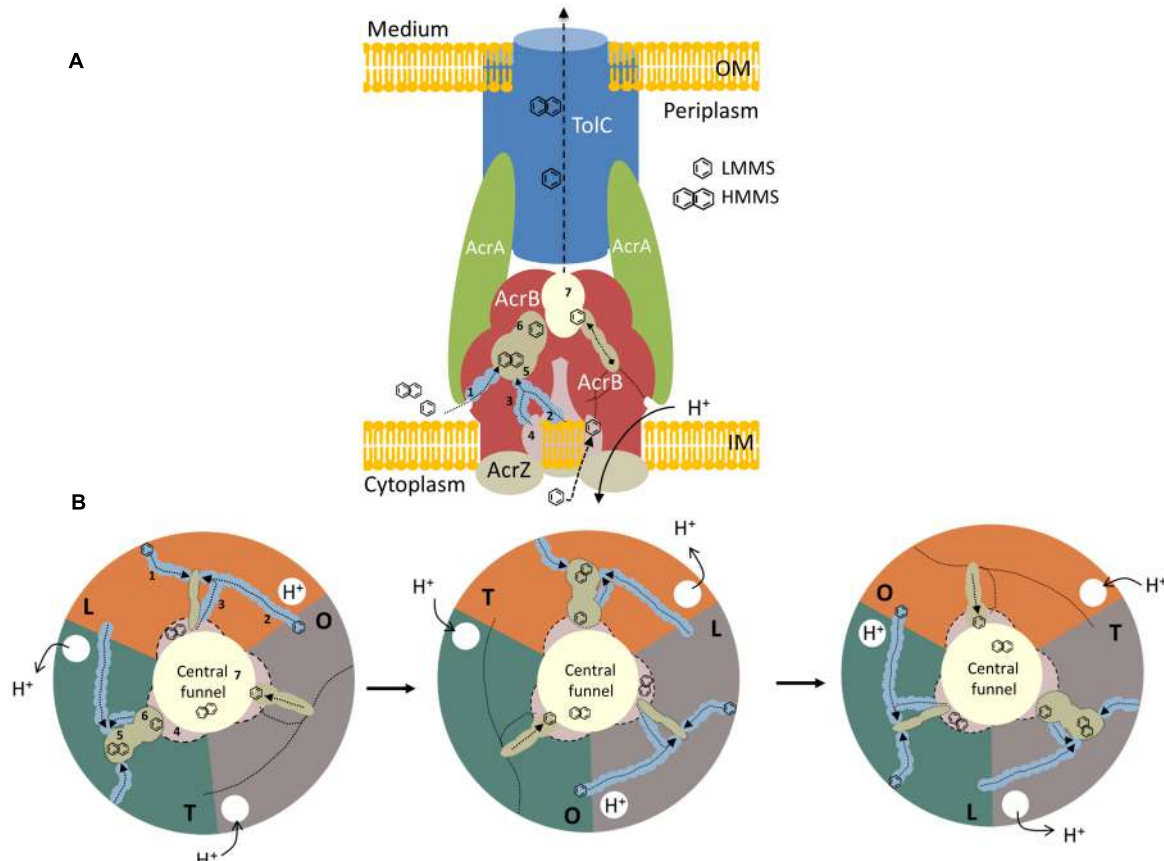


**FIGURE 2 | A model representation of AcrABZ-TolC efflux pump. (A)** Side view of a schematic model of a tripartite efflux system in Gram-negative bacteria. RND protein AcrB is described in red, the MFP, AcrA is indicated in green, and the OMP, TolC in blue. The small protein AcrZ is colored in beige. OM, outer membrane; IM, inner membrane. **(B)** Top view of the different stages of the ligand extrusion mechanism in AcrB RND efflux pump. Each color

represents a protomer of the AcrB protein. 1: lower external depression or cleft channel; 2: vestibule channel; 3: central cavity channel; 4: central cavity; 5: proximal binding pocket; 6: distal binding pocket; 7: central funnel. LMMS, low molecular mass substrates; HMMS, high molecular mass substrates. Adapted from (Murakami et al., 2002, 2006; Seeger et al., 2006; Husain et al., 2011; Nakashima et al., 2011).

can enter is located directly in the central cavity (**Figures 2A,B**; 4; Husain and Nikaido, 2010; Husain et al., 2011). The central cavity is involved in the transport of substrates from the cytosol (Yu et al., 2003). Once the substrate that derives from the cytoplasm or the periplasm binds to one of the channels, the binding pocket expands to accommodate the substrate. Once expanded, the substrate moves through the uptake channel, or tunnel, binding to the different locations within the multisite binding pocket (Murakami et al., 2006). The binding step occurs in the interior of the periplasmic domain at the tight protomer (T). High molecular mass substrates (HMMS), such as rifampicin or erythromycin, bind to the proximal binding pocket (**Figures 2A,B**; 5; Nakashima et al., 2011). Low molecular mass substrates (LMMS), as minocycline or doxorubicin, on the other hand, travel through the proximal pocket and bind further up on the distal pocket (**Figures 2A,B**; 6; Murakami et al., 2006). The extrusion of the substrate is then dependent on the last open protomer (O) of the AcrB trimer. Here, the conformation of the central helix of the protomer is changed due to the protonation closing the open channels and opening

the gate into the central funnel (**Figures 2A,B**; 7). Finally, the substrate is pushed out to the central funnel by the shrinking of the binding pocket where it will bind to the TolC domain and is subsequently extruded from the bacterial cell (Murakami et al., 2006; Seeger et al., 2006; Sennhauser et al., 2007; Nikaido and Pagès, 2012). An in depth review on the structure and transport of AcrB can be found elsewhere (Yu et al., 2003; Pos, 2009; Husain and Nikaido, 2010; Nakashima et al., 2011; Li et al., 2015).

The MFP AcrA (**Figure 2A**) is anchored to the inner membrane by the N-terminal lipid modification. This protein is composed of a membrane proximal (MP) domain, a  $\beta$ -barrel domain, a lipoyl domain and an  $\alpha$ -hairpin domain (Symmons et al., 2009). The later domain is known to interact with the outer membrane TolC whereas the first three domains are responsible for the interaction with AcrB (Elkins and Nikaido, 2003; Lobedanz et al., 2007; Kim et al., 2010a). Other studies show that AcrA is able to bind both RND and OMP proteins independently with nanomolar affinity (Tikhonova et al., 2011). AcrA oligomerisation and pH proved to be essential for AcrB

affinity (Tikhonova et al., 2009, 2011; Xu et al., 2011; Kim et al., 2010a, 2015). However, some thermodynamic interaction studies have shown that AcrA-TolC binds spontaneously whereas the interaction between AcrB and TolC is not thermodynamically favored (Touzé et al., 2004). AcrA function as a dimeric unit and each AcrA dimer has a propensity to form a trimer when in contact with an AcrB protomer, establishing a AcrA-AcrB stoichiometry of 6:3 (Tikhonova et al., 2011; Xu et al., 2011). The AcrA MP domain is also known to play an important role in the assembly of the tripartite efflux system (Ge et al., 2009; Weeks et al., 2010; Tikhonova et al., 2011).

The TolC outer membrane channel is made up of three TolC protomers that form a cannon shaped tunnel of 140 Å (Koronakis et al., 2000; **Figure 2A**). This channel makes the connection between the periplasmic space and the cell exterior through the outer membrane (Hinchliffe et al., 2013). The 12-stranded  $\beta$ -barrel, formed by four  $\beta$ -strands from each TolC protomer, are constitutively open to the external medium, whereas the periplasmic  $\alpha$ -barrel comprises 12  $\alpha$ -helices in an antiparallel arrangement, four from each protomer (Koronakis et al., 2000). Here an aspartate ring of residues establish a constriction that effectively closes the TolC pore to substrates (Higgins et al., 2004). TolC assumes a closed conformation when inactive. Only a small portion of TolC is used to support efflux activity and it is expressed at lower levels. The expression of AcrAB has no effect on TolC expression (Krishnamoorthy et al., 2013). The TolC protein is also part of others efflux systems such as the EmrAB-TolC or the MacAB-TolC of the MFS and ABC superfamilies, respectively, (Tanabe et al., 2009; Lu and Zgurskaya, 2012).

The assembly mechanism of the tripartite system is not fully understood, to date. Therefore, several models have been generated over the years. The *Adaptor Wrapping Model*, assumes that AcrB and TolC connect individually; plasmon surface resonance data also confirms this interaction (Tikhonova et al., 2011). TolC binds to the AcrB crown through the outer helices H3 and H4 (Weeks et al., 2010). As a result of this interaction, the inner helices H7 and H8 relax exposing the intraprotomer groove. The exposed intraprotomer groove is a high-affinity site for AcrA (Bavro et al., 2008). Binding to the exposed grooves of TolC cause alterations in the MP domain of AcrA (Krishnamoorthy et al., 2013); these conformational changes induce the opening of the TolC (Bavro et al., 2008). However, the partial opening of TolC, using a TolC mutant, rendered the tripartite system unstable and lead to disassembly of AcrAB-TolC efflux pump (Tikhonova et al., 2011). To date, there seems to be no consensus as to how the opening of TolC actually occurs.

The other model generated over the last years is the *Adaptor Bridging Model*. This model assumes no direct interaction between AcrB and TolC (Kim et al., 2010a; Xu et al., 2012; Du et al., 2014). Thermodynamic data has also shown that this interaction is not favored (Touzé et al., 2004). This model was generated based on the structure of other efflux systems with similar tripartite composition to AcrAB-TolC (Yum et al., 2009; Xu et al., 2012). These models also claim the fact that cross-linking interaction with cysteine only indicates that the

protein are in close proximity with each other; it does not mean that they are stable (Touzé et al., 2004). In fact, attempts at cross-linking have shown that the proteins do not form functional complexes (Kim et al., 2010a; Xu et al., 2011), or barely functional complexes (Du et al., 2014). In this model, AcrB and TolC are bridged in the periplasm through an AcrA hexamer (Xu et al., 2011; Du et al., 2014; Kim et al., 2015). When packed, AcrA protomers generate a funnel-like structure with a sealed central channel, closed to the periplasm (Du et al., 2014). The AcrA  $\alpha$ -helical hairpins interact with the periplasmic ends of the  $\alpha$ -helical coiled coils of TolC in an intermeshing-like cogwheel structure (Xu et al., 2011; Kim et al., 2015). The  $\beta$ -barrel and lipoyl domains of AcrA form a triangular hollow chamber, who's bottom opens into the funnel of AcrB (Xu et al., 2011; Du et al., 2014). The interaction with the  $\alpha$ -helical hairpins of AcrA change the conformation of the TolC hexamer to the open form (Du et al., 2014). TolC remains in this open form throughout the entire transport cycle.

Recently, a small protein AcrZ, formerly designated YbhT, was shown to interact with AcrB through the inner membrane (Hobbs et al., 2012). The *acrZ* gene is co-regulated by MarA, Rob and SoxS, the same regulators of AcrAB efflux pump. The gene is located between two molybdenum-flanking operons involved in molybdenum uptake and the regulation of molybdenum cofactor synthesis (see **Figure 1**). Structures such as tetracycline or acriflavine, or other substrates with several polycyclic features, are suggestive of the molybdenum cofactor. Enzymes such as xanthine dehydrogenase and aldehyde oxidoreductase (that requires a molybdenum cofactor) detoxify compounds that may be extruded through AcrB RND pump (Hobbs et al., 2012). The AcrZ protein was shown to help AcrAB-TolC complex to recognize and export chloramphenicol, tetracycline and puromycin (Hobbs et al., 2012). These authors suggested that AcrZ might trigger some conformational changes in the periplasmic domain affecting the recognition and capture of substrates with lower hydrophobicity.

AcrAB-TolC efflux system is known to be responsible for the extrusion of a broad range of compounds such as lipophilic antimicrobial drugs, i.e., penicillin G, cloxacillin, nafcillin, macrolides, novobiocin, linezolid, and fusidic acid (Nikaido, 2011); antibiotics (such as fluoroquinolones, cephalosporins, tetracyclines; Nikaido and Takatsuka, 2009); various dyes (i.e., crystal violet, acridine, acriflavine, ethidium, 6-rhodamine 6G); detergents [sodium dodecyl sulfate (SDS) and Triton X-100; Pos, 2009]; organic solvents (hexane, cyclohexane); steroid hormones (bile acids, estradiol, and progesterone) (Elkins and Mullis, 2006); essential oils (Fadli et al., 2014); and others (see **Table 1**). A common feature of all the substrates is that, to some extent, all contain lipophilic domains (Nikaido, 1996). However, the way these substrates interact with the phospholipid bilayer and the RND pumps is not yet completely defined.

AcrD, another acriflavine RND-type efflux pump, plays a similar role to AcrB. In contrast with the other acriflavine resistance efflux systems, *acrD* does not form an operon with

**TABLE 1 | Resistance-nodulation-cell division (RND) efflux pumps substrates and regulators.**

| Efflux pump | Substrates   | RND Regulator(s)  | Reference   |
|-------------|--|---|---|
| AcrAB-TolC  | $\beta$ -lactams, quinolones, tetracyclines, tigecycline, chloramphenicol, steroid hormones, lincosamides, benzene, cyclohexane, SDS, Triton X-100, rifampicin, bile salts, free fatty acids, geraniol, enterobactin, triclosan, chlorhexidine, quaternary ammonium compounds, acriflavine, ethidium bromide | AcrR<br>AcrS<br>SdiA<br>MarRAB<br>Rob<br>SoxS<br>CpxRA                | Perreten et al. (2001), Wang et al. (2001), Rahmati et al. (2002), Rosenberg et al. (2003), Hirata et al. (2004), Elkins and Mullis (2006), Poole (2007), Hirakawa et al. (2008), Lennen et al. (2013), Shah et al. (2013), Horiyama and Nishino (2014) |
| AcrAD-TolC  | Aminoglycosides, steroid hormones, enterobactin, $\beta$ -lactams, quinolones, Sodium dodecyl sulfate (SDS), deoxycholate  | BaeR<br>SdiA<br>CpxRA   | Nishino and Yamaguchi (2001), Wei et al. (2001), Hirakawa et al. (2003), Elkins and Mullis (2006), Poole (2007), Nishino et al. (2010), Horiyama and Nishino (2014), Kobayashi et al. (2014)  |
| AcrEF-TolC  | Quinolones, tigecycline, solvents  | H-NS<br>SdiA  | Jellen-Ritter and Kern (2001), Kobayashi et al. (2001), Wei et al. (2001), Hirata et al. (2004), Nishino and Yamaguchi (2004)   |
| MdtABC-TolC | Novobiocin, bile salts, enterobactin, quinolones, fosfomycin, benzalkonium, SDS, zinc, myricetin   | BaeSR<br>CpxRA  | Nishino and Yamaguchi (2001), Baranova and Nikaido (2002), Nagakubo et al. (2002), Hirakawa et al. (2003), Nishino et al. (2010), Kim and Nikaido (2012), Wang and Fierke (2013), Horiyama and Nishino (2014)   |
| MdtEF-TolC  | Erythromycin, doxorubicin, benzalkonium, SDS, deoxycholate, crystal violet, ethidium bromide, nitrosyl indole, rhodamine 6G, tetraphenylphosphonium bromide, free fatty acids  | H-NS<br>YdeO<br>CRP<br>GadX<br>ArcBA<br>GadE<br>EvgAS<br>RpoS<br>DsrA | Nishino and Yamaguchi (2001, 2002, 2004), Kobayashi et al. (2006), Nishino et al. (2008a,b, 2009, 2011), Zhang et al. (2011), Deng et al. (2013), Lennen et al. (2013)  |
| CusCFBA     | Silver, copper, fosfomycin, ethionamide, dinitrobenzene  | CusSR   | Nishino and Yamaguchi (2001), Conroy et al. (2010), Kim et al. (2011), Gudipaty et al. (2012)   |

the MFP gene *acrA* (Figure 1; Rosenberg et al., 2000). This gene is under the control of the regulons BaeR (Hirakawa et al., 2003), SdiA (Wei et al., 2001), and CpxRA (Nishino et al., 2010). With 1,037 amino acids and 66.1% homology with AcrB, AcrAD-TolC has a different substrate specificity mainly for hydrophilic substrates such as aminoglycosides (Rosenberg et al., 2000), negatively charged  $\beta$ -lactams (Kobayashi et al., 2014) and mild specificity for SDS, deoxycholate, novobiocin, cholic acid (Nishino and Yamaguchi, 2001), progesterone (Elkins and Mullis, 2006), and others. AcrD was used as a model to understand how RND pumps capture their substrates. This efflux pump was shown to capture aminoglycosides from both the periplasm and the cytoplasm (Aires and Nikaido, 2005). The results were then extrapolated in part to AcrB due to the close homology between both proteins. A chimeric study between AcrB and AcrD showed that the replacement of the two large external loops of AcrD with the equivalent loops of AcrB altered the substrate range of AcrD to a broader one, more typical of AcrB. Conversely, the replacement of the two large loops in AcrB with those of AcrD lead to an efflux pump that had a narrower substrate range, similar to that of an AcrD efflux pump. This demonstrated the importance these large periplasmic loops of AcrB and AcrD play in the substrate range of these pumps (Elkins and Nikaido, 2002).

AcrEF-TolC is also part of the acriflavine efflux system. The efflux system is encoded in an operon wherein the RND *acrF* gene is located together with the MFP gene *acrE*, with both genes under the control of the regulator *sdiA* (Wei et al., 2001). Histone-like proteins (e.g., H-NS, HU, IHF) are a key

component of the bacterial nucleoid and play an important role in global gene regulation (Nishino and Yamaguchi, 2004). The inactivation of H-NS increases the expression of AcrEF, indicating that H-NS represses the expression of AcrEF. The RND protein AcrF has 1,034 amino acids and 77.6% homology with AcrB, whereas AcrE has 385 amino acids and 69.3% homology with AcrA. Due to the close homology observed it is predicted that this system assembles in a similar manner as AcrAB.

The complex, AcrEF is postulated to be functionally identical to AcrAB due to its similar broad substrate range (Nishino and Yamaguchi, 2001). Nonetheless, *acrEF* expression is very low under laboratory conditions (Lau and Zgurskaya, 2005). Deletion *acrEF* produced no observable effect on the resistance phenotype in *E. coli* (Sulavik et al., 2001). Currently, it is still unclear under what physiologic conditions AcrEF is expressed.

The recombination of insertion sequence (IS) elements upstream of the *acrEF* operon increases the expression of the efflux system (Misra et al., 2015). Using an *acrB* mutant with increased expression of AcrEF the hypersensitivity to solvents generated by the mutant was suppressed (Kobayashi et al., 2001); the same pattern was also seen for fluoroquinolones (Jellen-Ritter and Kern, 2001).

The acriflavine efflux system is one of the most studied systems and presents a broad range of substrate resistance. Understanding how these tripartite systems act in different conditions has given us some insights that could be used to design and develop new inhibitor compounds.

## Multidrug Transport (Mdt) Efflux System

MdtABC-TolC is encoded in a single operon under the control of the two-component regulatory system, BaeSR (**Figure 1**; Nagakubo et al., 2002). During envelope stress this efflux system can also be activated by the CpxRA regulon (Nishino et al., 2010). The *mtdD* gene, which is also part of this operon, codes for a MFS transporter (Baranova and Nikaido, 2002). Nonetheless, this protein is not necessary for increased resistance to antimicrobials. Recently, MdtD has been associated with efflux of iron and citrate, being renamed as IceT (Frawley et al., 2013). MdtABC-TolC efflux system is responsible for the extrusion of substrates such as novobiocin, bile salts (Nagakubo et al., 2002), quinolones, fosfomycin, detergents (Nishino and Yamaguchi, 2001), zinc (Wang and Fierke, 2013), and myricetin (Kim and Nikaido, 2012).

The MdtABC-TolC efflux system presents a heterotrimeric conformation for the RND pump, in contrast to the pattern seen for AcrB, AcrD, AcrF, and CusA. The RND pump MdtBC, formerly known as YegNO, is composed by two MdtB protomers of 1,040 amino acids each, and one MdtC protomer with 1,025 residues (Kim et al., 2010b). Remarkably, these two protomers only show 49% similarity between them (Kim and Nikaido, 2012). In this case, each protomer has a specific function; MdtC is likely to be involved in substrate binding and extrusion whereas MdtB has been shown to induce conformational changes in the trimer, when the substrate binds to MdtC, leading to proton translocation (Kim and Nikaido, 2012). There is little structural information about this efflux system as there is no crystallographic data available to date. A homology model based on the AcrB crystal structure showed that MdtC has a broad tunnel beginning at the external cleft and continuing all the way to the interior edge of the binding pocket. The tunnel appears to narrow before it reaches the binding pocket (Kim and Nikaido, 2012). Based on this model, a substrate mechanism was predicted in which the substrate binds first to the peripheral site near the cleft. The binding of the substrate may induce proton translocation through the MdtB subunit(s), which will cause conformational changes mainly at the opening of the tunnel and the expansion of the binding pocket in the MdtC protomer, in a manner similar to what is observed in AcrAB (Kim and Nikaido, 2012).

MdtEF-TolC is the other known multidrug efflux system in this family, formerly referred to as YhiUV-TolC. The genes encoding this efflux system are located in an operon (**Figure 1**) under the control of *gadX* (Nishino et al., 2008b), *gadY* (Kobayashi et al., 2006) and *gadE* (Deng et al., 2013), which are regulators of acid resistance (**Table 1**). This operon can be activated in complex cascades or directly by several major regulators, such as EvgAS (Nishino and Yamaguchi, 2002); ArcBA (Deng et al., 2013); RpoS (Kobayashi et al., 2006); YedO (Nishino et al., 2009); or by the MdtEF repressor of cyclic AMP receptor protein (Nishino et al., 2008a), or the histone-like protein H-NS (Nishino and Yamaguchi, 2004). MdtEF efflux pump function is related with cell growth, its maximal expression level is achieved in late stationary phase of *E. coli* growth (Kobayashi et al., 2006).

Proteins MdtE and MdtF share 55 and 71% homology with AcrA and AcrB, respectively. Due to this fact the same conformational structure was assumed for the purpose of this review. MdtEF is known to induce resistance to oxacillin, cloxacillin, nafcillin, erythromycin, rhodamine 6G, and SDS under the controlled expression of the regulator, GadX (Nishino et al., 2008b). It can also induce resistance to benzalkonium, deoxycholate (Nishino and Yamaguchi, 2001), indole (Zhang et al., 2011), and others. In *E. coli*, MdtEF has an important role in cell growth under anaerobic conditions (Zhang et al., 2011). MdtEF mutants have shown susceptibility to indole nitrosative derivatives, a by-product formed when the bacterium metabolizes nitrate under anaerobic conditions. It was also observed that under respiratory stress MdtEF was able to extrude erythromycin (Zhang et al., 2011).

## Copper Transporting (Cus) Efflux System

The CusCFBA system is the only HME-RND identified in *E. coli* to date. It is responsible for the extrusion of silver ( $\text{Ag}^+$ ) and copper ( $\text{Cu}^+$ ). Although recognized for the extrusion of these two ions it was also found to induce resistance to fosfomycin (Nishino and Yamaguchi, 2001), dinitrophenol, dinitrobenzene, and ethionamide (Conroy et al., 2010). The *cus* genes, *cusCFBA*, are all located in the same operon (**Figure 1**) under the control of *cusR* and *cusS* encoding a response regulator and a histidine kinase, respectively, (Gudipaty et al., 2012). This efflux system plays an important role in  $\text{Cu}^+$  homeostasis in bacterial cells (Rademacher and Masepohl, 2012). The Cus system, like all the RND efflux pumps presents a tripartite structure or a tetrapartite structure, if CusF is taken into consideration. For the purpose of this review, the system will be considered as a tripartite system, as was the case for the AcrAB-TolC system and AcrZ.

The system is composed by the RND efflux pump (CusA); the MFP (CusB); and by the OMP (CusC). These proteins assemble together in a stoichiometry identical to the AcrB, CusA<sub>(3)</sub>:CusB<sub>(6)</sub>:CusC<sub>(3)</sub> (Su et al., 2011b; Delmar et al., 2014).

With 1,047 amino acids CusA was first resolved at 3.5 Å suggesting a homotrimer configuration. Each protomer is composed by 12 transmembrane  $\alpha$ -helices, four of each protruding into the cytoplasm and two into the periplasm (Long et al., 2010). Consequently,  $\text{Cu}^+$  and  $\text{Ag}^+$  were found to bind to the residues M573, M623, and M672 located at the bottom of the periplasmic cleft together with other conserved residues (Su et al., 2012). Once bound, both  $\text{Cu}^+$  and  $\text{Ag}^+$  appeared to induce significant conformational changes in both the periplasmic and transmembrane domains of CusA (Long et al., 2010; Su et al., 2012). The changes seemed to create a doorway for metal ions to enter the periplasmic domain of the pump. The cleft, which is initially closed, is open in the presence of  $\text{Ag}^+$  or  $\text{Cu}^+$  revealing the binding site. At the same time the changes caused by the binding may also relate to transmembrane signaling, which are thought to initiate proton translocation across the membrane (Delmar et al., 2013).

Four distinct methionine pairs have been identified on the inside of the channel formed by each protomer of the CusA pump. Three of these pairs: M410–M501, M403–M486, and M391–M1009 are found below the binding site in the transmembrane domain, and one, M271–M755, is located at the bottom of the periplasmic funnel. This channel, together with the three-methionine residues from the binding site, spans the entire length of each protomer. This represents a pathway for the transport of metal ions (Su et al., 2011a). Metal ions can enter through the binding site inside the cleft directly through the periplasmic cleft or *via* the cytoplasm through the methionine pairs within the transmembrane region. The metal ions bound at the methionine pair in the periplasmic funnel are released into the central funnel following the methionine pathway (Su et al., 2011a).

The second component of the Cus efflux system is the periplasmic membrane protein CusB. With 407 amino acids, it was first resolved at 3.4 Å (Su et al., 2009). Based on the crystal structure, it was initially thought to form a dimer. Subsequently, it has been shown that CusB forms a hexameric channel directly above the periplasmic domain of CusA (Su et al., 2011b; Long et al., 2012). The structure of the CusB hexamer mimics an inverted funnel and follows the same stoichiometry as AcrA, AcrB<sub>(3)</sub>:AcrA<sub>(6)</sub>:TolC<sub>(3)</sub>.

Four domains, three β-domains and one α-helical domain, compose each protomer of CusB. The first β-domain is located above the outer-leaflet of the inner membrane and it interacts directly with the CusA through the periplasmic domain (Su et al., 2011a). Both Ag<sup>+</sup> and Cu<sup>+</sup> bind to the CusB domain-1 at the residue positions M324, F358, and R368. The hexameric CusB channel is primarily created by β-barrels in the lower half, whereas the upper half is an entirely α-helical tunnel. The inner surface of the channel is predominantly negatively charged, which suggests a capacity to bind positively charged metal ions (Delmar et al., 2014). Methionine residues M21, M36, and M38 of CusB are most likely Cu<sup>+</sup> and Ag<sup>+</sup> binding sites (Bagai et al., 2007). These residues are located outside the periplasmic cleft of CusA, the same cleft that was shown to harbor the three-methionine binding sites. Therefore, CusB may transfer the bound metal ions at this location into the periplasmic cleft of CusA for extrusion (Su et al., 2011b).

CusF is a small chaperone protein of 110 amino acids and was first crystallized in 2005 at 1.5 Å resolution (Loftin et al., 2005). CusF exhibits a small five-stranded β-barrel composed of two antiparallel, three-stranded β-sheets packed orthogonally. Three conserved residues H36, M47, M49, and W44 located in β-strands 2 and 3, have been shown to interact with Cu<sup>+</sup> and Ag<sup>+</sup> (Loftin et al., 2007; Xue et al., 2008). Native mass spectrometry has shown that the N-terminal region of CusB can acquire Cu<sup>+</sup> from CusF (Meallman et al., 2012). It was proposed that under anaerobic conditions, due to the accumulation of Cu<sup>+</sup> and Ag<sup>+</sup> in the periplasm, there is a strong up-regulation of the metal chaperone CusF and that the former would work as a scavenger of metal ions and help fill all the available CusB binding sites (Kim et al., 2011; Chacón et al., 2014). The proposed model also suggests that CusB activates and deactivates the CusA pump depending on the ion levels in the periplasmic space. CusF interaction with CusB

appears to have an activating effect in this cascade, initiated by the opening of the periplasmic cleft.

The OMP of the Cus system, CusC, with 460 amino acids, was first crystallized in 2011 at a resolution of 2.3 Å (Kulathila et al., 2011). CusC assembles as a homotrimer creating a large cylindrical channel, the largest found in the outer membrane family. Structurally, the cannon shape is identical to TolC and OprM, however, CusC is believed to work only in the Cus efflux system (Delmar et al., 2014). The interior surface of the channel is highly electronegative allowing for the binding of positively charge ligands. The transmembrane domains appear to be open at the bottom entrance, whereas it appears to be closed at the far end by van der Waals interactions. Each protomer contains a tri-acylated N-terminal cysteine residue shown to be covalently linked to the outer membrane *via* a thioester bond (Kulathila et al., 2011; Delmar et al., 2013). In a docking model, CusC appears to interact with CusAB at the interior of the upper half of the channel formed by the α-helical domain of CusB, primarily through coiled-coil interaction (Long et al., 2012).

The Cus system is well characterized for Cu<sup>+</sup> and Ag<sup>+</sup>, nonetheless, the mechanism of action for other substrates needs to be further characterized.

## Functions of RND Efflux Pumps in *E. coli*

During growth, *E. coli* produces secondary metabolites that can be toxic to the cell. There are three ways of eliminating these metabolites. This can be achieved by inclusion of these metabolites into a second metabolic pathway; enzymatic degradation to non-toxic metabolites or extrusion of metabolites generated to the external environment. RND efflux pumps can also contribute to eliminate secondary metabolites. In a study using deleted genes for enterobactin biosynthesis (*entA* and *entE*), gluconeogenesis (*glpX*), cysteine biosynthesis (*cysH*), and purine biosynthesis (*purA*), the results showed no or diminished effect on the AcrAB promoter in an AcrB mutant strain (Ruiz and Levy, 2014). This suggests that this efflux pump is able to extrude compounds that are toxic or have a signaling role. In *E. coli*, the secretion of iron-chelating siderophore enterobactin from the periplasm is associated with AcrAB, AcrAD, and MdtABC RND efflux pumps (Horiyama and Nishino, 2014). Using a triple mutant *acrB*, *acrD*, and *mtdABC* a significant reduction in the extrusion of enterobactin from the cells was noted. Secretion of metabolites is therefore important for the proper development of the cell. Most of these metabolites regulate master regulators such as MarA or SoxS (Amaral et al., 2011). Therefore, based on these observations the sensor dosage hypothesis was developed. This hypothesis contemplates a homeostatic loop in which the intercellular concentration of metabolites reaches a certain threshold, at which they activate transcriptional regulators such as MarA, SoxS, and Rob (Rosner and Martin, 2009; Amaral et al., 2011). These regulators activate their target genes encoding proteins that function in the extrusion mechanism. When the basal levels of these metabolites are restored, the expression of the transcriptional regulators is restored also.

Considering the human host, in a food-borne infection scenario, *E. coli* has to transit through the human gastrointestinal (GI) tract in order to successfully colonize the intestine. To accomplish this it must survive pH variations and toxicity of the different environments. The presence of bile acids poses an additional barrier to bacterial survival. Bile acids are released into the duodenum and are present along the GI tract, affecting the cell membrane, and DNA of *E. coli* (Merritt and Donaldson, 2009). Bile salts are known to induce the expression of AcrAB-TolC in *E. coli* (Thanassi et al., 1997; Rosenberg et al., 2003) allowing the bacteria to survive in such environments. Other mammalian steroid hormones that are released in bile, also activate AcrB, AcrD, and MdtF RND pumps (Elkins and Mullis, 2006). Recent studies described the effect that bile salts have on alerting (signaling) *E. coli* for the entrance into the small intestine. In a transcriptomic study designed to further explore the effect of bile salts on *E. coli* O157:H7, these were found to induce significant changes in the activation of genes associated with iron scavenging and metabolism, thereby, preparing the bacteria to survive in an iron limiting environment (Hamner et al., 2013).

AcrD and AcrF RND efflux pumps were reported to be up-regulated when bacteria are in the sessile state, i.e., biofilm state. Inhibition of these pumps led to a decrease in biofilm formation caused by *E. coli*-causing UTI strains (Kvist et al., 2008). Some extracellular components of the *E. coli* biofilm matrix, such as cellulose, are hydrophilic (Beloin et al., 2008). As it is known AcrD have specificity for these substrates. AcrD mutants have shown to be unable to form biofilms (Matsumura et al., 2011); these results illustrate the importance of RND efflux pumps in the colonization processes.

Cell-to-cell communication plays an important role in bacterial stress and cell organization. *In vitro* assays with MDR *E. coli* using lomefloxacin and ceftazidime showed over-expression of *marA* and *sdiA* (Tavío et al., 2010). SdiA is believed to behave as a quorum sensor in *E. coli* (Shimada et al., 2014) that controls the expression of AcrAB (Rahmati et al., 2002). Although *E. coli* does not have N-acylhomoserine lactone system, these bacteria can detect quorum sensing signals secreted by other organisms. Understanding how RND efflux pumps interact with quorum sensing mechanisms is important for future development of new compounds capable of inhibiting biofilm structures and interfering with bacterial cell-to-cell communication.

## **“More In and Less Out” – How to Overcome Resistance Using Inhibitors of RND Pumps**

Once the structure of the RND efflux pumps was solved and the assembling mechanism determined it was possible to start the rational development of new compounds capable of inhibiting their function. This could be achieved due to the fact that all the RND efflux systems work in the same way, changing only their substrates. However, to our knowledge, there are no compounds capable of inhibiting all RND efflux pumps and that could be used at the present time in clinical practice.

The use of so-called EPIs in combination with antibiotics (designated as adjuvant therapy) has shown some interesting results in overcoming the innate and induced resistance of bacteria due to efflux (Bohnert and Kern, 2005). The adjuvant therapy can be tested by combining the action of an EPI with an antibiotic or a substrate of a given RND efflux pump at sub-inhibitory concentrations and measuring its efflux rate (Coldham et al., 2010). RND efflux pumps can be inhibited by different ways; for example by interfering with the PMF mechanism or by inhibiting/competing with the binding site of the RND pump.

Inhibition of the PMF can be achieved using a PMF uncoupler such as carbonyl cyanide *m*-chlorophenylhydrazone (CCCP; Viveiros et al., 2005; Ikonomidis et al., 2008). This compound is mainly used for the screening of RND efflux pumps activity. Other compound, Phenylalanine-Arginine- $\beta$ -naphthylamide (PA $\beta$ N) was identified as an EPI by assaying an array of compounds against *Pseudomonas aeruginosa* (Lomovskaya et al., 2001). A few years later, PA $\beta$ N was described as being not an inhibitor of RND efflux pumps, but rather a competitor (Viveiros et al., 2008). Recently, new data has shown that PA $\beta$ N acts as an inhibitor of AcrAB and AcrEF efflux systems when used in low concentrations. At higher concentrations this compound showed not only inhibitory activity toward the mentioned efflux pumps but also an effect in destabilizing the cell wall membrane (Misra et al., 2015). PA $\beta$ N was also found to bind to the upper portion of the central cavity and also the periplasmic domain to one side of the deep external cleft (Nikaido and Takatsuka, 2009). PA $\beta$ N is known to be a successful compound in reverting the resistance to tetracycline (Viveiros et al., 2005) and to macrolides when compared to other known EPIs (Kern et al., 2006).

In *E. coli*, compounds such as PA $\beta$ N, chloramphenicol and others have been shown to improve the efflux of cephalosporins (Kinana et al., 2013). This effect could be due to the fact that cephalosporins bind to a different site in the large binding pocket of the RND pump.

Naphthylpiperazines are also one type of RND inhibitor that could be used to target efflux pumps. Specifically, 1-(1-naphthylmethyl)-piperazine (NMP) is known to have an inhibitory effect on efflux pumps. When used in combination with fluoroquinolones this compound also showed a reduction in fluoroquinolone resistance in *E. coli* (Bohnert and Kern, 2005; Kern et al., 2006). A similar result was obtained when MDR *E. coli* of animal origin was assessed wherein NMP was able to reverse resistance to ciprofloxacin, tetracycline and florfenicol. However, NMP showed to be inefficient in reversing resistance to ampicillin (Marchetti et al., 2012).

The use of phenothiazines in combination with antibiotics has also been studied for potential reversal of bacterial resistance. Chlorpromazine (CPZ) and thioridazine (TZ), known antipsychotic drugs (Amaral and Molnar, 2012), have been shown to be active against *E. coli* (Viveiros et al., 2005). These compounds also showed to be able to reduce the resistance to aminoglycosides (Coutinho et al., 2010) as well as the capacity to be used for plasmid curing (Radhakrishnan et al., 1999; Spengler et al., 2003). Other recent compounds that should be considered include pimozide (Bohnert et al., 2013) or the

specifically designed MBX2319 (Opperman et al., 2014; Vargiu et al., 2014) that also proved to have a reducing effect in the resistance to some antibiotic classes; a similar effect to the one seen by the previously described EPIs.

Based on the studies described above it seems that the use of different EPIs conducts to different results depending on the antibiotic used in the combination tested. These differences are possibly due to the different binding sites of each antibiotic/EPI. Classification of the different EPIs based on their activity in the pump or in combination with the different antimicrobial classes could provide essential information for future research.

## Final Conclusion

The extensive use of antimicrobials has resulted in an increased pressure being exerted in different ecological niches. Data collected so far allow us to assume that the resistant profile seen is not only due to the extensive use of antimicrobials but also due to the innate capacity of the bacteria to extrude a broad range of substrates. It is therefore important to characterize efflux pumps and their mechanism of action, in different bacteria. Understanding how efflux mechanisms can contribute to quorum sensing is of paramount importance for the development of new molecules that can target key genes or proteins in this cascade.

## References

- Aires, J. R., and Nikaido, H. (2005). Aminoglycosides are captured from both periplasm and cytoplasm by the AcrD multidrug efflux transporter of *Escherichia coli*. *J. Bacteriol.* 187, 1923–1929. doi: 10.1128/JB.187.6.1923-1929.2005
- Alvarez-Ortega, C., Olivares, J., and Martínez, J. L. (2013). RND multidrug efflux pumps: what are they good for? *Front. Microbiol.* 4:7. doi: 10.3389/fmicb.2013.00007
- Amaral, L., Fanning, S., and Pagès, J.-M. (2011). Efflux pumps of gram-negative bacteria: genetic responses to stress and the modulation of their activity by pH, inhibitors, and phenothiazines. *Adv. Enzymol. Relat. Areas Mol. Biol.* 77, 61–108. doi: 10.1002/9780470920541.ch2
- Amaral, L., and Molnar, J. (2012). Why and how thioridazine in combination with antibiotics to which the infective strain is resistant will cure totally drug-resistant tuberculosis. *Expert Rev. Anti. Infect. Ther.* 10, 869–873. doi: 10.1586/eri.12.73
- Andersson, D. I., and Hughes, D. (2014). Microbiological effects of sublethal levels of antibiotics. *Nat. Rev. Microbiol.* 12, 465–478. doi: 10.1038/nrmicro3270
- Bagai, I., Liu, W., Rensing, C., Blackburn, N. J., and McEvoy, M. M. (2007). Substrate-linked conformational change in the periplasmic component of a Cu(I)/Ag(I) efflux system. *J. Biol. Chem.* 282, 35695–35702. doi: 10.1074/jbc.M703937200
- Baranova, N., and Nikaido, H. (2002). The baeSR two-component regulatory system activates transcription of the yegMNOB (mdtABCD) transporter gene cluster in *Escherichia coli* and increases its resistance to novobiocin and deoxycholate. *J. Bacteriol.* 184, 4168–4176. doi: 10.1128/JB.184.15.4168-4176.2002
- Bavro, V. N., Pietras, Z., Furnham, N., Pérez-Cano, L., Fernández-Recio, J., Pei, X. Y., et al. (2008). Assembly and channel opening in a bacterial drug efflux machine. *Mol. Cell* 30, 114–121. doi: 10.1016/j.molcel.2008.02.015
- Beloin, C., Roux, A., and Ghigo, J. M. (2008). *Escherichia coli* biofilms. *Curr. Top. Microbiol. Immunol.* 322, 249–289. doi: 10.1007/978-3-540-75418-3\_12
- Bohnert, J. A., and Kern, W. V. (2005). Selected arylpiperazines are capable of reversing multidrug resistance in *Escherichia coli* overexpressing RND efflux pumps. *Antimicrob. Agents Chemother.* 49, 849–852. doi: 10.1128/AAC.49.2.849-852.2005
- Bohnert, J. A., Schuster, S., and Kern, W. V. (2013). Pimozone inhibits the AcrAB-TolC efflux pump in *Escherichia coli*. *Open Microbiol. J.* 7, 83–86. doi: 10.2174/1874285801307100083
- Cagnacci, S., Gualco, L., Debbia, E., Schito, G. C., and Marchese, A. (2008). European emergence of ciprofloxacin-resistant *Escherichia coli* clonal groups O25:H4-ST 131 and O15:K52:H1 causing community-acquired uncomplicated cystitis. *J. Clin. Microbiol.* 46, 2605–2612. doi: 10.1128/JCM.00640-08
- Capita, R., Riesco-Peláez, F., Alonso-Hernando, A., and Alonso-Calleja, C. (2014). Exposure of *Escherichia coli* ATCC 12806 to sublethal concentrations of food-grade biocides influences its ability to form biofilm, resistance to antimicrobials, and ultrastructure. *Appl. Environ. Microbiol.* 80, 1268–1280. doi: 10.1128/AEM.02283-13
- Carraro, N., Matteau, D., Luo, P., Rodrigue, S., and Burrus, V. (2014). The master activator of IncA/C conjugative plasmids stimulates genomic islands and multidrug resistance dissemination. *PLoS Genet.* 10:e1004714. doi: 10.1371/journal.pgen.1004714
- Castanon, J. I. R. (2007). History of the use of antibiotic as growth promoters in European poultry feeds. *Poult. Sci.* 86, 2466–2471. doi: 10.3382/ps.2007-00249
- Centers for Disease Control and Prevention (CDC). (2006). Ongoing multistate outbreak of *Escherichia coli* serotype O157:H7 infections associated with consumption of fresh spinach—United States, September 2006. *MMWR. Morb. Mortal. Wkly. Rep.* 55, 1045–1046.
- Chacón, K. N., Mealman, T. D., McEvoy, M. M., and Blackburn, N. J. (2014). Tracking metal ions through a Cu/Ag efflux pump assigns the functional roles of the periplasmic proteins. *Proc. Natl. Acad. Sci. U.S.A.* 111, 15373–15378. doi: 10.1073/pnas.1411475111
- Coldham, N. G., Webber, M., Woodward, M. J., and Piddock, L. J. V. (2010). A 96-well plate fluorescence assay for assessment of cellular permeability and active efflux in *Salmonella enterica* serovar Typhimurium and *Escherichia coli*. *J. Antimicrob. Chemother.* 65, 1655–1663. doi: 10.1093/jac/dkq169
- Conroy, O., Kim, E.-H., McEvoy, M. M., and Rensing, C. (2010). Differing ability to transport nonmetal substrates by two RND-type metal exporters. *FEMS Microbiol. Lett.* 308, 115–122. doi: 10.1111/j.1574-6968.2010.02006.x

Regarding RND efflux pumps in *E. coli* the crystal structure of several pumps such as the MdtABC is crucial for the elucidation of the binding pockets composition as well as their substrates for these types of pumps.

In the future, the combined use of EPIs with antibiotics appears to be a promising therapy to be applied in the fight against antibiotic resistance. Therefore, the development of new inhibitor molecules based on the models generated by the crystal structure of the efflux pumps will allow performing a more target-specific inhibition.

## Acknowledgments

JA research is supported by Grant 11/F/051 provided by the Department of Agriculture, Food and the Marine (DAFM), Ireland, under the Food Institutional Research Measure (FIRM) Network and Team Building Initiative 2006.

MM and SF are members of the translocation consortium ([www.translocation.eu](http://www.translocation.eu)) that has received support from the Innovative Medicines joint Undertaking under Grant Agreement n°115525, resources which are composed of financial contribution from the European Union's seventh framework programme (FP/2007-2013) and EFPIA companies in kind contributions.

- Coutinho, H. D. M., Costa, J. G. M., Lima, E. O., Falcão-Silva, V. S., and Siqueira-Júnior, J. P. (2010). Increasing of the aminoglycoside antibiotic activity against a multidrug-resistant *E. coli* by *Turnera ulmifolia* L. and chlorpromazine. *Biol. Res. Nurs.* 11, 332–335. doi: 10.1177/1099800409340052
- Delmar, J. A., Su, C.-C., and Yu, E. W. (2013). Structural mechanisms of heavy-metal extrusion by the Cus efflux system. *Biometals* 26, 593–607. doi: 10.1007/s10534-013-9628-0
- Delmar, J. A., Su, C.-C., and Yu, E. W. (2014). Bacterial multidrug efflux transporters. *Annu. Rev. Biophys.* 43, 93–117. doi: 10.1146/annurev-biophys-051013-022855
- Deng, Z., Shan, Y., Pan, Q., Gao, X., and Yan, A. (2013). Anaerobic expression of the gadE-mdtEF multidrug efflux operon is primarily regulated by the two-component system ArcBA through antagonizing the H-NS mediated repression. *Front. Microbiol.* 4:194. doi: 10.3389/fmicb.2013.00194
- Du, D., Wang, Z., James, N. R., Voss, J. E., Klimont, E., Ohene-Agyei, T., et al. (2014). Structure of the AcrAB-TolC multidrug efflux pump. *Nature* 509, 512–515. doi: 10.1038/nature13205
- Elkins, C. A., and Mullis, L. B. (2006). Mammalian steroid hormones are substrates for the major RND- and MFS-type tripartite multidrug efflux pumps of *Escherichia coli*. *J. Bacteriol.* 188, 1191–1195. doi: 10.1128/JB.188.3.1191-1195.2006
- Elkins, C. A., and Nikaido, H. (2002). Substrate specificity of the RND-type multidrug efflux pumps AcrB and AcrD of *Escherichia coli* is determined predominantly by two large periplasmic loops. *J. Bacteriol.* 184, 6490–6498. doi: 10.1128/JB.184.23.6490-6499.2002
- Elkins, C. A., and Nikaido, H. (2003). Chimeric analysis of AcrA function reveals the importance of its C-terminal domain in its interaction with the AcrB multidrug efflux pump. *J. Bacteriol.* 185, 5349–5356. doi: 10.1128/JB.185.18.5349-5356.2003
- Fadli, M., Chevalier, J., Hassani, L., Mezrioui, N.-E., and Pagès, J.-M. (2014). Natural extracts stimulate membrane-associated mechanisms of resistance in Gram-negative bacteria. *Lett. Appl. Microbiol.* 58, 472–477. doi: 10.1111/lam.12216
- Fernandez-Recio, J., Walas, F., Federici, L., Venkatesh Pratap, J., Bavro, V. N., Miguel, R. N., et al. (2004). A model of a transmembrane drug-efflux pump from Gram-negative bacteria. *FEBS Lett.* 578, 5–9. doi: 10.1016/j.febslet.2004.10.097
- Fralick, J. A. (1996). Evidence that TolC is required for functioning of the Mar/AcrAB efflux pump of *Escherichia coli*. *J. Bacteriol.* 178, 5803–5805.
- Frawley, E. R., Crouch, M.-L. V., Bingham-Ramos, L. K., Robbins, H. F., Wang, W., Wright, G. D., et al. (2013). Iron and citrate export by a major facilitator superfamily pump regulates metabolism and stress resistance in *Salmonella Typhimurium*. *Proc. Natl. Acad. Sci. U.S.A.* 110, 12054–1209. doi: 10.1073/pnas.1218274110
- Ge, Q., Yamada, Y., and Zgurskaya, H. (2009). The C-terminal domain of AcrA is essential for the assembly and function of the multidrug efflux pump AcrAB-TolC. *J. Bacteriol.* 191, 4365–4371. doi: 10.1128/JB.00204-09
- Gilbert, P., and McBain, A. J. (2001). Biocide usage in the domestic setting and concern about antibacterial and antibiotic resistance. *J. Infect.* 43, 85–91. doi: 10.1053/jinf.2001.0853
- Gillings, M. R. (2014). Integrins: past, present, and future. *Microbiol. Mol. Biol. Rev.* 78, 257–277. doi: 10.1128/MMBR.00056-13
- Gudipaty, S. A., Larsen, A. S., Rensing, C., and McEvoy, M. M. (2012). Regulation of Cu(I)/Ag(I) efflux genes in *Escherichia coli* by the sensor kinase CusS. *FEMS Microbiol. Lett.* 330, 30–37. doi: 10.1111/j.1574-6968.2012.02529.x
- Gunn, J. S. (2001). Bacterial modification of LPS and resistance to antimicrobial peptides. *J. Endotoxin Res.* 7, 57–62. doi: 10.1177/09680519010070011001
- Hanner, S., McInerney, K., Williamson, K., Franklin, M. J., and Ford, T. E. (2013). Bile salts affect expression of *Escherichia coli* O157:H7 genes for virulence and iron acquisition, and promote growth under iron limiting conditions. *PLoS ONE* 8:e74647. doi: 10.1371/journal.pone.0074647
- Hassan, K. A., Elbourne, L. D. H., Li, L., Gamage, H. K. A. H., Liu, Q., Jackson, S. M., et al. (2015a). An ace up their sleeve: transcriptomic approach exposes the AceI efflux protein of *Acinetobacter baumannii* and reveals the drug efflux potential hidden in many microbial pathogens. *Front. Microbiol.* 6:333. doi: 10.3389/fmicb.2015.00333
- Hassan, K. A., Liu, Q., Henderson, P. J. F., and Paulsen, I. T. (2015b). Homologs of the *Acinetobacter baumannii* AceI transporter represent a new family of bacterial multidrug efflux systems. *MBio* 6, e01982-14. doi: 10.1128/mBio.01982-14
- Higgins, M. K., Eswaran, J., Edwards, P., Schertler, G. F. X., Hughes, C., and Koronakis, V. (2004). Structure of the ligand-blocked periplasmic entrance of the bacterial multidrug efflux protein TolC. *J. Mol. Biol.* 342, 697–702. doi: 10.1016/j.jmb.2004.07.088
- Hinchliffe, P., Symmons, M. F., Hughes, C., and Koronakis, V. (2013). Structure and operation of bacterial tripartite pumps. *Annu. Rev. Microbiol.* 67, 221–242. doi: 10.1146/annurev-micro-092412-155718
- Hirakawa, H., Nishino, K., Yamada, J., Hirata, T., and Yamaguchi, A. (2003). Beta-lactam resistance modulated by the overexpression of response regulators of two-component signal transduction systems in *Escherichia coli*. *J. Antimicrob. Chemother.* 52, 576–582. doi: 10.1093/jac/dkg406
- Hirakawa, H., Takumi-Kobayashi, A., Theisen, U., Hirata, T., Nishino, K., and Yamaguchi, A. (2008). AcrS/EnvR represses expression of the acrAB multidrug efflux genes in *Escherichia coli*. *J. Bacteriol.* 190, 6276–6279. doi: 10.1128/JB.00190-08
- Hirata, T., Saito, A., Nishino, K., Tamura, N., and Yamaguchi, A. (2004). Effects of efflux transporter genes on susceptibility of *Escherichia coli* to tigecycline (GAR-936). *Antimicrob. Agents Chemother.* 48, 2179–2184. doi: 10.1128/AAC.48.6.2179-2184.2004
- Hobbs, E. C., Yin, X., Paul, B. J., Astarita, J. L., and Storz, G. (2012). Conserved small protein associates with the multidrug efflux pump AcrB and differentially affects antibiotic resistance. *Proc. Natl. Acad. Sci. U.S.A.* 109, 16696–16701. doi: 10.1073/pnas.1210093109
- Horiyama, T., and Nishino, K. (2014). AcrB, AcrD, and MdtABC multidrug efflux systems are involved in enterobactin export in *Escherichia coli*. *PLoS ONE* 9:e108642. doi: 10.1371/journal.pone.0108642
- Husain, F., Bikhchandani, M., and Nikaido, H. (2011). Vestibules are part of the substrate path in the multidrug efflux transporter AcrB of *Escherichia coli*. *J. Bacteriol.* 193, 5847–5849. doi: 10.1128/JB.05759-11
- Husain, F., and Nikaido, H. (2010). Substrate path in the AcrB multidrug efflux pump of *Escherichia coli*. *Mol. Microbiol.* 78, 320–330. doi: 10.1111/j.1365-2958.2010.07330.x
- Ikonomidou, A., Tsakris, A., Kanellopoulou, M., Maniatis, A. N., and Pournaras, S. (2008). Effect of the proton motive force inhibitor carbonyl cyanide-m-chlorophenylhydrazone (CCCP) on *Pseudomonas aeruginosa* biofilm development. *Lett. Appl. Microbiol.* 47, 298–302. doi: 10.1111/j.1472-765X.2008.02430.x
- Jellen-Ritter, A. S., and Kern, W. V. (2001). Enhanced expression of the multidrug efflux pumps AcrAB and AcrEF associated with insertion element transposition in *Escherichia coli* mutants selected with a fluoroquinolone. *Antimicrob. Agents Chemother.* 45, 1467–1472. doi: 10.1128/AAC.45.5.1467-1472.2001
- Kern, W. V., Steinke, P., Schumacher, A., Schuster, S., von Baum, H., and Bohnert, J. A. (2006). Effect of 1-(1-naphthylmethyl)-piperazine, a novel putative efflux pump inhibitor, on antimicrobial drug susceptibility in clinical isolates of *Escherichia coli*. *J. Antimicrob. Chemother.* 57, 339–343. doi: 10.1093/jac/dki445
- Kim, E.-H., Nies, D. H., McEvoy, M. M., and Rensing, C. (2011). Switch or funnel: how RND-type transport systems control periplasmic metal homeostasis. *J. Bacteriol.* 193, 2381–2387. doi: 10.1128/JB.01323-10
- Kim, H.-M., Xu, Y., Lee, M., Piao, S., Sim, S.-H., Ha, N.-C., et al. (2010a). Functional relationships between the AcrA hairpin tip region and the TolC aperture tip region for the formation of the bacterial tripartite efflux pump AcrAB-TolC. *J. Bacteriol.* 192, 4498–4503. doi: 10.1128/JB.00334-10
- Kim, H.-S., Nagore, D., and Nikaido, H. (2010b). Multidrug efflux pump MdtBC of *Escherichia coli* is active only as a B2C heterotrimer. *J. Bacteriol.* 192, 1377–1386. doi: 10.1128/JB.01448-09
- Kim, H.-S., and Nikaido, H. (2012). Different functions of MdtB and MdtC subunits in the heterotrimeric efflux transporter MdtB(2)C complex of *Escherichia coli*. *Biochemistry* 51, 4188–4197. doi: 10.1021/bi300379y
- Kim, J.-S., Jeong, H., Song, S., Kim, H.-Y., Lee, K., Hyun, J., et al. (2015). Structure of the tripartite multidrug efflux pump AcrAB-TolC suggests an alternative assembly mode. *Mol. Cells* 38, 180–186. doi: 10.14348/molcells.2015.2277
- Kinana, A. D., Vargiu, A. V., and Nikaido, H. (2013). Some ligands enhance the efflux of other ligands by the *Escherichia coli* multidrug pump AcrB. *Biochemistry* 52, 8342–8351. doi: 10.1021/bi401303y
- Kobayashi, A., Hirakawa, H., Hirata, T., Nishino, K., and Yamaguchi, A. (2006). Growth phase-dependent expression of drug exporters in *Escherichia coli*

- and its contribution to drug tolerance. *J. Bacteriol.* 188, 5693–5703. doi: 10.1128/JB.00217-06
- Kobayashi, K., Tsukagoshi, N., and Aono, R. (2001). Suppression of hypersensitivity of *Escherichia coli* acrB mutant to organic solvents by integrational activation of the acrEF operon with the IS1 or IS2 element. *J. Bacteriol.* 183, 2646–2653. doi: 10.1128/JB.183.8.2646-2653.2001
- Kobayashi, N., Tamura, N., van Veen, H. W., Yamaguchi, A., and Murakami, S. (2014).  $\beta$ -Lactam selectivity of multidrug transporters AcrB and AcrD resides in the proximal binding pocket. *J. Biol. Chem.* 289, 10680–10690. doi: 10.1074/jbc.M114.547794
- Koronakis, V., Sharff, A., Koronakis, E., Luisi, B., and Hughes, C. (2000). Crystal structure of the bacterial membrane protein TolC central to multidrug efflux and protein export. *Nature* 405, 914–919. doi: 10.1038/35016007
- Krishnamoorthy, G., Tikhonova, E. B., Dhamdhare, G., and Zgurskaya, H. I. (2013). On the role of TolC in multidrug efflux: the function and assembly of AcrAB-TolC tolerate significant depletion of intracellular TolC protein. *Mol. Microbiol.* 87, 982–997. doi: 10.1111/mmi.12143
- Kulathila, R., Kulathila, R., Indic, M., and van den Berg, B. (2011). Crystal structure of *Escherichia coli* CusC, the outer membrane component of a heavy metal efflux pump. *PLoS ONE* 6:e15610. doi: 10.1371/journal.pone.0015610
- Kvist, M., Hancock, V., and Klemm, P. (2008). Inactivation of efflux pumps abolishes bacterial biofilm formation. *Appl. Environ. Microbiol.* 74, 7376–7382. doi: 10.1128/AEM.01310-08
- Lamikanra, A., Crowe, J. L., Lijek, R. S., Odetoyin, B. W., Wain, J., Aboderin, A. O., et al. (2011). Rapid evolution of fluoroquinolone-resistant *Escherichia coli* in Nigeria is temporally associated with fluoroquinolone use. *BMC Infect. Dis.* 11:312. doi: 10.1186/1471-2334-11-312
- Lau, S. Y., and Zgurskaya, H. I. (2005). Cell division defects in *Escherichia coli* deficient in the multidrug efflux transporter AcreF-TolC. *J. Bacteriol.* 187, 7815–7825. doi: 10.1128/JB.187.22.7815-7825.2005
- Lee, A., Mao, W., Warren, M. S., Mistry, A., Hoshino, K., Okumura, R., et al. (2000). Interplay between efflux pumps may provide either additive or multiplicative effects on drug resistance. *J. Bacteriol.* 182, 3142–3150. doi: 10.1128/JB.182.11.3142-3150.2000
- Lennen, R. M., Politz, M. G., Kruziki, M. A., and Pfleger, B. F. (2013). Identification of transport proteins involved in free fatty acid efflux in *Escherichia coli*. *J. Bacteriol.* 195, 135–144. doi: 10.1128/JB.01477-12
- Li, X.-Z., and Nikaido, H. (2009). Efflux-mediated drug resistance in bacteria: an update. *Drugs* 69, 1555–1623. doi: 10.2165/11317030-00000000-00000
- Li, X.-Z., Plésiat, P., and Nikaido, H. (2015). The challenge of efflux-mediated antibiotic resistance in Gram-negative bacteria. *Clin. Microbiol. Rev.* 28, 337–418. doi: 10.1128/CMR.00117-14
- Lobedanz, S., Bokma, E., Symmons, M. F., Koronakis, E., Hughes, C., and Koronakis, V. (2007). A periplasmic coiled-coil interface underlying TolC recruitment and the assembly of bacterial drug efflux pumps. *Proc. Natl. Acad. Sci. U.S.A.* 104, 4612–4617. doi: 10.1073/pnas.0610160104
- Loftin, I. R., Franke, S., Blackburn, N. J., and McEvoy, M. M. (2007). Unusual Cu(I)/Ag(I) coordination of *Escherichia coli* CusF as revealed by atomic resolution crystallography and X-ray absorption spectroscopy. *Protein Sci.* 16, 2287–2293. doi: 10.1110/ps.073021307
- Loftin, I. R., Franke, S., Roberts, S. A., Weichsel, A., Héroux, A., Montfort, W. R., et al. (2005). A novel copper-binding fold for the periplasmic copper resistance protein CusF. *Biochemistry* 44, 10533–10540. doi: 10.1021/bi050827b
- Lomovskaya, O., Warren, M. S., Lee, A., Galazzo, J., Fronko, R., Lee, M., et al. (2001). Identification and characterization of inhibitors of multidrug resistance efflux pumps in *Pseudomonas aeruginosa*: novel agents for combination therapy. *Antimicrob. Agents Chemother.* 45, 105–116. doi: 10.1128/AAC.45.1.105-116.2001
- Long, F., Su, C.-C., Lei, H.-T., Bolla, J. R., Do, S. V., and Yu, E. W. (2012). Structure and mechanism of the tripartite CusCBA heavy-metal efflux complex. *Philos. Trans. R. Soc. Lond. B Biol. Sci.* 367, 1047–1058. doi: 10.1098/rstb.2011.0203
- Long, F., Su, C.-C., Zimmermann, M. T., Boyken, S. E., Rajashankar, K. R., Jernigan, R. L., et al. (2010). Crystal structures of the CusA efflux pump suggest methionine-mediated metal transport. *Nature* 467, 484–488. doi: 10.1038/nature09395
- Lu, S., and Zgurskaya, H. I. (2012). Role of ATP binding and hydrolysis in assembly of MacAB-TolC macrolide transporter. *Mol. Microbiol.* 86, 1132–1143. doi: 10.1111/mmi.12046
- Lubelski, J., Konings, W. N., and Driessens, A. J. M. (2007). Distribution and physiology of ABC-type transporters contributing to multidrug resistance in bacteria. *Microbiol. Mol. Biol. Rev.* 71, 463–476. doi: 10.1128/MMBR.00001-07
- Marchetti, M. L., Errecalde, J., and Mestorino, N. (2012). Effect of (1-naphthylmethyl)-piperazine on antimicrobial agent susceptibility in multidrug-resistant isogenic and veterinary *Escherichia coli* field strains. *J. Med. Microbiol.* 61, 786–792. doi: 10.1099/jmm.0.040204-0
- Martins, A., Spengler, G., Rodrigues, L., Viveiros, M., Ramos, J., Martins, M., et al. (2009). pH Modulation of efflux pump activity of multi-drug resistant *Escherichia coli*: protection during its passage and eventual colonization of the colon. *PLoS ONE* 4:e6656. doi: 10.1371/journal.pone.0006656
- Masi, M., and Pagès, J.-M. (2013). Structure, function and regulation of outer membrane proteins involved in drug transport in Enterobacteriaceae: the OmpF/C - TolC case. *Open Microbiol. J.* 7, 22–33. doi: 10.2174/1874285801307010022
- Matsumura, K., Furukawa, S., Ogihara, H., and Morinaga, Y. (2011). Roles of multidrug efflux pumps on the biofilm formation of *Escherichia coli* K-12. *Biocontrol Sci.* 16, 69–72. doi: 10.4265/bio.16.69
- Matsumura, Y., Yamamoto, M., Nagao, M., Ito, Y., Takakura, S., and Ichiyama, S. (2013). Association of fluoroquinolone resistance, virulence genes, and IncF plasmids with extended-spectrum- $\beta$ -lactamase-producing *Escherichia coli* sequence type 131 (ST131) and ST405 clonal groups. *Antimicrob. Agents Chemother.* 57, 4736–4742. doi: 10.1128/AAC.00641-13
- Mealman, T. D., Zhou, M., Affandi, T., Chacón, K. N., Aranguren, M. E., Blackburn, N. J., et al. (2012). N-terminal region of CusB is sufficient for metal binding and metal transfer with the metallochaperone CusF. *Biochemistry* 51, 6767–6775. doi: 10.1021/bi300596a
- Merritt, M. E., and Donaldson, J. R. (2009). Effect of bile salts on the DNA and membrane integrity of enteric bacteria. *J. Med. Microbiol.* 58, 1533–1541. doi: 10.1099/jmm.0.014092-0
- Michael, C. A., Dominey-Howes, D., and Labbate, M. (2014). The antimicrobial resistance crisis: causes, consequences, and management. *Front. Public Health* 2:145. doi: 10.3389/fpubh.2014.00145
- Misra, R., Morrison, K. D., Cho, H. J., and Khuu, T. (2015). Importance of real-time assays to distinguish multidrug efflux pump inhibiting and outer membrane destabilizing activities in *Escherichia coli*. *J. Bacteriol.* doi: 10.1128/JB.02456-14 [Epub ahead of print].
- Money, P., Kelly, A. F., Gould, S. W. J., Denholm-Price, J., Threlfall, E. J., and Fielder, M. D. (2010). Cattle, weather and water: mapping *Escherichia coli* O157:H7 infections in humans in England and Scotland. *Environ. Microbiol.* 12, 2633–2644. doi: 10.1111/j.1462-2920.2010.02293.x
- Moon, D. C., Seol, S. Y., Gurung, M., Jin, J. S., Choi, C. H., Kim, J., et al. (2010). Emergence of a new mutation and its accumulation in the topoisomerase IV gene confers high levels of resistance to fluoroquinolones in *Escherichia coli* isolates. *Int. J. Antimicrob. Agents* 35, 76–79. doi: 10.1016/j.ijantimicag.2009.08.003
- Murakami, S., Nakashima, R., Yamashita, E., Matsumoto, T., and Yamaguchi, A. (2006). Crystal structures of a multidrug transporter reveal a functionally rotating mechanism. *Nature* 443, 173–179. doi: 10.1038/nature05076
- Murakami, S., Nakashima, R., Yamashita, E., and Yamaguchi, A. (2002). Crystal structure of bacterial multidrug efflux transporter AcrB. *Nature* 419, 587–593. doi: 10.1038/nature01050
- Nagakubo, S., Nishino, K., Hirata, T., and Yamaguchi, A. (2002). The putative response regulator BaeR stimulates multidrug resistance of *Escherichia coli* via a novel multidrug exporter system, MdtABC. *J. Bacteriol.* 184, 4161–4167. doi: 10.1128/JB.184.15.4161-4167.2002
- Nakashima, R., Sakurai, K., Yamasaki, S., Nishino, K., and Yamaguchi, A. (2011). Structures of the multidrug exporter AcrB reveal a proximal multisite drug-binding pocket. *Nature* 480, 565–569. doi: 10.1038/nature10641
- Nies, D. H. (2003). Efflux-mediated heavy metal resistance in prokaryotes. *FEMS Microbiol. Rev.* 27, 313–339. doi: 10.1016/S0168-6445(03)00048-2
- Nikaido, H. (1996). Multidrug efflux pumps of gram-negative bacteria. *J. Bacteriol.* 178, 5853–5859.
- Nikaido, H. (2011). Structure and mechanism of RND-type multidrug efflux pumps. *Adv. Enzymol. Relat. Areas Mol. Biol.* 77, 1–60. doi: 10.1002/9780470920541.ch1

- Nikaido, H., and Pagès, J.-M. (2012). Broad-specificity efflux pumps and their role in multidrug resistance of Gram-negative bacteria. *FEMS Microbiol. Rev.* 36, 340–363. doi: 10.1111/j.1574-6976.2011.00290.x
- Nikaido, H., and Takatsuka, Y. (2009). Mechanisms of RND multidrug efflux pumps. *Biochim. Biophys. Acta* 1794, 769–781. doi: 10.1016/j.bbapap.2008.10.004
- Nishino, K., Senda, Y., Hayashi-Nishino, M., and Yamaguchi, A. (2009). Role of the AraC-XylS family regulator YdeO in multi-drug resistance of *Escherichia coli*. *J. Antibiot. (Tokyo)* 62, 251–257. doi: 10.1038/ja.2009.23
- Nishino, K., Senda, Y., and Yamaguchi, A. (2008a). CRP regulator modulates multidrug resistance of *Escherichia coli* by repressing the mdtEF multidrug efflux genes. *J. Antibiot. (Tokyo)* 61, 120–127. doi: 10.1038/ja.2008.120
- Nishino, K., Senda, Y., and Yamaguchi, A. (2008b). The AraC-family regulator GadX enhances multidrug resistance in *Escherichia coli* by activating expression of mdtEF multidrug efflux genes. *J. Infect. Chemother.* 14, 23–29. doi: 10.1007/s10156-007-0575-Y
- Nishino, K., and Yamaguchi, A. (2001). Analysis of a complete library of putative drug transporter genes in *Escherichia coli*. *J. Bacteriol.* 183, 5803–5812. doi: 10.1128/JB.183.20.5803-5812.2001
- Nishino, K., and Yamaguchi, A. (2002). EvgA of the two-component signal transduction system modulates production of the YhiUV multidrug transporter in *Escherichia coli*. *J. Bacteriol.* 184, 2319–2323. doi: 10.1128/JB.184.8.2319-2323.2002
- Nishino, K., and Yamaguchi, A. (2004). Role of histone-like protein H-NS in multidrug resistance of *Escherichia coli*. *J. Bacteriol.* 186, 1423–1429. doi: 10.1128/JB.186.5.1423-1429.2004
- Nishino, K., Yamasaki, S., Hayashi-Nishino, M., and Yamaguchi, A. (2010). Effect of NlpE overproduction on multidrug resistance in *Escherichia coli*. *Antimicrob. Agents Chemother.* 54, 2239–2243. doi: 10.1128/AAC.01677-09
- Nishino, K., Yamasaki, S., Hayashi-Nishino, M., and Yamaguchi, A. (2011). Effect of overexpression of small non-coding DsrA RNA on multidrug efflux in *Escherichia coli*. *J. Antimicrob. Chemother.* 66, 291–296. doi: 10.1093/jac/dkq420
- Olesen, B., Hansen, D. S., Nilsson, F., Frimodt-Møller, J., Leihof, R. F., Struve, C., et al. (2013). Prevalence and characteristics of the epidemic multiresistant *Escherichia coli* ST131 clonal group among extended-spectrum beta-lactamase-producing *E. coli* isolates in Copenhagen, Denmark. *J. Clin. Microbiol.* 51, 1779–1785. doi: 10.1128/JCM.00346-13
- Opperman, T. J., Kwasny, S. M., Kim, H.-S., Nguyen, S. T., Housewright, C., D’Souza, S., et al. (2014). Characterization of a novel pyranopyridine inhibitor of the AcrAB efflux pump of *Escherichia coli*. *Antimicrob. Agents Chemother.* 58, 722–733. doi: 10.1128/AAC.01866-13
- Peltier, E., Vincent, J., Finn, C., and Graham, D. W. (2010). Zinc-induced antibiotic resistance in activated sludge bioreactors. *Water Res.* 44, 3829–3836. doi: 10.1016/j.watres.2010.04.041
- Pennington, T. H. (2014). *E. coli* O157 outbreaks in the United Kingdom: past, present, and future. *Infect. Drug Resist.* 7, 211–222. doi: 10.2147/IDR.S49081
- Perreten, V., Schwarz, F. V., Teuber, M., and Levy, S. B. (2001). Mdt(A), a new efflux protein conferring multiple antibiotic resistance in *Lactococcus lactis* and *Escherichia coli*. *Antimicrob. Agents Chemother.* 45, 1109–1114. doi: 10.1128/AAC.45.4.1109-1114.2001
- Piddock, L. J. V. (2006). Multidrug-resistance efflux pumps - not just for resistance. *Nat. Rev. Microbiol.* 4, 629–636. doi: 10.1038/nrmicro1464
- Poole, K. (2002). Mechanisms of bacterial biocide and antibiotic resistance. *J. Appl. Microbiol.* 92(Suppl. s1), 55S–64S. doi: 10.1046/j.1365-2672.92.5s1.8.x
- Poole, K. (2007). Efflux pumps as antimicrobial resistance mechanisms. *Ann. Med.* 39, 162–176. doi: 10.1080/07853890701195262
- Pos, K. M. (2009). Drug transport mechanism of the AcrB efflux pump. *Biochim. Biophys. Acta* 1794, 782–793. doi: 10.1016/j.bbapap.2008.12.015
- Rademacher, C., and Masepohl, B. (2012). Copper-responsive gene regulation in bacteria. *Microbiology* 158, 2451–2464. doi: 10.1099/mic.0.058487-0
- Radhakrishnan, V., Ganguly, K., Ganguly, M., Dastidar, S. G., and Chakrabarty, A. N. (1999). Potentiality of tricyclic compound thioridazine as an effective antibacterial and antiplasmid agent. *Indian J. Exp. Biol.* 37, 671–675.
- Radosavljevic, V., Finke, E.-J., and Belojevic, G. (2014). *Escherichia coli* O104:H4 outbreak in Germany—clarification of the origin of the epidemic. *Eur. J. Public Health* 25, 125–129. doi: 10.1093/ejphar/cku048
- Rahmati, S., Yang, S., Davidson, A. L., and Zechiedrich, E. L. (2002). Control of the AcrAB multidrug efflux pump by quorum-sensing regulator SdiA. *Mol. Microbiol.* 43, 677–685. doi: 10.1046/j.1365-2958.2002.02773.x
- Rosenberg, E. Y., Bertenthal, D., Nilles, M. L., Bertrand, K. P., and Nikaido, H. (2003). Bile salts and fatty acids induce the expression of *Escherichia coli* AcrAB multidrug efflux pump through their interaction with Rob regulatory protein. *Mol. Microbiol.* 48, 1609–1619. doi: 10.1046/j.1365-2958.2003.03531.x
- Rosenberg, E. Y., Ma, D., and Nikaido, H. (2000). AcrD of *Escherichia coli* is an aminoglycoside efflux pump. *J. Bacteriol.* 182, 1754–1756. doi: 10.1128/JB.182.6.1754-1756.2000
- Rosner, J. L., and Martin, R. G. (2009). An excretory function for the *Escherichia coli* outer membrane pore TolC: upregulation of marA and soxS transcription and Rob activity due to metabolites accumulated in tolC mutants. *J. Bacteriol.* 191, 5283–5292. doi: 10.1128/JB.00507-09
- Ruiz, C., and Levy, S. B. (2014). Regulation of acrAB expression by cellular metabolites in *Escherichia coli*. *J. Antimicrob. Chemother.* 69, 390–399. doi: 10.1093/jac/dkt352
- Seeger, M. A., Schieffner, A., Eicher, T., Verrey, F., Diederichs, K., and Pos, K. M. (2006). Structural asymmetry of AcrB trimer suggests a peristaltic pump mechanism. *Science* 313, 1295–1298. doi: 10.1126/science.11131542
- Sennhauser, G., Amstutz, P., Briand, C., Storchenecker, O., and Grüttner, M. G. (2007). Drug export pathway of multidrug exporter AcrB revealed by DARPin inhibitors. *PLoS Biol.* 5:e7. doi: 10.1371/journal.pbio.0050007
- Shah, A. A., Wang, C., Chung, Y.-R., Kim, J.-Y., Choi, E.-S., and Kim, S.-W. (2013). Enhancement of geranil resistance of *Escherichia coli* by MarA overexpression. *J. Biosci. Bioeng.* 115, 253–258. doi: 10.1016/j.jbiosc.2012.10.009
- Shimada, T., Shimada, K., Matsui, M., Kitai, Y., Igarashi, J., Suga, H., et al. (2014). Roles of cell division control factor SdiA: recognition of quorum sensing signals and modulation of transcription regulation targets. *Genes Cells* 19, 405–418. doi: 10.1111/gtc.12139
- Spengler, G., Miczák, A., Hajdú, E., Kawase, M., Amaral, L., and Molnár, J. (2003). Enhancement of plasmid curing by 9-aminoacridine and two phenothiazines in the presence of proton pump inhibitor 1-(2-benzoxazolyl)-3,3,3-trifluoro-2-propanone. *Int. J. Antimicrob. Agents* 22, 223–227. doi: 10.1016/S0924-8579(03)00207-3
- Su, C.-C., Long, F., Lei, H.-T., Bolla, J. R., Do, S. V., Rajashankar, K. R., et al. (2012). Charged amino acids (R83, E567, D617, E625, R669, and K678) of CusA are required for metal ion transport in the Cus efflux system. *J. Mol. Biol.* 422, 429–441. doi: 10.1016/j.jmb.2012.05.038
- Su, C.-C., Long, F., and Yu, E. W. (2011a). The Cus efflux system removes toxic ions via a methionine shuttle. *Protein Sci.* 20, 6–18. doi: 10.1002/pro.532
- Su, C.-C., Long, F., Zimmermann, M. T., Rajashankar, K. R., Jernigan, R. L., and Yu, E. W. (2011b). Crystal structure of the CusBA heavy-metal efflux complex of *Escherichia coli*. *Nature* 470, 558–562. doi: 10.1038/nature09743
- Su, C.-C., Yang, F., Long, F., Reynon, D., Routh, M. D., Kuo, D. W., et al. (2009). Crystal structure of the membrane fusion protein CusB from *Escherichia coli*. *J. Mol. Biol.* 393, 342–355. doi: 10.1016/j.jmb.2009.08.029
- Sulavik, M. C., Housewright, C., Cramer, C., Jiwani, N., Murgolo, N., Greene, J., et al. (2001). Antibiotic susceptibility profiles of *Escherichia coli* strains lacking multidrug efflux pump genes. *Antimicrob. Agents Chemother.* 45, 1126–1136. doi: 10.1128/AAC.45.4.1126-1136.2001
- Symmons, M. F., Bokma, E., Koronakis, E., Hughes, C., and Koronakis, V. (2009). The assembled structure of a complete tripartite bacterial multidrug efflux pump. *Proc. Natl. Acad. Sci. U.S.A.* 106, 7173–7178. doi: 10.1073/pnas.0900693106
- Tal, N., and Schuldiner, S. (2009). A coordinated network of transporters with overlapping specificities provides a robust survival strategy. *Proc. Natl. Acad. Sci. U.S.A.* 106, 9051–9056. doi: 10.1073/pnas.0902400106
- Tanabe, M., Szakonyi, G., Brown, K. A., Henderson, P. J. F., Nield, J., and Byrne, B. (2009). The multidrug resistance efflux complex, EmrAB from *Escherichia coli* forms a dimer in vitro. *Biochem. Biophys. Res. Commun.* 380, 338–342. doi: 10.1016/j.bbrc.2009.01.081
- Tavío, M. M., Aquili, V. D., Poveda, J. B., Antunes, N. T., Sánchez-Céspedes, J., and Vila, J. (2010). Quorum-sensing regulator sdiA and marA overexpression is involved in in vitro-selected multidrug resistance of *Escherichia coli*. *J. Antimicrob. Chemother.* 65, 1178–1186. doi: 10.1093/jac/dkq112

- Thanassi, D. G., Cheng, L. W., and Nikaido, H. (1997). Active efflux of bile salts by *Escherichia coli*. *J. Bacteriol.* 179, 2512–2518.
- Tikhonova, E. B., Dastidar, V., Rybenkov, V. V., and Zgurskaya, H. I. (2009). Kinetic control of TolC recruitment by multidrug efflux complexes. *Proc. Natl. Acad. Sci. U.S.A.* 106, 16416–16421. doi: 10.1073/pnas.090601106
- Tikhonova, E. B., Yamada, Y., and Zgurskaya, H. I. (2011). Sequential mechanism of assembly of multidrug efflux pump AcrAB-TolC. *Chem. Biol.* 18, 454–463. doi: 10.1016/j.chembiol.2011.02.011
- Tikhonova, E. B., and Zgurskaya, H. I. (2004). AcrA, AcrB, and TolC of *Escherichia coli* form a stable intermembrane multidrug efflux complex. *J. Biol. Chem.* 279, 32116–32124. doi: 10.1074/jbc.M402230200
- Touzé, T., Eswaran, J., Bokma, E., Koronakis, E., Hughes, C., and Koronakis, V. (2004). Interactions underlying assembly of the *Escherichia coli* AcrAB-TolC multidrug efflux system. *Mol. Microbiol.* 53, 697–706. doi: 10.1111/j.1365-2958.2004.04158.x
- Turlin, E., Heuck, G., Brandão, M. I. S., Szili, N., Mellin, J. R., Lange, N., et al. (2014). Protoporphyrin (PPIX) efflux by the MacAB-TolC pump in *Escherichia coli*. *Microbiologyopen* 3, 849–859. doi: 10.1002/mbo3.203
- Vargiu, A. V., Ruggerone, P., Opperman, T. J., Nguyen, S. T., and Nikaido, H. (2014). Molecular mechanism of MBX2319 inhibition of *Escherichia coli* AcrB multidrug efflux pump and comparison with other inhibitors. *Antimicrob. Agents Chemother.* 58, 6224–6234. doi: 10.1128/AAC.03283-14
- Viveiros, M., Jesus, A., Brito, M., Leandro, C., Martins, M., Ordway, D., et al. (2005). Inducement and reversal of tetracycline resistance in *Escherichia coli* K-12 and expression of proton gradient-dependent multidrug efflux pump genes. *Antimicrob. Agents Chemother.* 49, 3578–3582. doi: 10.1128/AAC.49.8.3578-3582.2005
- Viveiros, M., Martins, A., Paixão, L., Rodrigues, L., Martins, M., Couto, I., et al. (2008). Demonstration of intrinsic efflux activity of *Escherichia coli* K-12 AG100 by an automated ethidium bromide method. *Int. J. Antimicrob. Agents* 31, 458–462. doi: 10.1016/j.ijantimicag.2007.12.015
- Wang, D., and Fierke, C. A. (2013). The BaeSR regulon is involved in defense against zinc toxicity in *E. coli*. *Metallomics* 5, 372–383. doi: 10.1039/c3mt20217h
- Wang, H., Dzink-Fox, J. L., Chen, M., and Levy, S. B. (2001). Genetic characterization of highly fluoroquinolone-resistant clinical *Escherichia coli* strains from China: role of acrR mutations. *Antimicrob. Agents Chemother.* 45, 1515–1521. doi: 10.1128/AAC.45.5.1515-1521.2001
- Warner, D. M., and Levy, S. B. (2010). Different effects of transcriptional regulators MarA, SoxS and Rob on susceptibility of *Escherichia coli* to cationic antimicrobial peptides (CAMPs): rob-dependent CAMP induction of the marRAB operon. *Microbiology* 156, 570–578. doi: 10.1099/mic.0.033415-0
- Weeks, J. W., Celaya-Kolb, T., Pecora, S., and Misra, R. (2010). AcrA suppressor alterations reverse the drug hypersensitivity phenotype of a TolC mutant by inducing TolC aperture opening. *Mol. Microbiol.* 75, 1468–1483. doi: 10.1111/j.1365-2958.2010.07068.x
- Wei, Y., Lee, J. M., Smulski, D. R., and LaRossa, R. A. (2001). Global impact of sdiA amplification revealed by comprehensive gene expression profiling of *Escherichia coli*. *J. Bacteriol.* 183, 2265–2272. doi: 10.1128/JB.183.7.2265-2272.2001
- World Health Organization (WHO). (2014). *Antimicrobial Resistance: Global Report on Surveillance 2014*. Geneva: WHO.
- Xu, Y., Lee, M., Moeller, A., Song, S., Yoon, B.-Y., Kim, H.-M., et al. (2011). Funnel-like hexameric assembly of the periplasmic adapter protein in the tripartite multidrug efflux pump in gram-negative bacteria. *J. Biol. Chem.* 286, 17910–17920. doi: 10.1074/jbc.M111.238535
- Xu, Y., Moeller, A., Jun, S.-Y., Le, M., Yoon, B.-Y., Kim, J.-S., et al. (2012). Assembly and channel opening of outer membrane protein in tripartite drug efflux pumps of Gram-negative bacteria. *J. Biol. Chem.* 287, 11740–11750. doi: 10.1074/jbc.M111.329375
- Xue, Y., Davis, A. V., Balakrishnan, G., Stasser, J. P., Staehlin, B. M., Focia, P., et al. (2008). Cu(I) recognition via cation-pi and methionine interactions in CusF. *Nat. Chem. Biol.* 4, 107–109. doi: 10.1038/nchembio.2007.57
- Yang, D., Weatherspoon-Griffin, N., Kong, W., Hua, Z., and Shi, Y. (2014). The CpxR/CpxA two-component regulatory system upregulates the multidrug resistance cascade to facilitate *Escherichia coli* resistance to a model antimicrobial peptide. *J. Biol. Chem.* 289, 32571–32582. doi: 10.1074/jbc.M114.565762
- Yu, E. W., McDermott, G., Zgurskaya, H. I., Nikaido, H., and Koshland, D. E. (2003). Structural basis of multiple drug-binding capacity of the AcrB multidrug efflux pump. *Science* 300, 976–980. doi: 10.1126/science.1083137
- Yum, S., Xu, Y., Piao, S., Sim, S.-H., Kim, H.-M., Jo, W.-S., et al. (2009). Crystal structure of the periplasmic component of a tripartite macrolide-specific efflux pump. *J. Mol. Biol.* 387, 1286–1297. doi: 10.1016/j.jmb.2009.02.048
- Zgurskaya, H. I., and Nikaido, H. (2000). Cross-linked complex between oligomeric periplasmic lipoprotein AcrA and the inner-membrane-associated multidrug efflux pump AcrB from *Escherichia coli*. *J. Bacteriol.* 182, 4264–4267. doi: 10.1128/JB.182.15.4264-4267.2000
- Zhang, Y., Xiao, M., Horiyama, T., Zhang, Y., Li, X., Nishino, K., et al. (2011). The multidrug efflux pump MdtEF protects against nitrosative damage during the anaerobic respiration in *Escherichia coli*. *J. Biol. Chem.* 286, 26576–26584. doi: 10.1074/jbc.M111.243261

**Conflict of Interest Statement:** The authors declare that the research was conducted in the absence of any commercial or financial relationships that could be construed as a potential conflict of interest.

Copyright © 2015 Anes, McCusker, Fanning and Martins. This is an open-access article distributed under the terms of the Creative Commons Attribution License (CC BY). The use, distribution or reproduction in other forums is permitted, provided the original author(s) or licensor are credited and that the original publication in this journal is cited, in accordance with accepted academic practice. No use, distribution or reproduction is permitted which does not comply with these terms.



# PMQR genes *oqxAB* and *aac(6')Ib-cr* accelerate the development of fluoroquinolone resistance in *Salmonella typhimurium*

Marcus H. Wong<sup>1,2†</sup>, Edward W. Chan<sup>3†</sup>, Li Z. Liu<sup>1,2</sup> and Sheng Chen<sup>1,2\*</sup>

<sup>1</sup> Food Safety and Technology Research Centre, Hong Kong Polytechnic University – Shenzhen Research Institute, Shenzhen, China

<sup>2</sup> State Key Laboratory of Chirosciences, Department of Applied Biology and Chemical Technology, The Hong Kong Polytechnic University, Kowloon, China

<sup>3</sup> Department of Microbiology, The Prince of Wales Hospital – The Chinese University of Hong Kong, Shatin, China

## Edited by:

Attilio Vittorio Vargiu, Università di Cagliari, Italy

## Reviewed by:

Daniela Ceccarelli, University of Maryland, USA

Etnosa Igbinosa, University of Benin, Nigeria

Amit Kumar, Kansas State University, USA

## \*Correspondence:

Sheng Chen, State Key Laboratory of Chirosciences, Department of Applied Biology and Chemical Technology, The Hong Kong Polytechnic University, Hung Hom, Kowloon, China  
e-mail: sheng.chen@polyu.edu.hk

†Marcus H. Wong and Edward W. Chan have contributed equally to this work.

Emergence of multidrug-resistant *Salmonella typhimurium* strains, especially the ACSSuT and nalidixic acid R types, has significantly compromised the effectiveness of current strategies to control *Salmonella* infections, resulting in increased morbidity and mortality. Clinical *S. typhimurium* isolates recovered in Hong Kong during the period of 2005–2011 were increasingly resistant to ciprofloxacin (CIP) and antibiotics of the ACSSuT group. Our data revealed that *oqxAB* and *aac(6')Ib-cr* were encoded on plasmids of various sizes and the presence of these two elements together with a single *gyrA* mutation in *S. typhimurium* were sufficient to mediate resistance to CIP. Acquisition of the *oqxAB* and *aac(6')Ib-cr* encoding plasmids by *S. typhimurium* caused a fourfold increase in CIP minimal inhibitory concentration. Furthermore, the presence of *oqxAB* and *aac(6')Ib-cr* in *Salmonella* dramatically increased the mutation prevention concentration of CIP which may due to mutational changes in the drug target genes. In conclusion, possession of *oqxAB* and *aac(6')Ib-cr* encoding plasmid facilitate the selection of CIP resistant *S. typhimurium*, thereby causing a remarkable increase of CIP resistance among clinical *Salmonella* strains in Hong Kong.

**Keywords:** *S. typhimurium*, ciprofloxacin resistance, ACSSuT R type, *oqxAB*, *aac(6')Ib-cr*

## INTRODUCTION

Non-typhoidal *Salmonella* are among the principal bacterial pathogens implicated in food-borne gastroenteritis worldwide (Gomez et al., 1997). Antimicrobial agents are not usually required for treatment in salmonellosis but can be lifesaving in cases of severe or systemic infections, as well as treatment for elderly and immunocompromised patients (Hohmann, 2001). Multidrug resistance in *Salmonella* has been documented since 1980, a representative class of resistant organisms being the ACSSuT resistance type of *Salmonella typhimurium* DT104, which originated in the UK and spread rapidly to the US and other parts of the world (Centers for Disease Control and Prevention, 1997; Glynn et al., 1998; Markogiannakis et al., 2000). Hence fluoroquinolones and the extended-spectrum cephalosporins have become the drugs of choice for treatment of acute gastroenteritis caused by *Salmonella* and other enteric pathogens. Resistance toward quinolone and fluoroquinolone antimicrobials is mainly due to target mutations in quinolone resistance determining region (QRDR) of DNA gyrases (*gyrA* and *gyrB*) and Type IV topoisomerases (*parC* and *parE*), which subsequently prevent drugs from binding (Hawkey, 2003). Although high level fluoroquinolone-resistant *Salmonella* are known to be associated with specific serotypes of *Salmonella* and have been reported in scattered regions around the world, their prevalence remains low. This is probably due to the fact that the process of selection of double *gyrA* and single *parC* mutations is not very efficient. Nevertheless, several lines of evidence have suggested that emergence of multidrug

resistant non-typhoidal *Salmonella* strains has significant impact on the effectiveness of current strategies, including reduced efficacy of early empirical treatment to control and manage diseases associated with food-borne infections. These include reduced efficacy of early empirical treatment as well as limited choice of treatment.

Plasmid mediated quinolone resistance (PMQR) genes such as *qnrA*, *qnrB*, *qnrC*, *qnrD*, *qnrS*, *qepA*, and *aac(6')Ib-cr* have been increasingly reported in bacterial pathogens. The *qnr* type PMQR genes bind to DNA gyrase and topoisomerase to block the action of fluoroquinolones resulting in reduced susceptibility to fluoroquinolones (Tran et al., 2005). *QepA* encodes a MFS-type efflux pump which is able to excrete quinolone into extracellular space (Yamane et al., 2007). AAC(6')Ib-cr acetylates ciprofloxacin (CIP) and norfloxacin (Robicsek et al., 2006). It is postulated that these PMQR genes are able to contribute to the development of quinolone resistance in these organisms (Cattoir and Nordmann, 2009). Recently, a novel transmissible resistance-nodulation-division (RND) efflux pump *OqxAB*, which mediated resistance to olaquindox, chloramphenicol, nalidixic acid, and elevated minimal inhibitory concentrations (MICs) of other antimicrobial reagents including ampicillin, gentamicin, and CIP (MIC between 0.06 and 0.25 µg/ml), has been identified (Hansen et al., 2007). *OqxAB* was encoded on an IncX1 plasmid, pOLA52, harbored by a swine *Escherichia coli* isolate (Hansen et al., 2004). More recently, *OqxAB* was reported to be prevalent in organisms isolated from pork and pig farms in China

(Zhao et al., 2010; Liu et al., 2011; Wong and Chen, 2012), as well as from human food (18). On the other hand, the *oqxAB* gene has not been found in clinical isolates until recently, when it became detectable in clinical strains of *E. coli*, *Salmonella*, and *Klebsiella pneumoniae* (Kim et al., 2009; Park et al., 2012; Ruiz et al., 2012; Yuan et al., 2012). The functional and clinical significance of this and other PMQR genes such as *qnra*, *B*, *D*, and *S*, which have also become prevalent in clinical *Salmonella* isolates (Cavaco et al., 2009; Ferrari et al., 2011; Kim et al., 2013), remains unclear.

We have previously characterized 239 human clinical *S. typhimurium* isolates recovered from hospital patients in Hong Kong during the period of 2005–2011 for their susceptibilities to fluoroquinolones and other antibiotics and the prevalence of PMQR genes. Two PMQR genes, *oqxAB* and *aac(6')Ib-cr*, were found to exhibit close relationship with fluoroquinolone resistance in *S. typhimurium*. Approximately 44% of the *oqxAB*-positive *S. typhimurium* were resistant to CIP and around 89% of *oqxAB*, *aac(6')Ib-cr*-positive isolates were resistant to CIP, while only 11% of the *oqxAB*-negative isolates were resistant to CIP (Wong et al., 2013). In the current study, we want to investigate the direct association of *oqxAB/aac(6')Ib-cr* with the development of fluoroquinolone resistance in *S. typhimurium*. We confirm that *oqxAB* and *aac(6')Ib-cr* can mediate rapid development of fluoroquinolone resistance in *S. typhimurium* and could be a contributive factors accounting for the increasing prevalence of fluoroquinolone-resistant *Salmonella* in Hong Kong in recent years.

## MATERIALS AND METHODS

### BACTERIAL STRAINS

239 *S. typhimurium* previously described clinical isolates were included in this study (Wong et al., 2013).

### PCR AND TARGET GENE MUTATION SCREENING IN

#### *S. typhimurium*

The QRDRs of *gyrA* and *parC* were amplified by PCR as previously described (Chen et al., 2007), followed by determination of their nucleotide sequences and comparison to the wild-type *S. typhimurium* LT2 strain to identify target gene mutations in the test strains. The *gyrA* and *parC* sequences of four *Salmonella* isolates, S08-52, S10-9, S05-23, and S05-30, were submitted to GenBank with the accession numbers for *gyrA*, KM504240, KM504241, KM504242, and KM504243 and *parC*, KM513651, KM513652, KM513653, and KM513654. The association of Insertion sequence IS26 with *oqxAB* was determined by PCR using primers IS26-F(5'GCTGTTACGACGGGAGGAG) and oqx-R (5'GGAGACGAGGTTGGTATGGA).

### CONJUGATION EXPERIMENTS

A conjugative experiment was carried out as previously described (Jacoby et al., 2003) using sodium azide-resistant *E. coli* J53 strain as recipient. Briefly, overnight culture of donor and recipient strains were mixed and collected on a filter, which was subjected to overnight incubation on a blood agar plate. The mixture was then spread on double selective blood agar plates containing olaquindox (128 µg/ml) and sodium azide (100 µg/ml).

### S1-PFGE AND HYBRIDIZATION

S1-PFGE was conducted to determine the size of large plasmids. Briefly, agarose-embedded DNA was digested with S1 nuclease (New England BioLab) at 37°C for 1 h. The restriction fragments were separated by electrophoresis in 0.5 Tris-borate-EDTA buffer at 14°C for 18 h using a Chef Mapper electrophoresis system (Bio-Rad, Hercules, CA, USA) with pulse times of 2.16 to 63.8 s. Phage Lambda PFGE ladder (New England BioLab) was used as DNA size marker. The gels were stained with GelRed, and DNA bands were visualized with UV transillumination (Bio-Rad). Chromosomal and plasmid DNA of *S. typhimurium* strains were transferred and cross-linked onto nylon membrane and hybridized with a DIG-labeled *oqxAB* probe using DIG High Prime DNA Labeling and Detection Starter Kit I (Roche) following manufacturer's instructions to determine the localization of *oqxAB* and *aac(6')-Ib-cr* genes in *S. typhimurium* genetic materials.

### *oqxAB* CLONING, PLASMID TRANSFORMATION, AND PLASMID CURING

Cloning of *oqxAB* into pTrcHisB (Life Technologies) vector was done by PCR using primers pTrc-oqxAB-F (5'TTACTACTCGAGAATGAGCCTGCAAAAAAC) and pTrcoqxAB-R (5'AGGATCGAATTCCCTAGGCGGGCAGATCCTC). pTrc-*oqxAB* was transformed into *S. typhimurium* LT2. Plasmids from clinical strains were extracted by Qiagen Mini-prep kit, electroporated into *S. typhimurium* LT2 and a nalidixic acid and CIP susceptible *S. typhimurium* clinical strain 11–28, and selected on plates containing 32 µg/ml olaquindox. Plasmid curing was performed on clinical *S. typhimurium* strain 10–63 as previously described with slight modification (Sato et al., 2013). The strain was grown in 3 ml LB at 43°C for 2 weeks and selected on plates containing 0, 8, 16, 32 µg/ml olaquindox.

### MUTATION PREVENTION CONCENTRATION (MPC)

Mutation prevention concentration (MPC) of *oqxAB*, *aac(6')Ib-cr* positive, and negative strains was determined as described previously (Gebru et al., 2011, 2012). Briefly, MPC was determined by spreading  $1 \times 10^9$  cells on LB agar plates containing a range of concentration of CIP: 0, 0.05, 0.1, 0.25, 0.5, 1, 2, 4, 8, 16, 32 µg/ml. Plates containing CIP were incubated for up to 72 h, whereas CIP-free plates were incubated for 24 h. Viable counts on each plate were recorded. MPC was defined as the lowest antibiotic concentration at which no colonies were observed. For each strain, MPC was determined on the basis of the results of at least three independent experiments.

## RESULTS

### PMQRS AND SINGLE *GyrA* MUTATION MEDIATE DEVELOPMENT OF FLUOROQUINOLONE RESISTANCE IN *S. typhimurium*

To determine if *oqxAB* alone or the combination of *oqxAB* and *aac(6')Ib-cr* can contribute to fluoroquinolone resistance, the effect of interplay between *oqxAB*, *aac(6')Ib-cr*, and target mutations in mediating fluoroquinolone resistance phenotypes in *Salmonella* was studied. Among all *oqxAB* negative *S. typhimurium* organisms, the vast majority of those which exhibited CIP MIC  $\leq 0.05$  µg/ml had no mutation in the *gyrA* and *parC* genes. Single amino acid substitution (D87Y or D87N) in GyrA was often

detected in strains with CIP MIC between 0.1 and 1 µg/ml. Interestingly, two CIP-resistant isolates (CIP MIC = 1 µg/ml) showed only single mutation at D87Y. Double substitution in GyrA (S83F and D87Y or N) and a single substitution in ParC (S80I) were consistently detected in those with CIP MIC ≥2 µg/ml (Table 1). Among all *oqxAB* positive *S. typhimurium* strains, no mutation was detected in *gyrA* and *parC* in strains with CIP MIC ≤0.05 µg/ml; single mutation in GyrA (D87Y or D87N), but not in ParC, was detected in strains whose CIP MIC was between 0.25 and 2 µg/ml. Among all isolates which were positive to both *oqxAB* and *aac(6')Ib-cr*, single mutation in GyrA (D87Y or D87N), but not in ParC, was detected in strains whose CIP MIC was between 0.25 and 2 µg/ml, whereas most of the strains from this category exhibited CIP MIC ≥1 µg/ml. Comparative analysis of mutational and drug susceptibility data of *oqxAB* negative, *oqxAB* positive, and *oqxAB*, *aac(6')Ib-cr* positive strains showed that similar mutational profiles could result in drastically different CIP MIC, depending on whether the organism harbored the *oqxAB* or *oqxAB*, *aac(6')Ib-cr* genes. Strikingly, simultaneous presence of a single *gyrA* mutation and *oqxAB*, or both *oqxAB* and *aac(6')Ib-cr* genes, was sufficient to produce CIP resistance (CIP MIC = 1 µg/ml); however, double mutations in *gyrA* plus a single mutation in *parC* were required to mediate CIP MIC ≥2 µg/ml when *oqxAB* was absent. Importantly, around 98% of *oqxAB* positive *S. typhimurium* strains harbored mutations in the *gyrA* or *parC* genes, whereas less than 60% of *oqxAB* negative *S. typhimurium* strains had mutations in either or both of these two genes (Data not shown). Taken together, these findings suggest that acquisition of *oqxAB* or *oqxAB*, *aac(6')Ib-cr* by *S. typhimurium* could mediate selection of fluoroquinolone resistance in *S. typhimurium*.

#### TRANSFERABILITY AND GENETIC LOCATION OF *oqxAB*

Thirty randomly selected *oqxAB* positive *S. typhimurium* isolates were subjected to conjugation experiment to determine the transferability of the *oqxAB* gene that they harbored. Surprisingly,

none of the *S. typhimurium* strains tested was able to transfer this resistance element to *E. coli* J53 recipient strain through conjugation. S1-PFGE and Southern hybridization were performed on four *S. typhimurium* isolates and it showed that *oqxAB* and *aac(6')Ib-cr* were concurrently present on plasmids of various sizes in these *S. typhimurium* isolates, hybridization results of two of which were shown in Figure 1. In all the tested *S. typhimurium* isolates, the *oqxAB* gene was found to be flanked by the IS26 fragment in a manner similar to that of the

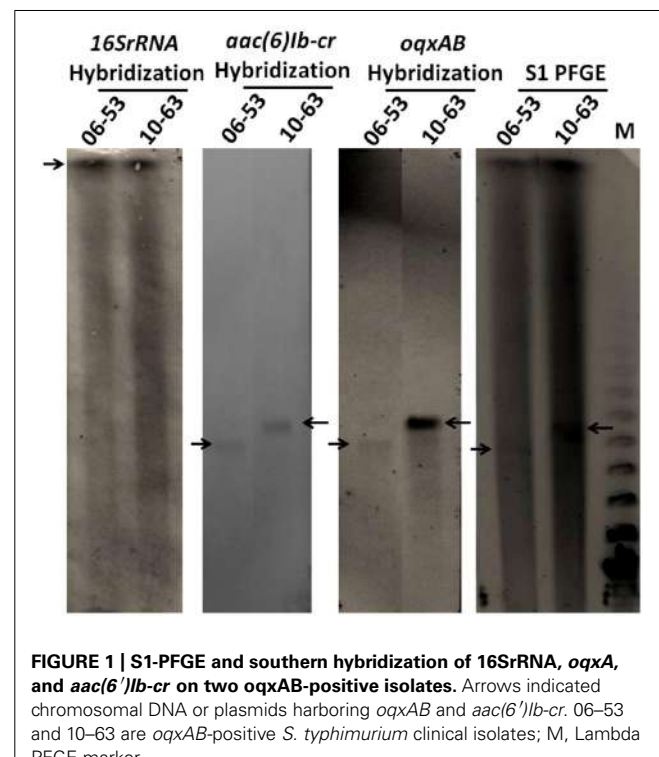


**FIGURE 1 | S1-PFGE and southern hybridization of 16SrRNA, *oqxAB*, and *aac(6')Ib-cr* on two *oqxAB*-positive isolates.** Arrows indicated chromosomal DNA or plasmids harboring *oqxAB* and *aac(6')Ib-cr*. 06–53 and 10–63 are *oqxAB*-positive *S. typhimurium* clinical isolates; M, Lambda PFGE marker.

**Table 1 | Presence of target mutations in different level of ciprofloxacin MIC of *oqxAB* positive and negative *Salmonella typhimurium* isolates.**

| CIP MIC | Clinical <i>S. typhimurium</i> |             |             |                 |                |             |                 |             |                                       |  |
|---------|--------------------------------|-------------|-------------|-----------------|----------------|-------------|-----------------|-------------|---------------------------------------|--|
|         | <i>oqxAB</i> –                 |             |             |                 | <i>oqxAB</i> + |             |                 |             | <i>oqxAB</i> +, <i>aac(6')Ib-cr</i> + |  |
|         | No. of isolates                | <i>gyrA</i> | <i>parC</i> | No. of isolates | <i>gyrA</i>    | <i>parC</i> | No. of isolates | <i>gyrA</i> | <i>parC</i>                           |  |
| ≤0.05   | 104                            | WT/D87N     | WT/S80R     | 1               | WT             | WT          | 0               |             |                                       |  |
| 0.1     | 24                             | D87N        | WT          | 0               |                |             | 2               | WT          | WT                                    |  |
| 0.25    | 14                             | D87N        | WT          | 1               | D87Y           | WT          | 1               | D87Y        | WT                                    |  |
| 0.5     | 18                             | D87N        | WT          | 3               | D87Y           | WT          | 3               | D87Y        | WT                                    |  |
| 1       | 2                              | D87Y        | WT          | 2               | D87Y           | WT          | 6               | D87Y        | WT                                    |  |
| 2       | 2                              | S83F, D87G  | S80R        | 3               | D87Y/D87N      | WT          | 35              | D87Y/D87N   | WT                                    |  |
| 4       | 0                              |             |             | 0               |                |             | 10              | D87Y        | WT                                    |  |
| 8       | 0                              |             |             | 0               |                |             | 0               |             |                                       |  |
| ≥16     | 8                              | S83F, D87G  | S80R        | 0               |                |             | 0               |             |                                       |  |
| Total   | 172                            |             |             | 10              |                |             | 57              |             |                                       |  |

pOLA52 plasmid as previously reported (Norman et al., 2008), suggesting that the *oqxAB* gene that was becoming prevalent in *S. typhimurium* could have been derived from the original transferable element located in pOLA52. To test this possibility, we performed PCR screening to determine if pOLA52 specific DNA sequences were prevalent among the test plasmids. To our surprise, however, none of the plasmids that carried *oqxAB* and *aac(6')Ib-cr* contained such sequences of pOLA52 (Data not shown).

#### CONTRIBUTION OF *oqxAB* AND *aac(6')Ib-cr* TO THE ELEVATED CIPROFLOXACIN MIC IN *S. typhimurium*

To directly prove the degree of contribution of *oqxAB* and *aac(6')Ib-cr* to the development of fluoroquinolone resistance in *S. typhimurium*, *oqxAB* was cloned into a pTrc expression vector and transformed into *S. typhimurium* LT2 strain. Compared to the original *oqxAB* negative *S. typhimurium* LT2 strain, pTrc-*oqxAB*- carrying *S. typhimurium* LT2 exhibited a CIP MIC of 0.25 µg/ml, with a 20-fold increase. However, *S. typhimurium* LT2 carrying pTrc-*oqxAB* showed much weaker growth than its parental counterpart, which was presumably due to the fitness cost caused by the over-expression of *oqxAB* in the host strain. To overcome this problem, the plasmids that carried *oqxAB* and *aac(6')Ib-cr* were extracted from different clinical *S. typhimurium* isolates and electroporated into *S. typhimurium* LT2 with no success. The plasmids were then electroporated into an *oqxAB*-negative *S. typhimurium* strain 11–28. Upon acquisition of such plasmid, the CIP MIC of this *S. typhimurium* strain increased by approximately fourfold (Table 2). To further prove the contribution of *oqxAB* and *aac(6')Ib-cr* to *S. typhimurium* fluoroquinolone resistance, the plasmid carrying such genes in a clinical *S. typhimurium* strain 10–63 was cured and it showed that the curing of the plasmid in 10–63 decreased the CIP MIC by approximately fourfold (Table 2). Taken together, our data had proven that *oqxAB* and *aac(6')Ib-cr* contributed to about four fold increase of CIP MIC in *S. typhimurium*. The MICs of other antibiotics were also determined for *S. typhimurium* that acquired

*oqxAB*, *aac(6')Ib-cr* encoding plasmids. In addition, it is shown that acquisition of *oqxAB* and *aac(6')Ib-cr* encoding plasmids ensured resistance to ampicillin, chloramphenicol, streptomycin, nalidixic acid, sulfamethoxazole, tetracycline, trimethoprim, and olaquindox in addition to the elevated CIP MIC (Table 2). This is also consistent to our previous finding that the presence of *oqxAB* in *S. typhimurium* was associated with the ACSSuT R phenotype. As much as 56% of *oqxAB*-positive *S. typhimurium* clinical isolates were resistant to ACSSuT, whereas only 14% of *oqxAB*-negative isolates were resistant to ACSSuT (Wong et al., 2013).

#### CONTRIBUTION OF *oqxAB* AND *aac(6')Ib-cr* TO ELEVATED MPC OF FLUOROQUINOLONE IN *S. typhimurium*

To validate the hypothesis that *oqxAB* and *aac(6')Ib-cr* contributed to mutation development, MPC of CIP were determined for *S. typhimurium* with and without *oqxAB*. As shown in Table 3, *oqxAB*, *aac(6')Ib-cr* positive clinical *Salmonella* isolates, 06–57, 07–43, and 08–11 exhibited much higher MPC of CIP than the *oqxAB*, *aac(6')Ib-cr*-negative *Salmonella* strains, 05–41, 07–54, and 10–25 (Table 3). Furthermore, although *Salmonella* 11–28 strain exhibited MPC for CIP of about 0.1 µg/ml, transformation of plasmids from other clinical *Salmonella* isolates carrying *oqxAB*, *aac(6')Ib-cr* to *Salmonella* 11–28 dramatically increased its MPC to 2~4 µg/ml. On the other hand, *Salmonella* 10–63 exhibited MPC of 8 µg/ml, yet the curing of the *oqxAB*, *aac(6')Ib-cr* encoding plasmid led to a slightly decreased MPC (4 µg/ml). The minimal effect of curing of *oqxAB*, *aac(6')Ib-cr* encoding plasmid on the MPC of 10–63 may be due to the fact that the long-term starvation stress used to cure the plasmid may have caused stress response to develop in the isolate, thereby indirectly contributing to the elevated MPC for strain.

Ten to 63 C. It has been shown that long-term starvation stress stimulates the stringent SOS response in bacteria, which is essential in bacteria for acquisition of mutations leading to resistance to some antibiotic drugs (Fung et al., 2010). Most importantly, compared to *Salmonella* 11–28 alone, which did not develop

**Table 2 | MIC profiles for *Salmonella* strains with various *oqxAB* and *aac(6')Ib-cr* -borne plasmids.**

| Strain  | MIC (µg/ml) |     |       |      |     |      |       |     |     |     |     |      |
|---------|-------------|-----|-------|------|-----|------|-------|-----|-----|-----|-----|------|
|         | AMP         | CRO | CIP   | NA   | TET | CHL  | SUL   | TRI | AMK | GEN | OLA | STE  |
| 11–28*  | ≤4          | ≤1  | 0.012 | 4    | 2   | ≤4   | ≤128  | ≤4  | ≤4  | ≤1  | 8   | 8    |
| P06–57# | ≥128        | ≤1  | 0.05  | 16   | 64  | ≥128 | ≥1024 | 32  | ≤4  | 32  | 128 | ≥128 |
| P07–43# | ≥128        | ≤1  | 0.05  | 32   | 64  | ≥128 | ≥1024 | 32  | ≤4  | 32  | 64  | ≥128 |
| P08–11# | ≥128        | ≤1  | 0.05  | 16   | 64  | ≥128 | ≥1024 | 32  | ≤4  | 32  | 64  | ≥128 |
| P10–9#  | ≥128        | ≤1  | 0.05  | 16   | 64  | ≥128 | ≥1024 | 32  | ≤4  | 32  | 128 | ≥128 |
| 10–63*  | ≥128        | ≤1  | 1     | ≥128 | 64  | ≥128 | ≥1024 | 32  | ≤4  | ≤1  | 512 | 32   |
| 10–63C  | 16          | ≤1  | 0.25  | ≥128 | 2   | ≥128 | ≥1024 | ≤4  | ≤4  | ≤1  | 16  | 8    |

AMP, ampicillin; CRO, ceftriaxone; CIP, ciprofloxacin; NA, Nalidixic acid; TET, tetracycline; CHL, chloramphenicol; SUL, sulfamethoxazole; TRI, trimethoprim; AMK, amikacin; GEN, gentamicin; STE, streptomycin; OLA, olaquindox.

\*Salmonella clinical isolates with various *oqxAB*, *aac(6')Ib-cr* background; #transformants with the transformation of *oqxAB*, *aac(6')Ib-cr* encoding plasmid from different clinical *Salmonella* isolates to parental *Salmonella* strain 11–28; C, *oqxAB*, *aac(6')Ib-cr* encoding plasmid cured strain.

**Table 3 | MICs of nalidixic acid (NA) and ciprofloxacin (CIP) and mutation prevention concentration (MPC) toward CIP of *Salmonella* isolates with various background of *oqxAB* and *aac(6')Ib-cr*.**

| Salmonella Isolate | <i>oqxAB</i> ,<br><i>aac(6')Ib-cr</i> | QRDR Mutations |      | MIC ( $\mu\text{g/ml}$ ) |       | MPC<br>( $\mu\text{g/ml}$ ) | GyrA mutation <sup>†</sup> | MPC/MIC |
|--------------------|---------------------------------------|----------------|------|--------------------------|-------|-----------------------------|----------------------------|---------|
|                    |                                       | GyrA           | ParC | NA                       | CIP   |                             |                            |         |
| 06-57*             | +                                     | WT             | WT   | 32                       | 0.1   | 2                           | NT                         | 20      |
| 07-43*             | +                                     | WT             | WT   | 16                       | 0.05  | 0.5                         | NT                         | 10      |
| 08-11*             | +                                     | WT             | WT   | 32                       | 0.1   | 1                           | NT                         | 10      |
| 05-41*             | -                                     | D87N           | WT   | 32                       | 0.025 | 0.1                         | NT                         | 4       |
| 07-54*             | -                                     | WT             | WT   | 16                       | 0.012 | 0.1                         | NT                         | 8       |
| 10-25*             | -                                     | WT             | WT   | 4                        | 0.025 | 0.1                         | NT                         | 4       |
| 11-28*             | -                                     | WT             | WT   | 4                        | 0.012 | 0.1                         | WT                         | 8       |
| p06-57#            | +                                     | WT             | WT   | 16                       | 0.05  | 4                           | D87N                       | 80      |
| p07-43#            | +                                     | WT             | WT   | 32                       | 0.05  | 2                           | WT                         | 40      |
| p08-11#            | +                                     | WT             | WT   | 16                       | 0.05  | 2                           | D87G                       | 40      |
| p10-9#             | +                                     | WT             | WT   | 16                       | 0.05  | 2                           | WT                         | 40      |
| 10-63*             | +                                     | D87N           | WT   | $\geq 128$               | 1     | 8                           | D87Y                       | 8       |
| 10-63c             | -                                     | D87N           | WT   | $\geq 128$               | 0.25  | 4                           | D87Y                       | 16      |

NA, Nalidixic acid; CIP, ciprofloxacin.

\*Salmonella clinical isolates with various *oqxAB*, *aac(6')Ib-cr* background; #transformants with the transformation of *oqxAB*, *aac(6')Ib-cr* encoding plasmids from different clinical *Salmonella* isolates to parental *Salmonella* strain 11-28; <sup>†</sup> GyrA mutation from strains that were selected after MPC assay and have CIP MIC between 0.5 and 4  $\mu\text{g/ml}$ ; c, *oqxAB*, *aac(6')Ib-cr* encoding plasmid cured strain; NT, Not tested.

*gyrA* mutation in MPC assay, *Salmonella* 11-28 transformed with *oqxAB*, *aac(6')Ib-cr* encoding plasmids from *Salmonella* 06-57 and 08-11 developed single mutation in *gyrA*, which may partly contributed to the increase of CIP MPC (Table 3). It is probably due to that the presence of *oqxAB* and *aac(6')Ib-cr* may enable *S. typhimurium* to survive under fluoroquinolone stress and facilitate subsequent development of target mutations. Nevertheless, these data confirm that *oqxAB*, *aac(6')Ib-cr* plays a key role in elevated CIP MIC and MPC, and hence resistance to fluoroquinolone in *S. typhimurium*.

## DISCUSSION

An important finding in this work is that the *oqxAB* and *aac(6')Ib-cr* gene products not only directly contribute to the elevated CIP MIC, but also enhance the ability of *S. typhimurium* to survive in an environment with high dose of CIP, which may in turn facilitate the development of fluoroquinolone resistance. The mechanism of fluoroquinolone resistance in *Salmonella* has conventionally been attributed to double mutations in *gyrA* with or without a single *parC* mutation (Casin et al., 2003; Chu et al., 2005). Unlike *E. coli* and *Campylobacter*, double *gyrA* mutations in *Salmonella* were rare and presumably difficult to acquire, therefore fluoroquinolone remained an effective treatment of choice for severe *Salmonella* infections. In this study, we demonstrated that acquisition of the *oqxAB* or *oqxAB*, *aac(6')Ib-cr* genes in *S. typhimurium*, could mediate development of resistance to CIP (CIP MIC  $\geq 1 \mu\text{g/ml}$ ). We postulate that the pump activities and enzymatic hydrolysis of fluoroquinolones enable the organisms to withstand antibiotic pressure for a prolonged period,

during which mutational changes can occur. Elevation of the antibiotic resistance potential of *Salmonella* is one way by which *oqxAB* can help the host strain to successfully launch clinical infection in human, leading to a dramatic increase in the proportion of *oqxAB* positive strains observable among clinical *Salmonella* isolates recovered in recent years (Wong et al., 2014). The increased prevalence of *oqxAB* positive *S. typhimurium* in clinical isolates also contributes directly to a higher percentage of fluoroquinolone resistance in clinical salmonella strains. In 2011, the proportion of the *oqxAB* positive *S. typhimurium* in Hong Kong that were found to be resistant to CIP reached 34% (Data not shown).

The fact that *oqxAB* could not be found in *S. typhimurium* until 2006 may be due to its poor ability to replicate in *Salmonella* initially; this notion is supported by the fact that transformation of *oqxAB*-borne plasmid to *S. typhimurium* did not elevate MIC of CIP in these strains and that direct expression of *oqxAB* into *S. typhimurium* had a fitness cost in this work (Hansen et al., 2007; Wong et al., 2013). Nevertheless, our data indicate that the *oqxAB* gene has adapted to co-exist in *S. typhimurium*. In this study, *oqxAB* were found to be associated with IS26 but not carried by pOLA52-like plasmids, suggesting *oqxAB* was excised from pOLA52 and integrated into other plasmids mediated by IS26 transposase. Since no *oqxAB* encoding plasmid in *Salmonella* has been sequenced, the mechanism underlying the co-existence of *oqxAB* and *aac(6')Ib-cr* in over 80% of the *oqxAB*-positive strain is not clear. The quick expansion of *oqxAB* and *aac(6')Ib-cr* positive, CIP-resistant *S. typhimurium* will pose huge threat to efforts of infection control of *Salmonella* infections. Urgent actions are

required to halt further transmission of the *oqxAB* positive strains in both environmental and clinical settings. In addition, it remains to be seen if *oqxAB* has been taken up by other bacterial species and whether it plays a role in the evolution of resistance and virulence traits of various bacterial pathogens. Findings in this work also highlight a need to investigate the impact of *oqxAB* in a wide range of foodborne and zoonotic pathogens.

## ACKNOWLEDGMENTS

We thank Dr. Julia Ling for her assistance in the collection of clinical *Salmonella* isolates in Hong Kong. This work was supported by the Chinese National Key Basic Research and Development (973) Program (2013CB127200) and the Health and Medical Research Fund of the Food and Health Bureau, The Government of Hong Kong (13121412 and 14130402 to Sheng Chen).

## REFERENCES

- Casin, I., Breuil, J., Darchis, J. P., Guelpa, C., and Collatz, E. (2003). Fluoroquinolone resistance linked to GyrA, GyrB, and ParC mutations in *Salmonella enterica Typhimurium* isolates in humans. *Emerg. Infect. Dis.* 9, 1455–1457. doi: 10.3201/eid0911.030317
- Cattoir, V., and Nordmann, P. (2009). Plasmid-mediated quinolone resistance in gram-negative bacterial species: an update. *Curr. Med. Chem.* 16, 1028–1046. doi: 10.2174/092986709787581879
- Cavaco, L. M., Hasman, H., Xia, S., and Aarestrup, F. M. (2009). qnrD, a novel gene conferring transferable quinolone resistance in *Salmonella enterica* serovar Kentucky and Bovismorbificans strains of human origin. *Antimicrob. Agents Chemother.* 53, 603–608. doi: 10.1128/AAC.00997-08
- Centers for Disease Control and Prevention. (1997). Multidrug-resistant *Salmonella* serotype *Typhimurium*—United States, 1996. *MMWR Morb. Mortal. Wkly. Rep.* 46, 308–310.
- Chen, S., Cui, S., McDermott, P. F., Zhao, S., White, D. G., Paulsen, I., et al. (2007). Contribution of target gene mutations and efflux to decreased susceptibility of *Salmonella enterica* serovar *typhimurium* to fluoroquinolones and other antimicrobials. *Antimicrob. Agents Chemother.* 51, 535–542. doi: 10.1128/AAC.00600-06
- Chu, C., Su, L. H., Chu, C. H., Baucheron, S., Cloeckaert, A., and Chiu, C. H. (2005). Resistance to fluoroquinolones linked to gyrA and par C mutations and overexpression of acrAB efflux pump in *Salmonella enterica* serotype *Choleraesuis*. *Microb. Drug Resist.* 11, 248–253. doi: 10.1089/mdr.2005.11.248
- Ferrari, R., Galiana, A., Cremades, R., Rodriguez, J. C., Magnani, M., Tognim, M. C., et al. (2011). Plasmid-mediated quinolone resistance by genes qnrA1 and qnrB19 in *Salmonella* strains isolated in Brazil. *J. Infect. Dev. Ctries.* 5, 496–498. doi: 10.3855/jidc.1735
- Fung, D. K., Chan, E. W., Chin, M. L., and Chan, R. C. (2010). Delineation of a bacterial starvation stress response network which can mediate antibiotic tolerance development. *Antimicrob. Agents Chemother.* 54, 1082–1093. doi: 10.1128/AAC.01218-09
- Gebru, E., Choi, M. J., Lee, S. J., Damte, D., and Park, S. C. (2011). Mutant-prevention concentration and mechanism of resistance in clinical isolates and enrofloxacin/marbofloxacin-selected mutants of *Escherichia coli* of canine origin. *J. Med. Microbiol.* 60, 1512–1522. doi: 10.1099/jmm.0.028654-0
- Gebru, E., Damte, D., Choi, M. J., Lee, S. J., Kim, Y. H., and Park, S. C. (2012). Mutant prevention concentration and phenotypic and molecular basis of fluoroquinolone resistance in clinical isolates and in vitro-selected mutants of *Escherichia coli* from dogs. *Vet. Microbiol.* 154, 384–394. doi: 10.1016/j.vetmic.2011.07.033
- Glynn, M. K., Bopp, C., Dewitt, W., Dabney, P., Mokhtar, M., and Angulo, F. J. (1998). Emergence of multidrug-resistant *Salmonella enterica* serotype *typhimurium* DT104 infections in the United States. *N. Engl. J. Med.* 338, 1333–1338. doi: 10.1056/NEJM199805073381901
- Gomez, T. M., Motarjem, Y., Miyagawa, S., Kafnerstein, F. K., and Stohr, K. (1997). Foodborne salmonellosis. *World Health Stat. Q.* 50, 81–89.
- Hansen, L. H., Jensen, L. B., Sorensen, H. I., and Sorensen, S. J. (2007). Substrate specificity of the OqxAB multidrug resistance pump in *Escherichia coli* and selected enteric bacteria. *J. Antimicrob. Chemother.* 60, 145–147. doi: 10.1093/jac/dkm167
- Hansen, L. H., Johannessen, E., Burmolle, M., Sorensen, A. H., and Sorensen, S. J. (2004). Plasmid-encoded multidrug efflux pump conferring resistance to olaquindox in *Escherichia coli*. *Antimicrob. Agents Chemother.* 48, 3332–3337. doi: 10.1128/AAC.48.9.3332-3337.2004
- Hawkey, P. M. (2003). Mechanisms of quinolone action and microbial response. *J. Antimicrob. Chemother.* 51(Suppl. 1), 29–35. doi: 10.1093/jac/dkg207
- Hohmann, E. L. (2001). Nontyphoidal salmonellosis. *Clin. Infect. Dis.* 32, 263–269. doi: 10.1086/318457
- Jacoby, G. A., Chow, N., and Waites, K. B. (2003). Prevalence of plasmid-mediated quinolone resistance. *Antimicrob. Agents Chemother.* 47, 559–562. doi: 10.1128/AAC.47.2.559-562.2003
- Kim, H. B., Wang, M., Park, C. H., Kim, E. C., Jacoby, G. A., and Hooper, D. C. (2009). *oqxAB* encoding a multidrug efflux pump in human clinical isolates of Enterobacteriaceae. *Antimicrob. Agents Chemother.* 53, 3582–3584. doi: 10.1128/AAC.01574-08
- Kim, J. H., Cho, J. K., and Kim, K. S. (2013). Prevalence and characterization of plasmid-mediated quinolone resistance genes in *Salmonella* isolated from poultry in Korea. *Avian Pathol.* 42, 221–229. doi: 10.1080/03079457.2013.779636
- Liu, B. T., Wang, X. M., Liao, X. P., Sun, J., Zhu, H. Q., Chen, X. Y., et al. (2011). Plasmid-mediated quinolone resistance determinants *oqxAB* and *aac(6')*-*lb-cr* and extended-spectrum beta-lactamase gene *blaCTX-M-24* co-located on the same plasmid in one *Escherichia coli* strain from China. *J. Antimicrob. Chemother.* 66, 1638–1639. doi: 10.1093/jac/dkr172
- Markogiannakis, A., Tassios, P. T., Lambiri, M., Ward, L. R., Kourea-Kremastinou, J., Legakis, N. J., et al. (2000). Multiple clones within multidrug-resistant *Salmonella enterica* serotype *Typhimurium* phage type DT104. The Greek nontyphoidal *Salmonella* study group. *J. Clin. Microbiol.* 38, 1269–1271.
- Norman, A., Hansen, L. H., She, Q., and Sorensen, S. J. (2008). Nucleotide sequence of pOLA52: a conjugative IncX1 plasmid from *Escherichia coli* which enables biofilm formation and multidrug efflux. *Plasmid* 60, 59–74. doi: 10.1016/j.plasmid.2008.03.003
- Park, K. S., Kim, M. H., Park, T. S., Nam, Y. S., Lee, H. J., and Suh, J. T. (2012). Prevalence of the plasmid-mediated quinolone resistance genes, *aac(6')*-*lb-cr*, *qepA*, and *oqxAB* in clinical isolates of extended-spectrum beta-lactamase (ESBL)-producing *Escherichia coli* and *Klebsiella pneumoniae* in Korea. *Ann. Clin. Lab. Sci.* 42, 191–197.
- Robicsek, A., Strahilevitz, J., Jacoby, G. A., Macielag, M., Abbanat, D., Park, C. H., et al. (2006). Fluoroquinolone-modifying enzyme: a new adaptation of a common aminoglycoside acetyltransferase. *Nat. Med.* 12, 83–88. doi: 10.1038/nm1347
- Ruiz, E., Saenz, Y., Zarazaga, M., Rocha-Gracia, R., Martinez-Martinez, L., Arlet, G., et al. (2012). *qnr*, *aac(6')*-*lb-cr* and *qepA* genes in *Escherichia coli* and *Klebsiella spp.*: genetic environments and plasmid and chromosomal location. *J. Antimicrob. Chemother.* 67, 886–897. doi: 10.1093/jac/dkr548
- Sato, T., Yokota, S., Uchida, I., Okubo, T., Usui, M., Kusumoto, M., et al. (2013). Fluoroquinolone resistance mechanisms in an *Escherichia coli* isolate, HUE1, without quinolone resistance-determining region mutations. *Front. Microbiol.* 4:125. doi: 10.3389/fmicb.2013.00125
- Tran, J. H., Jacoby, G. A., and Hooper, D. C. (2005). Interaction of the plasmid-encoded quinolone resistance protein Qnr with *Escherichia coli* DNA gyrase. *Antimicrob. Agents Chemother.* 49, 118–125. doi: 10.1128/AAC.49.1.118-125.2005
- Wong, M. H., and Chen, S. (2012). First detection of *oqxAB* in *Salmonella spp.* isolated from food. *Antimicrob. Agents Chemother.* 57, 658–660. doi: 10.1128/AAC.01144-12
- Wong, M. H., Yan, M., Chan, E. W., Biao, K., and Chen, S. (2014). Emergence of clinical *Salmonella Typhimurium* with concurrent resistant to ciprofloxacin, ceftriaxone and azithromycin. *Antimicrob. Agents Chemother.* 58, 3752–3756. doi: 10.1128/AAC.02770-13
- Wong, M. H., Yan, M., Chan, E. W., Liu, L. Z., Kan, B., and Chen, S. (2013). Expansion of *Salmonella Typhimurium* ST34 clone carrying multiple resistance determinants in China. *Antimicrob. Agents Chemother.* doi: 10.1128/AAC.01174-13 [Epub ahead of print].
- Yamane, K., Wachino, J., Suzuki, S., Kimura, K., Shibata, N., Kato, H., et al. (2007). New plasmid-mediated fluoroquinolone efflux pump, QepA, found in an *Escherichia coli* clinical isolate. *Antimicrob. Agents Chemother.* 51, 3354–3360. doi: 10.1128/AAC.00339-07
- Yuan, J., Xu, X., Guo, Q., Zhao, X., Ye, X., Guo, Y., et al. (2012). Prevalence of the *oqxAB* gene complex in *Klebsiella pneumoniae* and *Escherichia coli* clinical isolates. *J. Antimicrob. Chemother.* 67, 1655–1659. doi: 10.1093/jac/dks086

Zhao, J., Chen, Z., Chen, S., Deng, Y., Liu, Y., Tian, W., et al. (2010). Prevalence and dissemination of oqxAB in *Escherichia coli* isolates from animals, farmworkers, and the environment. *Antimicrob. Agents Chemother.* 54, 4219–4224. doi: 10.1128/AAC.00139-10

**Conflict of Interest Statement:** The authors declare that the research was conducted in the absence of any commercial or financial relationships that could be construed as a potential conflict of interest.

Received: 06 August 2014; accepted: 17 September 2014; published online: 02 October 2014.

*Citation:* Wong MH, Chan EW, Liu LZ and Chen S (2014) PMQR genes oqxAB and *aac(6')Ib-cr* accelerate the development of fluoroquinolone resistance in *Salmonella typhimurium*. *Front. Microbiol.* 5:521. doi: 10.3389/fmicb.2014.00521

This article was submitted to Antimicrobials, Resistance and Chemotherapy, a section of the journal *Frontiers in Microbiology*.

Copyright © 2014 Wong, Chan, Liu and Chen. This is an open-access article distributed under the terms of the Creative Commons Attribution License (CC BY). The use, distribution or reproduction in other forums is permitted, provided the original author(s) or licensor are credited and that the original publication in this journal is cited, in accordance with accepted academic practice. No use, distribution or reproduction is permitted which does not comply with these terms.

OPEN ACCESS

**Edited by:**

Keith Poole,  
Queen's University, Canada

**Reviewed by:**

Govindan Rajamohan,  
Council of Scientific and Industrial  
Research – Institute of Microbial  
Technology, India  
Ayush Kumar,  
University of Manitoba, Canada

**\*Correspondence:**

Ian T. Paulsen and Karl A. Hassan,  
Department of Chemistry  
and Biomolecular Sciences,  
Macquarie University, Eastern Road,  
Sydney, NSW 2109, Australia  
ian.paulsen@mq.edu.au;  
karl.hassan@mq.edu.au

**†Present address:**

Scott M. Jackson,  
Institute of Molecular Biology and  
Biophysics, ETH Zurich, Zurich,  
Switzerland

**Specialty section:**

This article was submitted to  
Antimicrobials, Resistance and  
Chemotherapy, a section of the  
journal Frontiers in Microbiology

**Received:** 12 February 2015

**Accepted:** 02 April 2015

**Published:** 22 April 2015

**Citation:**

Hassan KA, Elbourne LDH, Li L, Gamage HKAH, Liu Q, Jackson SM, Sharples D, Kolsto A-B, Henderson PJF and Paulsen IT (2015)

An ace up their sleeve:

a transcriptomic approach exposes  
the Acel efflux protein  
of *Acinetobacter baumannii*  
and reveals the drug efflux potential  
hidden in many microbial pathogens.

Front. Microbiol. 6:333.

doi: 10.3389/fmicb.2015.00333

# An ace up their sleeve: a transcriptomic approach exposes the Acel efflux protein of *Acinetobacter baumannii* and reveals the drug efflux potential hidden in many microbial pathogens

Karl A. Hassan<sup>1\*</sup>, Liam D. H. Elbourne<sup>1</sup>, Liping Li<sup>1</sup>, Hasinika K. A. H. Gamage<sup>1</sup>, Qi Liu<sup>1</sup>, Scott M. Jackson<sup>2†</sup>, David Sharples<sup>2</sup>, Anne-Brit Kolsto<sup>3</sup>, Peter J. F. Henderson<sup>2</sup> and Ian T. Paulsen<sup>1\*</sup>

<sup>1</sup> Department of Chemistry and Biomolecular Sciences, Macquarie University, Sydney, NSW, Australia, <sup>2</sup> Astbury Centre for Structural Molecular Biology, School of Biomedical Sciences, University of Leeds, Leeds, UK, <sup>3</sup> Laboratory for Microbial Dynamics, Department of Pharmaceutical Biosciences, School of Pharmacy, University of Oslo, Oslo, Norway

The era of antibiotics as a cure-all for bacterial infections appears to be coming to an end. The emergence of multidrug resistance in many hospital-associated pathogens has resulted in “superbugs” that are effectively untreatable. Multidrug efflux pumps are well known mediators of bacterial drug resistance. Genome sequencing efforts have highlighted an abundance of putative efflux pump genes in bacteria. However, it is not clear how many of these pumps play a role in antimicrobial resistance. Efflux pump genes that participate in drug resistance can be under tight regulatory control and expressed only in response to substrates. Consequently, changes in gene expression following antimicrobial shock may be used to identify efflux pumps that mediate antimicrobial resistance. Using this approach we have characterized several novel efflux pumps in bacteria. In one example we recently identified the *Acinetobacter* chlorhexidine efflux protein (Acel) efflux pump in *Acinetobacter*. Acel is a prototype for a novel family of multidrug efflux pumps conserved in many proteobacterial lineages. The discovery of this family raises the possibility that additional undiscovered intrinsic resistance proteins may be encoded in the core genomes of pathogenic bacteria.

**Keywords:** multidrug efflux systems, bacterial transmembrane pair, adaptive resistance, bacterial drug resistance, transcriptomics

## Introduction

Multidrug efflux pumps are a significant obstacle preventing the control of infections caused by pathogenic bacteria. Genes encoding these transporters have been found in all bacterial genomes sequenced, and the overexpression of just one can lead to the reduced efficacy of a range of structurally and mechanistically unrelated antimicrobials (Ren and Paulsen, 2007; Brzoska et al., 2013). Five families of transporters that include multidrug efflux systems have been studied extensively, and include representative proteins that have

been characterized biochemically and by tertiary structural analyses. These include the ATP-binding cassette (ABC) superfamily, the major facilitator superfamily (MFS), the resistance/nodulation/division (RND) superfamily, the small multidrug resistance (SMR) family, and the multidrug and toxic compound extrusion (MATE) family (Figure 1).

Significant longstanding difficulties surround identifying the physiological functions of these multidrug efflux transport proteins and determining which of the many pumps encoded by bacterial strains actually contribute to antimicrobial resistance (Piddock, 2006; Schindler et al., 2015). Studies have shown that these efflux pumps often have overlapping substrate recognition profiles (Tal and Schuldiner, 2009). Furthermore, it is not uncommon for a bacterial genome to encode a large number of efflux pumps that have predicted drug substrates, e.g., strains of *Bacillus cereus* encode more than 100 of these pumps accounting for more than 2% of their predicted protein coding potential (Ren and Paulsen, 2007; Simm et al., 2012). It is unlikely that all these pumps share the primary function of protection against toxic compounds, highlighting a need for higher throughput approaches to assess the physiological roles of individual proteins, be they in drug resistance, native housekeeping functions, or other cellular roles.

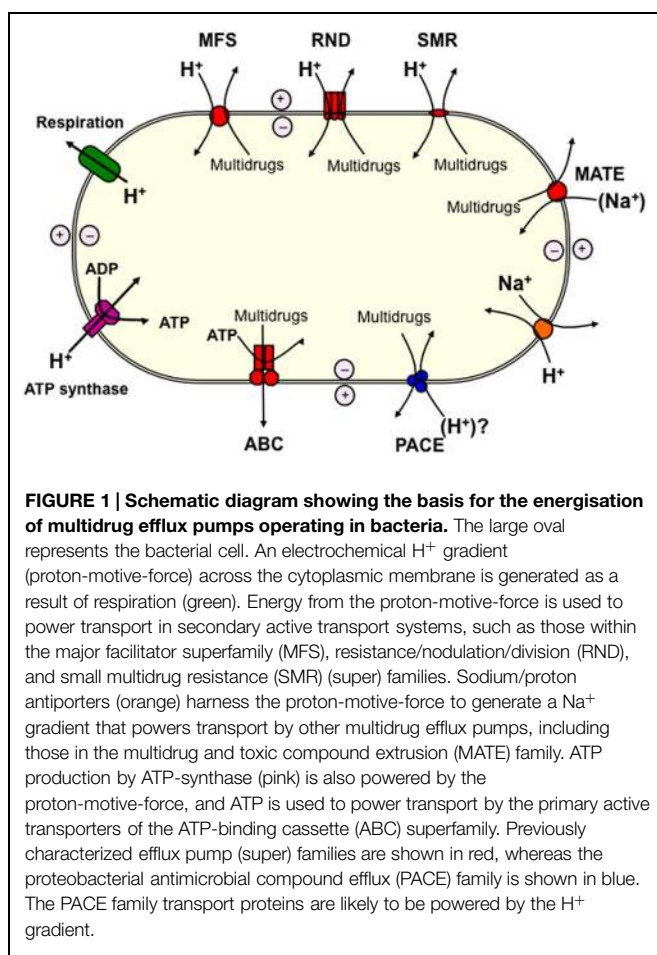


**FIGURE 1 | Schematic diagram showing the basis for the energisation of multidrug efflux pumps operating in bacteria.** The large oval represents the bacterial cell. An electrochemical  $H^+$  gradient (proton-motive-force) across the cytoplasmic membrane is generated as a result of respiration (green). Energy from the proton-motive-force is used to power transport in secondary active transport systems, such as those within the major facilitator superfamily (MFS), resistance/nodulation/division (RND), and small multidrug resistance (SMR) (super) families. Sodium/proton antiporters (orange) harness the proton-motive-force to generate a  $Na^+$  gradient that powers transport by other multidrug efflux pumps, including those in the multidrug and toxic compound extrusion (MATE) family. ATP production by ATP-synthase (pink) is also powered by the proton-motive-force, and ATP is used to power transport by the primary active transporters of the ATP-binding cassette (ABC) superfamily. Previously characterized efflux pump (super) families are shown in red, whereas the proteobacterial antimicrobial compound efflux (PACE) family is shown in blue. The PACE family transport proteins are likely to be powered by the  $H^+$  gradient.

## Efflux Pumps Participate in Intrinsic, Adaptive, and Acquired Resistance

Bacterial drug resistance can be divided into three general categories, intrinsic, adaptive, and acquired (Fernandez and Hancock, 2012). Depending on their mode(s) of regulation and their local genetic context, bacterial multidrug efflux pumps can be geared to participate in any of these three resistance categories. Intrinsic resistance stems from inherent properties of a bacterial cell and can occur as a result of high constitutive expression and activity of some multidrug efflux pumps. Adaptive resistance is related to physiological alterations that are induced by environmental changes and can occur when multidrug efflux pumps are expressed in response to antimicrobial substrates. Finally, acquired resistance can result from mutations promoting constitutive expression of an ordinarily tightly controlled endogenous multidrug efflux system, or when efflux pump genes are acquired on a mobile genetic element, such as a plasmid or phage.

## Adaptive Resistance Responses Identify Efflux Pumps that Mediate Drug Resistance

High-level expression of efflux pumps can have a negative impact on cell growth (Brzoska et al., 2013), resulting in a need to control the timing of efflux system expression to coincide with specific physiological requirements. As such, efflux pumps with physiological resistance functions may be characteristically expressed in response to drug substrates. These pumps may be part of an adaptive drug resistance response or part of general stress response regulons. For example, expression of the *adeAB* and *adeIJK* efflux pump genes in *Acinetobacter baumannii* (Hassan et al., 2013; our unpublished data), the *acrAB* and *acrF* genes in *Escherichia coli* (Shaw et al., 2003; Bailey et al., 2009), the *mexXY* and *mexCD* genes in *Pseudomonas aeruginosa* (Morita et al., 2014), the *norA* gene in *Staphylococcus aureus* (Kaatz and Seo, 2004), and the *bmr* gene in *Bacillus subtilis* (Ahmed et al., 1994), is induced in response to antimicrobial shock treatments.

The mode of regulation and regulatory cues of most efflux pumps are typically only investigated after their functional characterisation. However, global gene expression profiles that show heightened expression of putative efflux pump genes following drug or toxin shocks have provided the impetus to assess the drug resistance functions of these pumps. For example, members of our team recognized that an uncharacterised MFS exporter, BC4707, was expressed in response to bile salt shock in the human food-poisoning associated pathogen *Bacillus cereus*, and went on to characterize its role in drug resistance (Kristoffersen et al., 2007). The gene encoding BC4707 is conserved in the core genome of *B. cereus* and its deletion from *B. cereus* ATCC 14579 resulted in increased susceptibility to norfloxacin (Simm et al., 2012). Overexpression of BC4707 in *E. coli* BL21  $\Delta acrAB$  resulted in increased resistance to norfloxacin, ciprofloxacin, and kanamycin and fluorescence

transport assays showed that accumulation of norfloxacin is reduced by BC4707 in an energy dependent manner (Simm et al., 2012).

## Adaptive Resistance Responses Identify a New Class of Drug Efflux Pump

Extending from this work, we have exploited adaptive resistance responses to identify efflux pumps that may mediate drug resistance in hospital-acquired bacterial pathogens, with a focus on biocide resistance. For example, in recent work we conducted a transcriptomic study to examine the regulatory response of *A. baumannii* to a shock treatment with the synthetic biocide chlorhexidine (Hassan et al., 2013). Chlorhexidine is commonly applied in antibacterial soaps, mouthwashes and antisepsics, and is listed as an “Essential Medicine” by the World Health Organization. Chlorhexidine is a membrane active biocide and as such, multidrug efflux pumps are commonly associated with reduced levels of susceptibility (Russell, 1986; McDonnell and Russell, 1999). In line with the discussion above, the most highly overexpressed genes in our chlorhexidine shock treatment encoded AdeAB, components of a major tripartite RND multidrug efflux system in *A. baumannii* (Hassan et al., 2013). This efflux system has previously been shown to mediate resistance to a very broad range of antimicrobials and biocides, including chlorhexidine (Rajamohan et al., 2009). The overexpression of genes encoding AdeAB in response to chlorhexidine confirmed the role of this efflux system in adaptive resistance to chlorhexidine in *A. baumannii*. Apart from the genes encoding AdeAB, only one gene was highly (>10-fold) overexpressed in response to chlorhexidine. This gene was originally annotated as encoding a hypothetical membrane protein. Using biochemical approaches we showed that this protein is in fact a chlorhexidine resistance protein that functions via an active efflux mechanism (Hassan et al., 2013). We named this protein the *Acinetobacter chlorhexidine efflux protein I* (AceI).

## The AceI Transporter is a Prototype for a New Family of Bacterial Multidrug Efflux Systems

The AceI transport protein contains two tandem “Bacterial Transmembrane Pair” (BTP) protein domains defined within the Pfam database (Finn et al., 2014). There are more than 750 protein sequences containing this domain architecture listed in the Pfam database (version 27.0). Genes encoding these proteins are particularly common among proteobacterial lineages, but can also be found in the genomes of unrelated bacterial genera, including the Firmicutes and Actinobacteria. We have not yet identified these genes in the genomes of any archaeal or eukaryotic organisms.

We have recently characterized more than 20 homologs of the AceI transporter by heterologous expression in *E. coli* (Hassan

et al., 2015). These studies have demonstrated that many AceI homologs are able to provide resistance to an array of biocides in addition to chlorhexidine. For example, the VP1155 protein from *Vibrio parahaemolyticus* and Bcen2424\_2356 protein from *Burkholderia cenocepacia* each conferred increased resistance to chlorhexidine, benzalkonium, acriflavine, and proflavine, when expressed in *E. coli* (Hassan et al., 2015). Fluorescence transport assays conducted on cells expressing these and other AceI homologs that conferred resistance to acriflavine and proflavine, demonstrated that these compounds are actively exported from the cell by these transporters (Hassan et al., 2015). These results corroborate our earlier findings that chlorhexidine is actively transported by AceI (Hassan et al., 2013), and indicate that efflux is the mechanism of resistance operating in this group of proteins. Taken together all the observations suggest that these proteins comprise a new family of multidrug efflux pumps common amongst Proteobacterial lineages. We have named this family the Proteobacterial Antimicrobial Compound Efflux (PACE) family (**Figure 1**; Hassan et al., 2015).

## PACE Family Proteins are Encoded Within the Core Genome

Given that the PACE family represents a new class of resistance determinants, we were interested in gathering basic information regarding the mode of inheritance of these genes in bacteria. To this end, we examined their level of conservation within representative bacterial lineages following the basic premise that highly conserved genes within core bacterial genomes are expected to have been inherited vertically, whereas those in the accessory genome are likely to have been horizontally acquired.

We examined PACE family protein conservation in four  $\gamma$ -Proteobacterial species (*A. baumannii*, *P. aeruginosa*, *V. parahaemolyticus*, and *E. coli*) a  $\beta$ -Proteobacterial species (*B. cenocepacia*) and a member of the Firmicutes (*Veillonella parvula*). Annotated protein sequences from all complete and draft genomes of these species were downloaded from the NCBI Genbank database (October, 2014) and were queried using the BTP PfamHMM (Finn et al., 2014) in HMMER3 searches (Eddy, 2011). These searches determined that PACE family proteins are encoded in the pan-genomes of all six species examined. To determine the number of distinct orthologous groups of PACE family proteins in each species we performed a clustering analysis based on sequence identity (cluster stringency >90%) using cd-hit v4.6.1 (Fu et al., 2012). This analysis demonstrated that *A. baumannii* had three clusters (100, 96.7, and 0.3% conservation in 623 strains); *P. aeruginosa* had three clusters (99.5, 99.5, and 0.5% conservation in 197 strains); *V. parahaemolyticus* had one cluster (90.1% conservation in 101 strains); *E. coli* had 4 clusters (0.2, 0.1, 0.1, and 0.1% conservation in 1986 strains); *B. cenocepacia* had three clusters (100, 88.9, and 88.9% conservation in nine strains); and *V. parvula* had one cluster (100% conservation in four strains).

These data demonstrate that the pattern of PACE family protein conservation is variable between the species. For example, both *A. baumannii* and *P. aeruginosa* each encode two highly

conserved PACE family proteins present in virtually all sequenced strains, and one additional PACE protein encoded in one or two specific strains. Whereas, *V. parahaemolyticus* and *V. parvula* each encode only one highly conserved PACE protein, and *B. cenocepacia* encodes three highly conserved PACE proteins. Most *E. coli* strains do not encode a PACE family protein, although a small handful of strains encode one of four PACE protein variants. The highly conserved PACE family proteins encoded by *A. baumannii*, *P. aeruginosa*, *V. parahaemolyticus*, *B. cenocepacia*, and *V. parvula* are likely to constitute part of the core genome in these species and to have been inherited vertically rather than on mobile genetic elements. The almost complete lack of genes encoding PACE family proteins in *E. coli* strains suggests that these genes were lost early in the development of the *E. coli* lineage, but after its divergence from other  $\gamma$ -proteobacteria. In the few cases where *E. coli* strains were found to encode a PACE family protein, it was sometimes associated with mobile genetic elements suggesting that it had been acquired by horizontal gene transfer. The paucity of PACE genes in *E. coli* strains confirms our previous conclusion that *E. coli* is an excellent host to study the function of these proteins (Hassan et al., 2013).

## Physiological Substrates for PACE Family Transporters

To date, the substrates identified for PACE family transport proteins include synthetic biocides only, such as chlorhexidine, dequalinium, benzalkonium, proflavine, and acriflavine. The presence of these toxic biocides in the environments occupied by Proteobacteria is likely to have been negligible across evolutionary time, until perhaps the last 50–100 years when these compounds were applied in various industries. Given that the organisms encoding PACE family genes are likely to have diverged long before the development of this potential selective pressure, it is seems unlikely that biocides are the native physiological substrates of PACE efflux pumps. Nonetheless, these genes are transcriptionally responsive to at least one biocide, chlorhexidine in four species, *A. baumannii*, *A. baylyi*, *P. aeruginosa*, and *B. cenocepacia* (Nde et al., 2009; Coenye et al., 2011; Hassan et al., 2013), suggesting that chlorhexidine can serve as a mimic of their natural physiological substrate for inducing efflux pump expression.

## Regulatory Proteins Acting on PACE Efflux Pumps

In addition to antimicrobial resistance, the promiscuous substrate recognition profiles of multidrug efflux pumps allow them to participate in diverse physiological processes. For example, efflux systems in Gram-negative bacteria function in cell adherence, invasion, biofilm formation, virulence in animals and plants, and resistance to host encoded factors (Piddock, 2006). Consequently, the regulation of bacterial drug efflux systems can be highly complex and responsive to a range of cellular and

extracellular conditions. Complex regulation may be particularly apparent in efflux pumps, such as AceI and its homologs, which are encoded within core bacterial genomes. These genes are likely to have been present in these species for significant periods of evolutionary time, allowing fine-tuning of their expression in response to a range of environmental cues. A case in point, as summarized within the EcoCyc database (Keseler et al., 2013), transcription of the *acrAB* efflux system genes, within the core genome of *E. coli*, is controlled by at least seven distinct regulatory proteins, which are themselves subject to a range of regulatory pressures. These regulatory proteins are likely to integrate efflux pumps into the adaptive resistance responses observed in bacteria, as well as other pathways controlling their alternative physiological functions.

Regulators mediating the most direct control of genes encoding efflux pumps are often encoded locally – adjacent to and divergently transcribed from the gene(s) encoding the efflux system. These regulators, either activators or repressors, typically bind a similar spectrum of compounds to their cognate efflux pump with high affinity as a signal for transcriptional activation or relief of transcriptional repression. Some well characterized examples include AcrR, which controls transcription of the *E. coli* *acrAB* efflux pump genes (Li et al., 2007), and QacR, which controls *qacA/qacB* expression in *S. aureus* (Grkovic et al., 1998; Schumacher et al., 2001).

The PACE family transporters that we have studied to date are each encoded adjacent to a divergently transcribed LysR family regulator. To determine whether these regulators control the expression of their cognate PACE family gene, we used our established methods (Brzoska et al., 2013) to construct a

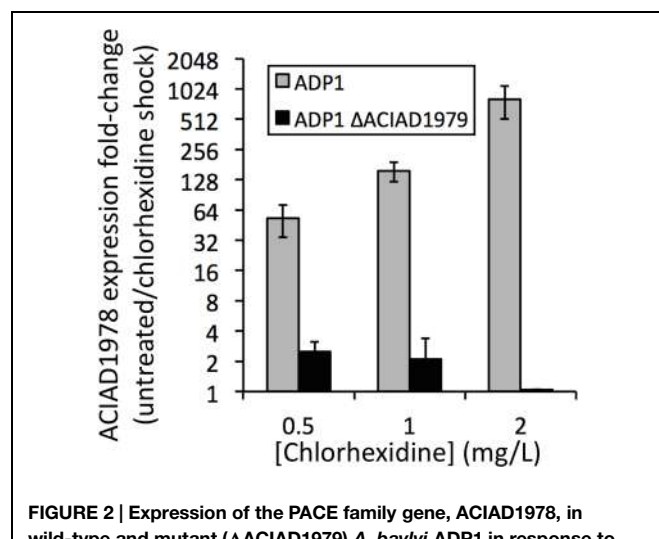


**FIGURE 2 | Expression of the PACE family gene, ACIAD1978, in wild-type and mutant ( $\Delta$ ACIAD1979) *A. baylyi* ADP1 in response to chlorhexidine shock treatments.** Cells were grown in LB broth to  $OD_{600} = 0.6$ , then split, with one half of each culture treated with chlorhexidine and the other half receiving no treatment. RNA was isolated and assessed by qRT-PCR following our established protocols (Brzoska and Hassan, 2014) to determine relative expression levels of ACIAD1978 in chlorhexidine treated and untreated samples. Error bars show the SEM. Changes in expression of ACIAD1978 were negligible in the ACIAD1979 mutant treated with 2 mg/L chlorhexidine, and thus the bar is difficult to see.

deletion mutant of the regulator gene ACIAD1979 in *A. baylyi* ADP1, which is encoded adjacent to the PACE family chlorhexidine resistance gene ACIAD1978. We examined the expression of ACIAD1978 in both the wild-type and the  $\Delta$ ACIAD1979 regulatory mutant in response to chlorhexidine shock treatments using quantitative real-time PCR analysis (Brzoska and Hassan, 2014). In the absence of chlorhexidine the expression of ACIAD1978 was similar in both strains. However, whereas increasing concentrations of chlorhexidine induced ACIAD1978 gene expression in the wild-type strain, chlorhexidine addition failed to induce ACIAD1978 expression in the  $\Delta$ ACIAD1979 mutant (Figure 2). These results suggest that the ACIAD1979 LysR family regulator functions as an activator of the PACE family gene ACIAD1978. We are currently investigating the role of LysR family proteins in controlling expression of PACE family pumps in other species and are determining whether the spectrum of ligands recognized by these regulators is closely linked to the substrate recognition profile of their cognate PACE family pump. It also remains to be determined whether the PACE-associated regulators control expression of other genes, or if there are distally encoded regulators that also modulate expression of PACE transporter genes.

## Conclusion and Future Directions

Transcriptomic analyses of antimicrobial shock treatments are valuable in identifying the potential resistance mechanisms operating in bacteria, including multidrug efflux pumps participating in the adaptive resistance response. Using transcriptomic analyses, we have defined roles for new efflux pumps and identified the PACE family of multidrug transport proteins, the first new family of drug efflux proteins discovered in over a decade.

Transporters within the PACE family are currently enigmas. We have identified drug substrates, such as chlorhexidine that are common to many of these pumps. Furthermore, PACE family gene expression is induced by chlorhexidine, a response that

is mediated via locally encoded regulators. This highlights a close relationship between the function of these pumps and their regulatory control. Since PACE family genes are encoded in the core genomes of bacterial lineages that diverged long ago, this functional-regulatory relationship is likely to have arisen early in the evolution of these proteins. However, the substrates/inducers that have been identified for PACE proteins are synthetic biocides that are likely to have been absent from the environment until the last 50–100 years. Therefore, it is unlikely that these biocides would have provided the selective pressure required to drive the functional or regulatory evolution of PACE family pumps. Consequently, a deeper understanding of these novel resistance proteins requires future investigations aimed at identifying their physiological substrate(s) and primary functional roles in bacteria.

The discovery of the PACE family opens up the possibility that there may be more novel efflux proteins waiting to be discovered. There are many hypothetical membrane proteins of unknown function encoded in all bacterial genomes. For example, even in the best-studied bacterial genome, *E. coli* K12, there are 409 membrane proteins of unknown function. At least some of these may represent entirely novel types of efflux pumps.

## Acknowledgments

This work was supported by National Health and Medical Research Council (Australia) Project Grant (1060895) to IP, KH, and PH and a Macquarie University Research Development Grant (9201401563) to KH and LE. Collaboration between the Australian and UK laboratories is supported by an EU International Research Staff Exchange Scheme BacMT 247634 (AK, PH, and IP). Additional travel support was provided by the Australian Academy of Science (IP). Work in the PH laboratory was supported by EU European Drug Initiative for Channels and Transporters Grant 201924, and also by a Leverhulme Trust Emeritus Award to PH.

## References

- Ahmed, M., Borsch, C. M., Taylor, S. S., Vázquez-Laslop, N., and Neyfakh, A. A. (1994). A protein that activates expression of a multidrug efflux transporter upon binding the transporter substrates. *J. Biol. Chem.* 269, 28506–28513.
- Bailey, A. M., Constantinidou, C., Ivens, A., Garvey, M. I., Webber, M. A., Coldham, N., et al. (2009). Exposure of *Escherichia coli* and *Salmonella enterica* serovar typhimurium to triclosan induces a species-specific response, including drug detoxification. *J. Antimicrob. Chemother.* 64, 973–985. doi: 10.1093/jac/dkp320
- Brzoska, A. J., and Hassan, K. A. (2014). Quantitative PCR for detection of mRNA and gDNA in environmental isolates. *Methods Mol. Biol.* 1096, 25–42. doi: 10.1007/978-1-62703-712-9\_3
- Brzoska, A. J., Hassan, K. A., De Leon, E. J., Paulsen, I. T., and Lewis, P. J. (2013). Single-step selection of drug resistant *Acinetobacter baylyi* ADP1 mutants reveals a functional redundancy in the recruitment of multidrug efflux systems. *PLoS ONE* 8:e56090. doi: 10.1371/journal.pone.0056090
- Coenye, T., Van Acker, H., Peeters, E., Sass, A., Buroni, S., Riccardi, G., et al. (2011). Molecular mechanisms of chlorhexidine tolerance in *Burkholderia cenocepacia* biofilms. *Antimicrob. Agents Chemother.* 55, 1912–1919. doi: 10.1128/AAC.01571-10
- Eddy, S. R. (2011). Accelerated profile HMM searches. *PLoS Comput. Biol.* 7:e1002195. doi: 10.1371/journal.pcbi.1002195
- Fernandez, L., and Hancock, R. E. (2012). Adaptive and mutational resistance: role of porins and efflux pumps in drug resistance. *Clin. Microbiol. Rev.* 25, 661–681. doi: 10.1128/CMR.00043-12
- Finn, R. D., Bateman, A., Clements, J., Coggill, P., Eberhardt, R. Y., Eddy, S. R., et al. (2014). Pfam: the protein families database. *Nucleic Acids Res.* 42, D222–D230. doi: 10.1093/nar/gkt1223
- Fu, L., Niu, B., Zhu, Z., Wu, S., and Li, W. (2012). CD-HIT: accelerated for clustering the next-generation sequencing data. *Bioinformatics* 28, 3150–3152. doi: 10.1093/bioinformatics/bts565
- Grkovic, S., Brown, M. H., Roberts, N. J., Paulsen, I. T., and Skurray, R. A. (1998). QacR is a repressor protein that regulates expression of the *Staphylococcus aureus* multidrug efflux pump QacA. *J. Biol. Chem.* 273, 18665–18673. doi: 10.1074/jbc.273.29.18665
- Hassan, K. A., Jackson, S. M., Penesyan, A., Patching, S. G., Tetu, S. G., Eijkelkamp, B. A., et al. (2013). Transcriptomic and biochemical analyses identify a family of chlorhexidine efflux proteins. *Proc. Natl. Acad. Sci. U.S.A.* 110, 20254–20259. doi: 10.1073/pnas.1317052110
- Hassan, K. A., Li, Q., Henderson, P. J. F., and Paulsen, I. T. (2015). Homologs of the *Acinetobacter baumannii* aceI transporter represent a new family of bacterial multidrug efflux systems. *mBio* 6, e01982–e01914. doi: 10.1128/mBio.01982-14

- Kaatz, G. W., and Seo, S. M. (2004). Effect of substrate exposure and other growth condition manipulations on *norA* expression. *J. Antimicrob. Chemother.* 54, 364–369. doi: 10.1093/jac/dkh341
- Keseler, I. M., Mackie, A., Peralta-Gil, M., Santos-Zavaleta, A., Gama-Castro, S., Bonavides-Martinez, C., et al. (2013). EcoCyc: fusing model organism databases with systems biology. *Nucleic Acids Res.* 41, D605–D612. doi: 10.1093/nar/gks1027
- Kristoffersen, S. M., Ravnum, S., Tourasse, N. J., Okstad, O. A., Kolsto, A. B., and Davies, W. (2007). Low concentrations of bile salts induce stress responses and reduce motility in *Bacillus cereus* ATCC 14579. *J. Bacteriol.* 189, 5302–5313. doi: 10.1128/JB.00239-07
- Li, M., Gu, R., Su, C. C., Routh, M. D., Harris, K. C., Jewell, E. S., et al. (2007). Crystal structure of the transcriptional regulator AcrR from *Escherichia coli*. *J. Mol. Biol.* 374, 591–603. doi: 10.1016/j.jmb.2007.09.064
- McDonnell, G., and Russell, A. D. (1999). Anitseptics and disinfectants: activity, action and resistance. *Clin. Microbiol. Rev.* 12, 147–179.
- Morita, Y., Tomida, J., and Kawamura, Y. (2014). Responses of *Pseudomonas aeruginosa* to antimicrobials. *Front. Microbiol.* 4:422. doi: 10.3389/fmicb.2013.00422
- Nde, C. W., Jang, H. J., Toghrol, F., and Bentley, W. E. (2009). Global transcriptomic response of *Pseudomonas aeruginosa* to chlorhexidine diacetate. *Environ. Sci. Technol.* 43, 8406–8415. doi: 10.1021/es9015475
- Piddock, L. J. (2006). Multidrug-resistance efflux pumps - not just for resistance. *Nat. Rev. Microbiol.* 4, 629–636. doi: 10.1038/nrmicro1464
- Rajamohan, G., Srinivasan, V. B., and Gebreyes, W. A. (2009). Novel role of *Acinetobacter baumannii* RND efflux transporters in mediating decreased susceptibility to biocides. *J. Antimicrob. Chemother.* 65, 228–232. doi: 10.1093/jac/dkp427
- Ren, Q., and Paulsen, I. T. (2007). Large-scale comparative genomic analyses of cytoplasmic membrane transport systems in prokaryotes. *J. Mol. Microbiol. Biotechnol.* 12, 165–179. doi: 10.1159/000099639
- Russell, A. D. (1986). Chlorhexidine: antibacterial action and bacterial resistance. *Infection* 14, 212–215. doi: 10.1007/BF01644264
- Schindler, B. D., Frempong-Manso, E., Demarco, C. E., Kosmidis, C., Matta, V., Seo, S. M., et al. (2015). Analyses of multidrug efflux pump-like proteins encoded on the *Staphylococcus aureus* chromosome. *Antimicrob. Agents Chemother.* 59, 747–748. doi: 10.1128/AAC.04678-14
- Schumacher, M. A., Miller, M. C., Grkovic, S., Brown, M. H., Skurray, R. A., and Brennan, R. G. (2001). Structural mechanisms of QacR induction and multidrug recognition. *Science* 294, 2158–2163. doi: 10.1126/science.1066020
- Shaw, K. J., Miller, N., Liu, X., Lerner, D., Wan, J., Bittner, A., et al. (2003). Comparison of the changes in global gene expression of *Escherichia coli* induced by four bactericidal agents. *J. Mol. Microbiol. Biotechnol.* 5, 105–122. doi: 10.1159/000069981
- Simm, R., Voros, A., Ekman, J. V., Sodring, M., Nes, I., Kroeger, J. K., et al. (2012). BC4707 is a major facilitator superfamily multidrug resistance transport protein from *Bacillus cereus* implicated in fluoroquinolone tolerance. *PLoS ONE* 7:e36720. doi: 10.1371/journal.pone.0036720
- Tal, N., and Schuldiner, S. (2009). A coordinated network of transporters with overlapping specificities provides a robust survival strategy. *Proc. Natl. Acad. Sci. U.S.A.* 106, 9051–9056. doi: 10.1073/pnas.0902400106

**Conflict of Interest Statement:** The authors declare that the research was conducted in the absence of any commercial or financial relationships that could be construed as a potential conflict of interest.

Copyright © 2015 Hassan, Elbourne, Li, Gamage, Liu, Jackson, Sharples, Kolsto, Henderson and Paulsen. This is an open-access article distributed under the terms of the Creative Commons Attribution License (CC BY). The use, distribution or reproduction in other forums is permitted, provided the original author(s) or licensor are credited and that the original publication in this journal is cited, in accordance with accepted academic practice. No use, distribution or reproduction is permitted which does not comply with these terms.



# Efflux-mediated fluoroquinolone resistance in the multidrug-resistant *Pseudomonas aeruginosa* clinical isolate PA7: identification of a novel MexS variant involved in upregulation of the *mexEF oprN* multidrug efflux operon

Yuji Morita <sup>\*</sup>, Junko Tomida and Yoshiaki Kawamura

Department of Microbiology, School of Pharmacy, Aichi Gakuin University, Nagoya, Japan

**Edited by:**

Keith Poole, Queen's University, Canada

**Reviewed by:**

Antonio Oliver, Hospital Son Dureta, Spain

Herbert P. Schweizer, Colorado State University, USA

Patrick Plesiat, University of Franche-Comté, France

**\*Correspondence:**

Yuji Morita, Department of Microbiology, School of Pharmacy, Aichi Gakuin University, 1-100 Kusumoto, Chikusa, Nagoya, Aichi 464-8650, Japan  
e-mail: yujmor@dpc.agu.ac.jp

The emergence of multidrug-resistant *Pseudomonas aeruginosa* has become a serious problem in medical settings. *P. aeruginosa* clinical isolate PA7 is resistant to fluoroquinolones, aminoglycosides, and most  $\beta$ -lactams but not imipenem. In this study, enhanced efflux-mediated fluoroquinolone resistance of PA7 was shown to reflect increased expression of two resistance nodulation cell division (RND)-type multidrug efflux operons, *mexEF oprN* and *mexXY oprA*. Such a clinical isolate has rarely been reported because MexEF-OprN-overproducing mutants often increase susceptibility to aminoglycosides apparently owing to impairment of the MexXY system. A mutant of PA7 lacking three RND-type multidrug efflux operons (*mexAB oprM*, *mexEF oprN*, and *mexXY oprA*) was susceptible to all anti-pseudomonas agents we tested, supporting an idea that these RND-type multidrug efflux transporters are molecular targets to overcome multidrug resistance in *P. aeruginosa*. *mexEF oprN*-upregulation in *P. aeruginosa* PA7 was shown due to a MexS variant harboring the Valine-155 amino acid residue. This is the first genetic evidence shown that a MexS variant causes *mexEF oprN*-upregulation in *P. aeruginosa* clinical isolates.

**Keywords:** *Pseudomonas aeruginosa*, efflux, *mexXY oprA*, *mexEF oprN*, *mexS*

## INTRODUCTION

*Pseudomonas aeruginosa* is a metabolically versatile bacterium that can cause a wide range of severe opportunistic infections in patients with serious underlying medical conditions (Gellatly and Hancock, 2013). Infections caused by *P. aeruginosa* often are hard to treat; inappropriate chemotherapy readily selects multidrug-resistant *P. aeruginosa* against which very few agents are effective (Morita et al., 2014; Poole, 2014). This so-called “antibiotic resistance crisis” has been compounded by the lagging in antibiotic discovery and development programs occurred in recent years, and is jeopardizing the essential role played by antibiotics in current medical practices (Rossolini et al., 2014). To combat this organism, it is very useful to understand its antimicrobial resistance mechanisms (see reviews such as Breidenstein et al., 2011; Poole, 2011; Morita et al., 2015).

The complete genome sequence of the multiresistant *P. aeruginosa* PA7 has been determined (Roy et al., 2010). The sequence of this strain, which exhibits resistance to fluoroquinolones (FQs), aminoglycosides, and various  $\beta$ -lactams but is susceptible to carbapenems (imipenem), includes typical FQ-resistance mutations in *gyrA* (Thr83Ile) and *parC* (Ser87Leu) (Roy et al., 2010). PA7 has additionally acquired a mutated *aacA4* gene, the product of which (AAC(6')-II) endows the strain with aminoglycoside (gentamicin and tobramycin) resistance (Roy et al., 2010). This clinical isolate is amenable to the construction of gene knock-out

mutations, thereby facilitating the analysis of molecular mechanisms of multidrug antimicrobial resistance in this isolate. Previously we showed that the effect of the modifying enzyme is enhanced by the MexXY resistance nodulation cell division (RND)-type multidrug efflux system, especially in the presence of divalent cations, providing high-level aminoglycoside resistance in *P. aeruginosa* (Morita et al., 2012b). This observation emphasizes the importance of the MexXY multidrug efflux system for aminoglycoside resistance in multidrug-resistant *P. aeruginosa* clinical isolates (Morita et al., 2012a).

Four members of the RND family of multidrug efflux systems, MexAB-OprM, MexCD-OprJ, MexEF-OprN, and MexXY have been implicated in FQ resistance in *P. aeruginosa* clinical isolates (Poole, 2011). As in other organisms, these RND family drug efflux transporters in *P. aeruginosa* operates as three-component pumps with an RND cytoplasmic membrane (CM) protein (MexB, MexD, MexF, and MexY) linked to an outer membrane channel-forming protein (OprM, OprJ, and OprN) by a CM-tethered periplasmic protein (MexA, MexC, MexE, and MexX) (Poole, 2013). Intriguingly PA7 possesses the *mexXY oprA* multidrug efflux operon of which *oprA* is missing in most *P. aeruginosa* strains (Roy et al., 2010). We showed that the MexXY can utilize either the OprA or OprM as an outer membrane component of the tripartite efflux pump (Morita et al., 2012b). Multidrug-resistant *P. aeruginosa* clinical isolates,

including carbapenem-resistant *P. aeruginosa*, often have been reported to be MexXY and/or MexAB-OprM overproducers (e.g., Hocquet et al., 2007; Cabot et al., 2011; Fuste et al., 2013; Khuntayaporn et al., 2013; Vatcheva-Dobrevska et al., 2013). FQ efflux is mediated by the MexAB-OprM system constitutively produced at moderate levels in wild-type *P. aeruginosa* PAO1 (Morita et al., 2001; Poole, 2013). Expression of *mexAB-oprM* is controlled directly or indirectly by three repressors encoded by the *mexR*, *nalC* and *nalD* genes, with inactivating mutations in any of these resulting in increased *mexAB-oprM* expression (Poole, 2011, 2013). In addition, *nfxB* and *nfxC* mutants (which overproduce components of the MexCD-OprJ and MexEF-OprN systems, respectively) are well-known as efflux-mediated FQ-resistant mutants of laboratory and clinical isolates of *P. aeruginosa*, although *nfxB* mutations appear to be rare in clinical settings (Poole, 2011). *nfxC* mutants also show increased resistance to carbapenems such as imipenem, not because MexEF-OprN accommodates these agents but because of a coordinated, MexT-dependent reduction of OprD production in such mutants (Poole, 2011, 2013). Hyperexpression of *mexEF-oprN* (and reduction in *oprD* expression) is also seen in laboratory isolates disrupted in the *mexS* gene, which encodes a putative oxidoreductase (a.k.a *qrh*) of unknown function (Sobel et al., 2005; Lamarche and Deziel, 2011). There are, however, no reports (to our knowledge) with experimental evidence of *mexEF-oprN*-expressing clinical isolates harboring mutations in *mexS* (Poole, 2013), although some studies suggested possible mutation of *mexS* in *nfxC*-type clinical isolates (e.g., Llanes et al., 2011; Fournier et al., 2013). The incidence of MexXY overproducers among clinical isolates has shown to be linked to the use of ciprofloxacin (Hocquet et al., 2008) and MexXY overproducers have been often reported to be one of major phenotypes in multidrug resistant clinical isolates (Morita et al., 2012a; Poole, 2013). However, MexXY-expressing FQ-resistance or its contribution to FQ-resistance in clinical settings has not well been studied compared to the other three pumps. In this study, we used reverse genetics to investigate the role of efflux-mediated FQ resistance in multidrug-resistant *P. aeruginosa* clinical isolate PA7.

## MATERIALS AND METHODS

### BACTERIAL STRAINS, PLASMIDS, AND GROWTH CONDITIONS

The bacterial strains and plasmids used in this study are listed in **Table 1**. Bacterial cells were grown in Luria (L) broth and on L agar (1.5%) under aerobic conditions at 37°C as previously described, unless otherwise indicated, with antibiotics as necessary (Morita et al., 2010). Bacterial growth was quantified by measuring the optical density at 600 nm on an Ultrospec 2100 Pro Spectrophotometer (GE Healthcare Corp., Tokyo, Japan), unless otherwise indicated. The plasmids pEX18Tc (Hoang et al., 1998), pYM101 (Morita et al., 2010), and their derivatives were maintained and selected using medium supplemented with 2.5–10 µg tetracycline ml<sup>-1</sup> for *E. coli* or 50–150 µg tetracycline ml<sup>-1</sup> for *P. aeruginosa*. The plasmids pUCP20T (Schweizer et al., 1996) and pFLP2 (Hoang et al., 1998) and their derivatives were maintained and selected using medium supplemented with 100 µg ampicillin ml<sup>-1</sup> for *E. coli* or 200 µg carbenicillin ml<sup>-1</sup> for *P. aeruginosa*.

**Table 1 | Bacterial strains and plasmids.**

| Strains or plasmids            | Relevant characteristics   | References                 |
|--------------------------------|--|----------------------------|
| <b>E. COLI</b>                 |  |                            |
| DH5α (PAGU <sup>9</sup> 121)   | For recombinant DNA manipulation   | Morita et al., 2010        |
| KAM3 (PAGU <sup>9</sup> 846)   | For recombinant DNA manipulation   | Morita et al., 1998        |
| S17-1 (PAGU <sup>9</sup> 856)  | For conjugational transfer   | Morita et al., 2006        |
| <b>P. AERUGINOSA</b>           |  |                            |
| PAO1 (PAGU 974)                | Wild type  | Morita et al., 2006        |
| PA7 (PAGU 1498)                | Multi-resistant clinical isolate   | Roy et al., 2010           |
| PAGU <sup>9</sup> 1565         | PA7 <i>ΔmexXY-oprA</i>   | Morita et al., 2012b       |
| PAGU <sup>9</sup> 1603         | PA7 <i>ΔmexAB-oprM</i>   | Morita et al., 2012b       |
| PAGU <sup>9</sup> 1748         | PA7 <i>ΔmexEF-oprN</i>   | This study                 |
| PAGU <sup>9</sup> 1641         | PA7 <i>ΔmexXY-oprA ΔmexAB-oprM</i>   | Morita et al., 2012b       |
| PAGU <sup>9</sup> 1751         | PA7 <i>ΔmexXY-oprA ΔmexEF-oprN</i>   | This study                 |
| PAGU <sup>9</sup> 1753         | PA7 <i>ΔmexAB-oprM ΔmexEF-oprN</i>   | This study                 |
| PAGU <sup>9</sup> 1756         | PA7 <i>ΔmexXY-oprA ΔmexAB-oprM ΔmexEF-oprN</i>   | This study                 |
| PAGU <sup>9</sup> 1793         | PA7 <i>ΔmexS</i>   | This study                 |
| PAGU <sup>9</sup> 1789         | PA7 <i>ΔmexT</i>   | This study                 |
| PAGU <sup>9</sup> 1867         | PA7 <i>mexS(V155A)</i>   | This study                 |
| DSM 1128 (PAGU 1504)           | Taxonomically PA7-related strain, wild-type  | Kiewitz and Tummeler, 2000 |
| K2153 (PAGU 1741)              | Clinical isolate   | Sobel et al., 2003         |
| K2376 (PAGU <sup>9</sup> 1834) | K2153 <i>ΔmexS</i>   | Fetar et al., 2011         |
| PAGU <sup>9</sup> 1850         | K2153 <i>ΔmexS attB::lacI<sup>q</sup>-P<sub>T7</sub></i>                               | This study                 |
| PAGU <sup>9</sup> 1851         | K2153 <i>ΔmexS attB::lacI<sup>q</sup>-P<sub>T7</sub>-mexS<sub>PA7</sub></i>            | This study                 |
| PAGU <sup>9</sup> 1844         | K2153 <i>ΔmexS attB::lacI<sup>q</sup>-P<sub>T7</sub>-mexS<sub>DSM 1128</sub></i>       | This study                 |
| PAGU <sup>9</sup> 1854         | K2153 <i>ΔmexS pUCP20T</i>   | This study                 |
| PAGU <sup>9</sup> 1855         | K2153 <i>ΔmexS pUCP20T::mexS<sub>PA7</sub></i>   | This study                 |
| PAGU <sup>9</sup> 1856         | K2153 <i>ΔmexS pUCP20T::mexS<sub>DSM 1128</sub></i>                                    | This study                 |
| PAGU <sup>9</sup> 1835         | K2153 <i>ΔmexT</i>   | Fetar et al., 2011         |
| PAGU <sup>9</sup> 1836         | K2153 <i>ΔmexF</i>   | Fetar et al., 2011         |
| K2942 (PAGU <sup>9</sup> 1837) | K2153 <i>ΔmexS ΔmexT</i>   | Fetar et al., 2011         |
| PAGU <sup>9</sup> 1852         | K2153 <i>ΔmexS ΔmexT attB::lacI<sup>q</sup>-P<sub>T7</sub></i>                         | This study                 |
| PAGU <sup>9</sup> 1846         | K2153 <i>ΔmexS ΔmexT attB::lacI<sup>q</sup>-P<sub>T7</sub>-mexT<sub>PA7</sub></i>      | This study                 |
| PAGU <sup>9</sup> 1845         | K2153 <i>ΔmexS ΔmexT attB::lacI<sup>q</sup>-P<sub>T7</sub>-mexT<sub>DSM 1128</sub></i> | This study                 |
| <b>PLASMID</b>                 |  |                            |
| pEX18Tc                        | Broad-host-range gene replacement vector   | Hoang et al., 1998         |
| pYM133                         | pEX18Tc:: <i>ΔmexEF-oprN</i>   | This study                 |
| pYM134                         | pEX18Tc:: <i>ΔmexS</i>   | This study                 |

(Continued)

**Table 1 | Continued**

| Strains or plasmids | Relevant characteristics                           | References             |
|---------------------|--|------------------------|
| pYM135              | pEX18Tc::ΔmexT                                     | This study             |
| pYM136              | pEX18Tc::ΔmexST                                    | This study             |
| pYM137              | pEX18Tc::mexS <sub>PA7</sub>                       | This study             |
| pYM138              | pEX18Tc::mexS <sub>PA7</sub> (V155A)               | This study             |
| pYM101              | <i>P. aeruginosa</i> chromosome integration vector | Morita et al., 2010    |
| pYM139              | pYM101::mexS <sub>PA7</sub>                        | This study             |
| pYM140              | pYM101::mexS <sub>DSM 1128</sub>                   | This study             |
| pYM141              | pYM101::mexT <sub>PA7</sub>                        | This study             |
| pYM142              | pYM101::mexT <sub>DSM 1128</sub>                   | This study             |
| pUCP20T             | Broad-host-range cloning vector                    | Schweizer et al., 1996 |
| pYM143              | pUCP20T::mexS <sub>PA7</sub>                       | This study             |
| pYM144              | pUCP20T::mexS <sub>DSM 1128</sub>                  | This study             |
| pFLP2               | Flp recombinase-producing plasmid                  | Hoang et al., 1998     |

### MOLECULAR BIOLOGY TECHNIQUES

Plasmid DNA isolation from *E. coli*, DNA purification, measuring DNA concentration, DNA digestion with restriction enzymes, DNA dephosphorylation, DNA ligation, isolation of chromosomal DNA from *P. aeruginosa*, PCR conditions, nucleotide sequencing, competent cell preparation from *E. coli*, transformation of *E. coli*, and transfer of plasmids into *P. aeruginosa* via conjugation were performed as described previously (Morita et al., 2010), unless otherwise indicated. DNA sequences and amino acid sequences were analyzed through 2012 to 2013 with Pseudomonas Genome Database (Winsor et al., 2011), Basic Local Alignment Search Tool (BLAST) (Boratyn et al., 2013), SWISS-MODEL (Bordoli et al., 2009), Sorting Tolerant From Intolerant (SIFT) BLINK (Kumar et al., 2009), and the software DNASIS Pro (Ver. 2.1; Hitachi, Japan).

### CLONING OF mexS AND mexT FROM *P. AERUGINOSA*

*mexS* and *mexT* from *P. aeruginosa* (without endogenous promoters) were amplified by PCR using the primers listed in Table 2. The purified *mexS* PCR product, digested with BamHI and HindIII, was cloned into similarly digested, dephosphorylated pUCP20T and pYM101, yielding pUCP20T::*mexS* and pYM101::*mexS*. The purified *mexT* PCR product, digested with EcoRI and BamHI, was cloned into similarly digested, dephosphorylated pUCP20T and pYM101, yielding pUCP20T::*mexT* and pYM101::*mexT*.

### CONSTRUCTION OF IN-FRAME DELETION MUTANTS FROM *P. AERUGINOSA*

In-frame deletion mutants of *mexEF-oprN*, *mexS*, and *mexT* from *P. aeruginosa* PA7 and its derivatives were constructed using the previously described *sacB*-based strategy (Morita et al., 2006, 2010). The plasmids and resulting *P. aeruginosa* mutants are listed in Table 1, while the primer pairs are listed in Table 2. The selection concentrations of tetracycline for the first homologous recombination event were adjusted to reflect the endogenous

tetracycline MICs for the *P. aeruginosa* strains. These constructs were confirmed by colony PCR.

### CONSTRUCTION OF THE ΦCTX-BASED SITE-SPECIFIC INTEGRANTS IN *P. AERUGINOSA*

For gene complementation experiments in *P. aeruginosa*, ΦCTX phage-based site-specific integrants were constructed using the integration-proficient, tightly controlled expression vector pYM101 and associated techniques (conjugative transfer, gene replacement at the chromosomal *attB* site, and curing of the unwanted plasmid backbone from the chromosome via the pFLP2-encoded Flp recombinase) as previously described (Morita et al., 2010).

### SITE-DIRECTED MUTAGENESIS OF mexS<sub>PA7</sub> IN THE CHROMOSOME OF *P. AERUGINOSA* PA7

An amino acid substitution (Val155Ala) mutation was introduced into the *mexS<sub>PA7</sub>* gene of the insert in the plasmid pUC20T::*mexS<sub>PA7</sub>*. Site-directed mutagenesis within a target plasmid was carried out according to Geiser et al. (2001) and Morita et al. (2009). A 50-μl mixture consisting of 50 ng of plasmid DNA, 0.25 μM of each mutagenic primer pair (Table 2), 0.2 mM each deoxynucleoside triphosphate, 1 mM MgSO<sub>4</sub>, 2.5 U of KOD Hot Start DNA polymerase -Plus- Ver.2 (TOYOBO Co. Ltd., Osaka, Japan), 1× KOD buffer, and 4.0% (vol/vol) dimethyl sulfoxide was heated to 94°C for 2 min followed by 18 cycles of 0.5 min at 94°C, 1 min at 60°C, and 5 min at 68°C. The resulting DNA products were purified as above, digested overnight with 10 U DpnI (Roche Diagnostics K.K., Tokyo, Japan) to eliminate template plasmid, and used to transform *E. coli* DH5α. Plasmids were recovered from individual transformants, and the *mexS* insert was sequenced to identify plasmids bearing the desired mutation. The *mexS* insert carrying the mutation was digested with BamHI and HindIII and cloned into similarly digested and dephosphorylated pEX18Tc to yield pEX18Tc::*mexS<sub>PA7</sub>*(V155A). The *mexS<sub>PA7</sub>*(V155A) mutation was gene replaced onto the chromosome of *P. aeruginosa* PA7 using the previously described *sacB*-based strategy (Morita et al., 2009, 2012b).

### ANTIBIOTIC SUSCEPTIBILITY ASSAY

The susceptibility of *P. aeruginosa* to antimicrobial agents in cation-adjusted Mueller–Hinton broth was assessed using the 2-fold serial microtiter broth dilution method described previously (Morita et al., 2012b). Minimal inhibitory concentrations (MICs) were defined as the lowest concentration of antibiotic resulting in visible inhibition of growth after 18 h of incubation at 37°C. MICs for the ΦCTX-based site-specific integrants were determined in the presence of the inducer 5 mM isopropyl-β-D-1-thiogalactopyranoside (IPTG). The categorization in susceptible, intermediate, and resistant was performed according to the interpretive standards of the Clinical and Laboratory Standards Institute (CLSI) (Patel et al., 2011).

### ANTIMICROBIAL AGENTS

Amikacin, ampicillin, carbenicillin, chloramphenicol, ciprofloxacin, norfloxacin, and tetracycline were purchased from Wako Pure Chemicals Industries, Ltd (Osaka, Japan). Moxifloxacin and levofloxacin were purchased from LKT

**Table 2 | Primers used in this study.**

| Primer                               | Sequence(5'-3')                             | Purpose   | References           |
|--------------------------------------|---|---|----------------------|
| EcoRI-mexE <sub>PA7</sub> -UF        | GAT CGA ATT CTG GCC TCG GGG GAA ATC T       | <i>mexEF oprN</i> genes disruption of <i>P. aeruginosa</i> PA7            | This study           |
| BamHI-mexE <sub>PA7</sub> -UR        | CTG AGG ATC CAT GCT TGA CTC CGC CAG TC      | <i>mexEF oprN</i> genes disruption of <i>P. aeruginosa</i> PA7            | This study           |
| BamHI-oprN <sub>PA7</sub> -DF        | CTG AGG ATC CTG AAC CGG CTA TCC CCG G       | <i>mexEF oprN</i> genes disruption of <i>P. aeruginosa</i> PA7            | This study           |
| Xhol-oprN <sub>PA7</sub> -DR         | GAT CCT CGA GCG CCG ACA GCG ATT GCC A       | <i>mexEF oprN</i> genes disruption of <i>P. aeruginosa</i> PA7            | This study           |
| BamHI-mexS <sub>PA7</sub> -F         | GAT CGG ATC CGA TGC ACT GCA GAG GTT TGC     | <i>mexS</i> gene cloning of <i>P. aeruginosa</i> PA7 and DSM 1128         | This study           |
| HindIII-mexS <sub>PA7</sub> -R       | CTA GAA GCT TCA ATC GGC GAC GTG GAT         | <i>mexS</i> gene cloning of <i>P. aeruginosa</i> PA7 and DSM 1128         | This study           |
| EcoRI-mexS <sub>PA7</sub> -UF        | GCT AGA ATT CAG TTC GTC GGT GTA GCT GA      | <i>mexS</i> gene disruption of <i>P. aeruginosa</i> PA7                   | This study           |
| BamHI-mexS <sub>PA7</sub> -UR        | CTA GGG ATC CGG ACA TCG CAA ACC TCT G       | <i>mexS</i> gene disruption of <i>P. aeruginosa</i> PA7                   | This study           |
| BamHI-mexS <sub>PA7</sub> -DF        | GCT AGG ATC CGT CGC CGA TTG AGG ACG AC      | <i>mexS</i> gene disruption of <i>P. aeruginosa</i> PA7                   | This study           |
| HindIII-mexS <sub>PA7</sub> -DR      | CTA GAA GCT TAG TAC ATC CAC GCG CAC CT      | <i>mexS</i> gene disruption of <i>P. aeruginosa</i> PA7                   | This study           |
| EcoRI-mexT <sub>PA7</sub> -F         | GAT CGA ATT CCC CTG GAA ACG AGG AAC         | <i>mexT</i> gene cloning of <i>P. aeruginosa</i> PA7 and DSM 1128         | This study           |
| BamHI-mexT <sub>PA7</sub> -R         | GAT CGG ATC CTC AGA GGC TGT CCG GGT C       | <i>mexT</i> gene cloning of <i>P. aeruginosa</i> PA7 and DSM 1128         | This study           |
| SacI-mexT <sub>PA7</sub> -UF         | GCT AGA GCT CTG GAA ACG ATC ACC CGC G       | <i>mexT</i> gene disruption of <i>P. aeruginosa</i> PA7                   | This study           |
| BamHI-mexT <sub>PA7</sub> -UR        | CTG AGG ATC CAT GGC GTT CCT CGT TTC C       | <i>mexT</i> gene disruption of <i>P. aeruginosa</i> PA7                   | This study           |
| BamHI-mexT <sub>PA7</sub> -DF        | GCT AGG ATC CGG ACA GCC TCT GAG TCA TCC ACG | <i>mexT</i> gene disruption of <i>P. aeruginosa</i> PA7                   | This study           |
| HindIII-mexT <sub>PA7</sub> -DR      | CTA GAA GCT TGC GAC CGC CGC CCT GGC TT      | <i>mexT</i> gene disruption of <i>P. aeruginosa</i> PA7                   | This study           |
| <i>mexS</i> <sub>PA7</sub> (V155A)-F | CTG ATC ACC GAG GCG GCG CGC ATG TAC GGG CC  | <i>mexS</i> (V155A) site directed mutagenesis of <i>P. aeruginosa</i> PA7 | This study           |
| <i>mexS</i> <sub>PA7</sub> (V155A)-R | GGC CCG TAC ATG CGC GCC GCC TCG GTG ATC AG  | <i>mexS</i> (V155A) site directed mutagenesis of <i>P. aeruginosa</i> PA7 | This study           |
| <i>mexTS</i> intergenic seq          | GCA CCA GGA CTT CCC CTG                     | DNA sequencing of <i>mexT-mexS</i> intergenic region                      | This study           |
| <i>uvrD</i> -F                       | ATCGACTTCCGAGCTGCTG                         | RT-PCR for <i>uvrD</i> gene of <i>P. aeruginosa</i>                       | Morita et al., 2012b |
| <i>uvrD</i> -R                       | CTGGAACTCGTCCACCAGGAT                       | RT-PCR for <i>uvrD</i> gene of <i>P. aeruginosa</i>                       | Morita et al., 2012b |
| <i>mexE</i> -F (RT)                  | CCA CCC TGA TCA AGG ACG AAG                 | RT-PCR for <i>mexE</i> gene of <i>P. aeruginosa</i>                       | This study           |
| <i>mexE</i> -R (RT)                  | CGG TAG ACG GTC TTG TTG TCG                 | RT-PCR for <i>mexE</i> gene of <i>P. aeruginosa</i>                       | This study           |
| <i>mexS</i> -F (RT)                  | AGG GCG TCA ATG TCA TCC TC                  | RT-PCR for <i>mexS</i> gene of <i>P. aeruginosa</i>                       | This study           |
| <i>mexS</i> -R (RT)                  | CTG CAG GTG CTT CTT GAA CG                  | RT-PCR for <i>mexS</i> gene of <i>P. aeruginosa</i>                       | This study           |
| <i>mexT</i> -F (RT)                  | TAT TGA TGC CGA ACC TGC TG                  | RT-PCR for <i>mexT</i> gene of <i>P. aeruginosa</i>                       | This study           |
| <i>mexT</i> -R (RT)                  | GGA GGA TCT TCG GCT TGC TG                  | RT-PCR for <i>mexT</i> gene of <i>P. aeruginosa</i>                       | This study           |
| <i>oprD</i> -F (RT)                  | ATT GCA CTG GCG GTT TCC                     | RT-PCR for <i>oprD</i> gene of <i>P. aeruginosa</i>                       | This study           |
| <i>oprD</i> -R (RT)                  | ATG AAC CCC TTC GCT TCG                     | RT-PCR for <i>oprD</i> gene of <i>P. aeruginosa</i>                       | This study           |
| <i>mexA</i> -F (RT)                  | GAC AAC GCT ATG CAA CGA ACG                 | RT-PCR for <i>mexA</i> gene of <i>P. aeruginosa</i>                       | This study           |
| <i>mexA</i> -R (RT)                  | AGC TCG GTA TTC AGC GTC ACC                 | RT-PCR for <i>mexA</i> gene of <i>P. aeruginosa</i>                       | This study           |

Laboratories, Inc. (St. Paul, MN, USA). Imipenem/cilastatin was purchased from Sandoz K.K. (Tokyo, Japan).

#### REAL-TIME QUANTITATIVE REVERSE TRANSCRIPTASE (qRT)-PCR

Overnight cultures of *P. aeruginosa* strains were diluted 1:100 in 10 ml, incubated with vigorous shaking at 37°C for 3–4 h, and harvested. Total RNA was stabilized with the RNA Protect Bacteria Reagent (Qiagen) and isolated with the RNeasy Mini Kit (Qiagen). The RNA samples were further treated with RQ1 RNase-Free DNase (Promega) and purified by using the RNeasy Mini Kit (Qiagen). Real-time qRT-PCR was performed with primer pairs internal to *uvrD*, *mexE*, *mexS*, *mexT*, and *oprD*

(**Table 2**) using the One Step SYBR PrimeScript RT-PCR kit II (TaKaRa) in a Thermal Cycler Dice real-time system (TaKaRa). The transcript levels of the target gene in a given strain were normalized to levels of *uvrD* and expressed as a ratio (fold change) to that observed in the parental PA7 strain. Gene expression values were calculated based on triplicate experiments.

#### NUCLEOTIDE SEQUENCE ACCESSION NUMBER

The nucleotide sequences of DNA regions containing *mexT* and *mexS* in *P. aeruginosa* DSM 1128 have been deposited in GenBank/EMBL/DDBJ with the accession number AB889539.

## RESULTS

### CONTRIBUTION OF RND MULTIDRUG EFFLUX SYSTEMS TO FQ RESISTANCE IN *P. AERUGINOSA* PA7

FQ resistance in *P. aeruginosa* PA7 was compared with the two FQ-susceptible strains, PAO1 (the standard laboratory strain) and DSM 1128 (a strain taxonomically related to PA7) (Morita et al., 2012b). The MICs of the FQs (ciprofloxacin, levofloxacin, moxifloxacin, and norfloxacin) for *P. aeruginosa* PA7, PAO1, and DSM 1128 are shown in **Table 3**. *P. aeruginosa* PA7 exhibited increased resistance (ca. 256-fold) to these FQs compared to *P. aeruginosa* PAO1 and DSM 1128. *P. aeruginosa* DSM 1128 showed the same level of resistance to the FQs as *P. aeruginosa* PAO1. Based on the interpretive standards of the CLSI (Patel et al., 2011), *P. aeruginosa* PA7 was considered highly resistant to these FQs. This observation is not surprising, because *P. aeruginosa* PA7 possesses typical target mutations, one in *gyrA* (Thr83Ile) and one in *parC* (Ser87Leu), well-known to be associated with FQ resistance (Lomovskaya et al., 1999). However, target mutations alone are not sufficient to explain high-level FQ resistance in *P. aeruginosa*; the additional effect of up-regulation of one of the four RND efflux pumps (MexXY-OprA, MexAB-OprM, MexCD-OprJ, or MexEF-OprN) is necessary (Lomovskaya et al., 1999; Bruchmann et al., 2013).

Previously we showed that the  $\Delta$ *mexXY oprA*  $\Delta$ *mexAB oprM* double mutant of PA7 was slightly more susceptible (ca. 2- to 4-fold) to ciprofloxacin, while retaining high-level resistance (MIC = 32  $\mu$ g/ml) to this antibiotic when compared to its parental strain (Morita et al., 2012b). That observation was inconsistent with data, derived via similar genetic analyses, in which a PAO1-derived  $\Delta$ *oprM gyrA parC* triple mutant (i.e., a strain deleted for *oprM* and carrying the target mutations) exhibited increased susceptibility (64-fold) to levofloxacin compared to an isogenic MexAB-OprM overexpressing (*nalB*) mutant, while exhibiting an MIC (0.5  $\mu$ g/ml) of levofloxacin similar to that of the wild-type PAO1 (0.25  $\mu$ g/ml) (Lomovskaya et al., 1999). We noted that deletion of *oprM* in PAO1 was expected to inactivate any efflux pumps that require OprM as an outer membrane factor (e.g., MexAB-OprM, MexXY-OprM, MexVW-OprM) (Morita et al., 2001; Li et al., 2003). We therefore hypothesized that

overexpression of other RND pumps such as MexCD-OprJ and MexEF-OprN was compensating for the effects of the *mexAB oprM mexXY oprA* double deficiency in PA7. As a first step in testing our hypothesis, we examined the primary sequences of the efflux system-encoding genes of PA7. Sequence analysis revealed the presence of *mexCD oprJ* (PSPA7\_0540-0539-0538) and *mexEF oprN* (PSPA7\_2745-2744-2743) homologs in *P. aeruginosa* PA7 (Roy et al., 2010), with predicted amino acid lengths (in PA7) and amino acid sequence identity and similarity [respectively; via BLAST of PA7 vs. PAO1-UW (Winsor et al., 2011)] as follows: MexC (387 aa; 88 and 95%), MexD (1043 aa; 95 and 98%), OprJ (475 aa; 89 and 93%); MexE (414 aa; 99 and 99%), MexF (1062 aa; 99 and 99%), and OprN (472 aa; 97 and 99%). As a second step in testing our hypothesis, we examined the regulation of these genes in PA7. qRT-PCR showed that expression of *mexE* was increased (ca. 22-fold) in PA7 compared to the wild-type strain DSM 1128. This observation indicated that FQ resistance in *P. aeruginosa* can be mediated by overexpression of the *mexEF oprN* operon, in addition to the previously reported overexpression of *mexXY oprA* due to mutation of the local repressor gene (*mexZ*) (Morita et al., 2012b).

We also observed that a  $\Delta$ *mexXY oprA*  $\Delta$ *mexAB oprM*  $\Delta$ *mexEF oprN* triple mutant derived from PA7 exhibited increased susceptibility to FQs (32–128-fold) compared to an isogenic  $\Delta$ *mexXY oprA*  $\Delta$ *mexAB oprM* double mutant, while exhibiting only mild elevation of FQ MIC (0.5–2  $\mu$ g/ml) compared to wild-type PAO1 and DSM 1128 (0.125–1  $\mu$ g/ml) (**Table 3**). Moreover, the triple mutant was much more sensitive (512-fold) to chloramphenicol than the double mutant, a further indicator of MexEF-OprN-mediated resistance (Sobel et al., 2005) (**Table 3**). We excluded a role for overexpression of *mexCD oprJ* in PA7, as judged by the susceptibilities of the mutant ( $\Delta$ *mexXY oprA*  $\Delta$ *mexAB oprM*  $\Delta$ *mexEF oprN* construct) to not only FQs but also to tetracycline and chloramphenicol, which are substrates of MexCD-OprJ (Poole et al., 1996).

To clarify the roles of MexXY-OprA, MexAB-OprM and MexEF-OprN multidrug efflux pumps in the FQ resistance of *P. aeruginosa* PA7, we constructed a series of deletion mutants of the three *mex* operons and examined their drug susceptibility

**Table 3 | Contribution of three RND efflux pumps to antimicrobial resistance of *P. aeruginosa* PA7.**

| Strain                 | Genotype   | MIC ( $\mu$ g/ml) of |      |      |     |     |      |     |
|------------------------|--|----------------------|------|------|-----|-----|------|-----|
|                        |  | CIP                  | NOR  | LVX  | MXF | AMK | CHL  | IPM |
| PA7 (PAGU 1498)        | Parent   | 64                   | 128  | 128  | 256 | 32  | 1024 | 2   |
| PAGU <sup>9</sup> 1565 | PA7 $\Delta$ <i>mexXY oprA</i>   | 32                   | 64   | 64   | 128 | 1   | 1024 | 2   |
| PAGU <sup>9</sup> 1603 | PA7 $\Delta$ <i>mexAB oprM</i>   | 64                   | 128  | 64   | 256 | 32  | 1024 | 2   |
| PAGU <sup>9</sup> 1748 | PA7 $\Delta$ <i>mexEF oprN</i>   | 32                   | 64   | 64   | 256 | 32  | 128  | 2   |
| PAGU <sup>9</sup> 1641 | PA7 $\Delta$ <i>mexXY oprA</i> $\Delta$ <i>mexAB oprM</i>                            | 32                   | 64   | 32   | 64  | 1   | 1024 | 2   |
| PAGU <sup>9</sup> 1751 | PA7 $\Delta$ <i>mexXY oprA</i> $\Delta$ <i>mexEF oprN</i>                            | 8                    | 16   | 8    | 32  | 1   | 256  | 2   |
| PAGU <sup>9</sup> 1753 | PA7 $\Delta$ <i>mexAB oprM</i> $\Delta$ <i>mexEF oprN</i>                            | 32                   | 64   | 32   | 128 | 32  | 16   | 2   |
| PAGU <sup>9</sup> 1756 | PA7 $\Delta$ <i>mexXY oprA</i> $\Delta$ <i>mexAB oprM</i> $\Delta$ <i>mexEF oprN</i> | 0.5                  | 0.5  | 0.5  | 2   | 1   | 4    | 2   |
| DSM 1128 (PAGU 1504)   | Wild type  | 0.125                | 0.25 | 0.25 | 1   | 0.5 | 32   | 1   |
| PAO1 (PAGU 974)        | Wild type  | 0.125                | 0.25 | 0.25 | 1   | 0.5 | 32   | 1   |

AMK, amikacin; CHL, chloramphenicol; CIP, ciprofloxacin; IPM, imipenem; LVX, levofloxacin; MXF, moxifloxacin; NOR, norfloxacin.

profiles (**Table 3**). We observed that the  $\Delta mexXY\text{-}oprA \Delta mexEF\text{-}oprN$  double deletion mutant was more susceptible (4-fold) than the  $\Delta mexAB\text{-}oprM \Delta mexXY\text{-}oprA$  double mutant and the  $\Delta mexAB\text{-}oprM \Delta mexEF\text{-}oprN$  double mutant (**Table 3**). These data suggested that the MexXY-OprA and MexEF-OprN systems make similar contributions to FQ resistance in *P. aeruginosa* PA7, each having an effect larger than that of MexAB-OprM. The apparent modest MexAB-OprM contribution to resistance of FQs and chloramphenicol in PA7 [PA7  $\Delta mexXY\text{-}oprA \Delta mexEF\text{-}oprN$  vs. PA7  $\Delta mexXY\text{-}oprA \Delta mexAB\text{-}oprM \Delta mexEF\text{-}oprN$ ] (**Table 3**) is typically observed in wild type *P. aeruginosa* such as PAO1 already shown in the previous results (e.g., PAO1  $\Delta mexXY$  vs. PAO1  $\Delta mexXY \Delta mexAB\text{-}oprM$ ) (e.g., Morita et al., 2001), implying that *mexAB\text{-}oprM* is expressed at moderate levels in PA7. We concluded that high-level FQ resistance in *P. aeruginosa* PA7 was due to overproduction of MexXY-OprA and MexEF-OprN, in addition to the typical target mutations.

#### MOLECULAR MECHANISMS OF *mexEF\text{-}oprN*-UPREGULATION IN *P. AERUGINOSA* PA7

The *mexEF\text{-}oprN* operon is quiescent in wild-type *P. aeruginosa* cells grown under standard laboratory conditions. In contrast, this operon is expressed in so-called *nfxC* mutants and in mutants defective in the *mexS* gene (previously known as *qrh*), a locus that encodes a putative oxidoreductase of as yet unknown function (Poole, 2013). Expression of *mexEF\text{-}oprN* is regulated by a transcriptional activator, MexT, a LysR family regulator (Kohler et al., 1999; Poole, 2013). *mexT* occurs upstream of *mexEF\text{-}oprN* and downstream of *mexS*, the latter gene also positively regulated by MexT (Kohler et al., 1999). Unusually, many so-called wild type strains possess inactive MexT (e.g., 8 bp insertion in *mexT* present in some PAO1 strains) (Maseda et al., 2000; Poole, 2013). The induction of *mexEF\text{-}oprN* contributes to multidrug resistance, albeit against a rather narrow range of antimicrobials including FQs, trimethoprim, and chloramphenicol (Poole, 2013). The enhanced resistance to imipenem of *nfxC* mutants or *mexS* deficient mutants results not from *mexEF\text{-}oprN* expression but the concomitant decrease in the level of outer membrane protein OprD (Poole, 2013), because OprD is an imipenem channel and serves as the primary route of entry of this antibiotic in *P. aeruginosa* (Trias and Nikaido, 1990). However, *P. aeruginosa* PA7 was reported to be susceptible to carbapenems, with MICs of 2 and 1  $\mu\text{g}/\text{ml}$  for imipenem and meropenem, respectively (Roy et al.,

2010). This observation of carbapenem susceptibility is somewhat paradoxical, given that a typical *nfxC* mutant or a *mexS* deficient mutant is expected to exhibit carbapenem resistance due to a coordinate, MexT-dependent reduction of OprD levels. We found that *P. aeruginosa* PA7 exhibited slight but reproducible elevation (2-fold) of resistance to imipenem compared to wild-type *P. aeruginosa* strains PAO1 and DSM 1128 (**Table 4**). Deletion of *mexS* in a PA7 background resulted in slightly increased expression of *mexE* (2-fold) and increased resistance to imipenem (4-fold) compared to PA7. Thus, PA7 appeared to exhibit susceptibility intermediate between that of wild type and a typical *nfxC* mutant. Deletion of *mexT* in a PA7 background resulted in drastically (>200-fold) decreased expression of *mexE* and *mexS* compared to PA7 (**Table 4**). Notably, expression of *mexS* in PA7  $\Delta mexT$  was more than 96-fold reduced compared to the wild-type DSM 1128 and PA7 *mexS* (V155A). This observation was consistent with a previous report (using  $\beta$ -galactosidase reporter assays) indicating that *mexS* (*qrh*) is constitutively expressed at a moderate level (Kohler et al., 1999; Poole, 2013).

We therefore determined the nucleotide sequences (ca. 2.4 kb) upstream of the *mexEF\text{-}oprN* operon in *P. aeruginosa* DSM 1128 (accession no. AB889539). This interval corresponds to the operon's cognate regulatory region, and includes the *mexS* and *mexT* loci. Comparison to the corresponding sequences from *P. aeruginosa* PA7 (data not shown) revealed that *MexS<sub>PA7</sub>* is encoded as an A155V variant, and *MexT<sub>PA7</sub>* as an A256T variant, compared to the DSM 1128 genome. In contrast, alanine-155 of MexS and alanine-256 of MexT are conserved among multiple laboratory and clinical strains, including PAO1, PA14, PAK, and K2153 (Sobel et al., 2005; Jin et al., 2011; Lamarche and Deziel, 2011). To test the function of the *mexS<sub>PA7</sub>* and *mexT<sub>PA7</sub>* loci, we amplified and cloned the individual *mexS* and *mexT* genes (without endogenous promoters) from *P. aeruginosa* PA7 and DSM 1128, and expressed the relevant genes in *P. aeruginosa* K2153  $\Delta mexS$  (*Fetar* et al., 2011) for a *mexS* complementation test or in K2153  $\Delta mexS \Delta mexT$  (Sobel et al., 2005; *Fetar* et al., 2011) for a *mexT* complementation test (**Table 5**). [As demonstrated by other researchers, *P. aeruginosa* K2153 and its derivatives are useful for the analysis of *mexEF\text{-}oprN*-dependent antimicrobial resistance as regulated by the MexT activator and MexS function (Sobel et al., 2005; *Fetar* et al., 2011)]. Interestingly, introduction of *mexS<sub>DSM 1128</sub>* or *mexS<sub>PA7</sub>* into the chromosome of K2153  $\Delta mexS$  did not provide complementation of  $\Delta mexS$  (**Table 5**). These data

**Table 4 | Relationship between antimicrobial resistance and *mexS\text{-}mexT*-mediated *mexEF\text{-}oprN* expression in *P. aeruginosa*.**

| Strains                | Genotype                | MIC ( $\mu\text{g}/\text{ml}$ ) of |       |     | Relative mRNA level |             |             |
|------------------------|-------------------------|------------------------------------|-------|-----|---------------------|-------------|-------------|
|                        |                         | CIP                                | CHL   | IPM | <i>mexE</i>         | <i>mexS</i> | <i>mexT</i> |
| PA7 (PAGU 1498)        | Parent                  | 128                                | 1024  | 2   | 1                   | 1           | 1           |
| PAGU <sup>9</sup> 1793 | PA7 $\Delta mexS$       | >128                               | >1024 | 8   | 2.0                 | nd          | 0.84        |
| PAGU <sup>9</sup> 1867 | PA7 <i>mexS</i> (V155A) | 64                                 | 256   | 1   | 0.053               | 0.57        | 0.74        |
| PAGU <sup>9</sup> 1789 | PA7 $\Delta mexT$       | 64                                 | 128   | 1   | < 0.005             | < 0.005     | nd          |
| DSM 1128 (PAGU 1504)   | Wild type               | 0.125                              | 32    | 1   | 0.046               | 0.48        | 1.1         |
| PAO1 (PAGU 974)        | Wild type               | 0.125                              | 32    | 1   | nd                  | nd          | nd          |

CHL, chloramphenicol; CIP, ciprofloxacin; IPM, imipenem; nd, not done.

**Table 5 | Functional characterization of *mexS* and *mexT* from *P. aeruginosa* PA7 and DSM 1128.**

| Strains                        | Genotype  | MIC ( $\mu\text{g/ml}$ ) |      |     |
|--------------------------------|---|--------------------------|------|-----|
|                                |   | CIP                      | CHL  | IPM |
| K2153 (PAGU 1741)              | Parent  | 0.5                      | 64   | 2   |
| K2376 (PAGU <sup>9</sup> 1834) | $\Delta m\text{exS}$  | 2                        | 2048 | 8   |
| PAGU <sup>9</sup> 1850         | $\Delta m\text{exS} attB::lacI^Q-P_{T7}$  | 2                        | 2048 | 8   |
| PAGU <sup>9</sup> 1851         | $\Delta m\text{exS} attB::lacI^Q-P_{T7}-m\text{exS}_{PA7}$                                | 2                        | 2048 | 8   |
| PAGU <sup>9</sup> 1844         | $\Delta m\text{exS}$<br>$attB::lacI^Q-P_{T7}-m\text{exS}_{DSM\ 1128}$                     | 2                        | 1024 | 8   |
| PAGU <sup>9</sup> 1854         | $\Delta m\text{exS} pUCP20T$  | 2                        | 2048 | 8   |
| PAGU <sup>9</sup> 1855         | $\Delta m\text{exS} pUCP20T::m\text{exS}_{PA7}$   | 1                        | 256  | 4   |
| PAGU <sup>9</sup> 1856         | $\Delta m\text{exS}$<br>$pUCP20T::m\text{exS}_{DSM\ 1128}$                                | 0.5                      | 64   | 2   |
| K2942 (PAGU <sup>9</sup> 1837) | $Dm\text{exS}\ \Delta m\text{exT}$  | 0.5                      | 64   | 2   |
| PAGU <sup>9</sup> 1852         | $\Delta m\text{exS}\ \Delta m\text{exT} attB::lacI^Q-P_{T7}$                              | 0.5                      | 64   | 2   |
| PAGU <sup>9</sup> 1846         | $\Delta m\text{exS}\ \Delta m\text{exT}$<br>$attB::lacI^Q-P_{T7}-m\text{exT}_{PA7}$       | 2                        | 2048 | 8   |
| PAGU <sup>9</sup> 1845         | $\Delta m\text{exS}\ \Delta m\text{exT}$<br>$attB::lacI^Q-P_{T7}-m\text{exT}_{DSM\ 1128}$ | 2                        | 2048 | 8   |

CHL, chloramphenicol; CIP, ciprofloxacin; IPM, imipenem.

5 mM IPTG was added to allow expression controlled by the  $P_{T7}$  promoter.

contrast previous instances in which we observed *attB*-site (i.e., single-copy) complementation for several other genes (Morita et al., 2010, 2012b). Presumably, in the present studies, failure to complement reflected insufficient *mexS* expression from the  $P_{T7}$  promoter in PAGU<sup>9</sup>1844, given that MexS<sub>DSM 1128</sub> is expected to be functional. Introduction of pUCP20T::*mexS*<sub>DSM 1128</sub> into *P. aeruginosa* K2153  $\Delta m\text{exS}$  yielded MICs identical to those of the K2153 *mexS*<sup>+</sup> parent; introduction of pUCP20T::*mexS*<sub>PA7</sub> yielded parent-like resistance to imipenem, but only partially restored resistance to ciprofloxacin and chloramphenicol (Table 5). Taken together, these results suggested that MexS<sub>PA7</sub> provides reduced function compared to MexS<sub>DSM 1128</sub>. Additionally it appears that the high levels of *mexS* expression are required to overcome the *nfxC*-type antimicrobial resistance.

Slightly increased expression of *mexS* was observed in *P. aeruginosa* PA7 compared to *P. aeruginosa* DSM 1128 (ca. 2-fold), while expression levels of *mexT* in *P. aeruginosa* PA7 were similar to those in *P. aeruginosa* DSM 1128 (ca. 0.9-fold) (Table 4). Introduction of *mexT*<sub>DSM 1128</sub> or *mexT*<sub>PA7</sub> into the chromosome of K2153  $\Delta m\text{exS}\ \Delta m\text{exT}$  yielded the *nfxC* phenotype (Table 5), suggesting that the A256T substitution in MexT is not a primary reason for overexpression of *mexEF oprN* in *P. aeruginosa* PA7. Using site-specific mutagenesis, we altered the plasmid-borne *mexS*<sub>PA7</sub> locus to encode a V155A version of the protein and replaced the endogenous PA7 chromosomal locus with the mutated gene. The PA7 *mexS*<sub>PA7(V155A)</sub> strain showed decreased *mexE* expression (0.053-fold compared to that of the PA7 parent), a value similar to that seen in DSM 1128 (0.034-fold compared to that of PA7) (Table 4). The PA7 *mexS*<sub>PA7(V155A)</sub> strain also showed decreased MICs for chloramphenicol (0.25-fold) (Table 4). Taken together with the complementation experiments, these data strongly suggested that the A155V substitution

in MexS<sub>PA7</sub> is the primary reason for increased expression of *mexEF oprN* and increased antimicrobial resistance in the PA7 strain.

## DISCUSSION

In this study, the multidrug-resistant clinical isolate PA7 was shown to exhibit increased expression of *mexEF oprN* as well as *mexXY oprA*. Although multidrug-resistant *P. aeruginosa* clinical isolates have often been reported to be MexXY overproducers (Morita et al., 2012a), clinical strains of *P. aeruginosa* overproducing MexEF-OprN and MexXY(-OprA) efflux pumps simultaneously have rarely been reported. In fact, PA7 was not a typical *nfxC* mutant (i.e., a MexEF-OprN overproducer), and instead expressed intermediate levels of *mexEF oprN*. We assume that simultaneous overproduction of MexEF-OprN and MexXY(-OprA) impairs *P. aeruginosa* growth, based on our observation that our PA7  $\Delta m\text{exS}$  construct (i.e., a simultaneous overproducer of MexEF-OprN and MexXY-OprA compared to the PA7 parent) was unstable even on L agar plates: colonies of the construct exhibited a non-uniform phenotype during growth on plates (data not shown). This observation is consistent with the increased susceptibility to aminoglycosides previously observed in MexEF-OprN-overproducing *nfxC* mutants, apparently owing to impairment of the MexXY system (Sobel et al., 2005).

Valine-155 of MexS<sub>PA7</sub> also was shown as the likely primary reason for increased production of MexEF-OprN in PA7. With the exception of *mexS*<sub>PA7</sub>, sequenced *P. aeruginosa* *mexS* genes (including those from PAO1, K2153, PA14, PAK, and DSM 1128) encode proteins with an alanine at residue 155 (Sobel et al., 2005; Jin et al., 2011; Lamarche and Deziel, 2011). The Ala155Val substitution is predicted by the SIFT algorithm (Kumar et al., 2009) not to affect the protein's function (data not shown). We hypothesize that MexS<sub>PA7</sub> retains function, albeit with decreased activity and/or altered regulation (e.g., allosteric), compared with the other MexS orthologs. In fact, there were few differences among the whole structures of MexS<sub>PA7</sub>, MexS<sub>PAO1</sub>, and MexS<sub>DSM 1128</sub> models developed by using the SWISS-MODEL program (data not shown) (Bordoli et al., 2009). MexS is a member of the cd08268: MDR2 family of the Conserved Domains Database (CDD) of the National Center for Biotechnology Information (NCBI) (Fargier et al., 2012) and alanine-155 corresponds to one of the putative NAD(P) binding sites featured in the MDR2 family.

In addition to antibiotic resistance, an *nfxC*-type mutation has been linked to reduced levels of homoserine lactone-dependent quorum sensing (QS)-regulated virulence factors, including pyocyanin, elastase, rhamnolipids, and *Pseudomonas Quinolone Signal* (PQS), and to reduced expression of type-III secretion system (TTSS) effector proteins (Kohler et al., 2001; Linares et al., 2005). QS is a cell-to-cell communication mechanism employing diffusible signal molecules (Jimenez et al., 2012), and the TTSS is a mechanism by which bacterial pathogens can deliver effectors directly into the cytoplasm of eukaryotic host cells (Hauser, 2009). We found that PA7 had reduced level of pyocyanin production, rhamnolipid production, and swarming activity compared to DSM 1128 and PAO1 (data not shown), consistent with the typical *nfxC* mutant phenotype (Jin et al., 2011). However, PA7

derivatives including PA7 *mexSPA7*(V155A) also showed almost the same activities of the QS regulated virulence factors with PA7 (data not shown), which suggests that the impaired QS-related phenotype is not derived from the *nfxC*-like phenotype in PA7. We presume that this lack of correlation reflects the absence from PA7 of TTSS-encoding genes and of the *mvfR* (*pqsR*) gene, which is known to encode a LysR-type transcriptional regulator that modulates the expression of multiple QS-regulated virulence factors (Deziel et al., 2005; Roy et al., 2010). These deficiencies might be the source of the *mexS* mutation and increased *mexEF-oprN* expression under oxidative stress, sulfide stress, or nitrosative stress (Juhas et al., 2004; Fetar et al., 2011; Fargier et al., 2012).

## ACKNOWLEDGMENTS

We thank Tadashi Kumazawa for his contribution. We thank Dr. Keith Poole (Queen's University, Canada) for providing the *P. aeruginosa* strains. This work was supported in part by a Grant-in-Aid for Young Scientists (B) (Kakenhi 23790106) and a Grant-in-Aid for Scientific Research (C) (Kakenhi 26460080) from the Japan Society for the Promotion of Science, and by a research grant from the Institute of Pharmaceutical Life Sciences, Aichi Gakuin University.

## REFERENCES

- Boratyn, G. M., Camacho, C., Cooper, P. S., Coulouris, G., Fong, A., and Ma, N. (2013). BLAST: a more efficient report with usability improvements. *Nucleic Acids Res.* 41, W29–W33. doi: 10.1093/nar/gkt282
- Bordoli, L., Kiefer, F., Arnold, K., Benkert, P., Battey, J., and Schwede, T. (2009). Protein structure homology modeling using SWISS-MODEL workspace. *Nat. Protoc.* 4, 1–13. doi: 10.1038/nprot.2008.197
- Breidenstein, E. B., De La Fuente-Nunez, C., and Hancock, R. E. (2011). *Pseudomonas aeruginosa*: all roads lead to resistance. *Trends Microbiol.* 19, 419–426. doi: 10.1016/j.tim.2011.04.005
- Bruchmann, S., Dotsch, A., Nouri, B., Chaberny, I. F., and Haussler, S. (2013). Quantitative contributions of target alteration and decreased drug accumulation to *Pseudomonas aeruginosa* fluoroquinolone resistance. *Antimicrob. Agents Chemother.* 57, 1361–1368. doi: 10.1128/aac.01581-12
- Cabot, G., Ocampo-Sosa, A. A., Tubau, F., Macia, M. D., Rodriguez, C., and Moya, B. (2011). Overexpression of AmpC and efflux pumps in *Pseudomonas aeruginosa* isolates from bloodstream infections: prevalence and impact on resistance in a Spanish multicenter study. *Antimicrob. Agents Chemother.* 55, 1906–1911. doi: 10.1128/aac.01645-10
- Deziel, E., Gopalan, S., Tampakaki, A. P., Lepine, F., Padfield, K. E., and Saucier, M. (2005). The contribution of *MvfR* to *Pseudomonas aeruginosa* pathogenesis and quorum sensing circuitry regulation: multiple quorum sensing-regulated genes are modulated without affecting *lasRI*, *rhlRI* or the production of N-acyl-L-homoserine lactones. *Mol. Microbiol.* 55, 998–1014. doi: 10.1111/j.1365-2958.2004.04448.x
- Fargier, E., Mac Aogain, M., Mooij, M. J., Woods, D. E., Morrissey, J. P., and Dobson, A. D. (2012). MexT functions as a redox-responsive regulator modulating disulfide stress resistance in *Pseudomonas aeruginosa*. *J. Bacteriol.* 194, 3502–3511. doi: 10.1128/jb.06632-11
- Fetar, H., Gilmour, C., Klinoski, R., Daigle, D. M., Dean, C. R., and Poole, K. (2011). *mexEF-oprN* multidrug efflux operon of *Pseudomonas aeruginosa*: regulation by the MexT activator in response to nitrosative stress and chloramphenicol. *Antimicrob. Agents Chemother.* 55, 508–514. doi: 10.1128/aac.00830-10
- Fournier, D., Richardot, C., Muller, E., Robert-Nicoud, M., Llanes, C., and Plesiat, P. (2013). Complexity of resistance mechanisms to imipenem in intensive care unit strains of *Pseudomonas aeruginosa*. *J. Antimicrob. Chemother.* 68, 1772–1780. doi: 10.1093/jac/dkt098
- Fuste, E., Lopez-Jimenez, L., Segura, C., Gainza, E., Vinuesa, T., and Vinas, M. (2013). Carbapenem-resistance mechanisms of multidrug-resistant *Pseudomonas aeruginosa*. *J. Med. Microbiol.* 62, 1317–1325. doi: 10.1099/jmm.0.058354-0
- Geiser, M., Cebe, R., Drewello, D., and Schmitz, R. (2001). Integration of PCR fragments at any specific site within cloning vectors without the use of restriction enzymes and DNA ligase. *Biotechniques* 31, 88–92.
- Gellatly, S. L., and Hancock, R. E. (2013). *Pseudomonas aeruginosa*: new insights into pathogenesis and host defenses. *Pathog. Dis.* 67, 159–173. doi: 10.1111/2049-632x.12033
- Hauser, A. R. (2009). The type III secretion system of *Pseudomonas aeruginosa*: infection by injection. *Nat. Rev. Microbiol.* 7, 654–665. doi: 10.1038/nrmicro2199
- Hoang, T. T., Karkhoff-Schweizer, R. R., Kutchma, A. J., and Schweizer, H. P. (1998). A broad-host-range Flp-FRT recombination system for site-specific excision of chromosomally-located DNA sequences: application for isolation of unmarked *Pseudomonas aeruginosa* mutants. *Gene* 212, 77–86.
- Hocquet, D., Berthelot, P., Roussel-Delvallez, M., Favre, R., Jeannot, K., and Bajoleit, O. (2007). *Pseudomonas aeruginosa* may accumulate drug resistance mechanisms without losing its ability to cause bloodstream infections. *Antimicrob. Agents Chemother.* 51, 3531–3536. doi: 10.1128/aac.00503-07
- Hocquet, D., Muller, A., Blanc, K., Plesiat, P., Talon, D., Monnet, D. L., et al. (2008). Relationship between antibiotic use and incidence of MexXY-OprM overproducers among clinical isolates of *Pseudomonas aeruginosa*. *Antimicrob. Agents Chemother.* 52, 1173–1175. doi: 10.1128/aac.01212-07
- Jimenez, P. N., Koch, G., Thompson, J. A., Xavier, K. B., Cool, R. H., and Quax, W. J. (2012). The multiple signaling systems regulating virulence in *Pseudomonas aeruginosa*. *Microbiol. Mol. Biol. Rev.* 76, 46–65. doi: 10.1128/mmbr.05007-11
- Jin, Y., Yang, H., Qiao, M., and Jin, S. (2011). MexT regulates the type III secretion system through MexS and PtrC in *Pseudomonas aeruginosa*. *J. Bacteriol.* 193, 399–410. doi: 10.1128/jb.01079-10
- Juhas, M., Wiehlmann, L., Huber, B., Jordan, D., Lauber, J., and Salunkhe, P. (2004). Global regulation of quorum sensing and virulence by VqsR in *Pseudomonas aeruginosa*. *Microbiology* 150, 831–841. doi: 10.1099/mic.0.26906-0
- Khuntayaporn, P., Montakantikul, P., Santanirand, P., Kiratisin, P., and Chomnawang, M. T. (2013). Molecular investigation of carbapenem resistance among multidrug-resistant *Pseudomonas aeruginosa* isolated clinically in Thailand. *Microbiol. Immunol.* 57, 170–178. doi: 10.1111/1348-0421.12021
- Kiewitz, C., and Tummler, B. (2000). Sequence diversity of *Pseudomonas aeruginosa*: impact on population structure and genome evolution. *J. Bacteriol.* 182, 3125–3135. doi: 10.1128/JB.182.11.3125-3135.2000
- Kohler, T., Epp, S. F., Curty, L. K., and Pechere, J. C. (1999). Characterization of MexT, the regulator of the MexE-MexF-OprN multidrug efflux system of *Pseudomonas aeruginosa*. *J. Bacteriol.* 181, 6300–6305.
- Kohler, T., Van Delden, C., Curty, L. K., Hamzehpour, M. M., and Pechere, J. C. (2001). Overexpression of the MexEF-OprN multidrug efflux system affects cell-to-cell signaling in *Pseudomonas aeruginosa*. *J. Bacteriol.* 183, 5213–5222. doi: 10.1128/JB.183.18.5213-5222.2001
- Kumar, P., Henikoff, S., and Ng, P. C. (2009). Predicting the effects of coding non-synonymous variants on protein function using the SIFT algorithm. *Nat. Protoc.* 4, 1073–1081. doi: 10.1038/nprot.2009.86
- Lamarche, M. G., and Deziel, E. (2011). MexEF-OprN efflux pump exports the *Pseudomonas* quinolone signal (PQS) precursor HHQ (4-hydroxy-2-heptylquinoline). *PLoS ONE* 6:e24310. doi: 10.1371/journal.pone.0024310
- Li, Y., Mima, T., Komori, Y., Morita, Y., Kuroda, T., and Mizushima, T. (2003). A new member of the tripartite multidrug efflux pumps, MexVW-OprM, in *Pseudomonas aeruginosa*. *J. Antimicrob. Chemother.* 52, 572–575. doi: 10.1093/jac/dkg390
- Linares, J. F., Lopez, J. A., Camafeita, E., Albar, J. P., Rojo, F., and Martinez, J. L. (2005). Overexpression of the multidrug efflux pumps MexCD-OprJ and MexEF-OprN is associated with a reduction of type III secretion in *Pseudomonas aeruginosa*. *J. Bacteriol.* 187, 1384–1391. doi: 10.1128/jb.187.4.1384-1391.2005
- Llanes, C., Kohler, T., Patry, I., Dehecq, B., Van Delden, C., and Plesiat, P. (2011). Role of the MexEF-OprN efflux system in low-level resistance of *Pseudomonas aeruginosa* to ciprofloxacin. *Antimicrob. Agents Chemother.* 55, 5676–5684. doi: 10.1128/aac.00101-11
- Lomovskaya, O., Lee, A., Hoshino, K., Ishida, H., Mistry, A., and Warren, M. S. (1999). Use of a genetic approach to evaluate the consequences of inhibition of efflux pumps in *Pseudomonas aeruginosa*. *Antimicrob. Agents Chemother.* 43, 1340–1346.

- Maseda, H., Saito, K., Nakajima, A., and Nakae, T. (2000). Variation of the *mexT* gene, a regulator of the MexEF-oprN efflux pump expression in wild-type strains of *Pseudomonas aeruginosa*. *FEMS Microbiol. Lett.* 192, 107–112. doi: 10.1111/j.1574-6968.2000.tb09367.x
- Morita, Y., Gilmour, C., Metcalf, D., and Poole, K. (2009). Translational control of the antibiotic inducibility of the PA5471 gene required for *mexXY* multidrug efflux gene expression in *Pseudomonas aeruginosa*. *J. Bacteriol.* 191, 4966–4975. doi: 10.1128/jb.00073-09
- Morita, Y., Kimura, N., Mima, T., Mizushima, T., and Tsuchiya, T. (2001). Roles of MexXY- and MexAB-multidrug efflux pumps in intrinsic multidrug resistance of *Pseudomonas aeruginosa* PAO1. *J. Gen. Appl. Microbiol.* 47, 27–32. doi: 10.2323/jgam.47.27
- Morita, Y., Kodama, K., Shiota, S., Mine, T., Kataoka, A., and Mizushima, T. (1998). NorM, a putative multidrug efflux protein, of *Vibrio parahaemolyticus* and its homolog in *Escherichia coli*. *Antimicrob. Agents Chemother.* 42, 1778–1782.
- Morita, Y., Narita, S., Tomida, J., Tokuda, H., and Kawamura, Y. (2010). Application of an inducible system to engineer unmarked conditional mutants of essential genes of *Pseudomonas aeruginosa*. *J. Microbiol. Methods* 82, 205–213. doi: 10.1016/j.mimet.2010.06.001
- Morita, Y., Sobel, M. L., and Poole, K. (2006). Antibiotic inducibility of the MexXY multidrug efflux system of *Pseudomonas aeruginosa*: involvement of the antibiotic-inducible PA5471 gene product. *J. Bacteriol.* 188, 1847–1855. doi: 10.1128/jb.188.5.1847-1855.2006
- Morita, Y., Tomida, J., and Kawamura, Y. (2012a). MexXY multidrug efflux system of *Pseudomonas aeruginosa*. *Front. Microbiol.* 3:408. doi: 10.3389/fmicb.2012.00408
- Morita, Y., Tomida, J., and Kawamura, Y. (2012b). Primary mechanisms mediating aminoglycoside resistance in the multidrug-resistant *Pseudomonas aeruginosa* clinical isolate PA7. *Microbiology* 158, 1071–1083. doi: 10.1099/mic.0.054320-0
- Morita, Y., Tomida, J., and Kawamura, Y. (2014). Responses of *Pseudomonas aeruginosa* to antimicrobials. *Front. Microbiol.* 4:422. doi: 10.3389/fmicb.2013.00422
- Morita, Y., Tomida, J., and Kawamura, Y. (2015). “Resistance and response to anti-pseudomonas agents and biocides,” in *Pseudomonas: New Aspects of Pseudomonas Biology*, eds J. Ramos, J. B. Goldberg, and A. Filloux (New York, NY: Springer), 173–187.
- Patel, J. B., Tenover, F. C., Turnidge, J. D., and Jorgensen, J. H. (2011). “Susceptibility test methods: dilution and disk diffusion methods,” in *Manual of Clinical Microbiology*, 10th Edn, eds J. Versalovic, K. C. Carroll, G. Funke, J. H. Jorgensen, M. L. Landry, and D. W. Warnock (Washington, DC: ASM Press), 1122–1143.
- Poole, K. (2011). *Pseudomonas aeruginosa*: resistance to the max. *Front. Microbiol.* 2:65. doi: 10.3389/fmicb.2011.00065
- Poole, K. (2013). “*Pseudomonas aeruginosa* efflux pumps,” in *Microbial Efflux Pumps: Current Research*, eds E. W. Yu, Q. Zhang, and M. H. Brown (Norfolk: Caiser Academic Press), 175–206.
- Poole, K. (2014). Stress responses as determinants of antimicrobial resistance in *Pseudomonas aeruginosa*: multidrug efflux and more. *Can. J. Microbiol.* 60, 783–791. doi: 10.1139/cjm-2014-0666
- Poole, K., Gotoh, N., Tsujimoto, H., Zhao, Q., Wada, A., and Yamasaki, T. (1996). Overexpression of the *mexC-mexD-oprJ* efflux operon in *nfxB*-type multidrug-resistant strains of *Pseudomonas aeruginosa*. *Mol. Microbiol.* 21, 713–724.
- Rossolini, G. M., Arena, F., Pecile, P., and Pollini, S. (2014). Update on the antibiotic resistance crisis. *Curr. Opin. Pharmacol.* 18c, 56–60. doi: 10.1016/j.coph.2014.09.006
- Roy, P. H., Tetu, S. G., Larouche, A., Elbourne, L., Tremblay, S., and Ren, Q. (2010). Complete genome sequence of the multiresistant taxonomic outlier *Pseudomonas aeruginosa* PA7. *PLoS ONE* 5:e8842. doi: 10.1371/journal.pone.0008842
- Schweizer, H. P., Klassen, T. R., and Hoang, T. T. (1996). “Improved methods for gene analysis and expression in *Pseudomonas*,” in *Molecular Biology of Pseudomonads*, eds T. Nakazawa, D. Haas, and S. Silver (Washington, DC: ASM Press), 229–237.
- Sobel, M. L., McKay, G. A., and Poole, K. (2003). Contribution of the MexXY multidrug transporter to aminoglycoside resistance in *Pseudomonas aeruginosa* clinical isolates. *Antimicrob. Agents Chemother.* 47, 3202–3207. doi: 10.1128/AAC.47.10.3202-3207.2003
- Sobel, M. L., Neshat, S., and Poole, K. (2005). Mutations in PA2491 (*mexS*) promote MexT-dependent *mexEF-oprN* expression and multidrug resistance in a clinical strain of *Pseudomonas aeruginosa*. *J. Bacteriol.* 187, 1246–1253. doi: 10.1128/jb.187.4.1246-1253.2005
- Trias, J., and Nikaido, H. (1990). Protein D2 channel of the *Pseudomonas aeruginosa* outer membrane has a binding site for basic amino acids and peptides. *J. Biol. Chem.* 265, 15680–15684.
- Vatcheva-Dobrevska, R., Mulet, X., Ivanov, I., Zamorano, L., Dobreva, E., and Velinov, T. (2013). Molecular epidemiology and multidrug resistance mechanisms of *Pseudomonas aeruginosa* isolates from Bulgarian hospitals. *Microb. Drug Resist.* 19, 355–361. doi: 10.1089/mdr.2013.0004
- Winsor, G. L., Lam, D. K., Fleming, L., Lo, R., Whiteside, M. D., and Yu, N. Y. (2011). Pseudomonas Genome Database: improved comparative analysis and population genomics capability for Pseudomonas genomes. *Nucleic Acids Res.* 39, D596–D600. doi: 10.1093/nar/gkq869

**Conflict of Interest Statement:** The authors declare that the research was conducted in the absence of any commercial or financial relationships that could be construed as a potential conflict of interest.

Received: 27 October 2014; paper pending published: 21 November 2014; accepted: 05 January 2015; published online: 21 January 2015.

Citation: Morita Y, Tomida J and Kawamura Y (2015) Efflux-mediated fluoroquinolone resistance in the multidrug-resistant *Pseudomonas aeruginosa* clinical isolate PA7: identification of a novel MexS variant involved in upregulation of the *mexEF-oprN* multidrug efflux operon. *Front. Microbiol.* 6:8. doi: 10.3389/fmicb.2015.00008

This article was submitted to Antimicrobials, Resistance and Chemotherapy, a section of the journal *Frontiers in Microbiology*.

Copyright © 2015 Morita, Tomida and Kawamura. This is an open-access article distributed under the terms of the Creative Commons Attribution License (CC BY). The use, distribution or reproduction in other forums is permitted, provided the original author(s) or licensor are credited and that the original publication in this journal is cited, in accordance with accepted academic practice. No use, distribution or reproduction is permitted which does not comply with these terms.

# Efflux pump-mediated drug resistance in *Burkholderia*

Nicole L. Podneacky<sup>1†</sup>, Katherine A. Rhodes<sup>1,2</sup> and Herbert P. Schweizer<sup>1,2\*</sup>

<sup>1</sup> Department of Microbiology, Immunology and Pathology, College of Veterinary Medicine and Biological Sciences, Colorado State University, Fort Collins, CO, USA, <sup>2</sup> Department of Molecular Genetics and Microbiology, College of Medicine, Emerging Pathogens Institute, Institute for Therapeutic Innovation, University of Florida, Gainesville, FL, USA

## OPEN ACCESS

### Edited by:

Keith Poole,  
Queen's University, Canada

### Reviewed by:

Veljo Kisand,  
University of Tartu, Estonia  
Giovanna Riccardi,  
University of Pavia, Italy

### \*Correspondence:

Herbert P. Schweizer,  
Department of Molecular Genetics  
and Microbiology, College  
of Medicine, Emerging Pathogens  
Institute, Institute for Therapeutic  
Innovation, University of Florida,  
Gainesville, FL 32610, USA  
hschweizer@ufl.edu

### †Present address:

Nicole L. Podneacky,  
Department of Pharmacy, Faculty  
of Health Sciences, UiT The Arctic  
University of Norway – Universitetet i  
Tromsø, 9037 Tromsø, Norway

### Specialty section:

This article was submitted to  
Antimicrobials, Resistance and  
Chemotherapy, a section of the  
journal Frontiers in Microbiology

Received: 10 February 2015

Paper pending published:  
06 March 2015

Accepted: 27 March 2015

Published: 14 April 2015

### Citation:

Podneacky NL, Rhodes KA and  
Schweizer HP (2015) Efflux  
pump-mediated drug resistance  
in *Burkholderia*.  
*Front. Microbiol.* 6:305.  
doi: 10.3389/fmicb.2015.00305

Several members of the genus *Burkholderia* are prominent pathogens. Infections caused by these bacteria are difficult to treat because of significant antibiotic resistance. Virtually all *Burkholderia* species are also resistant to polymyxin, prohibiting use of drugs like colistin that are available for treatment of infections caused by most other drug resistant Gram-negative bacteria. Despite clinical significance and antibiotic resistance of *Burkholderia* species, characterization of efflux pumps lags behind other non-enteric Gram-negative pathogens such as *Acinetobacter baumannii* and *Pseudomonas aeruginosa*. Although efflux pumps have been described in several *Burkholderia* species, they have been best studied in *Burkholderia cenocepacia* and *B. pseudomallei*. As in other non-enteric Gram-negatives, efflux pumps of the resistance nodulation cell division (RND) family are the clinically most significant efflux systems in these two species. Several efflux pumps were described in *B. cenocepacia*, which when expressed confer resistance to clinically significant antibiotics, including aminoglycosides, chloramphenicol, fluoroquinolones, and tetracyclines. Three RND pumps have been characterized in *B. pseudomallei*, two of which confer either intrinsic or acquired resistance to aminoglycosides, macrolides, chloramphenicol, fluoroquinolones, tetracyclines, trimethoprim, and in some instances trimethoprim+sulfamethoxazole. Several strains of the host-adapted *B. mallei*, a clone of *B. pseudomallei*, lack AmrAB-OprA, and are therefore aminoglycoside and macrolide susceptible. *B. thailandensis* is closely related to *B. pseudomallei*, but non-pathogenic to humans. Its pump repertoire and ensuing drug resistance profile parallels that of *B. pseudomallei*. An efflux pump in *B. vietnamiensis* plays a significant role in acquired aminoglycoside resistance. Summarily, efflux pumps are significant players in *Burkholderia* drug resistance.

**Keywords:** *Burkholderia*, antibiotics, resistance, efflux pump, adaptation

## The Genus *Burkholderia*

The genus *Burkholderia* comprises metabolically diverse and adaptable Gram-negative bacteria that are able to thrive in different, often adversarial, environments. Their metabolic versatility and adaptability is in part due to the coding capacity provided by large (7–9 Mb) genomes consisting of several chromosomes and in some species, e.g., *Burkholderia cenocepacia*, plasmids (Holden et al., 2004, 2009; Agnoli et al., 2012). Many members of the genus are clinically significant pathogens

with renowned virulence potential (Tegos et al., 2012) and drug resistance (Burns, 2007). In contrast to most other Gram-negative pathogens, *Burkholderia* species are intrinsically polymyxin resistant and therefore colistin cannot be used as drug of last resort (Loutet and Valvano, 2011). Despite clinical significance and recognized antibiotic resistance of *Burkholderia* species, characterization of efflux pumps lags significantly behind other non-enteric Gram-negative pathogens such as *Acinetobacter baumannii* and *Pseudomonas aeruginosa* (Nikaido and Pages, 2012). Many *Burkholderia* efflux systems have homologs in other Gram-negatives, including *A. baumannii* and *P. aeruginosa*, and it is now generally believed that the multidrug resistance exhibited by these opportunistic pathogens is largely attributable to the existence of similar efflux pumps in these organisms (Poole, 2001; McGowan, 2006). As with other Gram-negative bacteria, the relative roles that individual efflux pumps play in intrinsic or acquired antibiotic resistance in the respective *Burkholderia* species are in many instances difficult to discern for various reasons: (1) a subset of the pumps found in any organism usually exhibits a considerable degree of substrate promiscuity, i.e., they recognize and extrude chemically and structurally diverse compounds, which leads to similar multidrug resistance profiles; (2) many of the efflux systems are not expressed at significant levels in wild-type strains under laboratory conditions and there exists a significant knowledge gap regarding the environmental conditions under which efflux genes are expressed; and (3) well characterized clinical or laboratory isolates expressing or lacking the respective efflux pumps often do not exist or are difficult to obtain (Mima and Schweizer, 2010; Coenye et al., 2011; Biot et al., 2013; Buroni et al., 2014). In this review we will summarize the current state of knowledge of efflux pumps and their roles in antibiotic resistance in the genus *Burkholderia*, which have been characterized to various degrees in a few representative organisms.

### ***Burkholderia cepacia* Complex**

The *Burkholderia cepacia* complex (BCC) currently comprises 17 closely related species (Mahenthiralingam et al., 2005; Vanlaere et al., 2009; Vandamme and Dawyndt, 2011). Some BCC members exhibit beneficial aspects such as use in biocontrol, a practice that has since been abandoned because of the risk of infection of compromised individuals (Kang et al., 1998). Many are opportunistic pathogens, being particularly problematic for cystic fibrosis patients and immune compromised individuals. *B. cenocepacia* and *B. multivorans* account for 85% of all BCC infections (Drevinek and Mahenthiralingam, 2010). BCC infections are difficult to treat because of intrinsic antibiotic resistance and persistence in the presence of antimicrobials (Golini et al., 2004; Peeters et al., 2009; Rajendran et al., 2010; Jassem et al., 2011). *B. vietnamiensis* belongs to the BCC group and sporadically infects cystic fibrosis patients (Jassem et al., 2011).

### ***Burkholderia pseudomallei***

*Burkholderia pseudomallei* is a saprophyte and opportunistic pathogen endemic to tropical and subtropical regions of the world, and recent studies suggest that is more widespread than previously thought (Wiersinga et al., 2006, 2012, 2015; Currie

et al., 2010). Since the U.S. anthrax attacks in 2001 the bacterium has received increasing attention because of its biothreat potential (Cheng et al., 2005), a history dating back to its use with malicious intent in a Sherlock Holmes short story (Vora, 2002). In the U.S. it is a strictly regulated Tier 1 select agent, which must be handled in approved biosafety level 3 (BSL-3) laboratories. The bacterium is the etiologic agent of melioidosis, a difficult-to-treat multifaceted disease (Wiersinga et al., 2006, 2012). The disease affects at-risk patients, including those suffering from cystic fibrosis (Schulin and Steinmetz, 2001; Holland et al., 2002), non-cystic fibrosis bronchiectasis (Price et al., 2013), and diabetes (Simpson et al., 2003). *B. pseudomallei* infections are recalcitrant to antibiotic therapy because of the bacterium's intrinsic resistance due to expression of resistance determinants such as  $\beta$ -lactamase and efflux pumps, as well as contributing factors such as both intracellular and biofilm lifestyles (Schweizer, 2012b).

### ***Burkholderia mallei***

*Burkholderia mallei* is an obligate zoonotic pathogen and the etiologic agent of glanders, which has been used as a bioweapon (Cheng et al., 2005; Whitlock et al., 2007). This bacterium likely diverged from *B. pseudomallei* upon introduction into an animal host approximately 3.5 million years ago (Losada et al., 2010; Song et al., 2010). The ensuing in-host evolution through massive expansion of insertion (IS) elements, IS-mediated gene deletion, and genome rearrangement, and prophage elimination is likely also responsible for the generally increased antibiotic susceptibility of *B. mallei* when compared to *B. pseudomallei*, presumably due to inactivation of resistance determinants (Nierman et al., 2004).

### ***Burkholderia thailandensis***

*Burkholderia thailandensis* is closely related to *B. pseudomallei* (Brett et al., 1998). Although *B. thailandensis* has sporadically been shown to cause human disease (Glass et al., 2006), it is generally considered non-pathogenic and has often been used as a surrogate for antimicrobial compound and vaccine efficacy studies because the bacterium can be handled at BSL-2. Some strains are more closely related to *B. pseudomallei* than others. For instance, unlike the widely used *B. thailandensis* prototype strain E264 (Brett et al., 1998), strain E555 expresses the same capsular polysaccharide as *B. pseudomallei* (Sim et al., 2010). Since capsular polysaccharide is a potent immunogen this similarity was exploited in a vaccine study, which showed that immunization with live cells of this avirulent strain protects mice from challenge with a virulent *B. pseudomallei* strain (Scott et al., 2013).

### ***Burkholderia cenocepacia***

#### **Efflux Pumps and Drug Resistance**

Early reports provided mostly indirect evidence that *B. cenocepacia* efflux pumps play a role in drug efflux. The synergy between reduced outer membrane permeability and efflux was cited as a common theme of the increased resistance that non-fermenting Gram-negative bacteria like *A. baumannii*, *P. aeruginosa*, and *B. (ceno)cepacia* display (Hancock, 1998). An analysis

of the DsbA–DsbB disulfide bond formation system revealed that *dsbA* and *dsbB* mutation resulted increased susceptibilities to a variety of antibiotics (Hayashi et al., 2000). This led to the conclusion that the DsbA–DsbB system might be involved in the formation of a multidrug resistance system. Another early report described an outer membrane lipoprotein involved in multiple antibiotic (chloramphenicol, trimethoprim, and ciprofloxacin) resistance (Burns et al., 1996). This protein, OpcM, is the outer membrane channel of an efflux pump of the resistance nodulation cell division (RND) family that was subsequently named CeoAB-OpcM, which was shown to be inducible by salicylate and chloramphenicol (Nair et al., 2004). Efflux was also shown early on to play a role in fluoroquinolone resistance (Zhang et al., 2001).

Genome analysis and homology searches led to identification of an additional 14 open reading frames encoding putative components RND family efflux pumps (Guglierame et al., 2006). A summary of pertinent features of at least partially characterized *B. cenocepacia* RND efflux pumps and their relationships to RND systems in other *Burkholderia* species is presented in **Table 1**.

Expression of one of these, *orf2*, in *Escherichia coli* conferred resistance to several antibiotics (Guglierame et al., 2006). The roles of several RND transporters – RND-1, RND-3, and RND-4 – in intrinsic *B. cenocepacia* drug resistance was subsequently assessed by mutational analyses, which showed that RND-3 and RND-4, but not RND-1, contribute to *B. cenocepacia*'s intrinsic resistance to antibiotics and other inhibitory compounds (Buroni et al., 2009). A subsequent study comparing RND-4 and RND-9 single and double mutants confirmed the role that RND-4 plays in *B. cenocepacia*'s antibiotic resistance and also showed that RND-9 contributed only marginally to resistance (Bazzini et al., 2011b). Completion of the strain J2315 genome sequence showed that it encodes 16 RND efflux systems, which provides evidence for the biological relevance of these transporters in this bacterium and also enables global analyses of RND pump expression (Holden et al., 2009; Perrin et al., 2010; Bazzini et al., 2011a; Buroni et al., 2014). For example, deletion of the 16 putative RND operons from *B. cenocepacia* strain J2315 showed that these pumps play differential roles in the drug resistance of sessile (biofilm) and planktonic cells. These studies revealed that: (1)

**TABLE 1 | Partially characterized resistance nodulation cell division (RND) efflux pumps in *Burkholderia* species.**

| Species                         | Efflux pump | Gene names                     | Gene annotation             | Major substrates  | Reference  |
|---------------------------------|-------------|--------------------------------|-----------------------------|---|--|
| <i>Burkholderia cenocepacia</i> |             |                                |                             |   |  |
|                                 | RND-1       | NA                             | BCAS0591–BCAS0593           | Non-detectable  | Buroni et al. (2009)                             |
|                                 | RND-3       | NA <sup>1</sup>                | BCAL1674–BCAL1676           | Nalidixic acid, ciprofloxacin, tobramycin, chlorhexidine <sup>3</sup>           | Buroni et al. (2009, 2014), Coenye et al. (2011) |
|                                 | RND-4       | NA <sup>2</sup>                | BCAL2820–BCAL2822           | Aztreonam, chloramphenicol, fluoroquinolones, tobramycin                        | Bazzini et al. (2011b)                           |
|                                 | RND-8       | NA                             | BCAM0925–BCAM0927           | Tobramycin <sup>3</sup>   | Buroni et al. (2014)                             |
|                                 | RND-9       | NA                             | BCAM1945–BCAM1947           | Tobramycin <sup>3</sup> , chlorhexidine <sup>3</sup>                            | Coenye et al. (2011), Buroni et al. (2014)       |
|                                 | RND-10      | <i>ceoAB-opcM</i> <sup>4</sup> | BCAM2551–BCAM2549           | Chloramphenicol, fluoroquinolones, trimethoprim                                 | Nair et al. (2004)                               |
| <i>B. pseudomallei</i>          |             |                                |                             |   |  |
|                                 | AmrAB-OprA  | <i>amrAB oprA</i>              | BPSL1804–BPSL1802           | Aminoglycosides, macrolides, cethromycin  | Moore et al. (1999), Mima et al. (2011)          |
|                                 | BpeAB-OprB  | <i>bpeAB oprB</i>              | BPSL0814–BPSL0816           | Chloramphenical, fluoroquinolones, macrolides, tetracyclines <sup>5</sup>       | Chan et al. (2004), Mima and Schweizer (2010)    |
|                                 | BpeEF-OprC  | <i>bpeEF oprC</i>              | BPSS0292–BPSS0294           | Chloramphenical, fluoroquinolones, tetracyclines, trimethoprim <sup>6</sup>     | Kumar et al. (2006), Schweizer (2012a,b)         |
| <i>B. thailandensis</i>         |             |                                |                             |   |  |
|                                 | AmrAB-OprA  | <i>amrAB oprA</i>              | BTH_I2445–BTH_I2443         | Aminoglycosides, macrolides, tetracyclines                                      | Biot et al. (2013)                               |
|                                 | BpeAB-OprB  | <i>bpeAB oprB</i>              | BTH_I0680–BTH_I0682         | Tetracyclines   | Biot et al. (2013)                               |
|                                 | BpeEF-OprC  | <i>bpeEF oprC</i>              | BTH_I2106–BTH_I2104         | Chloramphenical, fluoroquinolones, tetracyclines, trimethoprim/sulfamethoxazole | Biot et al. (2011, 2013)                         |
| <i>B. vietnamiensis</i>         |             |                                |                             |   |  |
|                                 | AmrAB-OprM  | <i>amrAB oprM</i>              | Bcep1808_1574–Bcep1808_1576 | Aminoglycosides   | Jassem et al. (2014)                             |

NA, not applicable

<sup>1</sup>Corresponds to *B. pseudomallei amrAB oprA*

<sup>2</sup>Corresponds to *B. pseudomallei bpeAB oprB*

<sup>3</sup>Sessile (biofilm grown) cells only

<sup>4</sup>Corresponds to *B. pseudomallei bpeEF oprC*

<sup>5</sup>Low-level resistance in de-repressed ( $\Delta bpeR$ ) strains

<sup>6</sup>High-level resistance in regulatory mutants, e.g., *bpeT* carboxy-terminal mutations

RND-3 and RND-4 play important roles in resistance to various antibiotics, including ciprofloxacin and tobramycin, in planktonic populations; (2) RND-3, RND-8, and RND-9 protect from the antimicrobial effects of tobramycin in biofilm cells; and (3) RND-8 and RND-9 do not play a role in ciprofloxacin resistance (Buroni et al., 2014). An emerging theme from these studies is that RND-3 seems to play a major role in *B. cenocepacia*'s intrinsic drug resistance. It was suggested that mutations in the RND-3 regulator-encoding gene may be responsible for this pump's prevalent overexpression and accompanying high-level antibiotic resistance in clinical BCC isolates (Tseng et al., 2014).

Studies aimed at assessing chlorhexidine mechanisms in *B. cenocepacia* J2315 confirmed the differential roles that RND pumps play in biofilm versus planktonically grown cells. RND-4 contributed to chlorhexidine resistance in planktonic cells, whereas RND-3 and RND-9 played a role in chlorhexidine resistance in sessile cells (Coenye et al., 2011). Mutational analyses of 2-thiopyridine resistant mutants showed that RND-4 confers resistance to an anti-tubercular 2-thiopyridine derivative (Scoffone et al., 2014). The involvement of efflux pumps in tigecycline resistance was inferred from the potentiating effects of the efflux pump inhibitor (EPI) MC-207,110 on tigecycline's anti-*B. cenocepacia* activity (Rajendran et al., 2010).

Efflux pumps belonging to other families may also contribute to *B. cenocepacia*'s drug resistance. Experiments with an immunodominant antigen in cystic fibrosis patients infected with *B. cenocepacia* identified a drug efflux pump, BcrA, which is a member of the major facilitator superfamily (MFS). It was shown to confer tetracycline and nalidixic acid resistance when expressed in *E. coli* (Wigfield et al., 2002). Upregulation of an efflux pump resulted in resistance to the phosphonic acid antibiotic fosfomycin (Messiaen et al., 2011). This pump is a homolog of Fsr, a member of the MFS, which was previously shown to confer fosfomycin resistance on *E. coli* (Fujisaki et al., 1996; Nishino and Yamaguchi, 2001).

## Other Functions of *B. cenocepacia* RND Efflux Pumps

As with other Gram-negative bacteria, the function of *B. cenocepacia* efflux pumps extends beyond antibiotic resistance. In *B. cenocepacia*, these systems are involved in modulation of virulence-associated traits such as quorum sensing, biofilm formation, chemotaxis, and motility, as well as general physiological functions (Buroni et al., 2009; Bazzini et al., 2011a,b). A proteomic analysis of the effects of RND-4 gene deletion revealed about 70 differentially expressed proteins, most of which were associated with cellular functions other than drug resistance. This suggests that RND-4 plays a more general role in *B. cenocepacia*'s biology (Gamberi et al., 2013). Aside from the key role that efflux, especially RND-mediated efflux, plays in adaptation to antibiotic exposure (Bazzini et al., 2011b; Sass et al., 2011; Tseng et al., 2014), survival of *Burkholderia* species in various niche environments and accompanying conditions, e.g., the cystic fibrosis airways (Mira et al., 2011), marine habitats (Maravic et al., 2012), oxygen levels (Hemsley et al., 2014), exposure to noxious chemicals (Rushton et al., 2013), and other ecological niches (Liu et al.,

2015), involves to various degrees changes in efflux pump expression.

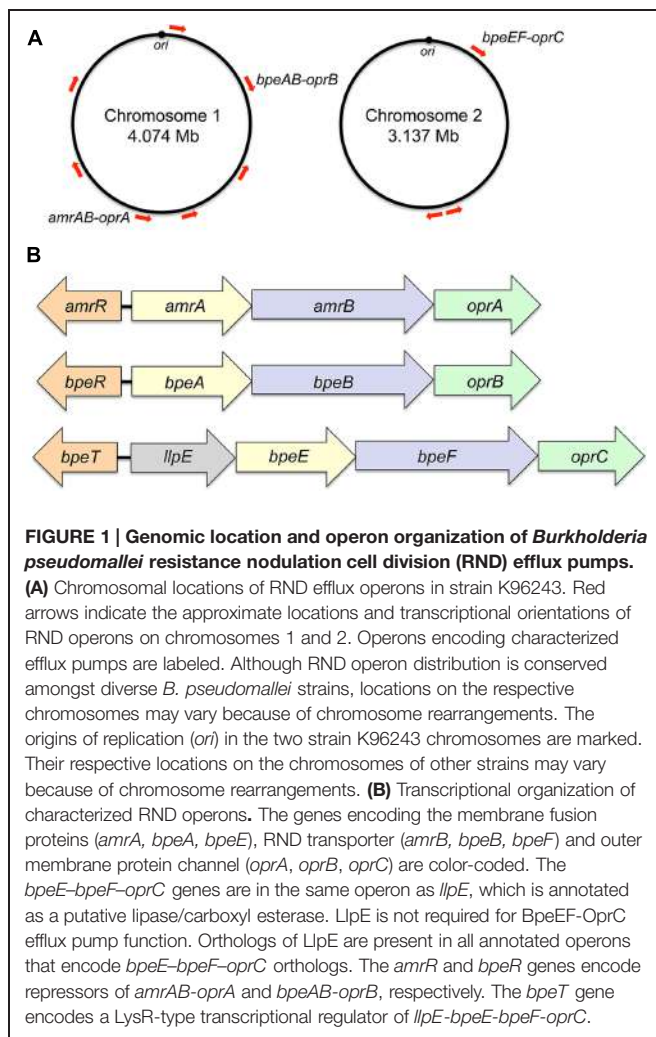
## *Burkholderia pseudomallei*

### Efflux Pumps and Drug Resistance

Initially, the presence of genomic DNA sequences in *B. pseudomallei* that hybridize with the multidrug resistance efflux gene *oprM* of *P. aeruginosa* was interpreted as evidence that efflux-mediated multidrug efflux systems may also be present in *B. pseudomallei* (Bianco et al., 1997). A recent survey of documented *B. pseudomallei* antibiotic resistance mechanisms indeed showed that efflux is the dominant mechanism affecting most classes of antibiotics (Schweizer, 2012b). Sequenced *B. pseudomallei* genomes encode numerous efflux systems, but as with other non-enteric bacteria only RND pumps have to date been shown to confer resistance to clinically significantly antibiotics. The K96243 and other *B. pseudomallei* genomes encode at least 10 RND systems, seven of which are encoded by chromosome 1 and three by chromosome 2 (Holden et al., 2004; **Figure 1A**). Although RND operon distribution is conserved amongst diverse *B. pseudomallei* strains, locations on the respective chromosomes may vary because of chromosome rearrangements. Bioinformatic analyses indicate that not all of the RND operons encode drug efflux pumps. For instance, one system seems to encode components of a general secretion (Sec) system. Although the presence of many RND systems can be detected in clinical and environmental isolates at the transcriptional (Kumar et al., 2008) and protein level (Schell et al., 2011), this expression is not necessarily linked to increased drug resistance. Meaningful studies to address their function are complicated because isogenic progenitor and/or comparator strains are generally not available. Further hindering efflux pump characterization are select agent guidelines, which restrict certain methods, such as selection of spontaneous drug resistant mutants that may display altered efflux expression profiles. These investigations are now facilitated by the availability of several *B. pseudomallei* strains, for instance Bp82 (Propst et al., 2010), which are excluded from select agent rulings. To date three RND drug efflux pumps – AmrAB-OprA, BpeAB-OprB, and BpeEF-OprC – have been characterized in some detail (**Figure 1B**). There is evidence that small molecule compounds such as MC-207,110, phenothiazine antipsychotics, and antihistaminic drugs like promazine can be used to potentiate antibiotic efficacy, primarily by inhibition of RND efflux pumps (Chan et al., 2007b).

### AmrAB-OprA

The AmrAB-OprA efflux pump was the first efflux pump described in *B. pseudomallei* (Moore et al., 1999). It is responsible for this organism's high-level intrinsic aminoglycoside and macrolide resistance (Moore et al., 1999; Viktorov et al., 2008). Rare (~1 in 1,000) naturally occurring aminoglycoside susceptible *B. pseudomallei* isolates have previously been identified (Trunck et al., 2009; Podin et al., 2014). They do not



express the AmrAB-OprA pump either due to regulatory mutations (Trunck et al., 2009), point mutations affecting the AmrB RND transporter amino acid sequence (Podin et al., 2014), or because the entire *amrAB oprM* operon is missing due to a genomic deletion (Trunck et al., 2009). Although the AmrAB-OprA efflux pump is expressed in prototype strains, exposure to antimicrobials can select for unknown mutations that cause its over-expression resulting in increased resistance. For instance, prototype strain 1026b is moderately susceptible [minimal inhibitory concentration (MIC) 4–8 µg/mL] to the ketolide cethromycin and exposure to this compound readily selects for highly resistant (MIC > 128 µg/mL) derivatives due to AmrAB-OprA over-expression (Mima et al., 2011). To date, AmrAB-OprA expression is the sole reported aminoglycoside and macrolide resistance mechanism observed in *B. pseudomallei*.

AmrAB is closely related to *P. aeruginosa* MexXY, which is expressed in some aminoglycoside resistant mutants and together with OprM constitutes a functional efflux pump (Mine et al., 1999; Sobel et al., 2003; Morita et al., 2012). MexXY associates with the *mexAB oprM* encoded OprM outer channel protein because the

*mexXY* operons of most *P. aeruginosa* strains do not encode a cognate outer membrane channel protein. However, some strains, e.g., *P. aeruginosa* PA7, encode a *mexAB oprA* operon akin and functionally equivalent to *B. pseudomallei amrAB oprA* (Morita et al., 2012).

### BpeAB-OprB

The BpeAB-OprB efflux pump was first described in strain KHW from Singapore (Chan et al., 2004) and subsequently characterized in Thai strain 1026b (Mima and Schweizer, 2010). It is not significantly expressed in wild-type strains. BpeAB-OprB expression is regulated by BpeR and *bpeR* mutants exhibit low-level chloramphenicol, fluoroquinolone, tetracycline, and macrolide resistance (Chan et al., 2004; Chan and Chua, 2005; Mima and Schweizer, 2010). Although the original studies with strain KHW indicated a role of BpeAB-OprB in aminoglycoside resistance (Chan et al., 2004), these results could not be confirmed with strain 1026b (Mima and Schweizer, 2010). At present, the observed differences in BpeAB-OprB substrate spectrum between strains KHW and 1026b are not understood. Because of the low levels of resistance bestowed by BpeAB-OprB and naturally occurring antibiotic resistant BpeAB-OprB over-expressing mutants have yet to be identified, the clinical significance of this pump remains unclear.

Although BpeAB-OprB is related to *P. aeruginosa* MexAB-OprM (Poole et al., 1993; Li et al., 1995; Mima and Schweizer, 2010), the respective features are quite divergent. While *P. aeruginosa* MexAB-OprM is widely expressed and responsible for this bacterium's intrinsic resistance to numerous antibacterial compounds (Poole et al., 1993; Li et al., 1995; Poole, 2001), *B. pseudomallei* BpeAB-OprB is not widely expressed and does seem to play only a minor role in this bacterium's resistance to antimicrobials.

### BpeEF-OprC

BpeEF-OprC was first identified as a chloramphenicol and trimethoprim efflux pump by expression in an efflux-compromised *P. aeruginosa* strain (Kumar et al., 2006). This pump is not expressed in *B. pseudomallei* wild-type strains, but only regulatory mutants. For instance, it is constitutively expressed in naturally occurring *bpeT* mutants (Hayden et al., 2012; Figure 2). When expressed, BpeEF-OprC confers high-level resistance to chloramphenicol, fluoroquinolones, tetracyclines, and trimethoprim. It is responsible for widespread trimethoprim resistance in clinical and environmental *B. pseudomallei* isolates (Podnecky et al., 2013). Pump expression is inducible by some pump substrates, which when present at sub MIC levels may lead to cross-resistance with other pump substrates (Schweizer, 2012a).

BpeEF-OprC is related to *P. aeruginosa* MexEF-OprN (Koehler et al., 1997), which shares properties such as substrate profiles and selection of pump-expressing regulatory mutants by chloramphenicol as previously demonstrated with both *P. aeruginosa* MexEF-OprN (Koehler et al., 1997) and *B. thailandensis* BpeEF-OprC (Biot et al., 2011).

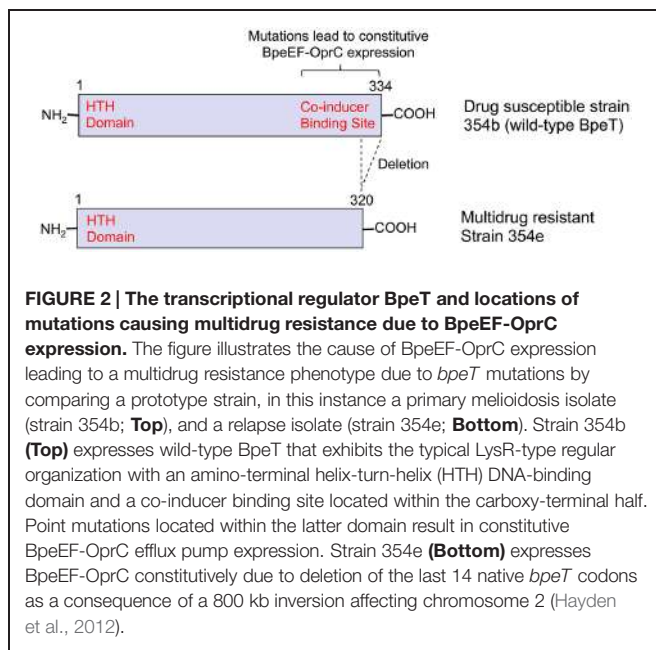


**FIGURE 2 |** The transcriptional regulator BpeT and locations of mutations causing multidrug resistance due to BpeEF-OprC expression.

**expression.** The figure illustrates the cause of BpeEF-OprC expression leading to a multidrug resistance phenotype due to *bpeT* mutations by comparing a prototype strain, in this instance a primary melioidosis isolate (strain 354b; **Top**), and a relapse isolate (strain 354e; **Bottom**). Strain 354b (**Top**) expresses wild-type BpeT that exhibits the typical LysR-type regular organization with an amino-terminal helix-turn-helix (HTH) DNA-binding domain and a co-inducer binding site located within the carboxy-terminal half. Point mutations located within the latter domain result in constitutive BpeEF-OprC efflux pump expression. Strain 354e (**Bottom**) expresses BpeEF-OprC constitutively due to deletion of the last 14 native *bpeT* codons as a consequence of a 800 kb inversion affecting chromosome 2 (Hayden et al., 2012).

## Other Functions of *B. pseudomallei* Efflux Pumps

Quorum sensing is an important determinant of virulence factor regulation in bacteria. Numerous studies with *P. aeruginosa* indicate the involvement of several RND pumps in quorum sensing and thus several virulence traits by being involved in transport of cell-to-cell signaling molecules and their inhibitors (Evans et al., 1998; Pearson et al., 1999; Koehler et al., 2001; Aendekerk et al., 2005; Hirakata et al., 2009; Tian et al., 2009). At least one efflux pump regulator, MexT, modulates expression of virulence factors, albeit independent of the function of the MexEF-OprN efflux pump whose expression it regulates (Tian et al., 2009). A *P. aeruginosa* MexAB-OprM deletion strain is also compromised in its ability to invade Madin–Darby canine kidney (MDCK) cells (Hirakata et al., 2009). Based on these findings with *P. aeruginosa*, several studies with *B. pseudomallei* explored the effects of efflux on quorum sensing and virulence. Studies with strain KHW showed that the BpeAB-OprB efflux pump was required: (1) for the secretion of the acyl homoserine lactones produced by this strain's quorum-sensing systems (Chan et al., 2007a); and (2) secretion of several virulence-associated determinants, including siderophore and biofilm formation (Chan and Chua, 2005), but these observations could not be confirmed with strain 1026b (Mima and Schweizer, 2010). Cell invasion of and cytotoxicity toward human A549 lung epithelial and THP-1 macrophage cell lines were significantly reduced in a KHW BpeAB-deficient strain (Chan and Chua, 2005). Adherence to A549 cells and virulence in the BALB/c mouse intranasal infection model were not affected in the AmrAB-OprA deficient Bp340 mutant, a derivative of strain 1026b (Campos et al., 2013). BALB/c mouse intranasal infection studies also showed that in addition to AmrAB-OprA, BpeAB-OprB, and BpeEF-OprC were not required for virulence (Propst, 2011; Schweizer, 2012a). The AmrAB-OprA efflux pump is also not required for efficient killing of *Caenorhabditis elegans* by *B. pseudomallei* (O'Quinn et al., 2001). The BpeAB-OprB pump has been implicated in being involved in spermidine homeostasis in strain KHW with exogenous spermidine and N-acetylspermidine activating *bpeA* transcription (Chan and Chua, 2010).

*elegans* by *B. pseudomallei* (O'Quinn et al., 2001). The BpeAB-OprB pump has been implicated in being involved in spermidine homeostasis in strain KHW with exogenous spermidine and N-acetylspermidine activating *bpeA* transcription (Chan and Chua, 2010).

## Efflux Pumps in other *Burkholderia* Species

### *Burkholderia mallei*

In part due to ongoing host evolution of this obligate pathogen, *B. mallei* is generally more susceptible to antimicrobials than its progenitor *B. pseudomallei*. For instance, many *B. mallei* strains are susceptible to aminoglycosides. In the ATCC 23344 prototype strain this susceptibility results from a 50 kb chromosomal deletion encompassing the *amrAB-oprA* operon (Nierman et al., 2004). Strains NCTC10229 and NCTC10247 are likely aminoglycoside susceptible because only remnants of the *amrAB-oprA* operon are present (Winsor et al., 2008). Genes and operons encoding other efflux pumps, including BpeAB-OprB and BpeEF-OprC, are present but whether they encode functional efflux systems remains to be established.

### *Burkholderia thailandensis*

One study indicated the presence of an MFS efflux pump, with an associated regulatory protein of the multiple antibiotic resistance regulator (MarR) family (Grove, 2010). However, expression of the efflux pump was only responsive to urate, xanthine, and hypoxanthine and thus the significance of this transporter in *B. thailandensis*' antibiotic resistance, if any, is unclear.

In contrast, the contributions of RND pumps to this bacterium's antibiotic resistance have been established. It was shown that chloramphenicol exposure selects for expression of an RND efflux pump, BpeEF-OprC, that also extrudes fluoroquinolones, tetracycline, and trimethoprim (Biot et al., 2011). Doxycycline selection resulted in mutants that either over-expressed AmrAB-OprA or BpeEF-OprC, and exhibited the multidrug resistance profiles associated with expression of these efflux pumps (Biot et al., 2013). Mutational analysis of these mutants suggested that BpeAB-OprB could at least partially substitute for absence of either AmrAB-OprA or BpeEF-OprC. Unlike other Gram-negative bacteria, cell envelope properties, efflux pump repertoire, and resulting drug resistance profile make *B. thailandensis* suitable as a *B. pseudomallei* BSL-2 surrogate for drug efficacy studies (Schweizer, 2012c).

### *Burkholderia vietnamiensis*

Transposon mutagenesis studies aimed at identification of polymyxin B susceptible mutants identified a gene encoding a NorM multidrug efflux protein (Fehlner-Gardiner and Valvano, 2002). While *norM* expression in an *E. coli* *acrAB* deletion mutant complemented its norfloxacin susceptibility, its inactivation in *B. vietnamiensis* only affected susceptibility to polymyxin but not other antibiotics.

Unlike other *Burkholderia* species, including most BCC members, the majority of environmental and clinical *B. vietnamensis* isolates are aminoglycoside susceptible (Jassem et al., 2011). Aminoglycoside resistance as a result of chronic infection or *in vitro* exposure to aminoglycosides is the result of the AmrAB-OprM efflux pump, which is most likely a homolog of *B. pseudomallei* and *B. thailandensis* AmrAB-OprA (Jassem et al., 2011, 2014). Of note is the observation that efflux pump expression in mutants that acquired resistance during infection was due to missense mutations in the *amrAB-oprM* regulator *amrR*, but not those mutants derived from antibiotic pressure *in vivo* (Jassem et al., 2014).

## Burkholderia Efflux Pump Mutants as Experimental Tools

The high-level intrinsic antibiotic resistance of many *Burkholderia* species complicates their genetic manipulation, use in studies of intracellular bacteria with the aminoglycoside protection assay, and drug efficacy studies. It has been shown that efflux-compromised mutants of *B. cenocepacia* and *B. pseudomallei* greatly facilitate genetic manipulation of these species, as well as cell invasion studies using the aminoglycoside protection assay (Dubarry et al., 2010; Hamad et al., 2010; Campos et al., 2013). Efflux-compromised strains of *B. thailandensis* and *B. pseudomallei* strains have also proved useful for study of the efflux propensity of novel antimicrobial compounds (Liu et al., 2011; Mima et al., 2011; Teng et al., 2013; Cummings et al., 2014).

## Conclusion

*Burkholderia* species are well adapted to life in diverse, often adversarial, environments including those containing antimicrobials. This adaptation is facilitated by large genomes that bestow on the bacteria the ability to either degrade or expel noxious chemicals. As a result, opportunistic infections by pathogenic members of this species are difficult to treat because of intrinsic antibiotic resistance and persistence in the presence of antimicrobials. Resistance is in large part attributable to efflux pump expression, mostly members of the RND family. While the last decade has seen significant progress in study of drug efflux in *Burkholderia* species, progress still lags significantly behind other opportunistic pathogens, e.g., *P. aeruginosa* and *A. baumannii*, where efflux pumps also play significant roles in intrinsic and acquired drug resistance.

There are some unique aspects of efflux systems in *Burkholderia* species that are without parallel and studies of these

may shed light on unique physiological functions of efflux pumps in these organisms. For instance, the first gene in the *bpeEF-oprC* operon, *llpE*, is co-transcribed with the genes encoding the BpeEF-OprC efflux pump components (Nair et al., 2004, 2005). Its deletion neither affects efflux pump function nor specificity for known antibiotic substrates. It is highly conserved throughout the *Burkholderia* genus and found in all sequenced genomes (Winsor et al., 2008). Based on homology, LlpE probably is an enzyme of the alpha/beta hydrolase family, recently annotated as a putative lipase/carboxyl esterase, and its conservation throughout the genus suggests an adaptation or survival benefit in a niche environment. The unique association of this enzyme with BpeEF-OprC and its role in *Burkholderia* biology warrant further studies of this enzyme.

When reviewing the *B. cenocepacia* efflux pump literature it becomes evident that efflux pump nomenclature in this species, especially that of the RND family is non-uniform and confusing (for instance CeoAB-OpcM, RND-1 to RND-16, BCA gene names, Mex1, orf, etc.), which makes comparisons with other Gram-negative bacteria unnecessarily cumbersome. As with other Gram-negative bacteria, the nomenclature initiated in *B. cenocepacia* by Dr. Jane Burns' laboratory in the early 2000s, i.e., CeoAB-OpcM (Nair et al., 2004), would make the most sense and it is a pity that it was not followed in subsequent studies.

## Author Contributions

NP, KR, and HS contributed to all aspects of the work, including, but not limited to, conception and design, acquisition and analysis of data, writing the manuscript, and final approval of the version to be published.

## Acknowledgments

The authors acknowledge the contributions of several talented graduate students (Katie Propst, Kyoung-Hee Choi, Lily Trunk, Carolina Lopez) and postdocs (Takeshi Mima, Ayush Kumar, Nawarat Somprasong) to efflux pump research performed in the Schweizer laboratory. We acknowledge Dr. Hillary Hayden from the University of Washington for providing sequence information on *B. pseudomallei* strains 354b and 354e. Work in the HPS laboratory was supported by grant AI065357 from the National Institute of Allergy and Infectious Diseases, National Institutes of Health, and contract HDTRA1-08-C-0049 from the United States Defense Threat Reduction Agency.

## References

- Aendekerk, S., Diggle, S. P., Song, Z., Hoiby, N., Cornelis, P., Williams, P., et al. (2005). The MexGHI-OpmD multidrug efflux pump controls growth, antibiotic susceptibility and virulence in *Pseudomonas aeruginosa* via 4-quinolone-dependent cell-to-cell communication. *Microbiology* 151, 1113–1125. doi: 10.1099/mic.0.27631-0
- Agnoli, K., Schwager, S., Uehlinger, S., Vergunst, A., Viteri, D. F., Nguyen, D. T., et al. (2012). Exposing the third chromosome of *Burkholderia cepacia* complex strains as a virulence plasmid. *Mol. Microbiol.* 83, 362–378. doi: 10.1111/j.1365-2958.2011.07937.x
- Bazzini, S., Udine, C., and Riccardi, G. (2011a). Molecular approaches to pathogenesis study of *Burkholderia cenocepacia*, an important cystic fibrosis opportunistic bacterium. *Appl. Microbiol. Biotechnol.* 92, 887–895. doi: 10.1007/s00253-011-3616-5

- Bazzini, S., Udine, C., Sass, A., Pasca, M. R., Longo, F., Emiliani, G., et al. (2011b). Deciphering the role of RND efflux transporters in *Burkholderia cenocepacia*. *PLoS ONE* 6:e18902. doi: 10.1371/journal.pone.0018902
- Bianco, N., Neshat, S., and Poole, K. (1997). Conservation of the multidrug resistance efflux gene oprM in *Pseudomonas aeruginosa*. *Antimicrob. Agents Chemother.* 41, 853–856.
- Biot, F. V., Lopez, M. M., Poyot, T., Neulat-Ripoll, F., Lignon, S., Caclard, A., et al. (2013). Interplay between three RND efflux pumps in doxycycline-selected strains of *Burkholderia thailandensis*. *PLoS ONE* 8:e84068. doi: 10.1371/journal.pone.0084068
- Biot, F. V., Valade, E., Garnotel, E., Chevalier, J., Villard, C., Thibault, F. M., et al. (2011). Involvement of the efflux pumps in chloramphenicol selected strains of *Burkholderia thailandensis*: proteomic and mechanistic evidence. *PLoS ONE* 6:e16892. doi: 10.1371/journal.pone.0016892
- Brett, P. J., Deshazer, D., and Woods, D. E. (1998). *Burkholderia thailandensis* sp. nov., a *Burkholderia pseudomallei*-like species. *Int. J. Syst. Bacteriol.* 48, 317–320. doi: 10.1099/00207713-48-1-317
- Burns, J. (2007). “Antibiotic resistance of *Burkholderia* spp.”, in *Burkholderia Molecular Microbiology and Genomics*, eds T. Coenye and P. Vandamme (Norfolk: Horizon Bioscience), 81–91.
- Burns, J. L., Wadsworth, C. D., Barry, J. J., and Goodall, C. P. (1996). Nucleotide sequence analysis of a gene from *Burkholderia (Pseudomonas) cepacia* encoding an outer membrane lipoprotein involved in multiple antibiotic resistance. *Antimicrob. Agents Chemother.* 40, 307–313.
- Buroni, S., Matthijs, N., Spadaro, F., Van Acker, H., Scuffone, V. C., Pasca, M. R., et al. (2014). Differential roles of RND efflux pumps in antimicrobial drug resistance of sessile and planktonic *Burkholderia cenocepacia* cells. *Antimicrob. Agents Chemother.* 58, 7424–7429. doi: 10.1128/AAC.03800-14
- Buroni, S., Pasca, M. R., Flannagan, R. S., Bazzini, S., Milano, A., Bertani, I., et al. (2009). Assessment of three Resistance-Nodulation-Cell Division drug efflux transporters of *Burkholderia cenocepacia* in intrinsic antibiotic resistance. *BMC Microbiol.* 9:200. doi: 10.1186/1471-2180-9-200
- Campos, C. G., Borst, L., and Cotter, P. A. (2013). Characterization of BcaA, a putative classical autotransporter protein in *Burkholderia pseudomallei*. *Infect. Immun.* 81, 1121–1128. doi: 10.1128/IAI.01453-12
- Chan, Y. Y., Bian, H. S., Tan, T. M., Mattmann, M. E., Geske, G. D., Igarashi, J., et al. (2007a). Control of quorum sensing by a *Burkholderia pseudomallei* multidrug efflux pump. *J. Bacteriol.* 189, 4320–4324. doi: 10.1128/JB.0003-07
- Chan, Y. Y., Ong, Y. M., and Chua, K. L. (2007b). Synergistic interaction between phenothiazines and antimicrobial agents against *Burkholderia pseudomallei*. *Antimicrob. Agents Chemother.* 51, 623–630. doi: 10.1128/AAC.0033-06
- Chan, Y. Y., and Chua, K. L. (2005). The *Burkholderia pseudomallei* BpeAB-OprB efflux pump: expression and impact on quorum sensing and virulence. *J. Bacteriol.* 187, 4707–4719. doi: 10.1128/JB.187.14.4707-4719.2005
- Chan, Y. Y., and Chua, K. L. (2010). Growth-related changes in intracellular spermidine and its effect on efflux pump expression and quorum sensing in *Burkholderia pseudomallei*. *Microbiology* 156, 1144–1154. doi: 10.1099/mic.0.032888-0
- Chan, Y. Y., Tan, T. M. C., Ong, Y. M., and Chua, K. L. (2004). BpeAB-OprB, a multidrug efflux pump in *Burkholderia pseudomallei*. *Antimicrob. Agents Chemother.* 48, 1128–1135. doi: 10.1128/AAC.48.4.1128-1135.2004
- Cheng, A. C., Dance, D. A., and Currie, B. J. (2005). Bioterrorism, glanders and melioidosis. *Euro. Surveill.* 10, E1–E2; author reply E1–E2.
- Coenye, T., Van Acker, H., Peeters, E., Sass, A., Buroni, S., Riccardi, G., et al. (2011). Molecular mechanisms of chlorhexidine tolerance in *Burkholderia cenocepacia* biofilms. *Antimicrob. Agents Chemother.* 55, 1912–1919. doi: 10.1128/AAC.01571-10
- Cummings, J. E., Beaupre, A. J., Knudson, S. E., Liu, N., Yu, W., Neckles, C., et al. (2014). Substituted diphenyl ethers as a novel chemotherapeutic platform against *Burkholderia pseudomallei*. *Antimicrob. Agents Chemother.* 58, 1646–1651. doi: 10.1128/AAC.02296-13
- Currie, B. J., Ward, L., and Cheng, A. C. (2010). The epidemiology and clinical spectrum of melioidosis: 540 cases from the 20 year Darwin prospective study. *PLoS Negl. Trop. Dis.* 4:e900. doi: 10.1371/journal.ptnd.0000900
- Drevinek, P., and Mahenthiralingam, E. (2010). *Burkholderia cenocepacia* in cystic fibrosis: epidemiology and molecular mechanisms of virulence. *Clin. Microbiol. Infect.* 16, 821–830. doi: 10.1111/j.1469-0691.2010.03237.x
- Dubarry, N., Du, W., Lane, D., and Pasta, F. (2010). Improved electrotransformation and decreased antibiotic resistance of the cystic fibrosis pathogen *Burkholderia cenocepacia* strain J2315. *Appl. Environ. Microbiol.* 76, 1095–1102. doi: 10.1128/AEM.02123-09
- Evans, K., Passador, L., Srikanth, R., Tsang, E., Nezezon, J., and Poole, K. (1998). Influence of the MexAB-OprM multidrug efflux system on quorum sensing in *Pseudomonas aeruginosa*. *J. Bacteriol.* 180, 5443–5447.
- Fehlner-Gardiner, C. C., and Valvano, M. A. (2002). Cloning and characterization of the *Burkholderia vietnamiensis* norM gene encoding a multi-drug efflux system. *FEMS Microbiol. Lett.* 215, 279–283. doi: 10.1111/j.1574-6968.2002.tb11403.x
- Fujisaki, S., Ohnuma, S., Horiuchi, T., Takahashi, I., Tsukui, S., Nishimura, Y., et al. (1996). Cloning of a gene from *Escherichia coli* that confers resistance to fosfomycin as a consequence of amplification. *Gene* 175, 83–87. doi: 10.1016/0378-1119(96)00128-X
- Gamberi, T., Rocchiccioli, S., Papaleo, M., Magherini, F., Citti, L., Buroni, S., et al. (2013). RND-4 efflux transporter gene deletion in *Burkholderia cenocepacia* J2315: a proteomic analysis. *J. Proteome Sci. Comp. Biol.* 2:1. doi: 10.7243/2050-2273-2-1
- Glass, M. B., Gee, J. E., Steigerwalt, A. G., Cavuoti, D., Barton, T., Hardy, R. D., et al. (2006). Pneumonia and septicemia caused by *Burkholderia thailandensis* in the United States. *J. Clin. Microbiol.* 44, 4601–4604. doi: 10.1128/JCM.01585-06
- Golini, G., Favari, F., Marchetti, F., and Fontana, R. (2004). Bacteriostatic and bactericidal activity of levofloxacin against clinical isolates from cystic fibrosis patients. *Eur. J. Clin. Microbiol. Infect. Dis.* 23, 798–800. doi: 10.1007/s10096-004-1216-3
- Grove, A. (2010). Urate-responsive MarR homologs from *Burkholderia*. *Mol. Biosyst.* 6, 2133–2142. doi: 10.1039/c0mb00086h
- Guglielmo, P., Pasca, M. R., De Rossi, E., Buroni, S., Arrigo, P., Manina, G., et al. (2006). Efflux pump genes of the resistance-nodulation-division family in *Burkholderia cenocepacia* genome. *BMC Microbiol.* 6:66. doi: 10.1186/1471-2180-6-66
- Hamad, M. A., Skeldon, A. M., and Valvano, M. A. (2010). Construction of aminoglycoside-sensitive *Burkholderia cenocepacia* strains for use in studies of intracellular bacteria with the gentamicin protection assay. *Appl. Environ. Microbiol.* 76, 3170–3176. doi: 10.1128/AEM.03024-09
- Hancock, R. E. W. (1998). Resistance mechanisms in *Pseudomonas aeruginosa* and other non-fermentative bacteria. *Clin. Infect. Dis.* 27(Suppl. 1), S93–S99. doi: 10.1086/514909
- Hayashi, S., Abe, M., Kimoto, M., Furukawa, S., and Nakazawa, T. (2000). The DsbA-DsbB disulfide bond formation system of *Burkholderia cepacia* is involved in the production of protease and alkaline phosphatase, motility, metal resistance, and multi-drug resistance. *Microbiol. Immunol.* 44, 41–50. doi: 10.1111/j.1348-0421.2000.tb01244.x
- Hayden, H. S., Lim, R., Brittnacher, M. J., Sims, E. H., Ramage, E. R., Fong, C., et al. (2012). Evolution of *Burkholderia pseudomallei* in recurrent melioidosis. *PLoS ONE* 7:e36507. doi: 10.1371/journal.pone.0036507
- Hemsley, C. M., Luo, J. X., Andreea, C. A., Butler, C. S., Soyer, O. S., and Titball, R. W. (2014). Bacterial drug tolerance under clinical conditions is governed by anaerobic adaptation but not anaerobic respiration. *Antimicrob. Agents Chemother.* 58, 5775–5783. doi: 10.1128/AAC.02793-14
- Hirakata, Y., Kondo, A., Hoshino, K., Yano, H., Arai, K., Hirotani, A., et al. (2009). Efflux pump inhibitors reduce the invasiveness of *Pseudomonas aeruginosa*. *Int. J. Antimicrob. Agents* 34, 343–346. doi: 10.1016/j.ijantimicag.2009.06.007
- Holden, M. T., Seth-Smith, H. M., Crossman, L. C., Sebaihia, M., Bentley, S. D., Cerdeno-Tarraga, A. M., et al. (2009). The genome of *Burkholderia cenocepacia* J2315, an epidemic pathogen of cystic fibrosis patients. *J. Bacteriol.* 191, 261–277. doi: 10.1128/JB.01230-08
- Holden, M. T. G., Titball, R. W., Peacock, S. J., Cerdeno-Tarraga, A. M., Atkins, T. P., Crossman, L. C., et al. (2004). Genomic plasticity of the causative agent of melioidosis, *Burkholderia pseudomallei*. *Proc. Natl. Acad. Sci. U.S.A.* 101, 14240–14245. doi: 10.1073/pnas.0403302101
- Holland, D. J., Wesley, A., Drinkovic, D., and Currie, B. J. (2002). Cystic fibrosis and *Burkholderia pseudomallei* infection: an emerging problem? *Clin. Infect. Dis.* 35, e138–e140. doi: 10.1086/344447
- Jassem, A. N., Forbes, C. M., and Speert, D. P. (2014). Investigation of aminoglycoside resistance inducing conditions and a putative AmrAB-OprM efflux

- system in *Burkholderia vietnamiensis*. *Ann. Clin. Microbiol. Antimicrob.* 13:2. doi: 10.1186/1476-0711-13-2
- Jassem, A. N., Zlosnik, J. E., Henry, D. A., Hancock, R. E., Ernst, R. K., and Speert, D. P. (2011). In vitro susceptibility of *Burkholderia vietnamiensis* to aminoglycosides. *Antimicrob. Agents Chemother.* 55, 2256–2264. doi: 10.1128/AAC.01434-10
- Kang, Y., Carlson, R., Sharpe, W., and Schell, M. A. (1998). Characterization of genes involved in biosynthesis of a novel antibiotic from *Burkholderia cepacia* BC11 and their role in biological control of *Rhizoctonia solani*. *Appl. Environ. Microbiol.* 64, 3939–3947.
- Koehler, T., Micheal-Hamzehpour, M., Henze, U., Gotoh, N., Curty, L. K., and Pechere, J. C. (1997). Characterization of MexE-MexF-OprN, a positively regulated multidrug efflux system of *Pseudomonas aeruginosa*. *Mol. Microbiol.* 23, 345–354. doi: 10.1046/j.1365-2958.1997.2281594.x
- Koehler, T., Van Delden, C., Kocjanic Curty, L., Hamzehpour, M. M., and Pechere, J.-C. (2001). Overexpression of the MexEF-OprN multidrug efflux system affects cell-to-cell signaling in *Pseudomonas aeruginosa*. *J. Bacteriol.* 183, 5213–5222. doi: 10.1128/JB.183.18.5213-5222.2001
- Kumar, A., Chua, K.-L., and Schweizer, H. P. (2006). Method for regulated expression of single-copy efflux pump genes in a surrogate *Pseudomonas aeruginosa* strain: identification of the BpeEF-OprC chloramphenicol and trimethoprim efflux pump of *Burkholderia pseudomallei* 1026b. *Antimicrob. Agents Chemother.* 50, 3460–3463. doi: 10.1128/AAC.00440-06
- Kumar, A., Mayo, M., Trunck, L. A., Cheng, A. C., Currie, B. J., and Schweizer, H. P. (2008). Expression of resistance-nodulation-cell division efflux pumps in commonly used *Burkholderia pseudomallei* strains and clinical isolates from Northern Australia. *Trans. R. Soc. Trop. Med. Hyg.* 102(Suppl. 1), S145–S151. doi: 10.1016/S0035-9203(08)70032-4
- Li, X. Z., Nikaido, H., and Poole, K. (1995). Role of MexA-MexB-OprM in antibiotic efflux in *Pseudomonas aeruginosa*. *Antimicrob. Agents Chemother.* 39, 1948–1953. doi: 10.1128/AAC.39.9.1948
- Liu, H., Ibrahim, M., Qiu, H., Kausar, S., Ilyas, M., Cui, Z., et al. (2015). Protein profiling analyses of the outer membrane of *Burkholderia cenocepacia* reveal a niche-specific proteome. *Microb. Ecol.* 69, 75–83. doi: 10.1007/s00248-014-0460-z
- Liu, N., Cummings, J. E., England, K., Slayden, R. A., and Tonge, P. J. (2011). Mechanism and inhibition of the FabI enoyl-ACP reductase from *Burkholderia pseudomallei*. *J. Antimicrob. Chemother.* 66, 564–573. doi: 10.1093/jac/dkq509
- Losada, L., Ronning, C. M., Deshazer, D., Woods, D., Fedorova, N., Kim, H. S., et al. (2010). Continuing evolution of *Burkholderia mallei* through genome reduction and large-scale rearrangements. *Genome Biol. Evol.* 2, 102–116. doi: 10.1093/gbe/evq003
- Loutet, S. A., and Valvano, M. A. (2011). Extreme antimicrobial peptide and polymyxin B resistance in the genus *Burkholderia*. *Front. Microbiol.* 2:159. doi: 10.3389/fmicb.2011.00159
- Mahenthiralingam, E., Urban, T. A., and Goldberg, J. B. (2005). The multifarious, multireplicon *Burkholderia cepacia* complex. *Nat. Rev. Microbiol.* 3, 144–156. doi: 10.1038/nrmicro1085
- Maravic, A., Skocibusic, M., Sprung, M., Samanic, I., Puizina, J., and Pavela-Vrancic, M. (2012). Occurrence and antibiotic susceptibility profiles of *Burkholderia cepacia* complex in coastal marine environment. *Int. J. Environ. Health Res.* 22, 531–542. doi: 10.1080/09603123.2012.67797
- McGowan, J. E. Jr. (2006). Resistance in non-fermenting gram-negative bacteria: multidrug resistance to the maximum. *Am. J. Infect. Control* 34, S29–S37; discussion S64–S73.
- Messiaen, A. S., Verbrugghen, T., Declerck, C., Ortmann, R., Schlitzer, M., Nelis, H., et al. (2011). Resistance of the *Burkholderia cepacia* complex to fosfomycin and fosfomycin derivatives. *Int. J. Antimicrob. Agents* 38, 261–264. doi: 10.1016/j.ijantimicag.2011.04.020
- Mima, T., and Schweizer, H. P. (2010). The BpeAB-OprB efflux pump of *Burkholderia pseudomallei* 1026b does not play a role in quorum sensing, virulence factor production, or extrusion of aminoglycosides but is a broad-spectrum drug efflux system. *Antimicrob. Agents Chemother.* 54, 3113–3120. doi: 10.1128/AAC.01803-09
- Mima, T., Schweizer, H. P., and Xu, Z.-Q. (2011). In vitro activity of cethromycin against *Burkholderia pseudomallei* and investigation of mechanism of resistance. *J. Antimicrob. Chemother.* 66, 73–78. doi: 10.1093/jac/dkq391
- Mine, T., Morita, Y., Kataoka, A., Mizushima, T., and Tsuchiya, T. (1999). Expression in *Escherichia coli* of a new multidrug efflux pump, MexXY, from *Pseudomonas aeruginosa*. *Antimicrob. Agents Chemother.* 43, 415–417.
- Mira, N. P., Madeira, A., Moreira, A. S., Coutinho, C. P., and Sa-Correia, I. (2011). Genomic expression analysis reveals strategies of *Burkholderia cenocepacia* to adapt to cystic fibrosis patients' airways and antimicrobial therapy. *PLoS ONE* 6:e28831. doi: 10.1371/journal.pone.0028831
- Moore, R. A., Deshazer, D., Reckseidler, S., Weissman, A., and Woods, D. E. (1999). Efflux-mediated aminoglycoside and macrolide resistance in *Burkholderia pseudomallei*. *Antimicrob. Agents Chemother.* 43, 465–470.
- Morita, Y., Tomida, J., and Kawamura, Y. (2012). MexXY multidrug efflux system of *Pseudomonas aeruginosa*. *Front. Microbiol.* 3:408. doi: 10.3389/fmicb.2012.00408
- Nair, B. M., Cheung, K. J. Jr., Griffith, A., and Burns, J. L. (2004). Salicylate induces an antibiotic efflux pump in *Burkholderia cepacia* complex genomovar III (*B. cenocepacia*). *J. Clin. Invest.* 113, 464–473. doi: 10.1172/JCI200419710
- Nair, B. M., Joachimiak, L. A., Chattopadhyay, S., Montano, I., and Burns, J. L. (2005). Conservation of a novel protein associated with an antibiotic efflux operon in *Burkholderia cenocepacia*. *FEMS Microbiol. Lett.* 245, 337–344. doi: 10.1016/j.femsle.2005.03.027
- Nierman, W. C., Deshazer, D., Kim, H. S., Tettelin, H., Nelson, K. E., Feldblyum, T., et al. (2004). Structural flexibility in the *Burkholderia mallei* genome. *Proc. Natl. Acad. Sci. U.S.A.* 101, 14246–14251. doi: 10.1073/pnas.0403306101
- Nikaido, H., and Pages, J. M. (2012). Broad-specificity efflux pumps and their role in multidrug resistance of Gram-negative bacteria. *FEMS Microbiol. Rev.* 36, 340–363. doi: 10.1111/j.1574-6976.2011.00290.x
- Nishino, K., and Yamaguchi, A. (2001). Analysis of a complete library of putative drug transporter genes in *Escherichia coli*. *J. Bacteriol.* 183, 5803–5812. doi: 10.1128/JB.183.20.5803-5812.2001
- O'Quinn, A. L., Wiegand, E. M., and Jeddelloh, J. A. (2001). *Burkholderia pseudomallei* kills the nematode *Caenorhabditis elegans* using an endotoxin-mediated paralysis. *Cell Microbiol.* 3, 381–393. doi: 10.1046/j.1462-5822.2001.0118.x
- Pearson, J. P., Van Delden, C., and Iglesias, B. H. (1999). Active efflux and diffusion are involved in transport of *Pseudomonas aeruginosa* cell-to-cell signals. *J. Bacteriol.* 181, 1203–1210.
- Peeters, E., Nelis, H. J., and Coenye, T. (2009). In vitro activity of cefazidime, ciprofloxacin, meropenem, minocycline, tobramycin and trimethoprim/sulfamethoxazole against planktonic and sessile *Burkholderia cepacia* complex bacteria. *J. Antimicrob. Chemother.* 64, 801–809. doi: 10.1093/jac/dkp253
- Perrin, E., Fondi, M., Papaleo, M. C., Maida, I., Buroni, S., Pasca, M. R., et al. (2010). Exploring the HME and HAE1 efflux systems in the genus *Burkholderia*. *BMC Evol. Biol.* 10:164. doi: 10.1186/1471-2148-10-164
- Podin, Y., Sarovich, D. S., Price, E. P., Kaestli, M., Mayo, M., Hii, K., et al. (2014). *Burkholderia pseudomallei* isolates from Sarawak, Malaysian Borneo, are predominantly susceptible to aminoglycosides and macrolides. *Antimicrob. Agents Chemother.* 58, 162–166. doi: 10.1128/AAC.01842-13
- Podneicky, N. L., Wuthiekanun, V., Peacock, S. J., and Schweizer, H. P. (2013). The BpeEF-OprC efflux pump is responsible for widespread trimethoprim resistance in clinical and environmental *Burkholderia pseudomallei* isolates. *Antimicrob. Agents Chemother.* 57, 4381–4386. doi: 10.1128/AAC.00660-13
- Poole, K. (2001). Multidrug efflux pumps and antimicrobial resistance in *Pseudomonas aeruginosa* and related organisms. *J. Mol. Microbiol. Biotechnol.* 3, 255–264.
- Poole, K., Krebes, K., McNally, C., and Neshat, S. (1993). Multiple antibiotic resistance in *Pseudomonas aeruginosa*: evidence for involvement of an efflux operon. *J. Bacteriol.* 175, 7363–7372.
- Price, E. P., Sarovich, D. S., Mayo, M., Tuanyok, A., Drees, K. P., Kaestli, M., et al. (2013). Within-host evolution of *Burkholderia pseudomallei* over a twelve-year chronic carriage infection. *MBio* 4:4. doi: 10.1128/mBio.00388-13
- Propst, K. L. (2011). *The Analysis of Burkholderia pseudomallei Virulence and Efficacy of Potential Therapeutics*. Ph.D. Dissertation, Colorado State University, Fort Collins, CO.
- Propst, K. L., Mima, T., Choi, K. H., Dow, S. W., and Schweizer, H. P. (2010). A *Burkholderia pseudomallei* ΔpurM mutant is avirulent in immune competent and immune deficient animals: candidate strain for exclusion from select agent lists. *Infect. Immun.* 78, 3136–3143. doi: 10.1128/IAI.01313-09

- Rajendran, R., Quinn, R. F., Murray, C., Mcculloch, E., Williams, C., and Ramage, G. (2010). Efflux pumps may play a role in tigecycline resistance in *Burkholderia* species. *Int. J. Antimicrob. Agents* 36, 151–154. doi: 10.1016/j.ijantimicag.2010.03.009
- Rushton, L., Sass, A., Baldwin, A., Dowson, C. G., Donoghue, D., and Mahenthiralingam, E. (2013). Key role for efflux in the preservative susceptibility and adaptive resistance of *Burkholderia cepacia* complex bacteria. *Antimicrob. Agents Chemother.* 57, 2972–2980. doi: 10.1128/AAC.00140-13
- Sass, A., Marchbank, A., Tullis, E., Lipuma, J. J., and Mahenthiralingam, E. (2011). Spontaneous and evolutionary changes in the antibiotic resistance of *Burkholderia cenocepacia* observed by global gene expression analysis. *BMC Genomics* 12:373. doi: 10.1186/1471-2164-12-373
- Schell, M. A., Zhao, P., and Wells, L. (2011). Outer membrane proteome of *Burkholderia pseudomallei* and *Burkholderia mallei* from diverse growth conditions. *J. Proteome Res.* 10, 2417–2424. doi: 10.1021/pr1012398
- Schulini, T., and Steinmetz, I. (2001). Chronic melioidosis in a patient with cystic fibrosis. *J. Clin. Microbiol.* 39, 1676–1677. doi: 10.1128/JCM.39.4.1676-1677.2001
- Schweizer, H. (2012a). “Mechanisms of *Burkholderia pseudomallei* antimicrobial resistance,” in *Melioidosis - A Century of Observation and Research*, ed. N. Ketheesan (Amsterdam: Elsevier), 229–238.
- Schweizer, H. P. (2012b). Mechanisms of antibiotic resistance in *Burkholderia pseudomallei*: implications for treatment of melioidosis. *Future Microbiol.* 7, 1389–1399. doi: 10.2217/fmb.12.116
- Schweizer, H. P. (2012c). When it comes to drug discovery not all Gram-negative bacterial biodefence pathogens are created equal: *Burkholderia pseudomallei* is different. *Microb. Biotechnol.* 5, 581–583. doi: 10.1111/j.1751-7915.2012.00334.x
- Scoffone, V. C., Spadaro, F., Udine, C., Makarov, V., Fondi, M., Fani, R., et al. (2014). Mechanism of resistance to an antitubercular 2-thiopyridine derivative that is also active against *Burkholderia cenocepacia*. *Antimicrob. Agents Chemother.* 58, 2415–2417. doi: 10.1128/AAC.02438-13
- Scott, A. E., Laws, T. R., D'elia, R. V., Stokes, M. G., Nandi, T., Williamson, E. D., et al. (2013). Protection against experimental melioidosis following immunization with live *Burkholderia thailandensis* expressing a manno-heptose capsule. *Clin. Vaccine Immunol.* 20, 1041–1047. doi: 10.1128/CVI.00113-13
- Sim, B. M., Chantratita, N., Ooi, W. F., Nandi, T., Tewhey, R., Wuthiekanun, V., et al. (2010). Genomic acquisition of a capsular polysaccharide virulence cluster by non-pathogenic *Burkholderia* isolates. *Genome Biol.* 11:R89. doi: 10.1186/gb-2010-11-8-r89
- Simpson, A. J., Newton, P. N., Chierakul, W., Chaowagul, W., and White, N. J. (2003). Diabetes mellitus, insulin, and melioidosis in Thailand. *Clin. Infect. Dis.* 36, e71–e72. doi: 10.1086/367861
- Sobel, M. L., McKay, G. A., and Poole, K. (2003). Contribution of the MexXY multidrug transporter to aminoglycoside resistance in *Pseudomonas aeruginosa* clinical isolates. *Antimicrob. Agents Chemother.* 47, 3202–3207. doi: 10.1128/AAC.47.10.3202-3207.2003
- Song, H., Hwang, J., Yi, H., Ulrich, R. L., Yu, Y., Nierman, W. C., et al. (2010). The early stage of bacterial genome-reductive evolution in the host. *PLoS Pathog.* 6:e100922. doi: 10.1371/journal.ppat.100922
- Tegos, G. P., Haynes, M. K., and Schweizer, H. P. (2012). Dissecting novel virulent determinants in the *Burkholderia cepacia* complex. *Virulence* 3, 234–237. doi: 10.4161/viru.19844
- Teng, M., Hilgers, M. T., Cunningham, M. L., Borchardt, A., Locke, J. B., Abraham, S., et al. (2013). Identification of bacteria-selective threonyl-tRNA synthetase substrate inhibitors by structure-based design. *J. Med. Chem.* 56, 1748–1760. doi: 10.1021/jm301756m
- Tian, Z. X., Mac Aogain, M., O'connor, H. F., Fargier, E., Mooij, M. J., Adams, C., et al. (2009). MexT modulates virulence determinants in *Pseudomonas aeruginosa* independent of the MexEF-OprN efflux pump. *Microb. Pathog.* 47, 237–241. doi: 10.1016/j.micpath.2009.08.003
- Trunck, L. A., Propst, K. L., Wuthiekanun, V., Tuanyok, A., Beckstrom-Sternberg, S. M., Beckstrom-Sternberg, J. S., et al. (2009). Molecular basis of rare aminoglycoside susceptibility and pathogenesis of *Burkholderia pseudomallei* clinical isolates from Thailand. *PLoS Negl. Trop. Dis.* 3:e0000519. doi: 10.1371/journal.pntd.0000519
- Tseng, S. P., Tsai, W. C., Liang, C. Y., Lin, Y. S., Huang, J. W., Chang, C. Y., et al. (2014). The contribution of antibiotic resistance mechanisms in clinical *Burkholderia cepacia* complex isolates: an emphasis on efflux pump activity. *PLoS ONE* 9:e104986. doi: 10.1371/journal.pone.0104986
- Vandamme, P., and Dawyndt, P. (2011). Classification and identification of the *Burkholderia cepacia* complex: Past, present and future. *Syst. Appl. Microbiol.* 34, 87–95. doi: 10.1016/j.syapm.2010.10.002
- Vanlaere, E., Baldwin, A., Gevers, D., Henry, D., De Brandt, E., Lipuma, J. J., et al. (2009). Taxon K, a complex within the *Burkholderia cepacia* complex, comprises at least two novel species, *Burkholderia contaminans* sp. nov. and *Burkholderia lata* sp. nov. *Int. J. Syst. Evol. Microbiol.* 59, 102–111. doi: 10.1099/ijts.0.001123-0
- Viktorov, D. V., Zakharova, I. B., Podshivalova, M. V., Kalinkina, E. V., Merinova, O. A., Ageeva, N. P., et al. (2008). High-level resistance to fluoroquinolones and cephalosporins in *Burkholderia pseudomallei* and closely related species. *Trans. R. Soc. Trop. Med. Hyg.* 102(Suppl. 1), S103–S110. doi: 10.1016/S0035-9203(08)70025-7
- Vora, S. K. (2002). Sherlock Holmes and a biological weapon. *J. R. Soc. Med.* 95, 101–103. doi: 10.1258/jrsm.95.2.101
- Whitlock, G. C., Estes, D. M., and Torres, A. G. (2007). Glanders: off to the races with *Burkholderia mallei*. *FEMS Microbiol. Lett.* 277, 115–122. doi: 10.1111/j.1574-6968.2007.00949.x
- Wiersinga, W. J., Birnie, E., Weehuizen, T. A., Alabi, A. S., Huson, M. A., In 't Veld, R. A., et al. (2015). Clinical, environmental, and serologic surveillance studies of melioidosis in Gabon, 2012–2013. *Emerg. Infect. Dis.* 21, 40–47. doi: 10.3201/eid2101.140762
- Wiersinga, W. J., Currie, B. J., and Peacock, S. J. (2012). Melioidosis. *N. Engl. J. Med.* 367, 1035–1044. doi: 10.1056/NEJMra1204699
- Wiersinga, W. J., Van Der Poll, T., White, N. J., Day, N. P., and Peacock, S. J. (2006). Melioidosis: insights into the pathogenicity of *Burkholderia pseudomallei*. *Nat. Rev. Microbiol.* 4, 272–282. doi: 10.1038/nrmicro1385
- Wigfield, S. M., Rigg, G. P., Kavari, M., Webb, A. K., Matthews, R. C., and Burnie, J. P. (2002). Identification of an immunodominant drug efflux pump in *Burkholderia cepacia*. *J. Antimicrob. Chemother.* 49, 619–624. doi: 10.1093/jac/49.4.619
- Winsor, G. L., Khaira, B., Van Rossum, T., Lo, R., Whiteside, M. D., and Brinkman, F. S. L. (2008). The *Burkholderia* genome database: facilitating flexible queries and comparative analyses. *Bioinformatics* 24, 2803–2804. doi: 10.1093/bioinformatics/btn524
- Zhang, L., Li, X. Z., and Poole, K. (2001). Fluoroquinolone susceptibilities of efflux-mediated multidrug-resistant *Pseudomonas aeruginosa*, *Stenotrophomonas maltophilia* and *Burkholderia cepacia*. *J. Antimicrob. Chemother.* 48, 549–552. doi: 10.1093/jac/48.4.549

**Conflict of Interest Statement:** The authors declare that the research was conducted in the absence of any commercial or financial relationships that could be construed as a potential conflict of interest.

Copyright © 2015 Podnecky, Rhodes and Schweizer. This is an open-access article distributed under the terms of the Creative Commons Attribution License (CC BY). The use, distribution or reproduction in other forums is permitted, provided the original author(s) or licensor are credited and that the original publication in this journal is cited, in accordance with accepted academic practice. No use, distribution or reproduction is permitted which does not comply with these terms.

# RND-type drug efflux pumps from Gram-negative bacteria: molecular mechanism and inhibition

Henrietta Venter<sup>1\*</sup>, Rumana Mowla<sup>1</sup>, Thelma Ohene-Agyei<sup>2</sup> and Shutao Ma<sup>3</sup>

<sup>1</sup> School of Pharmacy and Medical Sciences, Sansom Institute for Health Research, University of South Australia, Adelaide, SA, Australia, <sup>2</sup> Department of Pharmacology, University of Cambridge, Cambridge, UK, <sup>3</sup> Department of Medicinal Chemistry, School of Pharmaceutical Sciences, Shandong University, Jinan, China

## OPEN ACCESS

### Edited by:

Attilio Vittorio Vargiu,  
Università' di Cagliari, Italy

### Reviewed by:

Pierre Cornelis,  
Vrije Universiteit Brussel, Belgium  
Paolo Ruggerone,  
University of Cagliari, Italy

### \*Correspondence:

Henrietta Venter,  
School of Pharmacy and Medical Sciences, Sansom Institute for Health Research, University of South Australia, Frome Road, Adelaide, SA 5000, Australia  
rietie.venter@unisa.edu.au

### Specialty section:

This article was submitted to  
Antimicrobials, Resistance and Chemotherapy,  
a section of the journal  
*Frontiers in Microbiology*

Received: 26 January 2015

Paper pending published:

02 March 2015

Accepted: 12 April 2015

Published: 28 April 2015

### Citation:

Venter H, Mowla R, Ohene-Agyei T and Ma S (2015) RND-type drug efflux pumps from Gram-negative bacteria: molecular mechanism and inhibition.

*Front. Microbiol.* 6:377.

doi: 10.3389/fmicb.2015.00377

Drug efflux protein complexes confer multidrug resistance on bacteria by transporting a wide spectrum of structurally diverse antibiotics. Moreover, organisms can only acquire resistance in the presence of an active efflux pump. The substrate range of drug efflux pumps is not limited to antibiotics, but it also includes toxins, dyes, detergents, lipids, and molecules involved in quorum sensing; hence efflux pumps are also associated with virulence and biofilm formation. Inhibitors of efflux pumps are therefore attractive compounds to reverse multidrug resistance and to prevent the development of resistance in clinically relevant bacterial pathogens. Recent successes on the structure determination and functional analysis of the AcrB and MexB components of the AcrAB-TolC and MexAB-OprM drug efflux systems as well as the structure of the fully assembled, functional triparted AcrAB-TolC complex significantly contributed to our understanding of the mechanism of substrate transport and the options for inhibition of efflux. These data, combined with the well-developed methodologies for measuring efflux pump inhibition, could allow the rational design, and subsequent experimental verification of potential efflux pump inhibitors (EPIs). In this review we will explore how the available biochemical and structural information can be translated into the discovery and development of new compounds that could reverse drug resistance in Gram-negative pathogens. The current literature on EPIs will also be analyzed and the reasons why no compounds have yet progressed into clinical use will be explored.

**Keywords:** multidrug resistance, drug efflux, efflux pump inhibitor, Gram-negative, pathogen, antimicrobial resistance

## Introduction

Over the last two decades there has been a dramatic surge in the number of multidrug resistant bacteria, yet paradoxically the number of pharmaceutical companies developing new antimicrobial agents has dwindled during this same period. As a result, antibiotic resistance is now one of the world's most pressing health problems (WHO, 2014). Therefore, new treatments to combat drug resistant bacteria are urgently needed if we do not want to return to the high mortality rates associated with infections during the pre-antibiotic era (Bush et al., 2011; WHO, 2014).

Hospital acquired pathogens such as *Staphylococcus aureus*, *Klebsiella pneumoniae*, *Acinetobacter baumannii*, and *Pseudomonas aeruginosa* which can cause life-threatening infections display high levels of antibiotic resistance (Poole, 2011; Bassetti et al., 2013). Resistance of *K. pneumoniae*

to carbapenems, the last resort treatment for severe infections, of up to 54% of cases were reported (WHO, 2014).

Recently a few new antibiotics have been approved for the use against Gram-positive organisms (Butler and Cooper, 2011). However, infections caused by Gram-negative pathogens proved much harder to treat due to the very high intrinsic drug resistance displayed by Gram-negative organisms. This intrinsic drug resistance is due to presence of an outer membrane which acts as a permeability barrier and by the expression of drug efflux pumps.

Drug efflux pumps are protein complexes which reside in the membrane and remove antimicrobials and toxins, thereby lowering their concentration inside the cell to sub-toxic levels (Poole, 2004, 2005; Piddock, 2006a; Nikaido and Pages, 2012). These proteins recognize and expel a wide range of structurally diverse antibiotics with different mechanisms and sites of action. The clinical implication of this substrate promiscuity is the development of multidrug resistance where a pathogen displays resistance against multiple classes of antimicrobials.

Apart from antibiotics drug efflux proteins can also transport antiseptics and disinfectants (Chuanchuen et al., 2003; Sanchez et al., 2005; Mima et al., 2007; Pumbwe et al., 2007), detergents (including naturally occurring bile salts; Rosenberg et al., 2003; Lin et al., 2005), fatty acids (Lee and Shafer, 1999; Lennen et al., 2013), heavy metals (Silver and Phung, 1996; Walmsley and Rosen, 2009), solvents (White et al., 1997; Ramos et al., 2002; Segura et al., 2012), and virulence factors (Piddock, 2006b). Therefore, drug efflux pumps are also important constituents of bacterial pathogenesis, virulence, and biofilm formation (Hirakata et al., 2002, 2009; Piddock, 2006b; Ikonomidis et al., 2008; Martinez et al., 2009; Baugh et al., 2012, 2014; Amaral et al., 2014). In addition, micro-organisms can only acquire resistance in the presence of drug efflux pumps (Lomovskaya and Bostian, 2006; Ricci et al., 2006; Zhang et al., 2011; Piddock, 2014) as these non-specific pumps remove most compounds until the organism has had time to acquire resistance to an antibiotic through more specific adaptive mechanisms.

Despite their crucial role in bacterial pathogenesis and multidrug resistance there are currently no inhibitors for drug efflux pumps in clinical use. Therefore drug efflux pumps are attractive targets for inhibition. Efflux pump inhibitors (EPIs) will (a) synergise with currently used antibiotics, (b) restore the efficacy of antibiotics to which resistance has arisen, (c) reduce the incidence of emergence of drug-resistant pathogens, (d) reduce the ability of pathogens to infect the host as the inhibition of efflux attenuates the bacterium, and (e) prevent the development of highly drug resistant biofilms

## Drug Efflux Pumps in Gram-Negative Bacteria

Gram-negative pathogens rely on tripartite protein assemblies that span their double membrane to pump antibiotics from the cell. The tripartite complex consists of an inner membrane protein (IMP) of the resistance nodulation cell division (RND)

family, an outer-membrane protein (OMP), and a periplasmic membrane fusion protein (MFP) which connect the other two proteins (**Figure 1**). The inner-membrane protein catalyzes drug/H<sup>+</sup> antiport and is the part of the complex responsible for drug selectivity. The best studied tripartite drug efflux complexes are the AcrA-AcrB-TolC and MexA-MexB-OprM transporters from *Escherichia coli* and *P. aeruginosa*, respectively, (Du et al., 2013). The IMPs AcrB and MexB share 86% similarity and MexB can functionally substitute for AcrB (Krishnamoorthy et al., 2008; Welch et al., 2010). The asymmetric structure of the AcrB homotrimer and subsequent biochemical analysis revealed a functional rotating mechanism where the monomers cycle through the different states loose (L), tight (T), and open (O; Murakami et al., 2006; Seeger et al., 2006, 2008b). IMPs such as AcrB consist of a transmembrane domain and periplasmic domain. The drug efflux pathway from the periplasm/outer membrane leaflet through the periplasmic domain of AcrB has been the focus of many studies and are now relatively well-understood (Murakami, 2008; Seeger et al., 2008a; Eicher et al., 2009; Misra and Bavro, 2009; Nikaido and Takatsuka, 2009; Pos, 2009; Nikaido, 2011; Nikaido and Pages, 2012; Ruggerone et al., 2013a,b). Recently, it was also found that mutations at the cytoplasmic face of MexB affected transport of drugs with targets inside the cell (Ohene-Agyei et al., 2012). This raises the possibility that similar to the cytoplasmic pathway for Cu(II) in CusA (Delmar et al., 2014), MexB might also have the ability to remove antibiotics from the inner membrane leaflet/cytoplasm (Ohene-Agyei et al., 2012). Targeted geometric simulations showed that such a cytoplasmic pathway could be possible even though it would not necessarily out-compete the periplasmic channel for

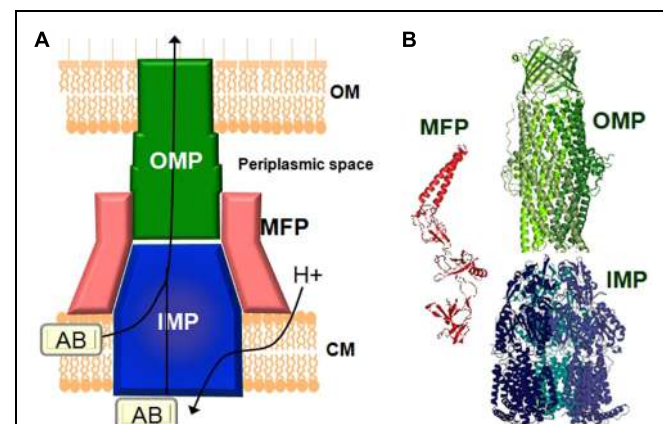


**FIGURE 1 | Schematic representation of a tripartite drug efflux complex. (A)** The complex consists of three proteins which span the inner-membrane (CM), the outer membrane (OM), and the periplasmic space. The inner-membrane protein (IMP), e.g., AcrB or MexB is responsible for substrate specificity and catalyzes  $\Delta\text{pH}$  dependent drug transport. Examples of the outer membrane protein (OMP) are TolC or OprM. The periplasmic membrane fusion protein (MFP), e.g., AcrA or MexA connects the IMP and the OMP. **(B)** Structures of the individual components of the efflux pump. The MexA (pdb: 2V4D), MexB (pdb: 2V50), and OprM (pdb: 1WP1) proteins from *Pseudomonas aeruginosa* are given as examples.

drug binding and transport (Phillips and Gnanakaran, 2015). Biochemical and structural analysis revealed that the periplasmic binding site in AcrB contains a shallow (proximal) and deep (distal) binding pocket separated by a switch loop (G-loop) consisting of residues 614–621 (Nakashima et al., 2011; Eicher et al., 2012; Cha et al., 2014). Conformational flexibility in this loop is necessary to move the substrate along the extended binding site. Mutations that change the small glycine residues in this loop to bulkier residues affects transport of larger macrolide antibiotics such as erythromycin while the activity toward smaller compounds such as novobiocin, ethidium, and chloramphenicol remained unaffected (Bohnert et al., 2008; Wehmeier et al., 2009; Nakashima et al., 2011, 2013; Eicher et al., 2012). Therefore, EPIs would most effectively inhibit the efflux of different antibiotics by interaction with the switch loop.

Due to the complexity of these macromolecular structures progress on elucidating their assembly and structure was slow. Only very recently Du et al. (2014) used a creative approach of genetic fusion proteins to solve the first structure of a partially active, fully assembled, tripartite pump in the presence of a modulatory partner. This structure of AcrA–AcrB–AcrZ–TolC shed light on long disputed subunit stoichiometries and revealed that the complex assembles in a 3 : 6 : 3 ratio of AcrB : AcrA : TolC with one monomer of AcrZ bound to each subunit of AcrB. The role of the small protein AcrZ is not clear, however, as it alters the substrate specificity of AcrB (Hobbs et al., 2012) it most likely plays a modulatory role.

The structural similarity between transporters from different Gram-negative organisms means that EPIs developed against, e.g., the AcrA–AcrB–TolC efflux pump from *E. coli* would most likely be effective against other pathogens also. Our current understanding of the structure and function of RND efflux pumps from Gram-negative bacteria could therefore provide the basis for the informed and efficient design of inhibitors against these protein complexes.

## Approaches to Inhibit Drug Efflux

The expression, function and assembly of drug efflux pumps of the RND class can be targeted in several ways (Figure 2).

### Targeting the Regulatory Network that Controls the Expression of Efflux Pumps as Levels of Pump Expression are Controlled by Activators and Repressors

Some progress has already been made in understanding the regulation of efflux pump expression, e.g., expression of AcrB from *Salmonella enterica* (Blair et al., 2014) and the regulation of efflux pump expression in *P. aeruginosa* (Wilke et al., 2008; Starr et al., 2012; Hay et al., 2013; Pursell and Poole, 2013; Lau et al., 2014). The expression levels of efflux pumps could be measured by real time PCR or with green fluorescent protein reporter fusions (Bumann and Valdivia, 2007; Ricci et al., 2012). Both these methods are amenable to high-throughput processing.

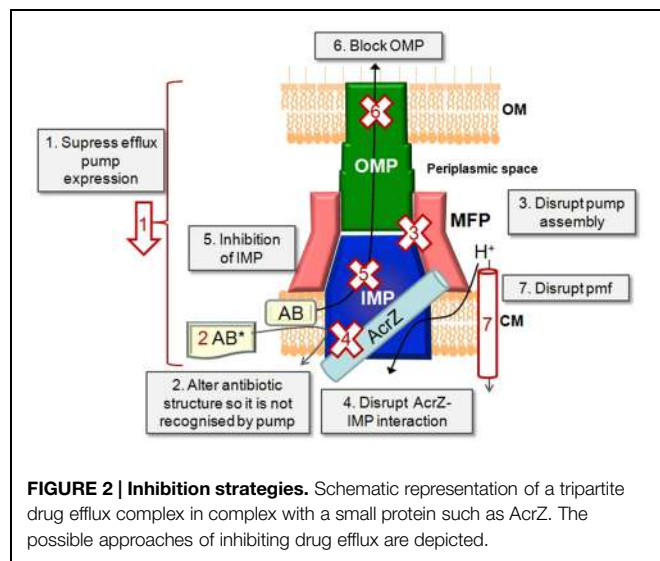


**FIGURE 2 | Inhibition strategies.** Schematic representation of a tripartite drug efflux complex in complex with a small protein such as AcrZ. The possible approaches of inhibiting drug efflux are depicted.

## Changing the Molecular Design of Old Antibiotics so that they are No Longer Recognized and Transported by the Efflux Pump

Given the wide range of compounds which could be recognized by drug efflux transporters, the plasticity in the binding sites, and the redundancy in aromatic residues in the binding pocket which could stabilize substrate binding (Du et al., 2013), this approach might prove a daunting task. In addition, altering the chemical structure of the antibiotic might render it less efficient against its intended cellular target. However, some progress has been made in this regard for a different class of drug efflux protein, the ATP binding cassette transporter, human P-glycoprotein where the substrate taxol was chemically modified so that P-glycoprotein no longer recognized it. This allowed the drug to cross the blood brain barrier and access its target receptor without being removed by P-glycoprotein (Rice et al., 2005).

### Preventing the Assembly of the Efflux Pump Components into a Functional Tripartite Pump by Targeting Protein–Protein Interfaces

This is a very promising approach which is still under-developed due to the lack of information of how tripartite pumps assemble. However, Tikhonova et al. (2011) showed that designed ankyrin repeat proteins (DARPins) could inhibit AcrAB-TolC function by inhibiting the interaction between AcrA and AcrB. The recent structure of a complete tripartite drug efflux pump and the information gained from that also opens up exciting new possibilities (Du et al., 2014). The interaction of purified protein components of the pump with each other can be measured with surface plasmon resonance (SPR). The ability of efflux pumps to assemble *in vivo* can be measured by cross-linking in whole cells with subsequent co-purifying of the pump components (Welch et al., 2010).

## Disrupting the Interaction Between AcrB and AcrZ

The exact role of AcrZ in drug efflux is still ill-defined. However, as AcrA–AcrB–TolC has a diminished ability to confer resistance to some drugs in the absence of AcrZ (Hobbs et al., 2012), this approach could be promising for restoring sensitivity to some antibiotics. Homologs of AcrZ are found in most Gram-negative bacteria, therefore the modulatory effect of RND class of transporters by small proteins is probably a widely conserved occurrence. The interaction between the IMP and a small protein such as AcrZ could be measured with SPR or with cross-linking in cells as mentioned above.

## Directly Blocking the IMP with a High Affinity Competing Substrate or Trapping the IMP in an Inactive Conformation

The recent crystal structure of AcrB and MexB bound to an inhibitor (Nakashima et al., 2013) and the advances in our understanding of how drugs are bound makes this option very attractive (see Efflux Pump Inhibitors Against Gram-Negative Bacteria Identified So Far). The ability of compounds to inhibit antibiotic efflux can be measured using drug accumulation or drug efflux assays (see Inhibition of Substrate Transport), while direct interaction between the test compound and the IMP component could be determined with isothermal calorimetry (ITC) or SPR (Tikhonova et al., 2011).

## Blocking the Exit Duct (the OMP)

A set of indole derivatives was designed based on the structure of TolC. These compounds were able to synergise with antibiotics and were reported to act on TolC specifically, presuming by preventing opening of the channel (Zeng et al., 2010). In addition, TolC from *E. coli* contains an electronegative entrance formed by an aspartate ring which is widely conserved throughout the TolC family and which could be a target for blocking by large cations (Andersen et al., 2002). The biggest challenge with this approach is achieving selectivity to the bacterial pores. Blocking of the OMP could be detected by inhibition of antibiotic efflux through the tripartite pump or by disruption of TolC-mediated conductance.

## Depleting the IMP From the Energy Needed to Drive the Drug/H<sup>+</sup> Antiport Reaction

The proton motive force (pmf) can easily be disrupted by the use of ionophores or compounds that disrupt the membrane integrity in one way or another. However, these effects are mostly not specific for bacterial membranes and hence compounds that act in this way would be cytotoxic to the host cells too. The magnitude of the pmf and the effect of test compounds on these could be determined by the use of fluorescent probes specific for the  $\Delta\Psi$  or  $\Delta\text{pH}$  components of the pmf (Venter et al., 2003).

## How Could EPIs be Identified?

Significant effort went into the biochemical and structural characterization of drug efflux proteins from Gram-negative bacteria.

Recent successes such as the structural determination of an intact pump and of IMPs bound to an inhibitor (Nakashima et al., 2013; Du et al., 2014) offer a solid platform for the rational design of EPIs using quantitative structure-activity relationship data (Ruggerone et al., 2013a; Wong et al., 2014; Figure 3).

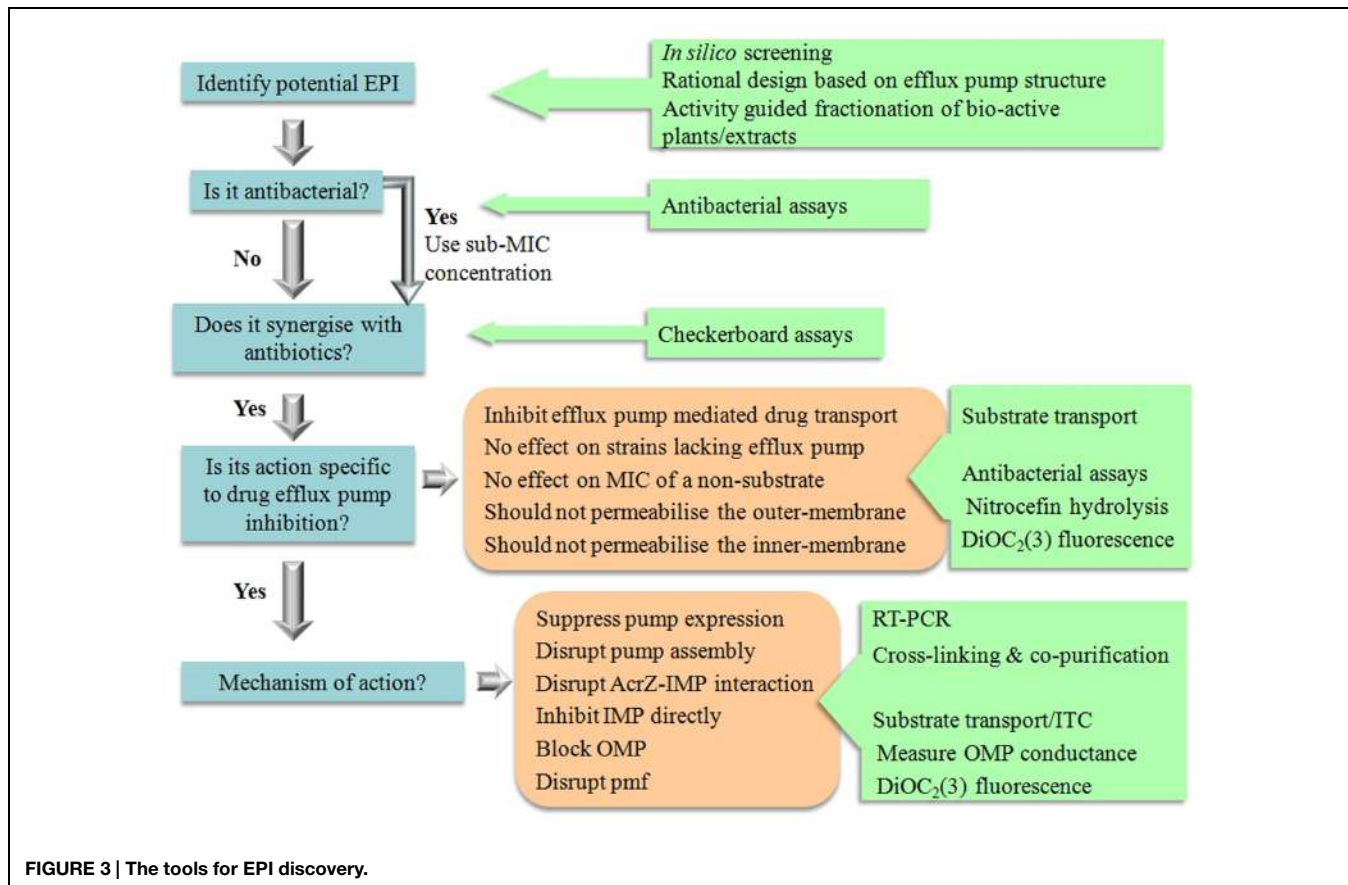
Recently we used *in silico* screening to identify compounds which would bind to AcrB with reasonable affinity. Of the roughly fifty compounds docked, six compounds were selected for further study. The docking allowed us to provide an order of efficiency of the compounds as potential EPIs. The biochemical data compared well with the predictions from the docking showing that *in silico* screening could be used as an effective screening tool to limit the amount of experiments needed or save on precious and hard earned purified natural products (Ohene-Agyei et al., 2014).

Another approach with good scope for success is investigating compounds purified from plants (Tegos et al., 2002). Traditional peoples have used plants to treat infections for 100s if not 1000s of years. In western medicine, plants are thus far an under-utilized source of chemical components in the treatment of infectious disease. Resistance to medicinal plant extracts have not been described yet and extracts of herbal medicines have been shown to potentiate antibiotic action in resistant pathogens (Garvey et al., 2011; Ohene-Agyei et al., 2014). Therefore, it is likely that as well as antibacterial chemicals, plants may also produce compounds that circumvent efflux-mediated resistance. Hence, activity guided fractionation can be used to identify the bio-active phytochemicals in plant extracts with EPI activity against Gram-negative organisms (Garvey et al., 2011).

## Tools for Studying Efflux Pump Inhibitors

The most significant problem in current screening campaigns for EPIs is that in many cases the synergism observed could be attributed to non-specific damage to the bacterial membrane. This would be a strong indicator the compound would have similar activity against mammalian cells and hence would be cytotoxic. This was clearly the case for the EPI Phe-Arg- $\beta$ -naphthylamide (PA $\beta$ N; Marquez, 2005; Lomovskaya and Zgurskaya, 2011).

Therefore, there need to be a thorough investigation in order to verify true EPI action (Figure 3). Compounds that permeabilise the membrane of Gram-negative organisms will always show synergism with antibiotics. For example, the modulatory effect of  $\alpha$ -tocopherol in multidrug resistant Gram-negative bacteria such as *P. aeruginosa* and *E. coli* could most probably be attributed to the effects of  $\alpha$ -tocopherol on the membrane (Andrade et al., 2014). It is therefore important that potential inhibitors are not only identified on their synergism with antibiotics, but that a subsequent biochemical assays are performed to determine that the compounds are truly acting by inhibiting drug efflux.



In order to qualify as an EPI a compound must be able to satisfy the following criteria as stipulated by Lomovskaya et al. (2001).

- (a) It must potentiate the activity of antibiotics to which a strain has developed resistance as a result of the expression of a drug efflux pump.
- (b) It should not have an effect on sensitive strains which lack the drug efflux pump.
- (c) It must not reduce the MIC of antibiotics which are not effluxed.
- (d) It must increase the level of accumulation and decrease the level of extrusion of compounds which are substrates of the efflux pump.
- (e) It must not permeabilise the outer membrane.
- (f) It must not affect the proton gradient across the inner membrane.

All the above criteria can be addressed with well-developed techniques as outlined below and in **Figure 3**, which would be amenable to scale-down for high throughput analysis.

### Measuring Synergism

The first thing to do is to determine the MIC of the test compound using standard broth dilution assays (Lomovskaya et al.,

2001; Welch et al., 2010; Ohene-Agyei et al., 2012, 2014). Ideally the compound should not be toxic to bacterial cells or only toxic at high concentrations. This would prevent resistance against the test compound from developing very quickly. The compound would then be used at concentrations below its MIC (usually  $4\times$  lower than the MIC) to test for synergism with antibiotics to which the organism has developed resistance. Synergism is best studied using checkerboard assays. These assays could be performed in a 96-well plate format with the antibiotic serially diluted along the ordinate and the test compound serially diluted along the abscissa (Lomovskaya et al., 2001; Orhan et al., 2005; Ohene-Agyei et al., 2014). The MIC of the antibiotic is determined in the presence of a range of different concentrations of the compound. Antibiotic-EPI interactions are subsequently classified on the basis of fractional inhibitory concentration (FIC). The FIC index is the sum of the FIC of each of the antibiotics, which in turn is defined as the MIC of the antibiotic when used in combination divided by the MIC of the antibiotic when used alone. The combination is considered synergistic when the  $\Sigma$ FIC is  $\leq 0.5$ , indifferent when the  $\Sigma$ FIC is  $> 0.5$  to  $< 2$ , and antagonistic when the  $\Sigma$ FIC is  $\geq 2$ .

### Ensuring the Compound has no Effect on Strains Which Lack the Drug Efflux Pump

An effective way of testing the effect of a compound on efflux pump mediated resistance is to use a wild-type antimicrobial

resistant strain and a sensitive strain with a genomic deletion of the IMP. Checkerboard assays can be performed on the wild type strain to determine if MIC drop toward that of sensitive strain. Conversely the compound should not have an effect on the MIC of the sensitive strain.

However, it is important not to use a strain with a TolC deletion. TolC is a multi-functional protein that operates with the majority of MFP-dependent transporters encoded in the genome of *E. coli* (Zgurskaya et al., 2011). Results from TolC minus cells would therefore be complicated by effects which are not related to active drug efflux (Ohene-Agyei et al., 2014).

### Inhibition of Substrate Transport

The ability of a potential EPI to inhibit substrate transport in a drug efflux pump can be measured by performing substrate accumulation assays or by measuring substrate efflux in the absence/presence of the putative EPI. Many fluorescent compounds are also substrates for drug efflux pumps. If these compounds undergo a change in fluorescence when bound to DNA/membrane lipids they can be used to measure the efflux activity of drug transporters. Many fluorescent compounds fulfill this role and are frequently used to measure drug efflux; examples are Hoechst 33342, berberine, ethidium bromide, TMA-DPH [1-(4-trimethylammoniumphenyl)-6-phenyl-1,3,5-hexatriene p-toluenesulfonate], *N*-phenylnaphthylamine and Nile Red which display enhanced fluorescence intensity when accumulated inside the cell or doxorubicin and rhodamine 6G for which accumulation inside cells results in quenching of the fluorescence signal (Lee et al., 2001; Lomovskaya et al., 2001; Seeger et al., 2008a,b; Ohene-Agyei et al., 2012, 2014; Cha et al., 2014). In drug accumulation assays the difference in rate of accumulation of the fluorescent compound between cells with and without an active efflux pump are used as an indication of efflux, since efflux will result in lower accumulation of compound. In drug efflux assays, the de-energized cells are pre-loaded with the fluorescent compound and then energized by the addition of glucose to catalyze drug efflux (observed as a drop in fluorescence). Drug influx assays are more straightforward and much quicker to perform than drug-efflux assays as de-energization and pre-loading can be time consuming. In addition, all the samples must be pre-loaded to the same level of fluorescence to avoid differences in efflux rate as a result of differences in the concentration of drug inside the cell. The main drawback of using fluorescent compounds to measure the effect of an EPI on drug efflux is that the potential EPI could be highly colored or fluorescent itself and thus interfere with the measurement. Recently, Bohnert et al. (2010) developed a method using Nile Red for efflux which are compatible with highly colored or fluorescent compounds.

### Testing of Outer Membrane Permeabilization

The most effective method to measure outer membrane permeabilization is the nitrocefin hydrolysis method. Nitrocefin is a chromogenic  $\beta$ -lactam which changes from yellow ( $\sim 380$  nm) to red ( $\sim 490$  nm) when it is hydrolyzed by the periplasmic  $\beta$ -lactamase, hence nitrocefin hydrolysis can be followed by

measuring the absorbance at 490 nm. If the test compound permeabilises the outer membrane, nitrocefin will diffuse more quickly over the membrane and hence the rate of nitrocefin hydrolysis will increase as a result (Lomovskaya et al., 2001; Ohene-Agyei et al., 2014). It is important to perform these assays in the presence of the ionophore CCCP to de-energize cells and prevent nitrocefin efflux.

### Testing of Inner Membrane Permeabilization

Several methods exist to measure permeabilization of the inner-membrane. A DNA stain which does not penetrate the membrane of intact bacterial cells and which will undergo an increase in fluorescence quantum yield when bound to DNA such as propidium iodide or SYTOX Green could be used (Roth et al., 1997; Nakashima et al., 2011). SYTOX Green would be preferred for its sensitivity as it undergoes a  $>500$ -fold enhancement in fluorescence emission when bound to DNA.

Other methods to measure the intactness of the bacterial inner membrane involve the use or measurement of the pmf in *E. coli*. Opperman et al. (2014), employed an assay based on the uptake of [*methyl-<sup>3</sup>H*]β-D-thiogalactopyranoside ([<sup>3</sup>H]TMG) by the LacY permease. The activity of the lactose permease is dependent on the pmf as it catalysis substrate/H<sup>+</sup> symport. Lomovskaya et al. (2001) probed the intracellular pH of *E. coli* cells by measuring the nuclear magnetic resonance (NMR) of the <sup>31</sup>P in the inner-membrane. Although both these two methods are effective they are quite time consuming and require access to specialist equipment. The magnitude of the individual components of the pmf can be measured directly by a simple fluorescence assay utilizing the fluorescent membrane potential probe 3,3'-diethyloxacarbocyanine iodide (DIOC<sub>2</sub>(3); Venter et al., 2003). Moreover, the DIOC<sub>2</sub>(3) assay can easily be adapted to 96-well format for the quick analysis of test compounds on the inner membrane in high-throughput screening.

### Use of a Non-Substrate

Another way of ruling out false positives and establishing that compounds do not act non-specifically is to measure the effect of the test compound on an antibiotic which is not an efflux pump substrate. For example our group used rifampicin, which is not transported by the AcrAB-TolC drug efflux pump from *E. coli* (Ohene-Agyei et al., 2014). The test compounds should not lower the MIC of rifampicin. Any reduction in the MIC of rifampicin would indicate that the compound does not potentiate antibiotic action by inhibition of efflux, but acts by indirect means such as permeabilization of the membrane.

### EPIs Against Gram-Negative Bacteria Identified so Far

The first EPI to be identified against RND pumps in Gram-negative bacteria was the peptidomimetic PA $\beta$ N, originally referred to as MC-2077110. PA $\beta$ N was identified in a screen for levofloxacin potentiators against resistant *P. aeruginosa*. Unfortunately, in addition to efflux pump inhibition it also

**TABLE 1 | Efflux pump inhibitors (EPIs) against Gram-negative pathogens.**

| Compound   | Source   | Protein/<br>Organism  | Actions <sup>1</sup>   | Essays performed  | Reference                                       |
|--|--|---|--|---|---|
| <b>Synthetic Compounds</b>                                     |  |   |  |   |   |
| Phe-Arg-<br>β-naphthylamide (PAβN;<br>MC-207,110)              | Synthetic  | MexAB-OprM,<br>MexCD-OprJ,<br>MexEF-OprN<br>( <i>Pseudomonas<br/>aeruginosa</i> ) | Synergise with<br>fluoroquinolones   | Antibacterial<br>Synergism<br>Substrate accumulation<br>Inhibition of efflux<br>Effect on<br>outer-membrane                       | Lomovskaya et al.<br>(2001)                     |
| 7-nitro-8-methyl-4-[2'-<br>(piperidinoethyl]<br>aminoquinoline | Alkylamino-quinolines                                  | AcrAB-TolC<br>( <i>Enterobacter<br/>aerogenes</i> )                               | Reduced MIC of Cam, Nor,<br>and Tet<br>Increased Cam uptake                              | Antibacterial<br>Synergism<br>Substrate accumulation  | Mallea et al. (2003)                            |
| 2,8-dimethyl-4-(2'-<br>pyrrolidinoethyl)-<br>oxyquinoline      | Alkoxy-quinoline<br>derivative                         | <i>E. aerogenes</i><br><i>Klebsiella<br/>pneumonia</i>                            | Reduced MIC of Nor, Tet,<br>Cam  | Substrate accumulation<br>Effect on membrane  | Chevalier et al. (2004)                         |
| 1-(1-Naphthylmethyl)-<br>piperazine<br>(NMP)                   | Synthetic  | AcrAB, AcrEF<br>( <i>Escherichia coli</i> )                                       | Reduction in MICs of Lev,<br>Oxa, Rif, Cam, Clr<br>Increased accumulation of<br>ethidium | Antibacterial<br>Substrate accumulation   | Kern et al. (2006)                              |
| New chloroquinoline<br>derivatives                             | Fluoroquinolones                                       | AcrAB-TolC<br>( <i>E. aerogenes</i> )   | Reduced MIC of Cam   | Antibacterial<br>Substrate accumulation   | Ghisalberti et al. (2006)                       |
| 3-amino-6-carboxyl-<br>indole,<br>3-nitro-6-amino-indole       | Designed and<br>synthesized based on<br>TolC structure | AcrAB-TolC<br>( <i>E. coli</i> )  | Reduced MIC of cam, tet,<br>ery, and cip   | Antibacterial<br>Synergism  | Zeng et al. (2010)                              |
| 4-(3-<br>morpholinopropylamino)-<br>quinazoline                | 4-alkylaminoquinazoline<br>derivatives                 | AcrAB-TolC<br>MexAB-OprM<br>( <i>E. coli</i><br><i>P. aeruginosa</i> )            | Reduced MIC of Cam, Nal,<br>Nor, and Spfx<br>Increased Cam uptake                        | Antibacterial<br>Synergism<br>Substrate accumulation  | Mahamoud et al. (2011)                          |
| MBX2319  | Synthetic<br>pyranopyridine                            | AcrB ( <i>E. coli</i> )   | Decreased MIC of Cip, Lev,<br>and Prl  | Docking<br>Time kill assay<br>Substrate accumulation<br>Effect on<br>outer-membrane<br>Effect on<br>inner-membrane                | Vargiu et al. (2014),<br>Opperman et al. (2014) |
| 2-substituted<br>benzothiazoles                                | Synthetic  | AdeABC<br>( <i>Acinetobacter<br/>baumannii</i> )                                  | Reduced MIC of cip   | Pharmacophore<br>hypothesis   | Yilmaz et al. (2014)                            |
| <b>Natural Compounds</b>                                       |  |   |  |   |   |
| EA-371α and EA-371δ  | <i>Streptomyces</i><br>MF-EA-371-NS1                   | MexAB-OprM<br>( <i>P. aeruginosa</i> )  | Reduce MIC of Lev  | Synergism<br>Substrate accumulation   | Lee et al. (2001)                               |
| Geraniol   | <i>Helichrysum italicum</i>                            | <i>E. coli</i><br><i>P. aeruginosa</i><br><i>A. baumannii</i>                     | Reduced MIC of β-lactams,<br>quinolones, and Cam   | Antibacterial<br>Synergism  | Lorenzi et al. (2009)                           |
| Plumbagin  | <i>Plumbago indica</i>                                 | AcrB ( <i>E. coli</i> )   | Reduced MIC of Ery, Cam,<br>TPP, SDS, tet<br>Inhibition of Nile Red efflux               | In silico screening<br>Antibacterial<br>Synergism<br>Non-substrate control<br>Inhibition of efflux<br>Effect on<br>outer-membrane | Ohene-Agyei et al.<br>(2014)                    |
| Nordihydroguaretic acid<br>(NDGA)                              | Creosote bush  | AcrB ( <i>E. coli</i> )   | Reduced MIC of Ery, Cam,<br>Nov, Tet, and TPP  |   |   |
| Shikonin   | <i>Lithospermum<br/>erythrorhizon</i>                  | AcrB ( <i>E. coli</i> )   | Reduced MIC of TPP   |   |   |
| (–)-epigallocatechin<br>gallate EGCG                           | Green tea  | <i>Campylobacter</i><br>spp.  | Reduced MIC to Ery and<br>Cip  | Antibacterial<br>Synergism  | Kurincic et al. (2012)                          |
| Curcumin   | <i>Curcuma longa</i><br>(Zingiberaceae)                | <i>P. aeruginosa</i>  | Reduced MIC Mem, Carb,<br>Caz, Gen, and Cip  | Antibacterial<br>Synergism  | Negi et al. (2014)                              |

(Continued)

**TABLE 1 | Continued**

| Compound   | Source  | Protein/<br>Organism   | Actions <sup>1</sup>  | Essays performed   | Reference                 |
|--|---|--|---|--|---------------------------|
| Lanatoside C and diadzein                            | Phytochemical                                   | AcrB, MexB<br>( <i>E. coli</i> ,<br><i>P. aeruginosa</i> )   | Reduced MIC of Lev and Carb<br>Increased accumulation of EtBr                               | High-throughput virtual screening<br>Synergism<br>Substrate accumulation | Aparna et al. (2014)      |
| 4-hydroxy- $\alpha$ -tetralone                       | <i>Ammannia</i> sp                              | <i>E. coli</i>   | Reduced MIC of Tet  | RT-PCR study<br><i>In silico</i> docking                                 | Dwivedi et al. (2014)     |
| <b>Non-antibacterial drugs</b>                       |   |  |   |  |                           |
| Trimethoprim and Epinephrine                         | Small heterocyclic or nitrogen-containing drugs | <i>S. typhimurium</i><br><i>E. cloacae</i><br><i>S. marcescens</i><br><i>P. aeruginosa</i><br><i>K. pneumoniae</i><br><i>E. coli</i> | Reduced MIC of Cip  | Antibacterial<br>Synergism<br>Substrate accumulation<br>Growth kinetics  | Piddock et al. (2010)     |
| Chlorpromazine, Amitriptyline, Trans-chlorprothixene | Non-antibiotic drugs                            | <i>P. aeruginosa</i>   | Reduced MIC of Pen, Cxm, and Tob  | Antibacterial<br>Synergism   | Kristiansen et al. (2010) |
| Sertraline   | Selective Serotonin Re-uptake Inhibitors        | AcrAB, AcrEF, MdtEF, and MexAB   | Inhibition of Nile Red efflux   | Inhibition of efflux<br>RT-PCR   | Bohnert et al. (2011)     |
| Artesunate   | Anti-malarial drug                              | AcrAB-TolC ( <i>E. coli</i> )  | Reduced MIC of $\beta$ -lactam antibiotic<br>Increased Dau uptake<br>Reduce mRNA expression | Antibacterial<br>Synergism<br>Substrate accumulation<br>RT-PCR           | Li et al. (2011)          |
| Pimozide   | Neuroleptic drug                                | AcrAB-TolC ( <i>E. coli</i> )  | Reduced MICs of Oxa and EtBr<br>Inhibition of Nile rRed efflux                              | Synergism<br>Substrate efflux  | Bohnert et al. (2013)     |

<sup>1</sup>Abbreviations used: Cam, Chloramphenicol; Carb, Carbanecillin; Caz, Ceftazidime; Cip, Ciprofloxacin; Clr, Clarithromycin; Cxm, Cefuroxime; Dau, Daunomycin; Ery, Erythromycin; EtBr, Ethidium Bromide; Gen, Gentamicin; Lev, Levofloxacin; Mem, Meropenem; Nal, Nalidixic acid; Nor, Norfloxacin; Oxa, Oxacillin; Pen, Penicillin; Prl, Piperacillin; Rif, Rifampicin; Spfx, Sparfloxacin; Tet, Tetracycline; Tob, Tobramycin; TPP, Triphenylphosphonium.

permeabilized the outer membrane (Lomovskaya et al., 2001). Derivatives of PA $\beta$ N with reduced toxicity, enhanced stability, and better solubility were developed and advanced to the pre-clinical stage, however, failed due to toxicity issues (Marquez, 2005; Lomovskaya et al., 2006; Lomovskaya and Zgurskaya, 2011; Bhardwaj and Mohanty, 2012).

The structural basis for the inhibition of the RND transporters has been recently described with the publication of the crystal structures of AcrB from *E. coli* and MexB from *P. aeruginosa* bound to a pyridopyrimidine derivative D13-D900 (Nakashima et al., 2013). The inhibitor binding almost overlapped with the binding of the substrates minocycline and doxorubicin, while part of the inhibitor inserted into a narrow phenylalanine rich region in the deep binding pocket, termed the hydrophobic trap by the authors. The authors suggested that the inhibitor competitively inhibit substrate binding and hinders the functional rotation of the efflux pumps.

As there is only one structure of a RND protein bound to an inhibitor published to date, docking, and molecular simulation studies were used to investigate the putative binding modes of other inhibitors such as PA $\beta$ N and NMP (Vargiu et al., 2014) while *in silico* screening also provided information on the binding of putative EPIS (Ohene-Agyei et al., 2014). Both PA $\beta$ N and NMP were predicted to interact with the switch

loop while D13-D900 and MBX2319 have more interactions with the hydrophobic trap first identified by Nakashima et al. (2013).

**Table 1** summarizes the compounds reported to act as EPIS against Gram-negative organisms so far. The term EPI is used loosely here as some of the included compounds were identified based on their synergism with one or more antibiotic while no further analysis was performed to study the mechanism of inhibition or rule out non-specific effects such as membrane permeabilization.

## Conclusion

There are various papers reporting the ability of crude extracts from plants or other organisms to reduce antibiotic resistance that were not dealt with in this review. As can be seen from **Table 1**, there is also a sizable amount of pure compounds which were able to synergise with antibiotics against drug resistant Gram-negative bacteria. However, the translation of these promising compounds into EPIS for clinical application is still lacking. The most probable reason for the discrepancies in lead compounds and final outcome is the deficiency of follow through from first identification of a compound with synergistic effects to identification of true EPI activity and providing a thorough

investigation into mechanism of action. With this review we aimed to summarize the current knowledge of how drug efflux can be inhibited.

The tools necessary to identify, test and characterize the mechanism of action of a putative EPI were also provided in order to aid the discovery and development of EPIs with which we would be able to stem the tide of multidrug resistant Gram-negative infections.

## References

- Amaral, L., Martins, A., Spengler, G., and Molnar, J. (2014). Efflux pumps of Gram-negative bacteria: what they do, how they do it, with what and how to deal with them. *Front. Pharmacol.* 4:168. doi: 10.3389/fphar.2013.00168
- Andersen, C., Koronakis, E., Hughes, C., and Koronakis, V. (2002). An aspartate ring at the TolC tunnel entrance determines ion selectivity and presents a target for blocking by large cations. *Mol. Microbiol.* 44, 1131–1139. doi: 10.1046/j.1365-2958.2002.02898.x
- Andrade, J. C., Moraes-Braga, M. F., Guedes, G. M., Tintino, S. R., Freitas, M. A., Menezes, I. R., et al. (2014). Enhancement of the antibiotic activity of aminoglycosides by alpha-tocopherol and other cholesterol derivates. *Biomed. Pharmacother.* 68, 1065–1069. doi: 10.1016/j.biopha.2014.10.011
- Aparna, V., Dineshkumar, K., Mohanalakshmi, N., Velmurugan, D., and Hopper, W. (2014). Identification of natural compound inhibitors for multidrug efflux pumps of *Escherichia coli* and *Pseudomonas aeruginosa* using *in silico* high-throughput virtual screening and *in vitro* validation. *PLoS ONE* 9:e101840. doi: 10.1371/journal.pone.0101840
- Bassetti, M., Merelli, M., Temperoni, C., and Astilean, A. (2013). New antibiotics for bad bugs: where are we? *Ann. Clin. Microbiol. Antimicrob.* 12, 22. doi: 10.1186/1476-0711-12-22
- Baugh, S., Ekanayaka, A. S., Piddock, L. J., and Webber, M. A. (2012). Loss of or inhibition of all multidrug resistance efflux pumps of *Salmonella enterica* serovar Typhimurium results in impaired ability to form a biofilm. *J. Antimicrob. Chemother.* 67, 2409–2417. doi: 10.1093/jac/dks228
- Baugh, S., Phillips, C. R., Ekanayaka, A. S., Piddock, L. J., and Webber, M. A. (2014). Inhibition of multidrug efflux as a strategy to prevent biofilm formation. *J. Antimicrob. Chemother.* 69, 673–681. doi: 10.1093/jac/dkt420
- Bhardwaj, A. K., and Mohanty, P. (2012). Bacterial efflux pumps involved in multidrug resistance and their inhibitors: rejuvenating the antimicrobial chemotherapy. *Recent Pat Antiinfect Drug Discov.* 7, 73–89. doi: 10.2174/157489112799829710
- Blair, J. M., Smith, H. E., Ricci, V., Lawler, A. J., Thompson, L. J., and Piddock, L. J. (2014). Expression of homologous RND efflux pump genes is dependent upon AcrB expression: implications for efflux and virulence inhibitor design. *J. Antimicrob. Chemother.* 70, 424–431. doi: 10.1093/jac/dku380
- Bohnert, J. A., Karamian, B., and Nikaido, H. (2010). Optimized Nile Red efflux assay of AcrAB-TolC multidrug efflux system shows competition between substrates. *Antimicrob. Agents Chemother.* 54, 3770–3775. doi: 10.1128/aac.00620-10
- Bohnert, J. A., Schuster, S., and Kern, W. V. (2013). Pimozone Inhibits the AcrAB-TolC Efflux Pump in *Escherichia coli*. *Open Microbiol. J.* 7, 83–86. doi: 10.2174/1874285801307010083
- Bohnert, J. A., Schuster, S., Seeger, M. A., Fahnrich, E., Pos, K. M., and Kern, W. V. (2008). Site-directed mutagenesis reveals putative substrate binding residues in the *Escherichia coli* RND efflux pump AcrB. *J. Bacteriol.* 190, 8225–8229. doi: 10.1128/jb.00912-08
- Bohnert, J. A., Szymaniak-Vits, M., Schuster, S., and Kern, W. V. (2011). Efflux inhibition by selective serotonin reuptake inhibitors in *Escherichia coli*. *J. Antimicrob. Chemother.* 66, 2057–2060. doi: 10.1093/jac/dkr258
- Bumann, D., and Valdivia, R. H. (2007). Identification of host-induced pathogen genes by differential fluorescence induction reporter systems. *Nat. Protoc.* 2, 770–777. doi: 10.1038/nprot.2007.78
- Bush, K., Courvalin, P., Dantas, G., Davies, J., Eisenstein, B., Huovinen, P., et al. (2011). Tackling antibiotic resistance. *Nat. Rev. Microbiol.* 9, 894–896. doi: 10.1038/nrmicro2693
- Butler, M. S., and Cooper, M. A. (2011). Antibiotics in the clinical pipeline in 2011. *J. Antibiot. (Tokyo)* 64, 413–425. doi: 10.1038/ja.2011.44
- Cha, H. J., Muller, R. T., and Pos, K. M. (2014). Switch-loop flexibility affects transport of large drugs by the promiscuous AcrB multidrug efflux transporter. *Antimicrob. Agents Chemother.* 58, 4767–4772. doi: 10.1128/aac.02733-13
- Chevalier, J., Bredin, J., Mahamoud, A., Mallea, M., Barbe, J., and Pages, J. M. (2004). Inhibitors of antibiotic efflux in resistant *Enterobacter aerogenes* and *Klebsiella pneumoniae* strains. *Antimicrob. Agents Chemother.* 48, 1043–1046. doi: 10.1128/AAC.48.3.1043-1046.2004
- Chuanchuen, R., Karkhoff-Schweizer, R. R., and Schweizer, H. P. (2003). High-level triclosan resistance in *Pseudomonas aeruginosa* is solely a result of efflux. *Am. J. Infect. Control* 31, 124–127. doi: 10.1067/mic.2003.11
- Delmar, J. A., Su, C. C., and Yu, E. W. (2014). Bacterial multidrug efflux transporters. *Annu. Rev. Biophys.* 43, 93–117. doi: 10.1146/annurev-biophys-051013-022855
- Du, D., Venter, H., Pos, K. M., and Luisi, B. F. (2013). “The machinery and mechanism of multidrug efflux in gram-negative bacteria,” in *Microbial Efflux Pumps: Current Research*, Chap. 3, eds E. W. Yu, Q. Zhang, and M. H. Brown (Ames, IA: Caister Academic Press), 35–48.
- Du, D., Wang, Z., James, N. R., Voss, J. E., Klimont, E., Ohene-Agyei, T., et al. (2014). Structure of the AcrAB-TolC multidrug efflux pump. *Nature* 509, 512–515. doi: 10.1038/nature13205
- Dwivedi, G. R., Upadhyay, H. C., Yadav, D. K., Singh, V., Srivastava, S. K., Khan, F., et al. (2014). 4-Hydroxy-alpha-tetralone and its derivative as drug resistance reversal agents in multi drug resistant *Escherichia coli*. *Chem. Biol. Drug Des.* 83, 482–492. doi: 10.1111/cbdd.12263
- Eicher, T., Brandstatter, L., and Pos, K. M. (2009). Structural and functional aspects of the multidrug efflux pump AcrB. *Biol. Chem.* 390, 693–699. doi: 10.1515/bc.2009.090
- Eicher, T., Cha, H. J., Seeger, M. A., Brandstatter, L., El-Delik, J., Bohnert, J. A., et al. (2012). Transport of drugs by the multidrug transporter AcrB involves an access and a deep binding pocket that are separated by a switch-loop. *Proc. Natl. Acad. Sci. U.S.A.* 109, 5687–5692. doi: 10.1073/pnas.1114944109
- Garvey, M. I., Rahman, M. M., Gibbons, S., and Piddock, L. J. (2011). Medicinal plant extracts with efflux inhibitory activity against Gram-negative bacteria. *Int. J. Antimicrob. Agents* 37, 145–151. doi: 10.1016/j.ijantimicag.2010.10.027
- Ghisalberti, D., Mahamoud, A., Chevalier, J., Baitiche, M., Martino, M., Pages, J. M., et al. (2006). Chloroquinolines block antibiotic efflux pumps in antibiotic-resistant *Enterobacter aerogenes* isolates. *Int. J. Antimicrob. Agents* 27, 565–569. doi: 10.1016/j.ijantimicag.2006.03.010
- Hay, T., Fraud, S., Lau, C. H., Gilmour, C., and Poole, K. (2013). Antibiotic inducibility of the mexXY multidrug efflux operon of *Pseudomonas aeruginosa*: involvement of the MexZ anti-repressor ArmZ. *PLoS ONE* 8:e56858. doi: 10.1371/journal.pone.0056858
- Hirakata, Y., Kondo, A., Hoshino, K., Yano, H., Arai, K., Hirotani, A., et al. (2009). Efflux pump inhibitors reduce the invasiveness of *Pseudomonas aeruginosa*. *Int. J. Antimicrob. Agents* 34, 343–346. doi: 10.1016/j.ijantimicag.2009.06.007
- Hirakata, Y., Sri Kumar, R., Poole, K., Gotoh, N., Suematsu, T., Kohno, S., et al. (2002). Multidrug efflux systems play an important role in the invasiveness of *Pseudomonas aeruginosa*. *J. Exp. Med.* 196, 109–118. doi: 10.1084/jem.20020005
- Hobbs, E. C., Yin, X., Paul, B. J., Astarita, J. L., and Storz, G. (2012). Conserved small protein associates with the multidrug efflux pump AcrB and differentially affects antibiotic resistance. *Proc. Natl. Acad. Sci. U.S.A.* 109, 16696–16701. doi: 10.1073/pnas.1210093109

## Acknowledgments

Work in HV's laboratory is funded by the University of South Australia, the Sansom Institute for Health Research and the Australian Research Council (Grant LE150100203 for screening of EPIs to HV). RM is the recipient of an Australian post-graduate award. HV and SM are co-recipients of a China–Australia Centre for Health Sciences Research Grant.

- Ikonomidis, A., Tsakris, A., Kanellopoulou, M., Maniatis, A. N., and Pournaras, S. (2008). Effect of the proton motive force inhibitor carbonyl cyanide-m-chlorophenylhydrazone (CCCP) on *Pseudomonas aeruginosa* biofilm development. *Lett. Appl. Microbiol.* 47, 298–302. doi: 10.1111/j.1472-765X.2008.02430.x
- Kern, W. V., Steinke, P., Schumacher, A., Schuster, S., von Baum, H., and Bohnert, J. A. (2006). Effect of 1-(1-naphthylmethyl)-piperazine, a novel putative efflux pump inhibitor, on antimicrobial drug susceptibility in clinical isolates of *Escherichia coli*. *J. Antimicrob. Chemother.* 57, 339–343. doi: 10.1093/jac/dki445
- Krishnamoorthy, G., Tikhonova, E. B., and Zgurskaya, H. I. (2008). Fitting periplasmic membrane fusion proteins to inner membrane transporters: mutations that enable *Escherichia coli* AcrA to function with *Pseudomonas aeruginosa* MexB. *J. Bacteriol.* 190, 691–698 doi: 10.1128/JB.01276-07
- Kristiansen, J. E., Thomsen, V. F., Martins, A., Viveiros, M., and Amaral, L. (2010). Non-antibiotics reverse resistance of bacteria to antibiotics. *In Vivo* 24, 751–754.
- Kurincic, M., Klancnik, A., and Smole Mozina, S. (2012). Effects of efflux pump inhibitors on erythromycin, ciprofloxacin, and tetracycline resistance in *Campylobacter* spp. isolates. *Microb. Drug Resist.* 18, 492–501. doi: 10.1089/mdr.2012.0017
- Lau, C. H., Krahn, T., Gilmour, C., Mullen, E., and Poole, K. (2014). AmgRS-mediated envelope stress-inducible expression of the mexXY multidrug efflux operon of *Pseudomonas aeruginosa*. *Microbiologyopen* 4, 121–135. doi: 10.1002/mbo3.226
- Lee, E. H., and Shafer, W. M. (1999). The farAB-encoded efflux pump mediates resistance of gonococci to long-chained antibacterial fatty acids. *Mol. Microbiol.* 33, 839–845. doi: 10.1046/j.1365-2958.1999.01530.x
- Lee, M. D., Galazzo, J. L., Staley, A. L., Lee, J. C., Warren, M. S., Fuernkranz, H., et al. (2001). Microbial fermentation-derived inhibitors of efflux-pump-mediated drug resistance. *Il Farmaco* 56, 81–85. doi: 10.1016/S0014-827X(01)01002-3
- Lennen, R. M., Politz, M. G., Kruziki, M. A., and Pfleger, B. F. (2013). Identification of transport proteins involved in free fatty acid efflux in *Escherichia coli*. *J. Bacteriol.* 195, 135–144. doi: 10.1128/jb.01477-12
- Li, B., Yao, Q., Pan, X. C., Wang, N., Zhang, R., Li, J., et al. (2011). Artesunate enhances the antibacterial effect of  $\beta$ -lactam antibiotics against *Escherichia coli* by increasing antibiotic accumulation via inhibition of the multidrug efflux pump system AcrAB-TolC. *J. Antimicrob. Chemother.* 66, 769–777. doi: 10.1093/jac/dkr017
- Lin, J., Cagliero, C., Guo, B., Barton, Y. W., Maurel, M. C., Payot, S., et al. (2005). Bile salts modulate expression of the CmeABC multidrug efflux pump in *Campylobacter jejuni*. *J. Bacteriol.* 187, 7417–7424. doi: 10.1128/jb.187.21.7417-7424.2005
- Lomovskaya, O., and Bostian, K. A. (2006). Practical applications and feasibility of efflux pump inhibitors in the clinic—vision for applied use. *Biochem. Pharmacol.* 71, 910–918. doi: 10.1016/j.bcp.2005.12.008
- Lomovskaya, O., Warren, M. S., Lee, A., Galazzo, J., Fronko, R., Lee, M., et al. (2001). Identification and characterization of inhibitors of multidrug resistance efflux pumps in *Pseudomonas aeruginosa*: novel agents for combination therapy. *Antimicrob. Agents Chemother.* 45, 105–116. doi: 10.1128/AAC.45.1.105-116.2001
- Lomovskaya, O., and Zgurskaya, H. I. (2011). *Efflux Pumps from Gram-negative Bacteria: From Structure and Function to Inhibition*. Norfolk, VA: Caister Academic press.
- Lomovskaya, O., Zgurskaya, H. I., Totrov, M., and Waitkins, W. J. (2006). Waltzing transporters and ‘the dance macabre’ between humans and bacteria. *Nat. Rev. Drug Discov.* 6, 56–65. doi: 10.1038/nrd2200
- Lorenzi, V., Muselli, A., Bernardini, A. F., Berti, L., Pages, J. M., Amaral, L., et al. (2009). Geraniol restores antibiotic activities against multidrug-resistant isolates from gram-negative species. *Antimicrob. Agents Chemother.* 53, 2209–2211. doi: 10.1128/aac.00919-08
- Mahamoud, A., Chevalier, J., Baitiche, M., Adam, E., and Pages, J. M. (2011). An alkylaminquinazoline restores antibiotic activity in Gram-negative resistant isolates. *Microbiology* 157(Pt. 2), 566–571. doi: 10.1099/mic.0.045716-0
- Mallea, M., Mahamoud, A., Chevalier, J., Alibert-Franco, S., Brouant, P., Barbe, J., et al. (2003). Alkylaminquinolines inhibit the bacterial antibiotic efflux pump in multidrug-resistant clinical isolates. *Biochem. J.* 376(Pt. 3), 801–805. doi: 10.1042/bj20030963
- Marquez, B. (2005). Bacterial efflux systems and efflux pumps inhibitors. *Biochimie* 87, 1137–1147. doi: 10.1016/j.biochi.2005.04.012
- Martinez, J. L., Sanchez, M. B., Martinez-Solano, L., Hernandez, A., Garmendia, L., Fajardo, A., et al. (2009). Functional role of bacterial multidrug efflux pumps in microbial natural ecosystems. *FEMS Microbiol. Rev.* 33, 430–449. doi: 10.1111/j.1574-6976.2008.00157.x
- Mima, T., Joshi, S., Gomez-Escalada, M., and Schweizer, H. P. (2007). Identification and characterization of TriABC-OpmH, a tricosan efflux pump of *Pseudomonas aeruginosa* requiring two membrane fusion proteins. *J. Bacteriol.* 189, 7600–7609. doi: 10.1128/JB.00850-07
- Misra, R., and Bavro, V. N. (2009). Assembly and transport mechanism of tripartite drug efflux systems. *Biochim. Biophys. Acta* 1794, 817–825. doi: 10.1016/j.bbapap.2009.02.017
- Murakami, S. (2008). Multidrug efflux transporter, AcrB—the pumping mechanism. *Curr. Opin. Struct. Biol.* 18, 459–465. doi: 10.1016/j.sbi.2008.06.007
- Murakami, S., Nakashima, R., Yamashita, E., Matsumoto, T., and Yamaguchi, A. (2006). Crystal structures of a multidrug transporter reveal a functionally rotating mechanism. *Nature* 443, 173–179. doi: 10.1038/nature05076
- Nakashima, R., Sakurai, K., Yamasaki, S., Hayashi, K., Nagata, C., Hoshino, K., et al. (2013). Structural basis for the inhibition of bacterial multidrug exporters. *Nature* 500, 102–106. doi: 10.1038/nature12300
- Nakashima, R., Sakurai, K., Yamasaki, S., Nishino, K., and Yamaguchi, A. (2011). Structures of the multidrug exporter AcrB reveal a proximal multisite drug-binding pocket. *Nature* 480, 565–569. doi: 10.1038/nature10641
- Negi, N., Prakash, P., Gupta, M. L., and Mohapatra, T. M. (2014). Possible role of curcumin as an efflux pump inhibitor in multi drug resistant clinical isolates of *Pseudomonas aeruginosa*. *J. Clin. Diagn. Res.* 8, Dc04–Dc07. doi: 10.7860/jcdr/2014/8329.4965
- Nikaido, H. (2011). Structure and mechanism of RND-type multidrug efflux pumps. *Adv. Enzymol. Relat. Areas Mol. Biol.* 77, 1–60. doi: 10.1002/9780470920541.ch1
- Nikaido, H., and Pages, J. M. (2012). Broad-specificity efflux pumps and their role in multidrug resistance of Gram-negative bacteria. *FEMS Microbiol. Rev.* 36, 340–363. doi: 10.1111/j.1574-6976.2011.00290.x
- Nikaido, H., and Takatsuka, Y. (2009). Mechanisms of RND multidrug efflux pumps. *Biochim. Biophys. Acta* 1794, 769–781. doi: 10.1016/j.bbapap.2008.10.004
- Ohene-Agyei, T., Lea, J. D., and Venter, H. (2012). Mutations in MexB that affect the efflux of antibiotics with cytoplasmic targets. *FEMS Microbiol. Lett.* 333, 20–27. doi: 10.1111/j.1574-6968.2012.02594.x
- Ohene-Agyei, T., Mowla, R., Rahman, T., and Venter, H. (2014). Phytochemicals increase the antibacterial activity of antibiotics by acting on a drug efflux pump. *Microbiologyopen* 3, 885–896. doi: 10.1002/mbo3.212
- Opperman, T. J., Kwasny, S. M., Kim, H. S., Nguyen, S. T., Houseweart, C., D’Souza, S., et al. (2014). Characterization of a novel pyranopyridine inhibitor of the AcrAB efflux pump of *Escherichia coli*. *Antimicrob. Agents Chemother.* 58, 722–733. doi: 10.1128/aac.01866-13
- Orhan, G., Bayram, A., Zer, Y., and Balci, I. (2005). Synergy tests by E test and checkerboard methods of antimicrobial combinations against *Brucella melitensis*. *J. Clin. Microbiol.* 43, 140–143. doi: 10.1128/jcm.43.1.140-143.2005
- Phillips, J. L., and Gnanakan, S. (2015). A data-driven approach to modeling the tripartite structure of multidrug resistance efflux pumps. *Proteins* 83, 46–65. doi: 10.1002/prot.24632
- Piddock, L. J. (2006a). Clinically relevant chromosomally encoded multidrug resistance efflux pumps in bacteria. *Clin. Microbiol. Rev.* 19, 382–402. doi: 10.1128/cmr.19.2.382-402.2006
- Piddock, L. J. (2006b). Multidrug-resistance efflux pumps? Not just for resistance. *Nat. Rev. Microbiol.* 4, 629–636. doi: 10.1038/nrmicro1464
- Piddock, L. J. (2014). Understanding the basis of antibiotic resistance: a platform for drug discovery. *Microbiology* 160, 2366–2373. doi: 10.1099/mic.0.082412-0
- Piddock, L. J., Garvey, M. I., Rahman, M. M., and Gibbons, S. (2010). Natural and synthetic compounds such as trimethoprim behave as inhibitors of efflux in Gram-negative bacteria. *J. Antimicrob. Chemother.* 65, 1215–1223. doi: 10.1093/jac/dkq079
- Poole, K. (2004). Efflux-mediated multiresistance in Gram-negative bacteria. *Clin. Microbiol. Infect.* 10, 12–26. doi: 10.1111/j.1469-0691.2004.00763.x
- Poole, K. (2005). Efflux-mediated antimicrobial resistance. *J. Antimicrob. Chemother.* 56, 20–51. doi: 10.1093/jac/dki71
- Poole, K. (2011). *Pseudomonas aeruginosa*: resistance to the max. *Front. Microbiol.* 2:65. doi: 10.3389/fmicb.2011.00065

- Pos, K. M. (2009). Drug transport mechanism of the AcrB efflux pump. *Biochim. Biophys. Acta* 1794, 782–793. doi: 10.1016/j.bbapap.2008.12.015
- Pumbwe, L., Wareham, D., Aduse-Opoku, J., Brazier, J., and Wexler, H. (2007). Genetic analysis of mechanisms of multidrug resistance in a clinical isolate of *Bacteroides fragilis*. *Clin. Microbiol. Infect.* 13, 183–189. doi: 10.1111/j.1469-0691.2006.01620.x
- Pursell, A., and Poole, K. (2013). Functional characterization of the NfxB repressor of the mexCD-oprJ multidrug efflux operon of *Pseudomonas aeruginosa*. *Microbiology* 159(Pt. 10), 2058–2073. doi: 10.1099/mic.0.069286-0
- Ramos, J. L., Duque, E., Gallegos, M.-T., Godoy, P., Ramos-González, M. I., Rojas, A., et al. (2002). Mechanisms of solvent tolerance in gram-negative bacteria. *Ann. Rev. Microbiol.* 56, 743–768. doi: 10.1146/annurev.micro.56.012302.161038
- Ricci, V., Busby, S. J., and Piddock, L. J. (2012). Regulation of RamA by RamR in *Salmonella enterica* serovar Typhimurium: isolation of a RamR superrepressor. *Antimicrob. Agents Chemother.* 56, 6037–6040. doi: 10.1128/aac.01320-12
- Ricci, V., Tzakas, P., Buckley, A., and Piddock, L. J. (2006). Ciprofloxacin-resistant *Salmonella enterica* serovar Typhimurium strains are difficult to select in the absence of AcrB and TolC. *Antimicrob. Agents Chemother.* 50, 38–42. doi: 10.1128/aac.50.1.38-42.2006
- Rice, A., Liu, Y., Michaelis, M. L., Himes, R. H., Georg, G. I., and Audus, K. L. (2005). Chemical modification of paclitaxel (Taxol) reduces P-glycoprotein interactions and increases permeation across the blood-brain barrier in vitro and in situ. *J. Med. Chem.* 48, 832–838. doi: 10.1021/jm040114b
- Rosenberg, E. Y., Bertenthal, D., Nilles, M. L., Bertrand, K. P., and Nikaido, H. (2003). Bile salts and fatty acids induce the expression of *Escherichia coli* AcrB multidrug efflux pump through their interaction with Rob regulatory protein. *Mol. Microbiol.* 48, 1609–1619. doi: 10.1046/j.1365-2958.2003.03531.x
- Roth, B. L., Poot, M., Yue, S. T., and Millard, P. J. (1997). Bacterial viability and antibiotic susceptibility testing with SYTOX green nucleic acid stain. *Appl. Environ. Microbiol.* 63, 2421–2431.
- Ruggerone, P., Murakami, S., Pos, K. M., and Vargiu, A. V. (2013a). RND efflux pumps: structural information translated into function and inhibition mechanisms. *Curr. Top. Med. Chem.* 13, 3079–3100. doi: 10.2174/15680266113136660220
- Ruggerone, P., Vargiu, A. V., Collu, F., Fischer, N., and Kandt, C. (2013b). Molecular dynamics computer simulations of multidrug RND efflux pumps. *Comput. Struct. Biotechnol. J.* 5:e201302008. doi: 10.5936/csbj.201302008
- Sanchez, P., Moreno, E., and Martinez, J. L. (2005). The biocide triclosan selects *Stenotrophomonas maltophilia* mutants that overproduce the SmeDEF multidrug efflux pump. *Antimicrob. Agents Chemother.* 49, 781–782. doi: 10.1128/AAC.49.2.781-782.2005
- Seeger, M. A., Diederichs, K., Eicher, T., Brandstatter, L., Schiefner, A., Verrey, F., et al. (2008a). The AcrB efflux pump: conformational cycling and peristalsis lead to multidrug resistance. *Curr. Drug Targets* 9, 729–749. doi: 10.2174/138945008785747789
- Seeger, M. A., von Ballmoos, C., Eicher, T., Brandstatter, L., Verrey, F., Diederichs, K., et al. (2008b). Engineered disulfide bonds support the functional rotation mechanism of multidrug efflux pump AcrB. *Nat. Struct. Mol. Biol.* 15, 199–205. doi: 10.1038/nsmb.1379
- Seeger, M. A., Schiefner, A., Eicher, T., Verrey, F., Diederichs, K., and Pos, K. M. (2006). Structural asymmetry of AcrB trimer suggests a peristaltic pump mechanism. *Science* 313, 1295–1298. doi: 10.1126/science.1131542
- Segura, A., Molina, L., Fillet, S., Krell, T., Bernal, P., Muñoz-Rojas, J., et al. (2012). Solvent tolerance in gram-negative bacteria. *Curr. Opin. Biotechnol.* 23, 415–421. doi: 10.1016/j.copbio.2011.11.015
- Silver, S., and Phung, L. T. (1996). Bacterial heavy metal resistance: new surprises. *Ann. Rev. Microbiol.* 50, 753–789. doi: 10.1146/annurev.micro.50.1.753
- Starr, L. M., Fruci, M., and Poole, K. (2012). Pentachlorophenol induction of the *Pseudomonas aeruginosa* mexAB-oprM efflux operon: involvement of repressors NalC and MexR and the antirepressor ArmR. *PLoS ONE* 7:e32684. doi: 10.1371/journal.pone.0032684
- Tegos, G., Stermitz, F. R., Lomovskaya, O., and Lewis, K. (2002). Multidrug pump inhibitors uncover remarkable activity of plant antimicrobials. *Antimicrob. Agents Chemother.* 46, 3133–3141. doi: 10.1128/AAC.46.10.3133-3141.2002
- Tikhonova, E. B., Yamada, Y., and Zgurskaya, H. I. (2011). Sequential mechanism of assembly of multidrug efflux pump AcrAB-TolC. *Chem. Biol.* 18, 454–463. doi: 10.1016/j.chembiol.2011.02.011
- Vargiu, A. V., Ruggerone, P., Opperman, T. J., Nguyen, S. T., and Nikaido, H. (2014). Molecular mechanism of MBX2319 inhibition of *Escherichia coli* AcrB multidrug efflux pump and Comparison with other inhibitors. *Antimicrob. Agents Chemother.* 58, 6224–6234. doi: 10.1128/aac.03283-14
- Venter, H., Shilling, R. A., Velamakanni, S., Balakrishnan, L., and Van Veen, H. W. (2003). An ABC transporter with a secondary-active multidrug translocator domain. *Nature* 426, 866–870. doi: 10.1038/nature02173
- Walmsley, A. R., and Rosen, B. P. (2009). *Transport Mechanisms of Resistance to Drugs and Toxic Metals Antimicrobial Drug Resistance*. Berlin: Springer, 111–120. doi: 10.1007/978-1-59745-180-2\_10
- Wehmeier, C., Schuster, S., Fahnerich, E., Kern, W. V., and Bohnert, J. A. (2009). Site-directed mutagenesis reveals amino acid residues in the *Escherichia coli* RND efflux pump AcrB that confer macrolide resistance. *Antimicrob. Agents Chemother.* 53, 329–330. doi: 10.1128/aac.00921-08
- Welch, A., Awah, C. U., Jing, S., van Veen, H. W., and Venter, H. (2010). Promiscuous partnering and independent activity of MexB, the multidrug transporter protein from *Pseudomonas aeruginosa*. *Biochem. J.* 430, 355–364. doi: 10.1042/BJ20091860
- White, D. G., Goldman, J. D., Demple, B., and Levy, S. B. (1997). Role of the acrAB locus in organic solvent tolerance mediated by expression of marA, soxS, or robA in *Escherichia coli*. *J. Bacteriol.* 179, 6122–6126.
- WHO. (2014). *Antimicrobial Resistance: Global Report on Surveillance 2014*. Available at: www.who.int/drugresistance/documents/surveillancereport/en/
- Wilke, M. S., Heller, M., Creagh, A. L., Haynes, C. A., McIntosh, L. P., Poole, K., et al. (2008). The crystal structure of MexR from *Pseudomonas aeruginosa* in complex with its antirepressor ArmR. *Proc. Natl. Acad. Sci. U.S.A.* 105, 14832–14837. doi: 10.1073/pnas.0805489105
- Wong, K., Ma, J., Rothnie, A., Biggin, P. C., and Kerr, I. D. (2014). Towards understanding promiscuity in multidrug efflux pumps. *Trends Biochem. Sci.* 39, 8–16. doi: 10.1016/j.tibs.2013.11.002
- Yilmaz, S., Altinkanat-Gelmez, G., Bolelli, K., Guneser-Merdan, D., Over-Hasdemir, M. U., Yildiz, I., et al. (2014). Pharmacophore generation of 2-substituted benzothiazoles as AdeABC efflux pump inhibitors in *A. baumannii*. *SAR QSAR Environ. Res.* 25, 551–563. doi: 10.1080/1062936x.2014.919357
- Zeng, B., Wang, H., Zou, L., Zhang, A., Yang, X., and Guan, Z. (2010). Evaluation and target validation of indole derivatives as inhibitors of the AcrAB-TolC efflux pump. *Biosci. Biotechnol. Biochem.* 74, 2237–2241. doi: 10.1271/bbb.100433
- Zhang, Q., Lambert, G., Liao, D., Kim, H., Robin, K., Tung, C. K., et al. (2011). Acceleration of emergence of bacterial antibiotic resistance in connected microenvironments. *Science* 333, 1764–1767. doi: 10.1126/science.1208747
- Zgurskaya, H. I., Krishnamoorthy, G., Ntreh, A., and Lu, S. (2011). Mechanism and function of the outer membrane channel tolC in multidrug resistance and physiology of enterobacteria. *Front. Microbiol.* 2:189. doi: 10.3389/fmicb.2011.00189

**Conflict of Interest Statement:** The authors declare that the research was conducted in the absence of any commercial or financial relationships that could be construed as a potential conflict of interest.

Copyright © 2015 Venter, Mowla, Ohene-Agyei and Ma. This is an open-access article distributed under the terms of the Creative Commons Attribution License (CC BY). The use, distribution or reproduction in other forums is permitted, provided the original author(s) or licensor are credited and that the original publication in this journal is cited, in accordance with accepted academic practice. No use, distribution or reproduction is permitted which does not comply with these terms.

# Recent advances toward a molecular mechanism of efflux pump inhibition

Timothy J. Opperman\* and Son T. Nguyen

Microbiotix, Inc., Worcester, MA, USA

## OPEN ACCESS

**Edited by:**

Keith Poole,  
Queen's University, Canada

**Reviewed by:**

Helen Zgurskaya,  
University of Oklahoma, USA

Rajeev Misra,  
Princeton University, USA

**\*Correspondence:**

Timothy J. Opperman,  
Microbiotix, Inc., One Innovation  
Drive, Worcester, MA 01605, USA  
toperman@microbiotix.com

**Specialty section:**

This article was submitted to  
Antimicrobials, Resistance  
and Chemotherapy,  
a section of the journal  
*Frontiers in Microbiology*

**Received:** 02 March 2015

**Paper pending published:**  
23 March 2015

**Accepted:** 21 April 2015

**Published:** 05 May 2015

**Citation:**

Opperman TJ and Nguyen ST (2015)  
Recent advances toward a molecular  
mechanism of efflux pump inhibition.  
*Front. Microbiol.* 6:421.  
doi: 10.3389/fmicb.2015.00421

Multidrug resistance (MDR) in Gram-negative pathogens, such as the Enterobacteriaceae and *Pseudomonas aeruginosa*, poses a significant threat to our ability to effectively treat infections caused by these organisms. A major component in the development of the MDR phenotype in Gram-negative bacteria is overexpression of Resistance-Nodulation-Division (RND)-type efflux pumps, which actively pump antibacterial agents and biocides from the periplasm to the outside of the cell. Consequently, bacterial efflux pumps are an important target for developing novel antibacterial treatments. Potent efflux pump inhibitors (EPIs) could be used as adjunctive therapies that would increase the potency of existing antibiotics and decrease the emergence of MDR bacteria. Several potent inhibitors of RND-type efflux pump have been reported in the literature, and at least three of these EPI series were optimized in a pre-clinical development program. However, none of these compounds have been tested in the clinic. One of the major hurdles to the development of EPIs has been the lack of biochemical, computational, and structural methods that could be used to guide rational drug design. Here, we review recent reports that have advanced our understanding of the mechanism of action of several potent EPIs against RND-type pumps.

**Keywords:** efflux pump inhibitor, mechanism of action, RND family pumps, AcrB, AcrD, MexB, *Escherichia coli*, *Pseudomonas aeruginosa*

## Introduction

The rise of multidrug resistant (MDR) Gram-negative pathogens poses a significant clinical problem. Apart from the acquisition of acquired resistance traits, such as transposons and plasmids encoding proteins that inactivate antibiotics, many of these organisms have increased resistance resulting from mutations that alter the expression of genes that are involved in intrinsic resistance to antibiotics (Nikaido and Pages, 2012). One of the major contributors to intrinsic resistance in Gram-negative bacteria are efflux pumps of the Resistance-Nodulation-Division (RND) family efflux in Gram-negative bacteria, which extrude a broad spectrum of antibiotics and biocides, including the fluoroquinolones (e.g., ciprofloxacin and levofloxacin),  $\beta$ -lactams (e.g., piperacillin, meropenem, and aztreonam; Piddock, 2006), tetracyclines (minocycline), oxazolidinones (linezolid), and  $\beta$ -lactamase inhibitors (e.g., clavulanate and sulbactam; Li et al., 1998; Nakae et al., 2000), from the periplasm to the outside of the cell. Because of their broad-substrate specificity, overexpression of the RND efflux pumps results in decreased susceptibility to diverse array of antibacterial agents and biocides (Nikaido and Pages, 2012). In addition, elimination of RND pumps in *Pseudomonas aeruginosa* by genetic deletion (Lomovskaya et al., 1999) or inhibition with a potent efflux pump inhibitor (EPI; Lomovskaya et al., 2001) decreases the frequency of resistance to levofloxacin.

In *Escherichia coli*, a functional RND pump (AcrAB-TolC) is required for the selection of mutations in the targets of fluoroquinolones (*gyrA* and *gyrB*) that give rise to fluoroquinolone resistance (Singh et al., 2012). Furthermore, RND pumps have been shown to play a role in virulence of the enteric pathogen *Salmonella enterica* serovar Typhimurium (Nishino et al., 2006), and EPIs that target RND pumps have been shown to inhibit biofilm formation in *E. coli* and *Klebsiella pneumoniae* (Kvist et al., 2008). Therefore, EPIs could be useful as adjunctive therapies with an antibiotic to improve antibacterial potency at low antibiotic concentrations, reduce the emergence of resistance, inhibit biofilm formation, and decrease virulence of enteric pathogens. Consequently, there has been considerable interest in developing EPIs of the RND family pumps.

Several potent EPIs that target the RND family pumps have been described in the literature (Van Bambeke et al., 2006), however, none have reached clinical development. A family of peptidomimetics, including PA $\beta$ N (MC-207 110), that exhibited potent inhibition of efflux pumps in *P. aeruginosa* has been developed for use as an adjunctive therapy (Renau et al., 1999, 2001, 2002, 2003; Lomovskaya et al., 2001; Watkins et al., 2003). Some of these inhibitors were validated using *in vivo* infection models (Renau et al., 1999, 2001; Watkins et al., 2003), however, they were abandoned because of toxicity (Lomovskaya and Bostian, 2006). The positive charged moieties that were required for activity in *P. aeruginosa* caused nephrotoxicity. In addition, a series of pyridopyrimidine EPIs that are specific for the MexAB efflux pump of *P. aeruginosa* was advanced to the preclinical stage (Nakayama et al., 2003a,b, 2004a,b; Yoshida et al., 2006a,b, 2007). However, the development of this series appears to have been halted. Finally, a pyranopyridine EPI, MBX2319, with potent activity against Enterobacteriaceae, but low activity vs. *P. aeruginosa*, has been described recently (Opperman et al., 2014). This compound is in the early stages of lead optimization and has not been tested for efficacy in animal models of infection. The difficulties encountered during the development of these varied classes of EPIs underscore some of the most significant challenges for developing EPIs for clinical use: potency, spectrum of activity, pharmacokinetics, and toxicity. Detailed knowledge of the mode of inhibition and the binding site of an EPI could facilitate the rational design of analogs with properties that could address these challenges.

There are significant challenges to mechanism of action (MOA) studies for EPIs vs. the RND family efflux pumps, many of which complicate their discovery and development. One of the major challenges is the structural complexity of the RND pumps, which are an integral membrane (IM) molecular machine that spans the inner membrane, periplasmic space, and the outer membrane. The RND family efflux pumps comprise a tripartite structure, consisting of an IM efflux transporter with broad-substrate specificity, an outer membrane channel that carries substrates from the pump through the outer membrane, and a periplasmic adapter protein. The major RND pumps in *E. coli* and *P. aeruginosa* are AcrAB-TolC and MexAB-OprM, respectively; AcrB/MexB are the IM pumps, AcrA/MexA are the membrane adapter protein, and TolC/OprM form the channel through the outer membrane. The pump subunits (AcrB and MexB) consist

of the following domains: (1) an IM domain comprised of 12 transmembrane helices that utilizes proton-motive force to drive the pumping action; (2), a porter domain comprised of the two large periplasmic loops that binds and extrudes substrates, and (3) a cap domain that binds to TolC [reviewed in Blair and Piddock (2009), Eicher et al. (2009), Pos (2009), Nikaido and Pages (2012)]. The three-dimensional structure of AcrB was first described as a symmetrical trimer, in which all subunits were in the same conformation (Murakami et al., 2002). Subsequently, an asymmetrical three-dimensional structure of AcrB was described (Murakami et al., 2006; Seeger et al., 2006; Sennhauser et al., 2007), in which the conformation of each subunit was different. Several lines of evidence indicate that the asymmetrical structure represents the biologically relevant form of the pump (Seeger et al., 2008; Takatsuka and Nikaido, 2009; Eicher et al., 2014). The conformations of the three subunits of the pump have been described as the Access (loose), Binding (tight), and Extrusion (open) subunits. The current model for the mechanism of the RND pumps is that each conformation represents a distinct step in the translocation pathway, in which each subunit successively assumes each of the conformations as substrates first interact with the pump in the Access conformation, are moved to the substrate binding pocket in the Binding conformation, and are then extruded into a central channel that leads to TolC as the binding pocket collapses en route to the Extrusion conformation. The entire process is driven by proton-motive force that is transduced by the IM domain of the protein (Su et al., 2006; Seeger et al., 2009; Takatsuka and Nikaido, 2009).

Of particular interest to the design of EPIs is the structure of the substrate binding pocket in the Binding protomer, also known as the distal binding site. The broad-substrate specificity of AcrB and MexB suggested that the substrate binding site would exhibit unique features that enable polyspecific, but not non-specific, binding of substrates. The substrate binding pocket was clearly defined when the three-dimensional structures of the asymmetric AcrB trimer with two pump substrates, minocycline and doxorubicin, bound to the Binding protomer were reported (Murakami et al., 2006). The substrate binding pocket comprised a large cavity lined with hydrophobic (Phe136 and Phe178, Phe610, Phe615, Phe617, and Phe628) and polar residues (Asn274 and Gln176). Minocycline and doxorubicin interacted with a distinct set of amino acid residues that line the deep binding pocket in the “Binding” subunit. Both compounds interacted mainly with hydrophobic residues through Van der Waals and ring-stacking interactions, and made hydrogen bonding interactions with the polar residues. However, minocycline and doxorubicin bound to slightly different regions of the binding pocket. Thus, the structure of the binding pocket with substrates explains the broad-substrate specificity of the pump, which is characterized by interactions based on generalized physical properties, such as hydrophobicity, and low binding affinities. Consequently, developing inhibitors that can bind to this site with high affinity is a major challenge.

Despite complexities of the RND family pumps, progress toward a better understanding of the MOA of several EPIs has been made on several fronts. In this article, we will review two aspects of the MOA studies of the major EPIs. Thus, the review

will be divided in two parts. First, we will review the various technologies that have been used to study the structure and function of RND family efflux pumps and how they have been, or could be applied to study the mechanism of EPIs. The technologies that will be discussed include genetic, biochemical, structural, and computational approaches. Second, we will review the major classes of EPIs in terms of their biological activities, stage of development, and what is known about their MOA, including at least three important developments. These include the first crystal structure of an EPI bound to two RND pumps (Nakashima et al., 2013), the first report of EPI-resistant mutants that map to the binding site of AcrB (Schuster et al., 2014), and the application of molecular dynamic (MD) simulations to model the binding sites of other EPIs (Vargiu and Nikaido, 2012; Vargiu et al., 2014).

## Approaches to Study the Mechanism of Action of EPIs

### Genetic Studies

The classic method for identifying the molecular target of an antibacterial agent is the select for resistant mutants and to map the mutations to the putative target. However, in the case of EPIs, this approach has proven to be very difficult for the following reasons. Because the majority of EPIs do not exhibit antibacterial activity, resistant mutants cannot be selected directly. Instead, mutants resistant to the EPI must be selected in the presence of an antibiotic or biocide that is a substrate of the pump, which provides the selective pressure. The selection for EPI-resistant mutants usually consists of an EPI and antibiotic at concentrations that would enable growth if a mutation resulted in resistance to the EPI. This selection scheme creates two problems. First, since the EPI and the antibiotic bind to the substrate binding pocket, it is possible that mutations result in decreased affinity for the EPI also reduce affinity for the antibiotic. This is particularly problematic for EPIs that are pump substrates or competitive inhibitors that bind to the same or an overlapping site in the binding pocket. Second, the presence of an antibiotic in the selection results in a high background of mutants with decreased susceptibility to the antibiotic due to mutations in genes that encode the antibiotic target or another intrinsic resistance mechanism, such as antibiotic influx (porin). Third, if EPI-resistant mutants are obtained in such a screen, they may be specific for the antibiotic used for selection. Finally, it is likely that the structure of the substrate binding pocket of the RND family pumps, which is large and contains potentially overlapping binding sites, decreases the probability of identifying resistant mutants. Indeed, site-directed mutations affecting the residues that were shown to interact with minocycline or doxorubicin in co-crystal structures do not significantly affect the minimal inhibitory concentrations (MICs) for these drugs, suggesting a plasticity in their interactions with the substrate binding pocket (Bohnert et al., 2008). Consequently, there have been no reports of the isolation of spontaneous EPI-resistant mutations in RND-family pumps (Lomovskaya and Bostian, 2006).

Site-directed mutagenesis and construction of hybrid pumps were used to map the substrate binding domain and the determinants of binding specificity. To map the substrate binding sites and determinants of substrate specificity, Elkins and Nikaido (2002) constructed chimeric pumps in which the periplasmic loops of AcrD and AcrB were replaced with the corresponding loops of AcrB and AcrD, respectively. The resulting chimeras exhibited the substrate specificities characteristic of the pump that was the source of the periplasmic loops, indicating that the functions of substrate binding and specificity reside in the periplasmic loops. The exchange of periplasmic loops between the following AcrB homologs yielded similar results: *P. aeruginosa* MexB and MexY (Eda et al., 2003), and AcrB and MexB (Tikhonova et al., 2002). Mao et al. (2002) selected mutants of AcrD with expanded substrate recognition, which mapped to the periplasmic loops comprising the porter domain. Kobayashi et al. (2014) replaced portions of the access binding site of AcrB with corresponding non-conserved portions of AcrD to identify residues that are responsible for the selectivity of AcrD for anionic  $\beta$ -lactam antibiotics, such as aztreonam, carbenicillin, and sulbenicillin. Building on the results of these studies, the authors used site-directed mutagenesis to construct an AcrB pump that conferred high-level resistance to anionic  $\beta$ -lactam antibiotics, a characteristic of AcrD. In addition, site-directed mutants of AcrB have been constructed to map residues in the deep binding pocket that play a key role in substrate recognition and extrusion (Bohnert et al., 2008). However, these types of experiments have not been used to determine residues important for the binding of EPIs.

In contrast, mutations responsible for EPI resistance were identified in *bmr*, a broad-substrate specificity efflux pump in *Bacillus subtilis* of the major facilitator superfamily (MFS), that reduced affinity for an inhibitor (reserpine), but did not affect affinity for the substrate (ethidium bromide; Ahmed et al., 1993). This was accomplished by randomly mutagenizing a strain carrying a plasmid-encoded copy of *bmr*, followed by a selection for mutants consisting of a serial passage in the presence of ethidium bromide and increasing concentrations of reserpine. The mutations were mapped to *bmr* and resulted in substitution of Val296 with Leu. The mutation reduced the affinity of reserpine for Bmr, but did not affect the efflux of ethidium bromide. It is not clear whether this mutation directly affects binding site or causes change in conformation that affects binding at a distance. Since the three-dimensional structure of *bmr* is not known, and the substrate binding site has not been identified, it is difficult to determine the significance of the resistance mutation. Nevertheless, this study demonstrated that it is possible to generate and select mutants in an efflux pump gene with reduced susceptibility to an EPI.

The isolation of the first EPI-resistance mutations in an RND-family pump was reported more than 20 years after the *bmr* resistance mutations were reported. After attempts to isolate mutants in *E. coli* that were resistant to 1-(1-naphthylmethyl)-piperazine (NMP) and PA $\beta$ N in a serial passage experiment, Schuster et al. (2014) randomly mutagenized the two large periplasmic loops of AcrB using error-prone PCR. They selected for mutants resistant to NMP and PA $\beta$ N in combination with

linezolid or clarithromycin, respectively, in a single step selection on agar plates. The authors isolated several mutants with reduced susceptibility to NMP that did not decrease the efflux activity of AcrB. When the NMP-resistant mutations were reconstructed using site-directed mutagenesis (alone and together), only a double mutant, in which Gly141 was substituted with Asp (G141D) and Asn282 was substituted with Tyr (N282Y), significantly affected susceptibility to NMP. As shown in **Figures 1A,B**, the mutated residues are located near the outer face of the distal substrate binding pocket near Phe610, which plays an key role in the extrusion process (Bohnert et al., 2008), and is across from the so-called “switch-loop” that separates the proximal (access) and the distal (substrate) binding sites (Nakashima et al., 2011; Eicher et al., 2012). The authors speculated that the G141D N282Y amino acid substitutions prevent the binding of NMP to the distal binding pocket. However, the substituted residues are not near the binding site of NMP that has been predicted by computational methods (Vargiu et al., 2014; see **Figure 1A**, and below for discussion), suggesting that the mutated residues may interfere with the action of NMP through an alternative mechanism. Interestingly, the mutated residues reduce susceptibility to NMP in the presence of linezolid only, the antibiotic used for selection. This strongly suggests that EPI-resistant mutants isolated in this type of screen are specific to the antibiotic used for the selection, and that the location of the substituted residues cannot be directly interpreted as being part of the EPI binding site. Because it is not known whether the NMP-resistant mutant of AcrB has decreased affinity for NMP, it is possible that the G141D N282Y amino acid substitutions enable the extrusion of linezolid while NMP is bound to the deep binding pocket. Further experiments are needed to fully understand the significance of this EPI-resistant mutant.

Consistent with the experience of other groups, Schuster et al. (2014) were unable to isolate mutants with reduced susceptibility to PA $\beta$ N, a substrate for RND-family pumps (Lomovskaya et al.,

2001; Bohnert et al., 2008). For EPIs that are substrates or competitive inhibitors, mutations that alter the binding site of the EPI may also affect the affinity for substrates, which could result in cell death if an antibiotic is used for selection. In addition, the plasticity of the binding site (see above) may also affect EPIs that are substrates. Although there are only two examples, it is tempting to speculate that there is a correlation between the mode of inhibition of an EPI and whether it is possible to isolate EPI-resistant mutations that map to the RND pump.

## Biochemical Studies

As mentioned above, the RND pumps are complex IM machines, which complicate the biochemical analysis of these proteins. Nevertheless, the development and use of biochemical systems for the study of the RND pumps have been reported, however, none have been used to analyze the mode of inhibition of EPIs. These studies are summarized below.

## Enzyme Activity Assays

Zgurskaya and Nikaido (1999) reported a biochemical system in which purified AcrB was reconstituted into proteoliposomes. Fluorescent derivatives of the lipids phosphatidylethanolamine labeled with NBD or rhodamine, which are AcrB substrates, were incorporated into proteoliposomes at concentrations high enough to for NBD fluorescence to be quenched by rhodamine. To prevent reincorporation of the substrate into proteoliposome, unlabeled liposomes were added the reaction mixture to act as lipid traps for labeled lipid substrate. Therefore, efflux activity results in an increase in the fluorescence of NBD. The efflux activity was dependent on the presence of a transmembrane proton gradient, and was stimulated by addition of AcrA through an unknown mechanism. The addition of known pump substrates inhibited efflux of labeled lipids through competition. The bile salts taurocholate and glycocholate were the strongest inhibitors, with IC<sub>50</sub> values ranging between 15 and 20  $\mu$ M. While this

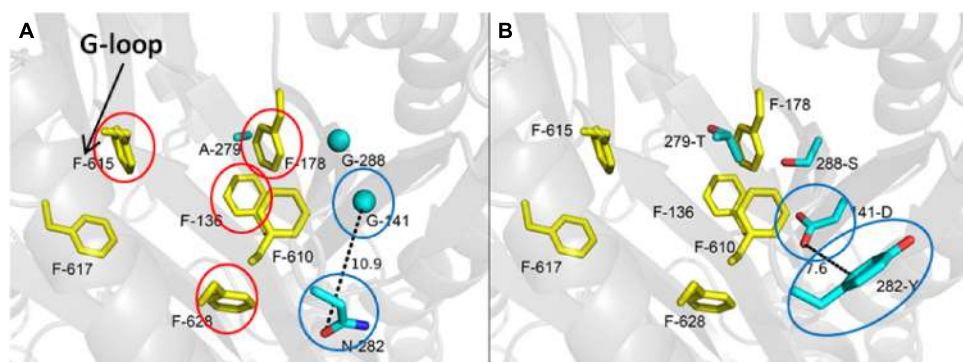


**FIGURE 1 |** The most frequently selected mutations that were isolated after *in vitro* random mutagenesis of the periplasmic domain of AcrB and linezolid/NMP selection are located in the distal binding pocket. **(A)** The wild type distal binding pocket of AcrB. The side chains of the wild-type residues that are substituted in the NMP-resistant mutant are shown as cyan sticks (glycines as cyan spheres), and distal binding pocket phenylalanine side chains are shown as yellow sticks. The view of the distal binding pocket is a side view from the periplasmic outer

face. The residues indicated with red circles are predicted to interact with NMP my molecular dynamic simulations (Vargiu et al., 2014). The location of the G-loop is indicated by the arrow. The residues indicated by the blue circles are those substituted in the G141D N282Y double mutant, which exhibits the strongest NMP-resistant phenotype. **(B)** The NMP-resistant distal binding pocket of AcrB. The residues indicated by the blue circles are those of the G141D N282Y double mutant. Reprinted with permission from Schuster et al. (2014).

biochemical system is amenable for the study of EPIs, it does not appear that this system has been used for this purpose. The reasons for this are not known. However, it is possible that there has been little interest in such assays, or that the assay is too difficult to implement.

### Cell-Based Efflux Pump Activity Assay

Nagano and Nikaido (2009) developed a cell-based assay that measures the efflux kinetics of the cephalosporin, nitrocefin, by the intact AcrAB-TolC pump. In this assay, the rate of nitrocefin hydrolysis by a periplasmic  $\beta$ -lactamase was measured spectrophotometrically. Using the Michaelis–Menten constants for the  $\beta$ -lactamase ( $K_M$  and  $V_{max}$ ), the rate of nitrocefin hydrolysis ( $V_h$ ) was used to determine the periplasmic concentration ( $C_p$ ) of nitrocefin. The rate of nitrocefin influx ( $V_{in}$ ) across the OM was determined experimentally as a function of the external concentration ( $C_o$ ). The difference between  $V_{in}$  and the measured rate of cephalosporin hydrolysis ( $V_h$ ) corresponds to the rate of efflux ( $V_e$ ) by AcrAB-TolC. By plotting  $V_e$  against  $C_p$  for nitrocefin, a curve that is indicative of Michaelis–Menten type kinetics was obtained, from which a  $K_M$  (6  $\mu$ M) and  $V_{max}$  (0.024 nmol/mg/s) were calculated. This assay format is broadly applicable to any  $\beta$ -lactam antibiotic that is a substrate of the periplasmic  $\beta$ -lactamases of *E. coli* (AmpC or TEM-1). Lim and Nikaido (2010) used this assay to determine the kinetic parameters for several penicillins and cephalosporins. Interestingly, the penicillins exhibited a stronger affinity for AcrAB-TolC than did the cephalosporins, and showed a kinetic behavior that indicated a strong positive cooperativity. Clearly, this assay format could have a wide utility in the analyses of efflux pump substrates and inhibitors.

The nitrocefin assay has been used to estimate the effects of an EPI (MBX2319) on the kinetic behavior of AcrAB-TolC (Opperman et al., 2014). The data demonstrated that MBX2319 (0.2  $\mu$ M) inhibited AcrAB-TolC, and the inhibition was due mainly to a large (4.4-fold) increase in the  $K_M$ . Higher concentrations of MBX2319 (1–10  $\mu$ M) completely inhibited nitrocefin efflux and prevented kinetic analyses. In contrast, PA $\beta$ N (1  $\mu$ M) had no effect on the efflux of nitrocefin, suggesting that this compound does not directly affect AcrB function at lower concentrations. The data suggest that MBX2319 competes with nitrocefin for a site in the binding pocket, or decreases its access to the binding site. This assay has proven to be useful for determining the effects of EPIs on the kinetic parameters of AcrAB-TolC, and could possibly be used to determine the mode of inhibition (competitive, non-competitive, and uncompetitive) of an EPI. In addition, the assay format could be adopted to measure the half maximal inhibitory concentration ( $IC_{50}$ ) of EPIs, which could be used to evaluate and prioritize experimental EPIs. The assay format has several advantages. It is versatile and does not require expensive reagents or equipment. However, because it is a cell-based assay, great care must be taken to control as many variables as possible to minimize variability. In addition, the calculations for  $V_{in}$  depend on several values (see Nagano and Nikaido, 2009) that may change depending on growth conditions or the bacterial strain that is used. Therefore, it is important to verify these values under the conditions that exist in your laboratory.

### Binding Assays

Several research groups have reported binding assays designed to measure the affinity of various substrates to the purified AcrB or MexB. While many of these methods could be used to study the interactions between EPIs and RND family pumps, there are only a few reports of these types of experiments. In addition, great care must be taken when performing or interpreting the results of these experiments, as the RND pumps are large and have multiple hydrophobic sites where non-specific interactions could occur. Therefore, proper negative controls should be included in each experiment.

The most promising technology for binding studies involving AcrB is isothermal titration calorimetry (ITC). Nakashima et al. (2013) measured the binding parameters of D13-9001, a pyranopyrimidine EPI (see below), to purified AcrB, MexB, and MexY using ITC. The data for the titration curves of D13-9001 for AcrB and MexB showed saturation at a stoichiometry of 1:1 (compound: trimer), indicating specific binding interactions. The  $K_D$  values of D13-9001 binding AcrB and MexB were 1.15 and 3.57  $\mu$ M, respectively. In contrast, no saturation binding in the titration curves for MexY, which is not inhibited by D13-9001, was observed. Another group used fluorescence polarization (FP) to study binding of substrate compounds, such as rhodamine 6G ( $5.5 \pm 0.9 \mu$ M), ethidium bromide ( $8.7 \pm 1.9 \mu$ M), ciprofloxacin ( $74.1 \pm 2.6 \mu$ M), and proflavin ( $14.5 \pm 1.1 \mu$ M), to AcrB (Su and Yu, 2007). However, neither of these studies included a negative control, such as a proton transduction deficient mutant, in which none of the subunits are in the Binding conformation. These results indicate that ITC and FP are useful tools for analyzing the affinity between EPIs and efflux pumps; however, they do not indicate where the EPIs bind to the pump.

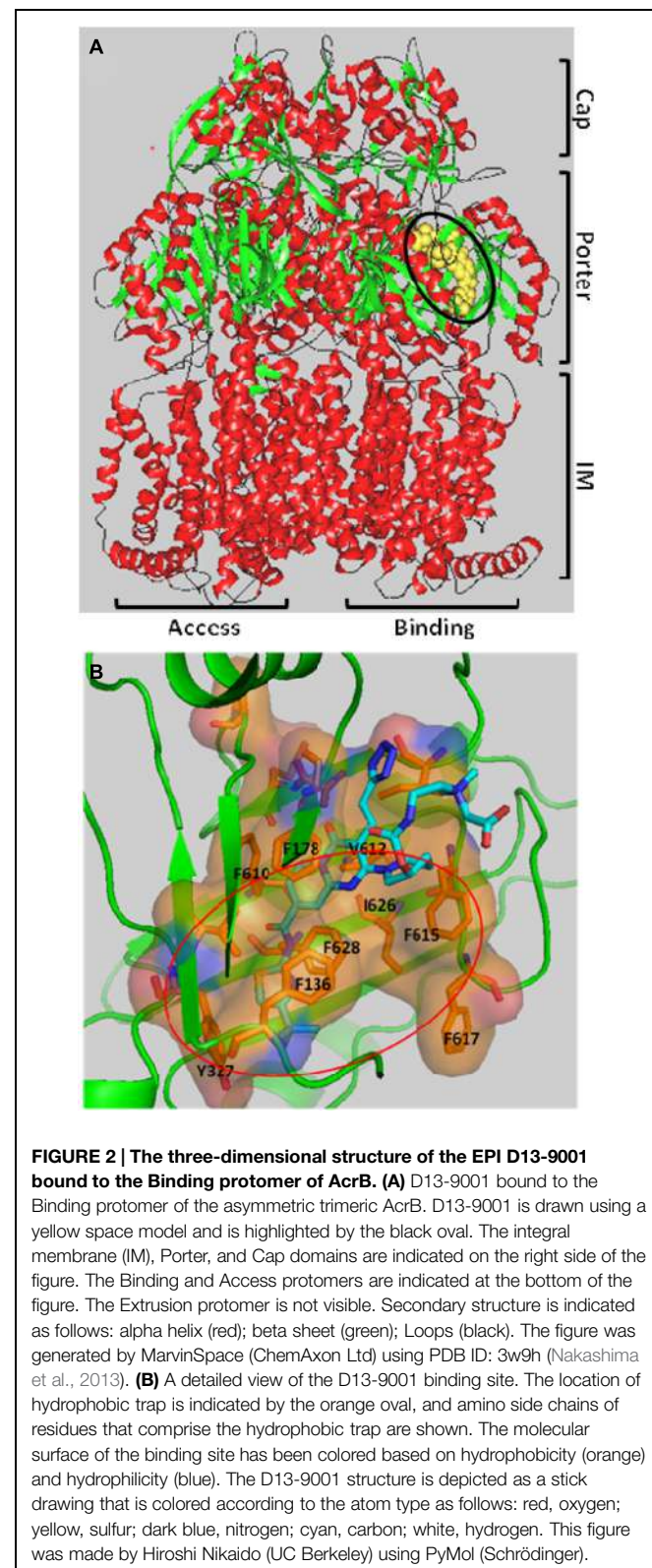
An experimental approach has been described, however, that could be used to identify binding sites for EPIs. This approach utilizes a pump substrate, usually a fluorescent dye molecule that carries a moiety that acts as a cross-linking agent by forming a covalent bond with a specific amino acid side chain, such as the free sulphydryl groups in Cys. This method was initially used to study the substrate binding specificity of the RND pump MexD by Mao et al. (2002). They used 2-(4'-maleimidylanilino)- naphthalene-6-sulphonic acid (MIANS) as the cross-linking reagent, which becomes fluorescent only after it reacts with sulphydryl groups, which enables the cross-linking reaction to be monitored by increased fluorescence. Amino acid residues that were predicted to play a role in substrate recognition were substituted with Cys, and the effect of MIANS on efflux of various substrates was measured. The pump was engineered to contain a single Cys residue. This method was later used to map the entire substrate path in the AcrB pump of *E. coli* (Husain and Nikaido, 2010; Husain et al., 2011). In these studies, residues that were predicted to line the substrate path were substituted with a Cys residue using site-directed mutagenesis, and the accessibility of each of these residues to a lipophilic fluorescent cross-linking reagent (Bodipy-FL-maleimide) was measured. In principle, this assay system could be used to map the binding sites of EPIs through the competitive exclusion of a fluorescent-cross linking agent by the inhibitor upon binding to the same site (competitive), or to an allosteric site binding (either

non-competitive or uncompetitive), which can be monitored by the accessibility of the Cys to the cross-linking reagent. The different modes of binding can be distinguished upon analysis of the binding kinetics. Indeed, this approach was used to obtain experimental support for hypotheses on the mechanism of substrate recognition in the deep binding pocket of AcrB, which were generated by *in silico* docking experiments (Takatsuka et al., 2010). Competition experiments were used to demonstrate that compounds predicted to bind to the “groove” of the substrate binding pocket compete with cross-linking reagent for a Cys residue in the groove, whereas, compounds predicted to bind lower in the site, or the so-called “cave,” did not compete. A covalently linked AcrB trimer, which would allow construction of mutant proteins in which a single subunit can assume the “binding” conformation, could prove to be useful in this type of study (Takatsuka and Nikaido, 2009; Zgurskaya, 2009). Despite the fact that this approach could be applied readily to the study of the interaction of EPIs with AcrB, it does not appear to have been used for this purpose. One problem with this approach is that it requires several AcrB variants, in which a single Cys substitution is introduced at several sites in the access and deep binding pockets of AcrB. In addition, the fluorescent cross-linking reagent must be a pump substrate. Fortunately, several such cross-linking compounds are available, such as MTS-rhodamine (Loo and Clarke, 2002), BODIPY-FL-maleimide (Husain et al., 2011), *N*-ethylmaleimide (Loo and Clarke, 2002; Guan and Kaback, 2007), or monobromobimane (Fluman et al., 2009). Thus, this approach could prove to be very useful for MOA studies for EPIs.

### X-ray Crystallography

Very few co-crystal structures of the asymmetric trimer of AcrB bound to substrates, and until recently, no co-crystal structures of an EPI bound to AcrB (see below) have been reported. As mentioned above, co-crystal structures for the substrates minocycline and doxorubicin bound to the deep binding pocket (Murakami et al., 2006) and erythromycin and rifampicin bound to the access binding site (Nakashima et al., 2011) of the asymmetric trimer have been reported. In contrast, several co-crystal structures of the symmetrical form of AcrB with substrates (ethidium bromide, rhodamine 6G, ciprofloxacin, nafcillin) and one EPI (PA $\beta$ N; Yu et al., 2005), as well as linezolid (Hung et al., 2013), have been published. However, the relevance of these structures is difficult to interpret as the pump is not in the conformation that is relevant biochemically. The paucity of co-crystal structures is probably the direct result of the difficulty in producing co-crystals. It is possible that the difficulties arise from the relatively low binding affinities of the substrates for the binding site.

Nakashima et al. (2013) reported a major breakthrough in the field when they published the first co-crystal structure of the pyridopyrimidine EPI D13-9001 (see Figures 2A,B) bound to AcrB (*E. coli*) and MexB (*P. aeruginosa*). The inhibitor, D13-9001, is a pyridopyrimidine compound that is a potent inhibitor of AcrB and MexB, but not of MexY (*P. aeruginosa*). The hydrophobic *tert*-butyl thiazolyl aminocarboxyl pyridopyrimidine moiety of D13-9001 binds tightly to a narrow depression, referred to as the hydrophobic trap, in the deep substrate binding pocket in the “Binding” protomer (see Figures 2A,B). The hydrophilic portion



of the compound extends into the substrate binding groove where it interacts with polar residues. A detailed description of the binding site can be found below. The location of the binding site and

the high affinity of D13-9001 suggested a MOA for this compound. The current hypothesis is that D13-9001 binds tightly to the hydrophobic trap and prevents the conformational changes that are needed for the proper activity of the pump (Nakashima et al., 2013). In addition, the hydrophilic portion of D13-9001 is expected to prevent binding of a wide range of substrates to the binding cleft. It is not clear why the co-crystal structure of D13-9001 is the only one that has been published. While it is not known how many other EPIs have been attempted, it is possible that D13-9001 has some properties that are amenable to X-ray crystallography, as relatively standard conditions for formation of co-crystals were used (Nakashima et al., 2013). However, the real significance of this work lies in the discovery of a binding site on AcrB for non-competitive (substrate) inhibitors that can be exploited for rational design of EPIs.

## Computational Methods

Because of the biochemical complexity of the RND family pumps and the difficulty of producing co-crystals, many researchers have turned to computational methods to explore the structure function relationships of AcrB and MexB. The computational systems that have been used to study RND family efflux pumps consist of algorithms that are designed to simulate the molecular interactions and conformational changes that comprise the current model for substrate recognition and extrusion. These systems range from relatively simple algorithms for docking compounds into the substrate binding pocket to complex MD simulations. Docking algorithms, such as AutoDock Vina (Trott and Olson, 2010), utilize the static binding site defined by a three-dimensional crystal or NMR structure in the absence of solvent to identify the most energetically favorable binding pose of a small molecule. In contrast, MD simulations attempt to reproduce the behavior of real molecules in motion in the presence of solvent. MD simulation consists of the numerical, step-by-step, solution of the classical equations of motion for each atom. A computer model of the protein is prepared from a three-dimensional protein structure, and the forces acting on each atom in the system atoms are then estimated using an equation that includes molecular ‘force fields,’ which model various bonded and non-bonded inter-atomic interactions. Several excellent reviews of the methodology of MD simulations for proteins have been published (Karplus and McCammon, 2002; Durrant and McCammon, 2011). Advances in technology have increased the predictive accuracy of these methods. For example, MD simulations of the enzyme-inhibitor complex between trypsin and the inhibitor benzamidine have produced binding predictions in which the root mean square deviation (rmsd) for the bound inhibitor was less than 2 Å as compared to the crystal structure (Buch et al., 2011). However, the current MD simulation methodologies are limited by high computational costs and by the approximations of the force fields used in the modeling.

The use of computational methods for the study of RND-family pumps and EPIs is made possible by the existence of high-resolution three-dimensional structures of RND-family pumps with and without substrates, such as AcrB (Murakami et al., 2006; Sennhauser et al., 2007; Nakashima et al., 2011, 2013) and MexB (Sennhauser et al., 2009; Nakashima et al., 2013), and supporting

biochemical data. Takatsuka et al. (2010) used docking experiments to examine the interaction of 30 compounds, including minocycline, doxorubicin, tetracycline, and levofloxacin with the distal substrate binding site of the binding protomer. They found that the substrates that were tested are predicted to bind to one of two regions of the binding pocket: a narrow groove at the distal end of the pocket, and a wider proximal region, which they called the cave region. The results of biochemical studies, including competition with the substrate nitrocefin and the fluorescent cross-linking dye fluorescein-5-maleimide (see above), provided support for the predictions of the docking experiment. Several studies that employ MD simulations to study the mechanism of substrate recognition and extrusion in AcrB and MexB have been reported. For example, MD simulations have been used to examine the mechanism of the peristaltic action of AcrB (Schulz et al., 2010; Yao et al., 2010; Fischer and Kandt, 2013; Schulz et al., 2015), to map the path of substrate from the periplasm to the central cavity (Imai et al., 2011), to study the role of water in substrate extrusion (Schulz et al., 2011) and proton transfer in the transmembrane domain (Fischer and Kandt, 2011), and the role of a key residue Phe 610 in extrusion (Vargiu et al., 2011). Several of these studies have been reviewed previously (Ruggerone et al., 2013a,b; Fischer et al., 2014). Because of the limitations posed by docking, MD simulations have been used to study substrate binding and specificity of AcrB (Vargiu and Nikaido, 2012; Yao et al., 2013) and MexB (Collu et al., 2012). In particular, Vargiu and Nikaido (2012) used MD simulations to examine the interaction between nine substrates and the distal binding pocket of AcrB in terms of the binding energy, hydrophobic surface-matching, and the residues involved in the process. Despite the potential inaccuracies resulting from the limitations of the system, the MD simulations enabled the assessment of the contribution of various residues in ligand binding and produced a much more realistic picture of the interaction of various ligands with AcrB, as compared to docking. These limitations include the following: (1) an inability to model the effect of the local environment in the binding site on the charge states of substrates, (2) the difficulties in estimating binding affinities due to the intrinsic limitations of the methodology used to calculate force fields, and (3) the absence of accessory proteins, such as AcrA (Nikaido, 2011) and AcrZ (Hobbs et al., 2012; Du et al., 2014), which may be required to form the active conformation of AcrB. The major advantages of the MD simulations include the presence of water molecules in the simulation and the flexibility of the distal binding site, which enables the modeling of binding interactions that are more realistic. For example, the binding site predicted for the bile salt taurocholate by MD simulations was similar to the one predicted by docking. However, MD simulation oriented the compound so that the hydrophobic and hydrophilic groups on the different sides of the planar structure were facing hydrophobic binding site residues or the solvent filled channel, respectively. Strong interactions between water molecules and most of the other substrates were observed, which are indicative of a more realistic binding prediction. This is illustrated by the binding pose of minocycline that was predicted by the MD simulation, which was in very good agreement with the crystallographic structure (Murakami et al., 2006; Eicher et al., 2012). The results of these

MD simulations demonstrate that this is a promising approach for studying substrate binding to RND-family pumps.

Computational models have also been used to study the interactions between EPIs and AcrB. The docking studies reported by Takatsuka et al. (2010) included the EPI NMP, which was predicted to bind to the “cave” region (see above) of distal binding pocket. Because of the low resolution of the docking model, Vargiu and Nikaido (2012) used MD simulations to study the interaction of NMP and PA $\beta$ N with AcrB (see Figures 3C,D). The results of the MD simulations for the EPIs NMP and PA $\beta$ N were markedly different from those of the substrate compounds that were included in the study. The EPIs were predicted to bind to a site that included the so-called “G-loop” or “switch loop” (Nakashima et al., 2011; Eicher et al., 2012; Cha et al., 2014),

which separates the distal and the proximal binding sites and is thought to be involved in the movement of substrates from the proximal to the distal site. In addition, the high resolution of the MD simulations enabled the identification of the amino acid residues that contributed to the binding energy. Recently, MD simulations have been used to evaluate the interaction between MBX2319 (see Figure 3A), a novel pyranopyridine EPI, and AcrB (Opperman et al., 2014). MBX2319 is predicted to bind to the same “hydrophobic trap” that was identified in the X-ray cocrystal structure of D13-9001 and AcrB (Nakashima et al., 2013). The data suggests that these compounds may share a common MOA. Based on the  $\Delta G_b$  values, the relative binding affinities of the EPIs were as follows: D13-9001 > MBX2319 > NMP and PA $\beta$ N, which is consistent with their relative potencies as EPIs. Finally,

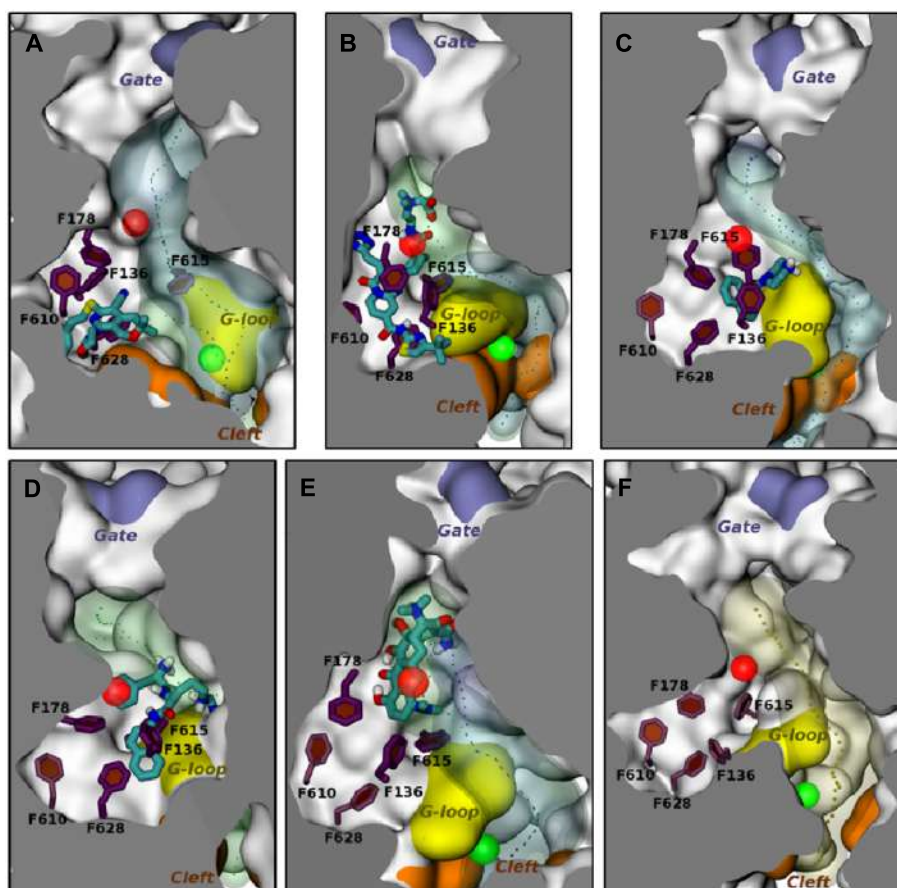


**FIGURE 3 | Molecular dynamic simulations of efflux pump inhibitors and minocycline (MIN) to the distal substrate binding pocket of the Binding protomer of AcrB.** The position of the various ligands used in this study with respect to the hydrophobic trap in protomer B in representative average structures of the complexes from MD simulations are shown. The structures of the ligands are depicted as stick drawings that colored according to the atom type (red, oxygen; yellow, sulfur; dark blue, nitrogen; cyan, carbon; white, hydrogen). The side chains of residues constituting the hydrophobic trap are depicted as stick drawings (thick if the residue is within 3.5 Å of the ligand, thinner otherwise). The rest of the protein is shown with molecular surface, colored in orange, yellow and iceblue at the PC1/PC2 Cleft, the G-loop tip and the exit Gate, respectively, and white elsewhere.

The channels leading to the proximity of the exit Gate (see Figure 1) and passing through residues of the DP are also shown in the presence and in the absence of the ligand, respectively, are shown as blue and green transparent surfaces. The centers of gravity of the points defining them are shown with points. The centers of mass of the access binding pocket (AP) and of the distal pocket (DP) are shown with green and red transparent spheres, respectively. No contiguous substrate translocation channel was found in the AcrB-PA $\beta$ N complex (D). The ligands are shown in the following panels: (A) MBX2319; (B) D13-9001; (C) NMP; (D) PA $\beta$ N; (E) MIN. (F) The substrate translocation channel of AcrB is shown in the ligand-free state to illustrate the representative average structure of the transporter. This figure was taken from Vargiu et al. (2014) and was modified slightly.

the computational protocol was able to reproduce the binding of minocycline and D13-9001 to AcrB that was observed in co-crystal structures with RMSD values of  $2.7 \pm 1.0$  and  $2.8 \pm 0.4$  Å (see **Figures 3B,E**), respectively, which increases the level confidence in the modeling results. Therefore, MD simulation is a promising approach to generate molecular hypotheses for the MOA of EPIs.

## An Overview of the Major Classes of EPIs and their Mechanism of Action

In this section, we will briefly review the important classes of EPIs that are active against the RND-family efflux pumps of Gram-negative bacteria. This section provides an overview of the biological activities of each EPI class and drug development-related issues (where appropriate). In addition, we will review the mechanistic action studies for each compound class.

### Peptidomimetic EPIs: PA $\beta$ N and the C-Capped Dipeptide Analogs

Renau et al. (1999), researchers at Microcide Pharmaceuticals and Daiichi Pharmaceutical Co. reported their discovery of the first inhibitor of RND transporters of Gram-negative bacteria, phenylalanyl arginyl  $\beta$ -naphthylamide (MC-207,110 or PA $\beta$ N, see **Figure 4**). This dipeptide compound was identified as a promising hit from a screening of 200,000 samples for small molecules that potentiate the antibacterial activity of levofloxacin against strains of *P. aeruginosa* overexpressing MexAB, MexCD, and MexEF pumps.

#### *In vitro*/spectrum of co-antibiotics

The EPI activity of PA $\beta$ N is strongly dependent on the nature of the antibiotic used as an indicator of pump activity, as measured as a shift in the MIC of the antibiotic (Lomovskaya et al., 2001). Specifically, at 20  $\mu$ M concentration, the potentiating effect of PA $\beta$ N on levofloxacin and erythromycin against a strain over-expressing MexAB-OprM was comparable to that of a MexAB-OprM deficient strain. It also exhibited strong potentiation for chloramphenicol, but only weak potentiation for carbenicillin, and none for ethidium bromide, one of the known substrates of MexAB-OprM pump. PA $\beta$ N did not potentiate antibiotics that are not substrates of MexAB-OprM pump, such as gentamicin and imipenem.

Other biological assays (Lomovskaya et al., 2001) showed that PA $\beta$ N also inhibits efflux of the AcrAB-TolC pump of *E. coli*, however, it is not very potent against this organism (Opperman et al., 2014). While PA $\beta$ N did not affect the proton gradient across the inner membrane, it increased permeability of the outer membrane of the PAM2035 strain, which lacks the functional MexAB-OprM pump, in a dose dependent manner. The permeabilizing effect of PA $\beta$ N was due to its dicationic character. However, the outer membrane activity was abolished by addition of magnesium salt. Although the effect on membrane integrity of PA $\beta$ N is less than that of polymyxin B, it is a toxicity concern.

#### Scaffold optimization

Because PA $\beta$ N is not very potent and unstable in murine and human serum, Renau et al. (1999, 2001) prepared over 500 analogs of PA $\beta$ N aiming to improve the potency (measured by Minimum Potentiation Concentration that decreases the MIC by 8-fold (MPC8) with levofloxacin) and serum stability. For structural optimization, the scaffold was divided into three parts: amino acid 1 and 2 (AA1, AA2) and the (amide) cap (**Figure 4**). Some of the main findings are: (i) an amino acid containing a basic side chain (as either AA1 or AA2) is needed for activity; (ii) Orn could replace Arg; (iii) replacement of Phe with homoPhe led to improved potency; (iv) methylation of the NH that links AA1 and AA2 led to increased serum stability; (v) replacement of L-amino acid with D-amino acid is acceptable and led to increased serum stability; (vi) replacing  $\beta$ -aminonaphthalene with 3-aminoquinoline as the cap group led to slightly reduced potency, but also less intrinsic antibacterial activity and less cytotoxic to mammalian cells. Overall, the analogs did not seem to be much more potent than PA $\beta$ N (the lowest MPC8 = 2.5  $\mu$ M for some compounds), but the stability in serum was significantly improved, enabling *in vivo* testing.

#### *In vivo* activity

Two analogs were selected for *in vivo* efficacy testing (**Figure 4**) that showed significant reduction on the growth of *P. aeruginosa* in a murine neutropenic thigh model when used in combination with levofloxacin (Renau et al., 1999, 2001). Specifically, compound L-Phe-(Me)-L-Orn- $\beta$ -Na at 30 mg/kg (intraperitoneally) in combination with levofloxacin (30 mg/kg, subcutaneously) led

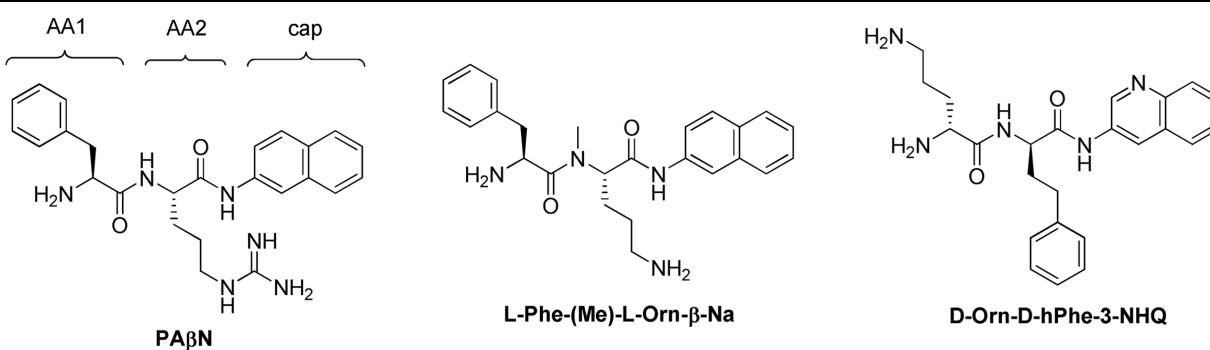


**FIGURE 4 |** Structures of PA $\beta$ N and selected analogs.

to 3-log reduction in colony forming units (cfu) for approximately 4 h, followed by regrowth. A single dose of either levofloxacin or test compound resulted in growth similar to the untreated controls. The immune-suppressed mice in this experiment were infected with *P. aeruginosa* PAM 1032 ( $1.0 \times 10^5$  cfu, intramuscularly).

### Mechanism of action

The vast majority of the MOA studies for this class of EPIs has been done using PA $\beta$ N. Lomovskaya et al. (2001) demonstrated that PA $\beta$ N is a substrate for RND pumps of *P. aeruginosa* (MexB, MexD, and MexF), suggesting that it acts as a competitive inhibitor of substrate binding and/or extrusion. PA $\beta$ N has been shown to increase the susceptibility of a MexAB-OprM-overproducing strain of *P. aeruginosa* to a wide range of antibiotics, such as levofloxacin, sparfloxacin, chloramphenicol, and erythromycin. However, it was significantly less effective when combined with tetracycline, carbenicillin, and ethidium bromide. If PA $\beta$ N is a competitive inhibitor, the spectrum of antibiotic potentiation may suggest that the binding sites of PA $\beta$ N may not overlap with these compounds. To date, there have been no reports of the isolation of mutants with reduced susceptibility to PA $\beta$ N with mutations that map to an RND-encoding pump gene.

Because of the lack of experimental evidence to shed light on the molecular mechanism of the EPI activity of PA $\beta$ N, Vargiu and Nikaido (2012) used MD simulations to examine the interaction between PA $\beta$ N and AcrB. As mentioned above, the results of MD simulation experiments predict that PA $\beta$ N binds with a relatively low affinity to the distal substrate binding site of AcrB and straddles the G-loop. PA $\beta$ N is predicted to interact mainly with the hydrophobic residues F136, F178, F615, and F628, but may interact with the hydrophilic residues Q176 and E673. Binding of PA $\beta$ N is predicted to cause a conformational change that shrinks the substrate extrusion channel in the distal binding pocket, which is where many substrates bind. Therefore, the results suggest two possible mechanisms, which may not be mutually exclusive. First, PA $\beta$ N prevents movement of the G-loop, which plays an important role in the movement of substrates from the proximal to the distal binding sites (Eicher et al., 2012; Cha et al., 2014). Second, the conformational change in the substrate extrusion channel prevents the binding of other substrates to this site. A docking study suggested that the conformational change induced by PA $\beta$ N reduced the affinity of minocycline (Vargiu et al., 2014), which supports the second possible MOA.

The first detailed description of the biological activity of PA $\beta$ N demonstrated that it has the additional MOA of altering the permeability of the outer membrane (Lomovskaya et al., 2001), although PA $\beta$ N was less potent (half maximal effect at  $\sim 70$   $\mu$ g/ml) than the polymyxin B nonapeptide (PMBN), an outer membrane-specific permeabilizing agent (Vaara and Vaara, 1983) that was used as a positive control. The increase in outer membrane permeability is expected to result in increased influx of antibiotics into the periplasm, which would increase susceptibility to an antibiotic substrate in an efflux-independent manner. However, the outer membrane activity of PA $\beta$ N was abolished by the addition of 1 mM Mg $^{2+}$ , but it is not clear whether Mg $^{2+}$

was effective at higher concentrations of PA $\beta$ N. The outer membrane activity of PA $\beta$ N and the effect Mg $^{2+}$  was also described recently by Lamers et al. (2013). Therefore, experiments with PA $\beta$ N should include 1 mM Mg $^{2+}$  to minimize the effect of the outer membrane activity.

### 1-(1-Naphthylmethyl)-Piperazine (NMP) and the Arylpiperazine Analogs

Bohnert and Kern (2005) reported the discovery of 1-(1-Naphthylmethyl)-piperazine (NMP, Figure 5) as an EPI against *E. coli*. The authors screened a library of *N*-heterocyclic compound library for potentiaters of levofloxacin against *E. coli* strains overexpressing *acrAB* and *acrEF* (2-DC14PS and 3-AG100MKX, respectively) and found some phenylpiperazine derivatives with activity. Further SAR study led to the synthesis of NMP, one of the most potent analogs. NMP (at 100  $\mu$ g/mL) caused an increase in the intracellular accumulation of levofloxacin. It also caused accumulation of ethidium bromide in a dose dependent manner (6.25–100  $\mu$ g/mL) in the pump overexpressing strains (2-DC14PS and HS414), but not in the pump-deficient strains (1-DC14PS and HS276), suggesting it was an inhibitor of the AcrAB and AcrEF efflux pumps. Because of low potency and the possibility that NMP acts as serotonin agonist, the likelihood that this EPI will be developed further as a adjunctive therapeutic agent is low (Zechini and Versace, 2009).

At 100  $\mu$ g/mL concentration, against *E. coli* strains overexpressing *acrAB* or *acrEF*, NMP potentiated levofloxacin by 8- to 16-fold, and by 4- to 8-fold for oxacillin, rifampin, chloramphenicol, and clarithromycin. It reduced the MIC of linezolid against the *acrEF*-overexpressing strain (2-DC14PS) by 32-fold, and by 8-fold against the *acrAB*-overexpressing strain (3-AG100MKX). Other fluoroquinolones (ciprofloxacin, norfloxacin, enoxacin, and pefloxacin), erythromycin, azithromycin, clindamycin, doxycycline, and nitrofurantoin, but not the ketolide telithromycin, glycopeptides, aminoglycosides, trimethoprim-sulfamethoxazole, and fosfomycin were potentiated by NMP (at 100  $\mu$ g/mL), as indicated by  $\geq 4$ -fold reduction of MIC against the 3-AG100MKX strain.

Testing against 60 clinical isolates of *E. coli* using NMP at 100  $\mu$ g/mL showed that this compound was moderately active in reversing MDR in clinical isolates of *E. coli* and could partially restore fluoroquinolone susceptibility (Kern et al., 2006). NMP caused reduction of MICs of levofloxacin, linezolid and ethidium bromide by  $\geq 4$ -fold in  $> 50\%$  of the isolates. Although its potentiation of linezolid was notable, the effect was not enough to make

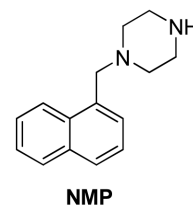


**FIGURE 5 | Structure of NMP.**

the isolates susceptible to this antibiotic. NMP also showed partial MDR reversal effects against other *Enterobacteriaceae* species, e.g., *E. aerogenes* and *K. pneumonia* (Schumacher et al., 2006), and *Acinetobacter baumannii* (Pannek et al., 2006). It was noticed that NMP and PA $\beta$ N showed markedly different preferences for antibacterial agents, as well as, the isolates that each could work with, suggesting they might inhibit different pumps, bind to different sites of the same pump(s), or act on different target(s).

### Mechanism of action

1-(1-Naphthylmethyl)-piperazine is widely used as a research reagent. Consequently, there is great interest in the MOA of this compound. Schuster et al. (2014) were the first group to successfully isolate AcrB mutants resistant to NMP. They screened a library of mutants in which the substrate binding and extrusion domain of AcrB were randomly mutagenized using error-prone PCR for mutants that were able to form colonies on plates containing NMP and linezolid. The authors isolated several mutants with reduced susceptibility to NMP that did not decrease function of the pump. Site-directed mutagenesis of wild-type *acrB* was used to verify the genetic basis for the NMP-resistant phenotype. Only a double mutant, in which Gly141 was substituted with Asp (G141D) and Asn282 was substituted with Tyr (N282Y), significantly affected susceptibility to NMP. The mutated residues are located near the outer face of the distal substrate binding pocket near Phe610 (see Figure 1A), which plays a key role in the extrusion process (Bohnert et al., 2008) and is across from the G-loop that separates the proximal (access) and the distal (substrate) binding sites (Nakashima et al., 2011; Eicher et al., 2012). The authors speculate that G141D N282Y amino acid substitutions prevent binding of NMP at a site near Phe610, where NMP is predicted to alter the specificity or the conformational changes of the binding pocket by acting on Phe610 in a non-competitive manner (see below). Interestingly, the NMP resistant phenotype was observed only in the presence of linezolid, and partial resistance in the presence of Hoechst 33342 and levofloxacin. The reason for this is unclear. However, as mentioned above, it is possible that the NMP resistant mutant enables the extrusion of linezolid when NMP is bound to a site that straddles the G-loop, which was predicted by MD simulations (see Figure 3C; Vargiu and Nikaido, 2012; Vargiu et al., 2014). The estimated binding energy is  $-10.6 \pm 7.9$  kcal/mol. The NMP binding site includes interactions with hydrophobic residues near the hydrophobic patch (F664 and F666) and G617 of the G-loop. This suggests the NMP

inhibits the action of AcrB by interfering with the movement of the G-loop, which has been shown to play important role in the extrusion of certain substrates (Eicher et al., 2012; Cha et al., 2014). As shown in Figure 1A, the binding site for NMP that was predicted by MD simulations does not include G141 and N282. Also, as is the case for PA $\beta$ N, NMP is predicted to induce a conformational change that results in a reduction of the width of the substrate binding cleft (Vargiu and Nikaido, 2012). Therefore, the amino acid substitutions in the NMP resistant mutant may prevent these NMP-induced conformational changes, allowing extrusion of linezolid when NMP is bound.

Despite the fact that NMP is used widely as a research reagent, two important questions about its activity have not been resolved. It has been stated in the literature that NMP is not a substrate of RND-family pumps, however, convincing data to support this statement have not been published. For example, Schuster et al. (2014) reported that the rate of intracellular accumulation of NMP (100  $\mu$ g/ml) was similar in an AcrB overexpressing strain, an AcrB-deficient strain, and NMP resistant mutants. Based on this result, the authors concluded that NMP is not a substrate (or a poor substrate) of AcrB (Schuster et al., 2014). However, the data was not presented in their paper. As discussed in the next section, these types of assays must be interpreted with caution when high concentrations of an EPI are present in the medium. Therefore, is not a trivial matter to determine whether an EPI is a substrate or non-substrate of an RND-family pump. Unlike PA $\beta$ N, additional mechanisms of action for NMP have not been reported. However, NMP exhibits antibacterial activity at a concentration of 400  $\mu$ g/ml (Bohnert and Kern, 2005), which is only 4-fold higher than the concentration at which it is used as an EPI. This indicates that this compound acts on an additional cellular target, resulting in growth inhibition. The most likely secondary target of NMP is the membrane, however, the effect this compound on membrane potential or integrity has not been reported.

### D13-9001 and the Pyridopyrimidinone Analogs

Yoshida et al. (2007) at Daiichi Pharmaceutical Co. and Essential Therapeutics described D13-9001 (Figure 6) as a MexAB-OprM specific pump inhibitor against *P. aeruginosa* with good solubility and *in vivo* activity. This report was the last of a seven article series starting from 2003, describing a systematic optimization of another screening hit compound (D1, Figure 6; Nakayama et al., 2003a,b, 2004a,b; Yoshida et al., 2006a,b). Compound D1

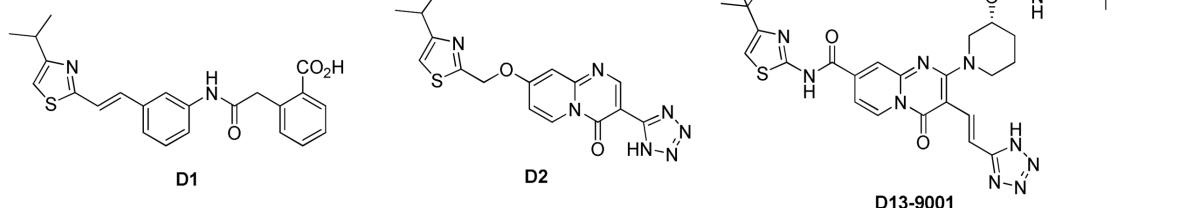


**FIGURE 6 | Structure of D13-9001 and its developmental precursors.**

only inhibited MexAB-OprM pump, and not the MexCD-OprJ, MexEF-OprN, or MexXY-OprM pumps. It exhibited very good MPC8 with levofloxacin ( $\leq 0.63 \mu\text{M}$ ) against a *P. aeruginosa* strain (PAM1723) that has overexpressed MexAB-OprM and disrupted MexCD-OprJ and MexEF-OprN. However, this compound was practically insoluble in water and showed no efficacy *in vivo*.

The poor *in vivo* performance of **D1** was attributed to its high affinity for serum albumin (>98% protein bound) and the increase in MPC8 (>10-fold shift) when serum was added. After some unsuccessful attempts at conservatively modifying the scaffold to improve pharmacokinetic properties, big changes were made by installing the quinolone and pyridopyrimidinone fragments to the mid-section of the scaffold. The pyridopyrimidinone analogs, such as **D2**, displayed higher MPC8 as compared to **D1** (5  $\mu\text{g/mL}$  for aztreonam and 10  $\mu\text{g/mL}$  for levofloxacin), but had lower affinity to serum protein and were effective *in vivo* (Nakayama et al., 2003b). Subsequent efforts to further optimize the scaffold for activity and pharmacokinetic properties led to the synthesis of D13-9001. This zwitterionic compound was soluble enough for *iv* administration (747  $\mu\text{g/mL}$  in pH 6.8 buffer), exhibited MPC8 = 2  $\mu\text{g/mL}$  for levofloxacin and aztreonam against the PAM1723 strain of *P. aeruginosa*. D13-9001 demonstrated acceptable PK profiles in rats and monkeys. It did not alter the serum level of aztreonam when both were given by *iv* (1000 mg/kg of aztreonam T, 1.25–20 mg/kg of D13-9001, 2 h infusion). In a lethal pneumonia model in rats (using PAM1020 strain), in combination with aztreonam (1000 mg/kg) D13-9001 (at 1.25–20 mg/kg) showed improved survival rates at the end of day seven.

### Mechanism of action

Nakashima et al. (2013) reported that D13-9001 does not perturb the inner or the outer membranes. In this same paper, the authors determined that D13-9001 is not a substrate of AcrB. They measured the time-dependent change in concentration of D13-9001 in the media containing either an AcrB overexpressing or an AcrB-deficient strain. Compounds that are not substrates accumulate in both strains, resulting in a decrease compound concentration in the media, while pump substrates will accumulate only in the AcrB-deficient strain. Using this assay, the authors concluded that D13-9001 is not a substrate. However, results of this nature should be interpreted with caution when the test compound is a potent EPI and is present at a high concentration (28.6  $\mu\text{M}$ ) in the medium. The high concentration of EPI is likely to inhibit AcrB, causing compound to accumulate in the AcrB overexpressing strain. Thus, potent EPIs would appear to be non-substrates, even when they are actually pump substrates. At this point, it is not clear whether D13-9001 is a non-substrate. This situation underscores the difficulties at present in determining whether EPIs are substrates using the available assays.

As mentioned above, Nakashima et al. (2013) elucidated the three-dimensional structure of the EPI D13-9001 bound to AcrB and MexB. The hydrophobic tert-butyl thiazolyl aminocarboxyl pyridopyrimidine moiety of D13-9001 binds tightly to a narrow depression, referred to as the hydrophobic trap, in the deep substrate binding pocket in the “Binding” protomer (see

**Figures 2A,B**). The hydrophobic trap branches off from the substrate translocation channel and is lined with hydrophobic residues (F136, F178, F610, F615, and F628). In addition, the tetrazole ring and the piperidine aceto-amino ethylene ammonio-acetate moiety interact with ionic and/or hydrophilic residues (N274, R620, Q176, and S180 in addition to aliphatic residues (I277 and L177) that are in the substrate translocation channel. The piperidine aceto-amino ethylene ammonio-acetate moiety extends into the substrate binding sites of both minocycline and doxorubicin. The crystal structure of the D13-9001 binding site in MexB was found to be similar to the binding site in AcrB, except that the conformation of the PAEA moiety in the substrate translocation channel was different. A homology model of the three-dimensional structure of MexY predicted that D13-9001 would not bind because F178 at the edge of the hydrophobic trap of AcrB/MexB has been replaced with a bulky W177 in MexY, which is predicted to prevent binding by steric hindrance. The model was confirmed when a site-directed mutant of MexY (W177F) was shown to be sensitive to inhibition by D13-9001. Conversely, D13-9001 does not bind to AcrB (F178W). As shown by ITC, D13-9001 binds tightly to AcrB and MexB with  $K_D$  values of 1.15 and 3.57  $\mu\text{M}$ , respectively. It is possible that the successful production of co-crystals with D13-9001 is due to the high affinity of this compound for AcrB and MexB. This EPI inhibits efflux of a broad range of compounds, presumably not by competitive inhibition (yet to be determined experimentally). The current hypothesis is that D13-9001 binds tightly to the hydrophobic trap and prevents the conformational changes that are needed for the proper activity of the pump (Nakashima et al., 2013). In addition, the presence of the hydrophilic portion of this EPI in the substrate binding channel is predicted to prevent substrate binding to this site. Therefore, this study has made a significant advance in the understanding of the mechanism of inhibition of an EPI, and has identified a previously unknown binding site in RND pumps that can be exploited for the rational design or optimization of EPIs. Because MD simulations (see **Figure 3B**) have been able to reproduce the structure of D13-9001 bound to AcrB (rmsd 2.8 Å; Vargiu et al., 2014), this tool may prove to be useful in evaluating novel EPIs.

### Pyranopyridines (MBX2319)

Opperman et al. (2014) at Microbiotix reported compound MBX2319 (**Figure 7**) as a novel inhibitor of the AcrAB efflux pump of *E. coli*. It was discovered from a high-throughput

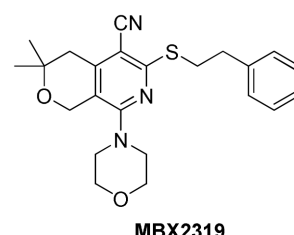


**FIGURE 7 | Structure of MBX2319.**

screening campaign designed to look for small molecules that potentiate ciprofloxacin against *E. coli*. Because the authors were not specifically looking for efflux inhibitors, the bacterial strain was not engineered to overexpress any transporters. MBX2319 had no intrinsic antibacterial activity ( $\text{MIC} \geq 100 \mu\text{g/mL}$ ), but exerted significant potentiating effects on antibiotics that are substrates of AcrB, such as fluoroquinolones,  $\beta$ -lactams, chloramphenicol, erythromycin, and linezolid at concentrations of 3.1–12.5  $\mu\text{g/mL}$ . Consistent with the proposed mechanism, MBX2319 did not affect MICs of antibiotics against *acrB*-deleted mutant or of antibiotics that are not AcrB pump substrates, e.g., gentamicin and carbenicillin. Further, MBX2319 caused increased intracellular accumulation of dye Hoechst 33342 and nitrocefin in a dose dependent manner in wild-type *E. coli* strains, but not the  $\Delta acrB$  and  $\Delta tolC$  strains. This inhibitor also worked against other *Enterobacteriaceae* species, i.e., *Shigella flexneri*, *K. pneumoniae*, *S. enterica* and *E. cloacae*. Against *P. aeruginosa* (ATCC 27854), MBX2319 reduced the MIC of cefotaxime (but not ciprofloxacin or levofloxacin) ca. 6-fold. However, the observation that PMBN increases the EPI activity of MBX2319 against *P. aeruginosa* indicates the outer membrane of this organism is the major obstacle to activity (Opperman et al. manuscript in preparation). Therefore, the pyranopyridines have the potential to be used as an adjunctive therapy against both *Enterobacteriaceae* and *P. aeruginosa*.

### Mechanism of action

Based on the results of MD simulations, MBX2319 is predicted to bind to the same “hydrophobic trap” (see **Figure 3A**) that was identified in the X-ray crystal structure of D13-9001 bound to AcrB (Nakashima et al., 2013). The pyridine ring of MBX2319 is predicted to make a ring-stacking interaction with the rings of F628 on one side and F136 on the other. The morpholinyl moiety is predicted to be in close proximity to Y327, and the phenylethylthiol group is loosely located in a hydrophobic pocket surrounded by F610, F628, P326, and Y327 (see **Figure 3A**). The prevalence of interactions with aromatic or aliphatic residues results in a calculated  $\Delta G_b$  of  $-12.5 \text{ kcal/mol}$ . Indeed, almost 70% of  $\Delta G_{\text{solv}}$  comes from residues belonging to the hydrophobic trap. As this region undergoes large conformational changes during the functional rotation of AcrB, binding of MBX2319 with high affinity could hinder these rearrangements (or those triggering the translocation of protons from the periplasm to the cytoplasm upon substrate binding). In addition, as a result of the interaction with the hydrophobic trap, the part of the distal binding site that forms a cleft, which is the binding site for minocycline and doxorubicin appears to shrink (compare **Figures 3A–F**), which may inhibit substrate binding. Indeed, results from the cell-based nitrocefin efflux assay (described above) demonstrated that at 0.2  $\mu\text{M}$  MBX2319 increased the apparent  $K_m$  of AcrB for nitrocefin by >4-fold (Opperman et al., 2014), suggesting, that the EPI altered the affinity of the substrate

for AcrB. Thus, the results of MD simulations are consistent with those of crystallographic methods and can be useful for the generation of molecular hypotheses for the MOA of EPIs that can be tested using genetic and biochemical experiments.

The EPI activity of MBX2319 appears to be specific for RND pump inhibition. MBX2319 does not exhibit intrinsic antibacterial activity ( $\text{MIC} \geq 100 \mu\text{M}$ ), so it is unlikely to act on a secondary non-specific target, such as the inner or outer membrane. This possibility is supported by experimental results that demonstrate MBX2319 does not perturb the proton gradient or integrity of the inner membrane, nor does it increase the permeability of the OM (Opperman et al., 2014).

### Future

Recent advances in methodologies have led to a greater understanding of the MOA of EPIs. In particular, the elucidation of a three-dimensional structure of the EPI D13-9001 bound to AcrB has resulted in hypotheses for the MOA of this compound. In addition, this structure has identified a previously unknown binding site of EPIs in the distal binding pocket, known as the hydrophobic pocket, which can be exploited for the rational design and optimization of novel EPIs with improved potency and spectrum of activity. Due to recent advances in technology, MD simulations have been able to reproduce the binding of two substrates and an EPI elucidated by crystallographic studies with a high degree of accuracy. This raises the possibility that this method could be used to evaluate novel inhibitors. Together, these advances could be useful in overcoming some of the major challenges in the discovery and development of clinically useful EPIs. One of the major challenges in the design of EPIs for Gram-negative is to make compounds that are able to traverse the OM and can bind to the RND pumps with high affinity. Penetration of the OM is controlled by porins, which prefer smaller hydrophilic and zwitterionic molecules. In contrast, the major RND pumps prefer larger hydrophobic molecules. By using rational drug design, however, it will be possible to identify suitable positions on EPIs to append charged groups that will improve OM penetration but will not decrease affinity for the pump.

### Acknowledgments

The authors would like to thank Hiroshi Nikaido for kindly preparing **Figure 2B**. This work was supported by the National Institute of Allergy and Infectious Diseases of the National Institutes of Health (grant R43 AI100332-01). The content of this article is solely the responsibility of the authors and does not necessarily represent the official views of the National Institutes of Health.

### References

- Ahmed, M., Borsch, C. M., Neyfakh, A. A., and Schuldiner, S. (1993). Mutants of the *Bacillus subtilis* multidrug transporter Bmr with altered sensitivity to the antihypertensive alkaloid reserpine. *J. Biol. Chem.* 268, 11086–11089.
- Blair, J. M., and Piddock, L. J. (2009). Structure, function and inhibition of RND efflux pumps in Gram-negative bacteria: an update.

- Curr. Opin. Microbiol.* 12, 512–519. doi: 10.1016/j.mib.2009.07.003
- Bohnert, J. A., and Kern, W. V. (2005). Selected arylpiperazines are capable of reversing multidrug resistance in *Escherichia coli* overexpressing RND efflux pumps. *Antimicrob. Agents Chemother.* 49, 849–852. doi: 10.1128/AAC.49.2.849-852.2005
- Bohnert, J. A., Schuster, S., Seeger, M. A., Fahnrich, E., Pos, K. M., and Kern, W. V. (2008). Site-directed mutagenesis reveals putative substrate binding residues in the *Escherichia coli* RND efflux pump AcrB. *J. Bacteriol.* 190, 8225–8229. doi: 10.1128/JB.00912-08
- Buch, I., Giorgino, T., and De Fabritiis, G. (2011). Complete reconstruction of an enzyme-inhibitor binding process by molecular dynamics simulations. *Proc. Natl. Acad. Sci. U.S.A.* 108, 10184–10189. doi: 10.1073/pnas.1103547108
- Cha, H. J., Muller, R. T., and Pos, K. M. (2014). Switch-loop flexibility affects transport of large drugs by the promiscuous AcrB multidrug efflux transporter. *Antimicrob. Agents Chemother.* 58, 4767–4772. doi: 10.1128/AAC.02733-13
- Collu, F., Vargiu, A. V., Dreier, J., Cascella, M., and Ruggerone, P. (2012). Recognition of imipenem and meropenem by the RND-transporter MexB studied by computer simulations. *J. Am. Chem. Soc.* 134, 19146–19158. doi: 10.1021/ja307803m
- Du, D., Wang, Z., James, N. R., Voss, J. E., Klimont, E., Ohene-Agyei, T., et al. (2014). Structure of the AcrAB-TolC multidrug efflux pump. *Nature* 509, 512–515. doi: 10.1038/nature13205
- Durrant, J. D., and McCammon, J. A. (2011). Molecular dynamics simulations and drug discovery. *BMC Biol.* 9:71. doi: 10.1186/1741-7007-9-71
- Eda, S., Maseda, H., and Nakae, T. (2003). An elegant means of self-protection in gram-negative bacteria by recognizing and extruding xenobiotics from the periplasmic space. *J. Biol. Chem.* 278, 2085–2088. doi: 10.1074/jbc.C200661200
- Eicher, T., Brandstatter, L., and Pos, K. M. (2009). Structural and functional aspects of the multidrug efflux pump AcrB. *Biol. Chem.* 390, 693–699. doi: 10.1515/BC.2009.090
- Eicher, T., Cha, H. J., Seeger, M. A., Brandstatter, L., El-Delik, J., Bohnert, J. A., et al. (2012). Transport of drugs by the multidrug transporter AcrB involves an access and a deep binding pocket that are separated by a switch-loop. *Proc. Natl. Acad. Sci. U.S.A.* 109, 5687–5692. doi: 10.1073/pnas.1114944109
- Eicher, T., Seeger, M. A., Anselmi, C., Zhou, W., Brandstatter, L., Verrey, F., et al. (2014). Coupling of remote alternating-access transport mechanisms for protons and substrates in the multidrug efflux pump AcrB. *eLife* 3:e03145. doi: 10.7554/eLife.03145
- Elkins, C. A., and Nikaido, H. (2002). Substrate specificity of the RND-type multidrug efflux pumps AcrB and AcrD of *Escherichia coli* is determined predominantly by two large periplasmic loops. *J. Bacteriol.* 184, 6490–6498. doi: 10.1128/JB.184.23.6490-6499.2002
- Fischer, N., and Kandt, C. (2011). Three ways in, one way out: water dynamics in the trans-membrane domains of the inner membrane translocase AcrB. *Proteins* 79, 2871–2885. doi: 10.1002/prot.23122
- Fischer, N., and Kandt, C. (2013). Porter domain opening and closing motions in the multi-drug efflux transporter AcrB. *Biochim. Biophys. Acta* 1828, 632–641. doi: 10.1016/j.bbapam.2012.10.016
- Fischer, N., Raunest, M., Schmidt, T. H., Koch, D. C., and Kandt, C. (2014). Efflux pump-mediated antibiotics resistance: insights from computational structural biology. *Interdiscip. Sci.* 6, 1–12. doi: 10.1007/s12539-014-0191-3
- Fluman, N., Cohen-Karni, D., Weiss, T., and Bibi, E. (2009). A promiscuous conformational switch in the secondary multidrug transporter MdfA. *J. Biol. Chem.* 284, 32296–32304. doi: 10.1074/jbc.M109.050658
- Guan, L., and Kaback, H. R. (2007). Site-directed alkylation of cysteine to test solvent accessibility of membrane proteins. *Nat. Protoc.* 2, 2012–2017. doi: 10.1038/nprot.2007.275
- Hobbs, E. C., Yin, X., Paul, B. J., Astarita, J. L., and Storz, G. (2012). Conserved small protein associates with the multidrug efflux pump AcrB and differentially affects antibiotic resistance. *Proc. Natl. Acad. Sci. U.S.A.* 109, 16696–16701. doi: 10.1073/pnas.1210093109
- Hung, L. W., Kim, H. B., Murakami, S., Gupta, G., Kim, C. Y. and Terwilliger, T. C. (2013). Crystal structure of AcrB complexed with linezolid at 3.5 angstrom resolution. *J. Struct. Funct. Genomics* 14, 71–75. doi: 10.1007/s10969-013-9154-x
- Husain, F., Bikhchandani, M., and Nikaido, H. (2011). Vestibules are part of the substrate path in the multidrug efflux transporter AcrB of *Escherichia coli*. *J. Bacteriol.* 193, 5847–5849. doi: 10.1128/JB.05759-11
- Husain, F., and Nikaido, H. (2010). Substrate path in the AcrB multidrug efflux pump of *Escherichia coli*. *Mol. Microbiol.* 78, 320–330. doi: 10.1111/j.1365-2958.2010.07330.x
- Imai, T., Miyashita, N., Sugita, Y., Kovalenko, A., Hirata, F., and Kidera, A. (2011). Functionality mapping on internal surfaces of multidrug transporter AcrB based on molecular theory of solvation: implications for drug efflux pathway. *J. Phys. Chem. B* 115, 8288–8295. doi: 10.1021/jp2015758
- Karplus, M., and McCammon, J. A. (2002). Molecular dynamics simulations of biomolecules. *Nat. Struct. Biol.* 9, 646–652. doi: 10.1038/nsb0902-646
- Kern, W. V., Steinke, P., Schumacher, A., Schuster, S., Von Baum, H., and Bohnert, J. A. (2006). Effect of 1-(1-naphthylmethyl)-piperazine, a novel putative efflux pump inhibitor, on antimicrobial drug susceptibility in clinical isolates of *Escherichia coli*. *J. Antimicrob. Chemother.* 57, 339–343. doi: 10.1093/jac/dki445
- Kobayashi, N., Tamura, N., Van Veen, H. W., Yamaguchi, A., and Murakami, S. (2014).  $\beta$ -Lactam selectivity of multidrug transporters AcrB and AcrD resides in the proximal binding pocket. *J. Biol. Chem.* 289, 10680–10690. doi: 10.1074/jbc.M114.547794
- Kvist, M., Hancock, V., and Klemm, P. (2008). Inactivation of efflux pumps abolishes bacterial biofilm formation. *Appl. Environ. Microbiol.* 74, 7376–7382. doi: 10.1128/AEM.01310-08
- Lamers, R. P., Cavallari, J. F., and Burrows, L. L. (2013). The efflux inhibitor phenylalanine-arginine beta-naphthylamide (PAbetaN) permeabilizes the outer membrane of gram-negative bacteria. *PLoS ONE* 8:e60666. doi: 10.1371/journal.pone.0060666
- Li, X. Z., Zhang, L., Sri Kumar, R., and Poole, K. (1998). Beta-lactamase inhibitors are substrates for the multidrug efflux pumps of *Pseudomonas aeruginosa*. *Antimicrob. Agents Chemother.* 42, 399–403.
- Lim, S. P., and Nikaido, H. (2010). Kinetic parameters of efflux of penicillins by the multidrug efflux transporter AcrAB-TolC of *Escherichia coli*. *Antimicrob. Agents Chemother.* 54, 1800–1806. doi: 10.1128/AAC.01714-09
- Lomovskaya, O., and Bostian, K. A. (2006). Practical applications and feasibility of efflux pump inhibitors in the clinic—a vision for applied use. *Biochem. Pharmacol.* 71, 910–918. doi: 10.1016/j.bcp.2005.12.008
- Lomovskaya, O., Lee, A., Hoshino, K., Ishida, H., Mistry, A., Warren, M. S., et al. (1999). Use of a genetic approach to evaluate the consequences of inhibition of efflux pumps in *Pseudomonas aeruginosa*. *Antimicrob. Agents Chemother.* 43, 1340–1346.
- Lomovskaya, O., Warren, M. S., Lee, A., Galazzo, J., Fronko, R., Lee, M., et al. (2001). Identification and characterization of inhibitors of multidrug resistance efflux pumps in *Pseudomonas aeruginosa*: novel agents for combination therapy. *Antimicrob. Agents Chemother.* 45, 105–116. doi: 10.1128/AAC.45.1.105-116.2001
- Loo, T. W., and Clarke, D. M. (2002). Location of the rhodamine-binding site in the human multidrug resistance P-glycoprotein. *J. Biol. Chem.* 277, 44332–44338. doi: 10.1074/jbc.M20843200
- Mao, W., Warren, M. S., Black, D. S., Satou, T., Murata, T., Nishino, T., et al. (2002). On the mechanism of substrate specificity by resistance nodulation division (RND)-type multidrug resistance pumps: the large periplasmic loops of MexD from *Pseudomonas aeruginosa* are involved in substrate recognition. *Mol. Microbiol.* 46, 889–901. doi: 10.1046/j.1365-2958.2002.03223.x
- Murakami, S., Nakashima, R., Yamashita, E., Matsumoto, T., and Yamaguchi, A. (2006). Crystal structures of a multidrug transporter reveal a functionally rotating mechanism. *Nature* 443, 173–179. doi: 10.1038/nature05076
- Murakami, S., Nakashima, R., Yamashita, E., and Yamaguchi, A. (2002). Crystal structure of bacterial multidrug efflux transporter AcrB. *Nature* 419, 587–593. doi: 10.1038/nature01050
- Nagano, K., and Nikaido, H. (2009). Kinetic behavior of the major multidrug efflux pump AcrB of *Escherichia coli*. *Proc. Natl. Acad. Sci. U.S.A.* 106, 5854–5858. doi: 10.1073/pnas.0901695106
- Nakae, T., Saito, K., and Nakajima, A. (2000). Effect of sulbactam on anti-pseudomonal activity of beta-lactam antibiotics in cells producing various levels of the MexAB-OprM efflux pump and beta-lactamase. *Microbiol. Immunol.* 44, 997–1001. doi: 10.1111/j.1348-0421.2000.tb02595.x
- Nakashima, R., Sakurai, K., Yamasaki, S., Hayashi, K., Nagata, C., Hoshino, K., et al. (2013). Structural basis for the inhibition of bacterial multidrug exporters. *Nature* 500, 102–106. doi: 10.1038/nature12300
- Nakashima, R., Sakurai, K., Yamasaki, S., Nishino, K., and Yamaguchi, A. (2011). Structures of the multidrug exporter AcrB reveal a proximal

- multisite drug-binding pocket. *Nature* 480, 565–569. doi: 10.1038/nature10641
- Nakayama, K., Ishida, Y., Ohtsuka, M., Kawato, H., Yoshida, K., Yokomizo, Y., et al. (2003a). MexAB-OprM-specific efflux pump inhibitors in *Pseudomonas aeruginosa*. Part 1: discovery and early strategies for lead optimization. *Bioorg. Med. Chem. Lett.* 13, 4201–4204. doi: 10.1016/j.bmcl.2003.07.024
- Nakayama, K., Ishida, Y., Ohtsuka, M., Kawato, H., Yoshida, K., Yokomizo, Y., et al. (2003b). MexAB-OprM specific efflux pump inhibitors in *Pseudomonas aeruginosa*. Part 2: achieving activity in vivo through the use of alternative scaffolds. *Bioorg. Med. Chem. Lett.* 13, 4205–4208. doi: 10.1016/j.bmcl.2003.07.027
- Nakayama, K., Kawato, H., Watanabe, J., Ohtsuka, M., Yoshida, K., Yokomizo, Y., et al. (2004a). MexAB-OprM specific efflux pump inhibitors in *Pseudomonas aeruginosa*. Part 3: optimization of potency in the pyridopyrimidine series through the application of a pharmacophore model. *Bioorg. Med. Chem. Lett.* 14, 475–479. doi: 10.1016/j.bmcl.2003.10.060
- Nakayama, K., Kuru, N., Ohtsuka, M., Yokomizo, Y., Sakamoto, A., Kawato, H., et al. (2004b). MexAB-OprM specific efflux pump inhibitors in *Pseudomonas aeruginosa*. Part 4: addressing the problem of poor stability due to photoisomerization of an acrylic acid moiety. *Bioorg. Med. Chem. Lett.* 14, 2493–2497. doi: 10.1016/j.bmcl.2004.03.007
- Nikaido, H. (2011). Structure and mechanism of RND-type multidrug efflux pumps. *Adv. Enzymol. Relat. Areas Mol. Biol.* 77, 1–60. doi: 10.1002/9780470920541.ch1
- Nikaido, H., and Pages, J. M. (2012). Broad-specificity efflux pumps and their role in multidrug resistance of Gram-negative bacteria. *FEMS Microbiol. Rev.* 36, 340–363. doi: 10.1111/j.1574-6976.2011.00290.x
- Nishino, K., Latifi, T., and Groisman, E. A. (2006). Virulence and drug resistance roles of multidrug efflux systems of *Salmonella enterica* serovar *Typhimurium*. *Mol. Microbiol.* 59, 126–141. doi: 10.1111/j.1365-2958.2005.04940.x
- Opperman, T. J., Kwasny, S. M., Kim, H. S., Nguyen, S., Housewright, C., D’souza, S., et al. (2014). Characterization of a novel pyranopyridine inhibitor of the AcrAB efflux pump of *Escherichia coli*. *Antimicrob. Agents Chemother.* 58, 722–733. doi: 10.1128/AAC.01866-13
- Pannek, S., Higgins, P. G., Steinke, P., Jonas, D., Akova, M., Bohnert, J. A., et al. (2006). Multidrug efflux inhibition in *Acinetobacter baumannii*: comparison between 1-(1-naphthylmethyl)-piperazine and phenyl-arginine-beta-naphthylamide. *J. Antimicrob. Chemother.* 57, 970–974. doi: 10.1093/jac/dkl081
- Piddock, L. J. (2006). Clinically relevant chromosomally encoded multidrug resistance efflux pumps in bacteria. *Clin. Microbiol. Rev.* 19, 382–402. doi: 10.1128/CMR.19.2.382–402.2006
- Pos, K. M. (2009). Drug transport mechanism of the AcrB efflux pump. *Biochim. Biophys. Acta* 1794, 782–793. doi: 10.1016/j.bbapap.2008.12.015
- Renau, T. E., Leger, R., Filanova, L., Flamme, E. M., Wang, M., Yen, R., et al. (2003). Conformationally-restricted analogues of efflux pump inhibitors that potentiate the activity of levofloxacin in *Pseudomonas aeruginosa*. *Bioorg. Med. Chem. Lett.* 13, 2755–2758. doi: 10.1016/S0960-894X(03)00556-0
- Renau, T. E., Leger, R., Flamme, E. M., Sangalang, J., She, M. W., Yen, R., et al. (1999). Inhibitors of efflux pumps in *Pseudomonas aeruginosa* potentiate the activity of the fluoroquinolone antibacterial levofloxacin. *J. Med. Chem.* 42, 4928–4931. doi: 10.1021/jm9904598
- Renau, T. E., Leger, R., Flamme, E. M., She, M. W., Gannon, C. L., Mathias, K. M., et al. (2001). Addressing the stability of C-capped dipeptide efflux pump inhibitors that potentiate the activity of levofloxacin in *Pseudomonas aeruginosa*. *Bioorg. Med. Chem. Lett.* 11, 663–667. doi: 10.1016/S0960-894X(01)00033-6
- Renau, T. E., Leger, R., Yen, R., She, M. W., Flamme, E. M., Sangalang, J., et al. (2002). Peptidomimetics of efflux pump inhibitors potentiate the activity of levofloxacin in *Pseudomonas aeruginosa*. *Bioorg. Med. Chem. Lett.* 12, 763–766. doi: 10.1016/S0960-894X(02)00006-9
- Ruggerone, P., Murakami, S., Pos, K. M., and Vargiu, A. V. (2013a). RND efflux pumps: structural information translated into function and inhibition mechanisms. *Curr. Top. Med. Chem.* 13, 3079–3100. doi: 10.2174/1568266113136660220
- Ruggerone, P., Vargiu, A. V., Collu, F., Fischer, N., and Kandt, C. (2013b). Molecular dynamics computer simulations of multidrug RND efflux pumps. *Comput. Struct. Biotechnol. J.* 5:e201302008. doi: 10.5936/csbj.201302008
- Schulz, R., Vargiu, A. V., Collu, F., Kleinekathofer, U., and Ruggerone, P. (2010). Functional rotation of the transporter AcrB: insights into drug extrusion from simulations. *PLoS Comput. Biol.* 6:e1000806. doi: 10.1371/journal.pcbi.1000806
- Schulz, R., Vargiu, A. V., Ruggerone, P., and Kleinekathofer, U. (2011). Role of water during the extrusion of substrates by the efflux transporter AcrB. *J. Phys. Chem. B* 115, 8278–8287. doi: 10.1021/jp200996x
- Schulz, R., Vargiu, A. V., Ruggerone, P., and Kleinekathofer, U. (2015). Computational study of correlated domain motions in the AcrB efflux transporter. *Biomed. Res. Int.* 2015:487298. doi: 10.1155/2015/487298
- Schumacher, A., Steinke, P., Bohnert, J. A., Akova, M., Jonas, D., and Kern, W. V. (2006). Effect of 1-(1-naphthylmethyl)-piperazine, a novel putative efflux pump inhibitor, on antimicrobial drug susceptibility in clinical isolates of Enterobacteriaceae other than *Escherichia coli*. *J. Antimicrob. Chemother.* 57, 344–348. doi: 10.1093/jac/dki446
- Schuster, S., Kohler, S., Buck, A., Dambacher, C., Konig, A., Bohnert, J. A., et al. (2014). Random mutagenesis of the multidrug transporter AcrB from *Escherichia coli* for identification of putative target residues of efflux pump inhibitors. *Antimicrob. Agents Chemother.* 58, 6870–6878. doi: 10.1128/AAC.03775-14
- Seeger, M. A., Schiefner, A., Eicher, T., Verrey, F., Diederichs, K., and Pos, K. M. (2006). Structural asymmetry of AcrB trimer suggests a peristaltic pump mechanism. *Science* 313, 1295–1298. doi: 10.1126/science.1131542
- Seeger, M. A., Von Ballmoos, C., Eicher, T., Brandstatter, L., Verrey, F., Diederichs, K., et al. (2008). Engineered disulfide bonds support the functional rotation mechanism of multidrug efflux pump AcrB. *Nat. Struct. Mol. Biol.* 15, 199–205. doi: 10.1038/nsmb.1379
- Seeger, M. A., Von Ballmoos, C., Verrey, F., and Pos, K. M. (2009). Crucial role of Asp408 in the proton translocation pathway of multidrug transporter AcrB: evidence from site-directed mutagenesis and carbodiimide labeling. *Biochemistry* 48, 5801–5812. doi: 10.1021/bi900446j
- Sennhauser, G., Amstutz, P., Briand, C., Storchenecker, O., and Grutter, M. G. (2007). Drug export pathway of multidrug exporter AcrB revealed by DARPin inhibitors. *PLoS Biol.* 5:e7. doi: 10.1371/journal.pbio.0050007
- Sennhauser, G., Bukowska, M. A., Briand, C., and Grutter, M. G. (2009). Crystal structure of the multidrug exporter MexB from *Pseudomonas aeruginosa*. *J. Mol. Biol.* 389, 134–145. doi: 10.1016/j.jmb.2009.04.001
- Singh, R., Swick, M. C., Ledesma, K. R., Yang, Z., Hu, M., Zechiedrich, L., et al. (2012). Temporal interplay between efflux pumps and target mutations in development of antibiotic resistance in *Escherichia coli*. *Antimicrob. Agents Chemother.* 56, 1680–1685. doi: 10.1128/AAC.05693-11
- Su, C. C., Li, M., Gu, R., Takatsuka, Y., Mcdermott, G., Nikaido, H., et al. (2006). Conformation of the AcrB multidrug efflux pump in mutants of the putative proton relay pathway. *J. Bacteriol.* 188, 7290–7296. doi: 10.1128/JB.00684-06
- Su, C. C., and Yu, E. W. (2007). Ligand-transporter interaction in the AcrB multidrug efflux pump determined by fluorescence polarization assay. *FEBS Lett.* 581, 4972–4976. doi: 10.1016/j.febslet.2007.09.035
- Takatsuka, Y., Chen, C., and Nikaido, H. (2010). Mechanism of recognition of compounds of diverse structures by the multidrug efflux pump AcrB of *Escherichia coli*. *Proc. Natl. Acad. Sci. U.S.A.* 107, 6559–6565. doi: 10.1073/pnas.1001460107
- Takatsuka, Y., and Nikaido, H. (2009). Covalently linked trimer of the AcrB multidrug efflux pump provides support for the functional rotating mechanism. *J. Bacteriol.* 191, 1729–1737. doi: 10.1128/JB.01441-08
- Tikhonova, E. B., Wang, Q., and Zgurskaya, H. I. (2002). Chimeric analysis of the multicomponent multidrug efflux transporters from gram-negative bacteria. *J. Bacteriol.* 184, 6499–6507. doi: 10.1128/JB.184.23.6499-6507.2002
- Trott, O., and Olson, A. J. (2010). AutoDock Vina: improving the speed and accuracy of docking with a new scoring function, efficient optimization, and multithreading. *J. Comput. Chem.* 31, 455–461. doi: 10.1002/jcc.21334
- Vaara, M., and Vaara, T. (1983). Sensitization of Gram-negative bacteria to antibiotics and complement by a nontoxic oligopeptide. *Nature* 303, 526–528. doi: 10.1038/303526a0
- Van Bambeke, F., Pages, J. M., and Lee, V. J. (2006). Inhibitors of bacterial efflux pumps as adjuvants in antibiotic treatments and diagnostic tools for detection of resistance by efflux. *Recent Pat. Antiinfect. Drug Discov.* 1, 157–175. doi: 10.2174/157489106777452692
- Vargiu, A. V., Collu, F., Schulz, R., Pos, K. M., Zacharias, M., Kleinekathofer, U., et al. (2011). Effect of the F610A mutation on substrate extrusion in the AcrB

- transporter: explanation and rationale by molecular dynamics simulations. *J. Am. Chem. Soc.* 133, 10704–10707. doi: 10.1021/ja202666x
- Variju, A. V., and Nikaido, H. (2012). Multidrug binding properties of the AcrB efflux pump characterized by molecular dynamics simulations. *Proc. Natl. Acad. Sci. U.S.A.* 109, 20637–20642. doi: 10.1073/pnas.1218348109
- Variju, A. V., Ruggerone, P., Opperman, T. J., Nguyen, S. T., and Nikaido, H. (2014). Molecular mechanism of MBX2319 inhibition of *Escherichia coli* AcrB multidrug efflux pump and comparison with other inhibitors. *Antimicrob. Agents Chemother.* 58, 6224–6234. doi: 10.1128/AAC.03283-14
- Watkins, W. J., Landaverry, Y., Leger, R., Litman, R., Renau, T. E., Williams, N., et al. (2003). The relationship between physicochemical properties, in vitro activity and pharmacokinetic profiles of analogues of diamine-containing efflux pump inhibitors. *Bioorg. Med. Chem. Lett.* 13, 4241–4244. doi: 10.1016/j.bmcl.2003.07.030
- Yao, X. Q., Kenzaki, H., Murakami, S., and Takada, S. (2010). Drug export and allosteric coupling in a multidrug transporter revealed by molecular simulations. *Nat. Commun.* 1, 117. doi: 10.1038/ncomms1116
- Yao, X. Q., Kimura, N., Murakami, S., and Takada, S. (2013). Drug uptake pathways of multidrug transporter AcrB studied by molecular simulations and site-directed mutagenesis experiments. *J. Am. Chem. Soc.* 135, 7474–7485. doi: 10.1021/ja310548h
- Yoshida, K., Nakayama, K., Kuru, N., Kobayashi, S., Ohtsuka, M., Takemura, M., et al. (2006a). MexAB-OprM specific efflux pump inhibitors in *Pseudomonas aeruginosa*. Part 5: carbon-substituted analogues at the C-2 position. *Bioorg. Med. Chem.* 14, 1993–2004. doi: 10.1016/j.bmcl.2005.10.043
- Yoshida, K., Nakayama, K., Yokomizo, Y., Ohtsuka, M., Takemura, M., Hoshino, K., et al. (2006b). MexAB-OprM specific efflux pump inhibitors in *Pseudomonas aeruginosa*. Part 6: exploration of aromatic substituents. *Bioorg. Med. Chem.* 14, 8506–8518. doi: 10.1016/j.bmcl.2006.08.037
- Yoshida, K., Nakayama, K., Ohtsuka, M., Kuru, N., Yokomizo, Y., Sakamoto, A., et al. (2007). MexAB-OprM specific efflux pump inhibitors in *Pseudomonas aeruginosa*. Part 7: highly soluble and in vivo active quaternary ammonium analogue D13-9001, a potential preclinical candidate. *Bioorg. Med. Chem.* 15, 7087–7097. doi: 10.1016/j.bmcl.2007.07.039
- Yu, E. W., Aires, J. R., Mcdermott, G., and Nikaido, H. (2005). A periplasmic drug-binding site of the AcrB multidrug efflux pump: a crystallographic and site-directed mutagenesis study. *J. Bacteriol.* 187, 6804–6815. doi: 10.1128/JB.187.19.6804-6815.2005
- Zechini, B., and Versace, I. (2009). Inhibitors of multidrug resistant efflux systems in bacteria. *Recent Pat. Antiinfect. Drug Discov.* 4, 37–50. doi: 10.2174/157489109787236256
- Zgurskaya, H. I. (2009). Covalently linked AcrB giant offers a new powerful tool for mechanistic analysis of multidrug efflux in bacteria. *J. Bacteriol.* 191, 1727–1728. doi: 10.1128/JB.01718-08
- Zgurskaya, H. I., and Nikaido, H. (1999). Bypassing the periplasm: reconstitution of the AcrAB multidrug efflux pump of *Escherichia coli*. *Proc. Natl. Acad. Sci. U.S.A.* 96, 7190–7195. doi: 10.1073/pnas.96.3.7190

**Conflict of Interest Statement:** Timothy J. Opperman and Son T. Nguyen are employees of Microbiotix, Inc.

Copyright © 2015 Opperman and Nguyen. This is an open-access article distributed under the terms of the Creative Commons Attribution License (CC BY). The use, distribution or reproduction in other forums is permitted, provided the original author(s) or licensor are credited and that the original publication in this journal is cited, in accordance with accepted academic practice. No use, distribution or reproduction is permitted which does not comply with these terms.

